THE PHOTOCHEMISTRY AND PHOTOSTABILIZATION POTENTIAL OF PLANT EXTRACTS ON SUNSCREEN ABSORBERS

by

MOSES ABEDNEGO OLLENGO

Submitted in fulfilment of the academic requirements for the degree of Doctor of Philosophy in the School of Chemistry and Physics, University of KwaZulu-Natal, Durban

December, 2014

In memory of my father Livingstone Olengo and mum Fejenia Shinali

ABSTRACT

The deleterious effects of ultraviolet (UV) radiation on outdoor workers and sunbathers cannot be over emphasised. To combat photoaging, skin wrinkling, photo-dermatitis, and various forms of skin cancer associated with UV radiation, photoprotection is necessary. The most convenient mode of protection is the use of sunscreens, presented in various cosmetic preparations. However, most of the commonly used sunscreens have been shown to photodegrade to less efficient light absorbing species whose toxicities are unknown. These photoproducts could be the cause of some of the observed hyperpigmentation and other skin disorders associated with topical cosmetic applications.

This thesis interrogates various sunscreens present in commercial sunscreen and skin-lightening preparations. Titanium dioxide was isolated, characterised and quantitated in twelve skin-lightening preparations because the amount, size and polymorph present determines its suitability as a sun protector. Anatase titanium dioxide is a known active photocatalyst and its nanoparticle penetration into viable tissues is likely to cause undesirable effects. A total of eight skin-lighteners had TiO_2 in quantifiable levels. The percent composition ranged between 2.83 – 12.47 % m/m. Four samples contained anatase TiO_2, three; rutile and one, a mixture of the two polymorphs. The particle size range of TiO_2 in these samples was from 16.23 – 58.70 nm indicating that all samples contained nano-TiO_2. The percentage composition of TiO_2 in sunscreen preparations was slightly higher (12.60 % m/m) than those in skin-lighteners. The amounts of organic absorbers in sunscreens and skin-lightening preparations were also measured in order to assess compliance with the health regulatory set maxima in various cosmetic preparations. The amount of organic absorbers in most skin-lightening preparations was found to be much lower than expected and none had the percentage composition indicated on the packet. The amounts of organic absorbers in the sunscreen preparations were within the allowed maximum limit allowed by health regulatory authorities. The amounts of organic absorbers were much higher than those in skin-lightening preparations.

The photostability of twenty two cosmetic sunscreen preparations was investigated, categorising those with plant extracts and those without plant extracts. The effect of plant extracts on common sunscreen absorbers was then examined. The products containing plant extracts demonstrated unique photostability compared with those without plant extracts. Some of the products contained liquorice and mulberry extracts and consequently it was of interest to investigate their contribution to the photostability observed. The effect of four plant extracts: grape seed extract, lavender oil, liquorice root extract, and mulberry extract on the photostability of 2-ethylhexyl-*p*-methoxycinnamate, benzophenone-3 and *tert*-butylmethoxy dibenzoylmethane was investigated. The mixture of each of these absorbers with the plant extracts singly and in combination demonstrated varying photoprotective potential. Three plant extracts (grape seed extract, mulberry extract and liquorice root extract) demonstrated photostabilization potential. In this work, lavender oil showed lower photostabilization potential. However, the irradiation of lavender oil in mixtures with sunscreen absorbers showed an increase in the number of photoproducts formed. Therefore, the addition of lavender oil in sunscreen preparations needs to be done with caution.

Plants are known sources of polyphenols perceived to be aggressive antioxidants and also show significant UV absorption. The antioxidant activity of some plant extracts and beverages was assayed

to ascertain their potential and suitability as free radical scavengers and synergistic absorbers. The total phenolic content in the plants and fruits investigated correlated positively with their corresponding antioxidant activity. The extracts also indicated significant UV absorption demonstrating possible use as UV absorbers.

Our work demonstrates for the first time the photostabilization potential of plant extracts on common UV absorbers in sunscreens and skin-lightening preparations. We have also shown that the incorporation of plant extracts may not require a combination of sunscreen absorbers to achieve broad-spectrum protection. Therefore, the reduction in the number of organic absorbers incorporated in a formulation is likely to decrease potential side-effects. Efforts have been made to profile the photoproducts in various plant extracts with a view of determining their identities as this is important for characterising their photo-toxicities in the future.

PREFACE

The experimental work described in this thesis was carried out in the School of Chemistry and Physics, University of KwaZulu-Natal, Durban, from October 2011 to December 2014, under the supervision of Professor B.S. Martincigh.

These studies represent original work by the author and have not otherwise been submitted in any form for any degree or diploma to any tertiary institution. Where use has been made of the work of others it is duly acknowledged in the text.

DECLARATION 1 – PLAGIARISM

I Moses Abednego Ollengo declare that

1. The research reported in thesis, except where otherwise indicated, is my original research.
2. This thesis has not been submitted for any degree or examination at any other University.
3. This thesis does not contain other person's data, pictures, graphs or other information, unless specifically acknowledged as being sourced from the persons.
4. This thesis does not contain other person's writing, unless specifically acknowledged as being sourced from other researchers. Where other written sources have been quoted, then:
    a. Their words have been re-written but, the general information attributed to them has been referenced
    b. Where their exact words have been used, then their writing has been placed in italics and inside quotation marks, and referenced.
5. This thesis does not contain text, graphics or tables copied and pasted from the internet, unless specifically acknowledged, and the source being detailed in the thesis and in the References sections.

Signed _____

DECLARATIONS 2 – PUBLICATIONS

DETAILS OF CONTRIBUTIONS TO PUBLICATIONS that form part and/or include research presented in this thesis.

Publication 1
Moses A. Ollengo and Bice S. Martincigh, Photostability, Photoproducts and Possible Photostabilization Mechanism of Sunscreens in Formulations (unpublished)

I planned, executed and wrote the initial draft manuscript under the supervision of Prof. BS Martincigh.

Publication 2
Moses A. Ollengo and Bice S. Martincigh, Trends in Sunscreen Formulation (unpublished)

I planned, executed and wrote the initial draft manuscript under the supervision of Prof. BS Martincigh.

Publication 3
Moses A. Ollengo and Bice S. Martincigh, The photostability of sunscreens in skin-lightening formulations in the South African market (unpublished)

I planned, executed and wrote the initial draft manuscript under the supervision of Prof. BS Martincigh.

Publication 4
Moses A. Ollengo and Bice S. Martincigh, *In-vitro* study of the photostabilizing potential of plant extracts on sunscreen absorbers (unpublished)

I planned, executed and wrote the initial draft manuscript under the supervision of Prof. BS Martincigh.

Publication 5
Moses A. Ollengo and Bice S. Martincigh, Quantitation and phases of titanium dioxide in skin-lightening products in the South African market (unpublished)

I planned, executed and wrote the initial draft manuscript under the supervision of Prof. BS Martincigh.

Publication 6
Moses A. Ollengo and Bice S. Martincigh, Grape seed extracts: an investigation of UV absorption potential and photostabilizing effect on three common sunscreen absorbers (unpublished).

I planned, executed and wrote the initial draft manuscript under the supervision of Prof. BS Martincigh.

Publication 7

Moses A. Ollengo and Bice S. Martincigh, The photostabilizing potential of mulberry extract on common sunscreen absorbers (unpublished).

I planned, executed and wrote the initial draft manuscript under the supervision of Prof. BS Martincigh.

Publication 8

Moses A. Ollengo and Bice S. Martincigh, The efficacy of Liquorice root extract in enhancing the UV stability of three commonly used sun-active agents (unpublished)

I planned, executed and wrote the initial draft manuscript under the supervision of Prof. BS Martincigh.

Publication 9

Moses A. Ollengo and Bice S. Martincigh, The effect of lavender oil on the photostability of commonly used sunscreen absorbers in suncare products (unpublished).

I planned, executed and wrote the initial draft manuscript under the supervision of Prof. BS Martincigh.

Publication 10

Moses A. Ollengo, Anis Mangenda and Bice S. Martincigh, Quantitation and Antioxidant Activity of Phenolic Acids from *Sutherlandia frutescens* (unpublished)

In this work Anis Mangenda did the experimental work on the isolation and quantitation of phenolic acids in cancer bush by HPLC analysis and the UV absorption potential of the cancer bush extract. Moses A. Ollengo determined the total phenolic content and antioxidant activity and also characterised three new phenolic compounds in the cancer bush by HPLC-MS under the supervision of Prof. BS Martincigh.

Publication 11

Moses A. Ollengo, Lynette Komarsamy, Georges J. Mturi and Bice S. Martincigh, Antioxidant Capacity of South African Beverages (unpublished)

This work was a contribution from three persons: Lynette Komarsamy provided HPLC profile of polyphenols in the fruit juices, Georges Mturi did the HPLC analysis of the tea samples and Moses Ollengo worked on the antioxidant activity of the beverages (teas and fruit juices). All persons were supervised by Prof. BS Martincigh.

Signed _____

CONFERENCE CONTRIBUTIONS

Oral presentation: Moses A. Ollengo and Bice S. Martincigh, The photostabilizing effect of mulberry extract on common sunscreen absorbers, South African Chemical Institute Postgraduate Colloquium, Pietermaritzburg, South Africa 28th October, 2014

Poster presentation: Moses A. Ollengo and Bice S. Martincigh, An investigation of the photostabilizing potential of plant extracts on sunscreen absorbers in skin-lightening products, The XXVth IUPAC Symposium on Photochemistry, Bordeaux, France 13th July - 18th July, 2014

Poster presentation: Moses A. Ollengo and Bice S. Martincigh, *In-vitro* study of photostabilizing potential of plant extracts on sunscreen absorbers in skin-lightening products, University of KwaZulu-Natal, College of Agriculture, Engineering and Science Research Day, Durban, South Africa 1st November, 2013

Oral presentation: Moses A. Ollengo and Bice S. Martincigh, The effect of plant extracts on the photostability of skin-lightening products containing sunscreen absorbers, 16th Biennual SACI Inorganic Chemistry Conference incorporating the Carman Physical Chemistry Symposium, Durban, South Africa 30th June - 4th July, 2013

Poster presentation: Moses A. Ollengo Ncoza C Ndlova and Bice S. Martincigh, Levels of Nano-TiO$_2$ in Selected Skin Lightening Products in South African Market, 4th Ethnic Skin and Hair, Congress Nairobi, Kenya 4th November – 9th November, 2012

Poster presentation: Moses A. Ollengo and Bice S. Martincigh, Levels of Titanium dioxide in Selected Skin-lightening Products in South African Market, University of KwaZulu-Natal, College of Agriculture, Engineering and Science Research Day, Pietermaritzburg, South Africa 29th October, 2012

Poster presentation: Moses A. Ollengo Ncoza C Ndlova and Bice S. Martincigh, Levels of Nano-TiO$_2$ in Selected Skin Lightening Products In South African Market, 3rd Continental Congress of the International Society of Dermatology and the 65th National Congress of the Dermatology Society of South Africa, Durban, South Africa, 24th October – 27th October, 2012

ACKNOWLEDGEMENTS

TABLE OF CONTENT

Chapter One

Introduction

Skin cancer is the most common form of human cancer and its incidence is increasing worldwide at an alarming rate. Most occurrences of skin cancer are thought to arise as a result of overexposure to solar ultraviolet (UV) radiation.

1.1   Solar ultraviolet radiation and its effects

For biological purposes solar UV radiation can be divided into three regions: ultraviolet C (UVC) from 100-280 nm, ultraviolet B (UVB) 280-315 nm, and ultraviolet A (UVA) 315-400 nm. The UVC since it contains the shortest wavelengths, is the most energetic and consequently the most damaging radiation (Kowalski 2009; de Gruijl et al. 1993). Fortunately it is absorbed mostly by the ozone in the stratosphere and does not fall on the earth's surface. This radiation is absorbed by the nucleic acid bases and hence can lead to genetic mutations and ultimately cancer.

UVB radiation greater than 290 nm falls on the earth's surface at sea level and constitutes about 5-10 % of the terrestrial solar UV radiation. This radiation is known to cause immune suppression, cataract formation, and other associated effects are inflammation, and formation of invasive and proliferating lesions called pterygia on the cornea. It is absorbed by nucleic acids and has the ability to directly cause genotoxic damage to DNA and finally skin cancer (Girard et al. 2002). The photochemical reactions of UVB on the skin, referred to as erythema, are the principal causes of UV induced tissue damage following solar exposures for any amount of time. The symptoms depend on the intensity and or length of the exposure. Chronic exposure to UVB causes photo-keratitis, wrinkling, photo-aging, acute erythema or oedema of the skin, basal cell carcinoma and squamous cell carcinomas and their precursors (de Gruijl et al. 1993). However, a moderate dose of UVB is necessary for production of vitamin D and vitamin K, that are very essential nutrients and antioxidants.

UVA radiation has the longest wavelength but penetrates deeper into the skin. At one point this radiation was thought to be harmless but now it is known to cause a wide variety of damaging biological effects. Because it reaches the viable tissues, UVA is thought to excite chromophores, such as flavins, quinone, porphyrins and melanin, which act as endogenous photosensitisers. The photosentization reactions lead to the formation of reactive oxygen species (ROS). The ROS and singlet oxygen ($^1O_2$) may react with DNA, generating DNA single- and double-strand breaks or induce the photoproduct 8-oxo-7,8-dihydro-2'-deoxyguanosine (8oxoG) in human skin (Baumler et al. 2012). These lesions have been linked to induction of mutations and apoptosis (Cortat et al. 2013). These attacks on the DNA could be the cause of immune system depression and the development of skin cancer, including melanoma (Garland et al. 2003). The photo-allergies and phototoxic reactions, as well as photo-dermatoses are mainly UVA induced (Fourtanier et al. 2012). This indirect DNA damage has also been fronted as the cause of malignant melanoma. More recent epidemiological data has shown that UVA radiation is involved in the genesis of cutaneous melanoma (Baumler et al. 2012; Autier et al. 2011). In addition, because UVA penetrates deeper it damages collagen fibres and destroys vitamin A. The current problem is that UVA forms the largest percentage (95 %) of the UV radiation that reaches the earth's surface. On most days of the year certain anatomic sites such as the top of the head, shoulders, arms, and faces are exposed. There is therefore need for photoprotection.

1.2   Photoprotective measures

The effect of UV radiation on outdoor workers and sunbathers cannot be over-emphasised. To combat photoaging, skin wrinkling, photo-dermatitis, and various forms of skin cancer associated with UV radiation, photoprotection is the only choice. The avoidance of the sun between 10 am and 4

pm, the known peak UV radiation period, by keeping under shade may not be a solution given the different lifestyles of people and rapidly changing social cultural perspectives. Various health regulatory bodies advocate the use of sunglasses, clothing, and hats but these too may not cover the entire skin especially with the rise in global temperatures. Hence, the most convenient mode of protection is the use of sunscreens, presented in various cosmetic preparations. Another problem is that among the Asian and African communities light skin is considered an element of beauty and so efforts are made to lighten the skin by inhibiting melanin formation, the intrinsic UV absorber. This practice makes the skin susceptible to deleterious UV effects. Consequently, these preparations require the incorporation of sunscreens to protect the lightened skin.

1.3 Sunscreen concerns

Sunscreens were originally designed to prevent erythema that is the reddening of the skin. They were not designed to prevent skin cancer. It has now been shown that they are effective against the development of cutaneous malignant melanoma (CMM) (Gallagher et al. 2000). Other current anticipated use of effective sunscreen is prevention of various deleterious UV effects such as immunosuppression, actinic keratosis, and UV-induced DNA damage, among others. However, most of the commonly used sunscreens have been shown to photodegrade (particularly in the UVA region) to less light absorbing species whose toxicities are unknown. Degraded sunscreens are no longer effective and the user remains inadvertently unprotected unless fresh sunscreen is applied. A serious concern for such photodegrading sunscreens is the fate of the photoproducts; currently know report about their phototoxicities exist. Such agents may induce adverse effects such as contact and photocontact allergic reactions. The other emerging challenge is the revelation that some sunscreens penetrate the skin (Gonzalez 2010; Gonzalez et al. 2006) posing an unknown systemic toxicity profile. There are reports from animal studies that speculate that some sunscreen agents may play a role in endocrine disruption (Schlumpf et al. 2004; Janjua et al. 2004) Hence the amounts of organic absorbers, sizes and forms of physical absorbers, like titanium dioxide have drawn significant attention. World health regulatory bodies have placed certain maximum values for the content of organic absorbers but no lower size limit of physical absorbers. These regulators lay no check on the form of titanium dioxide, yet anatase titanium dioxide is a well-known aggressive photocatalyst. This has the potential to penetrate to viable skin tissues if it is in the nano-range (Tiano et al. 2010).

Figures 1.1 and 1.2 show the common groups of organic sunscreens with varying UV absorption capacities. The derivatives of camphor, cinnamate, p-aminobenzoate and salicylate are known UVB absorbers whereas anthranilate and benzophenone derivatives absorb into the lower UVA1 region (340-400 nm). The commonly used UVA absorber is a derivative of dibenzoylmethane. This makes combinations of sunscreens inevitable in a bid to produce a broad-spectrum sunscreen product. This again opens other frontiers of unanswered questions. For example, *tert*-butylmethoxy dibenzoylmethane (BMDBM, commonly known as avobenzone) a common UVA absorber in combination with 2-ethylhexyl-p-methoxycinnamate (EHMC) gives a very photo-unstable product (Sayre et al. 2005; Dondi et al. 2006). Both chemical absorbers are known to lose UV absorption efficiency through isomerisation, and photodegradation. In addition, the triplet excited states of these absorbers are sufficiently close so that BMDBM can photosensitize EHMC causing it to isomerise and lose absorption efficiency (Sayre et al. 2005; Panday 2002). The quest for a stable and effective broad-spectrum sunscreen preparation therefore has become an elusive yet thought-stimulating question. Currently, various systems are under investigation, including plants extracts and other synthetic species, which would stabilize the approved organic absorbers.
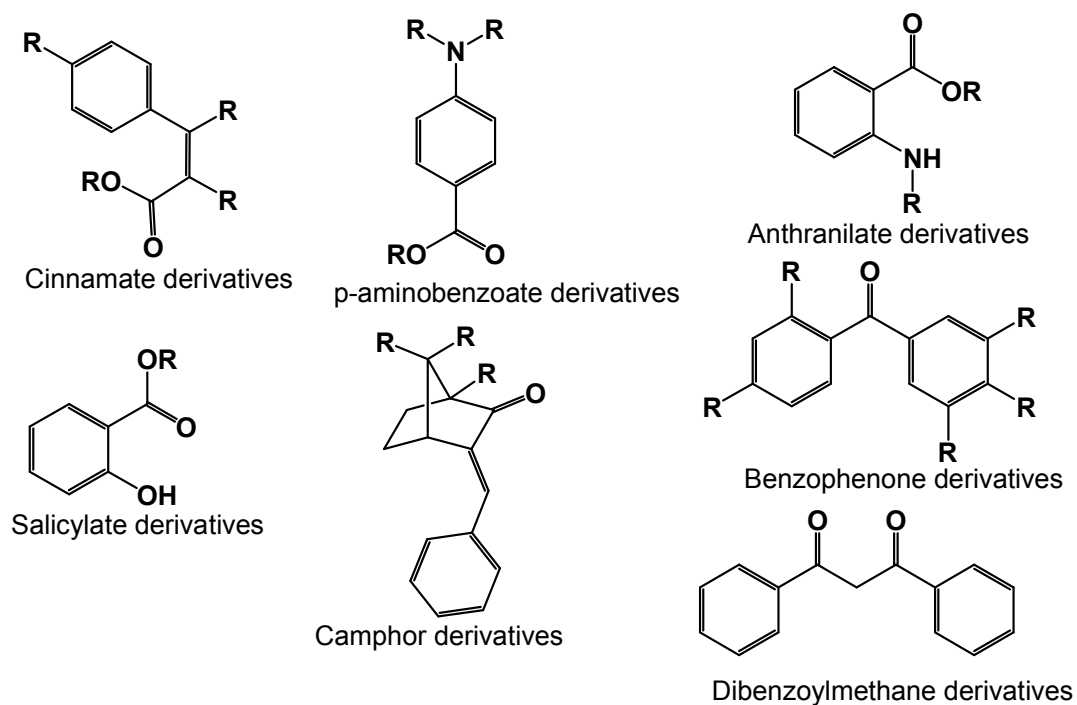
Figure 1.1: Common organic sunscreen absorber groups.
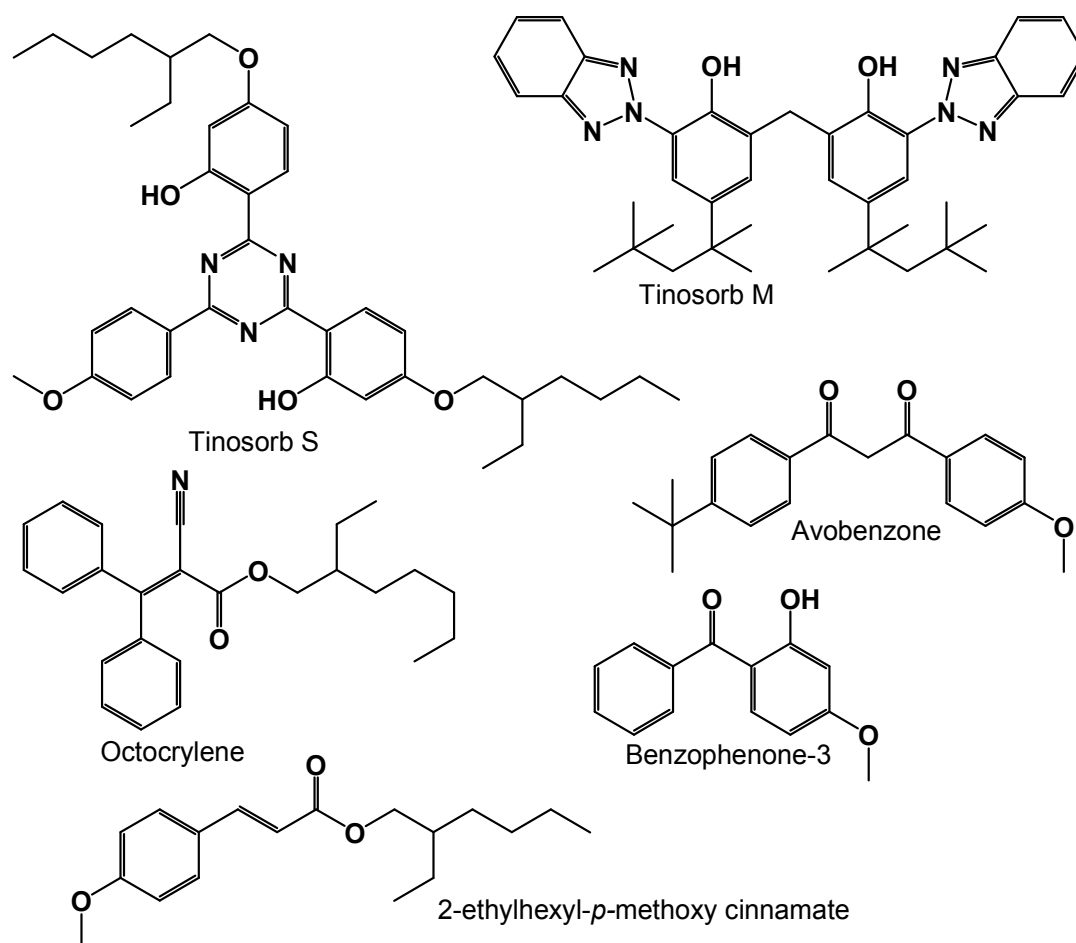
Figure 1.2: Frequently used sunscreens in cosmetic products.

1.4   Aim and objectives of this research

Due to the foregoing challenges, the aim of this work was to study the photochemistry and photostabilization potential of plant extracts on sunscreen absorbers. It is important to note that plants have found their niche in ethnopharmacology for ages now without reported adverse effects. Some of the phytochemicals in plants are good UV absorbers and have also shown very good antioxidant properties. Our study of the photostability of sunscreens in skin-lightening preparations demonstrated unique photostability for products containing plant extracts. This led us to speculate a possible enhancement of UV absorption from the plant extracts. Hence, the photo-activity of plant extracts projected itself as a worthwhile candidate for study with the aim to photostabilize commonly used sunscreens in the market. Therefore the aim of this work was to study the effect of common plant extracts added to the three most commonly used sunscreen agents, namely EHMC, benzophenone-3 (BP3) and BMDBM.

The above aim was achieved by undertaking the following objectives:

1. To determine the photostability of twenty two sunscreen products and twelve skin-lightening preparations upon exposure to solar radiation and to observe any differences between those that contained plants extracts and those without plant extracts.
2. To determine the levels of organic absorbers in the sunscreens and the skin-lightening preparations.
3. To quantitate, isolate, and characterise the polymorphs of titanium dioxide in the skin-lightening preparations and determine their particle size range.
4. To study the effect of plant extracts, namely, grape seed extract, mulberry extract, liquorice root extract and lavender oil on the photostability of: EHMC, BP3 and BMDBM.
5. To determine the total phenolic content, antioxidant activity and UV absorption potential of phenolic acids from a local herb: *Sutherlandia frutescens*, commonly known as cancer bush.
6. To quantitate the total phenolic content, antioxidant activity and identify the phenolic acids present in local beverages in order to inform on their suitability as dietary supplements to fight UV-induced systemic oxidative threats.

1.5   Overview of thesis structure

This thesis is written in paper/manuscript format and therefore consists of a series of self-contained chapters. To understand possible interactions of the common UV absorbers in complex matrices normally encountered in finished products we reviewed the literature on the photostability, photoproducts and possible photostabilization mechanism of sunscreens in formulations. This review is presented in Chapter Two. In order to achieve our aim we conducted a survey on the current trends in sunscreen formulations. We explored reports on the various strategies used so far and established missing links to the production of photostable products. A comprehensive coverage of this subject can be seen in Chapter Three. The photostability of twenty two cosmetic sunscreen preparations was investigated, categorising those with plant extracts and those without plant extracts. The effect of plant extracts on common sunscreen absorbers was then examined. The photostability was assessed by UV transmission spectrophotometry. The organic absorbers were characterised and quantitated by use of HPLC-PDA, HPLC-MS, GC-FID and GC-MS while ICP-OES was used for the physical absorbers and reflectors. The form of titanium dioxide present in these products was characterised by high resolution transmission electron microscopy (HR-TEM) and powder X-ray diffraction (PXRD). The two techniques were instrumental in the determination of not only the form of titanium dioxide but also the particle size. These reports can be seen as follows: the photostability of sunscreens in skin-lightening formulations in the South African market (Chapter Four), *in-vitro* study of the

photostabilizing potential of plant extracts on sunscreen absorbers (Chapter Five) and quantitation and particle size effects of titanium dioxide in skin-lightening products in the South African market (Chapter Six).

Previous work in our laboratory had shown that a polyphenolic extract of the cancer bush could photostabilize BMDBM degradation. On the basis of this observation and the unique spectral stability of the products containing plant extracts led us to investigate systems that could provide a lead to photostable sunscreen products. These reports are sequenced as: An investigation of the photostabilizing effect of grape seed extract on three common sunscreen absorbers (Chapter Seven), The photostabilizing potential of mulberry extract on common sunscreen absorbers (Chapter Eight), The efficacy of liquorice root extract in enhancing the UV stability of three commonly used sun-active agents (Chapter Nine), The effect of lavender oil on the photostability of commonly used sunscreen absorbers in suncare products (Chapter Ten).

South Africa is endowed with plant materials and has a long history of herbal use of plant extracts in traditional medicine. One such herb is *Sutherlandia frutescens* (cancer bush, CB). There is considerable interest in this herb for various medical reasons. We therefore investigated its polyphenolic content and quantitated the antioxidant activity of the phenolic acids in the cancer bush (Chapter Eleven). To demonstrate the UV absorption potential of the phenolic acids in CB; an extract was screened by standard spectrophotometric methods. Systemic antioxidant supplements are advocated as a remedy for various free radical mediated oxidative ailments. One easy way of introducing polyphenolic antioxidants is by consumption of antioxidant rich beverages. We investigated the antioxidant capacity of South African beverages (Chapter Twelve) to assess their nutritional value, a measure that could assist in determining their suitability as nutritional supplements. Efforts were made to characterise the active groups present in them by comparison of their UV spectra with library and literature matches. The fact that the polyphenols which are the main antioxidants in these beverages do have UV spectra is an indication that they are potent UV absorbers and hence suitable ingredients in sunscreen preparations and other cosmetic products.

1.6   Conclusion

The current work cross-examines various sunscreens present in commercial sunscreen and skin-lightening preparations. We report for the first time the photostabilization potential of plant extracts on common UV absorbers in sunscreens and skin-lightening preparations. We have also shown that the incorporation of plant extracts may not require a combination of sunscreen absorbers to achieve broad-spectrum protection. Therefore, the reduction in the number of organic absorbers incorporated in a formulation is likely to decrease potential side-effects. Efforts have been made to profile the photoproducts in various plant extracts with a view to determining their identities as this is important for characterising their photo-toxicities in the future.

References

Autier P, Doré J-F, Eggermont AM, Coebergh JW (2011) Epidemiological evidence that UVA radiation is involved in the genesis of cutaneous melanoma. Current Opinion in Oncology 23 (2):189-196

Baumler W, Regensburger J, Knak A, Felgentrager A, Maisch T (2012) UVA and endogenous photosensitizers - the detection of singlet oxygen by its luminescence. Photochemical and Photobiological Sciences 11 (1):107-117

Cortat B, Garcia CCM, Quinet A, Schuch AP, de Lima-Bessa KM, Menck CFM (2013) The relative roles of DNA damage induced by UVA irradiation in human cells. Photochemical and Photobiological Sciences 12 (8):1483-1495

de Gruijl FR, Sterenborg H, Forbes PD, Davies RE, Cole C, Kelfkens G, Vanweelden H, Slaper H, Vanderleun JC (1993) Wavelength dependence of skin-cancer induction by ultraviolet-irradiation of albino hairless mice. Cancer Research 53 (1):53-60

Dondi D, Albini A, Serpone N (2006) Interactions between different solar UVB/UVA filters contained in commercial suncreams and consequent loss of UV protection. Photochemistry and Photobiological Sciences 5 (9):835-843

Fourtanier A, Moyal D, Seite S (2012) UVA filters in sun-protection products: regulatory and biological aspects. Photochemistry and Photobiological Sciences 11 (1):81-89

Gallagher PR, Rivers KJ, Bajdik DC, Mclean ID, Coldman JA (2000) Broad-spectrum sunscreen use and the development of new nevi in white children: A randomized controlled trial. JAMA 283 (22):2955-2960

Garland CF, Garland FC, Gorham ED (2003) Epidemiologic evidence for different roles of ultraviolet A and B radiation in melanoma mortality rates. Ann Epidemiol 13:395-404

Girard PM, Francesconi S, Pozzebon M, Graindorge D, Rochette P, Drouin R, Sage E (2002) UVA-induced damage to DNA and proteins: direct versus indirect photochemical process. Journal of Physics 261 (1):1-10

Gonzalez H (2010) Percutaneous absorption with emphasis on sunscreens. Photochemical and Photobiological Sciences 9 (4):482-488

Gonzalez H, Farbrot A, Larko O, Wennberg AM (2006) Percutaneous absorption of the sunscreen benzophenone-3 after repeated wholebody applications, with and without ultraviolet irradiation. British Journal of Dermatology 154:337-340

Janjua NR, Mogensen B, Andersson A-M, Petersen JH, Henriksen M, Skakkebaek NE, Wulf HC (2004) Systemic Absorption of the Sunscreens Benzophenone-3, Octyl-Methoxycinnamate, and 3-(4-Methyl-Benzylidene) Camphor After Whole-Body Topical Application and Reproductive Hormone Levels in Humans. Journal of Investigative Dermatology 123 (1):57-61

Kowalski W (2009) Ultraviolet germicidal irradiation handbook UVGI for air and surface disinfection. 1:17-25

Panday R (2002) A photochemical investigation of two sunscreenabsorbers in a polar and non polar medium. MSc. Dissertation, University of KwaZulu-Natal, Durban, South Africa

Sayre MR, Dowdy CJ, Gerwig JA, Shields JW, Lloyd VR (2005) Unexpected photolysis of the sunscreen octinoxate in the presence of the sunscreen avobenzone. Photochemistry and photobiology 81:452-456

Schlumpf M, Schmid P, Durrer S, Conscience M, Maerkel K, Henseler M, Gruetter M, Herzog I, Reolon S, Ceccatelli R, Faass O, Stutz E, Jarry H, Wuttke W, Lichtensteiger W (2004) Endocrine activity and developmental toxicity of cosmetic UV filters—an update. Toxicology 205 (1–2):113-122

Tiano L, Armeni T, Venditti E, Barucca G, Mincarelli L, Damiani E (2010) Modified TiO(2) particles differentially affect human skin fibroblasts exposed to UVA light. Free Radical Biology and Medicine 49 (3):408-415

Chapter Two

Photostability, Photoproducts and Possible Photostabilization Mechanisms of Sunscreens in Formulations

Moses A. Ollengo and Bice S. Martincigh[*]

School of Chemistry and Physics, University of KwaZulu-Natal, Westville Campus, Private Bag X54001, Durban 4000, South Africa

*Corresponding author: Tel.:+27-31-2601394; Fax: +27-31-2603091; E-mail address: martinci@ukzn.ac.za

Abstract

Degradation of sunscreen agents when exposed to solar irradiation leads to a loss in the initial absorptive capacity. The resulting photoproducts and reactive intermediates of photo-unstable filter substances, if in direct contact with skin, may behave as photo-oxidants or promote phototoxic or photoallergic contact dermatitis. Moreover, ultrafine sunscreen-grade TiO_2, when irradiated with sunlight, is photocatalytically active and known to cause single- and double-strand breaks in DNA plasmids. In view of the above concerns and the need to improve sunscreen photostability their photophysics and photochemistry require careful study. The current work examines the photostability of the commonly used sunscreen absorbers and the fate of their photoproducts, if any. The possible strategies for photostabilization are also discussed.

Keywords: Photochemistry, photostability, sunscreens.

2.1   Introduction

Absorption of ultraviolet (UV) radiation by photoactive molecules either from the sun or artificial sources affects coatings containing photoactive substances. Active ingredients in cosmetic sunscreens are a mixture of UV filters designed to absorb, reflect or scatter the UVB rays (280–320 nm), UVA rays (320–400 nm) or both, and thereby reduce the amount of UV light reaching viable skin layers. There are two main types of sunscreen agents: organic UV absorbers and physical inorganic absorbers/reflectors. A key parameter for efficacy and safety of sunscreen products is a high photostability. Light-induced degradation leads to a reduction in the protection capacity during sun exposure and may generate potentially toxic species. It is important to photostabilize an electronically excited chromophore-containing organic molecule in order to provide sufficient UV protection. This can be accomplished by returning it to its ground state before undergoing a photochemical reaction destructive to its UV absorbing capability.

Photounstable UV filters may damage human skin either by behaving as exogenous sensitizers or by generating reactive intermediates (free radicals) during photolysis of the filter. The reactive intermediates may induce formation of reactive oxygen species (ROS) that further initiate destructive oxidative reactions or may bind to proteins or DNA. Secondly, a dose-dependent decrease of UVA absorptive capacity increases direct UVA-induced skin damage. Chemical photo-instability, accompanied by formation of photoproducts, free radicals, and ROS, may not only interact with other co-formulated ingredients of sunscreen products, but also skin constituents such as lipids, proteins, and nucleic acids (Crovara et al. 2012; Santo and Mezzena 2010). To prevent sunburns and protect people from serious skin damage sunscreens must be photostable and dissipate absorbed energy efficiently through photophysical and photochemical pathways ruling out formation of singlet oxygen ($^1O_2$), hydroxyl radicals ($^.OH$), and any other harmful reactive intermediates (Serpone et al. 2002). Interaction of photodegradation products with sunscreen excipients or skin components like sebum may lead to formation of new molecules with unknown toxicological properties (Gaspar and Maia Campos 2006). Several published reports demonstrate decomposition of several sunscreen agents under sunlight exposure and consequently they cannot maintain their initial absorptive capacity (Kockler et al. 2012; Mturi and Martincigh 2008; Gonzalez et al. 2007; Gaspar and Campos 2007).

Physical blockers like titanium dioxide (TiO_2), present in most skin care products are not spared. They have been shown to photo-induce degradation of organic sunscreens, enzymes, and DNA (Sayre et al. 2003). Illumination of TiO_2 suspensions with sunlight can degrade organic UV filters in a formulation (Egerton et al. 2007). Studies on the acute toxicity of TiO_2 nanoparticles in mammals indicate intra-tracheal instillation, intraperitoneal injection or oral instillation of TiO_2 particles to animals evoke inflammatory responses and histopathological changes (Saquib et al. 2012; Shukla et al. 2011; Naya et al. 2012; Zhang et al. 2010). In cultured macrophages, TiO_2 nanoparticles change the integrity of the cell membrane and phagocytic activity (Zhang et al. 2010). TiO_2, passing through the skin, is likely to interact with viable tissues since it carries with it absorbed UVA and UVB radiation and can generate hydroxyl radicals, posing possible undesirable mutagenic effects. Hence, the amount of TiO_2 in a formulation needs to be controlled. The European Cosmetic, Toiletry and Perfumery Association (COLIPA) has set the maximum allowable concentration as 25 % (m/m) (Atitaya et al. 2011). Dunford et al. (1997) showed using photo-excited TiO_2 specimens extracted from ten commercial sunscreens that TiO_2 can inflict similar DNA damage and similar direct strand breaks as do hydroxyl radicals in nuclei of whole human skin cells (Dunford et al. 1997). This confirms that ultrafine sunscreen-grade-TiO_2 irradiated with sunlight is photo-catalytically active and harmful causing single- and double-strand breaks in DNA plasmids.

An understanding of the photophysics and photochemistry of UV filter combinations is important to improve sunscreen photostability. In this context different systems have been investigated to enhance the photostability of UV filters, including sunscreen combinations, inclusion complexes with cyclodextrins, polymeric microspheres and nanoparticles (Iannuccelli et al. 2006; Alvarez-Roman et al. 2001). These approaches have been reported both by our group and other authors. The focus of this current work is to examine the photostability of sunscreen molecules and the fate of their photoproducts.

2.2   Photo-excitation and deactivation of sunscreen molecules

When exposed to UV light, photo-absorbing molecules can be decomposed or rearranged easily, because the absorbed energy (excitation energy) cannot be transferred efficiently into other forms, such as light or heat. The absorption of ultraviolet light by a chromophore-containing organic molecule causes excitation of an electron in the chromophore moiety from an initially occupied, low energy orbital to a higher energy, previously unoccupied orbital. The energy of the absorbed photon is used to energize an electron and cause it to "jump" to a higher energy orbital. Two excited electronic states arise from the electronic orbital configuration produced by UV light absorption. In one state, electron spins are paired (antiparallel) and in the other unpaired (parallel). The paired spin state has no resultant spin magnetic moment, possessed by unpaired spins state. A state with paired spins remains a single state in the presence of a magnetic field, and is termed a singlet state (S_1). On the other hand, a state with unpaired spins interacts with a magnetic field and splits into three quantized states, and is termed a triplet state (T_1). Because of these electronically excited states, chromophore-containing organic molecules are prone to degradation.

Several deactivation pathways of photo-excited molecules are known (see Fig 2.1). Since most photostability studies are done in solution, it is important to note in solution transition moments of molecules are random. The exciting such a system with linearly polarized light, will be efficient for molecules whose transition moments are at the time of excitation oriented similarly to the direction of polarization. The presence of a solvent induces symmetry distortion allowing spin-allowed, symmetry–forbidden electronic transitions to take place giving rise to extinction coefficients in the order of 10^{-2} to 10^{-4}. An increase in the population of the triplet excited state shows an effect dependent on the polarity of the solvent. Excited state molecules are chemically different species to their corresponding ground states and are energetically unstable and very short-lived. If an efficient dissipation of excited-state energy does not occur, chemical bonds of UV-absorbing molecules may be broken and new bonds formed, leading to an irreversible molecular change (Lee et al. 2004). Photolysis of these molecules may generate free radicals causing, directly or indirectly, skin damage (Scalia et al. 2002) for topically applied agents on the skin.

A photostable chromophore, as desired for a good sunscreen agent is one that is not destroyed during the process of deactivation and is repeatedly available to absorb more photons. The fundamental goal in maintaining photostability is to prevent the excited state molecule from acquiring sufficient activation energy during its lifetime to react at a rate competitive with other modes of excited state deactivation. There are several deactivation pathways: emission of a photon from the singlet excited state (fluorescence); emission of a photon from the triplet excited state (phosphorescence); internal conversion; intersystem crossing; energy transfer or via photochemical reaction. Figure 2.1 summarises these deactivation pathways classifying them into two main classes: the photochemical processes and photophysical pathways. The Jablonksi diagram (Fig. 2.2) shows the anticipated

energy transfers during the photophysical excited state decay. Ideally, all deactivation pathways compete with each other all the time. Those with the highest quantum yields and fastest rates predominate.
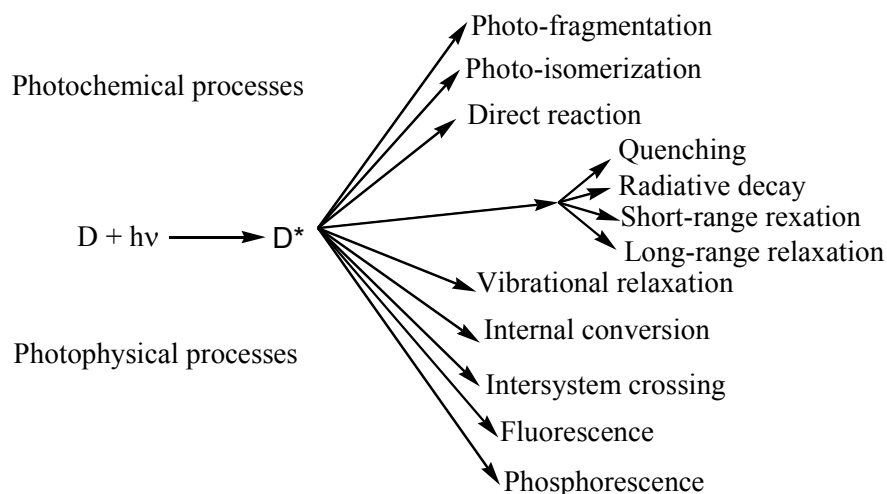
Figure 2.1: Summary of the deactivation pathways of an excited molecule.
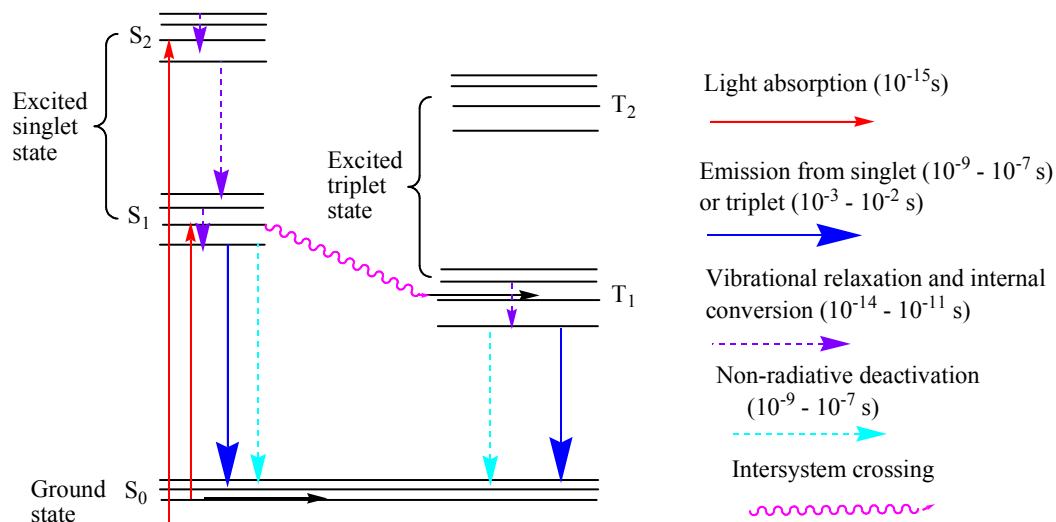
Figure 2.2: Jablonksi diagram for an organic molecule. Radiative processes and energy transfers are by in solid lines whereas non-radiative energy transfer processes are shown using dotted lines. Indicative timescales are shown, although they are molecule dependant. (http://photochemistryportal.net/home/index.php/category/principles/ (accessed on 3/7/2012)).

For organic-based filters, intersystem crossing is a crucial deactivation pathway because it populates the triplet excited state. This state has a longer lifetime, long enough to make the molecule acquire a diradical character making it particularly vulnerable to destructive chemical processes such as hydrogen and electron abstraction, cycloaddition, isomerisation and fragmentation. Photoisomerizations yield species that could be less light-absorbing than the parent species, and less useful as sunscreen agents. Photofragmentation processes cause absorbing molecules to dissociate into reactive fragments (*e.g.*, free radicals) or reactive intermediates. Formation of photo-adducts between active agents; such as thymine and thymidine bases have been reported. In addition, some active agents could increase the rate of formation of potentially carcinogenic DNA photoproducts (*e.g.* the cyclobutane-type pyrimidine dimers), on irradiation if they penetrate the cell nucleus. Or they can undergo photochemical changes (Fig. 1) resulting in a loss of UVA/UVB filtering ability.

Energy transfer from an excited molecule (donor) to another molecule (acceptor) deactivating a chromophore in the process is called quenching. The excited states of many organic compounds are efficiently quenched by the presence of oxygen, at rate constants several orders of magnitude faster than emission processes from the triplet state. But emission from the triplet is spin-forbidden, and hence has rate constants in the range of 10 to 10^3 dm^3 mol^{-1} s^{-1}, whereas oxygen quenching may take place at rate constants of the order of 10^9 dm^3 mol^{-1} s^{-1} (Wilkinson 1997). Quenching of an excited state is a significant process because it is usually a very efficient process. This can occur by two processes – electron transfer or energy transfer. In both cases, the excited state energy of the luminophore (luminescent species) is deactivated due to the presence of a quencher. Mostly quenchers operate on the triplet excited state of donors. However, quenching the singlet excited state is important because it will reduce the population of the triplet excited state molecule; the origin of destructive photochemical reactions. Under normal operating conditions such as room temperature (25 °C) or skin temperature (37 °C) increasing the concentration of acceptor molecules or quenchers increases the observed rate of energy transfer (Wilkinson 1997). Hence, increasing the quantum yield of quenching is likely to decrease the quantum yields of potentially destructive processes to the donor.

There are two mechanistic approaches in quenching of excited states of molecules. The first is induced dipole or coulombic interaction. Here the oscillating excited electron of a donor generates an electromagnetic field exciting one of the acceptor's electrons to a higher energy orbital. This action is distance dependent and is inversely proportional to the sixth power of the distance between donor and acceptor molecule. The second approach is collisional or exchange mechanisms. Here the donor and acceptor molecules are assumed to be close enough for their electron clouds to overlap. This permits an exchange of excited electron from donor and ground state electron from acceptor. Exchange only takes place if the donor is in the excited triplet state. After exchange, the donor returns to the ground state, and the acceptor is elevated to an excited state. The two mechanisms may, however, occur simultaneously in the singlet excited state.

Both coulombic and collisional mechanistic theories are related to energy transfer rates of a donor in a singlet excited state to an acceptor in the ground state. These rates are related to a quantity called the spectral overlap integral. The magnitude of the spectral overlap integral in turn is related to the probability that the donor and acceptor are energetically compatible (Adronov and Frechet 2000). The overlap integral J (cm^6 mol^{-1}) is given by

$$J = \int f_D(\nu)\varepsilon_A(\nu)\nu^{-4}d\nu$$

where $f_D(\nu)$ is the fluorescence intensity of the donor, $\varepsilon_A(\nu)$ is the molar extinction coefficient of the acceptor, and the overlap integral is calculated over the entire spectrum with respect to the frequency expressed in wavenumbers. This overlap integral represents the overlap between the donor emission spectrum and the acceptor absorption spectrum. It is closely correlated to the probability of energy transfer from the donor to the acceptor. Hence, the extent of spectral overlap between the fluorescence emission spectrum of the donor and the absorption of the acceptor determines the rate of energy transfer.

A plot of the fluorescent intensity of a compound as a function of the concentration of a potential acceptor (quencher), (Stern-Volmer analysis) can provide information for formulating a photostable sun care product. Given the fast rate of transitions in an singlet excited state (in the order of femto

seconds), observation that a process competes with fluorescence its good evidence that the process can effectively deactivate the photoactive molecule. Downstream processes such as intersystem crossing to the triplet excited state can then be avoided.

2.3   Classes of absorbers

Absorption of UV light accounts for about 85 % to 95 % of the photoprotective capacity of UV filters in cosmetic preparations. To date no single UV absorber shows significant absorption across both the UVB and UVA regions of the UV spectrum. Consequently the UV filters are classified depending on the region of the UV spectrum they absorb the most. This classification is based on the wavelength of maximum absorption it demonstrates in that region. Figure 2.3 shows common groups of organic sunscreens from which various UV absorbers are derived. The derivatives of camphor, cinnamate, *p*-aminobenzoate and salicylates are known UVB absorbers whereas anthranilates and benzophenone derivatives absorb into the lower UVA1 region (about 350 nm). The commonly used UVA absorber is a derivative of dibenzoylmethane. The agent, tert-butylmethoxy dibenzoylmethane (BMDBM), is known to degrade on exposure to UV light. This has necessitated the search for broad spectrum UV filters that will keep their absorptive efficacy without loss or breakdown to less absorbing chemical species.

Among the new promising UV filters are 2,2′-methanediyl*bis*[6-(2*H*-benzotriazol-2-yl)-4-(2,4,4-trimethylpentan-2-yl)phenol] (Tinosorb M) and 2,2′-[6-(4-methoxyphenyl)- 1,3,5-triazine-2,4-diyl] *bis*(5-[(2-ethylhexyl)oxy]phenol) (Tinosorb S). Their absorption efficacy is based on the stability of the aromatic ring systems and the auxochrome modification of the electron π-cloud of the phenyl rings. It is expected that a symmetric molecule having aromatic rings conjugated with carbonyl groups and electron-releasing groups substituted on the aromatic rings may afford that molecule photostability. In such a supramolecular assembly the energy dissipative processes via electron resonance delocalization upon absorption of a photon make it possible to deactivate sensitizers through energy transfer. As explained above the triplet-triplet energy transfers may to lead photoisomerisation deactivating an acceptor. This is likely to increase the photostability of a sunscreen molecule. Without intending to be limited to any particular mechanism by which such compounds are able to quench (accept the excited state energy) an excited photoactive compound (Beasley and Meyer 2010)

It is expected that the variation of the auxochromes around the phenyl rings may lead to photostabilization and subsequently present a different UV spectrum. However, these agents are relatively new and so not yet accepted in some other regions, for example in America (Oesterwalder and Herzog 2009). Hence lack of a single broad spectrum UV filter makes combinations of sunscreens inevitable in a bid to produce broad-spectrum sunscreen product. Figure 2.4 shows some of the commonly used sun active molecules and Table 2.1 documents the allowed levels of sunscreen absorbers (% m/m) in a single commercial product.
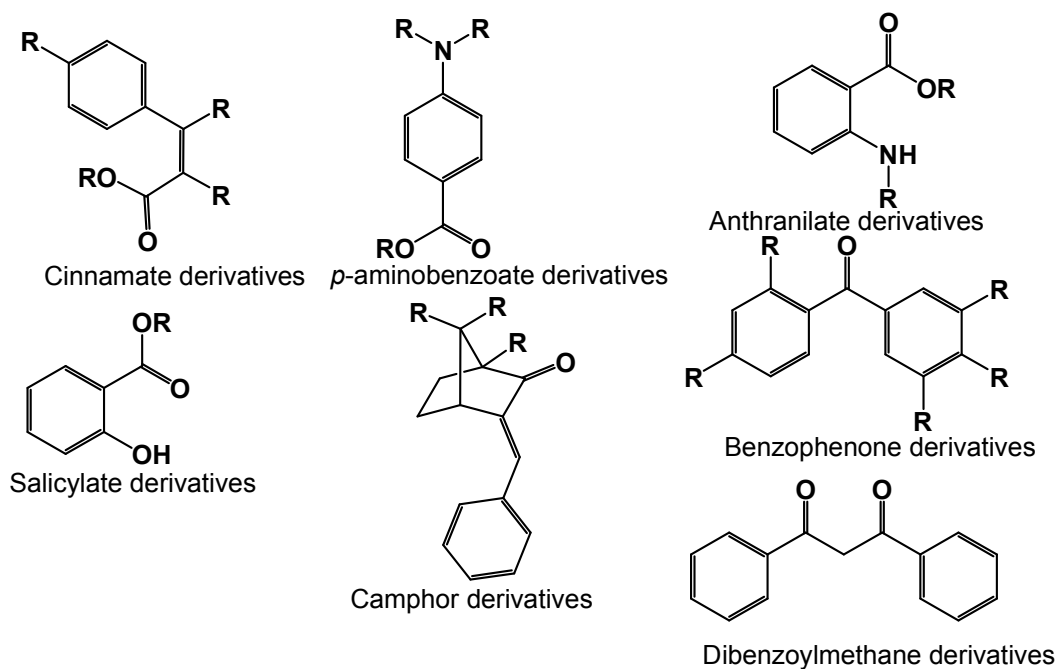
Figure 2.3: The common sunscreen families.
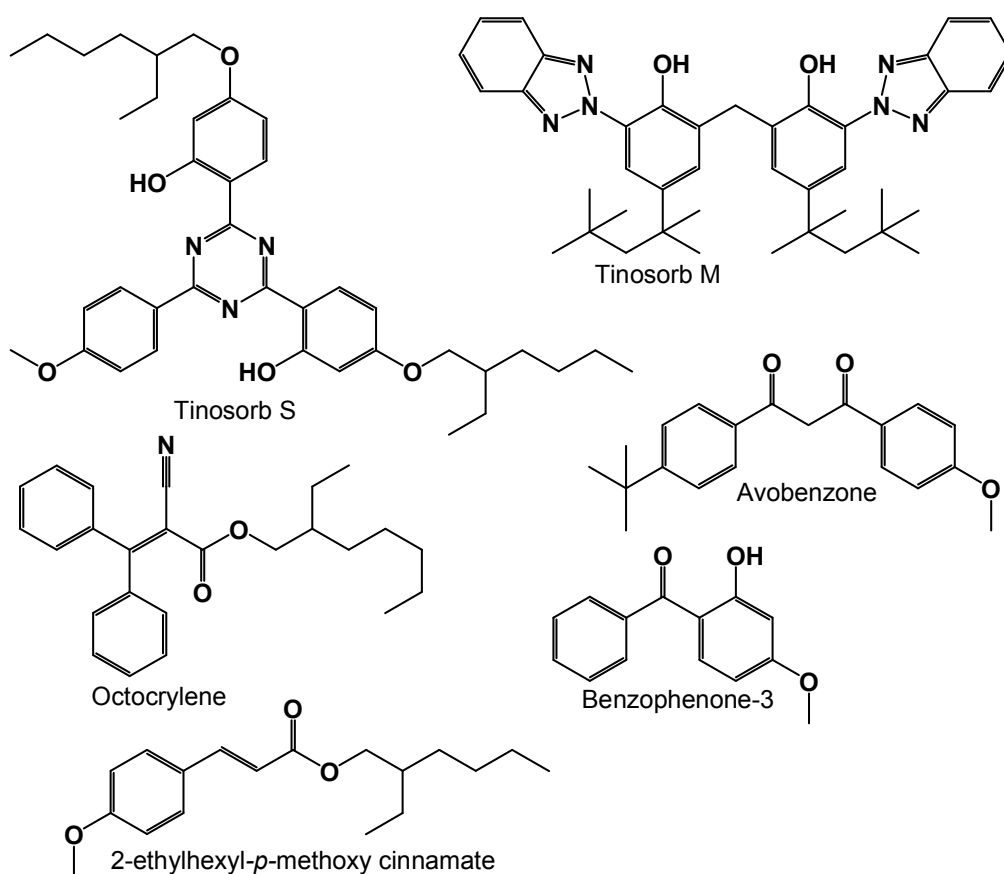
Figure 2.4: The common sunscreen molecules in cosmetic preparations.

Table 2.1: The list and maximal quantity (% m/m) of some of the sunscreen-active agents allowed in sunscreen products under the United States' Food and Drug Administration (US FDA), European COLIPA, Australian and Japanese Health authorities (Serpone et al. 2002; Oesterwalder and Herzog 2009; Krause et al. 2012).

.UV filter	Common name(s)	Absorption maximal λ/nm	FDA	EU	AUS	Japan
4-aminobenzoic acid	p-aminobenzoic acid	283	15	15	15	
3,3,5-trimethylcyclohexyl-2-hydroxybenzoate	Homosalate	306	15	10	15	10
2-ethylhexyl-2-hydroxybenzoate	Octyl salicylate, Octylsalate	307	5	5	5	10
4-hydroxy-2-methoxy-5-(oxo-phenylmethyl)benzenesulfonic acid	Sulisobenzone	286, 324	10	5	10	10
1-(4-methoxyphenyl)-3-(4-*tert*-butylphenyl)propane-1,3-dione	Avobenzone, tert- Butylmethoxy dibenzoylmethane	357	3	5	3	10
Methyl-2-aminobenzoate	Menthyl anthranilate	336	5	-	5	-
(2-hydoxy-4-methoxyphenyl)-phenylmethanone	Benzophenone-3, oxybenzone, 2-hydroxy-4-methoxybenzophenone	288,329	6	10	10	5
2-ethoxyethyl-3-(4-methoxyphenyl)propanoate	Cinoxate, 2-ethoxyethyl-4-methoxycinnamate	290	3			
2-ethylhexyl-2-cyano-3,3-diphenyl-2-propenoate	Octocrylene	303	10	10	10	10
2-ethylhexyl-4-(dimethylamino)benzoate	Padimate-O	311	8	8	8	10
2-Ethylhexyl-4-methoxy cinnamate	Octyl methoxycinnamate, octinoxate	311	7.5	10	10	20
(2-hydroxy-4-methoxyphenyl)-(2-hydroxyphenyl)methanone	Dioxybenzone, benzophenone-8	325	3			
Tris-(2-hydroxyethylammonium-2-hydroxybenzoate	Trolamine salicylate	298	12			
2-phenyl-*3H*-benzimidazole-5-sulfonic acid	Phenylbenzimidazole sulfonic acid	285, 333	4	8	3	4

2,2′-methanediylbis[6-(2*H*-benzotriazol-2-yl)-4-(2,4,4-trimethylpentan-2-yl)phenol]	Tinosorb M, Bisoctrizole	305, 360	TEA	10	10	10
2,2′-[6-(4-methoxyphenyl)- 1,3,5-triazine-2,4-diyl] bis(5-[(2-ethylhexyl)oxy]phenol)	Tinosorb S, Bemotrizinol	310, 343	TEA	10	3	10
Titanium(IV) oxide	Titanium dioxide	295	25	25	25	no limit
Zinc(II) oxide	Zinc Oxide	390	25	UR	20	no limit

TEA: Time and Extent Application (U.S. Food and Drug Administration application), UR: Under Review, COLIPA: European Cosmetics, Toiletry, and Perfumery Trade Association, EU: Europe, AUS: Australia.

2.3.1 Photostability and photoproducts of 4-tert-butyl-4′-methoxydibenzoylmethane

The most commonly used UVA absorber in broad-spectrum sunscreens is 4-*tert*-butyl-4′-methoxydibenzoylmethane (BMDBM). BMDBM exhibits high absorptivity in UVA region (λ$_{max}$ = 358 nm), but undergoes marked decomposition (Fig. 2.5) in sunlight leading to a decrease of the expected UV-protective level following sunscreen application.
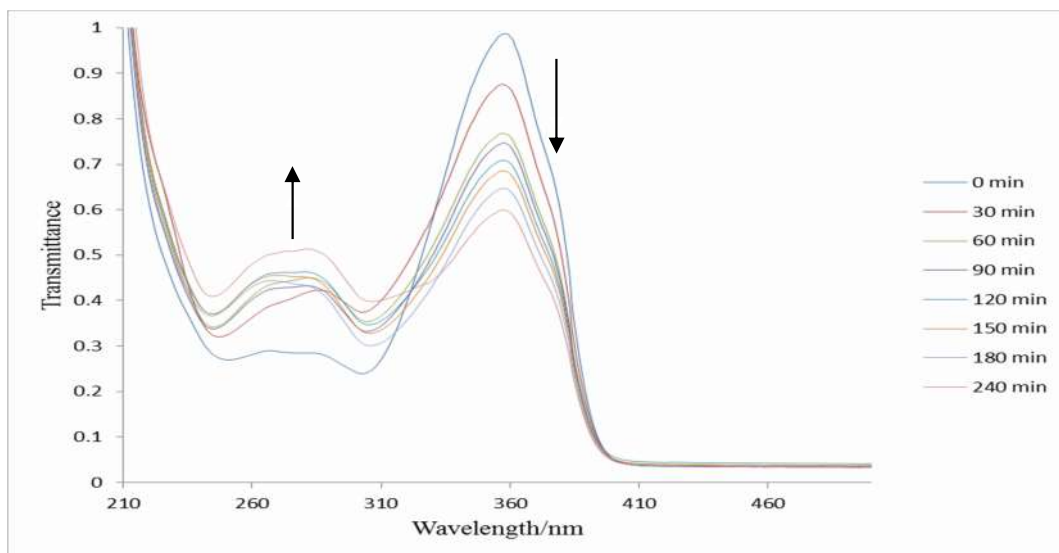
Figure 2.5: Characteristic degradation of BMDBM in methanol showing the decay of the enolate avobenzone at 360 nm and formation of the *keto* form at 260 nm upon increasing exposure to solar simulated radiation.

BMDBM, a derivative of dibenzoylmethane, has been widely reported to lose much of its UVA protective capability after irradiation through tautomerization (keto/enol tautomers) (see Fig. 2.6), fragmentation and photoproduct formation (Fig. 2.7). Many studies point at the polarity of the solvents as a major determinant for its stability. Dominating solute-solvent interactions arise from dipole-dipole interaction, lowering potential energies of all energy levels involved in absorption and excited state energy transfer processes. It is known that changes in solute-solvent interaction lead to solvatochromic shifts in absorption and fluorescence of the same fluorophore. The position of the absorption maximum wavelength and the strength of the absorption band depend sensitively on the electronic structure of a molecule.

In a solvent-dependant study BMDBM was shown to photo-degrade in non-polar solvents but showed photostability in polar solvents and the length of irradiation was shown to influence decomposition rates (Beasley and Meyer 2010; Schwack and Rudolph 1995). Roscher et al. (1994) showed that irradiation of BDBDM in cyclohexane yield *tert*-butylbenzene, *p-tert*-butylbenzoic acid and *p*-methoxybenzoic acid. Other products obtained were as result of the combination of BDBDM with the solvent giving cyclohexyl esters of *p*-methoxybenzoic acid, *p-tert*-butylbenzoic acid and methanoic acid. The solvent itself on photodegradation yielded: cyclohexanol, cyclohexanone and dicyclohexyl ether. In a more recent study by Mturi and Martincigh (2008), showed that the loss in photo-absorption efficacy of BDBDM dependent on the proticity of the solvent. They observed photoloss due to *keto - enol* tautomerisation of BMDBM in dimethylsulphoxide especially in the presence of oxygen and essentially photostable in methanol (Fig. 2.6). This agent also showed photodegradation to photoproducts absorbing mainly in UVC region depending on solvent polarity and independent of

oxygen. It is speculated that dibenzoylmethanes exists mainly in the chelated enol form in both non-polar and polar solvents, although the enol content is higher in polar solvents because of strong intramolecular hydrogen bonds (Tobita et al. 1995).
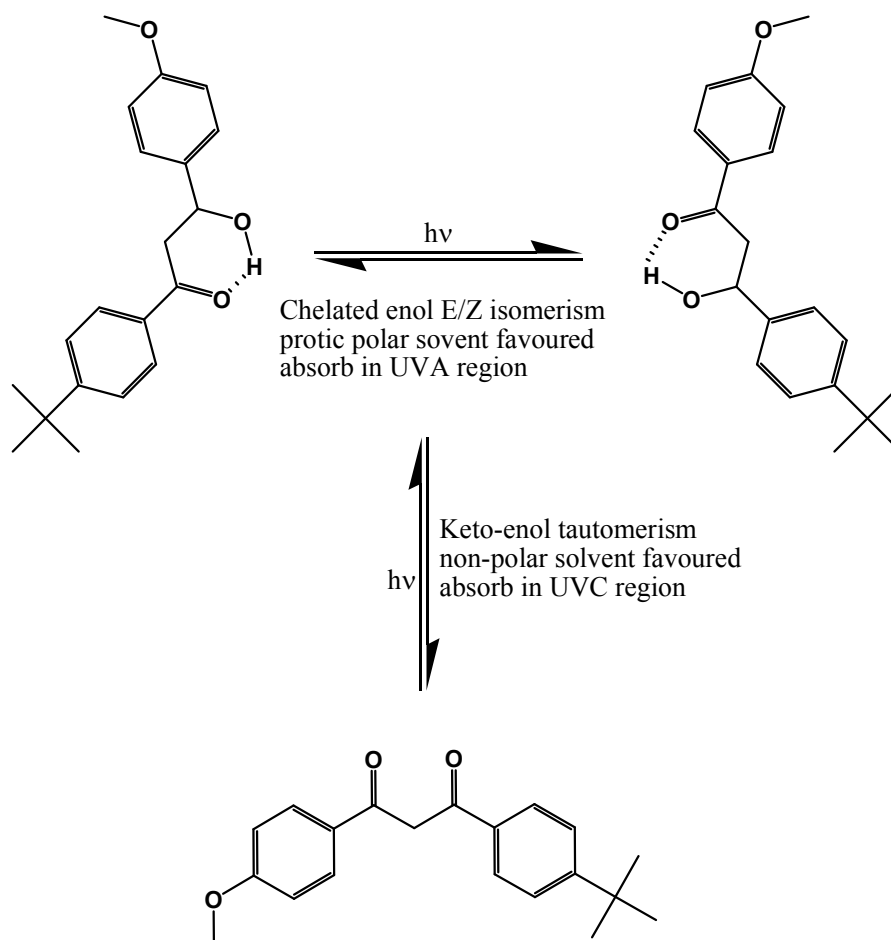
Figure 2.6: *Keto-enol tautomerism of BDBDM (Mturi and Martincigh 2008).*

The ketonization process is determined by a direct hydrogen transfer from the excited enol molecule, and after formation of an excited complex between one excited and one non-excited enol molecule. The low quantum yield of fluorescence of the enol-form molecule is explained by fast isomerization from the first excited singlet state (Yankov et al. 1988). The absorption of UVA light produces an excited enol state (S_1) whose main deactivation pathway involves an intramolecular hydrogen bond cleavage and a subsequent formation of a non-chelated enol (Z-isomer) (Fig. 2.6). This *enol* form shows a strong absorption band around 340–360 nm, while the keto form absorbs in the range 260–280 nm (Paris et al. 2009; Aspée et al. 2007). The photoreaction appears to proceed through an $n \sim \pi^*$ excited triplet state as indicated by the structure of the proposed photoproducts (Srei et al. 2008). However, the chelated enol form of dibenzoylmethanes shows strong characteristic absorption bands in the UVA region (315–380 nm) (Fig. 2.3) due to the $\pi - \pi^*$ transition of the chelated quasi-aromatic π-electron system (Yamaji et al. 2010). Though, phosphorescence intensity of diketone form and two chelated *enol* forms of β-diketones in solution depends largely on the solvent used (Yamaji et al. 2010; Paris et al. 2009).

The observed phosphorescence of the diketone form in polar solvents is similar to that of aromatic monoketones arising from a triplet ($\pi - \pi^*$) state. It can be argued that phosphorescence of one of the

two chelated *enol* forms in a nonpolar solvent is emitted from a triplet ($\pi - \pi^*$) state as suggested by the external and internal heavy atom effects (Paris et al. 2009). Consequently, irreversible photodegradation of BMBDM has been observed and related in part to a Norrish Type I process occurring from the diketone triplet state. These processes involve formation of transient enol isomers (rotamers). The chelated enol form of BMDBM has a wavelength of maximum absorption in the UVA region (360 nm) due to the $\pi - \pi^*$ transition of the chelated pseudo-aromatic π-electron system. However, BMDBM does not fluoresce in solution, indicating the presence of efficient non-radiative processes from the excited singlet states. This process is perceived to involve the formation of transient enol isomers. The rotamers formed, undergo structural rearrangement back to the chelated *enol* form in the dark (Yamaji et al. 2010; Paris et al. 2009). Lamola and Sharp (1966) suggested that a very fast radiationless decay takes place in molecules possessing an intramolecular hydrogen bond between the carbonyl oxygen and hydroxyl hydrogen. This may explain the shortness of the phosphorescence lifetime showing the lowest triplet state is probably mixed with some higher energy triplet state of $n - \pi^*$ type (Yamaji et al. 2010).

Since the diketone form of BMDBM has more luminescence than the chelated *enol* form of the β-diketo form, it is likely to generate singlet oxygen. The reaction of singlet oxygen with the enol form may lead to formation of oxygenation products. Photo-reactivity of singlet oxygen with the enol form leads to different types of peroxides and their cleavage products (Beasley and Meyer 2010; Schwack and Rudolph 1995). BMBDM has been shown to generate carbon-centred free radicals when illuminated with simulated sunlight causing in-vitro strand breaks in DNA and oxidative modifications in bovine serum albumin (Karlsson et al. 2009; Armeni et al. 2004). The energy of the UV light causing excitation of BMBDM is of same order of magnitude as its bond dissociation energies, thus breaking it into two primary reactive radical fragments. The photoproducts are proposed to originate from two radical precursors, either from a benzoyl radical or from a phenacyl radical (Fig. 2.7) (Mturi and Martincigh 2008; Schwack and Rudolph 1995).
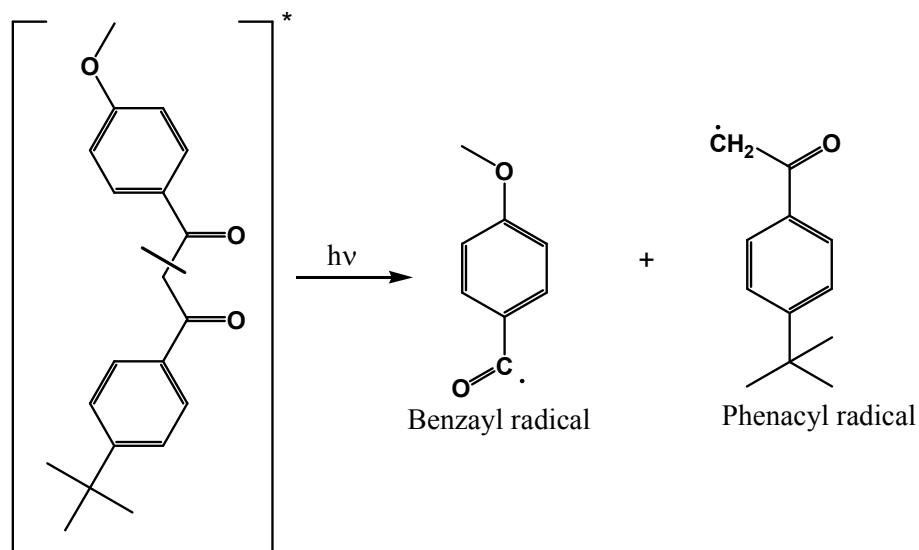
Figure 2.7: Proposed primary photochemical degradation of BMBDM (Schwack and Rudolph 1995; Mturi and Martincigh 2008).

Several reports show that photodegradation of BMBDM strongly depends on the presence of the 1,3-diketo forms and the enol-keto tautomerism (Figure 2.6) is seen as the primary mechanism of photolability (Chatelain and Gabard 2001) Any structural adjustment that favours stabilization of the enol form is likely to enhance the photostability of BMBDM. In a polar solvent prior to irradiation

BMBDM exists almost exclusively as the enol tautomer. A crystal structure investigation indicates this molecule is planar and the spatial distance between neighbouring oxygens is approximately 246 pm revealing a very strong intramolecular hydrogen bond (Bjarke et al. 2006). This has been observed and qualitatively assigned by Bjarke et al. (2006) as an infrared (IR) absorption in the region between 1700-1400 cm^{-1}. Hence, solvent solutions whose polarity will favour strengthening of the hydrogen bond should be considered as first line stabilizers of BMBDM.

2.3.2   Cinnamates

Cinnamates are esters of the cinnamic acid moiety found in cinnamon oil and balsam plants. They are potent UVB absorbers and hence used in sunscreen agents and cosmetics with sun protection efficacy. In particular, 2-ethylhexyl methoxycinnamate (EHMC), is the most commonly used. Apart from reported sensitization reactions of EHMC, it is absorbed into the skin and may promote generation of potentially harmful free radicals (Xu et al. 2001).

(*E*)-2-ethoxyethyl 3-(4-methoxyphenyl)acrylate   (*E*)-2-ethylhexyl 3-(4-methoxyphenyl)acrylate

2-ethylhexyl 2-cyano-3,3-diphenylacrylate
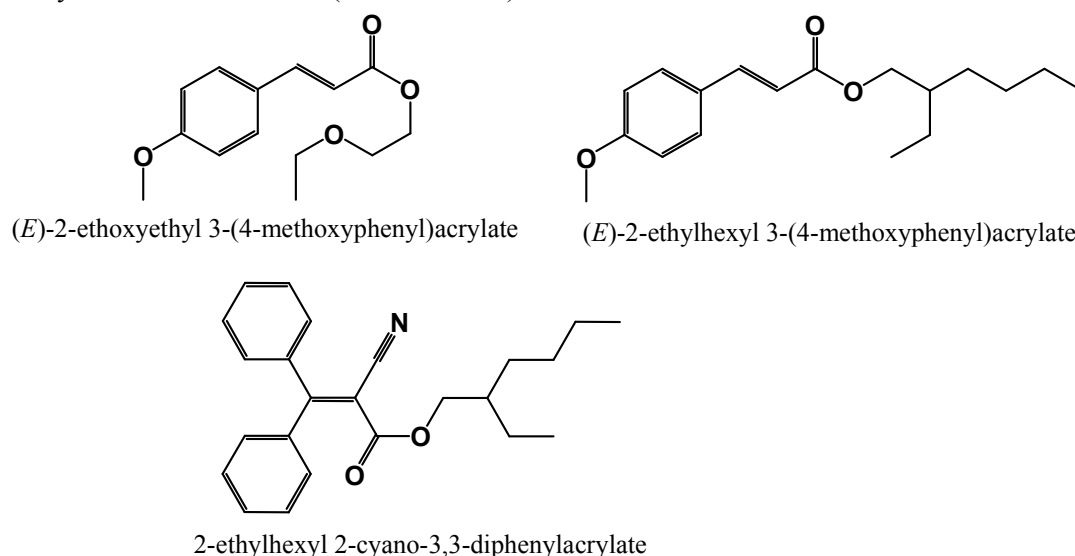
Figure 2.8: Cinnamate sunscreens commonly used in cosmetic preparations.

When exposed to sunlight, (*E*)-EHMC isomerizes to (*Z*)-EHMC with subsequent loss in absorption (Huong et al. 2007; Lyambila 2003) (Fig. 2.9). Studies show that the position of the equilibrium of photoisomerisation reaction depends upon the concentration of EHMC and the polarity of the solvent used (Pattanaargson et al. 2004; Lyambila 2003). The Z-isomer has a lower extinction coefficient (ε) and hence this reaction is accompanied by photoloss. Photodimers have been identified, and indicate that this sunscreen absorber can undergo [2+2] cycloaddition reactions with itself (Broadbent et al. 1996), that also reduce the efficacy of UV absorption of this agent (Fig. 2.10). There are reports that cinnamates seem to react easily with unsaturated molecules in their vicinity, such as squalene, unsaturated fatty acids or DNA bases on human skin (Hauri et al. 2004) An *in vitro* study on the possible photocycloaddition between EHMC and constituents of DNA by Ingouville (1995) returned no photo-adducts this led to the conclusion that photoreactions with DNA are likely to be very low. However, a subsequent study by Kowlaser (1998) detected formation of DNA photo-adducts with longer time of irradiation of EHMC with DNA nucleotides. This result points to the possibility of a photo-induced reaction between EHMC and DNA *in vivo*. Such a possibility may produce undesirable side-effects to unsuspecting sunscreen user.

The combination of the UVB filter, EHMC, and the UVA filter, BMBDM are commonly used in sunscreen products. But this combination is particularly photo-unstable (Sayre et al. 2005). A study

by Panday (2002) showed that BMBDM photosensitises the isomerisation of EHMC (Panday 2002). In a bid to photostabilize EHMC the influence of nanoparticle-based systems on the light-induced decomposition of the (*E*)-EHMC has been attempted with results indicating that loading (*E*)-EHMC nanoparticles may improve its photostability (Perugini et al. 2002).

Another cinnamate, octocrylene, is a known sensitizer upon UV absorption and has been reported to be a prime photoallergen (Avenel-Audran et al. 2010) of chemical absorbing sunscreens especially to people with sensitivities to cinnamates (Hanson et al. 2006). The associated sensitivity produces allergic contact dermatitis and photo-contact dermatitis.
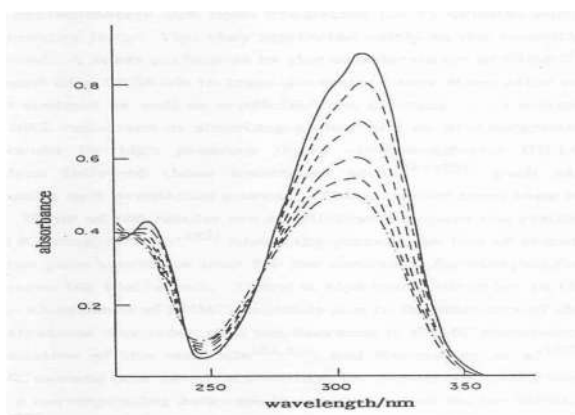
Fig. 2.9: Characteristic isomerization decay of EHMC.

Dimerisation of EHMC

Photoinduced (E-Z) isomerism of EHMC
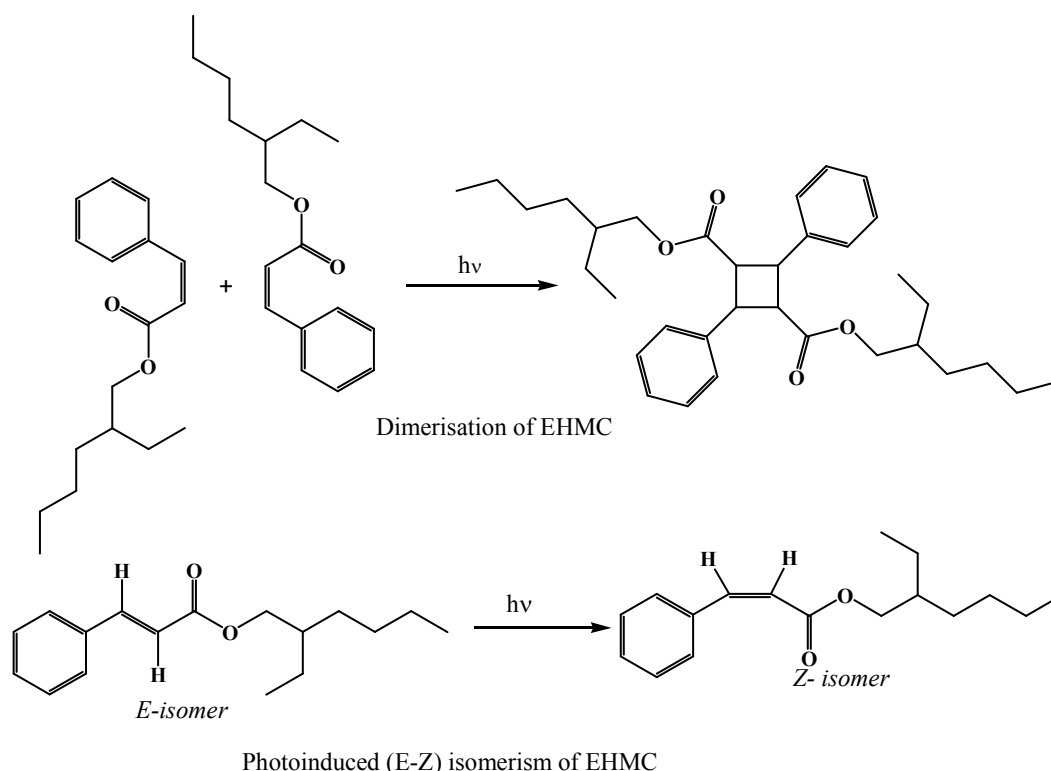
Figure 2.10: Photoinduced degradation of cinnamates sunscreens.

2.3.3   Tinosorb S

The rotation around the C=C double of the cinnamate moiety requires the molecule to acquire a diradical nature. The carbons change from sp^2 hybridization pseudo sp^3; this allows

photoisomerisation to occur. This requires sufficient energy synonymous with the excited triplet state. Hence, it is envisaged that addition of organic molecules that can quickly accept energy from such excited molecules will deprive them of the energy to undergo change in hybridization that allows photoisomerization. Such molecules are called photostabilisers. An example of a photostabilizing molecule is Tinosorb S. Tinosorb S (Fig. 2.11) is a photostable UVB and UVA sunscreen active with maximum absorption at 311 and 343 nm (Hexsel et al. 2008; Krause et al. 2012). It has a symmetric molecular symmetry and the presence of three aromatic rings conjugated with ether groups and electron-releasing groups. The hydroxyl groups substituted on the aromatic rings gives Tinosorb S an optimal structure for energy dissipative processes. This allows electron resonance delocalization upon absorption of a photon, and hence it is able to deactivate sensitizers through triplet–triplet energy transfer. Tinosorb S is a good energy acceptor that reversibly photo-isomerizes via hydrogen transfers to the triazine ring thus deactivating a photoexcited sensitizer. To return to its ground state it efficiently dissipates the accepted energy through intramolecular hydrogen transfer in the excited state re-forming the phenol followed by internal conversion and phosphorescence.
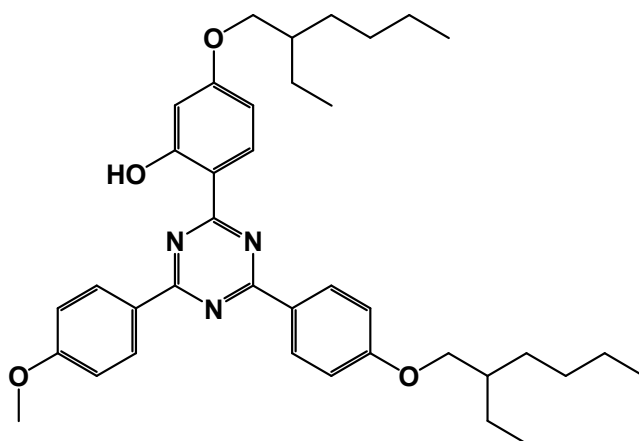
5-(2-ethylhexyloxy)-2-(4-(4-(2-ethylhexyloxy)phenyl)-6-(4-methoxyphenyl)-1,3,5-triazin-2-yl)phenol
Figure 2.11: Molecular structure of Tinosorb S.

2.3.4 Tinosorb M

The photo-absorbing molecule 2,2′-methanediylbis[6-(2H-benzotriazol-2-yl)-4-(2,4,4-trimethylpentan-2-yl)phenol] marketed by Ciba Speciality Chemicals as Tinosorb M and commonly referred to as bisoctrizole is a benzotriazole-based organic compound. It has two absorption maximum wavelengths: 305 nm and 360 nm, making it a broad-spectrum UV absorber, absorbing UVB as well as UVA rays. It shows poor solubility in both oil-based and aqueous based sunscreen preparations hence presenting itself as a hybrid UV absorber, and an organic UV reflector due to the microfine organic particles (< 200 nm) (Herzog et al. 2002). It shows very little photodegradation and has a stabilizing effect on other UV absorbers especially ethylhexyl methoxycinnamate. This is a highly symmetric molecule (Fig. 2.12) with nitrogen and oxygen atoms in close proximity. This close proximity may allow an intramolecular hydrogen transfer which is a known mechanism for excited state deactivation in organic molecules. This could in part explain the photostability of this agent. Studies on its percutaneous penetration indicate that in sunscreen formulation it has minimal skin penetration (Mavon et al. 2007). There are no *in vitro* estrogenic effects reports on this agent currently (Ashby et al. 2001).

Tinosorb M
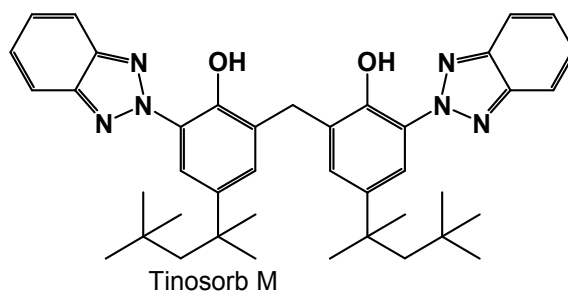
Fig. 2.12: The agent 2,2′-methanediylbis[6-(2*H*-benzotriazol-2-yl)-4-(2,4,4-trimethylpentan-2-yl)phenol].

2.3.5 Salicylates

The commonly used salicylate UV absorbers are homosalate and octyl salicylate. Both are esters of salicyclic acid with 3,3,5-trimetheylcyclohexanol and 2-ethylhexanol respectively (Fig. 2.13). They have been shown to be relatively photostable, absorbing UV light with wavelengths between 295 nm and 315 nm.
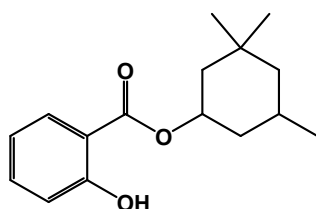
3,3,5-trimethylcyclohexyl 2-hydroxybenzoate
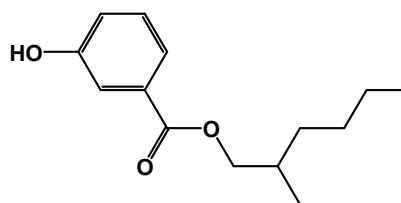
2-ethylhexyl 3-hydroxybenzoate

Figure 2.13: Commonly used salicylate screens in cosmetic preparations.

The cyclohexanol and 2-ethylhexanol portions of homosalate and ethylhexylsalicylate respectively are highly non-polar and this makes them hydrophobic reducing their solubility in water. Due to this hydrophobicity they are claimed to have limited skin penetration favouring accumulation in the lipophilic stratum corneum. It is this lipophilic barrier that prevents permeation of hydrophobic chemicals into the viable epidermis immediately below the stratum corneum (Chatelain et al. 2003). The epidermis is hydrophilic in nature and can act as a rate-limiting step in absorption of highly lipophilic topical applications. However, the absolute amount of a compound permeating the skin has been shown to depend on the carrier vehicle (Kim et al. 2014; Chatelain et al. 2003). Walters et al. (1997) showed that ethylhexylsalicylate has a high affinity for the lipid regions of the stratum corneum and its deeper permeation is limited by the hydrophilic nature of the viable epidermis. Other *in vitro* studies have reported anti-androgenic activity of ethylhexyl methoxycinnamate and homosalate by antagonizing dihydrotestosterone-induced androgen receptor activation in the human breast carcinoma cell line MDA-kb$_2$ (Hexsel et al. 2008; Krause et al. 2012). Despite the foregoing, topically applied salicyclic acid ester screens can be broken down to salicylic acid by nonspecific esterases in isolated non-viable skin (Boehnlein et al. 1994). Also salicylate esters topically applied on humans have been found in human excretes, but excretion rates depend on lipophilicity (Simonsen et al. 2002). Consequently, any permeation of these sunscreen agents should be avoided or their concentration kept low.

2.3.6   Camphor derivatives

Camphor derivatives (Fig. 2.14) are moderately effective UVB absorbers with maximum peak absorption at 300 nm (Hexsel et al. 2008). The photostable benzylidene camphor derivatives are effective UV filters for cosmetic applications whereas benzylidene malonate derivatives are UV absorbers used in the photoprotection of automotive coatings. Though these agents have very low phototransformation quantum yields, photoproducts have been reported upon sunlight exposure. It has been demonstrated that their photochemical behaviour is independent of the physicochemical environment (Beck et al. 1981) They have excited state lifetimes in the order of about 10^{-12}s, too short for them to react with neighbouring molecules (Beck et al. 1981). Studies indicate these compounds undergo very slight photodegradation and photoisomerization observed is speculated to be totally reversible (Beck et al. 1981). However, it has been shown that upon UV exposure, benzylidene malonate derivatives dimerize in substituted cyclobutane derivatives (Beck et al. 1981). The E-Z photoisomerization (Fig. 15) of most benzylidene camphor derivatives is independent of concentration and oxygen. This process is the single most important deactivation process occurring in these molecules (Douarre et al. 1995).

4-aminobenzylidene camphor

4-methylbenzylidene camphor

3-benzylidene camphor
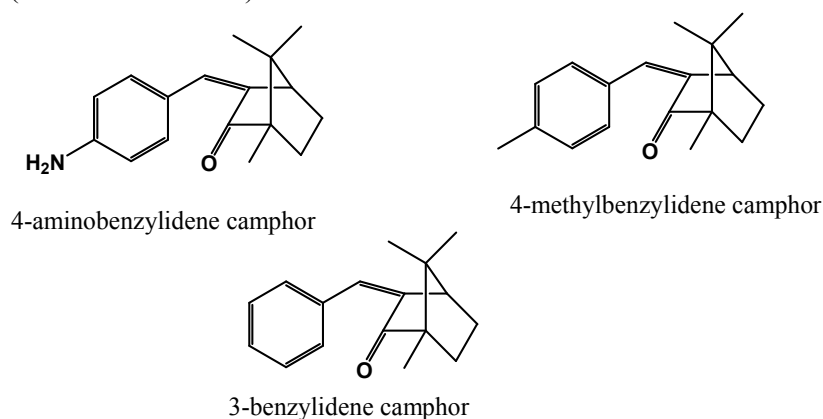
Figure 2.14: Commonly used camphor derivatives in sunscreen preparations.

In work by Douarre et al. (1995) photoproduct formation by 4-aminobenzylidene camphor required the presence of oxygen and an aqueous or acidic environment enhanced rapid back conversion of the photoproducts into the initial compounds. Beck et al. (1981) argued that a mixture of *E* and *Z* isomers acts as a UV filter due to the very short lifetime of their excited states, making these compounds excellent sunscreen agents. However, skin permeation of these particular agents into viable body tissues have been associated with endocrine disruptive effects in several animal studies (Krause et al. 2012).
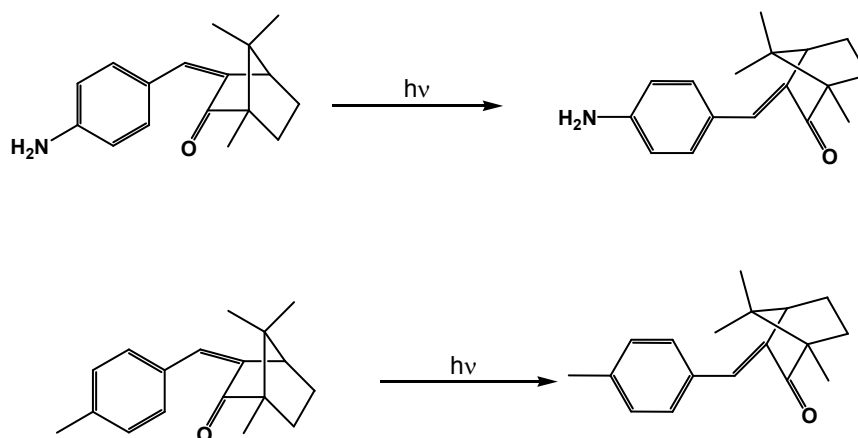
Figure 2.15: UV light induced isomerisation of camphor derivatives.

2.3.7 Benzophenones

Benzophenones (BPs) (Fig. 2.16) are known to be very stable on UV exposure on the basis of the molecular symmetry of the benzophenone (BP) moiety. However, it is that known under UV irradiation the carbonyl (C=O) group of BP participate in a rapid hydrogen abstraction reaction transforming it into an extremely powerful radical generator. Several reports indicate that BP is a potent photosensitizer of thymine dimers in deoxyribose nucleic acid (DNA) (Cuquerella et al. 2012). Recent reports indicate that some non-steroidal anti-inflammatory drugs (NSAIDs) having the BP moiety form thymine dimers when irradiated with DNA *in vitro* (Placzek et al. 2013). The medicinal compounds have also been shown to photosensitize double stranded supercoiled DNA making them to be prone to single-strand break formation (Sewlall 2003; Cuquerella et al. 2012). In addition, sunscreens of BP structure have been shown to yield endoperoxides depending on the polarity of the solvent. (2-hydroxy-4-methoxyphenyl)-phenylmethanone (BP3) is a common UV-filter in cosmetic sunscreen products. Its maximum permissible concentration in formulations is 6%. Transdermal absorption of BP3 in humans may reach 2%, as it is able to permeate the skin and reach the bloodstream after topical application. It has been found in urine after topical application (Hayden et al. 1997). A large amount of BP3 is absorbed, and accumulates in the body. It has also been shown to induce contact allergenic and photo-allergenic effects due to sensitization reactions (Gonzalez et al. 2006; Schram et al. 2007; Berne and Ros 1998). Male reproductive toxicity has been inconsistently reported in chronic high dose animal studies (Gonzalez et al. 2006; Coronado et al. 2008; Kunz et al. 2006). Studies also indicate the BP3 has weak estrogenic activity or weak anti-androgenic activity (Gonzalez et al. 2006; Kunz et al. 2006).

Recent work by Molina-Molina et al. (2008) in profiling of benzophenone derivatives by using fish and human estrogen receptor-specific *in vitro* bioassays considered 2,4-dihydroxybenzophenone (BP1), 2,2',4,4'-tetrahydroxybenzophenone (BP2), 2-hydroxyl-4-methoxybenzophenone (BP3), and; 2,4,4'-trihydroxybenzophenone (THB), all UV-absorbing chemicals, widely used in pharmaceuticals and sunscreens. All four benzophenone derivatives showed anti-androgenic activity in the order THB > BP2 > BP1 > BP3. Though, this study requires further investigation of their role as endocrine disrupters in humans and wildlife, these findings seem to corroborate studies by Heneweer et al. (2005), which indicated synergistic activation of oestrogen receptors. This led the authors to conclude that daily exposure to these sunscreen agents may have estrogenic effects in humans. Recent work by Kunisue et al. (2012) showed BP1 possesses an estrogenic activity higher than BP3. The authors speculate that exposure to elevated BP1 levels may be associated with endometriosis.

Schallreuter et al. (1996) showed that BP3 is rapidly photo-oxidized, yielding BP3 semiquinone, a potent electrophile. It may react with thiol groups on important anti-oxidant enzymes and substrates, such as thioredoxin reductase and reduced glutathione, respectively. Its rapid oxidation followed by inactivation of important antioxidant systems indicates this substance may be harmful to homeostasis of the epidermis. Cowley (1997) demonstrated BP3 can be photo-oxidized to its semiquinone by solar radiation in *vitro* and *in vivo*. The reactive intermediate then binds to thiolate groups in the epidermis and inactivates important anti-oxidant enzyme, thioredoxin reductase. With all these claims around there is need to minimize if not eliminate skin permeation of these UV filters. However, including BP3 in a dendritic structure may help in reducing its percutaneous absorption and improve excited state energy transfer to the core via triplet energy transfer in the dendritic structure (Chen et al. 2006). The presence of gold at the core of this structure may provide an effective triplet-triplet excited state energy quenching mechanism as well as gold itself acting as a physical blocker. The modified chemistry around this chromophore is likely to minimize detrimental effects.

benzophenone

bis(4-hydroxyphenyl)methanone

(2-hydroxy-4-methoxyphenyl)(2-hydroxyphenyl)methanone

(2-hydroxy-4-methoxyphenyl)(phenyl)methanone

2,3,4-trihydroxybenzophenone

5-benzoyl-4-hydroxy-2-methoxybenzenesulfonic acid

2,2'-dihydroxy-4-methoxybenzophenone
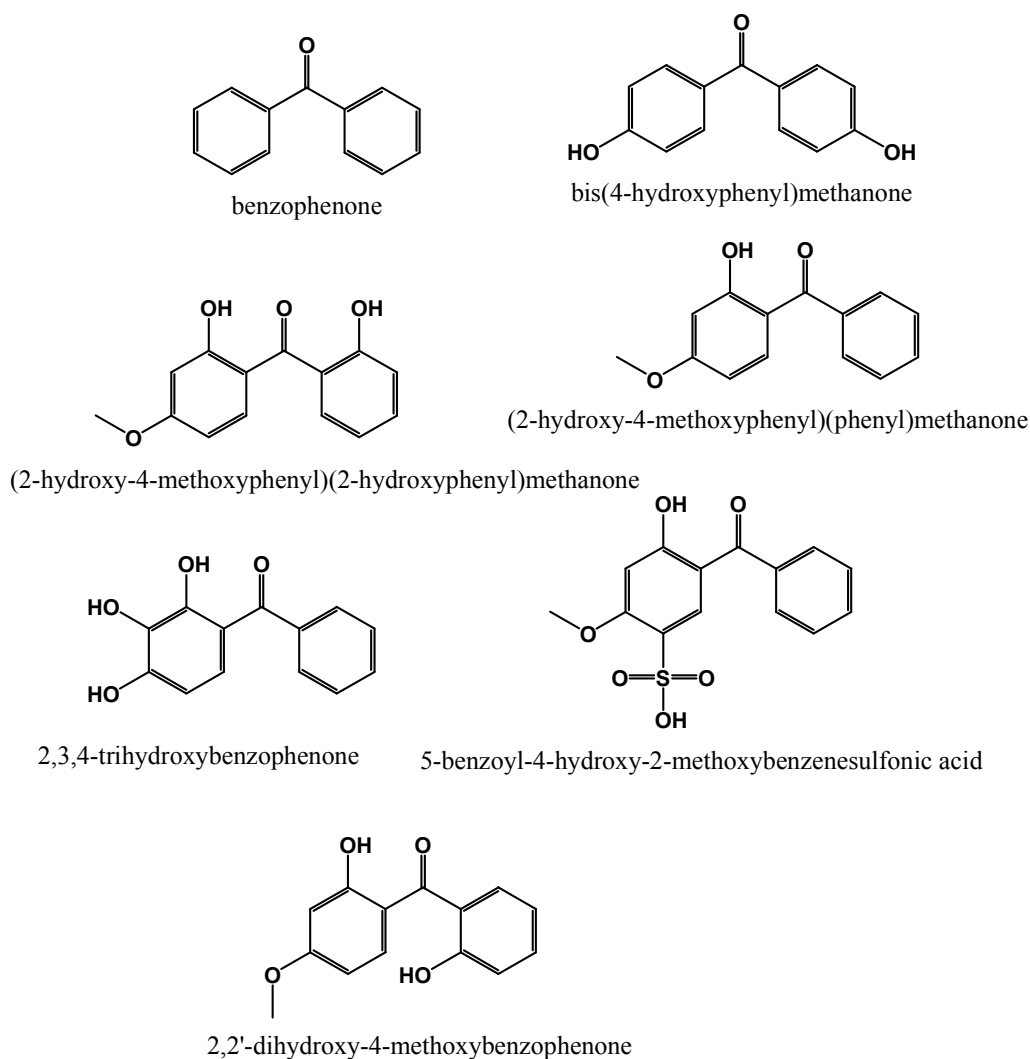
Figure 2.15: Benzophenone and some of its commonly used sunscreen derivatives.

2.3.8 *p*-Aminobenzoate derivatives

p-Aminobeinzoic acid (PABA) was idely used in sunscreens but it photosensitizes thymine dimers (Aliwell et al. 1994). These are precursors to skin cancer. A study by Sutherland and Griffin (1984) showed that it penetrate into cells and has been associated with photoallergicity and therefore it is no longer in used. However, the esters PABA are used as sunscreens. *p*-Aminobenzoate derivatives sunscreen agents are esters of 4-aminobenzoic acid (PABA). The potassium salt of (PABA) is used in the treatment of fibrotic skin disorders, such as Peyronie's disease and also occasionally prescribed as a management in a pill form for patients of irritable bowel syndrome to treat its associated gastrointestinal symptoms. However, PABA absorbs strongly in the UVB region of the spectrum and is reported to reduce deleterious effects of UV in mice (Ley and Fourtanier 1997). PABA has been shown to protect against skin tumors in rodents (Snyder and May 1975). The sunscreen efficacy of this UVB absorber can be deduced from the non-bonding electrons pair conjugated to the phenyl ring π-cloud. This allows for electron delocalization between the amine group and the carbonyl (C=O) group (Fig. 2.17). The ease of electron delocalization in a way photostabilizes the molecule. However, animal and *in vitro* studies have suggested that PABA might increase the risk of cellular UV damage. Secondly, the presence of the reactive amino group and carboxylic acid moieties makes easily form crystallizable products and hence may lead to clothing discolouration when used in

cosmetic preparations. The possible clothing discolouration problem, very oil solubility, and reported allergic responses associated with topical use of this agent have made it not suitable for skin application.

The water-insoluble PABA derivatives such as 2-ethylhexyl 4-(dimethylamino)benzoate (padimate-O) are currently used in some products. Padimate –O is an ester formed by the condensation of 2-ethylhexanol with dimethylaminobenzoic acid. Padimate O absorbs sufficiently in the UVB region and should thus prevent direct DNA damage. However, the excited padimate-O molecule has been shown to react with DNA leading to indirect DNA damage. *In vitro* studies have demonstrated the sunlight-induced mutagenicity of padimate-O (Knowland et al. 1993). The excited state padimate-O has been reported to photosensitize DNA in various *in vivo* studies thus considered photocarcinogenic (Gulston and Knowland 1999). There are contradictory reports from a number of *in vivo* studies conducted in hairless mice following topical application of padimate-O which no carcinogenic effects. These studies elude to the fact and that padimate-O reduces the frequency and the rate ofappearance of UV-induced skin tumours (Kligman et al. 1980; Bissett et al. 1991; Bissett and McBride 1996; Kerr 1998). However, padimate-O is known to penetrate human skin but its effects on human cells are not clear (Gulston and Knowland 1999).
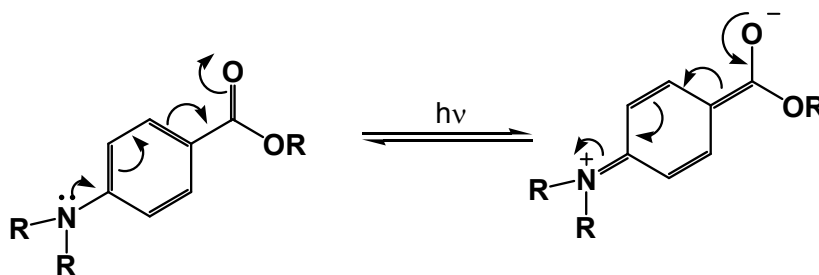
Figure 2.17: Resonance stabilization of p-aminobenzoic acid derivatives

2.4   Sunscreen mixtures: a photostabilization strategy

As a common practice at least two organic filters are used in sunscreen formulations with the intention to optimize the sunscreening effect in the UVB/UVA region. In a number of cases physical blockers are incorporated as well. These is because no single active agent, used at levels currently allowed, provides a high enough sun protection factor (SPF) or broad-spectrum absorption. Two extensively used representatives of such classes of chemical UV filters are cinnamates (UVB) and dibenzoylmethanes (UVA) (Dondi et al. 2006). Mixing absorbers aid formulators in producing high protection products without exceeding regulatory concentration maxima set by various countries. It also helps in overcoming limited solubility problems of absorbers and incompatibility with other ingredients.

It is desired that BMBDM remains intact chemically even over prolonged exposures to UVA irradiation. A number of articles have reported that BMBDM photodegradation can be retarded by the presence of other filters. Conversely, it can be accelerated if a photoreaction occurs between the two components. Formulation strategies to optimize BMBDM's photostability include: removal of incompatible ingredients, inclusion of other sunscreen actives with the ability to enhance BMBDM's photostability; and using non-sunscreen ingredients that have the capacity to photostabilize BMBDM through energy transfer mechanisms.

It has been shown that alkoxy crylenes, particularly methoxy crylenes, can return excited BMDBM from both an electronically excited S_1 and excited T_1 back to their ground state, thereby photostabilizing it. This formulation strategy was attempted by Deflandre et al. (1997) of which their cosmetic sunscreen composition contained at least 1% by weight of an α-cyano-β,β-diphenylacrylate, that photostabilizes BMBDM in a fatty phase. The authors showed that glycerol stearates, or isopropyl myristate in a mole ratio of α-cyano-β,β-diphenylacrylate to BMBDM of at least 0.8 gave a better stabilizing effect.

Several other methodologies have been developed in order to reduce the instability of BMBDM when exposed to sunlight, such as inclusion complexation with cyclodextrins, and incorporation in polymeric or lipid microparticles (Albertini et al. 2009). For instance Albertini et al. (2009) showed that entrapment of BMBDM in lipid microparticles, at high loading levels (>40%), represents an effective strategy to reduce the photolability of this UVA filter, but the limited (4–20 %, m/m) loading capacity is a disadvantage for the applicability to finished sunscreening preparations. Scalia et al. (2002) showed that their results indicated free radicals generated by BMBDM when exposed to simulated sunlight were effectively scavenged by inclusion complexation of BMBDM within hydroxypropyl-β-cyclodextrin. This indicates complexation of BMBDM with a cyclodextrin is another option to be considered.

The combination of EHMC and BMBDM in sunscreen formulations is not recommended in the US because of photoinstability and possible unfavourable synergistic interactions between these agents (Serpone et al. 2002). Photoadducts are formed between EHMC and photo-generated fragments of BMBDM (Serpone et al. 2002; Chatelain and Gabard 2001). Upon absorption of UV radiation, EHMC reacts with BMBDM photochemically in an irreversible manner, destroying the UV absorption properties of both molecules. The incompatibility of EHMC is believed to stem from presence of an exocyclic double bond, undergoing an allowed photochemical [2 + 2] cycloaddition reaction with BMDBM (Fig. 16) to form primary photoproducts that subsequently collapse to form arrange of degradation products (Beasley and Meyer 2010).
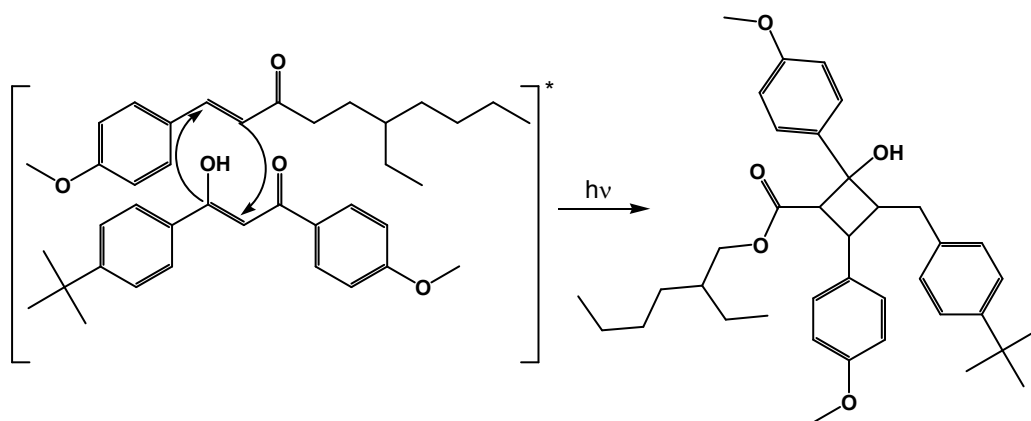
Figure 2.17: Possible photo-induced reaction mechanism between avobenzone and EHMC to produce a [2+2] cycloaddition product.

2.5   Conclusions

In conclusion the photophysics and the photochemical characteristics of sunscreens and their perceived photostabilizers need to be explored on a sun-active agent basis. The photochemical

response of a sunscreen agent may be influenced by the matrix in which is formulated and hence its absorption characteristics may be greatly affected.

Acknowledgement

References
Adronov A, Frechet MJJ (2000) Light-harvesting dendrimers. Chemical Communications:1701-1710

Albertini B, Mezzena M, Passerini N, Rodriguez L, Scalia S (2009) Evaluation of spray congealing as technique for the preparation of highly loaded solid lipid microparticles containing the sunscreen agent, avobenzone. Journal of Pharmaceutical Sciences 98 (8):2759-2769

Aliwell SR, Martincigh BS, Salter LF (1994) Photoproducts formed by near-UV irradiation of thymine in the presence of p-aminobenzoic acid. Journal of Photochemistry and Photobiology A 83 (3):223-228

Alvarez-Roman R, Barre G, Guy RH, Fessi H (2001) Biodegradable polymer nanocapsules containing a sunscreen agent: preparation and photoprotection. European Journal of Pharmaceutics and Biopharmaceutics 52:191-195

Armeni T, Damiani E, Battino M, Greci L, Principato G (2004) Lack of in vitro protection by a common sunscreen ingredient on UVA-induced cytotoxicity in keratinocytes. Toxicology 203 (1-3):165-178

Ashby J, Tinwell H, Plautz J, Twomey K, Lefevre PA (2001) Lack of Binding to Isolated Estrogen or Androgen Receptors, and Inactivity in the Immature Rat Uterotrophic Assay, of the Ultraviolet Sunscreen Filters Tinosorb M-Active and Tinosorb S. Regulatory Toxicology and Pharmacology 34 (3):287-291

Aspée A, Aliaga C, Scaiano JC (2007) Transient Enol Isomers of Dibenzoylmethane and Avobenzone as Efficient Hydrogen Donors toward a Nitroxide Pre-fluorescent Probe. Photochemistry and photobiology 83 (3):481-485

Atitaya S, Juwadee S, Atitaya S (2011) Particle size characterization of titanium dioxide in sunscreen products using sedimentation field-flow fractionation-inductively coupled plasma-mass spectrometry. Analytical and Bioanalytical Chemistry 399 (2):973-978

Avenel-Audran M, Dutartre H, Goossens A, et al. (2010) OCtocrylene, an emerging photoallergen. Archives of Dermatology 146 (7):753-757

Beasley D, Meyer T (2010) Characterization of the UVA Protection Provided by Avobenzone, Zinc Oxide, and Titanium Dioxide in Broad-Spectrum Sunscreen Products. American Journal of Clinical Dermatology 11 (6):413-421

Beck I, Deflandre A, Lang G, Arnaud R, Lemaire J (1981) Study of the photochemical behavior of sunscreens - benzylidene camphor and derivatives. International Journal of Cosmetic Science 3 (3):139-152

Berne B, Ros A-M (1998) 7 years experience of photopatch testing with sunscreen allergens in Sweden. Contact Dermatitis 38:61-64

Bissett DL, McBride JF (1996) Synergistic topical photoprotection by a combination of the iron chelator 2-furildioxime and sunscreen. Journal of the American Academy of Dermatology 35 (4):546-549

Bissett DL, McBride JF, Hannon DP, Patrick LF (1991) Time-dependent decrease in sunscreen protection against chronic photodamage in UVB-irradiated hairless mouse skin. Journal of Photochemistry and Photobiology B: Biology 9 (3–4):323-334

Bjarke KVH, Morten W, Jens S-L (2006) Intramolecuar hydrogen bonding. Spectroscopic and theoretical studies of vibrational transitions in dibenzoylmethane enol. Journal of Molecular Structure 790:74-79

Boehnlein J, Sakr A, Lichtin JL, Bronaugh RL (1994) Characterization of esterase and alcohol-dehydrogenase activity in skin - metabolism of retinyl palmitate to retinol (vitamin-a) during percutaneous-absorption. Pharmaceutical Research 11 (8):1155-1159

Broadbent KJ, Martincigh BS, Raynor WM, Salter FL, Moulder R, Sjoberg P, Markides EK (1996) Capillary supercritical fluid chromatography combined with atmospheric pressure chemical ionisation mass spectrometry for the investigation of photoproduct formation in the sunscreen absorber 2-ethylhexyl methoxycinnamate. Journal of Chromatography A 732:101-110

Chatelain E, Gabard B (2001) Photostabilization of Butyl methoxydibenzoylmethane (Avobenzone) and Ethylhexyl methoxycinnamate by Bis-ethylhexyloxyphenol methoxyphenyl triazine (Tinosorb S), a New UV Broadband Filter. Photochemistry and photobiology 74 (3):401-406

Chatelain E, Gabard B, Surber C (2003) Skin penetration and sun protection factor of five UV filters: effect of the vehicle. Skin Pharmacology and Applied Skin Physiology 16 (1):28-35

Chen J, Li S, Zhang L, Li Y-Y, Chen J, Yang G, Li Y (2006) Direct Observation of the Intramolecular Triplet-Triplet Energy Transfer in Poly(aryl ether) Dendrimers. Journal of Physical Chemistry B 110:4047-4053

Coronado M, De HH, Deng X, Rempel MA, Lavado R, Schlenk D (2008) Estrogenic activity and reproductive effects of the UV-filter oxybenzone (2-hydroxy-4-methoxyphenylmethanone) in fish. Aquatic Toxicology 90:182-187

Cowley JN (1997) The mechanistic photochemistry of 4-hydroxybenzophenone. MSc. Thesis, Queen's University, Ontario, Canada

Crovara AP, Astolfi P, Puglia C, Bonina F, Perrotta R, Herzog B, Damiani E (2012) On the assessment of photostability of sunscreens exposed to UVA irradiation: from glass plates to pig/human skin, which is best? Internationa Journal of Pharmaceutics 427 (2):217-223

Cuquerella MC, Lhiaubet-Vallet V, Cadet J, Miranda AM (2012) Benzophenone Photosensitised DNA Damage. Accounts of Chemical Research 45 (9):1558 - 1570

Deflandre A, Forestier S, Lang G, Richard H, Leduc M (1997) Photostable cosmetic sunscreens containing dibenzoylmethane derivative and dialkylbenzalmalonate. US5624663A,

Dondi D, Albini A, Serpone N (2006) Interactions between different solar UVB/UVA filters contained in commercial suncreams and consequent loss of UV protection. Photochemical & Photobiological Sciences 5 (9):835-843

Douarre L, Arnaud R, Lemaire J, Deflandre A, Richard H (1995) Photochemical study of para-substituted anilines. Journal of Photochemistry and Photobiology A: Chemistry 87:143 - 150

Dunford R, Salinaro A, Cai L, Serpone N, Horikoshi S, Hidaka H, Knowland J (1997) Chemical oxidation and DNA damage catalysed by inorganic sunscreen ingredients. FEBS Letters 418 (1–2):87-90

Egerton AT, Everall JN, Mattinsson AJ, Kessel ML, Tooley RI (2007) Interaction of TiO2 and nano-particles with organic UV absorbers. Journal of Photochemistry and Photobiology A: Chemistry 193 (1)

Gaspar LR, Campos PMBGM (2007) Photostability and efficacy studies of topical formulations containing UV-filters combination and vitamins A, C and E. International journal of pharmaceutics 343 (1–2):181-189

Gaspar LR, Maia Campos PMBG (2006) Evaluation of the photostability of different UV filter combinations in a sunscreen. International journal of pharmaceutics 307 (2):123-128

Gonzalez H, Farbrot A, Larkö O, Wennberg AM (2006) Percutaneous absorption of the sunscreen benzophenone-3 after repeated whole-body applications, with and without ultraviolet irradiation. British Journal of Dermatology 154 (2):337-340

Gonzalez H, Tarras-Wahlberg N, Stromdahl B, Juzeniene A, Moan J, Larko O, Rosen A, Wennberg A-M (2007) Photostability of commercial sunscreens upon sun exposure and irradiation by ultraviolet lamps. BioMedical Central Dermatology 7 (1):1-9

Gulston M, Knowland J (1999) Illumination of keratinocytes in the presence of the sunscreen ingredient padimate-O and through an SPF-15 sunscreen reduces direct photodamage to DNA but increases strand breaks. Mutations Research 444:49-60

Hanson KM, Gratton E, Bardeen CJ (2006) Sunscreen enhancement of UV-induced reactive oxygen species in the skin. Free Radical Biology and Medicine 41 (8):1205-1212

Hauri U, Lutolf B, Schlegel U, Hohl C (2004) Determination of photodegradation of UV filters in sunscreens by HPLC/DAD and HPLC/MS. Mitteilungen aus Lebensmitteluntersuchung und Hygiene 95:147-161

Hayden CGJ, Roberts MS, Benson HAE (1997) Systemic absorption of sunscreen after topical application. The Lancet 350 (9081):863-864

Heneweer M, Muusse M, van den Berg M, Sanderson JT (2005) Additive estrogenic effects of mixtures of frequently used UV filters on pS2-gene transcription in MCF-7 cells. Toxicology and Applied Pharmacology 208 (2):170-177

Herzog B, Mongiat S, Deshayes C, Neuhaus M, Sommer K, Mantler A (2002) In vivo and in vitro assessment of UVA protection by sunscreen formulations containing either butyl methoxy dibenzoyl methane, methylene bis-benzotriazolyl tetramethylbutylphenol, or microfine ZnO. International Journal of Cosmetic Science 24 (3):170-185

Hexsel LC, Bangert DS, Hebert AA, Henry LW (2008) Current sunscreen issues: 2007 Food and Drug Administration sunscreen labelling recommendations and combination sunscreen/insect repellent products. Journal of American Academy of Dermatology 59 (7):316 - 323

Huong PS, Andrieu V, Reynier J-P, Rocher E, Fourneron J-D (2007) The photoisomerization of the sunscreen ethylhexyl-p-methoxycinnamate and its influence on the sun protection factor. Journal of Photochemistry and Photobiology A: Chemistry 186:65-70

Iannuccelli V, Sala N, Tursilli R, Coppi G, Scalia S (2006) Influence of liposphere preparation on butyl-methoxydibenzoylmethane photostability. Europen Journal of Pharmacutics and Biopharmaceutics 63 (2):140-145

Ingouville AN (1995) The photochemical behaviour of the sunscreen absorber 2-ethylhexyl methoxycinnamate. MSc. Dissertation, University of Natal, , Durban, South Africa

Karlsson I, Hillerstrom L, Stenfeldt A-L, Martensson J, Borje A (2009) Photodegradation of Dibenzoylmethanes: Potential Cause of Photocontact Allergy of Sunscreens. Chemical Research in Toxicology 22:1881-1892

Kerr C (1998) The effects of two UVB radiation-absorbing sunscreens on UV radiation-induced carcinogenesis, suppression of the contact hypersensitivity response and histological changes in the hairless mouse. Mutation Research/Fundamental and Molecular Mechanisms of Mutagenesis 422 (1):161-164

Kim TH, Shin BS, Kim KB, Shin SW, Seok SH, Kim MK, Kim EJ, Kim D, Kim MG, Park ES, Kim JY, Yoo SD (2014) Percutaneous absorption, disposition, and exposure assessment of homosalate, a UV filtering agent, in rats. Journal of Toxicology and Environmental Health, Part A: Current Issues 77 (4):202-213

Kligman LH, Akin FJ, Kligman AM (1980) Sunscreens prevent ultraviolet photocarcinogenesis. Journal of the American Academy of Dermatology 3 (1):30-35

Knowland J, Mckenzie AE, McHugh JP, Cridland AN (1993) Sunlight-induced mutagenicity of a common sunscreen ingredient. FEBS Letters 324 (3):309-313

Kockler J, Oelgemoller M, Robertson S, Glass DB (2012) Photostabililty of sunscreens. Journal of Photochemistry and Photobiology C: Photochemistry Reviews 13:91-110

Kowlaser K (1998) Photoproduct formation in the irradiated sunscreen absorber 2-ethylhexyl methoxycinnamate. MSc. Dissertation, University of Natal, Durban, South Africa

Krause M, Kilt A, Blomberg JM, Soeborg T, Frederiksen H, Schlumpf M, Lichtensteiger W, Skakkebaek NE, Drzewiecki KT (2012) Sunscreens: are they beneficial for health? An overview of endocrine disrupting properties of UV-filters. International Journal of Andrology 35:424 - 436

Kunisue T, Chen Z, Louis GMB, Sundaram R, Hediger ML, Sun L, Kannan K (2012) Urinary Concentrations of Benzophenone-type UV Filters in U.S. Women and Their Association with Endometriosis. Environmental Science and Technology 46 (8):4624-4632

Kunz PY, Galicia HF, Fent K (2006) Comparison of In Vitro and In Vivo Estrogenic Activity of UV Filters in Fish. Toxicology Science 90:349-361

Lamola AA, Sharp LJ (1966) Environmental effects on excited states of O-hydroxy aromatic carbonyl compounds. Journal of Physical Chemistry 70 (8):2634-&

Lee J-S, Kim J-W, Kim J, Han S-H, Chang I-S (2004) Photochemical properties of UV-absorbing chemicals in phase-controlled polymer microspheres. Colloid and Polymer Science 283 (2):194-199

Ley DR, Fourtanier A (1997) Sunscreen protection against ultraviolet radiation-induced pyrimidine dimers in mouse epidermal DNA. Photochemistry and photobiology 65 (6):1007-1011

Lyambila W (2003) A study of photoinduced transformations of sunscreen chemical absorbers. PhD Thesis, University of KwaZulu-Natal, Durban

Mavon A, Miquel C, Lejeune O, Payre B, Moretto P (2007) In vitro Percutaneous Absorption and in vivo Stratum Corneum Distribution of an Organic and a Mineral Sunscreen. Skin Pharmacology and Physiology 20 (1):10-20

Molina-Molina J-M, Escande A, Pillon A, Gomez E, Pakdel F, Cavailles V, Olea N, Ait-Aissa S, Balaguer P (2008) Profiling of benzophenone derivatives using fish and human estrogen receptor-specific in vitro bioassays. Toxicology and Applied Pharmacology 232 (3):384-395

Mturi GJ, Martincigh BS (2008) Photostability of the sunscreening agent 4-*tert*-butyl-4'-methoxydibenzoylmethane (avobenzone) in solvents of different polarity and proticity Journal of Photochemistry and Photobiology A: Chemistry 200:410-420

Naya M, Kobayashi N, Ema M, Kasamoto S, Fukumuro M, Takami S, Nakajima M, Hayashi M, Nakanishi J (2012) In vivo genotoxicity study of titanium dioxide nanoparticles using comet assay following intratracheal instillation in rats. Regulatory Toxicology and Pharmacology 62 (1):1-6

Oesterwalder U, Herzog B (2009) Chemistry and properties of organic and inorganic UV filters. Clinical Guide to Sunscreens and Photoprotection. Informa Healthcare, New York, USA

Panday R (2002) A photochemical investigation of two sunscreenabsorbers in a polar and non polar medium. MSc. Dissertation, University of Natal, Durban, South Africa

Paris C, Lhiaubet-Vallet V, Jimenez O, Trullas C, Miranda MA (2009) A blocked diketo form of avobenzone: photostability, photosensitizing properties and triplet quenching by a triazine-derived UVB-filter. Photochemistry and photobiology 85 (1):178-184

Pattanaargson S, Munhapol T, Hirunsupachot P, Luangthongaram P (2004) Photoisomerization of octyl methoxycinnamate. Journal of Photochemistry and Photobiology A: Chemistry 161:269-274

Perugini P, Simeoni S, Scalia S, Genta I, Modena T, Conti B, Pavanetto F (2002) Effect of nanoparticle encapsulation on the photostability of the sunscreen agent, 2-ethylhexyl methoxycinnamate. International journal of pharmaceutics 246:37-45

Placzek M, Dendorfer M, Przybilla B, Gilbertz KP, Eberlein B (2013) Photosensitizing properties of compounds related to benzophenone. Acta Derm Venereol 93 (1):30-32

Roscher NM, Lindemann MKO, Kong SB, Cho CG, Jiang P (1994) Photodecomposition of Several Compounds Commonly Used as Sunscreen Agents. Journal of Photochemistry and Photobiology A: Chemistry 80 (1-3):417-421

Santo S, Mezzena M (2010) Photostabilisation Effect of Quercetin on the UV Filter Combination, Butyl Methoxydibenzoylmethane-Octyl Methoxycinnamate. Photochemistry and photobiology 86:273-278

Saquib Q, Al-Khedhairy AA, Siddiqui MA, Abou-Tarboush FM, Azam A, Musarrat J (2012) Titanium dioxide nanoparticles induced cytotoxicity, oxidative stress and DNA damage in human amnion epithelial (WISH) cells. Toxicology In Vitro 26 (2):351-361

Sayre MR, Dowdy CJ, Gerwig JA, Shields JW, Lloyd VR (2005) Unexpected photolysis of the sunscreen octinoxate in the presence of the sunscreen avobenzone. Photochemistry and photobiology 81:452-456

Sayre RM, Dowdy JC, Ricci A, Chretien MN, Scaiano JC (2003) Mineralization of organic sunscreens: interesting, but relevant? Comment and response. Photochemical and Photobiological Sciences 2 (10):1050-1051

Scalia S, Simeoni S, Barbieri A, Sostero S (2002) Influence of hydroxypropyl-beta-cyclodextrin on photoinduced free radical production by the sunscreen agent, butyl-methoxydibenzoylmethane. Journal of Pharmacy and Pharmacology 54 (11):1553-1558

Schallreuter KU, J.M W, Farwell DW, Moore J, Edwards HGM (1996) Oxybenzone oxidation following solar irradiation of skin: Photoprotection versus antioxidant inactivation. Journal of Investigative Dermatology 106 (3):583 - 586

Schram SE, Glesne LA, Warshaw EM (2007) Allergic contact cheilitis from benzophenone-3 in lip balm and fragrance/flavorings. Dermatitis 18:221-224

Schwack W, Rudolph T (1995) Photochemistry of dibenzoyl methane UVA filters Part 1. Journal of Photochemistry and Photobiology B: Biology 28:229-234

Serpone N, Salinaro A, Emeline AV, Horikoshi S, Hidaka H, Zhao JC (2002) An in vitro systematic spectroscopic examination of the photostabilities of a random set of commercial sunscreen lotions and their chemical UVB/UVA active agents. Photochemical and Photobiological Sciences 1 (12):970-981

Sewlall A (2003) DNA cleavage photoinduced by benzophenone based sunscreens. MSc. Dissertation, University of Natal, Durban, South Africa

Shukla RK, Sharma V, Pandey AK, Singh S, Sultana S, Dhawan A (2011) ROS-mediated genotoxicity induced by titanium dioxide nanoparticles in human epidermal cells. Toxicology in Vitro 25 (1):231-241

Simonsen L, Petersen BM, Groth L (2002) *In-vivo* skin penetration of salicyclic compounds in hairless rats. European Journal of Pharmaceutical Sciences 17:95 - 104

Snyder DS, May M (1975) Ability of PABA to protect mammalian skin from ultraviolet light-induced skin tumors and actinic damage. The Journal of Investigative Dermatology 65:543-546

Srei PH, Emmanuelle R, Jean-Dominique F, Laurence C, Valerie M, Hot B, Veronique A (2008) Photoreactivity of the sunscreen butylmethoxydibenzoylmethane (DBM) under various

experimental conditions. Journal of Photochemistry and Photobiology A: Chemistry 196:106-112

Sutherland JC, Griffin KP (1984) p-Aminobenzoic acid can sensitize the formation of pyrimidine dimers in DNA: direct chemical evidence. Photochemistry and Photobiololgy 40 (3):391-394

Tobita S, Ohba J, Nakagawa K, Shizuka H (1995) Recovery mechanism of the reaction intermediate produced by photoinduced cleavage of the intramolecular hydrogen bond of dibenzoylmethane. Journal of Photochemistry and Photobiology A: Chemistry 92 (1-2):61-67

Walters KA, Brain KR, Howes D, James VJ, Kraus AL, Teetsel NM, Toulon M, Watkinson AC, Getting SD (1997) Percutaneous Penetration of Octyl Salicylate from Representative Sunscreen Formulations through Human Skin *In Vitro*. Food and Chemical Toxicology 35:1219 - 1225

Wilkinson F (1997) Quenching of electronically excited states by molecular oxygen in fluid solution. Pure and Applied Chemistry 69 (4):851-856

Xu C, Green A, Parisi A, Parsons PG (2001) Photosensitization of the Sunscreen Octyl p-Dimethylaminobenzoate by UVA in Human Melanocytes but not in Keratinocytes. Photochemistry and photobiology 73 (6):600-604

Yamaji M, Cecilia P, Miguel AM (2010) Steady-state and laser flash photolysis studies on photochemical formation of 4-t*ert*-butyl-4'-methoxydibenzoylmethane from its derivative *via* the Norrish Type II reaction in solution. Journal of Photochemistry and Photobiology A: Chemistry 209:153 - 157

Yankov P, Saltiel S, Petkov I (1988) Photoketonization and excited state relaxation of dibenzoylmethane in non-polar solvents. Journal of Photochemistry and Photobiology A: Chemistry 41 (2):205-214

Zhang R, Niu Y, Li Y, Zhao C, Song B, Li Y, Zhou Y (2010) Acute toxicity study of the interaction between titanium dioxide nanoparticles and lead acetate in mice. Environmental Toxicology and Pharmacology 30 (1):52-60

Chapter Three

Trends in Sunscreen Formulations

Moses A. Ollengo and Bice S. Martincigh[*]

School of Chemistry and Physics, University of KwaZulu-Natal, Westville Campus, Private Bag X54001, Durban 4000, South Africa

*Corresponding author. Tel.:+27-31-2601394; Fax: +27-31-2603091; E-mail address: martinci@ukzn.ac.za

Abstract

There are different methods of combating the deleterious effects of ultraviolet radiation (UV): sunscreens formulated with filters as well as clothing. It is known that exposure of keratinocytes to 15 minutes of UVA radiation leads to substantial cell mortality and a decrease in protein content. Thus, the consequences of exposure to UV radiation and its correlation with cancer development have triggered a public education campaign promoting the use of sunscreens. A broad variety of different creams, dispersions, emulsions, gels, ointments, lotions, milks, sprays, tonics and hydrogels are available in the market that use various UV-filter systems. Several inorganic and organic compounds have been explored and are employed for protection from harmful UV radiation. A lot of research is ongoing with a view of investigating ways of reducing the skin penetration of the sunscreen active ingredients, oxidative stress management and evaluation of different types of vehicles for topical dermal delivery. This review aims at exploring the current formulations as well as to point out novel approaches for suncare product development and presentation.

3.1   Introduction

Ozone, a minority constituent in the earth's atmosphere, is a major absorber of ultraviolet (UV) radiation (Sklar et al. 2013). As has been shown anthropogenic emissions, for example, of chlorofluorocarbons can deplete stratospheric ozone, giving rise to an ozone hole. A decrease in atmospheric ozone is expected to significantly increase levels of UV on the earth's surface (Bowden 2004). The main public concern regarding the ozone hole has been the effect of increased surface UV radiation on human health. It is well documented that UV radiation is harmful to skin and can cause helioderma and cancers (Abarca and Casiccia 2002). Publicized strategies for combating UV radiation are: sun avoidance during peak hours (10 am to 4 pm), clothing and sunscreens formulated with filters.

Solar UV radiation incident on the earth's surface can be divided into two regions: UVB (290-320 nm) and UVA (320-400 nm). Both types are harmful to human skin, damaging both the skin surface and inner structure of skin when taking prolonged sunbaths. The skin is the largest organ of the body and constitutes 16 % of the body weight, with a surface area of 1.8 m^2. It has several functions; most important being that it is a physical barrier to the environment, allowing and limiting inward and outward passage of water, electrolytes and various substances. It provides protection against micro-organisms, UV radiation, toxic agents, and mechanical insults**.** Though structurally consistent throughout the body, the skin varies in thickness depending on anatomical site and age of an individual. The epidermis is the outer layer, serving as the physical and chemical barrier between the interior and exterior body environment. Because UVB rays are of shorter wavelength they only reach the epidermal layer causing sunburn. Most of the UVB radiation is absorbed by the stratum corneum on the epidermis surface (Fig. 3.1). This stratum corneum is a layer of dead cells; the skin visible layer (Lautenschlager et al. 2007). There is evidence from animal studies that UVB induces the disruption of the epidermal barrier function (Jiang et al. 2006). However, UVB radiation has been shown to play a critical role in the synthesis of vitamin D. Dermis is the deeper layer providing the structural support it is a loose connective tissue layer beneath the epidermis and subcutis or hypodermis is an important depot of fat. Topically applied UV filters should be localized in the outermost part of the stratum corneum without infiltration to deeper viable tissues (Felton et al. 2002).
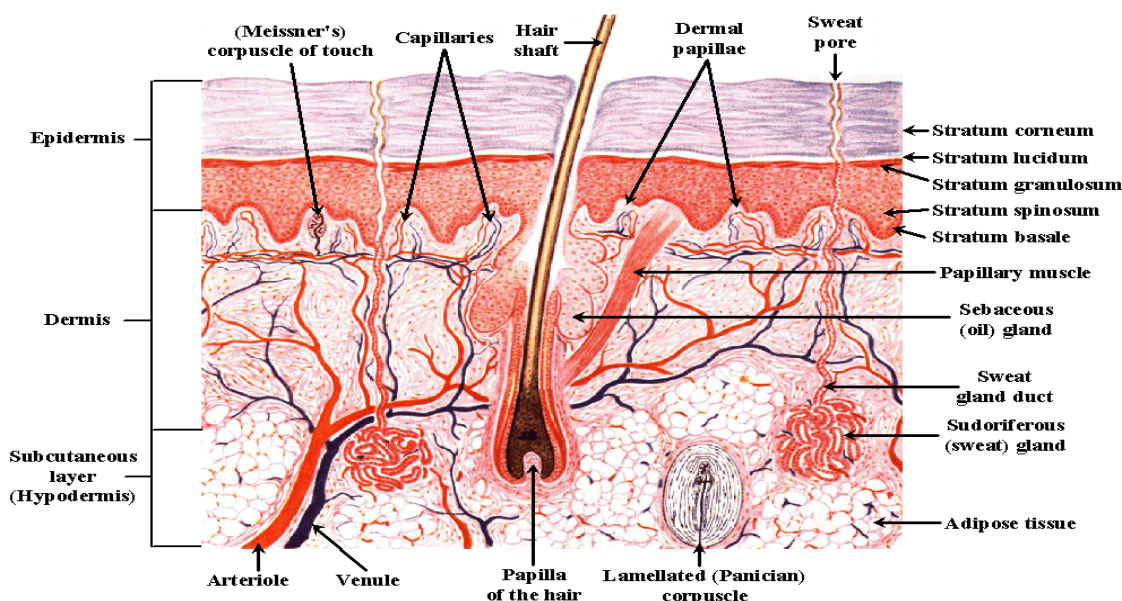
Figure 3.3: The structure of the skin (http://csmrsoldier.com/2013/09/06/adventures-skin-trade/ accessed on 12-12-2014)

Its known that compared with UVB, UVA radiation is a tenfold more efficient oxidative stress generator causing lipid peroxidation linked to plasma membrane damage (Damiani et al. 2006). *In vitro* studies indicate UVA generates a peroxidative process in cultured human skin fibroblasts and in keratinocytes, a radical process that alters the plasma membrane. Exposure of keratinocytes to 15 min UVA radiation has been shown to result in substantial cell mortality and a protein content decrease (Armeni et al. 2004). Such physiological changes have adverse effects on the overall skin structure and serves to initiate various skin maladies.

The cancer induction mechanism by UVA and UVB radiation is well documented. Absorption of UVA and UVB radiation causes pyrimidine bases in the DNA molecule to form dimers (González et al. 2008); resulting in transcription errors during DNA replication. The malignant type of cancer manifests tumours as a consequence of abnormal proliferating skin cells. The uncontrollable growth of these cells leads to melanoma tumours forming. Melanoma is a cancerous skin tumour, produced by cells in the skin that give it pigment (melanin), cells called melanocytes. Melanoma begins as a dark skin lesion and may spread rapidly to other skin areas and within the body (Besaratinia and Pfeifer 2008). Usually, melanoma skin cancer is caused by longer, deeper penetrating UVA rays. They penetrate the dermal layer and cause elastosis (loss of structural support and elasticity of the skin) (Atitaya et al. 2011). Melanomas are therefore linked to UVA radiation but other experiments on opossums suggest a larger role for UVB (van der Leun and de Gruijl 2002). Consequently both UVA and UVB radiation have therefore been linked to skin cancer, whether malignant or benign (Abarca and Casiccia 2002). The most lethal of the skin cancers, cutaneous malignant melanoma, is more commonly associated with sporadic burning exposure to solar radiation. There are several indications that UVA might have an important role in the pathogenesis of melanoma (Lautenschlager et al. 2007). But sunburns are taken as a measure of overexposure to solar radiation and they have been identified as a risk factor for the development of melanoma. It is on the basis of sunburns; primarily due to UVB that implicates UVB as a potential contributing factor to the pathogenesis of melanoma. To this end there is a great deal of controversy regarding the relationship between UVA exposure and the development of melanoma (Wang et al. 2001). Nonetheless, cutaneous malignant melanoma is one of the fastest increasing cancers and UV radiation is strongly linked in its etiology (De Fabo et al. 2004). Cutaneous malignant melanoma is more prevalent among light-skinned people (Abarca and Casiccia 2002).

The other solar radiation associated skin conditions are basal and squamous cell carcinomas, which are common forms of skin cancer in humans. These cancers (BCC and SCC) are relatively mild and rarely fatal, although the treatment of squamous cell carcinoma sometimes requires extensive reconstructive surgery. Other UV radiation induced skin disorders are: photoaging; actinic keratosis; lupus vulgaris (tuberculosis of the skin), and psoriasis or vitiligo (a discontinuous depigmentation of the skin). Hence, sun protection is an inevitable choice, and suitable vehicles are required to deliver the sunscreen ingredient onto the skin or in clothing fabric.

3.2   Sunscreen carriers

The consequences of exposure to UV radiation and the correlation with cancer development have triggered a public education campaign promoting the use of sunscreens. Solar UV filters present in sunscreens are intended to absorb, reflect, or refract ultraviolet radiation. A broad variety of different creams, dispersions, emulsions, gels, ointments, lotions, milks, sprays, tonics and hydrogels are available in the market making use of a variety of UV-filter systems. A number of factors determine the choice of vehicle used in delivering a suncare product. These considerations are: target sun protection factor (SPF), skin type, cost of materials, level of water resistance, desired packaging, and

aesthetic value.

Emulsions are more popular, being termed creams or lotions depending on their degree of viscosity; though no clear-cut distinction between a cream and a lotion exists. However, both are easier to spread on the skin and dispense from bottles. Due to ease of surface dispersion it is possible to achieve a uniform thickness, non-transparent sunscreen film and hence minimum ingredient interaction with sunscreen-active components. It is because of these factors that make emulsion formulations to afford higher SPF values. However, emulsions are difficult to stabilize especially at elevated temperatures, creating a favourable environment for microbial contamination and risking product breakdown. Undeniably emulsions are the best medium that gives skin suppleness and a smooth silky feel.

Oils have the advantage of ease of formulation and excellent product stability. Given that most sunscreen ingredients are lipophilic in nature dissolution in oils makes their manufacture simpler compared to emulsions. Application of oils on the skin yields a thinner, uniform layer, and a transparent film screen greatly reducing SPF. It has been demonstrated that oils, like mineral oils, have a hypochromic shift effect on UV filters as a result of interactions with nonpolar esters that constitute the most popular sunscreens (Kwok et al. 2008). Chemical reactions between esters in sunscreen oils may produce products likely to react with the plastic casing housing a product. This offers an additional cost effect rolled over to consumers, since suitable packaging is required.
Gels, on the other hand, present as crystal clear films when spread on the skin give an impression of high purity, class and fashion. There are four classes of gels: aqueous, hydro-alcoholic, micro-emulsion and gelled-oleaginous (oily anhydrous). Each of these vehicles have corresponding disadvantages, for example, aqueous gels are prone to wash off when exposed to water or perspiration. Use of a high concentration of surfactants makes the finished product both expensive and time-consuming. Hydro-alcoholic gels give a good cooling effect on the skin. Most lipophilic screens are soluble in ethanol thus additional solubilizers are not required. However, the main limitations of this vehicle are water wash-ability and eye itch due to the high levels of alcohol. Volatility of alcohol is another challenge demanding special packaging thereby increasing the cost of production. Micro-emulsion gels have particle sizes in the range of < 0.5 μm. They afford an elegant feel to the skin creating a smooth, thick and uniform film when dispersed on the skin. A challenge with this mode of sunscreen presentation is the use of high emulsifier levels known to irritate and increase wash-ability. Oily gels are produced by crystallizing a combination of mineral oils and sunscreens with special silica making them clear. This vehicle is not very popular due to cost of production.

Popular among the feminine gender is the need to cover smaller sections of the body, such as the lips or nose; here sunscreen-sticks comes in handy. Most sticks are composed of oils and oil-soluble sun-active ingredients thickened by incorporation of waxes and petrolatum, thereby enhancing water resistance (Kwok et al. 2008). For outdoor workers the vehicle of choice is ointments; they are hard to remove or wash away but aesthetically not appealing due to their oily and greasy nature. Other vehicles in the market are mousses and aerosols but associated sun protection factors are much less. All vehicles discussed above have to carry several inorganic and organic compounds employed to absorb or scatter/reflect deleterious UV radiation. The quantity of these compounds in commercial sun protection formulations is generally decided by the SPF. A given sunscreen product must have a minimum SPF of less than the number of active sunscreen ingredients used in combination multiplied by two (Jain and Jain 2010).

Since both UVB and UVA radiation are carcinogens, sunscreen products should achieve broad-spectrum protection, that is, UVA and UVB protection. Problems of photoinstability of such products have been reported (Mturi and Martincigh 2008; Azusa et al. 2009; Kockler et al. 2012) and consequently the photostability of the protective molecules needs to be optimized. Any photo-generated reactive species should be quenched before photochemical damage occurs. Suncare chemicals are classified into two main classes: physical blockers and chemical absorbers.

Physical blockers, in sufficient amount and monodispersed on the skin surface should reflect or scatter all UV, visible and infrared radiation. The most commonly used physical blockers are titanium oxide, zinc oxide and red petrolatum. In most formulations they are used in conjunction with chemical absorbers to achieve high SPF factors. Other forms of metal oxides and dopants are being investigated to enhance sun protection and increase aesthetic value of formulations (Herling et al. 2013). Chemical absorbers, on the other hand, are classified depending on the type of radiation they protect that is either UVA or UVB. Sunscreen ingredients that absorb in the UVA range (315-400 nm) are classified as UVA absorbers. Examples are derivatives of benzophenone, anthranilate; and dibenzoylmethane. Those absorbing between 290-315 nm, for example salicylates, cinnamates, camphor derivatives and *p*-amino benzoic acid derivatives, are classified as UVB absorbers (Atitaya et al. 2011).

The chemical environment in which a sunscreen absorber is packaged greatly determines its UV absorptivity. Acidic chemical absorbers in alkaline conditions favour formation of anions that tend to increase electron delocalization. This decreases the energy required for electronic transitions in the UV region and thus a shift to longer wavelength is observed (bathochromic shift). Similarly, *tert*-butylmethoxy dibenzoylmethane (BMDBM) a common UVA absorber has been shown to stabilize in polar protic environments that favour the chelated *enol* form (Mturi and Martincigh 2008) that enhances its absorptivity in the UVA region. Several other published works show a relationship between the chemical structure and efficacy of UV filters. For example, 4-methylbenzylidene camphor (4-MBC), a UV filter with a high molar absorption coefficient of above 20000 dm^3 mol^{-1} cm^{-1} absorbs in the UVB range of 290-300 nm. This molecule owes its photostability to the reversible photo-isomerization (Fig. 3.2). A chemical environment that would favour carbonyl-hydrogen abstraction is therefore likely to interfere with the reversibility of the isomerisation and hence induce a loss in photostability.
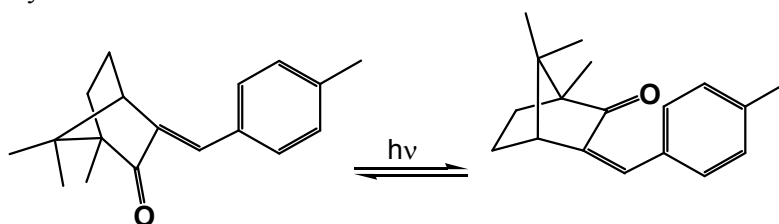
Figure 3.4 Photo-isomerization of 4-methylbenzylidene camphor (Shaath 2010).

UVA (315-400 nm) penetrates to deeper layers of the skin damaging DNA and tissue via production of reactive oxygen species (ROS) (Setlow et al. 1993). In addressing the effects of UVA damage it has been necessary to search for broad-spectrum UV radiation filters. A common UVA absorber used BMDBM, is known to be inherently photolabile and requires special selection of formula ingredients to provide photostable protection (Wang et al. 2008). Innovative stabilizing strategies for BMDBM have been investigated. Chaudhuri et al. (2006) showed diethylhexyl syringylidene malonate as a potent stabilizer of BMDBM and effective antioxidant. Recently Santo and Mezzena (2010)

demonstrated that addition of quercetin to the sunscreen formulation significantly reduced the photodegradation of the combination of BMDBM and EHMC, a mixture known to be photolabile.

The photodegradation of suncare molecule produces by-products that are potentially dangerous, since they may induce sensitization and skin irritation. Several techniques are available to reduce photodegradation. These include:

- Use of different UV filters in the same product, to enhance the synergistic effect,
- Incorporation of specific stable UV filters that absorb at a specific wavelength, and
- Protecting the active ingredient by complexing or encapsulation.

This review aims at exploring current formulations and pointing out novel approaches for suncare product development and presentation.

3.3 Quality of suncare product

To optimize the functions of the integument, sunscreens must have minimal dermal absorption, if any, for good protection (Wissing and Müller 2002a). Absorption and skin penetration of sunscreens may induce phototoxic reactions increasing the risk of photoallergic effects (Chawla and Mrig 2009) . Benzophenone-3 (BP3) has been reported to have been recovered as unchanged BP3 and its metabolites in the urine after topical application (Gonzalez et al. 2006; Hayden et al. 1997). Concerns arising from the skin permeation of these substances are the possible estrogenic potency of these sunscreens and their components. A recent study demonstrated changes in hormone (estradiol and testosterone) levels of participants after topical application of popular sunscreens (Gordon et al. 2005; Schlecht et al. 2004; Jarry et al. 2004). A recent *in vivo* study on endocrine active components of sunscreens showed that 4-MBC, EHMC and BP3 indicated high estrogenicity in uterine wet weight, cell height, and cell proliferation assays (Schlumpf et al. 2004; Schlecht et al. 2004; Jarry et al. 2004).

While safety of the sunscreen product is important, there are other factors that a commercial sunscreen product should meet. These factors include water resistance; high tolerance, and pleasant product feel on the skin. An ideal suncare formulation should delicately balance these vital aspects without compromising safety by way of skin penetration. Efforts have therefore been made to reduce skin penetration of sunscreen active ingredients, including an evaluation of different vehicle types (Felton et al. 2002). An increase in formulation viscosity (Cross et al. 2001), or incorporation of UV filters in nanoparticles (Felton et al. 2002), or complexation with cyclodextrins (Morabito et al. 2011; Vyas et al. 2008), are perceived as viable solutions. Also, the addition of antioxidants reduces oxidative stress associated with some of the sunscreen ingredients. For instance, Hanson et al. (2006) demonstrated that sunscreens, octocrylene (OCT), EHMC and BP3, enhanced the production of UV-induced ROS in the skin above that produced naturally by epidermal chromophores under UV irradiation. The stabilizing mechanisms: encapsulation or complexation may sustain efficacy, and antioxidants incorporated may trap free radicals formed thereby limiting photochemical damage (Nesseem 2011). In addition, a suitable sunscreen delivery system that decreases the amount and the photolability of organic sun-active ingredients, is needed to maintain product efficacy.

The current trend is to encapsulate active ingredients in various media. An encapsulated system consists of a particle totally surrounded by a matrix. In this case the particle is theoretically totally isolated from its surroundings. This makes the undesired properties of the active sunscreening agent, such as contact and photo-contact allergic dermatitis, to be masked. Encapsulation converts organic sunscreen into particulates and isolates the sunscreen from the skin, minimizing ingredient interaction. More so, it allows the use of oil soluble actives in oil-free systems with a greater range of solubility

(Jain and Jain 2010). This is likely to reduce the interaction between oils and sunscreen esters hence limiting attack on the plastic casing.

3.4 Nanoencapsulation

Solid lipid nanoparticles (SLN) are emerging as a carrier system for sunscreens. SLN are produced by replacing the liquid-lipid (oil) of an oil in water (o/w) emulsion by a solid lipid or a blend of solid-lipids. The lipid-particle matrix is solid at both room and body temperature (Müller et al. 2000; Puri et al. 2010). For purposes of topical application, the SLN are reported to favour skin hydration, modified active agents release, and may avoid systemic uptake (Puri et al. 2010) of topically applied active agent. Lipid nanoparticles are known to enhance the chemical stability of compounds sensitive to light, oxidation and hydrolysis. SLNs are advantageous in comparison with conventional o/w emulsions because they exhibit a zero-order release profile of organic components. The slow active molecule release from SLNs yields a longer-lasting sunscreen (Wissing and Müller 2002b; Pardeike et al. 2009) enhanced by the synergistic effect of offering both UV protection and photostability. This results in a reduced need for high concentrations of potentially photo-carcinogenic photo-active molecules without sacrificing the SPF (Carlotti et al. 2005). A study by Mueller et al. (2002) showed that SLN acting as a physical UV blocker resulted in improved UV protection in combination with BP3 at low concentrations. A more recent report indicates that solid-liquid microspheres (SLMs) could be excellent carriers of BP3 in order to decrease release and penetration rate of this UV absorber (Mestres et al. 2010). The SLMs have also been shown not only to decrease skin penetration of EHMC but also to improve it photostability (Yener et al. 2003). This served to corroborate an earlier study that indicated nanoparticle-based systems could enhance the photostability of the sunscreen agent, *trans*-EHMC (Perugini et al. 2002).

The advantage of SLNs is based upon their ability to reflect and scatter incoming UV radiation. It has been shown that the scattering properties of SLNs depend on the degree of crystallinity. More crystalline SLNs have a greater ability to reflect and scatter radiation (Wissing and Müller 2002b). Solid-lipid nanoparticles have emerged as an alternative to other novel delivery approaches. Because of various advantages, including feasibility of incorporation in lipophilic and hydrophilic drugs, improved physical stability, low cost compared to liposomes, and ease of scale-up and manufacturing (Mandawgade and Patravale 2008), SLNs are regarded as new topical delivery systems for pharmaceutical and cosmetic active ingredients (Müller et al. 2002; Müller et al. 2000). By being particulate, they remain on the skin forming a thin film layer sufficient to prevent trans-epidermal water loss (Wissing and Müller 2001; Jenning et al. 2000) and significantly increasing SPF. An SPF 50 was reported after encapsulation of titanium dioxide into SLNs (Villalobos-Hernández and Müller-Goymann 2005). This indicates that encapsulation of inorganic sunscreens into SLNs is a promising approach to obtain well tolerated sunscreens with high SPF. Another competing encapsulation mechanism is the use of cyclodextrins.

3.5 Cyclodextrin complexation

Cyclodextrins are toroidal-shaped cyclic oligosaccharides with a hydrophilic outer surface and hydrophobic hollow interior. Cyclodextrins can entrap a vast number of lipophilic compounds into their hydrophobic cavity, depending on their size and molecular structure. For this reason cyclodextrins behave as hosts and hydrophobic species are guests. The driving force for such an inclusion process is the enthalpy contribution arising from non-covalent hydrophobic interactions (Loftsson and Masson 2001; Szejtli 1998; Szejtli 2004). The basic physicochemical characteristics of

cyclodextrins have been used extensively to improve physicochemical and pharmaceutical properties: solubility, stability and bioavailability of administered drug molecules.

The photodegradation studies on encapsulated BMDBM in cyclodextrins showed a significant reduction of the light-induced decomposition of BMDBM (Scalia et al. 2006; Iannuccelli et al. 2006; Scalia et al. 1998). This led the authors to conclude that incorporation of BMDBM in the cyclodextrin complex form could be more effective in enhancing this sunscreen. Another photostabilization potential of cyclodextrin complexation with sunscreens was demonstrated with the reduction in the light-induced decomposition of 4-MBC (Scalia et al. 2007). Experiments on the skin permeation of BMDBM have also shown that encapsulation of this agent in cyclodextrins markedly reduces its epidermal concentration. It was also demonstrated that the encapsulation limits direct contact of the sunscreen and of its reactive photolytic products with the skin viable tissues (Simeoni et al. 2004). Other systems of the sunscreen formulation target not only the photostabilization of the sunscreen agent but also scavenging of ROS generated by some agents. This is by addition of antioxidants.

3.6   Addition of antioxidants

External sources of ROS initiation include UV light, ozone, cigarette smoke, dietary quinones and quinoid drugs. Photo-induced singlet oxygen is produced by absorption of incident light of particular wavelengths by excitable endogenous molecules (Rogiers et al. 2006). Transferred energy promotes an electron in an adjacent triplet (unexcited) oxygen molecule, to a singlet excited state. Generated ROS interacts primarily with the skin and eyes. A different phenomenon occurs in plants excessive exposure to UV radiation triggering production of non-photosynthetic pigments for example cinnamic acid derivatives and flavonoids. Flavonoids have many positive effects on various cell layers of skin, namely, antioxidant, anti-allergic and anti-inflammatory effects. The antioxidant capacity of flavones is attributed to the high reactivity of the hydroxyl substituent, with the number of hydroxyl groups on the β-ring being correlated to ROS scavenging capability (Al Shaal et al. 2011; Gavin and Durako 2011). These compounds are known to be responsible for blocking UV radiation in addition to their antioxidant activity (Gavin and Durako 2011). The flavanoids are discussed at length in the section under plant extracts.

Antioxidants contain many free electrons transferable to unpaired electrons in radicals. The antioxidants, vitamins C and E, pycnogenol and β-carotene have shown a synergistic effect in combination with sunscreen ingredients (Morabito et al. 2011). Chemically, ascorbic acid (vitamin C), an alpha-ketolactone at physiological pH, is oxidized to dehydro-L-ascorbic acid. This intermediate compound after donation of one electron forms ascorbate, a stable free radical. Water soluble ascorbate, an effective free radical scavenger, interacts with a variety of free radicals intracellularly and extracellularly. Vitamin C is known to regenerate α-tocopherol, a most stable form of vitamin E. The vitamins C and E in topical applications show reduced UVB-induced skin wrinkling and delay the onset of skin tumours (Rogiers et al. 2006). The addition of botanical antioxidants and vitamins C and E to a broad-spectrum sunscreen may further decrease UV-induced damage compared with sunscreens alone. These agents have been shown to enhance protection against UV-induced epidermal thickening (Matsui et al. 2009).

UVA induces tissue damage via production of radical oxygen species. Topical application of antioxidants in sunscreens can potentially neutralize UVA-induced free radicals (Wang et al. 2011). It is speculated that topical supplementation of antioxidants can provide additional protection to

neutralize ROS from both endogenous and exogenous sources (Chen et al. 2012; Matsui et al. 2009). Topical antioxidants have shown the potential to diminish the ROS generated from the UVA radiation. An in *vivo* study by Wu et al. (2011) demonstrated that antioxidants may contribute significantly to sun protection when added to a broad-spectrum sunscreen agent and applied topically on human skin. Hence, the addition of antioxidants in cosmetics may help to prevent wrinkles and reduce ageing caused by UV radiation. It is therefore envisaged that the inclusion of antioxidants in UV filter formulations could be an effective photoprotective strategy. Another class of antioxidants of interest is carotenoids.

The carotenoids, beta-carotene, lutein and lycopene, are considered to be of prime importance for reduction in skin aging and the risk of cancer development (Meinke et al. 2010). Though carotenoids are produced by other photosynthetic organisms, in plants they play two major roles: light-harvesting and photoprotection. Their photoprotective ability requires a minimum of nine conjugated double bonds in their chemical structure (Krinsky and Johnson 2005). Photoprotection is achieved by deactivating excited singlet oxygen to yield the triplet carotenoid excited state and triplet oxygen in the ground-state, thus acting as a singlet oxygen quencher (Biesalski et al. 1996). The carotenoids are natural effective antioxidants because of their ability to scavenge and trap peroxyl radicals. It has been shown that a dietary mixture of β-carotene, lutein and lycopene, protects against UV-induced erythema (Heinrich et al. 2006; Sies and Stahl 2004). Darvin et al. (2011) have shown topical, systemic and combined antioxidant treatments induce statistically significant increases of antioxidant levels in human skin. Worthy to note is that due to blue light filtering, carotenoids are suitable components in a suncare formulation. Other secondary metabolites with the ability to scavenge free radicals and absorb UV radiation are the polyphenols. These form the bulk of plant extracts.

3.7   Plant extracts

Biological antioxidants can be categorized into two classes: enzymatic antioxidants that include superoxide dismutase, catalase and glutathione, and nonenzymatic antioxidants such as tocopherol, ascorbate and beta-carotene discussed earlier. Plants produce a variety of antioxidants against molecular damage from ROS. Phenolics comprise the major class of plant-derived antioxidants. Among the various phenolic compounds, flavonoids are perhaps most important group (Chen et al. 2008).

Flavonoids (or bioflavonoids) are a group of about 4000 naturally occurring compounds ubiquitous in all vascular plants. They are important for normal growth, development and defence of plants. Flavanoids found in several medicinal plant and herbal remedies have been used in folk medicine around the world. The use of plants containing flavonoids, either alone or in combination is popularised by consumer demand for compounds of natural origin. Attention has been given to dietary plants containing this class of molecules as natural cancer chemopreventive compounds (Ren et al. 2003). Very recently Vijayalakshmi et al. (2013) demonstrated that flavonoid possessed potent anticancer properties against breast cancer cells.

Besides scavenging UV-induced free radicals and inhibiting propagation of lipid peroxidative chain reactions, flavonoids provide a UV protective effect as therefore UV-absorbing organic molecules (Fent et al. 2010). Flavonoids are known to possess good anti-inflammatory activity both in humans and animals and recently their topical application has met considerable interest. For example a rutin derivative is known to prevent acute hind limb limphedema in rats, and hamamelis distillate has been shown to suppresses human UV radiation-induced erythema (Deters et al. 2001). Various other

flavonoids show good inhibitory activity against croton oil-induced mouse ear or paw oedema (Fent et al. 2010). Flavonoids are claimed to prevent photo-oxidative stress in skin. It is therefore important to investigate plant extracts containing these substances and associated physicochemical stability after inclusion in topical formulations. Several authors have demonstrated the antioxidant activity *in vitro* or *in vivo* of some plant extracts (Pulido et al. 2000; Sarla et al. 2011).

Topical administration of antioxidants has recently proved to represent a successful strategy for protecting the skin against UV-mediated oxidative damage (Coronado et al. 2008; Berne and Ros 1998). However, there is no data on the efficacy following inclusion in sunscreening preparations and the influence on the physicochemical stability of such a formulation. Despite the overwhelming evidence of the role of flavonoids in the protection of skin from oxidative injury, their antioxidative role in topical preparations remains subject to investigation. These tasks require a thorough screening of plants extracts for their photoprotective efficacy in sunscreen formulation.

Work on extracts of seeds of *Coffea arabica*, flower buds of *Syzygium aromaticum*, bark of *Cinnamomium burmanii* and leaf of *Ocimum tenuiflorum* showed good antioxidant properties and UV absorption capacity (Shekar et al. 2012). Other studies have shown that green and black tea polyphenols ameliorate adverse skin reactions following UV exposure (Anitha 2012). Recently *in vitro* and *in vivo* studies on *Garcinia brasiliensis* epicarp extract indicated a great potential for use of these extracts as a sunscreen additive for topical formulations when incorporated in UV filters (Figueiredo et al. 2014). Most importantly a biflavonoid fraction from *Araucaria angustifolia* needles has been shown to be an effective singlet oxygen ($^1O_2$) quencher. Thereby demonstrating potential to protect plasmid DNA against single strand break (ssb) caused by $^1O_2$ or Fenton reaction and to inhibit Fenton or UV radiation-induced lipoperoxidation in phosphatidylcholine liposomes (Yamaguchi et al. 2005). In an investigation by Violante et al. (2009) on photoprotection of the dry ethanolic extract of *L. pacari,* the extract showed wavelength of maximum absorption in UVB (315 nm) and extract of *O. hirsutissima* indicated an absorption maximum in the UVA region. However, these extracts presented sun protection factor (SPF) ≥ 2 and therefore considered not very good sun-protective agents on their own (Violante et al. 2009). Interestingly the *Polypodium leucotomos* extract as a component of sunscreen moistures has been shown to prevent photodecomposition of *trans*-urocanic acid (*t*-UCA), inhibit UV-induced deleterious effects of TiO_2 and to protect skin cells and endogenous molecules directly involved in skin immunosurveillance (Capote et al. 2006). The plant phytochemicals hesperetin and naringenin (flavonoids) have also been demonstrated to be potent topical photoprotective agents but their topical activity require optimization using suitable penetration enhancers (Saija et al. 1998).

The citrus and rosemary extracts have recently have been shown to have protective effects on UV-induced damage in the human skin. The authors speculated that combination of the extracts may have synergistic effects in decreasing UVB-induced intracellular ROS and preventing DNA damage. This group concluded that the combination of citrus and rosemary extracts may be suitable ingredients for oral photoprotection (Perez-Sanchez et al. 2014). Another study has also shown good correlation between SPF and phenolic contents (Ebrahimzadeh et al. 2014) though no correlations between SPF and flavonoid contents or antioxidant activity has so far been established. An earlier work from our laboratories had indicated that polyphenols have significant UV absorption and that polyphenols from *Sutherlandia frutescens* (cancer bush) may photostabilize BMDBM (Mturi 2005). From these findings it can be speculated that plant extracts can be used alone or as additives in other sunscreen formulations to enhance sunscreen product performance. Other organisms besides plants, also

generate metabolites that absorb in the UV range with promising stability. Amongst these are the fungal metabolites resembling amino acids.

3.8 Mycosporine-like amino acids

The generic name, mycosporine, is given to fungal metabolites absorbing at 310 nm or 320 nm formed by a cyclohexenone ring conjugated with a nitrogen substituent of an amino acid or amino alcohol. Mycosporine-like amino acids generally consist of an imine derivative mycosporine containing an amino cyclohexenimine chromophore (Conde et al. 2000). Mycosporine-like amino acids (MAAs) are UV-absorbing pigments. Structurally distinct MAAs have been identified in taxonomically diverse organisms (Matsui et al. 2011). They are biosynthesized via the shikimate pathway in a manner similar to the biosynthesis of UV-absorbing flavanoids in terrestrial plants discussed above. Only fungi and algae can synthesize MAAs. One adaptation of marine organisms to prevent UV-induced damage is to synthesize MAAs that strongly absorb within the UV region. MAAs, with maximum absorption around 310–360 nm, have been hypothesized to act as sunscreens and thus reduce the harmful effects of UV radiation (Carignan et al. 2009).

Their high absorptivity ranges from the mycosporine-glycine wavelength of absorption at 310 nm to palythene with a wavelength of absorption at 350 nm (Sinha et al. 2002). Oxocarbonyl-MAAs such as mycosporine–glycine and mycosporine–taurine, have reported antioxidant activity against cellular damage induced by high levels of ROS in organisms exposed to different oxidative stresses (Carignan et al. 2009). MAAs and scytonemin can be good candidates in UVA sunscreen formulations given their strong absorption in the UVA region. There is some evidence from cyanobacteria regarding the UV sunscreen role of mycosporine-like compounds (Garcia-Pichel et al. 1993). Indeed, the first claimed patent for the incorporation MAAs in personal care products was by Llewellyn and Galley (2002), they used mycosporine-2 glycine as a sunscreen in a cream formulation. Recently another cream comprising of MAAs has been claimed by the inventors to have good UV absorption and free radical scavenging abilities (Zhang et al. 2014). These preparations are, however, not featured prominently in the market to the best of our knowledge. There are also other compounds synthetic in nature though not light-absorbing but good free radical scavengers: hindered amine light stabilizers.

3.9 Hindered amine light stabilizers

Hindered amine light stabilizers (HALS) are usually derivatives of 2,2,6,6-tetramethylpiperidine (secondary and tertiary amines or amino ethers) (Geuskens and McFarlane 1999). They have been extensively employed to stabilize polymers and prevent photo-oxidation. Though, HALS, are effective in protection of surface coatings, they do not absorb UV light (Hodgson and Coote 2010). Hindered amines after transformation to the N-oxyl radical can quench the fluorescence of a chromophore by an intramolecular radiationless process. Paramagnetic N-oxyls are effective quenchers of excited singlet states of aromatic hydrocarbons by intermolecular electron-exchange interactions between the donor-aromatic hydrocarbon in the excited state and the N-oxyl radical in the ground state (Búcsiová et al. 2000). Nitroxides are extremely effective modulators of processes mediated by paramagnetic species, such as radicals and transition metals. The reaction of the N-oxyl radical with other radicals results in the formation of a non-photoactive diamagnetic product (Búcsiová et al. 2000). In biological systems it has been demonstrated that the nitroxide Tempol (a HALS) affords protection against UV radiation in a transgenic murine fibroblast culture model of cutaneous photoaging (Armeni et al. 2004). A proper investigation is required to evaluate their potential applicability in cosmetic products. But it is prudent to consider antioxidants, such as

nitroxides, as they may be useful additives in sunscreen formulations for protection against photo-carcinogenesis and photoaging in skin. However, other carrier systems need proper exploration especially in the possible role they could play as singlet and triplet quenchers. Such systems include the dendrimers discussed below.

3.10   Dendrimer-nanoparticle-incorporation

Dendrimers are highly branched, synthetic polymers with layered architectures that show promise in several biomedical applications. Dendrimers are core–shell nanostructures with precise architecture and low polydispersity; their molecular size and shape are controllable. Recent studies demonstrating their controllable properties, which include toxicity, crystallinity, structural flexibility pattern, size, chirality and biocompatibility, are important parameters influencing their application in biomedicine (Luo et al. 2011; Nanjwade et al. 2009). Dendrimers are composed of a core molecule, hyperbranches regularly extending outward, with terminal groups of defined molecular weight and size. Higher generation dendrimers take a spherical shape, and can encapsulate metal complexes, nanoparticles, or other inorganic and organic guest molecules (Astuc et al. 2010).

Noble metal nanoparticles exhibit a distinct absorption band within the UV-visible region known as the surface plasmon band. This is a property that may be utilized in the physical blocking of UV radiation if they are well dispersed on the surface of the skin. Dendrimers are well suited for hosting metal nanoparticles because dendrimer templates are fairly uniform in composition and structure and yield well defined nanoparticle replicas. Nanoparticles stabilized by encapsulation within dendrimers may not agglomerate (Liu and Fréchet 1999). Encapsulated nanoparticles are confined primarily by steric factors making the bulk of the surface available for localized surface plasmon resonance. Terminal groups on the dendrimer periphery can be tailored to control the solubility of the hybrid nanocomposites and used to anchor bioactive agents on the applied surface.

One very important aspect of dendrimers is their monodispersity. This ensures that the encapsulated guest does not agglomerate which occurs with most nanoparticles in biological systems. Dendritic encapsulation may allow isolation of active agents from, for instance, dermal contact. Most applications are achieved by drug molecules bonding covalently with functional groups on the dendrimer surface. It is claimed most dendrimers do not trigger the immune system when injected or used topically and exhibit very low cytotoxicity. The uniform size solubility controlled by the choice of modifiable surface group functionality (Lee et al. 2005), and available internal cavities make them suitable as nanoparticle carriers for sunscreen preparations.

Benzophenone derivatives and particularly BP3 is frequently used in sunscreen preparations. This agent is known to induce photosentization reactions in the excited state (Kumasaka et al. 2014). From fluorescence studies by Miura et al. (2007) for excited nano-incorporated stilbene; and benzophenone in a dendritic structure, they showed that singlet–singlet energy transfer (SSET) from the stilbene core to the benzophenone units can take place more efficiently in dendrimers. Another study targeting excited triplet state quenching of benzophenone indicated that there can be an efficient triplet-triplet energy transfer (TTET) from the benzophenone periphery to the stilbene core. This photochemical energy transfer results in the stilbene core isomerization subsequent to deactivation of benzophenone in the dendrimer shell (Miura et al. 2007). This showed benzophenone to be stabilized by this synergistic interaction co-hosted in the dendrimer structure. This incorporation of benzophenone in the dendritic structure may limit its possible permeation into viable tissues. Benzophenones and other

organic filters have also been intercalated in layered double hydroxides and have shown promising results.

3.12 Hydrotalcite sunscreen intercalation

Hydrotalcites (HTlc) are an uncommon type of lamellar solid bearing positively charged lamellae and exchangeable anions in the interlamellar region. They are represented by the general formula:

$$[M^{z+}_{1-x}M^{3+}(OH)_2]^{b+}[A^{n-}_{b/n}].mH_2O$$
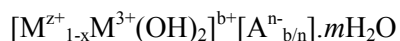
where M^{3+} can be Al, Cr, Fe, and M^{2+} can be Mg, Zn, Ni, Co; x ranges from 0.2 to 0.4. A^{n-} is an exchangeable inorganic or organic anion that compensates the positive charge of the layer, m are moles of solvent, usually co-intercalated water.

Most structures correspond to a natural hydrotalcite; magnesium–aluminum hydroxycarbonate; occurring in nature in foliated and knobby plates or fibrous masses. Its formula is $Mg_6Al_2(OH)_{16}CO_3 \cdot 4H_2O$; it exhibits a well-known CdI_2-type structure: hexagonal close-packing of hydroxyl ions, with all octahedral sites every two interlayers occupied by Mg^{2+} ions. Partial $Mg^{2+}:Al^{3+}$ substitution gives rise to positively charged layers, thus leading to location of anions in unoccupied interlayers. An intercalated anion can be replaced by another via an ion-exchange mechanism. Thus, the interlayer region of a lamellar host can be considered a micro-vessel where an anionic molecule may be stored (Caminade et al. 2005). By way of anion exchange or direct synthesis procedures capitalizing on the ease of "dissolution–reconstruction" of HTlc (Thomsen et al. 2006) it is possible to prepare intercalation compounds. A large variety of anionic species both inorganic and organic can be hosted. The guest species are protected from oxidation and UV radiation and their properties are modulated by guest–guest and host–guest interactions.

Intercalation of sunscreen agents in hydrotalcites has been attempted with positive results for instance the intercalation between UV absorber 5-benzoyl-4-hydroxy-2-methoxybenzenesulfonic acid (4BHF) and ZnAl-hydrotalcite lamellae was shown to greatly improve its photostability and SPF (Perioli et al. 2007; He et al. 2004). The photosensitizing effect of PABA was reported to be greatly reduced, and photoprotection range increased, when intercalated with the consequence that cutaneous reactions and allergy problems were shown to be eliminated (Perioli et al. 2006a). another organic UV filter, cinnamic acid and p-methoxycinnamic acid intercalated into Zn_2Al layered double hydroxides (Zn_2Al-LDHs) showed excellent UV absorption ability and very limited skin-sunscreen contact making them safe sunscreen materials (Sun et al. 2007). The intercalation of 2-phenyl-1H-benzimidazole-5-sulfonic acid in HTlc was shown to offer longer photoprotection efficacy, filter photostabilization and avoidance of a close contact between skin and filter, with consequent elimination of allergy problems and photocross reactions (Perioli et al. 2006b). The only task is to identify a suitable vehicle to carry it most likely a gel or even a lotion are preferred. A number of recent patents involving intercalation of UV absorbers include one by Matsufuji and Shimizu (2014), this authors claim their composite pigment can provide enhanced UV filtering effects low skin penetration, and optionally enhanced colouring effects. This was demonstrated that the intercalation enhances absorption of UVA and UVB of the sunscreen agent Tinosorb M in a formulation (Matsufuji et al. 2014). Hydrotalcites have advantage of ease of availability; and direct synthesis from soluble salts hence lower cost of production.

3.13   Conclusions

The photostability of a sunscreen formulation is not determined by the constituent UV absorbers alone. The photochemical interactions of individual UV absorbers with solvents, antioxidants, and other additives may significantly influence the products' photochemical response. A suitable cosmetic product presented either as an oil/water or water/oil emulsion in creams or in lotions should meet the minimum requirements of reducing/eliminating ROS generation and providing broad-spectrum UV protection. This review has discussed the means by which this can be achieved. The sunscreen absorbers can be encapsulated in SLN, HTLcs, and/or CDs in order to improve their efficacy. The incorporation sunscreens in dendrimer assemblies may prove a novel strategy for improving their photostability. Plant extract and antioxidant additions to the sunscreen formulation may also provide much better viable alternatives because apart from being synergistic UV absorbers, they may also scavenge UV-induced ROS.

References

Abarca JF, Casiccia CC (2002) Skin cancer and ultraviolet-B radiation under the Antarctic ozone hole: southern Chile, 1987–2000. Photodermatology, Photoimmunology and Photomedicine 18 (6):294-302

Al Shaal L, Shegokar R, Müller RH (2011) Production and characterization of antioxidant apigenin nanocrystals as a novel UV skin protective formulation. International journal of pharmaceutics 420 (1):133-140

Anitha T (2012) Medicinal plants used in protection. Asian Journal of Pharmaceutical and Clinical Research 5 (3):35-38

Armeni T, Damiani E, Battino M, Greci L, Principato G (2004) Lack of in vitro protection by a common sunscreen ingredient on UVA-induced cytotoxicity in keratinocytes. Toxicology 203 (1-3):165-178

Astuc D, Boisselier E, Omelas C (2010) Dendrimer designed for functions: from physical, photophysical and supramolecular properties to applications in sensing, catalysis, molecular electronics, photonics, and nanomedicine. Chemical Reviews 110:1857-1959

Atitaya S, Juwadee S, Atitaya S (2011) Particle size characterization of titanium dioxide in sunscreen products using sedimentation field-flow fractionation-inductively coupled plasma-mass spectrometry. Analytical and Bioanalytical Chemistry 399 (2):973-978

Azusa K, Nozomi O, Mikio Y (2009) Optical and Electron Paramagnetic Resonance Studies of the Excited States of 4-*tert*-Butyl-4'-Methoxydibenzoylmethane and 4-*tert*-Butyl-4'-Methoxydibenzoylpropane. Journal of Physical Chemistry 113:13492-13497

Berne B, Ros A-M (1998) 7 years experience of photopatch testing with sunscreen allergens in Sweden. Contact Dermatitis 38:61-64

Besaratinia A, Pfeifer GP (2008) Sunlight ultraviolet irradiation and BRAF V600 mutagenesis in human melanoma. Human Mutation 29 (8):983-991

Biesalski HK, Hemmes C, Hopfenmuller W, Schmid C, Gollnick HPM (1996) Effects of Controlled Exposure of Sunlight on Plasma and Skin Levels of β-Carotene. Free Radical Research 24 (3):215-224

Bowden GT (2004) Prevention of non-melanoma skin cancer by targeting ultraviolet-B-light signalling. Nature Reviews Cancer 4 (1):23-35

Búcsiová Lu, Chmela Š, Hrdlovič P (2000) Preparation, photochemical stability and photostabilising efficiency of adducts of pyrene and hindered amine stabilisers in iPP matrix. Polymer Degradation and Stability 71 (1):135-145

Caminade A-M, Laurent R, Majoral J-P (2005) Characterization of dendrimers. Advanced Drug Delivery Reviews 57 (15):2130-2146

Capote R, Alonso-Lebrero JL, Garcia F, Brieva A, Pivel JP, Gonzalez S (2006) Polypodium leucotomos extract inhibits trans-urocanic acid photoisomerization and photodecomposition. Journal of Photochemistry and Photobiology B: Biology 82 (3):173-179

Carignan MO, Cardozo KHM, Oliveira-Silva D, Colepicolo P, Carreto JI (2009) Palythine–threonine, a major novel mycosporine-like amino acid (MAA) isolated from the hermatypic coral Pocillopora capitata. Journal of Photochemistry and Photobiology B: Biology 94 (3):191-200

Carlotti ME, Sapino S, Vione D, Pelizzetti E, Ugazio E, Morel S (2005) Study on the Photostability of Octyl-p-Methoxy Cinnamate in SLN. Journal of Dispersion Science and Technology 26 (6):809-816

Chaudhuri R, Puccetti G, Marchio F, Lascu Z (2006) Methods for stabilizing ingredients within cosmetics, personal care and household products. US Patent US 07150876

Chawla HM, Mrig S (2009) Simultaneous quantitative estimation of oxybenzone and 2-ethylhexyl-4-methoxycinnamate in sunscreen formulations by second order derivative spectrophotometry. J Anal Chem 64 (6):585-592

Chen L-P, Hong S-G, Hou H-Q (2008) Theoretical Study on the Mechanism of Sonogashira Coupling Reaction. Chinese Journal of Structural Chemistry 27 (11):1404-1411

Chen L, Hu YJ, Wang QS (2012) The role of antioxidants in photoprotection: A critical review. Journal of American Academy of Dermatology 67:1013-1024

Conde FR, Churio MS, Previtali CM (2000) The photoprotector mechanism of mycosporine-like amino acids. Excited-state properties and photostability of porphyra-334 in aqueous solution. Journal of Photochemistry and Photobiology B: Biology 56 (2-3):139-144

Coronado M, De HH, Deng X, Rempel MA, Lavado R, Schlenk D (2008) Estrogenic activity and reproductive effects of the UV-filter oxybenzone (2-hydroxy-4-methoxyphenylmethanone) in fish. Aquatic Toxicology 90:182-187

Cross ES, Jiang R, Benson AEH, Roberts SM (2001) Can increasing the viscosity of formulations be used to reduce the human skin penetration of the sunscreen oxybenzone? The Journal of Investigative Dermatology 117 (1):147-150

Damiani E, Rosati L, Castagna R, Carloni P, Greci L (2006) Changes in ultraviolet absorbance and hence in protective efficacy against lipid peroxidation of organic sunscreens after UVA irradiation. Journal of Photochemistry and Photobiololgy B: Biology 82 (3):204-213

Darvin ME, Fluhr JW, Schanzer S, Richter H, Patzelt A, Meinke MC, Zastrow L, Golz K, Doucet O, Sterry W, Lademann J (2011) Dermal carotenoid level and kinetics after topical and systemic administration of antioxidants: Enrichment strategies in a controlled in vivo study. Journal of Dermatological Science 64 (1):53-58

De Fabo EC, Noonan FP, Fears T, Merlino G (2004) Ultraviolet B but not Ultraviolet A Radiation Initiates Melanoma. Cancer Research 64 (18):6372-6376

Deters A, Dauer A, Schnetz E, Fartasch M, Hensel A (2001) High molecular compounds (polysaccharides and proanthocyanidins) from Hamamelis virginiana bark: influence on human skin proliferation and differentiation and influence on irritated skin. Phytochemistry 58:949-958

Ebrahimzadeh MA, Enayatifard R, Khalili M, Ghaffarloo M, Saeedi M, Yazdani Charati J (2014) Correlation between Sun Protection Factor and Antioxidant Activity, Phenol and Flavonoid Contents of some Medicinal Plants. Iranian Journal of Pharmaceutical Research 13 (3):1041-1047

Felton LA, Wiley CJ, Godwin DA (2002) Influence of hydroxypropyl-beta-cyclodextrin on the transdermal permeation and skin accumulation of oxybenzone. Drug Development And Industrial Pharmacy 28 (9):1117-1124

Fent K, Zenker A, Rapp M (2010) Widespread occurrence of estrogenic UV-filters in aquatic ecosystems in Switzerland. Environmental Pollution 158:1817-1824

Figueiredo SA, Pinto Vilela FM, da Silva CA, Cunha TM, dos Santos MH, Vieira Fonseca MJ (2014) In vitro and in vivo photoprotective/photochemopreventive potential of Garcinia brasiliensis epicarp extract. Journal of Photochemistry and Photobiology B: Biology 131:65-73

Garcia-Pichel F, Wingard EC, Castebholz WR (1993) Evidence regarding the UV sunscreen role of a mycosporine-like in the cyanobacterium Gloeocapsa sp. Applied and Environmental Microbiology 59 (1):170-178

Gavin NM, Durako MJ (2011) Localization and antioxidant capacity of flavonoids from intertidal and subtidal *Halophila johnsonii* and *Halophila decipiens*. Aquatic Botany 95 (3):242-247

Geuskens G, McFarlane DM (1999) Study of some parameters responsible for the efficiency of hindered amine light stabilizers. Journal of Vinyl and Additive Technology 5 (4):186-194

Gonzalez H, Farbrot A, Larkö O, Wennberg AM (2006) Percutaneous absorption of the sunscreen benzophenone-3 after repeated whole-body applications, with and without ultraviolet irradiation. British Journal of Dermatology 154 (2):337-340

González S, Fernández-Lorente M, Gilaberte-Calzada Y (2008) The latest on skin photoprotection. Clinics in Dermatology 26 (6):614-626

Gordon DJ, Chu CA, Chu DM, Matherly C, Denison SM, Grune G, Clark CG (2005) Estrogenic potency of many popular sunscreens and it's "non-active" components detected using the lumi-cell ER bioassay. ISPAC-General, Dioxin 1145:2685-2689

Hanson KM, Gratton E, Bardeen CJ (2006) Sunscreen enhancement of UV-induced reactive oxygen species in the skin. Free Radical Biology and Medicine 41 (8):1205-1212

Hayden CGJ, Roberts MS, Benson HAE (1997) Systemic absorption of sunscreen after topical application. The Lancet 350 (9081):863-864

He Q, Yin S, Sato T (2004) Synthesis and photochemical properties of zinc–aluminum layered double hydroxide/organic UV ray absorbing molecule/silica nanocomposites. Journal of Physics and Chemistry of Solids 65 (2-3):395-402

Heinrich U, Tronnier H, Stahl W, Béjot M, Maurette JM (2006) Antioxidant Supplements Improve Parameters Related to Skin Structure in Humans. Skin Pharmacology and Physiology 19 (4):224-231

Herling T, Seilert M, Jung K (2013) Cerium dioxide: Future UV-filter in sunscreen. International Journal for Applied Science 139 (5):10-14

Hodgson JL, Coote ML (2010) Clarifying the Mechanism of the Denisov Cycle: How do Hindered Amine Light Stabilizers Protect Polymer Coatings from Photo-oxidative Degradation? Macromolecules 43 (10):4573-4583

Iannuccelli V, Sala N, Tursilli R, Coppi G, Scalia S (2006) Influence of liposphere preparation on butyl-methoxydibenzoylmethane photostability. Europen Journal of Pharmacutics and Biopharmaceutics 63 (2):140-145

Jain SK, Jain NK (2010) Multiparticulate carriers for sun-screening agents. International Journal of Cosmetic Science 32 (2):89-98

Jarry H, Christoffel J, Rimoldi G, Koch L, Wuttke W (2004) Multi-organic endocrine disrupting activity of the UV screen benzophenone 2 (BP2) in ovariectomized adult rats after 5 days treatment. Toxicology 205 (1–2):87-93

Jenning V, Gysler A, Schäfer-Korting M, Gohla SH (2000) Vitamin A loaded solid lipid nanoparticles for topical use: occlusive properties and drug targeting to the upper skin. European Journal of Pharmaceutics and Biopharmaceutics 49 (3):211-218

Jiang SJ, Chen JY, Lu ZF, Yao J, Che DF, Zhou XJ (2006) Biophysical and morphological changes in the stratum corneum lipids induced by UVB irradiation. Journal of Dermatological Science 44 (1):29-36

Kockler J, Oelgemoller M, Robertson S, Glass DB (2012) Photostabililty of sunscreens. Journal of Photochemistry and Photobiology C: Photochemistry Reviews 13:91-110

Krinsky NI, Johnson EJ (2005) Carotenoid actions and their relation to health and disease. Molecular Aspects of Medicine 26 (6):459-516

Kumasaka R, Kikuchi A, Yagi M (2014) Photoexcited States of UV Absorbers, Benzophenone Derivatives. Photochemistry and photobiology 90 (4):727-733

Kwok WM, Guan X, Chu LM, Tang W, Phillips DL (2008) Observation of Singlet Cycloreversion of Thymine Oxetanes by Direct Photolysis. Journal of Physical Chemistry B 112:11794-11797

Lautenschlager S, Wulf HC, Pittelkow MR (2007) Photoprotection. Lancet 370 (9586):528-537

Lee CC, MacKay JA, Fréchet JMJ, Szoka FC (2005) Designing dendrimers for biological applications. Nature Biotechnology 23 (12):1517-1526

Liu M, Fréchet JMJ (1999) Designing dendrimers for drug delivery. Pharmaceutical Science and Technology Today 2 (10):393-401

Llewellyn C, Galley E (2002) Personal care compositions containing mycosporine-like amino acids as sunscreens. WO2002039974A1,

Loftsson T, Masson M (2001) Cyclodextrins in topical drug formulations: theory and practice. International journal of pharmaceutics 225 (1–2):15-30

Luo K, Li C, Wang G, Nie Y, He B, Wu Y, Gu Z (2011) Peptide dendrimers as efficient and biocompatible gene delivery vectors: Synthesis and in vitro characterization. Journal of Controlled Release 155 (1):77-87

Mandawgade SD, Patravale VB (2008) Development of SLNs from natural lipids: Application to topical delivery of tretinoin. International journal of pharmaceutics 363 (1–2):132-138

Matsufuji S, Shimizu M (2014) Composite pigment and method for preparing the same. WO2014010101A1,

Matsufuji S, Shimizu M, Lalloret F, Willien M (2014) Composite pigment and method for preparing the same for cosmetic uses. WO2014010099A1,

Matsui K, Nazifi E, Kunita S, Wada N, Matsugo S, Sakamoto T (2011) Novel glycosylated mycosporine-like amino acids with radical scavenging activity from the cyanobacterium Nostoc commune. Journal of Photochemistry and Photobiology B: Biology 105 (1):81-89

Matsui MS, Hsia A, Miller JD, Hanneman K, Scull H, Cooper KD, Baron E (2009) Non-Sunscreen Photoprotection: Antioxidants Add Value to a Sunscreen. Journal of Investigative Dermatology Sympossium Proceedings 14 (1):56-59

Meinke MC, Darvin ME, Vollert H, Lademann J (2010) Bioavailability of natural carotenoids in human skin compared to blood. European Journal of Pharmaceutics and Biopharmaceutics 76 (2):269-274

Mestres JP, Duracher L, Baux C, Vian L, Marti-Mestres G (2010) Benzophenone-3 entrapped in solid lipid microspheres: formulation and in vitro skin evaluation. International journal of pharmaceutics 400 (1-2):1-7

Miura Y, Momotake A, Shinohara Y, Wahadoszamen M, Nishimura Y, Arai T (2007) The first observation of the effect of dendritic structure to produce the triplet excited state of the core stilbene by dendron excitation. Tetrahedron Letters 48 (4):639-641

Morabito K, Shapley NC, Steeley KG, Tripathi A (2011) Review of sunscreen and the emergence of non-conventional absorbers and their applications in ultraviolet protection. International Journal of Cosmetic Science 33 (5):385-390

Mturi GJ, Martincigh BS (2008) Photostability of the sunscreening agent 4-*tert*-butyl-4'-methoxydibenzoylmethane (avobenzone) in solvents of different polarity and proticity Journal of Photochemistry and Photobiology A: Chemistry 200:410-420

Mturi JG (2005) An investigation of the photostabilisation of the sunscreen absorbers by plant polyphenols. MSc. Dissertation, University of KwaZulu-Natal, Durban, South Africa

Mueller RH, Radtke M, Wissing SA (2002) Solid lipid nanoparticles (SLN) and nanostructured lipid carriers (NLC) in cosmetic and dermatological preparations. Advanced Drug Delivery Reviews 54 (Suppl. 1):S131-S155

Müller RH, Mäder K, Gohla S (2000) Solid lipid nanoparticles (SLN) for controlled drug delivery – a review of the state of the art. European Journal of Pharmaceutics and Biopharmaceutics 50 (1):161-177

Müller RH, Radtke M, Wissing SA (2002) Solid lipid nanoparticles (SLN) and nanostructured lipid carriers (NLC) in cosmetic and dermatological preparations. Advanced Drug Delivery Reviews 54, Supplement (0):S131-S155

Nanjwade BK, Bechra HM, Derkar GK, Manvi FV, Nanjwade VK (2009) Dendrimers: emerging polymers for drug-delivery systems. European Journal of Pharmaceutical Sciences 38 (3):185-196

Nesseem D (2011) Formulation of sunscreens with enhancement sun protection factor response based on solid lipid nanoparticles. International Journal of Cosmetic Science 33 (1):70-79

Pardeike J, Hommoss A, Muller RH (2009) Lipid nanoparticles (SLN, NLC) in cosmetic and pharmaceutical dermal products. International journal of pharmaceutics 366 (1-2):170-184

Perez-Sanchez A, Barrajon-Catalan E, Caturla N, Castillo J, Benavente-Garcia O, Alcaraz M, Micol V (2014) Protective effects of citrus and rosemary extracts on UV-induced damage in skin cell model and human volunteers. Journal of Photochemistry and Photobiology B: Biology 136:12-18

Perioli L, Ambrogi V, Bertini B, Ricci M, Nocchetti M, Latterini L, Rossi C (2006a) Anionic clays for sunscreen agent safe use: photoprotection, photostability and prevention of their skin penetration. European Journal of Pharmaceutics and Biopharmaceutics 62 (2):185-193

Perioli L, Ambrogi V, Rossi C, Latterini L, Nocchetti M, Costantino U (2006b) Use of anionic clays for photoprotection and sunscreen photostability: Hydrotalcites and phenylbenzimidazole sulfonic acid. Journal of Physics and Chemistry of Solids 67 (5-6):1079-1083

Perioli L, Nocchetti M, Ambrogi V, Latterini L, Rossi C, Costantino U (2007) Sunscreen immobilization on ZnAl-hydrotalcite for new cosmetic formulations. Microporous Mesoporous Materials 107 (1-2):180-189

Perugini P, Simeoni S, Scalia S, Genta I, Modena T, Conti B, Pavanetto F (2002) Effect of nanoparticle encapsulation on the photostability of the sunscreen agent, 2-ethylhexyl methoxycinnamate. International journal of pharmaceutics 246:37-45

Pulido R, Bravo L, Saura-Calixto F (2000) Antioxidant activity of dietary polyphenols as determined by a modified ferric reducing/antioxidant power assay. Journal of Agricultural and Food Chemistry 48 (8):3396-3402

Puri D, Bhandari A, Sharma P, Choudhary D (2010) Lipid nanoparticles (SLN, NLC): A novel approach for cosmetic and dermal pharmaceutical. Journal of Global Pharma Technology 2 (5):1-15

Ren W, Qiao Z, Wang H, Zhu L, Zhang L (2003) Flavonoids: Promising anticancer agents. Medicinal research reviews 23 (4):519-534

Rogiers V, Sanner T, White IR, Engelen vJ, Revuz J, Rastogi SC, Platzek T, Marty JP, Liden C, Kapoulas V, Jazwiec-Kanyion B, Degen G, Chambers C (2006) Opinion on Benzophenone-3. S38, vol 1069. European Commission: Health and Consumer Protection Directorate-General, Brussels

Saija A, Tomaino A, Trombetta D, Giacchi M, De Pasquale A, Bonina F (1998) Influence of different penetration enhancers on in vitro skin permeation and in vivo photoprotective effect of flavonoids. International journal of pharmaceutics 175:85-94

Santo S, Mezzena M (2010) Photostabilisation Effect of Quercetin on the UV Filter Combination, Butyl Methoxydibenzoylmethane-Octyl Methoxycinnamate. Photochemistry and photobiology 86:273-278

Sarla S, Prakash MA, Apeksha R, Subhash C (2011) Free Radical Scavenging (DPPH) and Ferric Reducing Ability (FRAP) of *Aphanamixis polystachya* (Wall) Parker. International Journal of Drug Development and Research 3 (4):271 - 274

Scalia S, Tursilli R, Bianchi A, Nostro PL, Bocci E, Ridi F, Baglioni P (2006) Incorporation of the sunscreen agent, octyl methoxycinnamate in a cellulosic fabric grafted with β-cyclodextrin. International journal of pharmaceutics 308 (1–2):155-159

Scalia S, Tursilli R, Iannuccelli V (2007) Complexation of the sunscreen agent, 4-methylbenzylidene camphor with cyclodextrins: Effect on photostability and human stratum corneum penetration. Journal of pharmaceutical and biomedical analysis 44 (1):29-34

Scalia S, Villani S, Scatturin A, Vandelli MA, Forni F (1998) Complexation of the sunscreen agent, butyl-methoxydibenzoylmethane, with hydroxypropyl-b-cyclodextrin. International journal of pharmaceutics 175:205-213

Schlecht C, Klammer H, Jarry H, Wuttke W (2004) Effects of estradiol, benzophenone-2 and benzophenone-3 on the expression pattern of the estrogen receptors (ER) alpha and beta, the estrogen receptor-related receptor 1 (ERR1) and the aryl hydrocarbon receptor (AhR) in adult ovariectomized rats. Toxicology 205 (1–2):123-130

Schlumpf M, Schmid P, Durrer S, Conscience M, Maerkel K, Henseler M, Gruetter M, Herzog I, Reolon S, Ceccatelli R, Faass O, Stutz E, Jarry H, Wuttke W, Lichtensteiger W (2004) Endocrine activity and developmental toxicity of cosmetic UV filters—an update. Toxicology 205 (1–2):113-122

Setlow RB, Grist E, Thompson K, Woodhead AD (1993) Wavelengths effective in induction of malignant-melanoma. Proceedings of the National Academy of Sciences of the United States of America 90 (14):6666-6670

Shaath NA (2010) Ultraviolet filters. Photochemistry and Photobiological Sciences 9 (4):464-469

Shekar M, Shetty S, Lekha G, Mohan K (2012) Evaluation of in vitro antioxidant property and radio protective effect of the constituent medicinal plants of Herbal sunscreen formulation. International Journal of Pharmaceutical Frontier Research 2 (2):90-96

Sies H, Stahl W (2004) Carotenoids and UV protection. Photochemical and Photobiological Sciences 3 (8):749-752

Simeoni S, Scalia S, Benson HAE (2004) Influence of cyclodextrins on in vitro human skin absorption of the sunscreen, butyl-methoxydibenzoylmethane. International journal of pharmaceutics 280 (1–2):163-171

Sinha RP, Sinha JP, Groniger A, Hader DP (2002) Polychromatic action spectrum for the induction of a mycosporine-like amino acid in a rice-field cyanobacterium, Anabaena sp. Journal of Photochemistry and Photobiology B: Biology 66 (1):47-53

Sklar LR, Almutawa F, Lim HW, Hamzavi I (2013) Effects of ultraviolet radiation, visible light, and infrared radiation on erythema and pigmentation: a review. Photochemical and Photobiological Sciences 12 (1):54-64

Sun W, He Q, Luo Y (2007) Synthesis and properties of cinnamic acid series organic UV ray absorbents–interleaved layered double hydroxides. Materials Letters 61 (8-9):1881-1884

Szejtli J (1998) Introduction and General Overview of Cyclodextrin Chemistry. Chemical Reviews 98 (5):1743-1754

Szejtli J (2004) past, present and future of cyclodextrins. Pure Applied Chemistry 76 (10):1825-1845

Thomsen V, Schatzlein D, Mercuro D (2006) Interelement corrections in spectrochemistry. Spectroscopy 21:32,34-38,40

van der Leun JC, de Gruijl FR (2002) Climate change and skin cancer. Photochemical & Photobiological Sciences 1 (5):324-326

Vijayalakshmi A, Kumar PR, Sakthi Priyadarsini S, Meenaxshi C (2013) In Vitro Antioxidant and Anticancer Activity of Flavonoid Fraction from the Aerial Parts of Cissus quadrangularis Linn. against Human Breast Carcinoma Cell Lines. Journal of Chemistry 2013:1-9

Villalobos-Hernández JR, Müller-Goymann CC (2005) Novel nanoparticulate carrier system based on carnauba wax and decyl oleate for the dispersion of inorganic sunscreens in aqueous media. European Journal of Pharmaceutics and Biopharmaceutics 60 (1):113-122

Violante MPI, Souza MI, Venturini LC, Ramalho FSA, Santos ANR, Ferrari M (2009) Avaliacao in vitro da atividade fotoprotetora de extratos vegetais do cerrado de Mato Grosso. Brazilian Journal of Pharmacognosy 19 (2A):452-457

Vyas A, Saraf S, Saraf S (2008) Cyclodextrin based novel drug delivery systems. J Incl Phenom Macrocycl Chem 62 (1-2):23-42

Wang SQ, Osterwalder U, Jung K (2011) Ex vivo evaluation of radical sun protection factor in popular sunscreens with antioxidants. Journal of the American Academy of Dermatology 65 (3):525-530

Wang SQ, Setlow R, Berwick M, Polsky D, Marghoob AA, Kopf AW, Bart RS (2001) Ultraviolet A and melanoma: a review. Journal of American Academy of Dermatology 44 (5):837-846

Wang SQ, Stanfield JW, Osterwalder U (2008) In vitro assessments of UVA protection by popular sunscreens available in the United States. Journal of the American Academy of Dermatology 59 (6):934-942

Wissing SA, Müller RH (2001) A novel sunscreen system based on tocopherol acetate incorporated into solid lipid nanoparticles. International Journal of Cosmetic Science 23 (4):233-243

Wissing SA, Müller RH (2002a) The development of an improved carrier system for sunscreen formulations based on crystalline lipid nanoparticles. International journal of pharmaceutics 242 (1–2):373-375

Wissing SA, Müller RH (2002b) Solid lipid nanoparticles as carrier for sunscreens: in vitro release and in vivo skin penetration. Journal of Controlled Release 81 (3):225-233

Wu Y, Matsui MS, Chen JZS, Jin X, Shu CM, Jin GY, Dong GH, Wang YK, Gao XH, Chen HD, Li YH (2011) Antioxidants add protection to a broad-spectrum sunscreen. Clinical and Experimental Dermatology 36 (2):178-187

Yamaguchi LF, Vassao DG, Kato MJ, Di Mascio P (2005) Biflavonoids from Brazilian pine Araucaria angustifolia as potentials protective agents against DNA damage and lipoperoxidation. Phytochemistry 66 (18):2238-2247

Yener G, Incegul T, Yener N (2003) Importance of using solid lipid microspheres as carriers for UV filters on the example octyl methoxy cinnamate. International journal of pharmaceutics 258 (1-2):203-207

Zhang C, Miao Z, Wu H, Chen L, Zhu Y, Chen D, Wu W (2014) Multi-efficacy sunscreen cream containing sargassum polysaccharide, mycosporine-like amino acid and sargassum polyphenol with good ultraviolet absorption and free radical scavenging abilities, and application thereof. CN103720625A,

Chapter Four

The photostability of sunscreens in skin-lightening formulations in the South African market

Moses A. Ollengo and Bice S. Martincigh[*]

School of Chemistry and Physics, University of KwaZulu-Natal, Westville Campus, Private Bag X54001, Durban 4000, South Africa

*Corresponding author: Tel.:+27-31-2601394; Fax: +27-31-2603091; E-mail address: martinci@ukzn.ac.za

Abstract

The photochemical stability of common sunscreens in skin-lightening preparations was investigated in order to assess the products' efficacy in photoprotection. The percentage composition of the organic absorbers was determined by use of reversed-phase-HPLC. The physical absorber, titanium dioxide, was quantitated by means of ICP-OES. The percentage compositions of most UV filters were found within the set maximum allowed limits of the various health regulatory bodies. The amounts of most of the sunscreen agents in the skin-lightening preparation were very low and no percentage composition was indicated on the product packages for comparison. Such low amounts may not be sufficient to offer any significant photoprotection. The photostability experiments were performed by application of a thin layer of the product on a quartz plate and exposing it to sunlight. The application density was kept at ~ 1.0 mg cm^{-2}. The spectral transmission measurements were recorded on a UV-vis spectrophotometer after every hour of exposure for a total duration of five to seven hours. Skin-lightening preparations with sunscreens but without plant extracts showed an increase in transmittance with increasing exposure to solar irradiation. This photo-instability is due to degradation and photoisomerisation of the UV absorbers. However, skin-lightening products that contained plant extracts together with sunscreens showed a drop in transmittance in the long wavelength region. The effect could be associated with the formation of highly conjugated photoproducts hence the high long wavelength absorption. We conclude that inclusion of plant extracts in the skin-lightening preparations is likely to photostabilize the sunscreen absorbers. Thus, the photoprotection offered is likely to be enhanced but further investigation and profiling of the photo-toxicities of the photochemical products formed needs to be performed.

Keywords: Sunscreens, skin-lighteners, photostability, plant extracts.

4.1 Introduction

Skin-lightening is widely practiced worldwide but more so in sub-Saharan Africa, Asia and the Middle East. It involves the use of chemical substances in an attempt to lighten skin tone or provide an even skin complexion. These chemicals reduce the concentration of melanin, the pigment responsible for skin colour. Several cosmetic preparations have been shown to be effective in skin-lightening, while some have been proved to be toxic or have debateable safety profiles, in certain ethnic groups. Some of these cosmetic preparations are used for medical reasons especially in depigmenting specific zones on the skin with abnormally high pigmentation such as moles and birthmarks. Another medical condition of interest is vitiligo in which case the unaffected skin may be lightened to achieve a more uniform appearance. However, a prolonged use of skin-lightening agents has been associated with increase in pigmentation in the joints of the fingers, toes, buttocks and ears. It is observed that the skin of the face may become thinned and the area around the eyes may have increased pigmentation causing a 'bleach panda effect' (Olumide 2010).

Melanin, the primary determinant of skin, hair, and eye colour plays a critical role in photoprotection due to its ability to absorb ultraviolet (UV) radiation (Lin and Fisher 2007; Costin and Hearing 2007). Melanin is synthesised in the body via a process referred to as melanogenesis (Fig. 4.1). Melanogenesis is a complex enzyme-controlled process, which when disturbed gives rise to various types of pigmentation defects, which are classified as hypo or hyperpigmentation and the occurrence of these defects is independent of the number of melanocytes (Fistarol and Itin 2010; Lin and Fisher 2007; Park et al. 2009). Most skin-lightening agents reduce the amount of melanin formation by inhibiting tyrosinase. Tyrosinase is the rate-limiting enzyme for the synthesis of melanin (Chang 2012), thus inhibiting its formation inhibits melanogenesis.
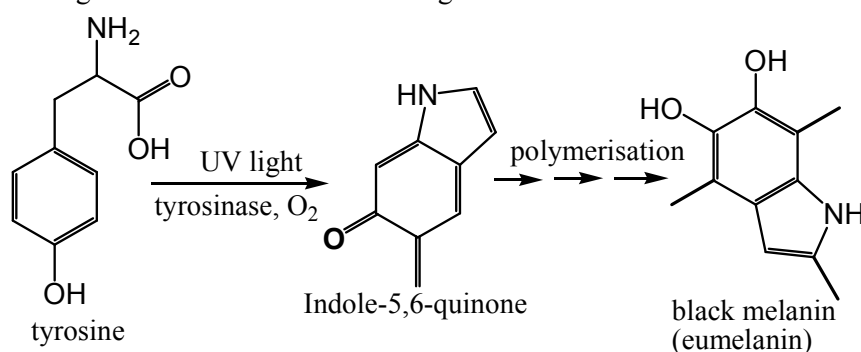
Figure 4.5: Tyrosinase controlled melanogenesis for the formation of eumelanin.

There are several topical cosmetic or medically prescribed chemicals that inhibit melanin formation. For instance tretinoin has been shown to be effective in treating skin discolouration (Bhawan 1996). Users of tretinoin have to avoid sunlight, because it makes the skin more sensitive to UVA (320-400 nm) and UVB (290-320 nm) radiation. A common skin-lightener is hydroquinone. This is medically regarded as the primary topical ingredient for inhibiting melanin production (Ball Arefiev and Hantash 2012; Musashi et al. 2009; Dadzie and Petit 2009). Hydroquinone lightens the skin by disrupting the synthesis and production of melanin hyperpigmentation. It has been banned in some countries because of fears of a cancer risk (Dadzie and Petit 2009). Active compounds isolated from plants, such as arbutin, aloesin, gentisic acid, flavonoids, hesperidin, licorice (specifically glabridin), niacinamide, yeast derivatives, and polyphenols, inhibit melanogenesis without melanocytotoxicity by different mechanisms (Zhu and Gao 2008). The plant extracts that have been shown to contain arbutin are: *Broussonetia papyrifera* (paper mulberry), *Uva ursi* (bearberry), *Mitracarpus scaber* extract, extract, *Morus bombycis* (mulberry), and *Morus alba* (white mulberry). These plant extracts

are considered safe alternatives and are commonly used as depigmenting agents to make the skin fairer. These arbutin is a form of hydroquinone which has been shown to be an efficient skin-lightening agent (Jun et al. 2008).

Other agents of botanical origin include kojic acid, which has been shown to be effective for inhibiting melanin production (Moon et al. 2001) but photo-unstable in cosmetic preparations. It is thought to cause allergic contact dermatitis (Serra-Baldrich et al. 1998) and skin irritation. Azelaic acid has been shown to be effective for skin discolourations (Baliña and Graupe 1991) as well as inhibiting melanin production (Rendon et al. 2006). Glutathione is an antioxidant that inhibits melanin synthesis by quenching of free radicals and peroxides that contribute to tyrosinase activation and melanin formation. The alpha hydroxy acids (AHAs): lactic acid and glycolic acid, have also been shown to inhibit melanin production apart from their actions as exfoliants on skin.

Medically prescribed skin-lightening agents of synthetic origin are monobenzone and mequinol. It is reported that monobenzone may cause destruction of melanocytes and permanent depigmentation. Hence, monobenzone is not recommended for skin conditions other than vitiligo but some users abuse it. The overall effect of the skin-lightening agents on the skin is the destruction of the natural defence system against UV radiation. In some cases the skin structure is also destroyed making such a skin vulnerable to the assaults of UVB and UVA radiation. Therefore, the skin needs photoprotection and that is why most of the skin-lightening preparations should incorporate sunscreens.

Sunscreens (both organic and physical) are compounds that absorb or reflect UV radiation and thereby prevent or minimize the deleterious effects of the solar radiation on the skin. However, some of the chemical absorbers photo-degrade and the subsequent photo-loss reduces the photoprotection. The photoinstability of these agents is more pronounced in the UVA region. The other concern is the safety of these products as the toxicities of the resulting photoproducts are unknown. Some of the agents have been shown to form photoproducts that may be harmful to the homeostasis of the skin (Schallreuter et al. 1996). It is therefore of interest to assess the photostabilities of these products and the quantities of the active ingredients in the final commercial products.

The aim of the present work was to investigate the photostability of sunscreens in skin-lightening and suncare products containing plant extracts. The target is to establish their robustness on long time sun exposure and suitability for outdoor activity users. The specific objectives were to firstly quantify the amounts of the UV absorbers in the cosmetic preparations. The amounts of these agents in these cosmetic agents are of concern as they may help in mapping some of observed dermal effects associated with skin-lightening preparations. The Second objective was to examine the photostabilities, of the products upon solar exposure. For most skin-lightening preparations there are no amounts of sunscreens indicated on the packages of the products. Also, no report exists on the levels of the sun-screening agents in these skin-lightening preparations and their effectiveness. To the best of our knowledge this is the first report of the amounts of sun-active agents in skin-lightening preparations. The analysis of these agents in commercial products is important for quality control and for monitoring the observance of the existing legislation.

4.2 Materials and Methods

4.2.1 Reagents

The sunscreens 2-ethylhexyl-p-methoxycinnamate (EHMC), benzophenone-3 (BP3), 4-*tert*-butyl-4'-methoxy-dibenzylmethane (BMBDM), was purchased from BASF, and 1-phenyl-1-pentanone (valerophenone) (99.8%) was purchased from Sigma-Aldrich, dodecane (99.9 %) was bought from Fluka Chemie, acetone (99.8 %) was from Riedel-de Haen. HPLC grade methanol and acetonitrile was purchased from BDH HiperSolv^{TM} Chemicals, Ltd. Sulphuric acid (H_2SO_4) and potassium hydrogen sulphate ($KHSO_4$) were purchased from BDH Chemicals Ltd. Ultra-pure water was freshly dispensed from a Milli-Q$^®$ water purification system (Millipore, Bedford, MA, USA) for each day of analysis. Titanium dioxide (TiO_2) was from SAARCHEM Pty Ltd. Twelve skin-lightening products containing UV filters were purchased from the retail store in Durban South Africa.

4.2.2 Preparation of solutions

4.2.2.1 Standard solutions

All stock standard solutions of the three organic UV absorbers were prepared fresh each day of analysis. Stock solutions of EHMC, BP3 and BMDBM were prepared by dissolving 32.5-40 mg in 20 mL of methanol, and ultrasonicated for 1 hour and then diluted to 25 mL with methanol in a volumetric flask. For the purposes of determining the linearity range, working standard solutions were prepared in the concentration range of 4.37–273 μM for BMDBM, 3.12–499 μM for BP3, and 4.86–778 μM for EHMC.

4.2.2.2 Sample preparation

The analysis of EHMC, BP3, and BMDBM in the skin-lightening samples was performed by dissolving ~ 150 mg of the samples in 30 mL of methanol, ultrasonicated in a water-bath for 1 hour and then diluted to 100 mL volume in a standard flask with methanol. Working solutions were then prepared from this stock solution by imposing a tenfold dilution factor to achieve an approximate UV filter content of about 10-200 μM or more. The prepared solutions were filtered through 0.45 μm Millex LCR syringe filters prior to injection into the HPLC system.

4.2.3 High performance liquid chromatographic analysis

The HPLC system consisted of a solvent delivery pump (Waters 600), an auto sampler (Perkin Elmer 200 series), a photodiode array detector (Waters 996) and chromatography software (Millennium version 2.10 from Waters, Milford, MA, USA). The analysis of EHMC, BMDBM, and BP3 was performed under isocratic elution with methanol–water (84:16, v/v) at a flow rate of 1 mL min^{-1} on a reversed phase C-12 column (Phenomenex Synergi 4μ Max-RP 80 Å, 150 mm x 4.6 mm). A 20 μL aliquot of the sample was injected on the column. The mobile phase was auto-degassed with helium at a rate of 30 mL min^{-1} continually during each run. The chromatograms were recorded at 286, 310, and 358 nm. The isocratic elution run time was set for 15 min.

4.2.4 Validation of Analytical method

The method validation experiments were performed by spiking ~150 mg of three pre-analysed commercial sunscreen products with 9-10 mg of the pure sunscreen absorbers. The spiked samples were dissolved in methanol and made up in the same way as described in Section 4.2.2.2. The

solutions were filtered through a 0.45 μm Millex LCR syringe filter before a further dilution was made to achieve a final concentration of ~80-200 μM by using the auto-sampler. The prepared solutions were subjected to the same chromatographic conditions as described in Section 4.2.3. The linearity of the employed method was determined by using a five point external calibration method. The regression equations were obtained through un-weighted least squares linear regression analysis, by using the peak areas as a function of concentration. In order to assess the repeatability of the analytical procedure, an intra-day and inter-day analysis was performed by injecting authentic standard solutions onto the chromatograph. The amounts of each standard were then computed by using the calibration curves. Each experiment was repeated three times. The analysis of TiO2 and the corresponding results are described in Chapter Six.

4.2.5   Photostability experiments

All the photostability studies were done on a clear sunny day. The windy conditions were avoided to minimize aerosol accumulation on the quartz plates which greatly interferes with the spectral transmittance of the applied sample. The accumulation of aerosols on the quartz plates carrying the sample causes scattering of light which was found to distort the spectral characteristics of the applied sample. The products surface application density of ~ 1.0 mg cm^{-2} was used; the ideal recommended application density is 2 mg cm^{-2} for children and 1.5 mg cm^{-2} for adults (Maier et al. 2001). However, in practice consumers apply much less than the recommended value for aesthetic reasons. The products were applied on a quartz plate by using a gloved finger saturated with the product. To achieve a uniform thin film the finger was moved in a circular fashion outward from the center. The quartz plates were allowed to dry in the dark, reweighed and then exposed to sunlight. The spectral changes were recorded every hour on a Perkin Elmer Lambda 35 UV-vis dual beam spectrophotometer for a total duration five to seven hours.

4.2.7.1   Actinometric studies

To determine the amount of UV radiation falling on the quartz plates and therefore interacting with the applied sunscreen absorbers, the decrease in the concentration of the chemical actinometer valerophenone, with time was used. It is known that valerophenone undergoes a Norrish Type II photodegradation reaction with quantum yield close to unity. It is reported that the valerophenone photoreaction has a quantum yield (Φ) in aqueous solution of (290-330 nm) 0.98 ± 0.04 (Klan et al. 2000). Therefore, the actinic flux incident on the applied sunscreen absorbers was calculated by assuming a quantum yield of 0.98. The UV dose received by the absorbers was then calculated and expressed as the standard erythemal dose (SED). The SED corresponds to 100 J m^{-2} (Lucas et al. 2006) weighted at 297 nm, this is deemed representative of the *in vivo* solar UV dose received because it is independent of the skin type unlike the minimal erythemal dose (MED – 200 J m^{-2}) (Zepp et al. 1998; Stalgis-Bilinski et al. 2011; Lucas et al. 2006) that causes reddening of the skin.

The reduction in the concentration of valerophenone with irradiation time was followed by means of gas chromatography-flame ionisation detection (GC-FID). To improve the precision and accuracy of the actinometric data of the GC quantitative analysis an internal standard that does not undergo photoreaction under the current experimental conditions was used. The internal standard used in this work was a straight chain alkane; dodecane. A mass of 16.55 mg of valerophenone and 17.37 mg of dodecane was dissolved in acetone and made up to 100 mL to make 1.02×10^{-3} mol dm^{-3} of solution of each in the same standard flask. The high concentration of valerophenone used in this work was

aimed at making the valerophenone photodegradation kinetics approximately zero order. Zero order reactions are independent of the concentration of the reactants.

A fixed volume (3 mL) of the prepared solution was accurately pipetted and transferred in a 1 cm pathlength quartz cuvette. The tightly sealed cuvette was then placed in ice in a petri-dish to avoid possible evaporation during sun exposure. The petri-dish and its contents were placed in a specially cut out trough at the centre of the eight quartz plate troughs containing the quartz plates with applied sunscreen products (Fig. 4.2). Fresh actinometric solution was pipetted and exposed for every hour of exposure of the skin-lightening product. After which a 1 µL of this solution was injected into the GC-FID chromatograph to monitor the remaining concentration of valerophenone.

The GC-FID used was a Shimadzu GC-2010, fitted with auto-sampler AOC 20i and a flow unit type AFC-2010. A SGE BP X5 (5% phenylpolysilphenylene-siloxane) capillary column of length 30 m, internal diameter 0.25 mm and film thickness 0.25 µm was used. The make-up gas was nitrogen/air flowing at 30 mL min^{-1}, the carrier gas was hydrogen gas at a flow rate of 47 mL min^{-1} and air flowing at 400 mL min^{-1}. The injection port was set at 250 °C and the oven temperature program was 80 °C held for 2 min then increased at 20 °C min^{-1} to 230 ºC and held there for 2 min. The detector temperature was 280 °C and the auto-sampler was set to inject a volume of 1 µL in splitless mode. The velocity flow control mode was adopted keeping the pressure at 80.7 kPa, the total flow rate at 5.0 mL min^{-1}, the column flow of 0.90 mL min^{-1}, and a linear velocity of 25.3 mL s^{-1}.

Figure 4.6: Experimental set-up for the actinometric measurements and photostability studies.

To minimise detector response and sensitivity variability a relative response factor (RRF) was calculated every day as follows:

$$RRF = \frac{M_{dodecane} \times S_{valerophenone}}{M_{valerophenone} \times S_{dodecane}}$$

Where $M_{valerophenone}$ and $M_{dodecane}$ are the masses of valerophenone and dodecane respectively, and $S_{valerophenone}$ and $S_{dodecane}$ are the GC signals (peak areas) of valerophenone and dodecane respectively. The RRF was firstly determined and used in the determination of the amount of valerophenone

remaining after each exposure time. A plot of concentration against the time yields a linear curve. The slopes of the hourly plots were used to determine the irradiance incident on the samples for each hour and time of the day. The total irradiance of each experimental day was also determined.

4.2.7.2   Actinometric data analysis

The slope k_0 (mol L^{-1} s^{-1}) from the valerophenone concentration vs time curve and the quantum yield, Φ (0.98) were used to calculate the incident solar intensity, I_0 (einstein L^{-1} s^{-1}), for the photo-degradation of valerophenone.

$$I_0 = \frac{k_0}{\Phi}$$

since I_0 is the rate at which the photons of light are falling on the actinometric solution. It can be shown that the total photon flux, F_0 (W m^{-2}) can be computed from the expression

$$F_0 = \frac{I_0 V N_A E_\lambda}{A}$$

where F_0 is the photon flux, V is the volume (dm^3), and A is the area (m^2) of the exposed actinometric solution, N_A is Avogadro's number of particles; E_λ (Joule photon^{-1}) is the energy of photon of wavelength λ. The energy of a photon can be obtained from the relation

$$E_\lambda = \frac{hc}{\lambda}$$

where h is the Planck's constant (6.626 × 10^{-34} m^2 kg s^{-1}) and c is the speed of light (3.0 x 10^8 m s^{-1}) and λ is the average wavelength over which the actinometric measurements are made; 290-330 nm for this particular experiment

The SED (J m^{-2}) value for each hour of irradiation was then calculated as a product of irradiation time in seconds, T and F_0 divided by 100.

$$SED = \frac{F_0 T}{100}$$

4.3   Results

It was of interest to quantify the active sunscreen ingredients in the skin-lightening products and then to determine the photostability of these products. The skin-lightening preparations contained one or more of the three organic sunscreen absorbers, namely EHMC, BP3 and BMDBM, and the physical absorber TiO$_2$. Some preparations did not include sunscreen absorbers among the list of ingredients on the product label. Moreover, even those that listed the sunscreening agents on the product label none indicated the amount of the absorbers incorporated.

4.3.1   Levels of sunscreen agents in skin-lightening products

The chromatographic detection and quantitation of the UV filters was done at the wavelength of maximum absorption of each UV filter. Identification of each UV absorber was done by comparison of its retention time and UV spectrum with those of known standards. A typical chromatogram of the three UV filters in a single preparation obtained under these conditions is shown in Figure 4.3. Linear calibration curves were obtained for each UV filter by using five standard solutions. The correlation coefficients of each calibration curve were ≅ 0.99. In this study, the limit of detection (LOD) and the limit of quantitation (LOQ) were calculated based on the slope (b) of the calibration curves and the standard deviation ($S_{y/x}$) of the slope of the regression lines according to the formula: LOD = 3($S_{y/x}$/b),

LOQ = 10(S$_{y/x}$/b) (Miller and Miller 1984). The calculated LOD values for BP3, BMDBM, and EHMC were 0.100, 0.014 and 0.076 µM, respectively. The calculated LOQ values were 0.333, 0.045, and 0.253 µM, respectively. Tables 4.1 and 4.2 summarise the calibration data and intra- and inter-day analysis. Recoveries from spiked samples were in the range 97–104 % depending on the used matrix. Due to the complex matrix of cosmetics deviations in the results are expected. The summary of analytical parameters used in the analysis of the UV filter is presented in Tables 4.1 and 4.2 whereas the levels of UV filters in the 12 skin-lightening preparations analysed are presented in Table 4.3. Most products contained all three organic UV filters thereby affording broad-spectrum protection. Products H and J did not contain BP3. The other exceptions were samples K and L that contained only the physical blocker; TiO$_2$. These samples (K and L) also had no ingredients indicated on their packets. The samples A, D, F and H did not contain titanium dioxide, a physical blocker.
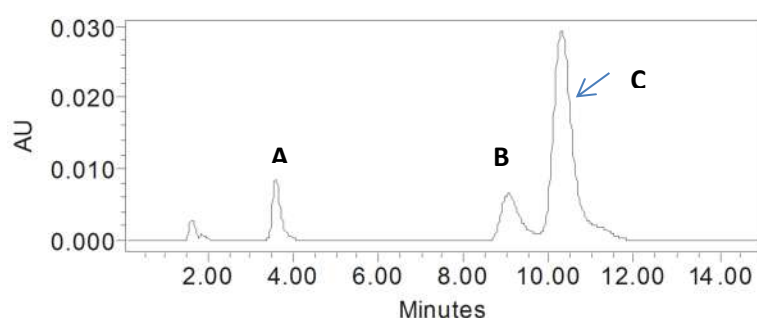
Figure 4.7: HPLC chromatogram of sample **A** showing the UV filters: BP3 (A), BMDBM (B) and EHMC (C). A reversed phase C-12 column (Phenemonex Synergi 4µ Max-RP 80 Å, 150 mm × 4.6 mm) was used with mobile of methanol-water (84:16 % v/v). The injection volume was 20 µL and flow rate set at 1 mL min^{-1}, The detection wavelength was 310 nm.

Table 4.2: The summary of linear regression of calibration data for the sunscreen absorbers.

Parameters	BMBDM	BP3	EHMC
Calibration range/µM	4.37 - 273	3.12 - 499	4.86 - 778
Slope/10^{10}	3.31	1.37	2.15
Error of the slope/10^8	1.49	4.56	5.46
R^2	0.9997	0.9741	0.9879
LOD/µM	0.014	0.100	0.076
LOQ/µM	0.045	0.333	0.253

The LOD is calculated as $3S_{y/x}b^{-1}$ ($S_{y/x}$ is the standard error of the slope and b is the slope of the calibration line) and LOQ is given as 3.33(LOD).

Table 4.3: A summary of the intra- and inter-day instrumental response analysis.

Sunscreen absorber	Conc./µM	Intra-day (n = 5)			Inter-day (n = 5)		
		Found/µM	RSD/%	Recovery/%	Found/µM	RSD/%	Recovery/%
BMBDM	30	30.23 ± 0.95	3.14	100.8	29.57 ± 1.01	3.42	98.6
BP3	60	59.87 ± 0.33	0.55	99.8	60.1 ± 0.56	0.93	100.2
EHMC	50	50.12 ± 0.05	0.10	100.2	49.68 ± 0.96	1.93	99.4

Recovery/% = (mean of found concentration/theoretical amount) × 100 % and RSD/% = (SD/mean concentration) × 100 %

Table 4.4: The percentage amounts of the sunscreens in the investigated skin-lightening preparations from the South African market.

Sample	BMDBM/ % m/m	BP3/% m/m	EHMC/%m/m	TiO$_2$/% m/m
A	0.221 ± 0.002	1.10 ± 0.02	2.49 ± 0.005	-
B	0.066 ± 0.007	9.44 ± 0.03	20.97 ± 0.09.0	6.90 ± 0.05
C	0.432 ± 0.003	0.87 ± 0.04	1.93 ± 0.08	2.83 ± 0.07
D	0.422 ± 0.001	0.85 ± 0.03	2.31 ± 0.08	-
E	1.84 ± 0.015	0.39 ± 0.08	7.02 ± 0.06	7.47 ± 1.2
F	0.214 ± 0.01	0.35 ± 0.01	7.00 ± 0.05	-
G	0.163 ± 0.001	0.35 ± 0.007	1.52 ± 0.08	5.65 ± 0.05
H	1.92 ± 0.06	-	8.20 ± 0.04	-
I	0.50 ± 0.06	0.40 ± 0.009	1.85 ± 0.02	3.35 ± 0.03
J	1.70 ± 0.01	-	6.46 ± 0.03	2.86 ± 0.06
K	0	0	0	3.73 ± 0.07
L	0	0	0	3.04 ± 0.06
Max. COLIPA value % (m/m)	5	10	10	25%; > 100 nm
USA*	3	6	7.5	25
AUS*	5	10	10	25
Japan*	10	5	20	no limit

BMDBM – butylmethoxy dibenzoylmethane, EHMC – 2-ethylhexyl-*p*-methoxycinnamate, BP3 - benzophenone-3,
 *from (Krause et al. 2012; Oesterwalder and Herzog 2009; Serpone et al. 2002)
Sunscreens below the detection limit but which may have been present are indicated as zero those that were not present were indicated as dash (-).

4.3.2 Photostability of the skin-lightening products

The photostability of sunscreen products determines their effectiveness, since the decomposition of the UV filters under sunlight exposure reduces their expected screening capacity. Hence, in order to ensure adequate photoprotection during usage, the photochemical behaviour of sunscreen agents needs to be investigated under conditions that mimic those encountered in the finished sun-care preparation. In this work we investigated the photostability of skin-lightening preparations. These products contained majorly the sunscreens: EHMC, BP3 and BMDBM. Some of the samples contained plant extracts labelled on the packet as constituents constituting the preparation. Each product was tested by smearing on a quartz plate. The samples for instance A containing: EHMC, BMDBM and BP3, at an application density of 1.096 mg cm^{-2} showed photodegradation (Fig. 4.4). The same effect was observed for other skin-lightening products. For instance, sample G incorporating EHMC, BP3, BMDBM, and TiO_2 also photodegraded (Fig. 4.5). This observation implied that despite the presence of a physical absorber and reflector of radiation, the samples suffered photo-loss upon solar exposure. The only way we can tell that the UV filters are photo-unstable is by decrease of the absorptive capacity because of photo-instability of the absorbers resulting in an increase of the transmitted radiation especially UVA region, (see Fig 4.4 and Fig. 4.5). Products A and G were similar in composition save for titanium dioxide in sample G. Both samples contain the UVA absorber, BMDBM which is known to be photolabile particularly in aprotic media. It undergoes phototautomerisation from the *enol-* form that absorbs at 360 nm to the *keto-* form that absorbs at 260 nm. In addition, in nonpolar media it is known to photodegrade. A contained slightly more of the absorber than G but A was photostable in the UVB region whereas G exhibited a small photoloss in this region. However, both were markedly unstable in the longer wavelength region. Other products that showed similar behaviour see Supplementary Materials Figures S4.1 – S4.4.

However, samples containing plant extracts showed a different trend on continued exposure. These samples most of them showed first an initial increase in percent transmittance and then a drop. An indication of gain in photostability after an initial photoloss. For example E, a composed of EHMC, BP3, BMDBM, TiO_2, mulberry extracts, grape extracts, liquorice extracts, sexifrage extracts and scutelleria root extracts kojic acid and kojic diplamitate showed, drop in transmittance with increasing solar exposure (Fig. 4.6). The application density on this plate was 1.002 mg cm^{-2}. The drop in transmittance is an indication of an increase in absorption efficacy. We concluded from this observation and from other skin-lightening preparations even those containing the TiO_2, that plants extracts have a positive effect on photostability. For another example is sample B, Figure 4.7 shows the transmittance spectra of a preparation containing EHMC, BP3, BMDBM, TiO_2, citronellol, coumarin, gereniol, limonene, and linalool at an application density of 1.010 mg cm^{-2} with increasing absorptive potential. Table 4.4 summarise the constituents of the samples investigated and the effect of solar exposure applied on the transmission characteristics when the products were applied on the quartz plates.
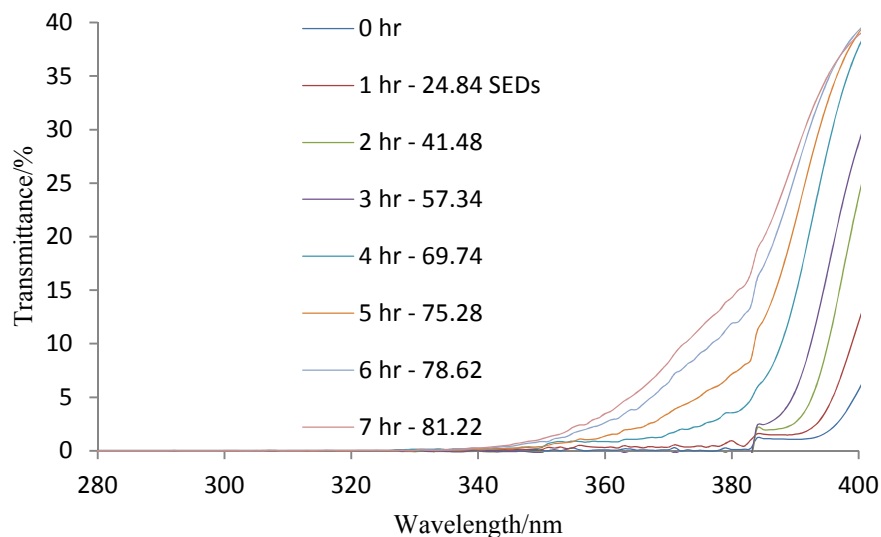
Figure 4.8: Photochemical degradation of skin-lightener A containing BMDBM, EHMC, and BP3. The application density was 1.096 mg cm^{-2} smeared on a quartz plate. The spectra were recorded on a Perkin Elmer Lambda 35 UV-vis dual beam spectrophotometer.
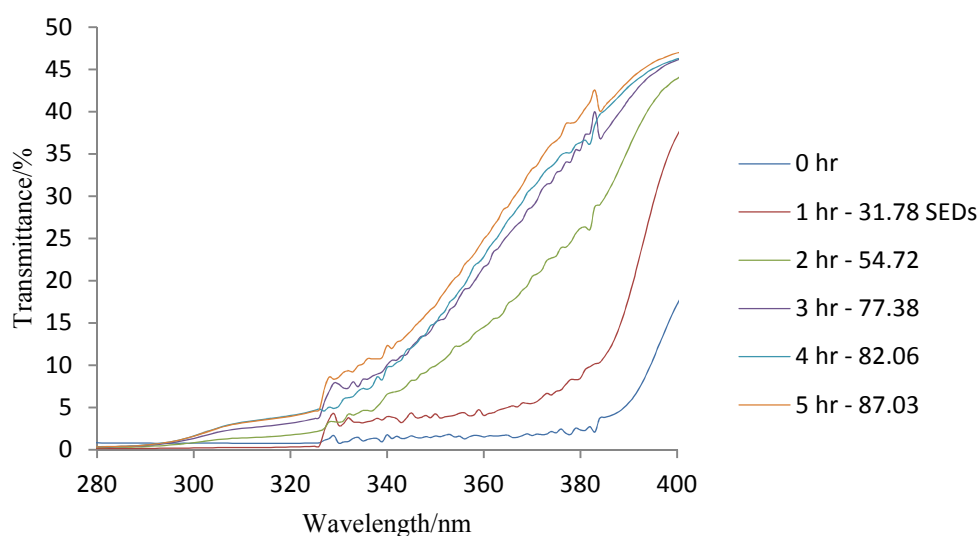
Figure 4.9: Photodegradation of skin lightening preparation G under solar irradiation, the sunscreens present are and EHMC, BP3, BMDBM and TiO$_2$. The application density was 1.021 mg cm^{-2} smeared on quartz plate and spectra recorded on a Perkin Elmer lambda 35 UV-vis dual beam spectrophotometer.
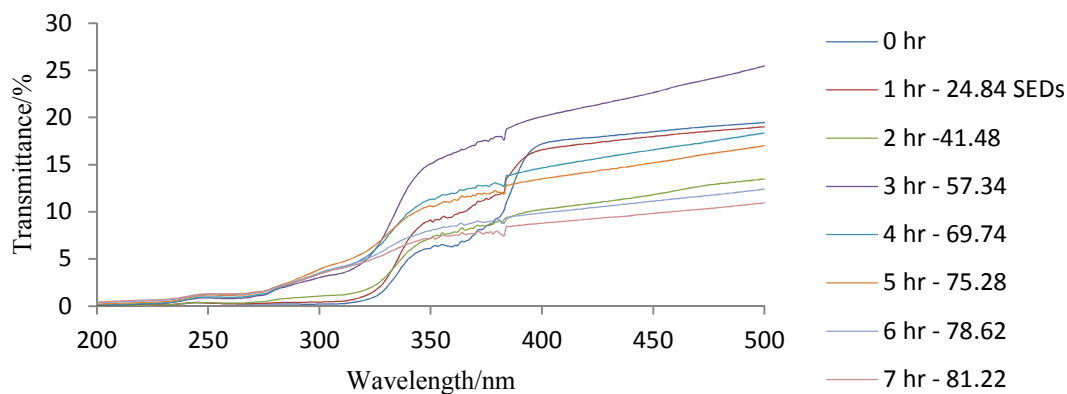
Figure 4.10: Transmission spectra of skin lightening preparation E containing the sunscreen agents, EHMC, BP3, BMDBM and TiO_2 with plant extracts of mulberry, liquorice, grape, sexifrage, and scutelleria and kojic acid, and kojic dipalmitate. The sunscreens incorporated are: avobenzone and ethylhexylmethoxy cinnamate. The product was applied on quartz glass plate at an application density 1.002 mg cm^{-2} and spectra recorded on a Perkin Elmer Lambda 35 UV-vis dual beam spectrophotometer.

Table 4.5: The constituents of the investigated skin lightening preparations as listed on product labels and their effect on light transmission.

Skin-lightening Product	Sunscreen Present	Antioxidant present	Plant Extracts	Other Additives	Effect on transmission due to solar exposure
A	EHMC BMDBM BP3	Tocopheryl acetate	Soy protein sulfonate	Phenoxyethanol	Increase
B	EHMC BP3 BMDBM TiO_2	Tocopheryl acetate	Citronellol Coumarin Geraniol Limonene Linalool	Hydrolysed milk protein Phenoxyethanol	Drop
C	EHMC BMDBM BP3 TiO_2		Mulberry extract Grape extract Sexifrage extract Scutelleria root extract Jojoba oil Avocado oil Niacinamide	Sweet almond milk Mineral oil	Drop
D	EHMC BMDBM BP3		Javetri extract Kasturimanjal extract Kesar extract Raktachandan extract	Glycerin	Drop
E	EHMC BP3 BMDBM TiO_2	Tocopheryl acetate Lactic acid	Mulberry extract Grape extract Liquorice extract Sexifrage extract Scutelleria root		Drop

			Kojic acid Kojic dipalmitate		
F	EHMC BP3 BMDBM		Almond oil Cucumber extract Liquorice extract Aloe vera extract Saffron extract Germ oil	Phenoxyethanol Methyl paraben propyl paraben	Drop
G	EHMC BMDBM BP3 TiO$_2$	Tocopheryl acetate Sodium ascorbate phosphate	Niacinamide	Milk cream Methyl paraben	Increase
H	EHMC BMDBM	Butylated hydoxytoluene	Licorice extract Sunflower seed oil Niacinamide	Allantoin Methyl paraben propyl paraben	Drop
I	EHMC BP3 BMDBM TiO$_2$	Propyl gallate	Licorice extract Aspergillus ferment	Diazolidynyl urea Methyl paraben Propyl paraben	Drop

4.4   Discussion

Most UV filters investigated had UV filter concentrations that fell within the allowed maximum limits of the health regulatory bodies in Japan, United States of America and the European Union, apart from sample B (Table 4.4). The concentration of EHMC ranged from 1.85 – 20.97 % m/m with a mean concentration for the analysed samples of 4.98 % m/m. The concentration range of benzophenone-3 was 0.35 – 9.44 % m/m and mean concentration of 1.72 % m/m. The concentration range for BMDBM was from 0.221 – 1.92 % m/m and a percent composition of 0.65 % m/m. . The amounts of BMDM in most samples were much lower than anticipated. Only one sample, B, had a concentration of EHMC that was found to exceed even the 20 % (m/m) maximum allowed concentration in Japan. In comparison with levels found in the commercial sunscreen products in the market, the average composition of all organic absorbers in the products were lower than expected (Table 4.5).

Table 4.5: A comparison of the percent composition of organic UV filters in skin-lightening preparations quantified and UV filters in commercial sunscreens products

UV filter	Present work Av % m/m	Av. % m/m from Kim et al. (2011)	Av. % m/m from Bunhu (2006)
EHMC	4.98	6.77	6.15
BP3	1.72	4.25	3.72
BMDBM	0.65	2.01	1.67

This work demonstrates that it is possible to photo-stabilize sunscreen molecules in certain formulations and photodegradation in others. For instance, the products A and G contained BP3, a photostable absorber, which absorbs in the short wavelength UVA region and hence masks part of the BMDBM photoloss. However, the lowest excited triplet state (T_1) energy of BP3 (E_{T1} = 2.98 eV) (Kumasaka et al. 2014) is higher than that of the UVA absorber, BMDBM (E_{T1} = 2.53 eV) (Mendrok-Edinger 2009; Kumasaka et al. 2014), and UVB absorber EHMC (E_{T1} = 2.42 eV) (Kikuchi et al. 2010; Kumasaka et al. 2014). This makes BP3 a possible triplet energy donor to BMDBM and EHMC in the mixture of these UV absorbers. Hence the photosensitized BMDBM and EHMC may undergo [2+2] cycloaddition reactions yielding less absorbing photoproducts. This could result in the rapid loss in photo-absorption observed. EHMC is known to photoisomerise upon irradiation from the *trans*- to *cis*-isomer and thereby lose some of its efficacy. It is also known that BMDBM photosensitizes the photoisomerisation of EHMC from the trans- to cis- and the cis-isomer is less efficient absorber of the UVB radiation. Formulation G could suffer another drawback due to the photocatalytic effect of TiO_2 since it has been shown that the presence of TiO_2 can mineralize organic absorbers (Egerton et al. 2008; Dondi et al. 2006). It can therefore be argued that the photo-unstable UV filters may be harmful to human skin due to unknown photoproducts formed.

The inclusion of plant extracts seems to confer stability to the incorporated sun-active molecules though further research is needed to confirm or elucidate the mechanism of the conferred photostability. Notable case was the samples with plant phytochemicals; they showed remarkable improvement with increasing period of exposure to sunlight. Sample B on its label indicated that it contained citronellol, coumarin. gereniol, limonene and linalool. These are known compounds found in most plant species. These compounds have some level of unsaturation within their carbon skeleton. We envisage that upon exposure to UV radiation they are likely to participate in photo-induced cyclization reactions and possible dimerization with net increase in π - π conjugation. This claim requires further investigation, to establish the excited states involved and the resultant chromophoric

species formed. It is interesting to note that the UV filter combination of BMDBM and EHMC, which is known to be photo-unstable, they demonstrated unusual photostability in skin-lightening preparation containing plant extracts (Fig. 4.6 and Fig 4.7). The plant extracts incorporated may play a role in stabilizing the products and enhancing their absorptive capacity. This is what causes the decrease in transmittance.

BMDBM, while it is one of the few organic sunscreening agents that affords photoprotection in the long wavelength UVA range, is photo-unstable as can be seen in the sharp increase in spectral transmittance between 330 and 350 nm due to photo-degradation to less absorbing products. However, in this work skin lightening products with plant extracts showed a fall in this region. The photostability of BMDBM has been shown to be partly depended on the polarity of the solvent. BMDBM undergoes photodegradation in a nonpolar environment (Schwack and Rudolph 1995), by reactive radical formation of benzoyl and phenacyl radicals. This reaction yield photoproducts that are less absorbing within the UVB and UVA range. However, in a polar protic environment BMDBM tends to participate in *keto-enol* tautomeric isomerization via excited carbonyl hydrogen abstraction reaction with the solvent or other hydrogen donors in the environment. The *enol* form of BMDBM has a wavelength of maximum absorption at 358 nm making it a better UVA absorber. The formation of the *keto* form of BMDBM which has maximum absorption at 260 nm greatly weakens its usefulness as UV protecting molecule. This occurs in a polar aprotic environment. Hence the *keto-enol* tautomerism of this molecule plays a role on its photo-absorption. This polarity and proticity dependent photostability of BMDBM was shown by Mturi and Martincigh (2008). Because of the improved photostability of these compounds in the skin-lightening preparations containing plant extracts, we propose that the phenolic compounds present in the plant extracts may create a favourable polar environment to enhance the *enol* form of BMDBM.

On the other hand, the *trans-cis* photo-isomerization of EHMC results in a loss of some of its absorbing ability. This is because the *cis* isomer has a shorter molar absorption coefficient, and thus a lower UV absorption efficacy. Apart from these photo-induced structural transformations that bring about the photo-loss of the cinnamic group, the triplet excited state of the cinnamic chromophore is lower than the excited state of the dibenzoylmethane derivative (Kikuchi et al. 2010; Mendrok-Edinger 2009). Hence, it may undergo photosensitized isomerization in the presence of BMDBM. The resultant effect is an enhanced photo-loss because of the greater formation of the *cis*-isomer which is a less efficient absorber of UVB radiation. From the foregoing analysis, therefore, a combination of BMDBM with EHMC is expected to be inherently photo-unstable. The observed photostability is thus of great interest, because the decrease in transmittance was shown in the presence of both BMDBM and EHMC. This leads us to conclude that phytochemicals play a role in stabilizing both UV filters. A probable mechanism of photostabilization of sunscreen agents by these phenolic compounds could be by way of a vibrational deactivation mechanism or via participation in hydrogen abstraction reactions.

The photostability of skin-lightening preparation E containing the plant extracts: mulberry, liquorice, grape, sexifrage, and scutelleria extracts could be explained interms of the presence of plants extracts. This view could be reinforced by the fact that the only sunscreens incorporated are EHMC and BMDBM (Fig.4.7). The problem with this mixture is that it becomes difficult to determine the exact contribution of each of the different extracts. The phytochemical compositions across different plant species are different and therefore there are likely to be antagonistic, or some other form of, reactions that may reduce the products efficacy. Hence, each extract requires investigation singularly in order to evaluate its worth in photoprotection.

The use of natural products with properties known to rejuvenate and protect the skin from environmental pollution, chemicals, atmospheric temperature fluctuation, UVA and UVB radiation, wrinkling, hyperpigmentation (excessive tanning) and inflammation has been on the rise in cosmetic industry. The other likely benefit of incorporating plants extracts in skin-lightening preparations with sunscreens is the radical scavenging ability of polyphenolic substances. Several reports suggest that naturally occurring unsaturated fatty acids and phenolic compounds have free radical scavenging properties. This approach is likely to mitigate not only the effects of UV long-wave radiation but also contribute to the nourishing of skin tone.

The possible photostabilizing potential of plant extracts in cosmetics, other than the widely reported antioxidant activity has not been extensively explored. However, there a is some evidence show the UV filtering ability of some of these natural phytochemicals. Rancan et al. (2002) showed that usnic acid a naturally occurring dibenzofuran derivative found in several lichen species, had the best UVB filtering effect, with an *in vivo* protection factor similar to Nivea Sun Spray LSF 5. This group found most of the isolated compounds to have good photo-absorption efficacy compared to EHMC. However, caution must be exercised because although some of these compounds are indeed UV-active they may photodegrade. In the work by (Sobarzo-Sanchez et al. (2012)) they showed that boldine, has a UV light-filtering property relevant to photoprotective action, but noted that the photoproducts were toxic to nauplii of *Artemia salina.*

A light complexion is the desire of all users of skin-lightening preparations. However, a bleached skin is more susceptible to UV effects and hence other product related risks must be minimized. Hence, more effective formulations containing herbal components for topical application require a better understanding of the fate of the photochemical products. More so the inclusion of other UV filters in such a formulation require investigation of various chemical interactions. Currently no law exists that guides the incorporation of the various herbal components in cosmetic preparations. The regulatory authorities need to frame some laws concerned with the safety, efficacy and quality assessment of these newer herbal cosmeceuticals.

4.5 Conclusions

The aim of this study was to investigate the photostability of sunscreens in skin-lightening preparations. Two categories of these products were investigated in this work: photodegradation of sunscreen in skin-lighteners and sunscreens in skin-lighteners with plant extracts. All the products containing sunscreens without plant extracts showed photodegradation. Skin-lightening preparations with plant extracts showed a decrease in the spectral transmittance in the long wavelength region. This behaviour is likely to confer product photostability and effective photoprotection to the user. However, further investigation is required to determine the photo toxicities of the photoproducts formed.

References

Baliña LM, Graupe K (1991) The Treatment of Melasma 20% Azelaic Acid versus 4% Hydroquinone Cream. International Journal of Dermatology 30 (12):893-895

Ball Arefiev KL, Hantash BM (2012) Advances in the treatment of melasma: a review of the recent literature. Dermatology and Surgery 38 (7, Pt. 1):971-984

Bhawan J (1996) Short- and long-term histologic effects of topical tretinoin on photodamaged skin. International Journal of Dermatology 37:286-292

Bunhu T (2006) An Assessment of the Photostability of South African Commercial Sunscreens. MSc Dissertation, University of KwaZulu-Natal, Durban, South Africa

Chang T-S (2012) Natural Melanogenesis Inhibitors Acting Through the Down-Regulation of Tyrosinase Activity. Materials 5 (12):1661-1685

Costin G-E, Hearing VJ (2007) Human skin pigmentation: melanocytes modulate skin color in response to stress. The FASEB Journal 21 (4):976-994

Dadzie OE, Petit A (2009) Skin bleaching: highlighting the misuse of cutaneous depigmenting agents. J Eur Acad Dermatol Venereol 23 (7):741-750

Dondi D, Albini A, Serpone N (2006) Interactions between different solar UVB/UVA filters contained in commercial suncreams and consequent loss of UV protection. Photochemistry and Photobiological Sciences 5 (9):835-843

Egerton A, Everall JN, Mattinson AJ, Kessell ML, Tooley RI (2008) Interaction of TiO_2 nano-particles with organic UV absobers. Journal of Photochemistry and Photobiology A: Chemistry 193:10 - 17

Fistarol SK, Itin PH (2010) Disorders of Pigmentation. Journal der Deutschen Dermatologischen Gesellschaft 8 (3):187-202

Jun S-Y, Park K-M, Choi K-W, Jang M, Kang H, Lee S-H, Park K-H, Cha J (2008) Inhibitory effects of arbutin-β-glycosides synthesized from enzymatic transglycosylation for melanogenesis. Biotechnol Lett 30 (4):743-748

Kikuchi A, Yukimaru S, Oguchi N, Miyazawa K, Yagi M (2010) Excited triplet state of a UV-B absorber, octyl methoxycinnamate. Chemical Letters 39 (6):633-635

Kim K, Mueller J, Park Y-B, Jung H-R, Kang S-H, Yoon M-H, Lee J-B (2011) Simultaneous determination of nine UV filters and four preservatives in suncare products by High Performance Liquid Chromatography Journal of Chromatographic Science 49:554-558

Klan P, Janosek J, Kriz Z (2000) Photochemistry of valerophenone in solid solutions. Journal of Photochemistry and Photobiology A: Chemistry 134 (1-2):37-44

Krause M, Kilt A, Blomberg JM, Soeborg T, Frederiksen H, Schlumpf M, Lichtensteiger W, Skakkebaek NE, Drzewiecki KT (2012) Sunscreens: are they beneficial for health? An overview of endocrine disrupting properties of UV-filters. International Journal of Andrology 35:424 - 436

Kumasaka R, Kikuchi A, Yagi M (2014) Photoexcited States of UV Absorbers, Benzophenone Derivatives. Photochemistry and photobiology 90 (4):727-733

Lin JY, Fisher DE (2007) Melanocyte biology and skin pigmentation. Nature 445 (7130):843-850

Lucas R, McMichael T, Smith W, Amstrong B (2006) Solar ultraviolet radiation: Global burden of disease from ultraviolet radiation. In: Pruss-Ustun A, Zeeb H, Mathers C, Repacholi M (eds) Environmental Burden of Disease

Maier H, Schauberger G, Brunnhofer K, Honigsmann H (2001) Change of ultraviolet absorbance of sunscreens by exposure to solar-simulated radiation. Journal of Investigative Dermatology 117 (2):256-262

Mendrok-Edinger C (2009) The quest for avobenzone stabilizers and sunscreen photostability. CosmeticsToiletries 124 (2):47

Miller JC, Miller JN (1984) Statistics for Analytical Chemistry. Wiley, New York

Moon KY, Ahn KS, Lee J, Kim YS (2001) Kojic acid, a potential inhibitor of NF-kappa B activation in transfectant human HaCaT and SCC-13 cells. Archives of Pharmacology Research 24 (4):307-311

Mturi GJ, Martincigh BS (2008) Photostability of the sunscreening agent 4-*tert*-butyl-4'-methoxydibenzoylmethane (avobenzone) in solvents of different polarity and proticity Journal of Photochemistry and Photobiology A: Chemistry 200:410-420

Musashi M, Hirata K, Yamaguchi Y (2009) Composition for external application on skin, and skin-whitening cosmetic containing hydroquinone and lyotropic liquid crystal. WO2009096481A1,

Oesterwalder U, Herzog B (2009) Chemistry and properties of organic and inorganic UV filters. Clinical Guide to Sunscreens and Photoprotection. Informa Healthcare, New York, USA

Olumide YM (2010) Use of skin lightening creams. BMJ 341

Park HY, Kosmadaki M, Yaar M, Gilchrest BA (2009) Cellular mechanisms regulating human melanogenesis. Cell Mol Life Sci 66 (9):1493-1506

Rancan F, Rosan S, Boehm K, Fernandez E, Hidalgo ME, Quihot W, Rubio C, Boehm F, Piazena H, Oltmanns U (2002) Protection against UVB irradiation by natural filters extracted from lichens. Journal of Photochemistry and Photobiology B: Biology 68:133-139

Rendon M, Berneburg M, Arellano I, Picardo M (2006) Treatment of melasma. Journal of the American Academy of Dermatology 54 (5, Supplement 2):S272-S281

Schallreuter UK, Wood MJ, Farwell WD, Moore J, Edwards GMH (1996) Oxybenzone oxidation following solar irradiation of skin: photoprotection versus antioxidant inactivation. Journal of Investigative Dermatology 106:583-586

Schwack W, Rudolph T (1995) Photochemistry of dibenzoyl methane UVA filters Part 1. Journal of Photochemistry and Photobiology B: Biology 28:229-234

Serpone N, Salinaro A, Emeline AV, Horikoshi S, Hidaka H, Zhao JC (2002) An in vitro systematic spectroscopic examination of the photostabilities of a random set of commercial sunscreen lotions and their chemical UVB/UVA active agents. Photochemical and Photobiological Sciences 1 (12):970-981

Serra-Baldrich E, Tribô MJ, Camarasa JG (1998) Allergic contact dermatitis from kojic acid. Contact Dermatitis 39 (2):86-87

Sobarzo-Sanchez E, Soto PG, Rivera CV, Sanchez G, Hidalgo ME (2012) Applied biological and physicochemical activity of isoquinoline alkaloids: oxoisoaporphine and boldine. Molecules 17:10958-10970

Stalgis-Bilinski LK, Boyages J, Salisbury LE, Dunstan RC, Henderson IS, Talbot LP (2011) Burning daylight: balancing vitamin D requirements with sensible sun exposure. The Medical Journal of Australia 194 (7):345-348

Zepp RG, Gumz MM, Miller WL, Gao H (1998) Photoreaction of valerophenone in aqueous solution. Journal of Physical Chemistry A 102 (28):5716-5723

Zhu W, Gao J (2008) The use of botanical extracts as topical skin-lightening agents for the improvement of skin pigmentation disorders. Journal of Investigative Dermatology Sympossium Proceedings 13 (1):20-24

Supplementary Materials
Photodegradation of Skin-lightening preparations without plant extracts
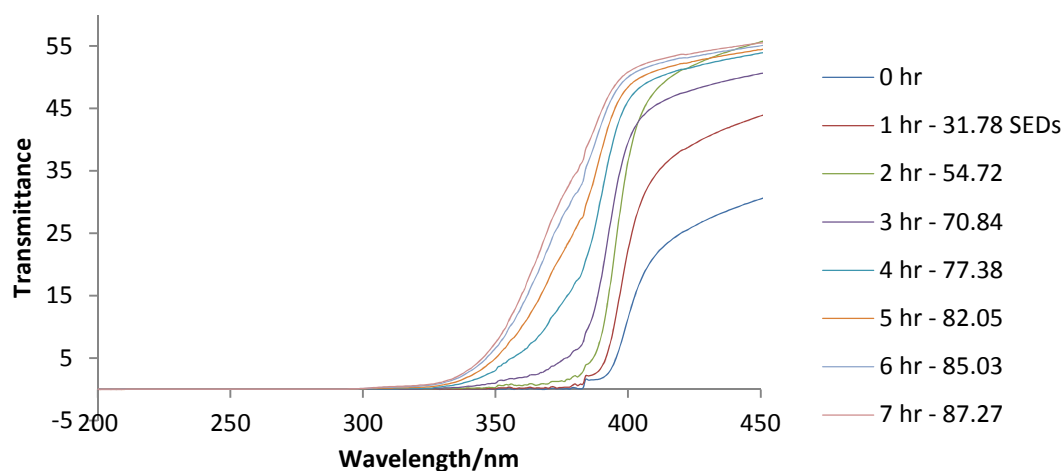
Figure S4.1: Photochemical degradation of skin-lightener A (repeat) containing BMDBM, EHMC, and BP3. The application density was 1.096mg cm^{-2} smeared on quartz glass plate. The spectra were recorded on a Perkin Elmer Lambda 35 UV-Vis spectrophotometer.
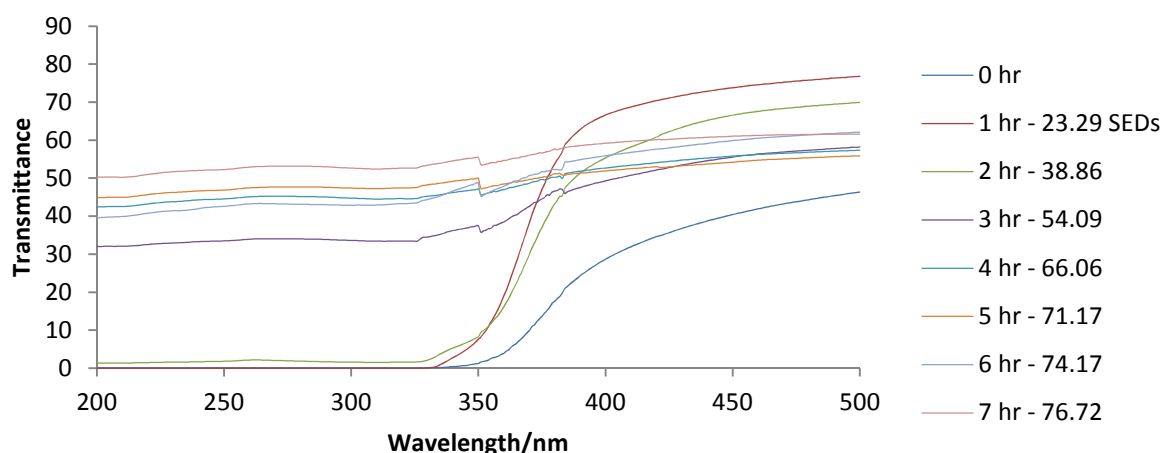
Figure S4.2: Photochemical degradation of skin-lightener **K** containing BMDBM, EHMC, and TiO$_2$ no ingredients were indicated on the packet the sunscreens were characterised on the basis of their retention time and UV spectra match with authentic standards on HPLC but were below quantitation limit. The physical blocker TiO$_2$ was determined by its emission line at 337 nm on ICP-OES and XRD. The application density was 1.096mg cm^{-2} smeared on quartz glass plate. The spectra were recorded on a Perkin Elmer Lambda 35 UV-vis dual beam spectrophotometer.
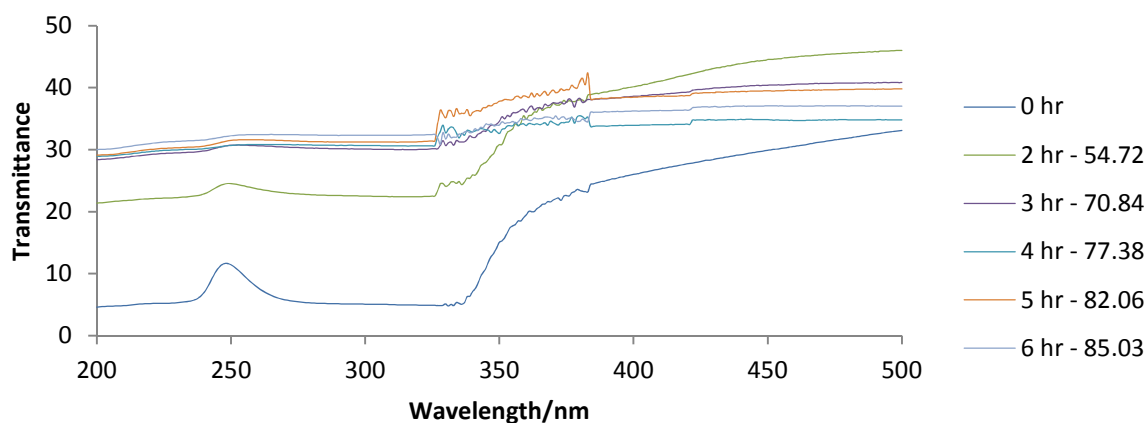
Figure S4.3: Photochemical degradation of skin-lightener L containing BMDBM, EHMC and TiO_2 the organic sunscreen agents were identified by match of their retention time and UV spectra with the corresponding standards from the HPLC data. The quantities were below the limit of quantitation hence not included in the results table. The application density was 0.090 mg cm^{-2} smeared on quartz glass plate. The spectra were recorded on a Perkin Elmer Lambda 35 UV-vis dual beam spectrophotometer.

Photostability of skin-lighteners with plant extracts
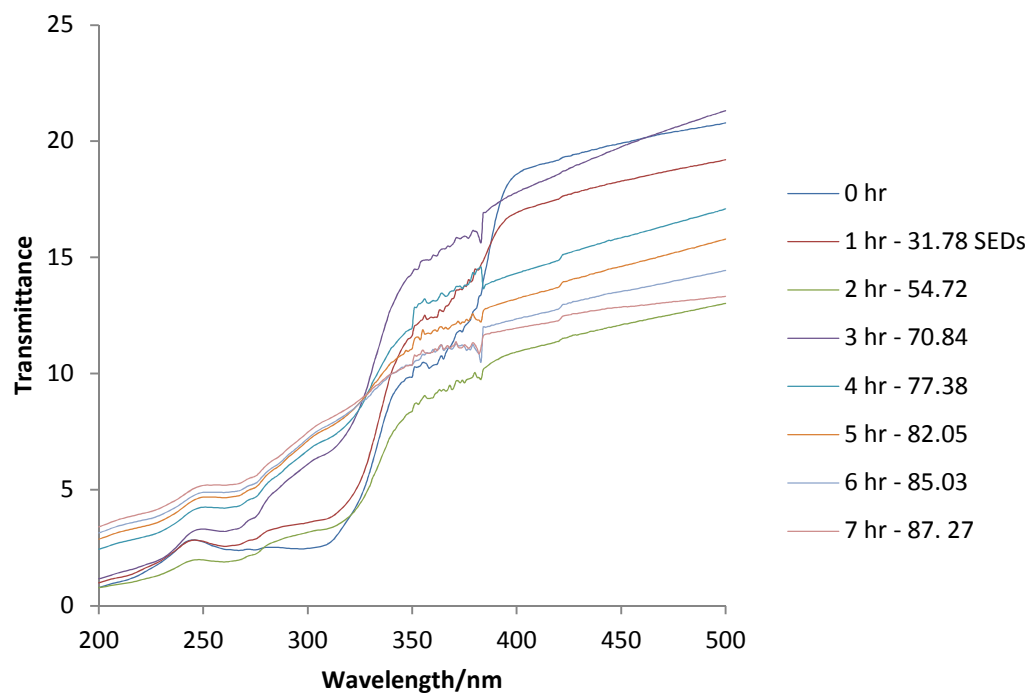
Figure S4.4: Photochemical degradation of skin-lightener **D** containing BMDBM, BP3 and EHMC. The plant extracts are: javeti extracts, kasturimanjal extracts, kesar extracts, and raktachandan extracts. The application density was 1.01 mg cm^{-2} smeared on quartz glass plate. The spectra were recorded on a Perkin Elmer Lambda 35 UV-vis dual beam spectrophotometer.
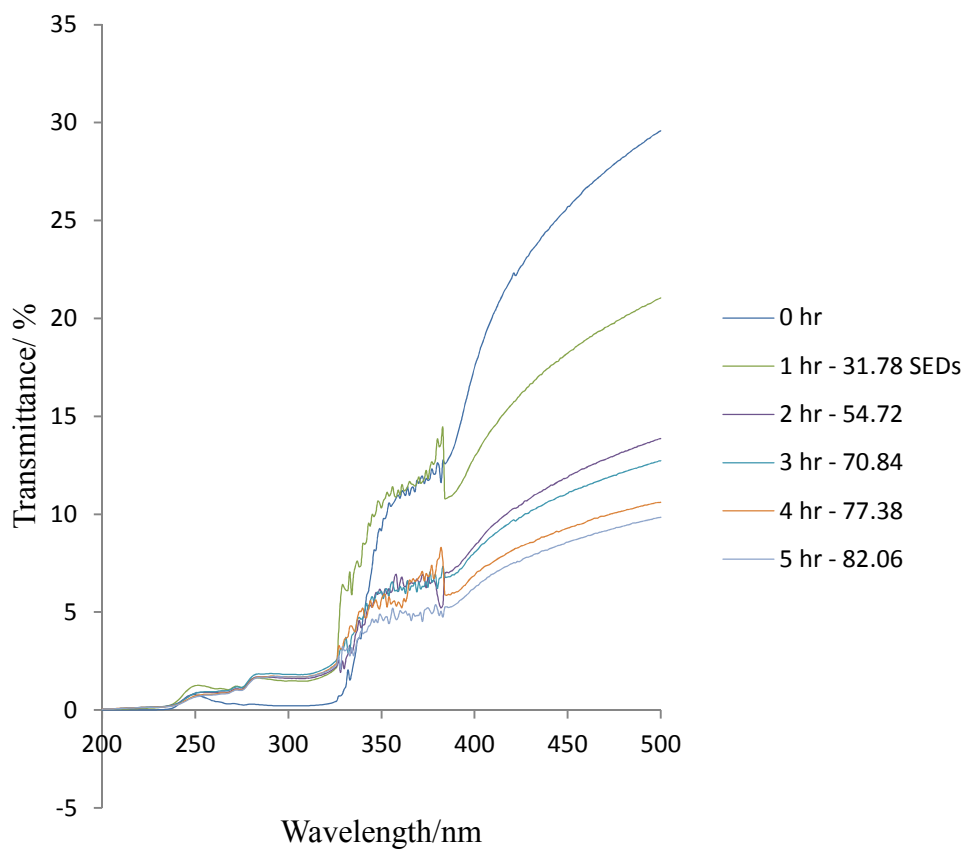
Figure S4.5: Photochemical degradation of skin-lightener **C** containing EHMC, BP3, BMDBM, and TiO_2. The plant extracts are: mulberry extracts, grape seed extracts, avocado oil, saxifrage extracts, jojoba seed oil, and scutelleria root extracts. The application density was 1.096mg cm^{-2} smeared on quartz glass plate. The spectra were recorded on a Perkin Elmer Lambda 35 UV-vis dual beam spectrophotometer.
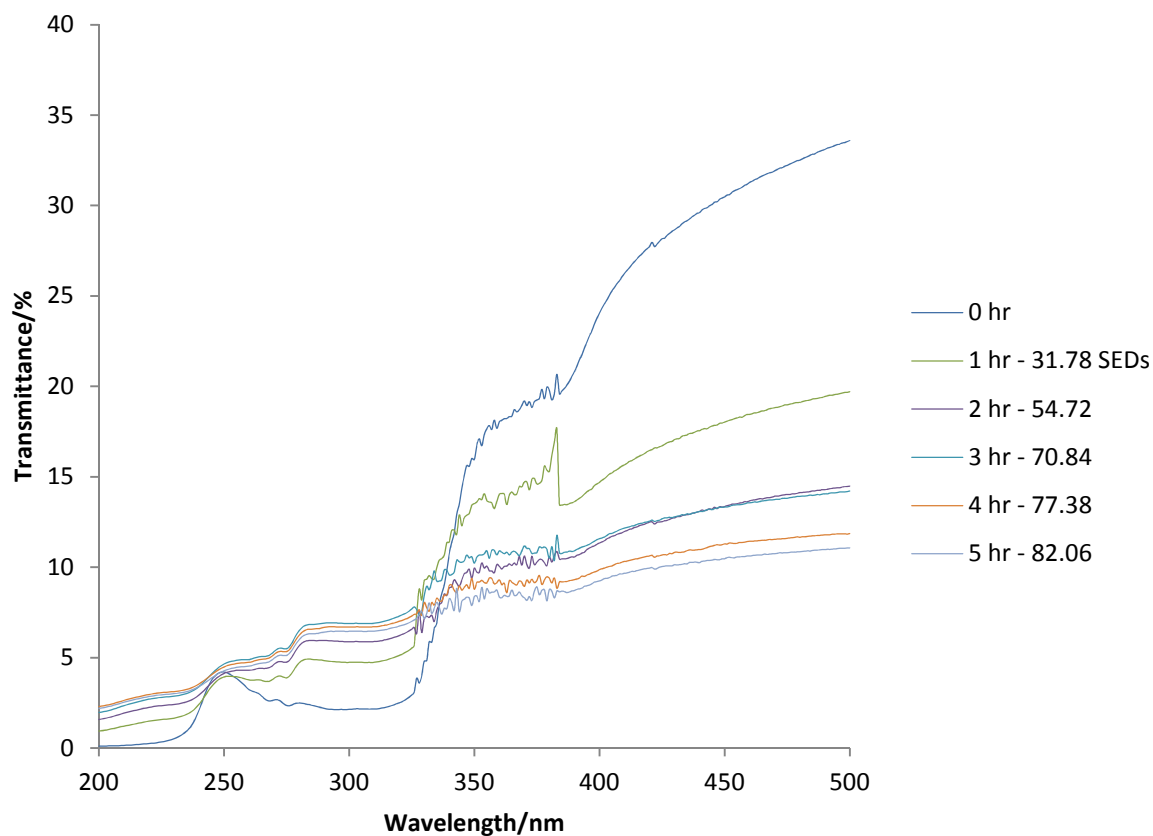
Figure S4.6: Photochemical degradation of skin-lightener F containing BMDBM, EHMC and BP3. The plant extracts in the preparation are: almond oil, cucumber extract, liquorice extract, vetiver extract, aloe vera extract, saffron extract, and germ oil. The application density was 1.001 mg cm^{-2} smeared on quartz glass plate. The spectra were recorded on a Perkin Elmer Lambda 35 UV-Vis spectrophotometer.

Calibration curves for BMDBM, EHMC and BP3 analysis
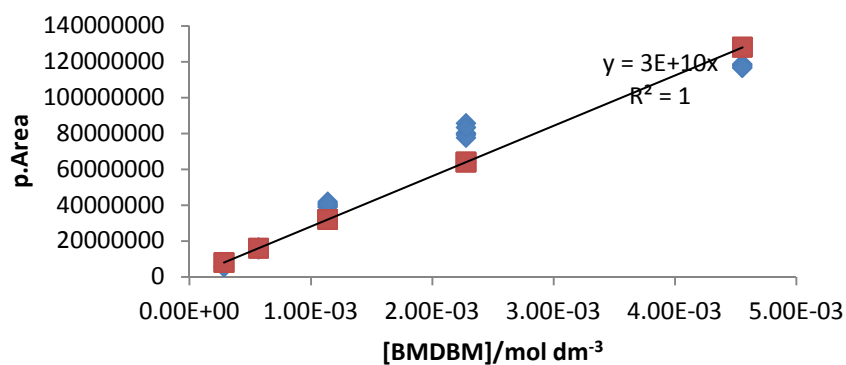
Figure S4.7.1: HPLC calibration curve for the determination of BMDBM in sunscreen preparations. The chromatographic conditions were: A reversed-phase C-12 Phenomenex Synergi 4μ Max-RP 80 Å column (150 mm × 4.6 mm), a mobile phase composition of methanol-water (84:16, v/v) at a flow rate of 1 mL min^{-1} and detection wavelength of 358 nm at ambient temperatures.
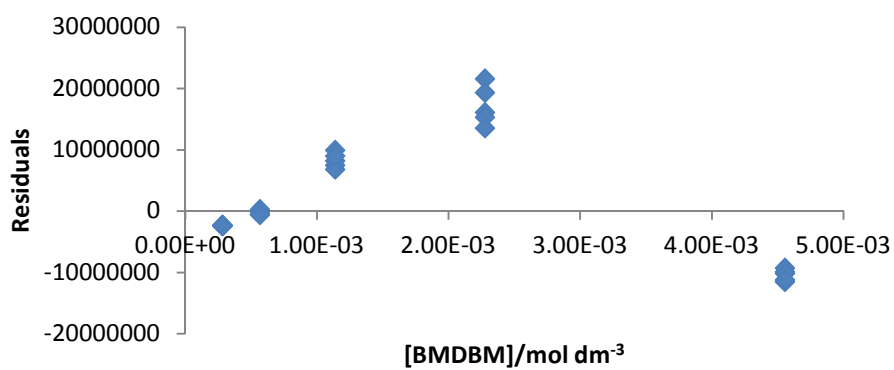
Figure S4.7.2: Residual plot for BMDBM
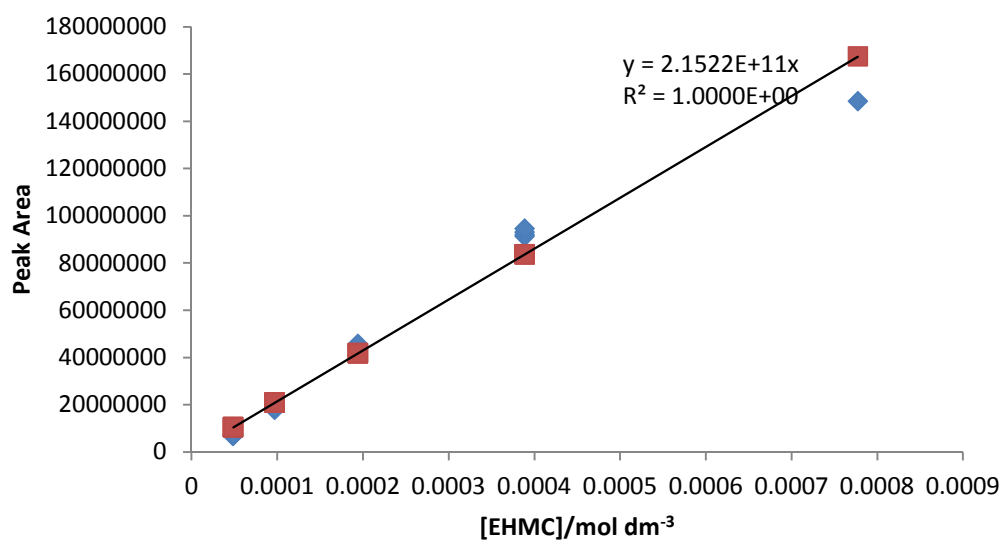
Figure S4.8.1: HPLC calibration curve for the determination of EHMC in sunscreen preparations. The chromatographic conditions were: A reversed-phase C-12 Phenomenex Synergi 4μ Max-RP 80 Å column (150 mm × 4.6 mm), a mobile phase composition of methanol-water (84:16, v/v) at a flow rate of 1 mL min^{-1} and detection wavelength of 310 nm at ambient temperatures.
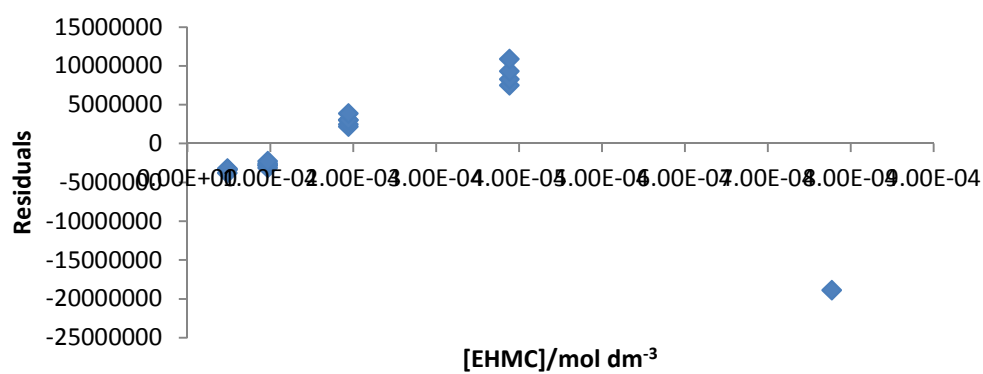
Figure S4.8.2.: Residuals plot for EHMC
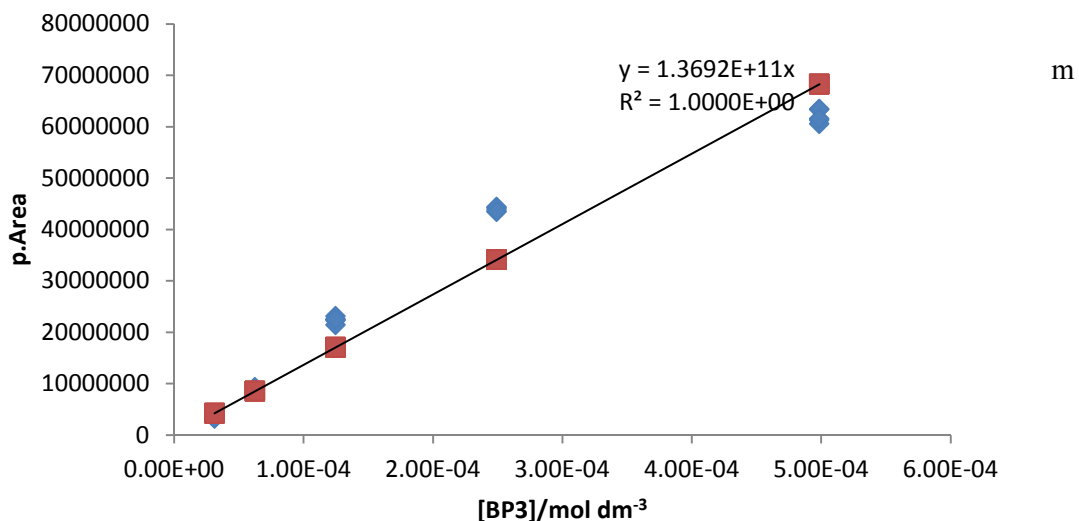
Figure S4.9.1: HPLC calibration curve for the determination of BP3 in sunscreen preparations. The chromatographic conditions were: A reversed-phase C-12 column Phenomenex Synergi 4μ Max-RP 80 Å, (150 mm × 4.6 mm), a mobile phase composition of methanol-water (84:16, v/v) at a flow rate of 1 mL min^{-1} and detection wavelength of 286 nm at ambient temperatures.
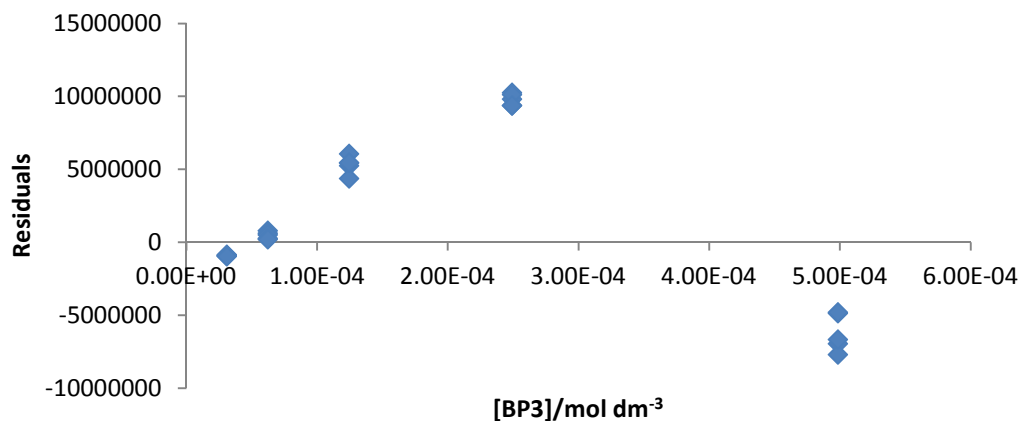
Figure S4.9.2: Residual plot for BP3
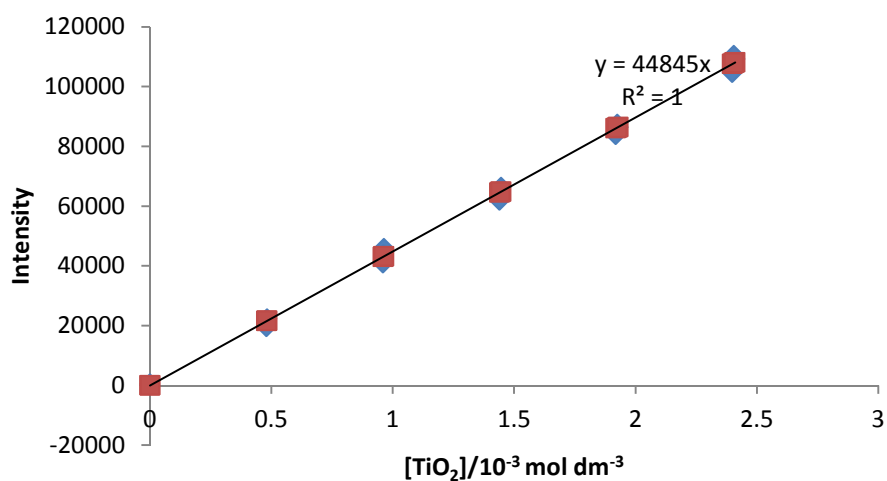
Figure S4.10: The calibration curve for quantitation of TiO_2 on ICP-OES operating conditions were: argon gas flow rate of 1.5 litres (L) min^{-1}, auxiliary and nebulizer gas flows at 0.2 L min^{-1} and 0.8 L min^{-1} respectively. The pump flow rate was set at 1.5 mL min^{-1} while plasma radiofrequency working at 1300 W and data acquired at wavelength of 337.279 nm.

Table S5.1: The actinometric data used in this work.

Time/hr	Time/s	Dod/Area	Val/Area	Val/Dod	RRF	Conc. Rem. Val/M	k_0/mol/L/s	I_0/einstein/L/s	F_0/ W/m²	cum F_0/ W/m²	SED/ J/m²
0	0	3097493	2386120	0.77	346.27	0.0023					
1	3600	2981028	1202842	0.40	346.27	0.0013	2.94E-07	3.00E-07	0.88	0.88	31.78
2	7200	2658511	640280	0.24	346.27	0.00081	2.12E-07	2.16E-07	0.64	1.52	54.72
3	10800	2816061	597626	0.21	346.27	0.00072	1.49E-07	1.52E-07	0.45	1.97	70.84
4	14400	3285889	1539600	0.47	346.27	0.0015	6.05E-08	6.18E-08	0.18	2.15	77.37
5	18000	2835763	1419040	0.50	346.27	0.0016	4.33E-08	4.42E-08	0.13	2.28	82.05
6	21600	2746013	1549284	0.56	346.27	0.0017	2.76E-08	2.81E-08	0.08	2.36	85.03
7	25200	2816500	1652425	0.59	346.27	0.0018	2.07E-08	2.12E-08	0.06	2.42	87.27

Time/hr	Time/s	Dod/Area	Val/Area	Val/Dod	RRF	Conc. Rem. Val/M	k_0/mol/L/s	I_0/einstein/L/s	F_0/ W/m²	Cum F_0/W/m²	SED/ J/m²
0	0	3175693	2440150	0.77	346.27	0.0023					
1	3600	2911686	1464313	0.50	346.27	0.0016	2.13E-07	2.17E-07	0.64	0.64	23.00
2	7200	2931436	1176494	0.40	346.27	0.0013	1.47E-07	1.50E-07	0.44	1.08	38.90
3	10800	2620407	626855	0.24	346.27	0.0008	1.41E-07	1.44E-07	0.42	1.51	54.18
4	14400	2771025	587049	0.21	346.27	0.0007	1.11E-07	1.14E-07	0.33	1.84	66.24
5	18000	3341469	1552749	0.46	346.27	0.0015	4.87E-08	4.97E-08	0.15	1.99	71.50
6	21600	2874821	1607794	0.56	346.27	0.0017	2.80E-08	2.85E-08	0.08	2.07	74.52
7	25200	2916500	1752425	0.60	346.27	0.0018	1.91E-08	1.95E-08	0.06	2.13	76.59

Time/hr	Time/s	Dod/Area	Val/Area	Val/Dod	RRF	Conc. Rem. Val/M	k_0/mol/L/s	I_0/einstein/L/s	F_0/ W/m²	Cum F_0/w/m²	SED/ J/m²

Time/hr	Time/s	Dod/Area	Val/Area	Val/Dod	RRF	Conc. Rem. Val/M	k_0/mol/L/s	I_0/einstein/L/s	F_0/ W/m^2	Cum F_0/w/m^2	SED/ J/m^2
0	0	3192328	2440010	0.76	346.27	0.0023					
1	3600	2935894	1474930	0.50	346.27	0.0016	2.10E-07	2.14E-07	0.63	0.63	22.70
2	7200	2889846	1185579	0.41	346.27	0.0013	1.42E-07	1.45E-07	0.43	1.06	38.04
3	10800	2792634	670371	0.24	346.27	0.0008	1.40E-07	1.43E-07	0.42	1.48	53.18
4	14400	2939027	618242	0.21	346.27	0.0007	1.11E-07	1.13E-07	0.33	1.81	65.18
5	18000	3529809	1654131	0.48	346.27	0.0015	4.74E-08	4.84E-08	0.14	1.95	70.30
6	21600	2852753	1573089	0.55	346.27	0.0017	2.85E-08	2.90E-08	0.085	2.04	73.38
7	25200	2906500	1710025	0.59	346.27	0.0018	2.06E-08	2.10E-08	0.06	2.10	75.59

Time/hr	Time/s	Dod/Area	Val/Area	Val/Dod	RRF	Conc. Rem. Val/M	k_0/mol/L/s	I_0/einstein/L/s	F_0/ W/m^2	Cum F_0/w/m^2	SED/ J/m^2
0	0	3001347	2285707	0.76	346.27	0.0023					
1	3600	3007162	1516639	0.50	346.27	0.0016	2.06E-07	2.11E-07	0.62	0.62	22.29
2	7200	2806170	1148953	0.41	346.27	0.0013	1.41E-07	1.44E-07	0.42	1.04	37.54
3	10800	2675593	647278	0.24	346.27	0.0008	1.39E-07	1.42E-07	0.42	1.46	52.55
4	14400	2801497	605620	0.22	346.27	0.0007	1.09E-07	1.11E-07	0.33	1.79	64.36
5	18000	3253306	1516008	0.47	346.27	0.0015	4.74E-08	4.84E-08	0.14	1.93	69.48
6	21600	2982271	1666095	0.56	346.27	0.0017	2.71E-08	2.77E-08	0.08	2.01	72.41
7	25200	3006500	1690001	0.56	346.27	0.0017	2.36E-08	2.40E-08	0.07	2.08	74.96

Time/hr	Time/s	Dod/Area	Val/Area	Val/Dod	RRF	Conc. Rem. Val/M	k_0/mol/L/s	I_0/einstein/L/s	F_0/ W/m^2	Cum F_0/w/m^2	SED/ J/m^2
0	0	3197784	2462296	0.77	346.27	0.0023					
1	3600	3166929	1587121	0.50	346.27	0.0016	2.16E-07	2.20E-07	0.65	0.65	23.29
2	7200	2999845	1243110	0.41	346.27	0.0013	1.43E-07	1.46E-07	0.43	1.07	38.70
3	10800	2741937	653762	0.24	346.27	0.0008	1.42E-07	1.45E-07	0.43	1.50	54.05
4	14400	2857733	621259	0.22	346.27	0.0007	1.11E-07	1.13E-07	0.33	1.83	66.02
5	18000	3321061	1554092	0.47	346.27	0.0015	4.85E-08	4.95E-08	0.15	1.98	71.25
6	21600	3052704	1707927	0.56	346.27	0.0017	2.82E-08	2.87E-08	0.08	2.06	74.29
7	25200	3046502	1690001	0.55	346.27	0.0017	2.44E-08	2.49E-08	0.07	2.14	76.93

Time/hr	Time/s	Dod/Area	Val/Area	Val/Dod	RRF	Conc. Rem. Val/M	k0/mol/L/s	I0/einstein/L/s	F0/ W/m2	Cum F0/w/m2	SED/ J/m2
0	0	3108668	2386294	0.77	346.27	0.0023					
1	3600	3054880	1523849	0.50	346.27	0.0016	2.16E-07	2.20E-07	0.65	0.65	23.29
2	7200	2951782	1205207	0.41	346.27	0.0013	1.44E-07	1.47E-07	0.43	1.08	38.86
3	10800	2673674	642339	0.24	346.27	0.0008	1.41E-07	1.44E-07	0.42	1.50	54.07
4	14400	2906023	624182	0.22	346.27	0.0007	1.11E-07	1.13E-07	0.33	1.84	66.06
5	18000	3478178	1643913	0.47	346.27	0.0015	4.73E-08	4.83E-08	0.14	2.00	71.17
6	21600	3048413	1708304	0.56	346.27	0.0017	2.77E-08	2.83E-08	0.083	2.06	74.17
7	25200	3046512	1710001	0.56	346.27	0.0017	2.37E-08	2.41E-08	0.07	2.13	76.72

Time/hr	Time/s	Dod/Area	Val/Area	Val/Dod	RRF	Conc. Rem. Val/M	k_0/mol/L/s	I_0/einstein/L/s	F_0/ W/m^2	Cum F_0/w/m^2	SED/ J/m^2
0	0	3202837	2526506	0.79	346.27	0.0024					
1	3600	2980481	1496463	0.50	346.27	0.0016	2.30E-07	2.35E-07	0.69	0.69	24.84
2	7200	3135265	1269250	0.41	346.27	0.0013	1.54E-07	1.57E-07	0.46	1.15	41.48
3	10800	2685361	643784	0.24	346.27	0.0008	1.47E-07	1.50E-07	0.44	1.59	57.34
4	14400	2887630	624869	0.22	346.27	0.0007	1.15E-07	1.17E-07	0.34	1.94	69.74
5	18000	3369275	1579386	0.47	346.27	0.0015	5.14E-08	5.24E-08	0.15	2.09	75.28
6	21600	2882010	1606799	0.56	346.27	0.0017	3.10E-08	3.16E-08	0.09	2.18	78.62
7	25200	2882100	1667854	0.58	346.27	0.0018	2.41E-08	2.46E-08	0.07	2.26	81.22

Chapter Five

In-vitro study of the photostabilizing potential of plant extracts on sunscreen absorbers in commercial sunscreen formulations

Moses A. Ollengo and Bice S. Martincigh[*]

School of Chemistry and Physics, University of KwaZulu-Natal, Westville Campus, Private Bag X54001, Durban 4000, South Africa.

*Corresponding author: Tel.:+27-31-2601394; Fax: +27-31-2603091; E-mail address: martinci@ukzn.ac.za

Abstract

The photostabilizing potential of plant extracts on sunscreen absorbers in commercial sunscreen products was investigated. The amounts of the ultraviolet (UV) filters in these products were determined in order to check compliance with applicable regulatory requirements. A reversed-phase high performance liquid chromatographic method (RP–HPLC), with photodiode array (PDA) detection was used for the simultaneous determination of 2-ethylhexyl-*p*-methoxycinnamate (EHMC), benzophenone-3 (BP3), 2,2′-methanediylbis[6-(2*H*-benzotriazol-2-yl)-4-(2,4,4-trimethylpentan-2-yl)phenol] (MBBT), octocrylene (OCT), 2,2′-[6-(4-methoxyphenyl)-1,3,5-triazine-2,4-diyl]bis(5-[(2-ethylhexyl)oxy]phenol) (BEMT) and *tert*-butylmethoxy dibenzoylmethane (BMDBM). The external standard calibration curves were linear with $R^2 \geq 0.998$. The recovery of these six chemical UV filters from the spiked samples was 98.3–101.5 %. The physical absorbers: titanium dioxide (TiO_2) and zinc oxide (ZnO) were also quantified by means of inductively coupled plasma-optical emission spectrometry (ICP-OES). Their recoveries were in the range of 98.8–99.5 %. All samples contained UV filters within the accepted maximum limits set by various health regulatory authorities. The photostability experiment was performed by applying the product with a ~1.0 mg cm^{-2} of the product surface density on a quartz plate and exposing the plate to sunlight. The spectral changes were recorded every hour on a UV-vis spectrophotometer. The products containing plant extracts showed remarkable photostability compared with products without plant extracts irrespective of the percentage composition of the UV filters in the products. We conclude that plants extracts may contribute synergistically, or otherwise, to the observed photostability.

5.1   Introduction

The destruction of stratospheric ozone layer, the main absorber of ultraviolet (UV) radiation, by various anthropogenic emissions has been identified as the cause of an increase in erythema, burning, dehydration, photo-dermatoses, photoaging and skin cancer in recent years. The UV spectrum is divided into three regions on the basis of the wavelength range: UVC (100–280 nm), UVB (280–315 nm) and UVA (315–400 nm). The UVA region is further subdivided into UVA2 (315–340 nm) and UVA1 (340–400 nm).   The amount of solar UV radiation reaching the Earth's surface is approximately 90–99 % UVA and 1–10 % UVB (Serge 2008; Perrson et al. 2002).

The direct interaction of UVB radiation with cellular DNA has been cited as the primary cause of photocarcinogenesis via the formation of cyclobutane pyrimidine dimers and thymine glycols. Though, the UVB effects have been shown to be mainly restricted to the epidermis. For example, erythema (redness of the skin) is due to sunburn mainly associated with UVB (Sklar et al. 2013). This is a cutaneous inflammatory reaction that can be accompanied by warmth and tenderness; severe cutaneous erythema may cause blister formation (Casetti et al. 2011). The deeper penetrating UVA radiation may be much more harmful and therefore further investigation on its role in photocarcinogenesis is relevant. The major consequence of cumulative UVA radiation is reported as generation of reactive oxygen species (ROS) which may induce cancer through other reactions like generating oxidized DNA base derivatives (Cortat et al. 2013; Fourtanier et al. 2012). One of the DNA base derivatives is 8-hydroxydeoxyguanosine, and the other effect of oxidant species is alteration of tumour suppressor genes, like p53 (Vielhaber et al. 2006; Seite et al. 2000). Several reports demonstrate in the human fibroblast model, the induction of 8-hydroxydeoxyguanosine after radiation from UVA2 (>334 nm) up to near visible light (434 nm). It is evident that UVA radiation directly affects the dermal compartment and is thought to be the major cause responsible for photoaging of human skin (Fourtanier et al. 2012). A number of studies have shown that UVA1 causes destructive effects in human dermal fibroblasts, by induction of cytokines, matrix metalloproteinases, and mtDNA mutations (Kanavy and Gerstenblith 2011). The induction of collagenase: matrix metalloproteinase-1 (MPP-1) responsible for degradation of collagen-type 1, the major constituent of the connective tissue, is considered most significant. This is because the extent of collagen-type 1 reduction has been correlated with photodamage in human skin (Perrson et al. 2002; Vielhaber et al. 2006). The only remedy is to limit exposure of the human skin to UV radiation by use of protective clothing or stay under shade to avoid solar radiation or use sunscreens.

The use of cosmetic products containing UV filters has been advocated by health authorities as the first line of defence against solar radiation-induced damages such as photo-aging, skin cancer and other dermal immunological related complications (Sambandan and Ratner 2011; Kockler et al. 2012). UV filters are organic or inorganic compounds that mitigate the deleterious effects of sunlight and are incorporated in a variety of pharmaceutics and cosmetics such as sunscreen creams, lotions and sprays and other products. The need for high photo-absorption efficiency of sunscreen products against both UVB and UVA has sparked great interest in the development of cosmetic preparations and sunscreening agents. A list of approved UV filters and their maximum allowed concentrations in commercial products has been set by regional health regulatory authorities around the world. For example, Table 5.1 shows maximum allowed concentrations by COLIPA and FDA and some of the average organic absorber concentrations quantified by Kim et al. (2011) and those quantitated by Bunhu (2006) from the South African market.

The lipophilicity of most of the available organic UV filters cannot be ignored as they may accumulate in human subjects (Hagedorn-Leweke and Lippold 1995; Cameron and Michael 1997;

Jiang et al. 1999) as well as other biotic systems (Poiger et al. 2004; Manova et al. 2013). Recently Cuquerella et al. (2012) demonstrated that benzophenone (BP) may photosensitize DNA reactions or its building blocks. Their results showed that irradiation of the BP chromophore in the presence of DNA or its components led to nucleobase oxidations, cyclobutane pyrimidine dimer formation, single strand-breaks, and DNA-protein cross-links. This finding may imply that photostable BP UV filter derivatives like benzophenone-3 (BP3), may initiate such reactions when in contact with viable tissues. In fact, Salter et al. (1993) showed that the UV filter Uvinul DS49, a derivative of BP, photosensitized the formation of thymine dimer *in vitro*. Moreover, a number of organic UV filters have been shown to undergo photochemical transformation including isomerization resulting in the formation of photoproducts whose toxicity potentials are yet to be established (Schwack and Rudolph 1995; Ingouville 1995; Broadbent et al. 1996). There has therefore been a growing need to photostabilize these agents in cosmetic preparations. One of the ways is by incorporation of plant extracts.

Plant extracts contain mostly phenolic compounds possessing one or more aromatic rings with one or more hydroxyl groups (Dai and Mumper 2010). These compounds are known to offer photoprotection to plants and have been shown to be good antioxidants. These secondary metabolites have also been shown to have chemo-protective effects against oxidative stress-mediated disorders (Soobrattee et al. 2005). The photoprotective effect of some of these extracts has been demonstrated (Yamaguchi et al. 2005) and observed that they could reduce UVB-induced erythema and associated early events in murine and human skin (Zhao et al. 1999). However, the direct effect of these plant extracts on the photostability of sunscreen absorbers in commercial sunscreen products has not been reported.

Several working groups have reported analytical techniques for determining UV filters in sunscreen products. These include analytical methods based on separation and/or quantification by using UV–vis spectroscopy (Chisvert et al. 2002), gas chromatography (Ikeda et al. 1990), and high-performance liquid chromatography (HPLC) (Bunhu 2006; Scalia et al. 2006; Gaspar and Campos 2007). Reversed-phase HPLC is the most common method for the simultaneous analysis of several UV filters in pharmaceutics and cosmetics. Bunhu (2006) separated and quantified ten sunscreen agents 2-ethylhexyl-*p*-methoxycinnamate (EHMC), benzophenone-3 (BP3), tert-butylmethoxy dibenzoylmethane (BMDBM), octylsalicylate (OS), methybenzylidene camphor (MBC), octyldimethyl aminobenzoate (ODAB), phenylbenzimidazole sulphonic acid (ensulizole) methylene MBBT, BEMT, and OCT in South African commercial sunscreens (some of them are shown in Fig. 1). Though the amounts of these agents in these cosmetic preparations are of concern and may help in mapping some of observed dermal effects associated with cosmetic preparations, the effect of plant extracts on their photostability has not been examined. For the first time we report the effect of plant extracts on the photostability of suncare agents in selected sunscreen preparations from the South African market. The investigation on the photostability of these agents in commercial suncare products is important for evaluation of the quality of the photoprotection conferred.
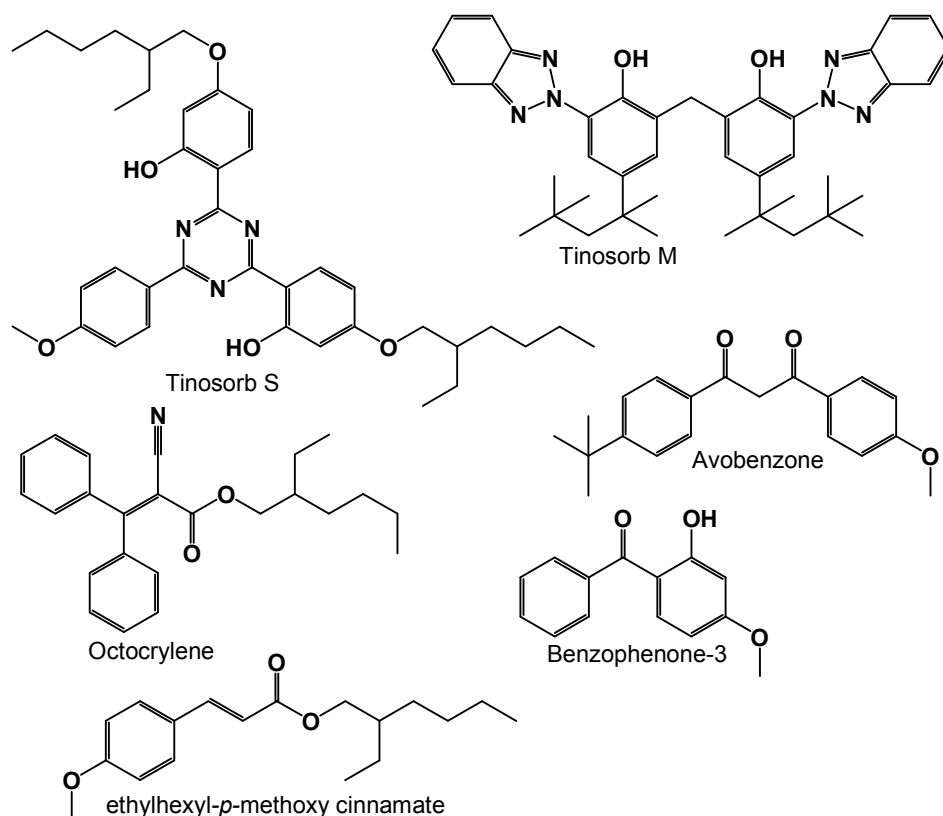
Figure 5.9: Some common organic sunscreen agents.

Table 5.6: Levels of UV-filters and in 101 commercial sun-care products reported by Kim et al. (2011) and 22 sunscreens reported by Bunhu (2006) expressed in % (m/m).

Sunscreens	Kim et al. (2011) Frequently used Conc	Kim et al. (2011) Av. Conc.	Bunhu (2006) Av. Conc	Max. Allowed Conc. (Korea)	Max. Allowed Conc* COLIPA	Max. Allowed Conc* FDA
EHMC	3.08~8.16	6.77	6.15	7.50	10	7.5
IAMC	0.33~7.79	2.91	2.32	10	10	3
EHS	1.78~5.33	4.2	3.41	5	5	5
MBC	2.01~4.96	3.42	3.06	5	5	5
BP3	3.04~5.37	4.25	3.72	5	10	6
EDAB	2.23~5.71	4.46	-	8	8	8
OCT	1.13~6.75	3.53	3.89	10	10	10
BMDBM	0.49~3.41	2.01	1.67	5	5	3

* Maximum allowed concentrations/% (m/m) by COLIPA and FDA (Krause et al. 2012; Oesterwalder and Herzog 2009; Serpone et al. 2002).

5.2 Materials and Methods

5.2.1. Chemicals and reagents

The solvents, acetonitrile (ACN) and methanol (MeOH) of HPLC-grade, were purchased from Merck KGaA and dimethyl formamide (DMF) from Merck KGaA. Ultra-pure water was freshly dispensed from a Milli-Q® water purification system (Millipore, Bedford, MA, USA) for each day of analysis. The six chemical UV filters of analytical purity were purchased as follows: MBBT and BEMT were a kind gift from Ciba Speciality Chemicals Ltd; 2-ethylhexyl-*p*-methoxcinnmate (EHMC) and *tert*-butylmethoxy dibenzoylmethane (BMDBM) were a kind donation from BASF, octocrylene (OCT) and benzophenone-3 (BP3) was from Sigma-Aldrich Sulphuric acid (H_2SO_4) and potassium hydrogen sulphate ($KHSO_4$) were purchased from BDH Chemicals Ltd. TiO_2 was bought from SAARCHEM Pty Ltd and ZnO and 1000 mg dm^{-3} Zn^{+2} ion standard solutions were purchased from Merck KGaA. The sunscreen products were purchased from retail stores in Durban, South Africa.

5.2.2. Quantitation of organic UV absorbers

5.2.2.1. Preparation of standard solutions

All standard stock solutions of the six organic UV absorbers were prepared fresh each day of analysis. The solutions of MBBT and BEMT were prepared by dissolving 15-20 mg of the UV filter in 30 mL DMF, ultrasonicated in a water bath for 1 hour and made up to volume with methanol so that their concentration was about 500 µM. Stock solutions of OCT, EHMC, BP3 and BMDBM with a concentration of about 1000 µM each were prepared by dissolving 10-15 mg of each UV filter in 30 mL of methanol, and ultrasonicated for 1 hour and then diluted to 50 mL with methanol. For the purposes of determining the linearity working range, working standard solutions were prepared in the concentration range of 6.11–196 µM for MBBT, 2.45–157 µM for BEMT, 11.2–360 µM for OCT, 4.37–273 µM for BMDBM, 3.12–499 µM for BP3, and 4.86–778 µM for EHMC by using the HPLC autosampler.

5.2.2.2. Sample preparation

Quantitation of all the organic UV filters in the sunscreen products was performed by using external standard calibration curves. Samples containing MBBT and BEMT products were prepared by dissolving ~150 mg of the cream in 30 mL DMF, ultrasonicated in a water bath for 1 hour, and made to 50 mL in a volumetric flask with methanol. From this stock solution a volume of 2 mL of these samples was diluted to 10 mL with the mobile phase so that the final expected concentration of the chemical UV filters in the injected solutions was approximately 80–100 µM depending on the absorber. Samples that gave higher concentrations more than the calibration range were re-diluted. All experiments were performed in triplicate. The analysis of BMDBM, BP3, OCT and EHMC in the sunscreen samples was performed by dissolving ~ 150 mg of the samples in 30 mL of methanol, ultrasonicated in a water bath for 1 hour, and then diluted to 50 mL in a standard flask with methanol. Working solutions were then prepared from this stock solution by imposing a tenfold dilution factor to achieve an approximate UV filter content of about 10-200 µM or more. The prepared solutions were filtered through 0.45 µm Millex LCR syringe filters before injection into the HPLC system.

5.2.2.3 Chromatographic conditions

A reversed-phase C-12 Phenomenex Synergi 4µ Max-RP 80 Å column (150 mm × 4.6 mm) was used. The mobile phase for the analysis of MBBT, and BEMT standards and samples was:

methanol–acetonitrile (90:10 % v/v). The analysis of EHMC, BMDBM, OCT and BP3 was done with a mobile phase composition of methanol-water (84:16 % v/v), for both standards and samples. All the mobiles phases were purged with helium at a rate of 30 mL min^{-1} continually during each run. The flow rate of the mobile phases was 1.0 mL min^{-1}, and the injection volume was 20 µL. All the separations were performed at ambient temperatures. The chromatograms were detected at 286, 304, 310, 342, and 358 nm. The isocratic elution run time was set for 30 min.

5.2.2.4   Validation of chromatographic method

The method validation experiments were performed in three different sunscreen products by using the external standard method and prepared similarly. Briefly ~150 mg of a pre-analysed sunscreen product was spiked with 10-15 mg of a UV filter and prepared as described in Section 5.2.2. The prepared solutions were filtered through 0.45 µm Millex LCR syringe filters before injection into the HPLC system.

5.2.3   Quantitation of physical blockers

The quantitation and validation of the quantitation method for the analysis of TiO$_2$ was carried out as described in Chapter Six, Sections 6.2.2.1 to 6.2.2.3. The zinc standards in the range of 10 mg dm^{-3}-100 mg dm^{-3} were prepared from a 1000 mg dm^{-3} commercial standard solution.

5.2.3.1   Preparation of ZnO samples

Masses of samples in range 0.4 -0.6 g were weighed into a fused silica crucible, placed into an electrical furnace with the temperature set at 600 ºC for three hours to give a carbon free ash. The ash was allowed to cool in a desiccator for 10 min, and then about 0.5 g of KHSO$_4$ was added. The crucible with residue ash and KHSO$_4$ was heated over Bunsen burner for 15 min to fuse the mixture. The molten product was then dissolved in hot, concentrated H$_2$SO$_4$ and the solution transferred to a beaker. This solution was strongly heated to ensure complete solubilization of the ZnO. Sample solutions were then diluted with deionised water to 100 mL. A ten-fold dilution was done for samples with higher counts above the calibration standards. All samples were filtered through 0.45 µm Millex LCR syringe filters before aspiration into the ICP-OES, each sample was analysed in triplicate.

5.2.3.2   ICP-OES experiment

The TiO$_2$ and ZnO in the samples were quantified by means of ICP-OES. The ICP-OES spectrometer (Perkin Elmer Optima 5300 DV), fitted with an auto-sampler, was programmed to sample each standard and sample five times. The instrument was operated in radial view mode. Other operating conditions were: argon gas at a flow rate of 1.5 L min^{-1}, auxiliary and nebulizer gas flows at 0.2 L min^{-1} and 0.8 L min^{-1} respectively. The pump flow rate was set at 1.5 mL min^{-1} while the plasma radiofrequency was working at 1300 W in radial view mode and the analysis was monitored at 206 nm for ZnO and 337 nm for TiO$_2$.

5.2.3.3   Validation of ICP-OES method

The validation of the ICP-OES method was done as detailed in Chapter Six, Section 6.2.2.3.

5.2.4 Data analysis

Calibration curves for all UV filters were constructed for quantitation of the sunscreen absorbers in the products. Regression equations were obtained through un-weighted least squares linear regression analysis, by using peak areas as a function of their concentration on Microsoft Excel 2007.

5.2.5 Photostability experiments

The photostability experiments were carried out as described in Chapter Four, Section 4.2.6.

5.2.6 Actinometric studies

The actinometric studies were carried out as detailed in Chapter Four, Section 4.2.7.1.

5.2.6.1 Actinometric data analysis

The analysis of the actinometric data was performed as described in Chapter Four Section 4.2.7.2.

5.3 Results

A total of eleven commercial sunscreen products were quantitated and their photostability investigated.

5.3.1 Quantitation of absorbers

In this work, six organic absorbers and two physical absorbers were quantified. Some of the products contained other absorbers but these were not quantified because standards were not readily available. However, all were present in the HPLC chromatograms. Each organic UV filter was quantified at the wavelength of its maximum absorption and physical blockers, TiO_2 and ZnO, were quantified at their preferred wavelengths of emission. The chromatogram in Fig. 5.2 shows a typical separation of the OCT, MBBT and BEMT standards and the corresponding UV spectra used in the identification. This chromatogram was obtained with a mobile phase of methanol-acetonitrile (90:10 % v/v). The calibration curves of the UV filters were linear in the investigated concentration ranges ($R^2 \cong 0.99$). The analytical parameters of representative calibration curves are summarised in Table 5.2. To validate this method the mean recovery of the UV filters from the spiked samples was calculated and results are shown in Table 5.3. To check on instrument signal stability during the period of analysis an intra- and inter-day analysis of authentic standards was done. A high level of precision was realized ≥ 99 % for the intra- and inter-day analysis (Table 5.4). The statistical limit of detection (LOD) is defined as the analyte concentration that gives a signal equal to $y_b + 3.3\,S_b$, where y_b is the signal of the blank and S_b is its standard deviation. Similarly, the limit of quantitation (LOQ) is given as $y_b + 10\,S_b$. However, for the un-weighted least-squares method it is recommended in practice to use the standard deviation of the slope ($S_{y/x}$) (Miller and Miller 1984) instead of S_b

Thus

$$LOD = 3.3\,S_{y/x}/b$$

and

$$LOQ = 10\,S_{y/x}/b$$

where b is the slope of the regression line.

The amounts of the UV filters found in this work were all within the allowed maxima set by COLIPA and FDA. However, some samples had much lower amounts than anticipated. For instance in B1,

B2, B3 and B4 the amount of BMDBM was below the limit of quantitation and so the respective amounts are indicated as zero (Table 5.5). The amount of BP3 was in the range of 2.69 – 5.37 % (m/m), EHMC ranged from 0.28 – 3.62 % (m/m), OCT ranged from 0.68 – 4.02 % m/m, MBBT ranged from 2.65 – 7.93 % (m/m) and BEMT ranged from 3.79 – 6.07 % (m/m). The sunscreen products; P1 – P3 containing plant extracts had much lower concentration of the UV filters, EHMC and BMDBM. The levels of BEMT and MBBT for those products that had them were sufficiently comparable to the allowed amounts by COLIPA and FDA. The amount of TiO_2 in these samples ranged from 0.72 – 12.60 % (m/m) an average slightly higher than those found in skin-lightening preparations (see Chapter Six). The quantitation of ZnO in other sunscreens products served as a control because the percentage composition was indicated on the packs unlike those that contained TiO_2. The experimental values were very close to the packet label an indication that the packet labels represented the actual concentration of ZnO (Table 6). The levels of organic absorbers in the samples containing ZnO had previously been reported by Lyambila (2003) and therefore not included in this work, however, levels of ZnO were not done and in this work they ranged from 5.03 – 8.61 % (m/m).
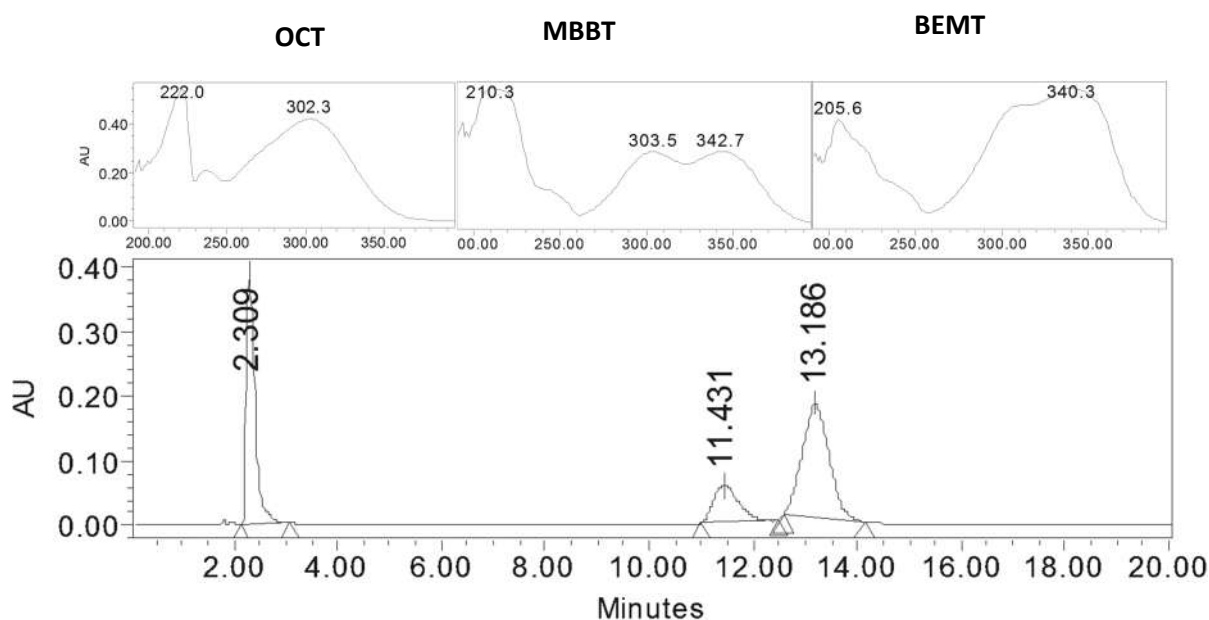
Figure 5.10: A typical HPLC chromatogram of OCT at retention time 2.309 minute, MBBT at 11.431 minute, and BEMT at 13.186 minutes on a reversed-phase C-12 Phenomenox synergi column (150 mm × 4.6 mm). The injection volume was 20 μL at a flow rate of 1 mL min^{-1} in isocratic elution mode of MeOH-ACN (90:10 v/v). The chromatogram was monitored at 304 nm.

Table 5.7: Summary of analytical parameters for representative calibration curves of the UV filters in the sunscreenproducts.

UV filter	Retention time/min	Standards range/μM	Slope	R^2	LOD/ μM	LOQ/ μM
BP3 [a]	3.73 - 3.83	3.12 - 4 99	1.37×10^{11}	0.987	0.1001	0.33
OCT [a]	8.88 - 8.90	5.90 - 189	1.29×10^{11}	9881	0.14	0.470
BMDBM [a]	9.77 – 10.37	4.37 - 273	3.31×10^{11}	0.9998	0.0132	0.044
EHMC [a]	11.00 - 11.40	4.86 - 778	2.15×10^{11}	0.9939	0.076	0.253
MBBT [b]	11.45 - 11.52	6.11- 196	2.64×10^{10}	0.9962	0.066	0.220
BEMT [b]	13.19 - 13.56	2.45 - 157	4.17×10^{10}	0.9784	0.191	0.637
TiO_2 [c]	-	0.48 - 2.5 [d]	4.49×10^4	0.9997	0.0187	0.0623
ZnO [c]	-	10.0 - 100.0 [e]	1.15×10^5	0.9999	0.0077	0.0256

[a] Chromatographic conditions: A reversed-phase C-12 Phenomenex Synergi 4μ Max-RP 80 Å column (150 mm × 4.6 mm); mobile phase: methanol–water (84:16 % v/v).
[b] Chromatographic conditions: A reversed-phase C-12 Phenomenex Synergi 4μ Max-RP 80 Å column (150 mm × 4.6 mm); mobile phase: methanol–acetonitrile (90:10 % v/v).
[c] Determined on a Perkin Elmer Optima 5300 DV ICP-OES in radial view mode monitored at 337.279 nm for TiO_2 and 206 nm for ZnO.
[d] the units are mol dm^{-3}, and [e] mg dm^{-3}.
The LOD is calculated as $3S_{y/x}b^{-1}$ ($S_{y/x}$ is the standard error of the slope and b is the slope of the calibration line) and LOQ is given as 3.33(LOD).

Table 5.8: Validation studies of the eight UV absorbers added to the test formulation.

UV absorber	Spiked mass/g	Recovery/% (m/m)
BMDBM	0.095 ± 0.021	100.5 ± 1.32
BP3	1.007 ± 0.147	99.7 ± 0.59
EHMC	0.0428 ± 0.0125	99.8 ± 1.01
OCT	0.035 ± 0.009	101.5 ± 4.39
MBBT	0.041 ± 0.011	99.5 ± 1.93
BEMT	0.020 ± 0.002	98.3 ± 2.48
TiO_2	0.021 ± 0.005	98.8 ± 0.46
ZnO	0.032 ± 0.0041	99.5 ± 0.99

($n = 5$) Each determination is mean ± SD.

Table 5.9: A summary of intra- and inter-day instrumental response analysis.

Sunscreen absorber	Conc./µM	Intra-day ($n = 5$)			Inter-day ($n = 5$)		
		Found/µM	RSD/%	Accuracy/%	Found/µM	RSD/%	Accuracy/%
BMBDM[a]	30	30.23 ± 0.95	3.14	100.8	29.57 ± 1.01	3.42	98.6
BP3[a]	60	59.87 ± 0.33	0.55	99.8	60.1 ± 0.56	0.93	100.2
EHMC[a]	50	50.12 ± 0.05	0.10	100.2	49.68 ± 0.96	1.93	99.4
BEMT[b]	20	19.99 ± 0.11	0.55	100.0	20.02 ± 0.12	1.00	100.1
MBBT[b]	40	39.98 ± 0.35	0.88	100.0	40.12 ± 0.85	0.60	100.3
OCT[a]	70	70.55 ± 0.46	0.65	100.8	69.85 ± 1.04	1.49	99.8
TiO_2	2 [d]	2.01 ± 0.02	0.10	100.5	2.01 ± 0.02	0.10	100.5
ZnO	80 [d]	80.80 ± 0.40	0.50	101.0	79.39 ± 0.06	0.08	99.2

Recovery/% = (mean of found concentration/theoretical amount) × 100 % and RSD/% = (SD/mean concentration) × 100 %,

n is the sample population, SD is standard deviation, and RSD is the relative standard deviation.

[a] Chromatographic conditions: A reversed-phase C-12 Phenomenex Synergi 4µ Max-RP 80 Å column (150 mm × 4.6 mm); mobile phase, methanol–water (84:16 v/v).

[b] Chromatographic conditions: A reversed-phase C-12 Phenomenex Synergi 4µ Max-RP 80 Å column (150 mm × 4.6 mm); mobile phase, methanol–acetonitrile (90:10 v/v).

[c] Determined on Perkin Elmer Optima 5300 DV ICP-OES in a radial view mode monitored at 337.279 nm for TiO_2 and 206 nm for ZnO.

[d] the units are mg dm^{-3}.

Table 5.10: The percentage levels of sunscreen agents in commercial sunscreen products containing plant extracts determined by HPLC.

SAMPLE	BMDBM[a]/% (m/m)	BP3[a]/% (m/m)	EHMC[a]/% (m/m)	OCT[a]/% (m/m)	MBBT[b]/% (m/m)	BEMT[b]/% (m/m)	TiO$_2$[c]/% (m/m)
XD	2.33 ± 0.21	4.25 ± 0.32	3.11 ± 0.45	-	-	-	-
PB	3.05 ± 0.65	2.69 ± 0.12	3.62 ± 0.92	4.02 ± 0.46	-	3.85 ± 0.63	-
B1	0	-	3.02 ± 0.08	-	2.65 ± 0.19	-	7.70 ± 0.09
B2	0	-	0	-	7.93 ± 1.90	-	8.81 ± 0.03
B3	0	-	-	-	2.81 ± 0.64	-	-
B4	0	-	0	-	3.15 ± 1.23	-	12.60 ± 0.21
P1	0.59 ±0.002	-	0.28 ± 0.0003	0.68 ± 0.002	-	5.62 ± 0.01	0.70 ± 0.01
P2	0.124 ± 0.004	5.37 ± 0.29	0.41 ± 0.0003	3.61 ± 0.19	-	-	7.43 ± 0.02
P3	0.26 ± 0.0004	5.01 ± 0.15	0.33 ± 0.007	2.65 ± 0.03	-	3.79 ± 0.04	1.50 ± 0.01
P4	2.49 ± 0.03	4.41 ± 0.15	-	2.75 ± 0.02	-	6.07 ± 0.11	0
P6	2.38 ± 0.81	-	-	2.47 ± 0.05	-	-	0.72 ± 0.04

(n = 5) Each measurement is average value ± SD.

[a] Chromatographic conditions: A reversed-phase C-12 Phenomenex Synergi 4μ Max-RP 80 Å column (150 mm × 4.6 mm); mobile phase: methanol–water (84:16 % v/v).

[b] Chromatographic conditions: A reversed-phase C-12 Phenomenex Synergi 4μ Max-RP 80 Å column (150 mm × 4.6 mm); mobile phase: methanol–acetonitrile (90:10 % v/v).

[c] Determined on a Perkin Elmer 5300 DV ICP-OES in a radial view mode monitored at 337.279 nm for TiO$_2$.

The amounts of sunscreen absorber detected but below the quantitation limit in this method are indicated as zero (0) and those without particular sunscreen absorber are indicated -.

Table 5.11: The percentage composition of zinc oxide in some selected sunscreen products in the market.

Sample ID	Product name	SPF	Zinc oxide/% (m/m)	Packet labelled Zinc oxide % (m/m)
SAU4	Banana boat ultra	30+	8.33 ± 0.63	8
SAU5	Banana boat sensitive skin	30+	8.74 ± 0.41	8
SAU6	Banana boat faces	30+	8.40 ± 0.39	8
SAU8	Triplegard		7.09 ± 0.17	7
SAU12	Solar block	30+	6.97 ± 0.08	6
SAU14	Banana boat kids	30+	8.61 ± 0.64	8
SAU16	UV triplegard kids lotion	30+	7.19 ± 0.95	6.06
SAU17	UV triplegard kids	30+	6.93 ± 0.10	7.07
SAU19	The cancer council of Australia - children	30+	6.17 ± 0.55	7
SAU21	Triplegard sun stick	30+	4.84 ± 0.54	5
SAU24	Triplegard lip balm	30+	5.03 ± 0.27	5

(n = 5) Each determination is mean ± SD.

The amounts of organic absorbers in these products and their photostabilities had previously been reported by Lyambila (2003).

5.3.2   Photostability of sunscreens products without plant extracts

The sunscreen products investigated in this work mainly contained the following agents: BEMT, MBBT, homosalate (HMS), ethylhexyl salicylate (EHS), ethylhexyl triazine (EHT), ensulizole, OCT, EHMC, BP3, BMDBM and one product contained terephthalylidene dicamphor sulphonic acid (TDSA). A number of them carried more than one sunscreen agent including the plant extracts. Most sunscreen products containing no plant extracts, showed a characteristic degradation but with some showing a notable photostability. This could be attributed to the inclusion of the photostable sunscreen absorbers: MBBT and BEMT, for example sample PB (Fig. 5.3). This sunscreen product, PB contained OCT, HMS, BP3, BMDBM and BEMT a combination that is envisaged to offer very high stability in the UVB and UVA regions (Fig. 5.3) making it a broad-spectrum photoprotective product. The very stable agent BEMT could explain its spectral stability in the UVA region. However, the sunscreen product XD (Fig 5.4), containing EHMC, BMDBM, BP3, and ensulizole showed a sudden increase in light transmittance under two hours of exposure. This is less the time,

normally recommended for reapplication. The sudden increase indicates high photoinstability in both UVB and UVA regions. The transmittance of great amounts of UVB and UVA radiation is potentially dangerous because, both UVB and UVA are defined as carcinogenic factors by the IARC (1992) and sub-erythemogenic UVA doses have been shown to be responsible for various biological effects, including induction of photoallergic complications, and skin photodamage. In addition, as a result of photochemical reactions, short-lived reactive photoproducts formed may react with biomolecules and give rise to potentially mutagenic products. This product is therefore quite unstable and harmful to the unsuspecting consumer.

Most sunscreens products showed similar photodegradation reported previously by Bunhu (2006). The problem with these commercial sunscreen products is that the percentage compositions of these sunscreens are not indicated on the pack and our HPLC analysis of some of these samples returned very low values. This implies the sunscreen composition may be inadequate to offer sufficient photoprotection. It is imperative that sufficient amounts of the ingredients be packaged and the percentage composition indicated on the pack. Table 5.7 summarizes the compositions of the sunscreen products investigated and their photo-transmission response.
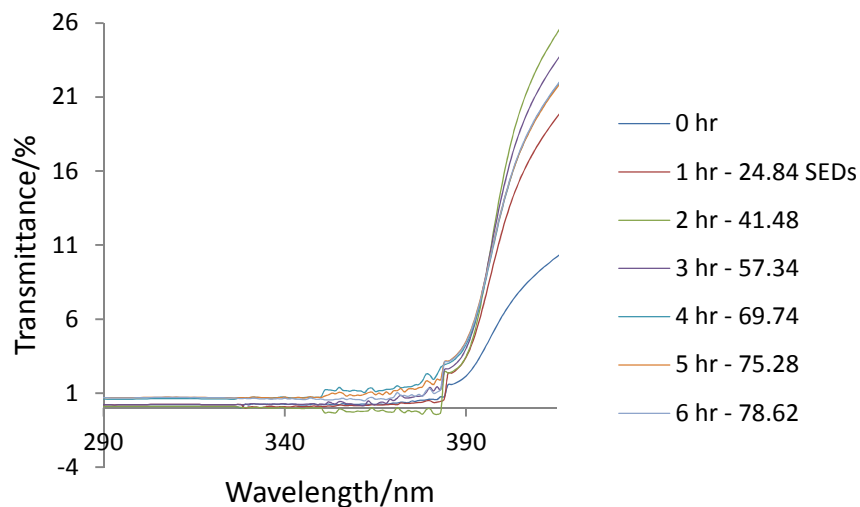
Figure 5.11: The photostability of the sunscreen PB without plant extracts applied on quartz plate (1.12 mg cm^{-2}) exposed to sunlight. The spectra were recorded on Perkin Elmer Lambda 35 UV-vis spectrophotometer.
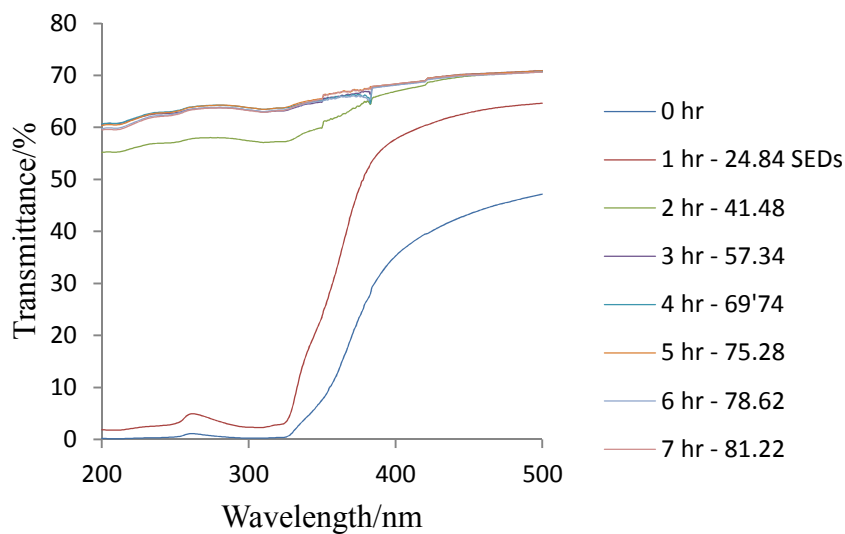
Figure 5.13: Photodegradation of sunscreen preparation XD containing EHMC, BP3, BMDBM and ensulizole. The application density was 1.33 mg cm^{-2}. The product was applied on quartz plate and the spectra recorded on a Perkin Elmer lambda 35 UV-vis dual beam spectrophotometer.

5.3.3 Photostability of Sunscreens with plant extracts

The sample P1 was indicated to contain the chemical absorbers OCT, BMDBM and BEMT, EHS, and the physical absorber and reflector TiO_2. The plant extract present was listed to be *Simmondsa chinensis* (Jojoba seed oil). When the quartz plates with sample P1 applied was exposed to sunlight the transmission characteristics appeared to drop in the long wavelength region (Fig. 5.5). The significant drop in the long wavelength could be due to the high degree of conjugated unsaturation of new photoproducts. These spectral modifications indicate the conversion of phytochemicals and the incorporated chemical absorbers to other forms, which might be UVA-absorbing. These changes are however, small possibly due to inclusion of stable chemical absorbers like BEMT and the physical absorber TiO_2. The overall conclusion is that either way exposure of this product to solar radiation causes chemical changes that could be accompanied with complete new products formed. The formed photo-induced chemical species have different photo-absorption characteristics. The spectral transmission behaviour varied from product to product in terms of magnitude of photo-absorption in the UVA2 and UVA1. The product P3 containing the sunscreen agents OCT, EHMC, BP3, HMS, EHS, BMDBM, BEMT and TiO_2 had *vinifera* (grape) seed extract, *vaccinium oxycoccos* (cranberry) extract and Lycium Chinese fruit extract incorporated. This product showed pronounced drops in percent light transmission across the UV spectrum (Fig. 5.6). The samples P2, P4, and P6 had much lower spectral change characteristics showing broad-spectrum protection; these products contained various plant extracts (see Supplementary Materials). The product P2 contained jojoba seed oil and *Buddleja davidii* extracts but the offered photoprotection was perceived lower as it allowed light to pass through across the entire spectrum. Product P6 proved to be very good sunscreen formulation in the seven hour continuous exposure. This product contained OCT, BMDBM, EHT, FeO, TiO_2, TDSA and *Cocos nucifera* extract. The product showed remarkable increase in absorption of light indicated by drop in transmission to well below 2 % at 400 nm (see Table 5.7 and Supplementary Material S5.10). The effect of physical absorbers in these sunscreen products could not be verified because the spectral behaviour of the products was not significantly different when compared to those without physical absorbers (eg P4 and P4).
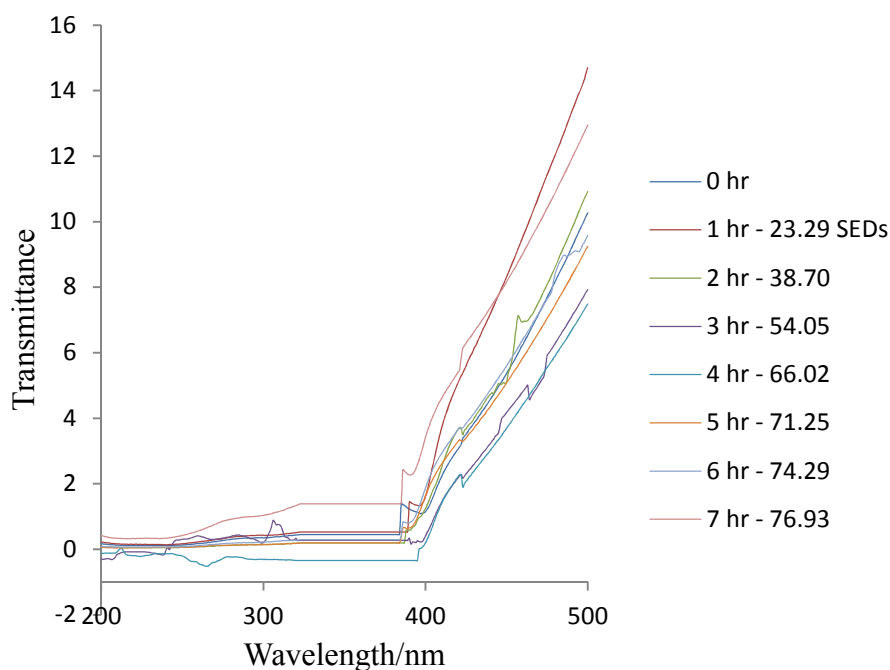
Figure 5.13: Spectral changes of sample P1 applied on quartz plate (1.03 mg cm^{-2}) exposed to sun light. The product was applied on quartz glass plate and spectra recorded on Perkin Elmer Lambda 35 UV-vis dual beam spectrophotometer.
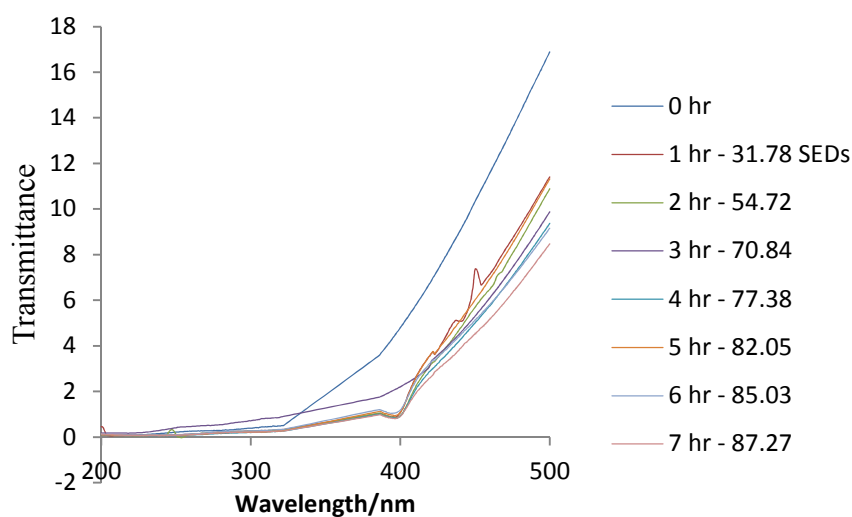
Figure 5.13: Transmittance spectra of sample P3 applied on quartz plate (0.99 mg cm^{-2}) exposed to sun light. The product was applied on quartz glass plate and spectra recorded on a Perkin Elmer lambda 35 UV-Vis dual beam spectrophotometer.

Table 5.12: The composition of the sunscreen products used in the study and their effect upon solar exposure.

Sunscreen product code	Product name	Sunscreen present	Antioxidant present	Plant Extracts	Effect on transmission due to solar exposure
XD	Xeroderm (SPF 34)	EHMC BMDBM BP3 Ensulizole	Tocopherol acetate		Sharp increase in light transmission
PB	Piz buin	OCT HMS BP3 BMDBM BEMT	Tocopheryl acetate		Small Increase
P1	Garnier Ambre Solaire (SPF 50+)	TiO_2 BEMT EHS BMDBM OCT		*Simmondsa chinensis* extract (Jojoba seed oil)	Drop
P2	Techni block	OCT EHMC EHS BMDBM BP3 TiO_2		*Buddleja davidii* extract Jojoba seed oil	Drop
P3	Everysun family (SPF 40)	OCT EHMC BP3 HMS EHS BMDBM BEMT TiO_2		*Vinifera* (grape) seed extract *Vaccinium oxycoccos* (cranberry) extract *Lycium* Chinese fruit extract	Drop
P4	Tropitone (SPF 30)	OCT EHS HMS BP3 BMDBM BEMT Tin Oxide TiO_2		*Cocos nucifera Gardenia tahitensis*	Drop

P6	Garnier amber solaire (SPF 30)	OCT BMDBM EHT FeO TiO$_2$ TDSA		*Cocos nucifera*	Drop
B1	Disaar (SPF 60)	EHMC MBBT BMDBM EHT TiO$_2$		Green tea	Small drop
B2	Disaar (SPF 90)	EHMC MBBT BMDBM EHT TiO$_2$	Tocopheryl acetate Ascprbyl tetraisopalmitate	O-cymen-5-ol	Increase
B3	Disaar (SPF 60/90)	EHMC MBBT BMDBM EHT TiO$_2$	Tocopheryl acetate Ascprbyl tetraisopalmitate Trehalose Propylene glycol	O-cymen-5-ol	Increase
B4	Disaar beauty skin cream (SPF 60)	EHMC MBBT BMDBM EHT TiO$_2$	Propylene glycol Tocopheryl acetate Ascprbyl tetraisopalmitate	O-cymen-5-ol	Increase

5.4   Discussion

UV radiation is reported to be largely responsible for the most damaging effects of sunlight on the skin. The commonly used sunscreens are used to absorb this radiation because they show good absorption in this region. It is known exposure of the skin to UV light gives rise to the formation of active oxygen intermediates (Mefferth et al., 1976; Fuchs and Packar, 1991) and lipid peroxidation products increases greatly in chronically sun-exposed human skin (Mefferth et al., 1976). Therefore, a topical application that shows great potential of attenuating or absorbing UV light presents a good remedy for deleterious UV effects.

The products investigated in this work showed varying degrees of photoprotection depending on the chemical composition and the plant extracts incorporated. Plants are known to have varying phytochemical compositions based on species and even on geographical location. It is not surprising that the photochemical behaviours of these products are different. The phytochemicals present in these plants play a major role in protecting the plant itself against UV radiation as well preventing oxidative damage to the plant tissues induced by UV light. Major plant phytochemicals known to inhibit photo-induced radical chain reactions are flavonoids. Besides scavenging UV-induced radicals and so stopping propagation of lipid peroxidative chain reactions, flavonoids may provide their protective effect against UV radiation by acting as strong UV-absorbing sunscreens. This group

of compounds belongs to the larger class of compounds referred to as polyphenols, which are natural antioxidants and are known to provide protection against UV irradiation-induced cytotoxicity.

A product P3 in this work showed much longer wavelength protection compared to other products under study. This product is labelled to contain *vinifera* seed extract, cranberry extract and lycium Chinese fruit extract. The actual composition of these extracts in this product while it is unknown to us but the chemical compositions of each of the extract are known. The major chemical component of *vinifera* seed extract are anthocyanins (Bagchi et al. 2000; Santosh 2008) which are known antioxidant and strong UV absorbers (Rancan et al. 2002). Product P2 showed relatively lower photoprotection of the products investigated, however, because of the inclusion of the plant extracts we expect less UV induced effects because of polyphenols present from the plant extracts. This product contains *Buddleja davidii* extract which has been shown to be rich in flavonoid related compounds (Fan et al. 2008) and Jojoba seed oil. This observation opens another question of possible antagonistic effects between the phytochemical components in the extracts and the incorporated sunscreen agents.

It is reported that UVA radiation penetrates deeply into the skin (Tyrrell, 1991); therefore, after topical application, antioxidant molecules may provide the skin with satisfactory photoprotection only if they are able to permeate through the stratum corneum and, therefore reach deeper skin layers. The permeability barrier of the skin is determined by the stratum corneum, which is viewed as the main obstacle against the penetration of exogenous substances through the skin. Products P4 and P6 contained among other ingredients *Cocos nucifera* extract. This particular extract is reported to contain various phytochemicals like vitamins (Yong et al. 2009). These compounds are known to permeate deeply into the skin, and hence are likely to offer systemic protection against UVA induced free radical reactions. Recently quercetin (a flavonoid) was shown to be able to permeate through the stratum corneum and, so, to penetrate into deeper skin layers. Results from the work by Marquele-Oliveira et al. (2007) showed that antioxidant compounds present in propolis extract were able to reach the lower layers of skin. This conclusion was informed by observed antioxidant activity in the viable epidermis of pig skin and in the whole hairless mouse skin. These findings suggest that topically applied antioxidants could be excellent candidates for successful employment as protective agents in certain skin diseases caused, initiated or exacerbated by sunlight irradiation (Bonina et al. 1996). Nevertheless, evaluation of cutaneous permeation and *in vivo* efficacy of formulations containing plant extracts are necessary in order to confirm their use for skin photoprotection. Topical administration of antioxidants has recently proved to represent a successful strategy for protecting the skin against UV-mediated oxidative damage (Chen et al. 2012). This approach has been shown to provide an efficient way to enrich the endogenous cutaneous protection system, and thus may be a successful strategy for diminishing UV radiation-mediated oxidative damage on the skin (Saija et al. 1998).

It has been widely reported that polyphenols prevent photo-oxidative stress in the skin, it would be important to know if plant extracts containing these substances maintain their action after inclusion in topical formulations. Another important parameter to study is how they may interfere with the physical stability of the formulation. This thought line is motivated by a recent work by Mambro and Fonseca (2005), whose result suggested that plant extracts could be active against one free radical but fail to protect the skin against other reactions mediated by free radicals. These authors observed sufficient antioxidant activity of polyphenols via chemiluminescence assay but same compounds could not inhibit lipid peroxidation. These polyphenols are also susceptible to temperature and

humidity action, and their stability profile and biological activity are strongly related and affected by processing and storage conditions.

5.5 Conclusions

The aim of this study was to investigate the photostability of sunscreens preparations containing plant extracts. Two categories of commercial sunscreens were investigated in this work: sunscreens products without plant extracts and those with plants extracts or phytochemicals. All the products containing sunscreens without plant extracts showed photodegradation. Those preparations with plant extracts showed a decrease in spectral transmittance in both the short and long wavelength regions. The broad-spectrum photo-absorption demonstrated may enhance a products' efficacy in UV protection and minimize or eliminate deleterious UV effects. There was notable spectral lability in some products in both short and long wavelength region of the UV spectrum. This implies formation of photochemical species of diverse structural morphology. This warrants further research to ascertain photo-toxicities of these new photochemical products.

References

Bagchi D, Bagchi M, Stohs SJ, Das DK, Ray SD, Kuszynski CA, Joshi SS, Pruess H (2000) Free radicals and grape seed proanthocyanidin extract: importance in human health and disease prevention. Toxicology 148 (2):187-197

Bonina F, Lanza M, Montenegro L, Puglisi C, Tomaino A, Trombetta D, Castelli F, Saija A (1996) Flavanoids as potential protective agents against photo-oxidative skin damage. International journal of pharmaceutics 145:87-94

Broadbent KJ, Martincigh BS, Raynor WM, Salter FL, Moulder R, Sjoberg P, Markides EK (1996) Capillary supercritical fluid chromatography combined with atmospheric pressure chemical ionisation mass spectrometry for the investigation of photoproduct formation in the sunscreen absorber 2-ethylhexyl methoxycinnamate. Journal of Chromatography A 732:101-110

Bunhu T (2006) An Assessment of the Photostability of South African Commercial Sunscreens. MSc Dissertation, University of KwaZulu-Natal, Durban, South Africa

Cameron GJH, Michael SR (1997) Systematic absorption of sunscreen after topical application. Lancet 350 (9081):863-865

Casetti F, Miese A, Mueller ML, Simon JC, Schempp CM (2011) Double trouble from sunburn: UVB-induced erythema is associated with a transient decrease in skin pigmentation. Skin Pharmacology and Physiology 24 (3):160-165

Chen L, Hu YJ, Wang QS (2012) The role of antioxidants in photoprotection: A critical review. Journal of American Academy of Dermatology 67:1013-1024

Chisvert A, Vidal MT, Salvador A (2002) Sequential injection analysis for benzophenone-4 and phenylbenzimidazole sulphonic acid in sunscreen sprays by solid-phase extraction coupled with ultraviolet spectrometry. Analytica Chimica Acta 464:295-301

Cortat B, Garcia CCM, Quinet A, Schuch AP, de Lima-Bessa KM, Menck CFM (2013) The relative roles of DNA damage induced by UVA irradiation in human cells. Photochemical and Photobiological Sciences 12 (8):1483-1495

Cuquerella MC, Lhiaubet-Vallet V, Cadet J, Miranda AM (2012) Benzophenone Photosensitised DNA Damage. Accounts of Chemical Research 45 (9):1558 - 1570

Dai J, Mumper RJ (2010) Plant Phenolics: Extraction, Analysis and Their Antioxidant and Anticancer Properties. Molecules 15 (10):7313-7352

Fan P, Hay A-E, Marston A, Hostettmam K (2008) Acetycholinesterase-inhibitory activity of linarin from Buddleja davidii, structure-activity relationships of related flavonoids, and chemical investigation of buddleja nitida. Pharmaceutical Biology 46 (9):596-601

Fourtanier A, Moyal D, Seite S (2012) UVA filters in sun-protection products: regulatory and biological aspects. Photochemistry and Photobiological Sciences 11 (1):81-89

Gaspar LR, Campos PMBGM (2007) Photostability and efficacy studies of topical formulations containing UV-filters combination and vitamins A, C and E. International journal of pharmaceutics 343 (1–2):181-189

Hagedorn-Leweke U, Lippold BC (1995) Absorption of sunscreens and other compounds through human skin in vivo: derivation of a method to predict maximum fluxes. Pharmaceutical Research 12 (9):1354-1360

IARC IAfRoC (1992) IARC monographs on the evaluation of carcinogenic risks to humans. Solar and ultraviolet radiation. IARC Monograph of Evaluation of Carcinogenic Risks to Humans 55:1-316

Ikeda K, Suzuki S, Watanabe Y (1990) Determination of sunscreen agents in cosmetic products by gas chromatography and gas chromatography-mass spectrometry. Journal of Chromatography 513:321-326

Ingouville AN (1995) The photochemical behaviour of the sunscreen absorber 2-ethylhexyl methoxycinnamate. MSc. Dissertation, University of Natal, , Durban, South Africa

Jiang R, Roberts MS, Collins DM, Benson HA (1999) Absorption of sunscreens across human skin: an evaluation of commercial products for children and adults. British Journal of clinical Pharmacology 48:635-637

Kanavy HE, Gerstenblith MR (2011) Ultraviolet radiation and melanoma. Seminars in Cutaneous Medicine and Surgery 30 (4):222-228

Kim K, Mueller J, Park Y-B, Jung H-R, Kang S-H, Yoon M-H, Lee J-B (2011) Simultaneous determination of nine UV filters and four preservatives in suncare products by High Performance Liquid Chromatography Journal of Chromatographic Science 49:554-558

Kockler J, Oelgemoller M, Robertson S, Glass DB (2012) Photostabililty of sunscreens. Journal of Photochemistry and Photobiology C: Photochemistry Reviews 13:91-110

Krause M, Kilt A, Blomberg JM, Soeborg T, Frederiksen H, Schlumpf M, Lichtensteiger W, Skakkebaek NE, Drzewiecki KT (2012) Sunscreens: are they beneficial for health? An overview of endocrine disrupting properties of UV-filters. International Journal of Andrology 35:424 - 436

Lyambila W (2003) A study of photoinduced transformations of sunscreen chemical absorbers. PhD Thesis, University of Natal, Durban, South Africa

Mambro MDV, Fonseca JVM (2005) Assays of physical stability and antioxidant activity of a topical formulation added with different plant extracts. Journal of pharmaceutical and biomedical analysis 37:287-295

Manova E, Goetz vN, Hauri U, Bogdal C, Hungerbuhler (2013) Organic UV in personal care products in Switzerland: A survey of occurrence and concentrations. International Journal of Hygiene and Environmental Health 216:508-514

Marquele-Oliveira F, Fonseca YM, de Freitas O, Fonseca MJV (2007) Development of topical functionalized formulations added with propolis extract: Stability, cutaneous absorption and in vivo studies. International of Journal of Pharmaceutics 342:40-48

Miller JC, Miller JN (1984) Statistics for Analytical Chemistry. Wiley, New York

Oesterwalder U, Herzog B (2009) Chemistry and properties of organic and inorganic UV filters. Clinical Guide to Sunscreens and Photoprotection. Informa Healthcare, New York, USA

Perrson EA, Edstrom WD, Backvall H, Lundeberg J, Ponten F, Ros A-M, Williams C (2002) The mutagenic effect of ultraviolet-A1 on human skin demonstrated by sequencing the p53 gene in single keratinocytes. Photodermatology, Photoimmunology and Photomedicine 18:287-293

Poiger T, Buser H-R, Balmer EM, Bergqvist P-A, Muller DM (2004) Occurrence of UV filter compounds from sunscreens in surface waters: regional mass balance in two Swiss lakes. Chemosphere 55:951-963

Rancan F, Rosan S, Boehm K, Fernandez E, Hidalgo ME, Quihot W, Rubio C, Boehm F, Piazena H, Oltmanns U (2002) Protection against UVB irradiation by natural filters extracted from lichens. Journal of Photochemistry and Photobiology B: Biology 68:133-139

Saija A, Tomaino A, Trombetta D, Giacchi M, De Pasquale A, Bonina F (1998) Influence of different penetration enhancers on in vitro skin permeation and in vivo photoprotective effect of flavonoids. International journal of pharmaceutics 175:85-94

Salter LF, Martincigh BS, Bolton K, Aliwell SR, Clemmett SJ (1993) Thymine Dimer Formation Mediated by the Photosensitizing Properties of Pharmaceutical Constituents. In: Swenberg C, Horneck G, Stassinopoulos EG (eds) Biological Effects and Physics of Solar and Galactic Cosmic Radiation, vol 243A. NATO ASI Series. Springer US, pp 63-70

Sambandan RD, Ratner D (2011) Sunscreens: An overview and update. Journal of American Academy of Dermatology 64 (4):748-758

Santosh KK (2008) Grape seed proanthocyanidines and skin cancer prevention: Inihibition of oxidative stress and protection of immune system. Molecular Nutrition and Food Research 52 (Suppl 1):S71-S76

Scalia S, Tursilli R, Bianchi A, Lo Nostro P, Bocci E, Ridi F, Baglioni P (2006) Incorporation of the sunscreen agent, octyl methoxycinnamate in a cellulosic fabric grafted with beta-cyclodextrin. International journal of pharmaceutics 308 (1-2):155-159

Schwack W, Rudolph T (1995) Photochemistry of dibenzoyl methane UVA filters Part 1. Journal of Photochemistry and Photobiology B: Biology 28:229-234

Seite S, Moyal D, Verdier M-P, Hourseau C, Fourtanier A (2000) Accumulated p53 protein and UVA protection level of sunscreens. Photodermatology, Photoimmunology and Photomedicine 16:3-9

Serge F (2008) Rationale for sunscreen development. Journal of American Academy of Dermatology 58:133-138

Serpone N, Salinaro A, Emeline AV, Horikoshi S, Hidaka H, Zhao JC (2002) An in vitro systematic spectroscopic examination of the photostabilities of a random set of commercial sunscreen lotions and their chemical UVB/UVA active agents. Photochemical and Photobiological Sciences 1 (12):970-981

Sklar LR, Almutawa F, Lim HW, Hamzavi I (2013) Effects of ultraviolet radiation, visible light, and infrared radiation on erythema and pigmentation: a review. Photochemical and Photobiological Sciences 12 (1):54-64

Soobrattee MA, Neergheen VS, Luximon-Ramma A, Aruoma OI, Bahorun T (2005) Phenolics as potential antioxidant therapeutic agents: mechanism and actions. Mutation Research 579 (1-2):200-213

Vielhaber G, Grether-Beck S, Koch O, Johncock W, Krutmann J (2006) Sunscreens with absorption maximum of 360 nm provide optimal protection against UVA1-induced expression of matrix metalloproteinase-1, interleukin-1, and interleukin-6 in human dermal fibroblasts. Photochemistry and Photobiological Sciences 5:275-282

Yamaguchi LF, Vassao DG, Kato MJ, Di Mascio P (2005) Biflavonoids from Brazilian pine Araucaria angustifolia as potentials protective agents against DNA damage and lipoperoxidation. Phytochemistry 66 (18):2238-2247

Yong JW, Ge L, Ng YF, Tan SN (2009) The chemical composition and biological properties of coconut (Cocos nucifera L.) water. Molecules 14 (12):5144-5164

Zhao JF, Jin XH, E YP, Zheng ZS, Zhang YJ, Athar M, DeLeo VA, Mukhtar H, Bickers DR, Wang ZY (1999) Photoprotective effect of black tea extracts against UVB-induced phototoxicity in skin. Photochemistry and photobiology 70 (4):637-644

Supplementary Materials
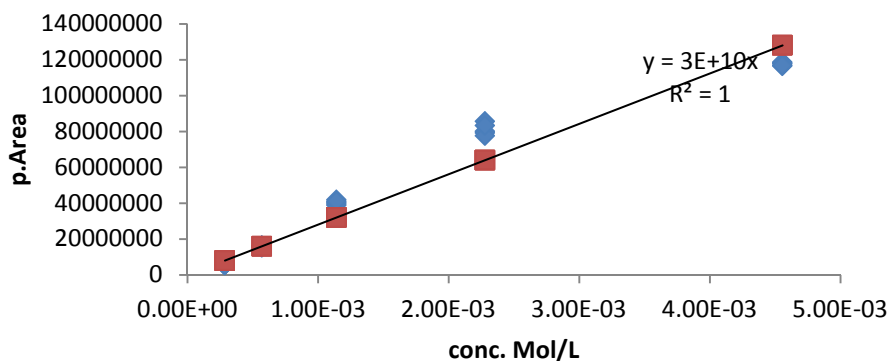
Figure S5.1: HPLC calibration curve for the determination of BMDBM in sunscreen preparations. The chromatographic conditions were: A reversed-phase C-12 Phenomenex Synergi 4μ Max-RP 80 Å column (150 mm × 4.6 mm), a mobile phase composition of methanol-water (84:16, v/v) at a flow rate of 1 mL min^{-1} and detection wavelength of 358 nm at ambient temperatures.
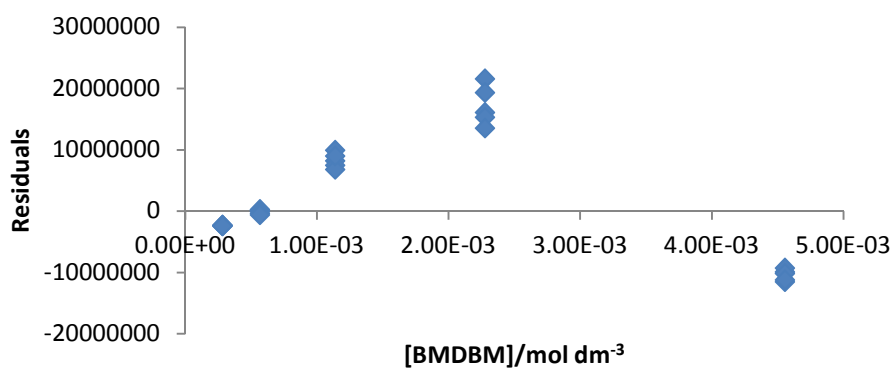
Figure S5.2: Residual plot for BMDBM
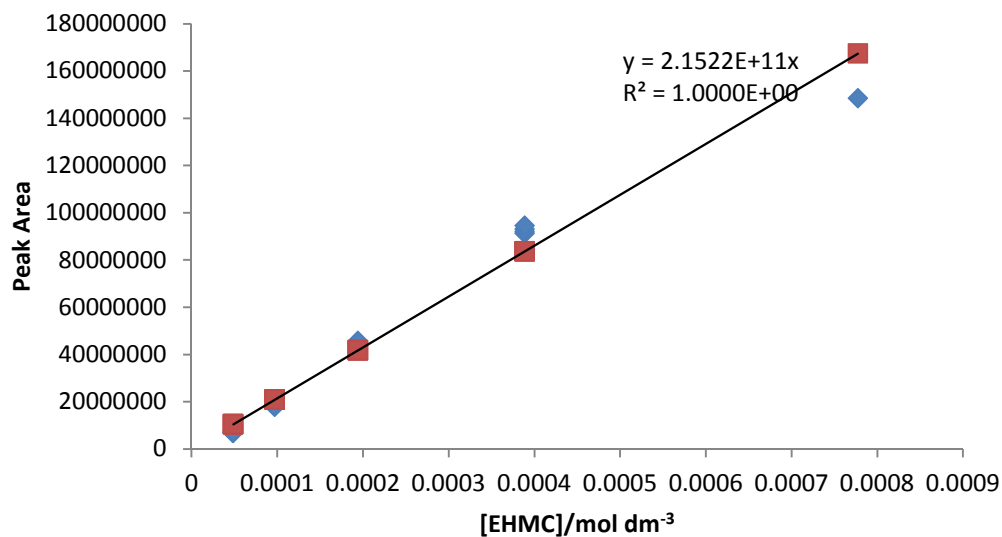
Figure S5.2.1: HPLC calibration curve for the determination of EHMC in sunscreen preparations. The chromatographic conditions were: A reversed-phase C-12 Phenomenex Synergi 4μ Max-RP 80 Å column (150 mm × 4.6 mm), a mobile phase composition of methanol-water (84:16, v/v) at a flow rate of 1 mL min^{-1} and detection wavelength of 310 nm at ambient temperatures.
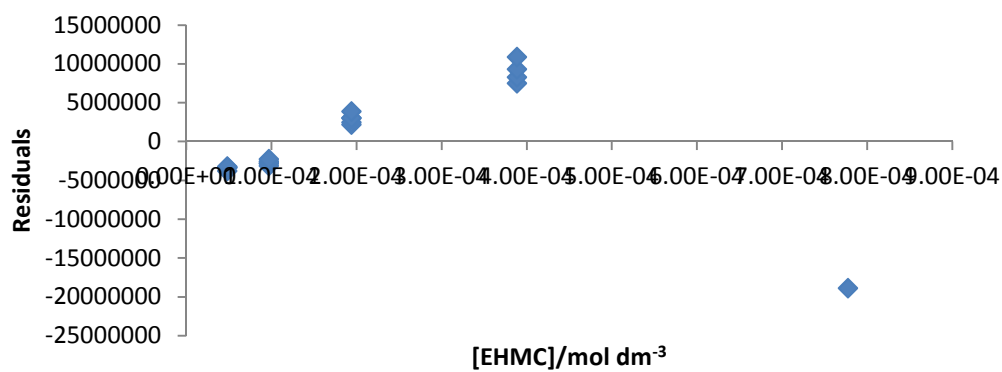
Figure S5.2.2.: Residuals plot for EHMC
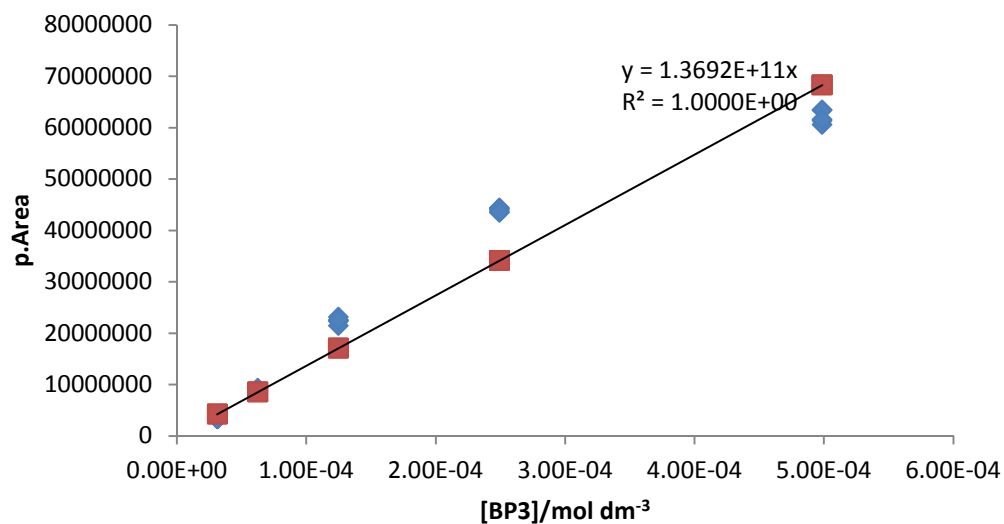
Figure S5.3.1: HPLC calibration curve for the determination of BP3 in sunscreen preparations. The chromatographic conditions were: A reversed-phase C-12 column Phenomenex Synergi 4μ Max-RP 80 Å, (150 mm × 4.6 mm), a mobile phase composition of methanol-water (84:16, v/v) at a flow rate of 1 mL min^{-1} and detection wavelength of 286 nm at ambient temperatures.
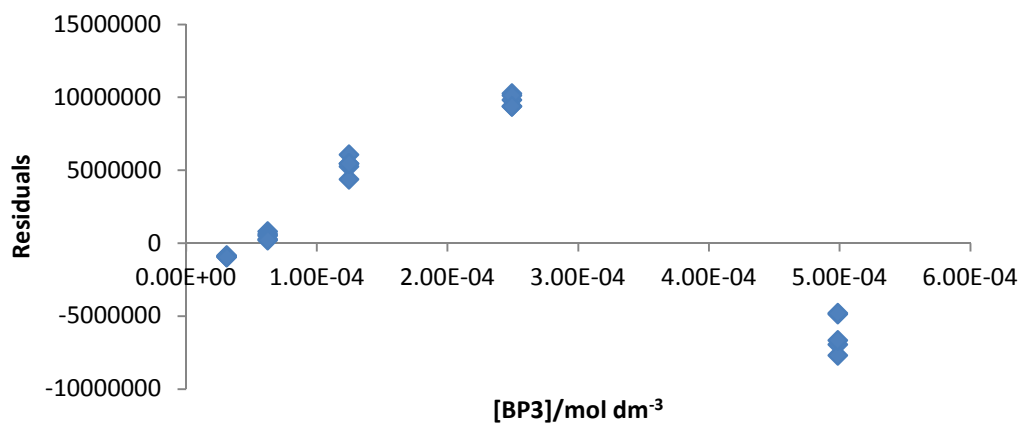
Figure S5.3.2: Residual plot for BP3
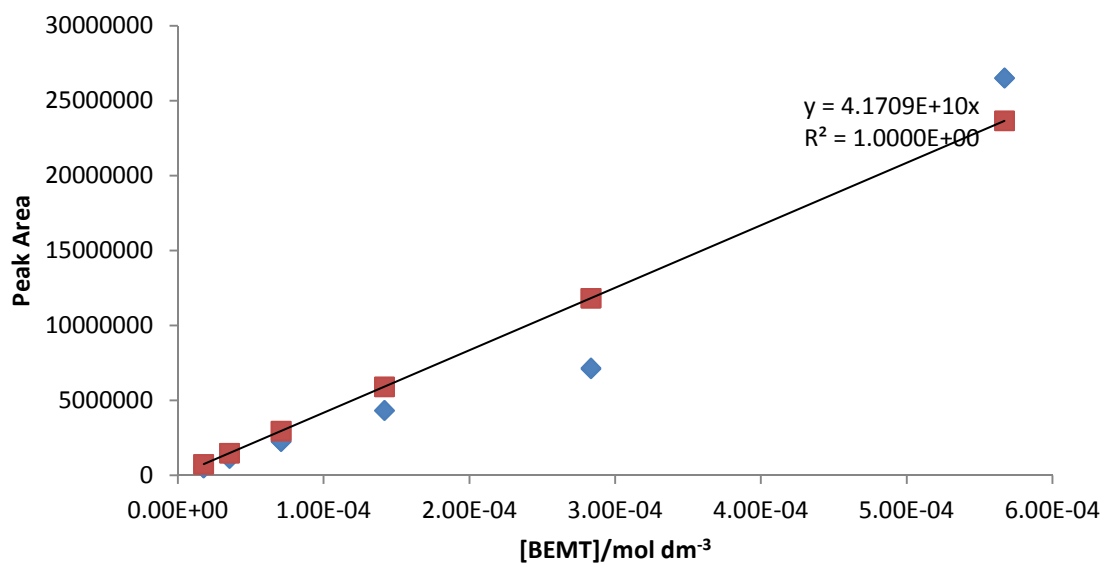
Figure S5.4.1: HPLC calibration curve for the determination of BEMT in sunscreen preparations. The chromatographic conditions were: A reversed-phase C-12 column Phenomenex Synergi 4μ Max-RP 80 Å, (150 mm x 4.6 mm), a mobile phase composition of methanol-water (90.10 v/v) at a flow rate of 1 mL min^{-1} and detection wavelength of 342 nm at ambient temperatures.
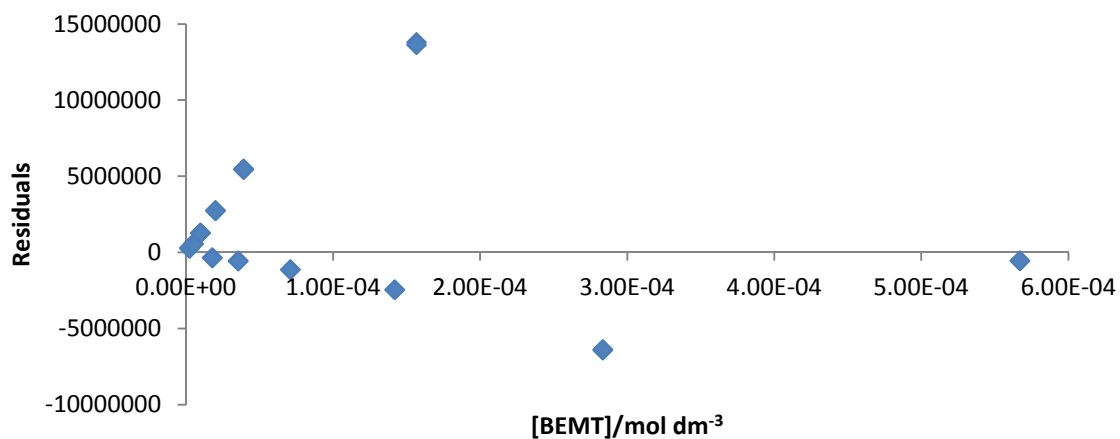
Figure S5.4.2: Residual plot for BEMT
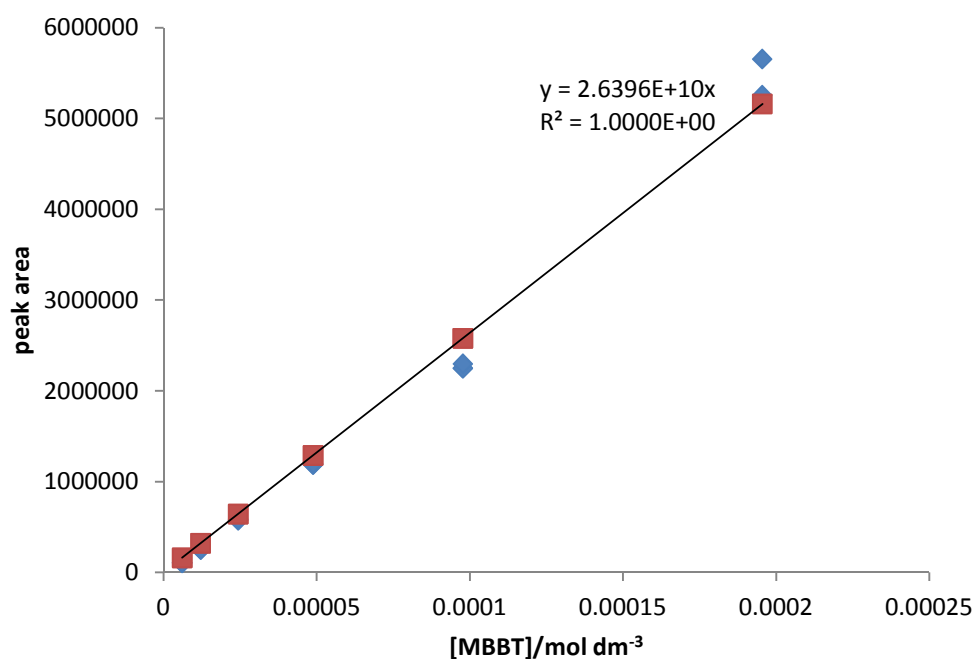
Figure S5.5.1: HPLC calibration curve for the determination of MBBT in sunscreen preparations. The chromatographic conditions were: A reversed-phase C-12 column Phenomenex Synergi 4μ Max-RP 80 Å, (150 mm × 4.6 mm), a mobile phase composition of methanol-water (90.10 v/v) at a flow rate of 1 mL min^{-1} and detection wavelength of 342 nm at ambient temperatures.
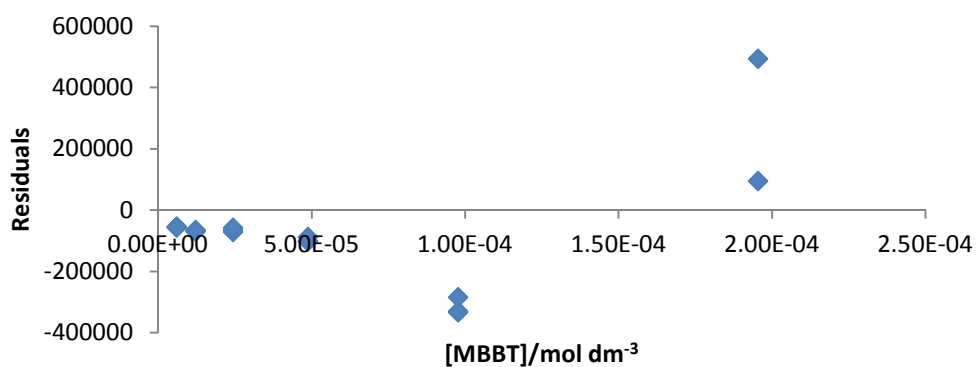
Figure S5.5.2:: Residual plot for MBBT.
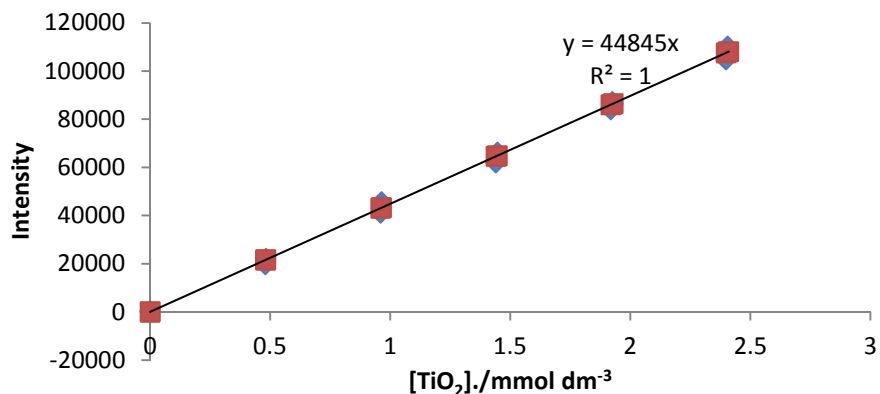
Figure S5.6.1: The calibration curve for quantitation of TiO_2 on ICP-OES operating conditions were: argon gas flow rate of 1.5 litres (L) min^{-1}, auxiliary and nebulizer gas flows at 0.2 L min^{-1} and 0.8 L min^{-1} respectively. The pump flow rate was set at 1.5 mL min^{-1} while plasma radiofrequency working at 1300 W and data acquired at 337.279 nm wavelength.
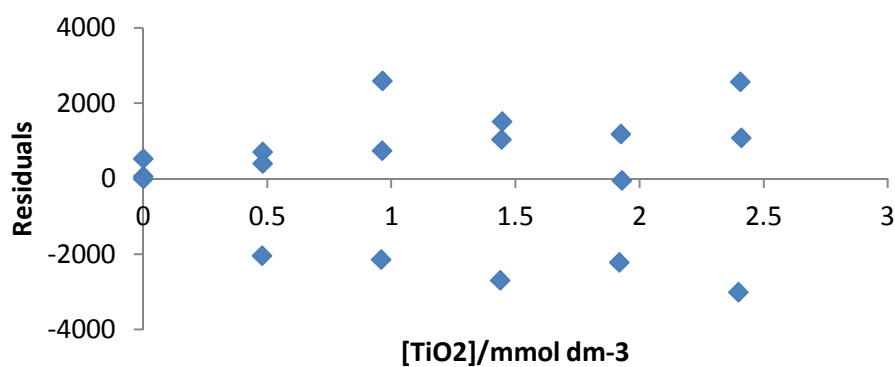
Figure S5.6.2: Residual plot for TiO_2
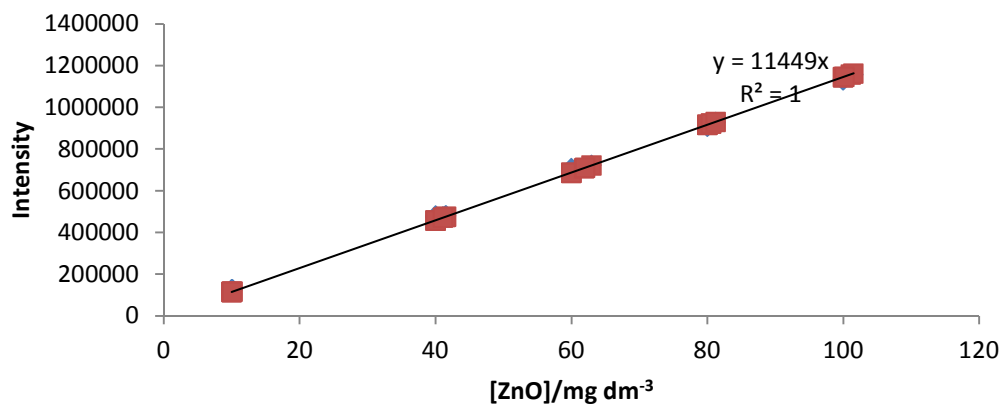
Figure S5.7.1: The calibration curve for quantitation of ZnO on ICP-OES operating conditions were: argon gas flow rate of 1.5 L min^{-1}, auxiliary and nebulizer gas flows at 0.2 L min^{-1} and 0.8 L min^{-1} respectively. The pump flow rate was set at 1.5 mL min^{-1} while plasma radiofrequency working at 1300 W and data acquired at 206 nm wavelength.
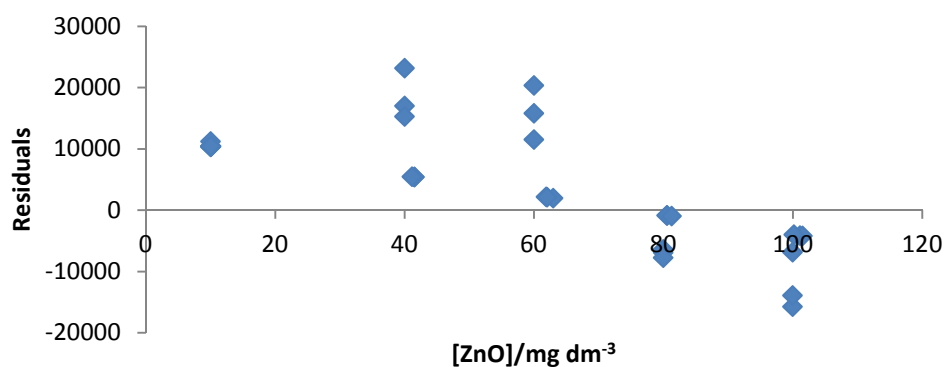
Figure S5.7.2: Residual plot for ZnO.

Photostability experiments for sunscreens with plant extracts
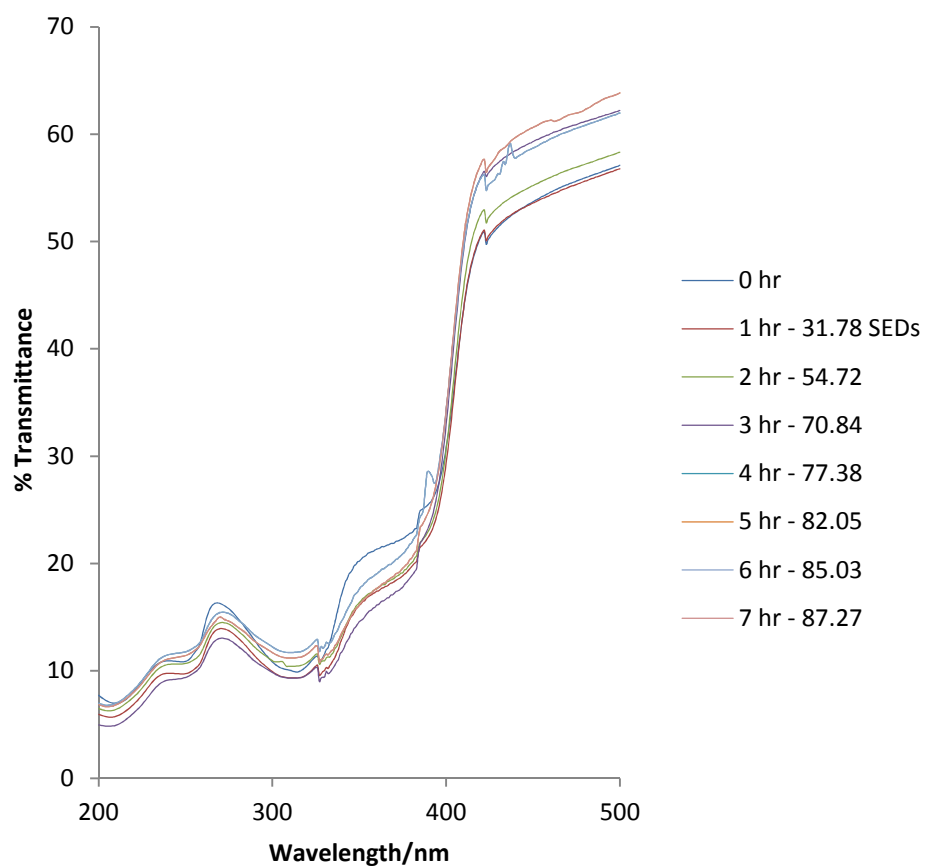
Figure S5.8: Spectral changes of sample P2 applied on quartz plate (1.02 mg cm^{-2}) exposed to sun light. The product was applied on quartz glass plate and spectra recorded on Perkin Elmer lambda 35 UV-Vis spectrophotometer.
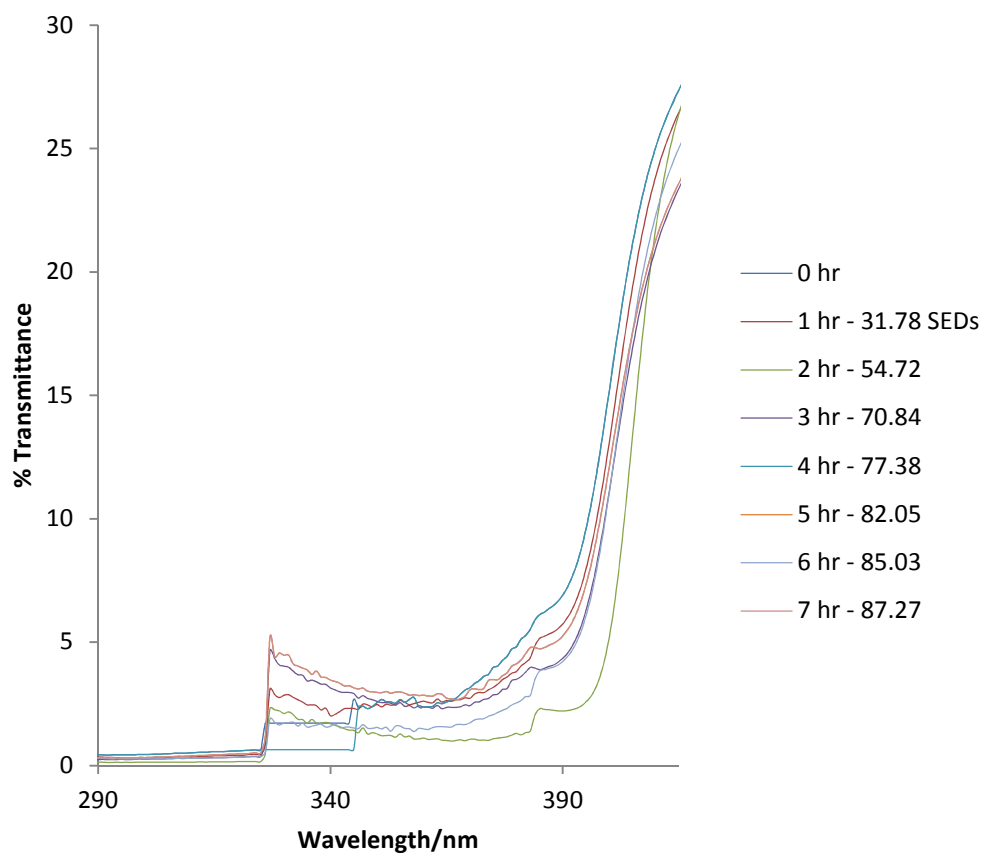
Figure S5.9: Spectral changes of sample P4 applied on quartz plate (1.00 mg cm^{-2}) exposed to sun light. The product was applied on quartz glass plate and spectra recorded on Perkin Elmer lambda 35 UV-Vis spectrophotometer.
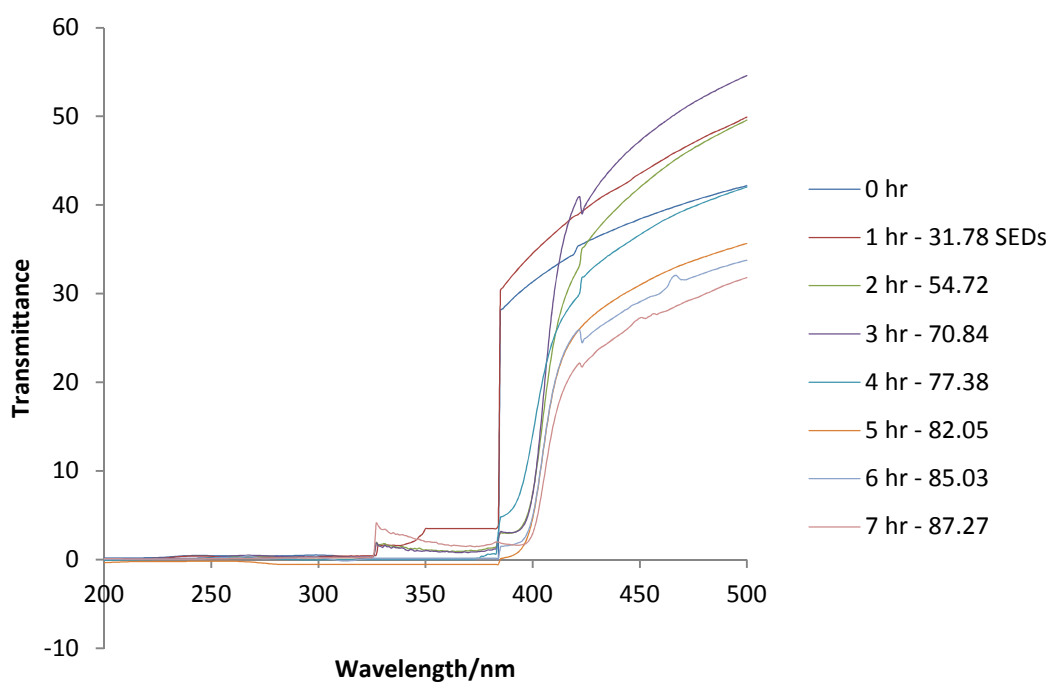
Figure S5.10: Spectral changes of sample P6 applied on quartz plate (1.12 mg cm^{-2}) exposed to sun light. The product was applied on quartz glass plate and spectra recorded on Perkin Elmer lambda 35 UV-Vis spectrophotometer.
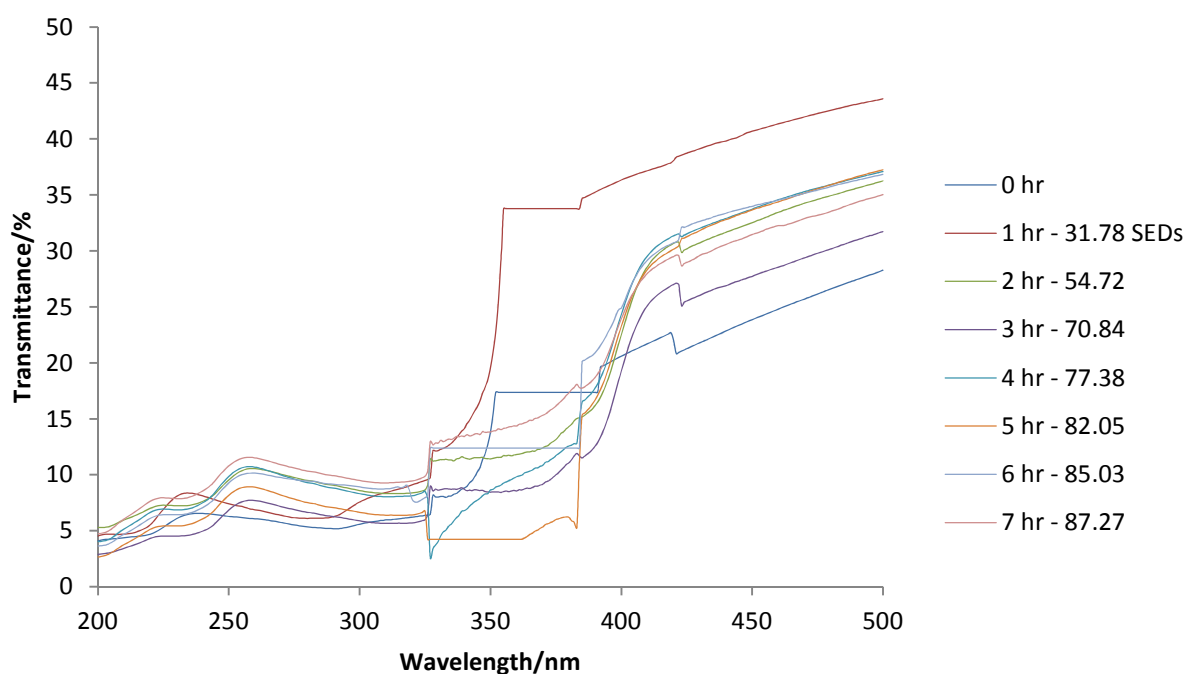
Figure S5.11: Spectral changes of sample B1 applied on quartz plate (1.03 mg cm^{-2}) exposed to sun light. The product was applied on quartz glass plate and spectra recorded on Perkin Elmer lambda 35 UV-Vis spectrophotometer.

Table S5.1: Recovery data for sunscreen analysis.

BMDBM	BP3	EHMC	BEMT	MBBT	OCT
85702617	49558373	51761148	82619914	67893224	93540756
86319709	50184832	52140932	82296827	68488281	93174878
85470431	49494526	52149613	82403375	68488256	94073428
85836085	47384756	51997817	82645404	68528015	93798580
84924711	48510880	51935928	81535279	67181774	93372005
85696080	49756460	51951388	82536263	69161773	93372000
86575973	49090651	52045120	82535270	67161779	93372116

Table S5.2: The actinometric data used in this work.

Time/hr	Time/s	Dod/Area	Val/Area	Val/Dod	RRF	Conc. Rem. Val/M	k_0/mol/L/s	I_0/einstein/L/s	F_0/ W/m^2	cum F_0/ W/m^2	SED/ J/m^2
0	0	3097493	2386120	0.77	346.27	0.0023					
1	3600	2981028	1202842	0.40	346.27	0.0013	2.94E-07	3.00E-07	0.88	0.88	31.78
2	7200	2658511	640280	0.24	346.27	0.00081	2.12E-07	2.16E-07	0.64	1.52	54.72
3	10800	2816061	597626	0.21	346.27	0.00072	1.49E-07	1.52E-07	0.45	1.97	70.84
4	14400	3285889	1539600	0.47	346.27	0.0015	6.05E-08	6.18E-08	0.18	2.15	77.37
5	18000	2835763	1419040	0.50	346.27	0.0016	4.33E-08	4.42E-08	0.13	2.28	82.05
6	21600	2746013	1549284	0.56	346.27	0.0017	2.76E-08	2.81E-08	0.08	2.36	85.03
7	25200	2816500	1652425	0.59	346.27	0.0018	2.07E-08	2.12E-08	0.06	2.42	87.27

Time/hr	Time/s	Dod/Area	Val/Area	Val/Dod	RRF	Conc. Rem. Val/M	k_0/mol/L/s	I_0/einstein/L/s	F_0/ W/m^2	Cum F_0/W/m^2	SED/ J/m^2
0	0	3175693	2440150	0.77	346.27	0.0023					
1	3600	2911686	1464313	0.50	346.27	0.0016	2.13E-07	2.17E-07	0.64	0.64	23.00
2	7200	2931436	1176494	0.40	346.27	0.0013	1.47E-07	1.50E-07	0.44	1.08	38.90
3	10800	2620407	626855	0.24	346.27	0.0008	1.41E-07	1.44E-07	0.42	1.51	54.18
4	14400	2771025	587049	0.21	346.27	0.0007	1.11E-07	1.14E-07	0.33	1.84	66.24
5	18000	3341469	1552749	0.46	346.27	0.0015	4.87E-08	4.97E-08	0.15	1.99	71.50
6	21600	2874821	1607794	0.56	346.27	0.0017	2.80E-08	2.85E-08	0.08	2.07	74.52
7	25200	2916500	1752425	0.60	346.27	0.0018	1.91E-08	1.95E-08	0.06	2.13	76.59

Time/hr	Time/s	Dod/Area	Val/Area	Val/Dod	RRF	Conc. Rem. Val/M	k_0/mol/L/s	I_0/einstein/L/s	F_0/ W/m^2	Cum F_0/w/m^2	SED/ J/m^2
0	0	3192328	2440010	0.76	346.27	0.0023					
1	3600	2935894	1474930	0.50	346.27	0.0016	2.10E-07	2.14E-07	0.63	0.63	22.70
2	7200	2889846	1185579	0.41	346.27	0.0013	1.42E-07	1.45E-07	0.43	1.06	38.04
3	10800	2792634	670371	0.24	346.27	0.0008	1.40E-07	1.43E-07	0.42	1.48	53.18
4	14400	2939027	618242	0.21	346.27	0.0007	1.11E-07	1.13E-07	0.33	1.81	65.18
5	18000	3529809	1654131	0.48	346.27	0.0015	4.74E-08	4.84E-08	0.14	1.95	70.30
6	21600	2852753	1573089	0.55	346.27	0.0017	2.85E-08	2.90E-08	0.085	2.04	73.38
7	25200	2906500	1710025	0.59	346.27	0.0018	2.06E-08	2.10E-08	0.06	2.10	75.59

Time/hr	Time/s	Dod/Area	Val/Area	Val/Dod	RRF	Conc. Rem. Val/M	k_0/mol/L/s	I_0/einstein/L/s	F_0/ W/m^2	Cum F_0/w/m^2	SED/ J/m^2
0	0	3001347	2285707	0.76	346.27	0.0023					
1	3600	3007162	1516639	0.50	346.27	0.0016	2.06E-07	2.11E-07	0.62	0.62	22.29
2	7200	2806170	1148953	0.41	346.27	0.0013	1.41E-07	1.44E-07	0.42	1.04	37.54
3	10800	2675593	647278	0.24	346.27	0.0008	1.39E-07	1.42E-07	0.42	1.46	52.55
4	14400	2801497	605620	0.22	346.27	0.0007	1.09E-07	1.11E-07	0.33	1.79	64.36
5	18000	3253306	1516008	0.47	346.27	0.0015	4.74E-08	4.84E-08	0.14	1.93	69.48
6	21600	2982271	1666095	0.56	346.27	0.0017	2.71E-08	2.77E-08	0.08	2.01	72.41
7	25200	3006500	1690001	0.56	346.27	0.0017	2.36E-08	2.40E-08	0.07	2.08	74.96

Time/hr	Time/s	Dod/Area	Val/Area	Val/Dod	RRF	Conc. Rem. Val/M	k_0/mol/L/s	I_0/einstein/L/s	F_0/ W/m^2	Cum F_0/w/m^2	SED/ J/m^2
0	0	3197784	2462296	0.77	346.27	0.0023					
1	3600	3166929	1587121	0.50	346.27	0.0016	2.16E-07	2.20E-07	0.65	0.65	23.29
2	7200	2999845	1243110	0.41	346.27	0.0013	1.43E-07	1.46E-07	0.43	1.07	38.70
3	10800	2741937	653762	0.24	346.27	0.0008	1.42E-07	1.45E-07	0.43	1.50	54.05
4	14400	2857733	621259	0.22	346.27	0.0007	1.11E-07	1.13E-07	0.33	1.83	66.02
5	18000	3321061	1554092	0.47	346.27	0.0015	4.85E-08	4.95E-08	0.15	1.98	71.25
6	21600	3052704	1707927	0.56	346.27	0.0017	2.82E-08	2.87E-08	0.08	2.06	74.29
7	25200	3046502	1690001	0.55	346.27	0.0017	2.44E-08	2.49E-08	0.07	2.14	76.93

Time/hr	Time/s	Dod/Area	Val/Area	Val/Dod	RRF	Conc. Rem. Val/M	k0/mol/L/s	I0/einstein/L/s	F0/ W/m2	Cum F0/w/m2	SED/ J/m2
0	0	3108668	2386294	0.77	346.27	0.0023					
1	3600	3054880	1523849	0.50	346.27	0.0016	2.16E-07	2.20E-07	0.65	0.65	23.29
2	7200	2951782	1205207	0.41	346.27	0.0013	1.44E-07	1.47E-07	0.43	1.08	38.86
3	10800	2673674	642339	0.24	346.27	0.0008	1.41E-07	1.44E-07	0.42	1.50	54.07
4	14400	2906023	624182	0.22	346.27	0.0007	1.11E-07	1.13E-07	0.33	1.84	66.06
5	18000	3478178	1643913	0.47	346.27	0.0015	4.73E-08	4.83E-08	0.14	2.00	71.17
6	21600	3048413	1708304	0.56	346.27	0.0017	2.77E-08	2.83E-08	0.083	2.06	74.17
7	25200	3046512	1710001	0.56	346.27	0.0017	2.37E-08	2.41E-08	0.07	2.13	76.72

Time/hr	Time/s	Dod/Area	Val/Area	Val/Dod	RRF	Conc. Rem. Val/M	k_0/mol/L/s	I_0/einstein/L/s	F_0/ W/m^2	Cum F_0/w/m^2	SED/ J/m^2
0	0	3202837	2526506	0.79	346.27	0.0024					
1	3600	2980481	1496463	0.50	346.27	0.0016	2.30E-07	2.35E-07	0.69	0.69	24.84
2	7200	3135265	1269250	0.41	346.27	0.0013	1.54E-07	1.57E-07	0.46	1.15	41.48
3	10800	2685361	643784	0.24	346.27	0.0008	1.47E-07	1.50E-07	0.44	1.59	57.34
4	14400	2887630	624869	0.22	346.27	0.0007	1.15E-07	1.17E-07	0.34	1.94	69.74
5	18000	3369275	1579386	0.47	346.27	0.0015	5.14E-08	5.24E-08	0.15	2.09	75.28
6	21600	2882010	1606799	0.56	346.27	0.0017	3.10E-08	3.16E-08	0.09	2.18	78.62
7	25200	2882100	1667854	0.58	346.27	0.0018	2.41E-08	2.46E-08	0.07	2.26	81.22

Chapter Six

Quantitation and phases of titanium dioxide in skin-lightening products in the South African market

Moses A. Ollengo and Bice S. Martincigh*

School of Chemistry and Physics, University of KwaZulu-Natal, Westville Campus, Private Bag X54001, Durban 4000, South Africa

*Corresponding author: Tel.:+27-31-2601394; Fax: +27-31-2603091; E-mail address: martinci@ukzn.ac.za

Abstract

Titanium(IV) oxide (TiO_2) is used as a physical blocker of ultraviolet (UV) radiation in many skin-care products. Absorption of TiO_2 through the skin is likely to interact with viable tissues because UV radiation absorption generates toxic reactive oxygen species such as hydroxyl radicals. Studies on the acute toxicity of TiO_2 nanoparticles in mammals indicate that intra-tracheal instillation, intraperitoneal injection or oral instillation of TiO_2 particles to the animals evoke an inflammatory response as well as certain histopathological changes. Ultrafine particles of the anatase form of titanium dioxide, which are smaller than 0.1 microns, are pathogenic. In this work eight skin-lighteners containing TiO_2 from South African market were studied. The TiO_2 was extracted by a fusion technique and quantified by inductively coupled plasma-optical emission spectrometry (ICP-OES). Sequential solvent extraction was employed to isolate TiO_2 particles for characterisation by means of high resolution transmission electron microscopy (HR-TEM) and powder X-ray diffraction (PXRD). All samples considered in this study meet agreeable TiO_2 % (m/m) levels as specified by all health regulatory bodies. Both forms of TiO_2: anatase and rutile, were found to be present. Most samples contained nano-TiO_2 in the particle size range of 16.23 nm to 51.47 nm that could possibly lead to detrimental effects. The fact that the anatase form, known for its photocatalytic activity, was present, is a cause for concern.

Keywords: Quantitation, anatase, rutile, nano-TiO_2

6.1 Introduction

Physical blockers like titanium dioxide (TiO_2) present in most skin care products have been shown to photo-induce degradation of organic sunscreens, enzymes, and DNA (Egerton et al. 2008; Sayre et al. 2003). Studies on the acute toxicity of TiO_2 nanoparticles in mammals indicate intra-tracheal instillation, intraperitoneal injection or oral instillation of TiO_2 particles to animals evoke inflammatory response and histopathological changes (Chen et al. 2010). In cultured macrophages, TiO_2 nanoparticles change the integrity of cell membrane and phagocytic activity (Zhang et al. 2010). A study showed reduction in cell viability, morphological alterations, a compromised antioxidant system, intracellular ROS production, and significant DNA damage in cells exposed to TiO_2 nanoparticles signifying the potential of nanoparticles to induce cytotoxicity and genotoxicity in cultured human amnion epithelial (WISH) cells (Saquib et al. 2012).

TiO_2 absorbs about 70 % of incident UV, and in viable aqueous environments this may lead to generation of hydroxyl radicals. These free radicals may initiate oxidative reactions presenting possible undesirable mutagenic effects. Hidaka et al. (1997) demonstrated that, if the sunscreen agent TiO_2 illuminated with appropriate UV light it interacts with DNA or RNA and is, can cause serious damage. This confirms that ultrafine sunscreen-grade TiO_2 irradiated with sunlight is photocatalytically active. A recent study showed that even some modified TiO_2 particles specifically developed and marketed for sun-care, skin-care, and colour cosmetic formulations, still retain photocatalytic activity (Tiano et al. 2010). Mild cytotoxic response of TiO_2 nanoparticles has been reported and linked to induction of DNA damage. Shukla et al. (2011) observed significant induction in micronucleus formation, reduction in glutathione, concomitant increase in lipid hydroperoxide and reactive oxygen species (ROS) generation demonstrating mild cytotoxic potential. Though induced ROS and oxidative stress may lead to oxidative DNA damage, micronucleus formation may form the basic mechanism of TiO_2 nanoparticle genotoxicity (Shukla et al. 2011).

Oxidative and nitrative stress causes nitration of the protein tyrosine, a post-translational modification linked to the onset or progression of diseases, such as cardiovascular diseases neurodegenerative diseases, and inflammation. The presence of tyrosine nitration in diseased conditions is an indication of the generation of peroxynitrite ($ONOO^-$) *in vivo* produced from the very fast reaction of nitric oxide (NO) and superoxide ($O_2^{\cdot-}$) radical. Tyrosine nitration is reported in several cutaneous pathological effects: contact hypersensitivity, systemic sclerosis, cutaneous inflammation, and thermal injury (Lu et al. 2008). Lu et al. (2008) recently demonstrated the physiological potential of nano-TiO_2 to photocatalyse protein nitration in mouse skin homogenate. The anatase form of TiO_2 can greatly increase the formation of free radicals when exposed to sunlight and water in sunscreens. Studies indicate nano-anatase TiO_2 (1-100 nm) is highly photo-reactive, and thus hazardous. Nano-anatase TiO_2 in sunscreens was shown to react with sunlight and break down coatings on steel roofs at a rate 100-fold more than normal sunlight (Barker and Branch 2008). With the same effectiveness nano-anatase is likely to attack viable tissues if it comes in contact.

The major concern of the nano-particulate range of TiO_2 in cosmetics is for infants and children with thinner, developing skin and people having broken skin. The skin could be broken due to contact dermatitis, eczema, acne or other skin conditions, making it susceptible to particles coming in contact with living cells. Nano particulate TiO_2 is widely used in sunscreen products to boost the SPF. Another area of application is in skin-lightening preparations. Skin-lighteners are designed to reduce the formation of melanin in the skin and thus the skin is left without adequate protection from the deleterious effects of UV radiation. Consequently, these products contain TiO2 to afford braod-spectrum protection. From the foregoing it is apparent that the amount, particle size, and form of

TiO_2 in a formulation needs to be controlled; European cosmetic, toiletry and perfumery association (COLIPA) set the maximum allowable concentration of TiO_2 in sunscreens as 25% (m/m) (Atitaya et al. 2011). However, most health regulatory bodies worldwide to date do not specify particle size limits. In the present work we set to isolate, quantitate, and characterize the phases of titanium dioxide present in skin-lightening products in the South African market.

6.2   Materials and Methods

6.2.1   Reagents

Titanium dioxide (TiO_2) (99.8 % – Analytical Reagent Grade) from Riedel-de Haën A.G., Seelze-Hannover, was used for the preparation of standard solutions. Analytical grade sulphuric acid (H_2SO_4) (98.0 %) was supplied by Associated Chemical Enterprises (Pty) Ltd, Johannesburg, South Africa, and BDH Chemicals Ltd, Poole, England. Potassium hydrogen sulphate ($KHSO_4$) was supplied by BDH Chemicals Ltd, Poole, England. A total of eight skin-lightening products containing TiO_2 were purchased from retail outlets in Durban, South Africa.

6.2.2   Quantitation of TiO_2

6.2.2.1   Preparation of standard solutions

A mass of 0.05 g of TiO_2 (> 99 %) was weighed and dissolved in 100 mL of hot concentrated H_2SO_4 (> 98 %), with constant stirring for 12 h to make a standard stock solution of 300 mg mL^{-1} of Ti^{4+}. The stock solution was used to make working standards in the range 2 mg dm^{-3}– 10 mg dm^{-3}.

6.2.2.2   Preparation of samples

Masses of the skin-lightening samples in range of 0.4 -0.6 g were weighed into a fused silica crucible and placed into an electrical furnace (Natalab supplies, South Africa) with the temperature set at 600 ºC for three hours to give a carbon-free ash. The ash was allowed to cool in a desiccator for 10 min, and then about 0.5 g of $KHSO_4$ was added to it. The crucible containing the ash residue and $KHSO_4$ was heated over a Bunsen burner for 15 min to fuse the mixture. The molten product was then dissolved in hot, concentrated H_2SO_4 and the solution transferred to a beaker. This solution was strongly heated to ensure complete solubilization of the TiO_2. The sample solutions were then diluted with deionised water to 100 mL. A ten-fold dilution was done for samples that did not fall within the range of the calibration standards. All samples were analysed in triplicate.

6.2.2.3   Inductively coupled plasma-optical emission spectroscopy analysis

An inductively coupled plasma optical emission spectrometer Perkin Elmer (Optima 5300 DV) fitted with an auto-sampler was used for the quantitation of TiO_2 and the data was processed by Perkin Elmer WinLab32 software. The instrument was programmed to sample each standard and sample five times in radial view mode. Other operating conditions were: argon gas flow rate of 1.5 L min^{-1}, auxiliary and nebulizer gas flows at 0.2 L min^{-1} and 0.8 L min^{-1} respectively. The pump flow rate was set at 1.5 mL min^{-1} with the plasma radiofrequency working at 1300 W. The data were acquired at a wavelength of 337.279 nm.

6.2.2.4   Method validation

The method validation was done by spiking a TiO_2-free sample with about 10 mg of TiO_2. A mass of ~ 0.150 g of the spiked sample was accurately weighed into a fused silica crucible. The crucible was then put in an electrical furnace at 600 °C for three hours after which it was placed in a desiccator for 10 min to cool. To the cooled carbon-free ash residue a mass of 0.50 g of $KHSO_4$ was added and fused over a Bunsen burner for 15 min. The molten product was dissolved in hot, concentrated H_2SO_4 and made up to 100 mL with deionized water it was then subjected to a ten-fold dilution. The diluted sample was subjected to ICP-OES analysis. The standards were analysed in between sample runs to check on instrument signal response and precision. An intra- and inter-day analysis was performed based on the precision of the standards analysis within the day of analysis and between days of analysis.

6.2.2.5   Data analysis

The calibration data was analysed with Microsoft Excel© 2007 tool pack. The limit of detection (LOD) and limit of quantitation (LOQ) was calculated from the results of the linear calibration curve of the standards. The results were expressed as mean ± SD.

6.2.3   Characterisation of TiO_2

6.2.3.1   Extraction of TiO_2

Samples containing TiO_2 were washed with solvents of varying polarity indices in order to isolate crystalline particles. A mass of ~ 0.2 g of the sample was weighed into a beaker and washed firstly in 200 mL dimethyl formamide with ultranisonication for 2 h. The solvent with the dissolved organics was filtered through Whatman 1 filter paper and the remaining solid residue was then re-washed with fresh solvent in the order: methanol, acetone, and chloroform. The order varied depending on the sample matrix. Each wash was similarly filtered until crystalline TiO_2 could be observed. The isolated crystals were then dried in an electric oven at 100 °C for one hour.

6.2.3.2   Characterisation by PXRD

PXRD analyses was done by using a Bruker D8 Advance diffractometer equipped with an Anton Paar XRK 900 reaction chamber, a TCU 750 temperature control unit, with CuK_α radiation at 40 mA; 40 kV and 1.5405 Å. The diffractograms were collected over a 2θ of 10.000° -89.893° range at a goniometric velocity of 0.034° min^{-1} at 25°C. The spectral data was accumulated and processed by using Diffrac^{plus} basic XRD Wizard2.8 software. The diffraction peaks of crystalline phases were compared with standard anatase and rutile reported in the JCPDS database. The particle size of TiO_2 extracted by the sequential solvent system was estimated from the width, of diffraction peaks, calculated by using Scherrer's equation:

$$\tau = \frac{K\lambda}{\beta cos\theta}$$

where K is Scherrer's constant (0.89): shape factor, λ is the X-ray wavelength used (1.5405 Å), β is the width at half maximum intensity (FWHM) in radians of the diffraction peak measured at 2θ, θ is the Bragg angle, and τ is mean size of the crystalline particles.

6.2.3.3   Characterisation by high resolution transmission electron microscopy

Samples for high resolution transmission electron microscopy (HR-TEM) observation were prepared by dispersing the extracted TiO_2 powders in an absolute ethanol solution under ultrasonic irradiation. The dispersed TiO_2 was then deposited on carbon-copper grids. The crystallite sizes and shapes were observed by HR-TEM on a JEOL JEM-2100 microscope at 200 kV. The structure resolution of the microscope was set at 0.2 nm.

6.3   Results

The TiO_2 content of the eight skin-lightening products investigated in this work was determined by ICP-OES. The analytical method had a linear working from 0.48 to 2.5 mmol dm^{-3} as observed from the calibration curve of the standards (see Supplementary Materials Fig. S6.19). The correlation coefficient of the calibration curve (determined in triplicate) was 0.999.

Table 1 shows the amounts, particle size, and phases of the TiO_2 analysed in this work. The LOD was calculated by using equation 6.1:

$$LOD = 3S_{y/x}/b \qquad\qquad\qquad 6.1$$

where $S_{y/x}$ is the standard error of the slope and b is the slope of the calibration curve (Thomsen et al. 2003). The was 0.06518 mg dm^{-3}. The LOQ from this data was calculated using equation 6.2:

$$LOQ = 3.3\, LOD. \qquad\qquad\qquad 6.2$$

The limit of detection at this wavelength was 0.2151 mg dm^{-3}. The recovery test using spiked samples gave a mean recovery of 98.8 % and the signal stability was determined by the intra- and inter-day analysis. The intra-day analysis using an authentic standard gave an RSD % of 0.10 % and an inter-day value of 0.10 % thereby indicating very high precision.

The percentage composition of titanium dioxide in this samples was in the range of 2.83 % to 12.47 % (Table 1). These were all well below the COLIPA allowable 25 % (m/m) maximum concentration of titanium dioxide in a cosmetic formulation (Atitaya et al. 2011). Most of the samples of the samples contained approximately 3 % (m/m) TiO_2, which when compared with the maximum allowed limit is low.

The PXRD characterisation of the samples gave signals at 2θ values: 25.22, 37.73, 38. 45, 47.82 and 54.95° characteristic of anatase, at 27.33 37.73, 41.10, 54.10 and 68.69° characteristic of the rutile phase of TiO_2 (see Figure 6.1 and Supplementary Materials S6.2 – 6.14). The crystallite size estimation was based on the Scherrer equation. The Scherrer formula can provide a good estimate of the particle size but a variety of factors can contribute to the width of a diffraction peak. Besides crystallite size, the most important of these are usually inhomogeneous strain and instrumental effects. If all of these other contributions to the peak width were zero, then the peak width would be determined solely by the crystallite size and the Scherrer formula would apply.   If the other contributions to the width are non-zero, then the crystallite size can be larger than that predicted by the Scherrer formula, with the peak broadening coming from the other factors. The eight samples gave crystallite sizes in the range of 16.23 nm to 58.38 nm (see Table 1). These all fall within the nano-dimension.

Analysis of the high resolution transmission electron microscopy images also revealed grain sizes in the nano range (see Figure 6.2 and 6.3 and Supplementary Materials Fig. S6.1 – S6.15). This range is useful for attenuation of UV radiation. Attenuation is the combined effect of absorbing and scattering of incident light. Because nano-TiO_2 absorbs more UV light than it scatters compared with pigmentary grade TiO_2, it is preferred in most sunscreen preparations. Also, in this size range it does not produce a whitening effect on the skin and thus it is more aesthetically appealing. The two methods of characterisation, thus proved helped useful in crystallite size approximation. However, the measurement from the HR-TEM depend on the particle dispersion and it is not apparent on the form of TiO_2 being measured. Whereas with the PXRD both particle size and form of TiO_2 could be obtained by library match. In this work three samples displayed pure anatase signals indicating that the samples contained majorly anatase and four displayed rutile signals. One sample however, showed mixed signals of anatase and rutile thereby showing a mixture of the two in the samples (see Supplementary Materials 6S.10 Table 6.1.

Table 6.13: Average percentage concentration, particle size and phase of TiO_2 in the skin-lightening samples.

Sample	*TiO_2 % (m/m)	Particle size/nm	Phase of TiO_2
B	6.90 ± 0.01	16.23 ± 0.31	Rutile/anatase
E	7.47 ± 1.24	26.39 ± 1.79	Rutile
G	5.65 ± 0.01	45.03 ± 1.27	Rutile
L	3.04 ± 0.01	22.86 ± 4.14	Rutile
C	2.83 ± 0.01	44.42 ± 2.00	Anatase
I	3.35 ± 0.00	58.70 ± 0.38	Anatase
J	2.86 ± 0.01	42.59 ± 5.35	Anatase
K	3.73 ± 0.01	51.67 ± 6.56	Anatase

* Each value is an average of three replicates (mean ± SD).
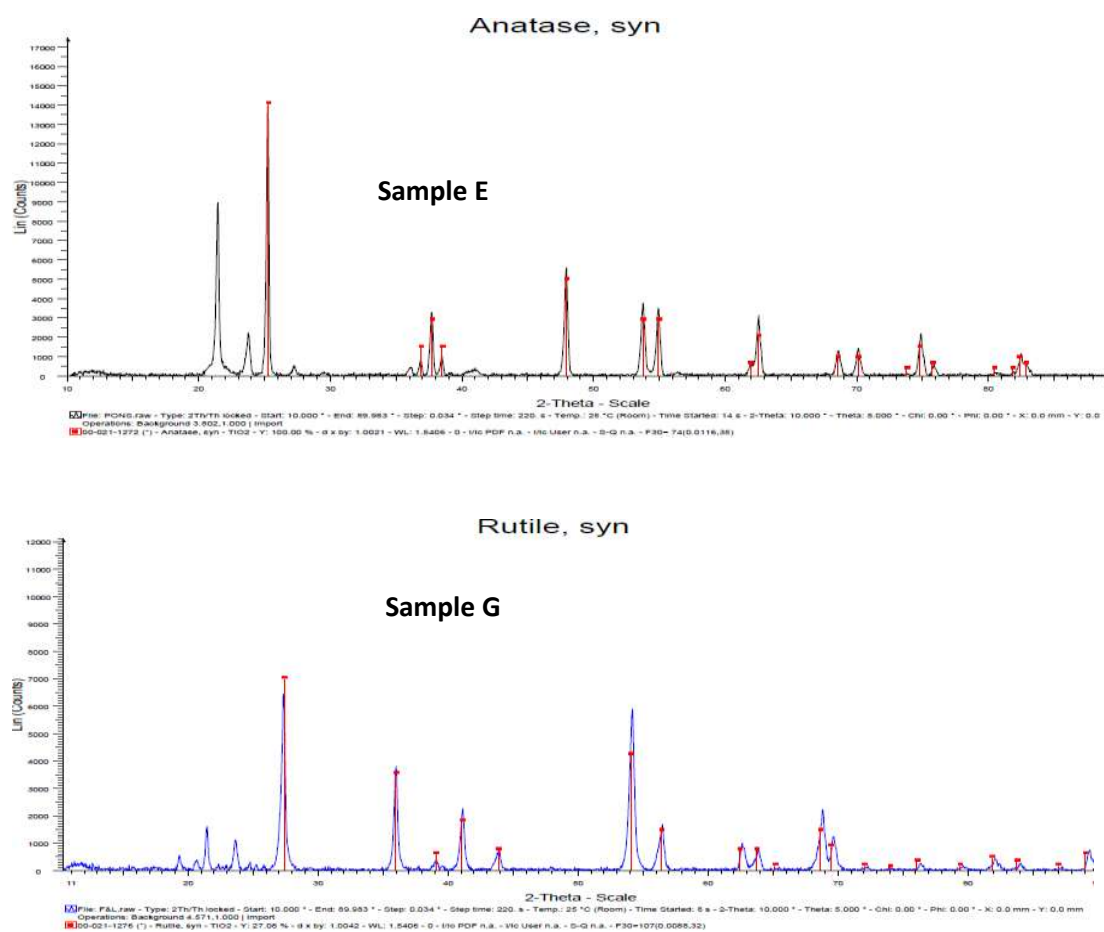
Figure 6.14: X-ray diffactogram for sample E (anatase) and sample G (rutile) superimposed on library difractograms of anatase and rutile.
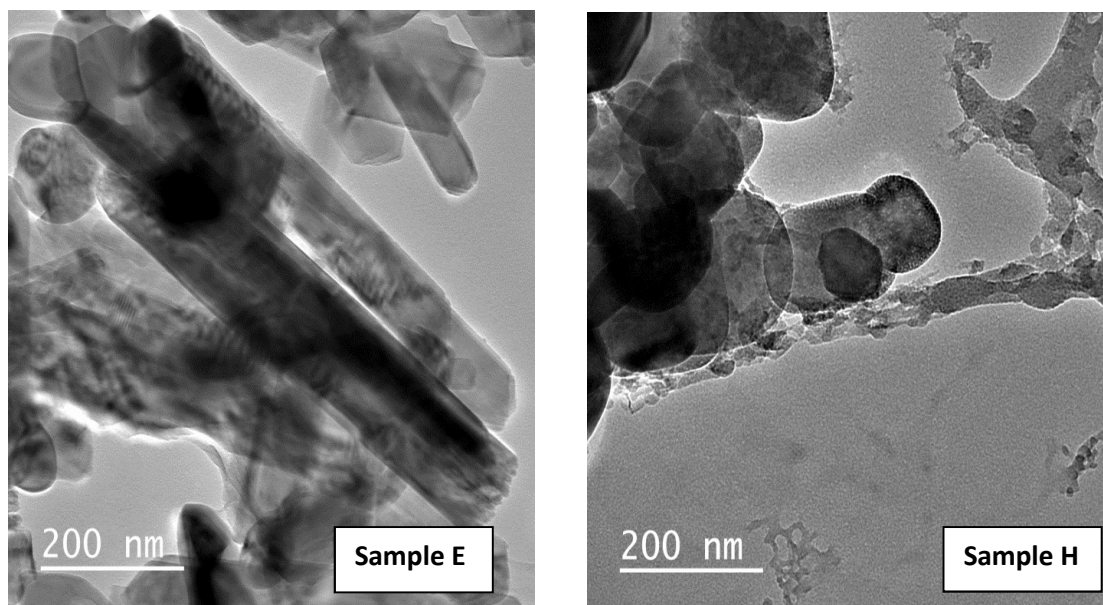
Figure 6.2: HRTEM images of samples E and showing well-defined crystalline TiO$_2$.
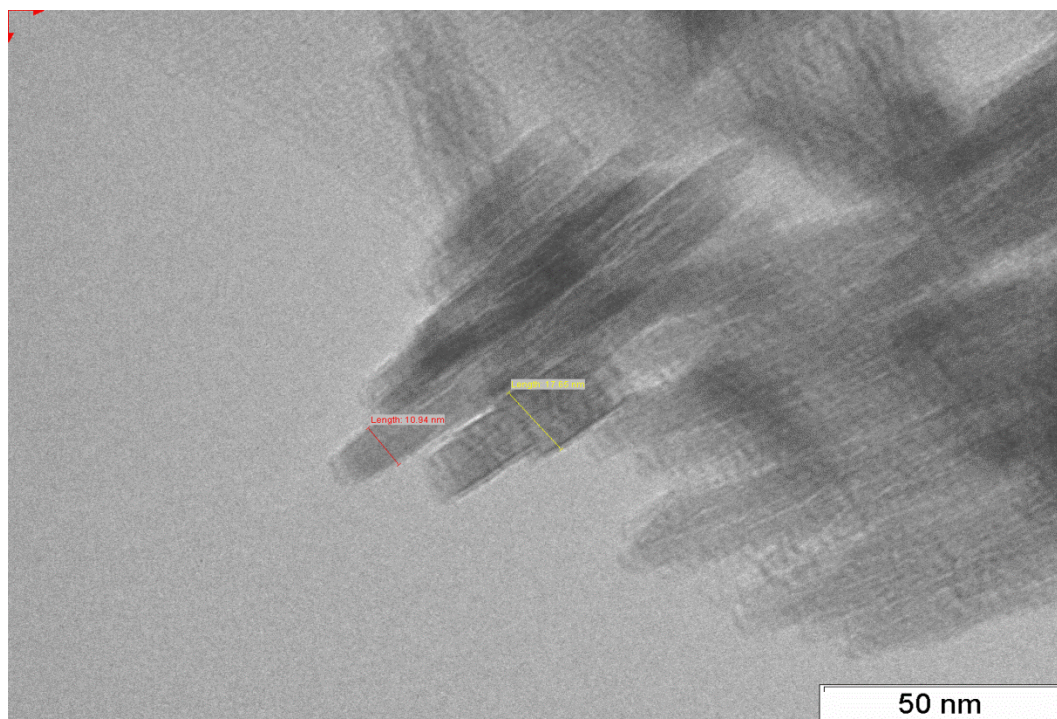
Figure 6.15: Particle size measurement for sample A observed using high-resolution transmission electron microscopy

6.4 Discussion

Samples investigated in this work contained TiO_2 acting as a sunscreen. The high refractive index of TiO_2 makes it useful for this purpose. The refractive indices of the rutile and anatase forms of TiO_2 are 2.75 and 2.54 respectively (Vayssieres et al. 2011). In this work the crystallite size range was from 16.23 – 69.10 nm (Table 1) as determined by PXRD. The particles of TiO_2 in the size range < 100 nm are referred to us nano-TiO_2 and those > 100 nm are known as pigmentary-TiO_2. The nano-TiO_2 have shown to be excellent UV filters or blockers because they have strong UV light absorbing capabilities and resistance to discolouration under UV irradiation. This advantage enhances its stability and ability to protect the skin from UV light (Morganti 2010). Hence, nano-TiO_2 particles are frequently used in cosmetics because they scatter visible light less than pigmentary-TiO_2 while still providing UV protection. The majority of sunscreens intended for infants or people with delicate skin use are often based on TiO_2 and/or ZnO, because these physical UV filters are believed to cause less skin irritation than other UV absorbing agents.

However, nano-TiO_2 is naturally photocatalytic because when they absorb UV light electrons are excited and promoted for anatase to the conduction band across the 3.2 eV band gap. This excitation is induced by UV light of wavelengths below 385 nm. The excited electrons promoted from the valence band (v_b) to the conduction band (c_b) generate two mobile charged species; negatively charged single electrons (e^-) and positively charged spaces called holes (h^+) (equation 1). The electron and hole pair (e^-/h^+) (equation 2) may recombine or migrate rapidly to the particle surface. At the surface the electrons and holes may participate in chemical reactions with adsorbed chemical species. There are two possible reactions that may take place at the surface. The e^- may react with dissolved oxygen gas (O_2) and h^+ with hydroxyl (OH^-) ions or water (H_2O), to form superoxide (O_2^-) or hydroxyl ($^.OH$) radicals:

$$TiO_2 + h\nu \rightarrow TiO_2 \ (e^-/h^+) \tag{1}$$
$$TiO_2 \ (e^-/h^+) \rightarrow e^- \ (c_b) + h^+ \ (v_b) \tag{2}$$
$$e^- \ (c_b) + O_2 \rightarrow O_2^{.-} \tag{3}$$
$$h^+ \ (v_b) + OH^- \rightarrow \ ^.OH \tag{4}$$
$$h^+ \ (v_b) + H_2O \rightarrow \ ^.OH + H^+ \tag{5}$$
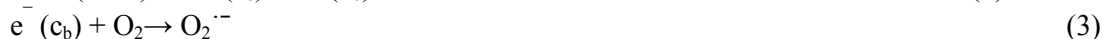
The O_2^- and, in particular, the $^.OH$ radicals formed are the active agents for the degradation of organic compounds:
$$^.OH \text{ or } O_2^{.-} + \text{substrate} \rightarrow \text{photo-oxidized products} \quad \text{(Bunhu et al. 2011).} \tag{6}$$
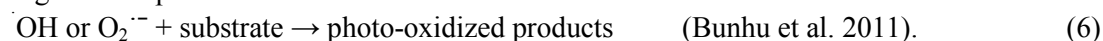
Also, the excited electrons may return to their ground state, emitting energy, or escape from the particle (equation 2). Escaped electrons may initiate oxidative reactions in nearby molecules, generating free radicals (equation 3 - 5). Free radicals may cause further damage to skin cells or interact with other sunscreen components producing chemical species with undesirable effects (equation 6). The fear is that this could lead to cancer in the skin.

The probability of photo-electron promotion and generation of e^-/h^+ pairs is the phase of the nano-TiO_2 crystal. In this work, both phases of TiO_2, namely, anatase and rutile were identified in the skin-lightening products. It is known that rutile is more photostable than anatase. This arises from the size dependence on the orbital character of the conduction band of anatase TiO_2 nano-crystals. It is known that the appearance and predominance of unoccupied states derived from the hybridization of the antibonding Ti 4s and O 2p band is observed when the nanoparticle size approaches the exciton radius

(ca. 1 nm). Such extended hydridization of O 2p with Ti 4s compared to narrow directional 3d in rutile demonstrates a confinement effect in anatase TiO_2 nano-crystals, a factor in electron excitation upon UV irradiation. The presence of s-hybridized band gap states controls the interfacial electron transfers and reduces the back reaction (Vayssieres et al. 2011). This may create an avalanche of escaped electrons that may attack viable skin cells via generation of free radicals as illustrated above. On this account, rutile should be the preferred phase of TiO_2 for use in cosmetic preparations. In this study samples C, D E and H showed characteristic peaks of te anatase in the XRD diffractograms (see Figure 1 and Suplementary Materials Fig. S6.6, S6.10, S6.12) an evidence that anatase is still used in some skin-lightening preparations. The forms of TiO_2 present in these samples were not indicated on the packet labels. This is a major concern because anatase TiO_2 is a very active photocatalyst and should not be used in cosmetic preparations. Secondly, as shown by Tiano et al. (2010) even surface-modified TiO2 still retains photocatalytic activity.

The question of percutaneous penetration of TiO_2 has drawn a lot of attention especially after topical application. Table 6.2 shows the relationship between particle size and possible viable tissue penetration by the nano-range particles. In the worst case scenario the particle range of TiO_2 found in this work (16 – 59 nm, Table 6.1) are likely to enter viable tissue should they be in contact with any of these body tissues

Table 6.14: Particle size and entry into the human body

Nanoparticle Size/nm	Entry Point
70	Alveolar surface of lung
50	cells
30	Central nervous system
20	No data yet

(http://www.organicmakeup.ca/titaniumdioxide.asp (accessed on 14/10/2012)

Animal studies indicate that subjects who routinely apply sunscreens with micronized TiO_2 show that the skin can absorb microfine particles (Naya et al. 2012; Lu et al. 2008). The samples investigated in this work all have TiO_2 in the nano-range (< 100 nm) (Table 6.1). The penetration of nano-TiO_2 into the cells may lead to photocatalysis within the cell, causing DNA damage after exposure to sunlight.

Kumazawa et al. (2002) and Tamura et al. (2002) have shown that a Ti^{+4} solution stimulates neutrophils and increases the quantity of released O_2^- anions. The authors showed that the cytotoxic effect of Ti particles is size dependent, and that they must be smaller than that of cells. Animal model studies have shown the ingested titanium accumulates in the liver DNA leading to histopathological changes and hepatocyte apoptosis (Dunford et al. 1997; Saquib et al. 2012).

However, some studies show that there is no deeper penetration of topically applied TiO_2 into viable skin tissue (Lademann et al. 1999). The same study indicated that there is possible penetration of TiO_2 into the open skin parts around the follicles. This is a pointer that compromised skin surface may be susceptible to TiO_2 penetration. The effects of viable tissue incorporated TiO_2 include induction of ROS reactions that can lead to DNA mutations and cell death (Rahman et al. 2002). There are reports that TiO_2 particles isolated from commercial sunscreen products induced DNA strand-breaks and other lesions in DNA plasmids and in human cells (Dunford et al. 1997). It can therefore be inferred that the presence of TiO_2 in sunscreen formulations can initiate or lead to photo-oxidative damage of the skin. Though, other investigations have shown that coarse or fine particles of

TiO$_2$ to be safe and effective at deflecting and absorbing UV light, protecting the skin (Donathan and Thomas 2011; Sadrieh et al. 2010). But consumers should avoid using products with nano-pigments, either in sunscreens or colour cosmetics if they have any wounds or broken skin. Such preparations should be used with caution on the children where the skin is thinner and more permeable.

Most of the investigated products in this work contained a combination of TiO$_2$ with organic UV-filters tert-butylmethoxy dibeznoylmethane, 2-ethylhexy-*p*-methoxy cinnamate, and benzophenone-3. There is the possibility that TiO$_2$ may photocatalyse the photodegradation of these UV filters. Several reports indicate loss of photo-absorption efficacy of these UV filters in the presence of TiO$_2$ (Ricci et al. 2003). The photoproducts resulting from the TiO$_2$ photocatalysed reactions of the organic UV filters lead to a loss of photoprotection and potential risk to the skin. In addition, the toxicities of the resulting photoproducts are not known.

To inhibit the effects of TiO$_2$ on the organic macromolecules and other substrates the surface of the TiO$_2$ may require deactivation. The surface deactivation of nano-TiO$_2$ like the once found in this work may afford thin film uniform surface coating on the particles. However, such surface modifications have been found inefective in photo-oxidative reactions (Tiano et al. 2010). The structural modification of the TiO$_2$ crystalline lattice by introduction of impurities has been shown to reduce photo-activity of TiO$_2$. The choice of the transition metal (dopant) determines the photo-response of the doped TiO$_2$. Recently, it was demonstrated that manganese-doped TiO$_2$ had enhanced UVA absorption, less degradation of other organic constituents of the formulation and a reduction in free radical generation (Wakefield et al. 2004). However, there is no guarantee that surface coating or doping completely deactivates TiO$_2$.

6.5 Conclusions

The aim of this study was to isolate, characterise and quantitate the amount of TiO$_2$ present in the eight skin-lightening preparations. The percentage composition of TiO$_2$ in these skin-lightening agents was found to be in the range 2.83 % to 12.47 % (m/m). Both anatase and rutile forms of TiO$_2$ were found present in nano range (16.23 nm to 51.67 nm). Since anatase TiO2 is a potent photocatalyst it should not be used in such topical skin preparations. This is more so since it has been shown that surface modification does not eliminate this photocatalytic activity.

References

Atitaya S, Juwadee S, Atitaya S (2011) Particle size characterization of titanium dioxide in sunscreen products using sedimentation field-flow fractionation-inductively coupled plasma-mass spectrometry. Analytical and Bioanalytical Chemistry 399 (2):973-978

Barker PJ, Branch A (2008) The interaction of modern sunscreen formulations with surface coatings. Progress in Organic Coatings 62 (3):313-320

Bunhu T, Kindness A, Martincigh BS (2011) Determination of titanium dioxide in commercial sunscreens by inductively coupled plasma-optical emission spectroscopy. South African Journal of Chemistry 64:139-143

Chen J, Zhou H, Santulli CA, Wong SS (2010) Evaluating Cytotoxicity and Cell Uptake from the Presence of Variously Processed TiO$_2$ Nanostructured morphologies. Chem Res Toxicol 23:871 - 879

Donathan GB, Thomas AM (2011) Characterisation of the UVA protection Provided by Avobenzone, Zinc Oxide and Titanium Dioxide in Broad-Spectrum sunscreen Products. American Journal of Clinical Dermatology 11 (6):413-421

Dunford R, Salinaro A, Cai L, Serpone N, Horikoshi S, Hidaka H, Knowland J (1997) Chemical oxidation and DNA damage catalysed by inorganic sunscreen ingredients. FEBS Letters 418 (1–2):87-90

Egerton A, Everall JN, Mattinson AJ, Kessell ML, Tooley RI (2008) Interaction of TiO$_2$ nano-particles with organic UV absobers. Journal of Photochemistry and Photobiology A: Chemistry 193:10 - 17

Hidaka H, Horikoshi S, Serpone N, Knowland J (1997) In vitro photochemical damage to DNA, RNA and their bases by an inorganic sunscreen agent on exposure to UVA and UVB radiation. Journal of Photochemistry and Photobiology A: Chemistry 111:205-2013

Kumazawa R, Watari F, Takashi N, Tanimura Y, Uo M, Totsuka Y (2002) Effects of Ti ions and particles on neutrophil function and morphology. Biomaterials 23 (17):3757-3764

Lademann J, Weigmann HJ, Rickmeyer C, Barthelmes H, Schaefer H, Mueller G, Sterry W (1999) Penetration of titanium dioxide microparticles in a sunscreen formulation into the horny layer and the follicular orifice. Skin Pharmacology and Applied Skin Physiology 12 (5):247-256

Lu N, Zhu Z, Zhao X, Tao R, Yang X, Gao Z (2008) Nano titanium dioxide photocatalytic protein tyrosine nitration: A potential hazard of TiO$_2$ on skin. Biochemical and Biophysical Research Communications 370 (4):675-680

Morganti P (2010) Use and potential of nanotechnology in cosmetic dermatology. Clinical, Cosmetic and Investigational Dermatology 3:5-13

Naya M, Kobayashi N, Ema M, Kasamoto S, Fukumuro M, Takami S, Nakajima M, Hayashi M, Nakanishi J (2012) In vivo genotoxity study of titanium dioxide nanoparticles using comet assay following intratracheal instillation in rats. Regulatory Toxicology and Pharmacology 62 (1):1-6

Rahman Q, Lohani M, Dopp E, Pemsel H, Jonas L, Weiss DG, Schiffmann D (2002) Evidence that ultrafine titanium dioxide induces micronuclei and apoptosis in Syrian hamster embryo fibroblasts. Environmental Health Perspectives 110 (8):797-800

Ricci A, Chretien MN, Maretti L, Scaiano JC (2003) TiO$_2$-promoted mineralization of organic sunscreens in water suspension and sodium dodecyl sulfate micelles. Photochemical and Photobiological Sciences 2 (5):487-492

Sadrieh N, Wokovich AM, Gopee NV, Zheng JW, Haines D, Parmiter D, Siitonen PH, Cozart CR, Patri AK, McNeil SE, Howard PC, Doub WH, Buhse LF (2010) Lack of Significant Dermal Penetration of Titanium Dioxide from Sunscreen Formulations Containing Nano- and Submicron-Size TiO2 Particles. Toxicological Sciences 115 (1):156-166

Saquib Q, Al-Khedhairy AA, Siddiqui MA, Abou-Tarboush FM, Azam A, Musarrat J (2012) Titanium dioxide nanoparticles induced cytotoxicity, oxidative stress and DNA damage in human amnion epithelial (WISH) cells. Toxicology *In Vitro* 26 (2):351-361

Sayre RM, Dowdy JC, Ricci A, Chretien MN, Scaiano JC (2003) Mineralization of organic sunscreens: interesting, but relevant? Comment and response. Photochemical and Photobiological Sciences 2 (10):1050-1051

Shukla RK, Sharma V, Pandey AK, Singh S, Sultana S, Dhawan A (2011) ROS-mediated genotoxicity induced by titanium dioxide nanoparticles in human epidermal cells. Toxicology in Vitro 25 (1):231-241

Tamura K, Takashi N, Kumazawa R, Watari F, Totsuka Y (2002) Effects of particle size on cell function and morphology in titanium and nickel. Materials Transactions 43 (12):3052-3057

Thomsen V, Schatzlein D, Mercuro D (2003) Limits of detection in spectroscopy. Spectroscopy 18:112-114

Tiano L, Armeni T, Venditti E, Barucca G, Mincarelli L, Damiani E (2010) Modified TiO_2 particles differentially affect human skin fibroblasts exposed to UVA light. Free Radical Biology and Medicine 49 (3):408-415

Vayssieres L, Persson C, Guo JH (2011) Size effect on the conduction band orbital character of anatase TiO_2 nanocrystals. Applied Physics Letters 99 (18):183101

Wakefield G, Lipscomb S, Holland E, Knowland J (2004) The effects of manganese doping on UVA absorption and free radical generation of micronised titanium dioxide and its consequences for the photostability of UVA absorbing organic sunscreen components. Photochemical and Photobiological Sciences 3 (7):648-652

Zhang R, Niu Y, Li Y, Zhao C, Song B, Li Y, Zhou Y (2010) Acute toxicity study of the interaction between titanium dioxide nanoparticles and lead acetate in mice. Environmental Toxicology and Pharmacology 30 (1):52-60

Supplementary Materials

The high resolution electron microscopy images TiO_2 in the investigated samples and their corresponding XRD difractograms.
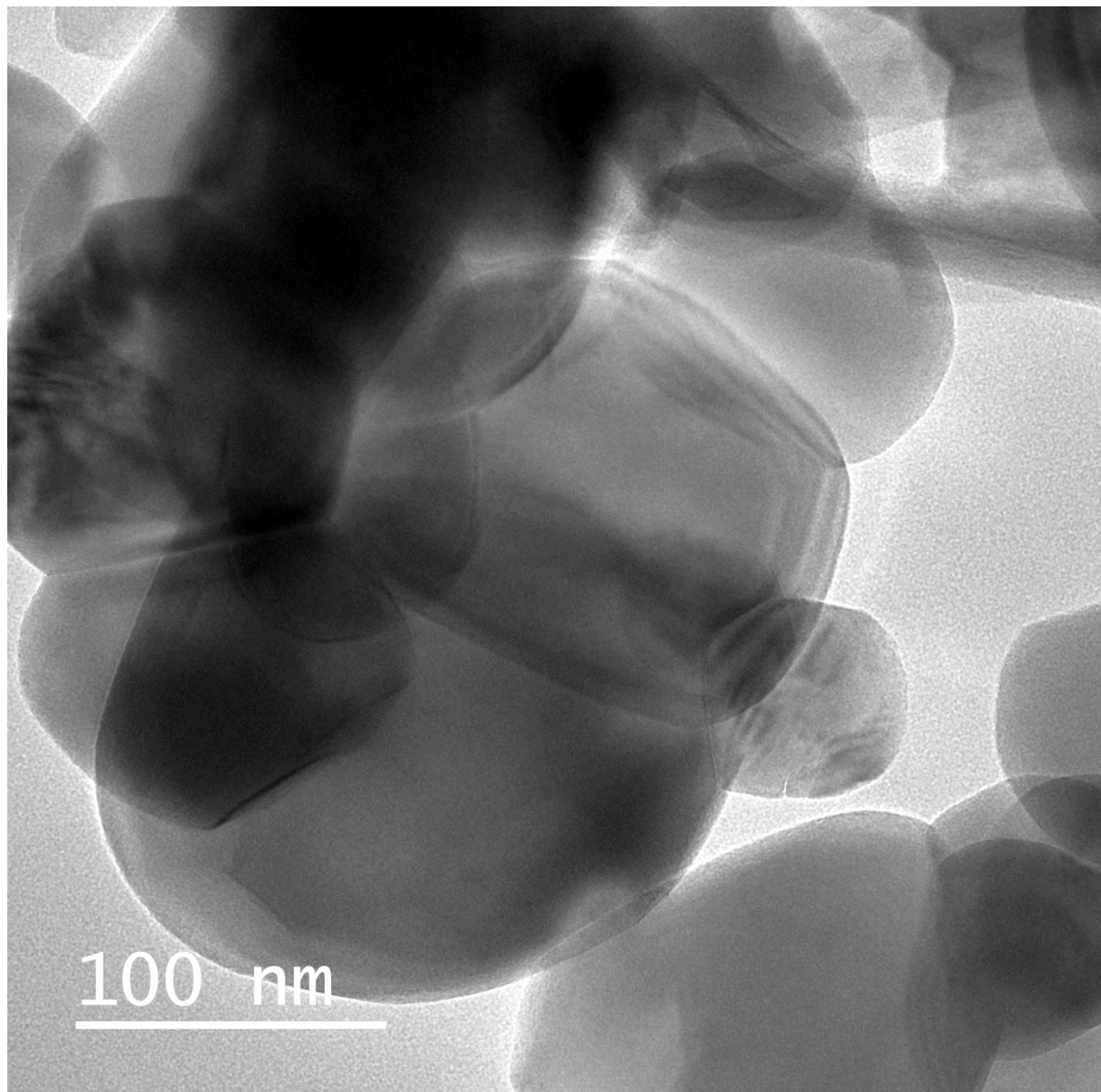
Figure S6.1: High resolution electron microscopy image of sample C observed using high-resolution transmission electron microscopy (HRTEM) on a JEOL JEM-2100 at 200 kV. Structure resolution of microscope was set at 0.2 nm.
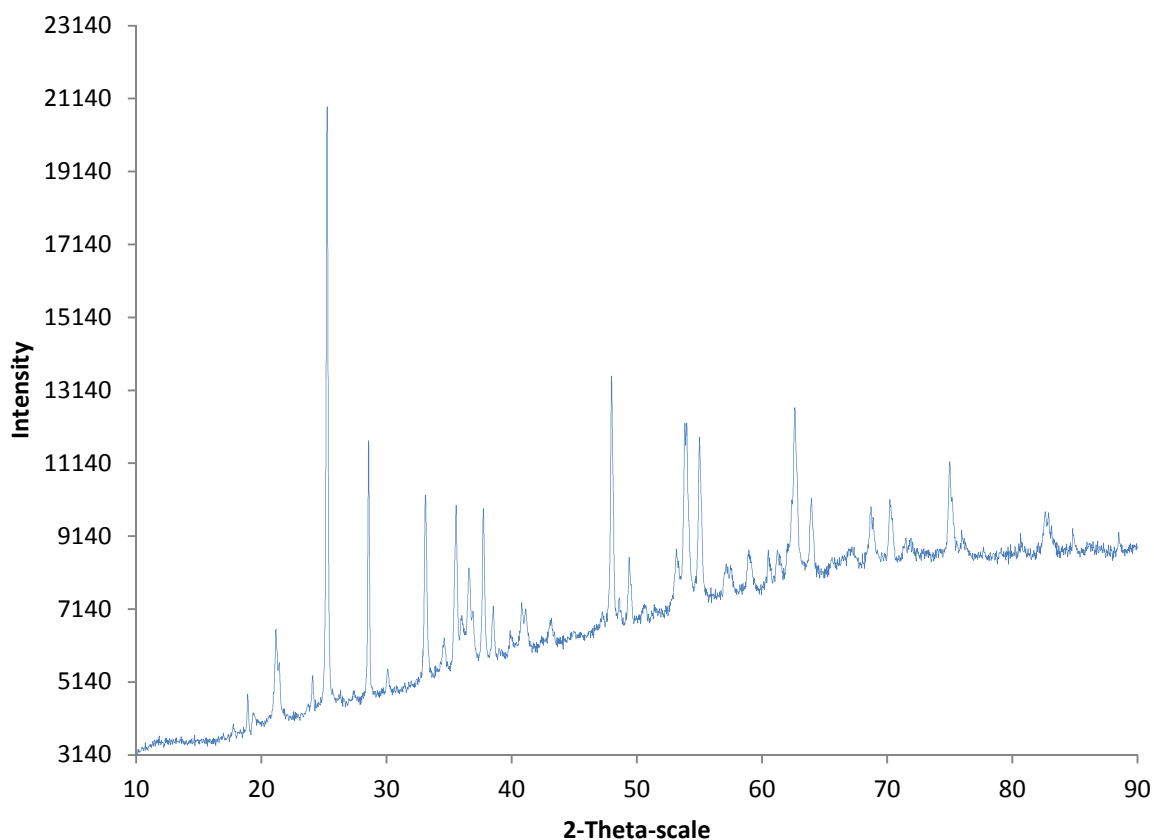
Figure S.2: X-ray diffactogram for sample C dried in an electric oven at 100℃ for one hour. Instrument settings were 2Th/Th locked - Start: 10.000 ° - End: 89.983 ° - Step: 0.034 ° - Step time: 220. s - Temp.: 25 °C (Room) - Time Started: 8 s - 2-Theta: 10.000 ° - Theta: 5.000 ° - χ: 0.00 ° - ψ: 0.00 ° - X: 0.0 mm - Y: 0.0 mm - Operations: Background 0.068,1.000 with Enhanced background 6.761,1.000 and wavelength set at 1.5406 nm.
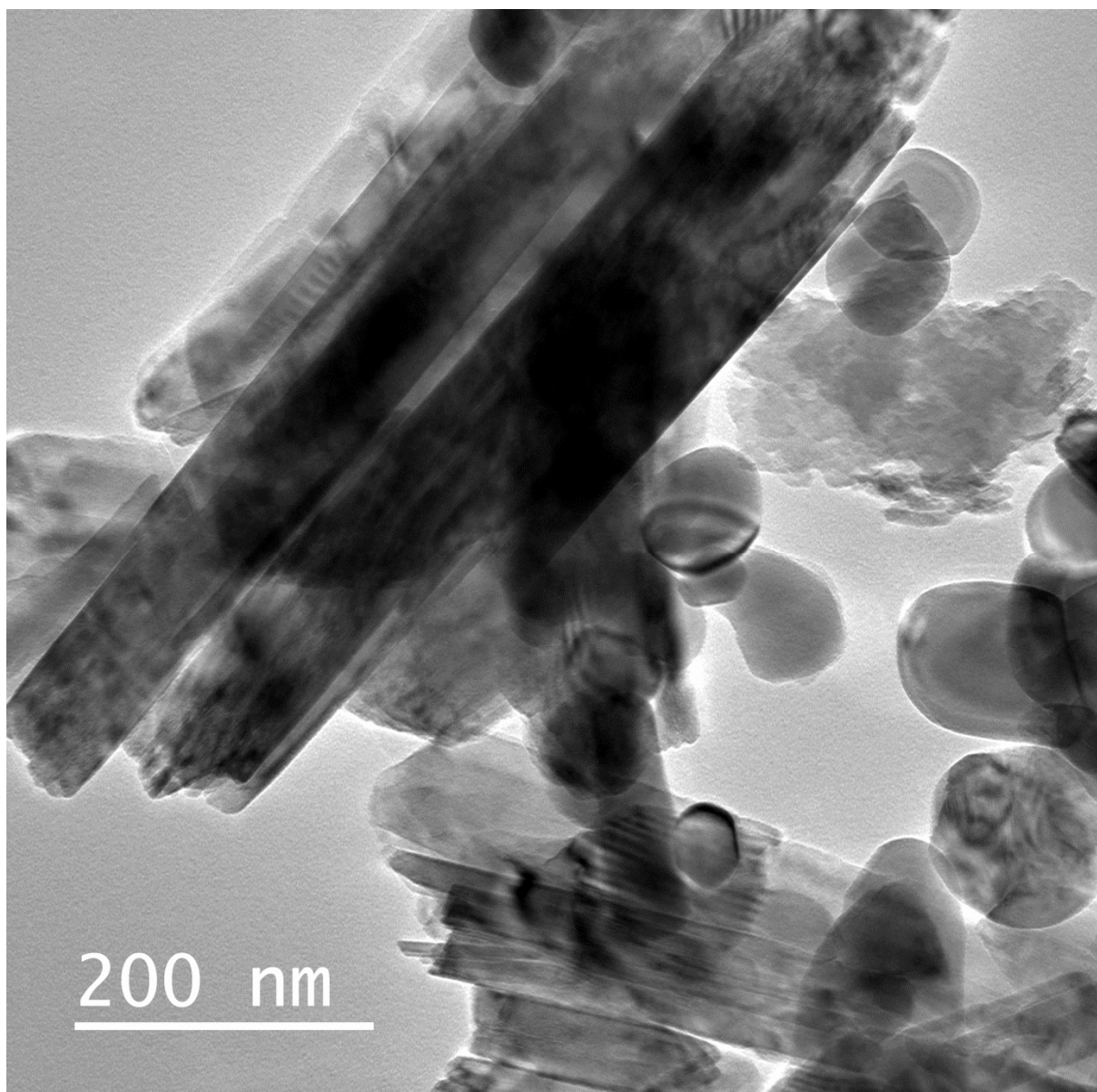
Figure S6.3: High resolution electron microscopy image of sample D observed using high-resolution transmission electron microscopy (HRTEM) on a JEOL JEM-2100 at 200 kV. Structure resolution of microscope was set at 0.2 nm.
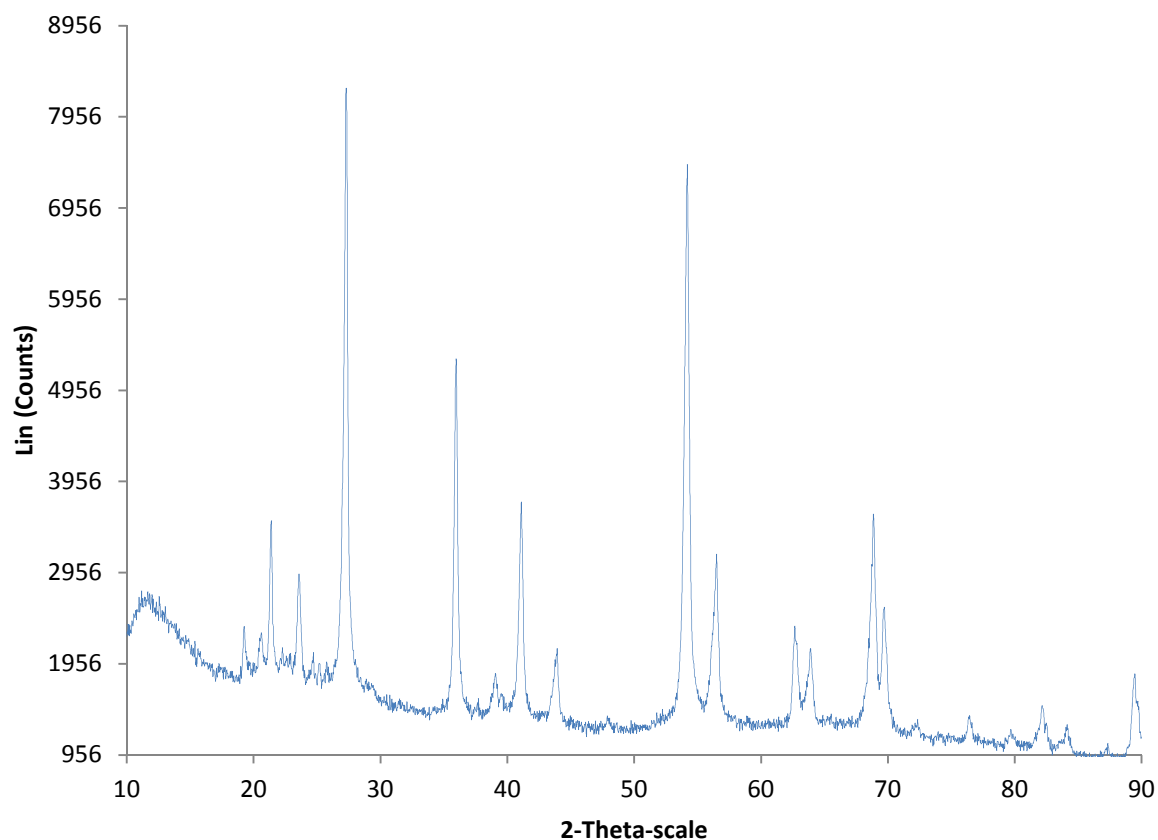
Figure S6.4: X-ray diffactogram for sample D dried in an electric oven at 100 ℃ for one hour. Instrument settings were 2Th/Th locked - Start: 10.000 ° - End: 89.983 ° - Step: 0.034 ° - Step time: 220. s - Temp.: 25 °C (Room) - Time Started: 8 s - 2-Theta: 10.000 ° - Theta: 5.000 ° - χ: 0.00 ° - ψ: 0.00 ° - X: 0.0 mm - Y: 0.0 mm - Operations: Background 0.068,1.000 with Enhanced background 6.761,1.000 and wavelength set at 1.5406 nm.
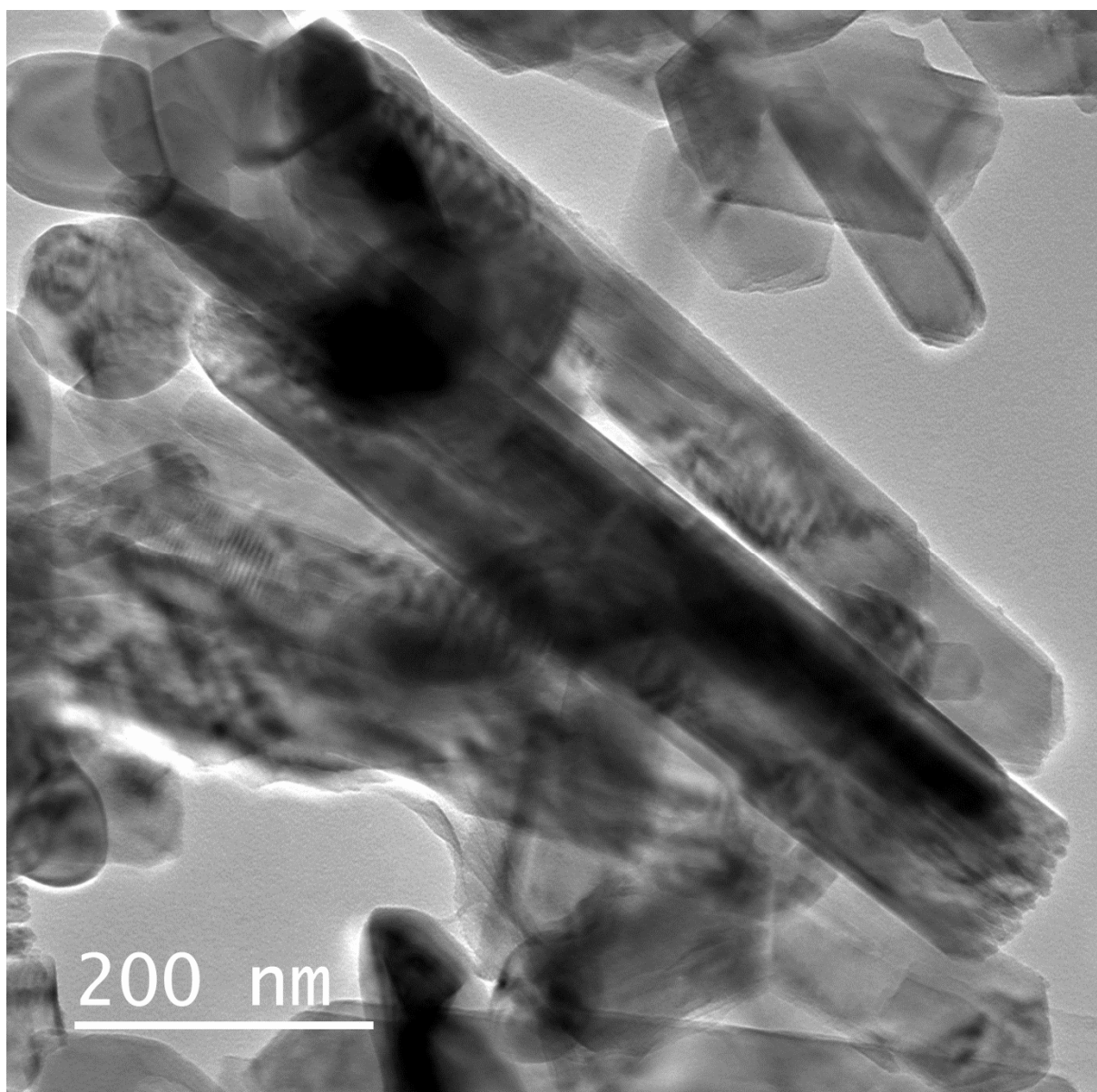
Figure S6.5: High resolution electron microscopy image of sample E observed using high-resolution transmission electron microscopy (HRTEM) on a JEOL JEM-2100 at 200 kV. Structure resolution of microscope was set at 0.2 nm.
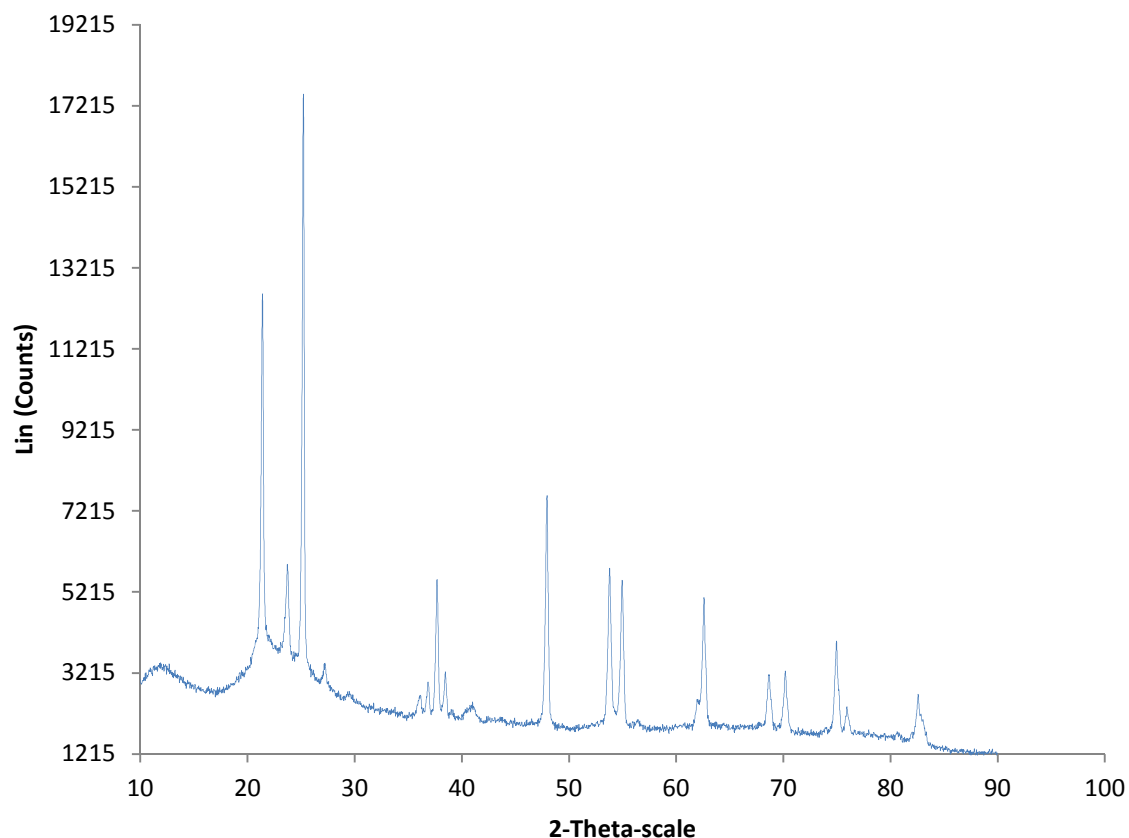
Figure S6.6: X-ray diffactogram for sample E dried in an electric oven at 100℃ for one hour. Instrument settings were 2Th/Th locked - Start: 10.000 ° - End: 89.983 ° - Step: 0.034 ° - Step time: 220. s - Temp.: 25 °C (Room) - Time Started: 8 s - 2-Theta: 10.000 ° - Theta: 5.000 ° - χ: 0.00 ° - ψ: 0.00 ° - X: 0.0 mm - Y: 0.0 mm - Operations: Background 0.068,1.000 with Enhanced background 6.761,1.000 and wavelength set at 1.5406 nm.
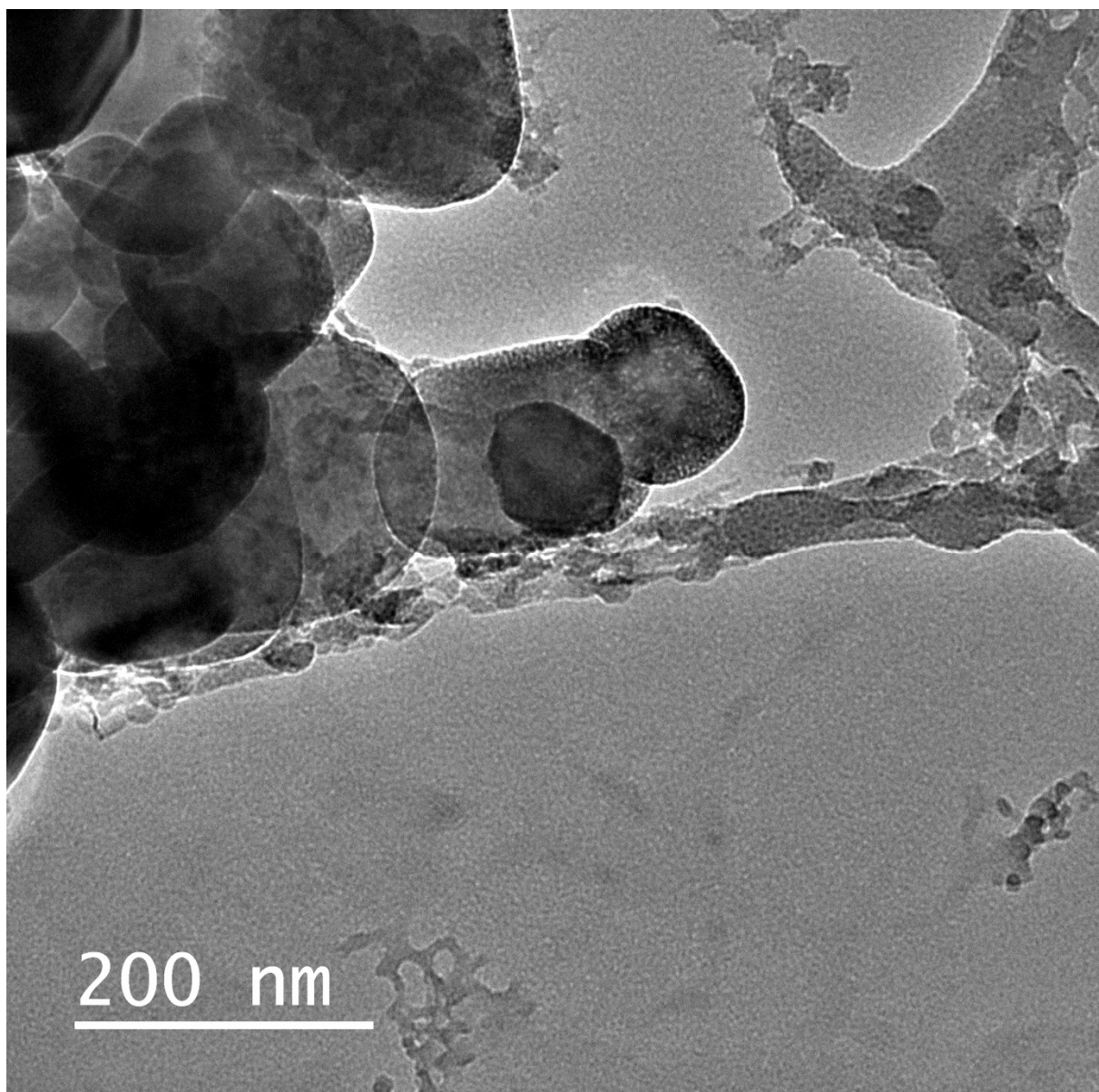
Figure S6.7: High resolution electron microscopy image of sample H observed using high-resolution transmission electron microscopy (HRTEM) on a JEOL JEM-2100 at 200 kV. Structure resolution of microscope was set at 0.2 nm.
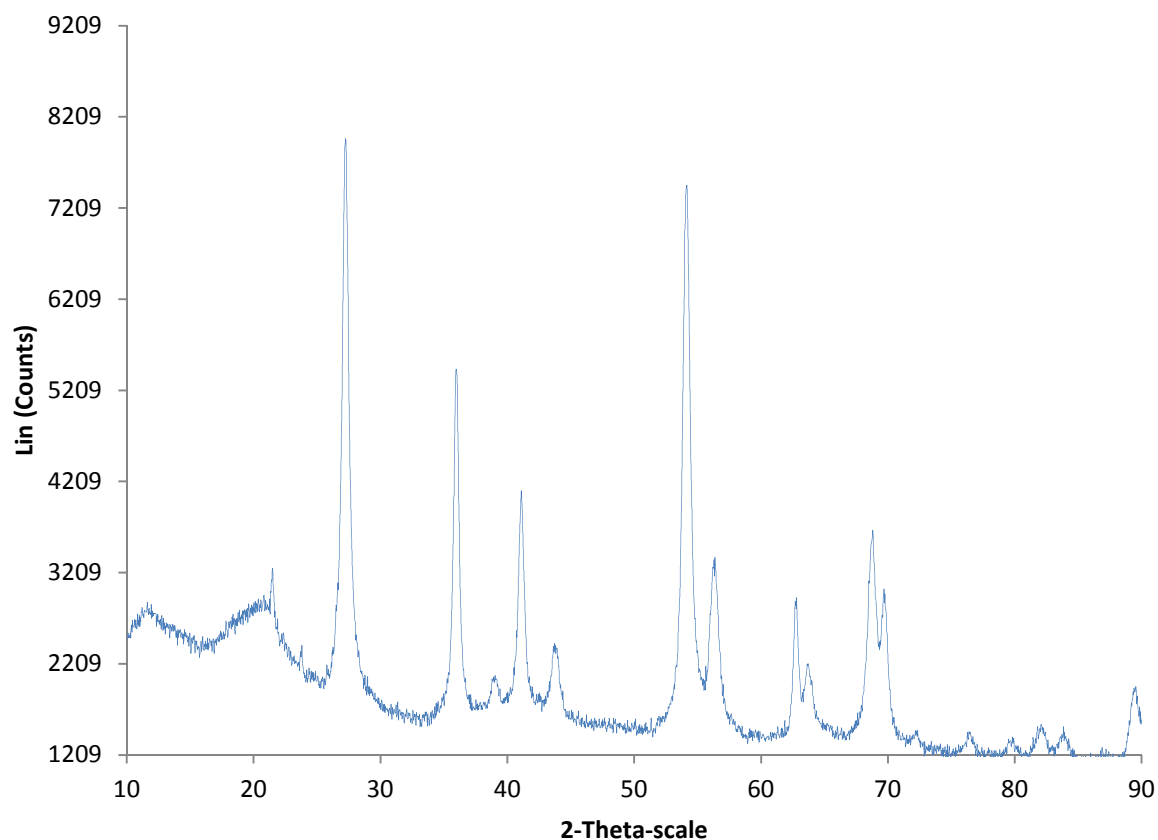
Figure S6.8: X-ray diffactogram for sample H dried in an electric oven at 100℃ for one hour. Instrument settings were 2Th/Th locked - Start: 10.000 ° - End: 89.983 ° - Step: 0.034 ° - Step time: 220. s - Temp.: 25 °C (Room) - Time Started: 8 s - 2-Theta: 10.000 ° - Theta: 5.000 ° - χ: 0.00 ° - ψ: 0.00 ° - X: 0.0 mm - Y: 0.0 mm - Operations: Background 0.068,1.000 with Enhanced background 6.761,1.000 and wavelength set at 1.5406 nm.
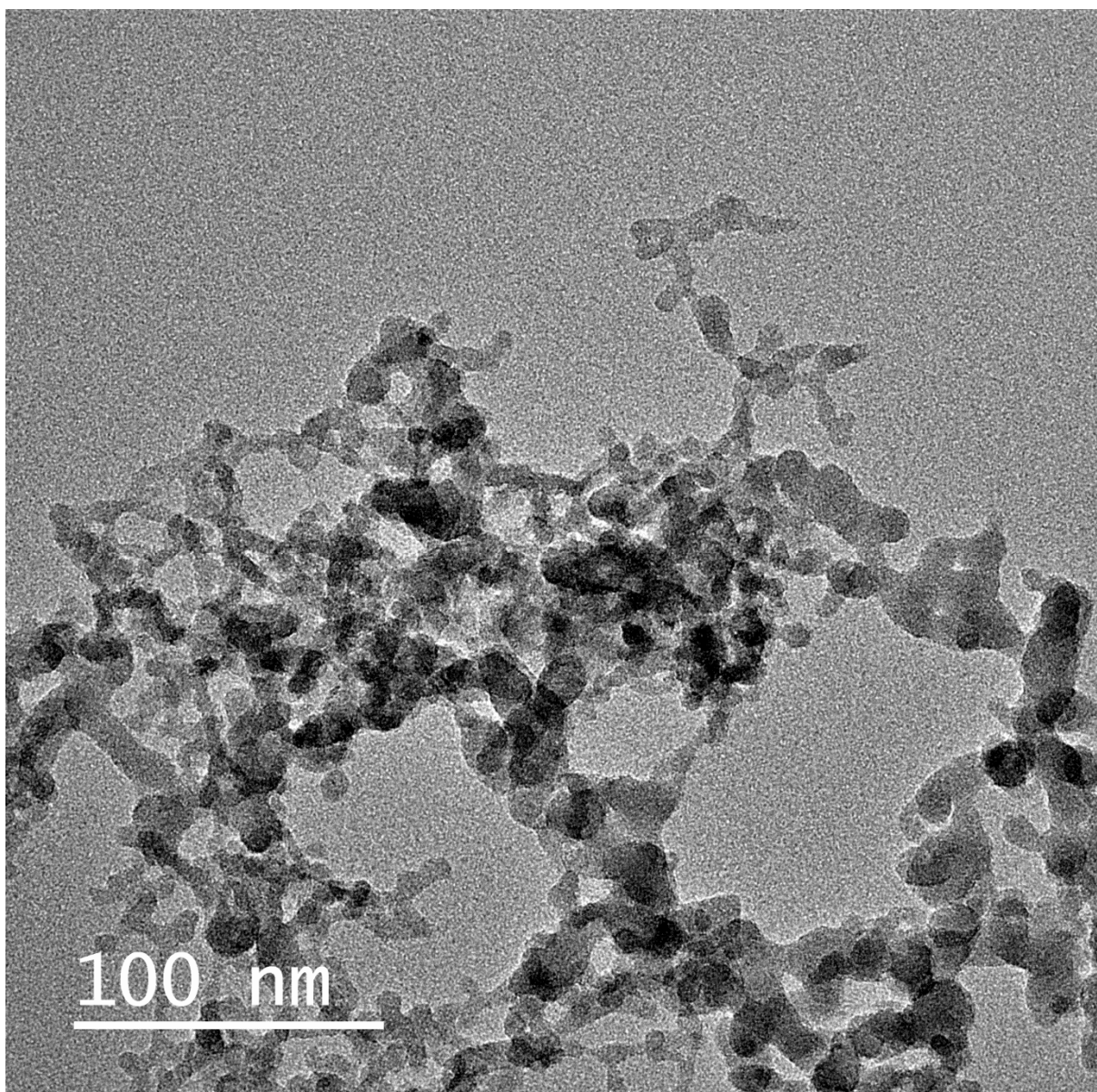
Figure S6.9: High resolution electron microscopy image of sample A observed using high-resolution transmission electron microscopy (HRTEM) on a JEOL JEM-2100 at 200 kV. Structure resolution of microscope was set at 0.2 nm.
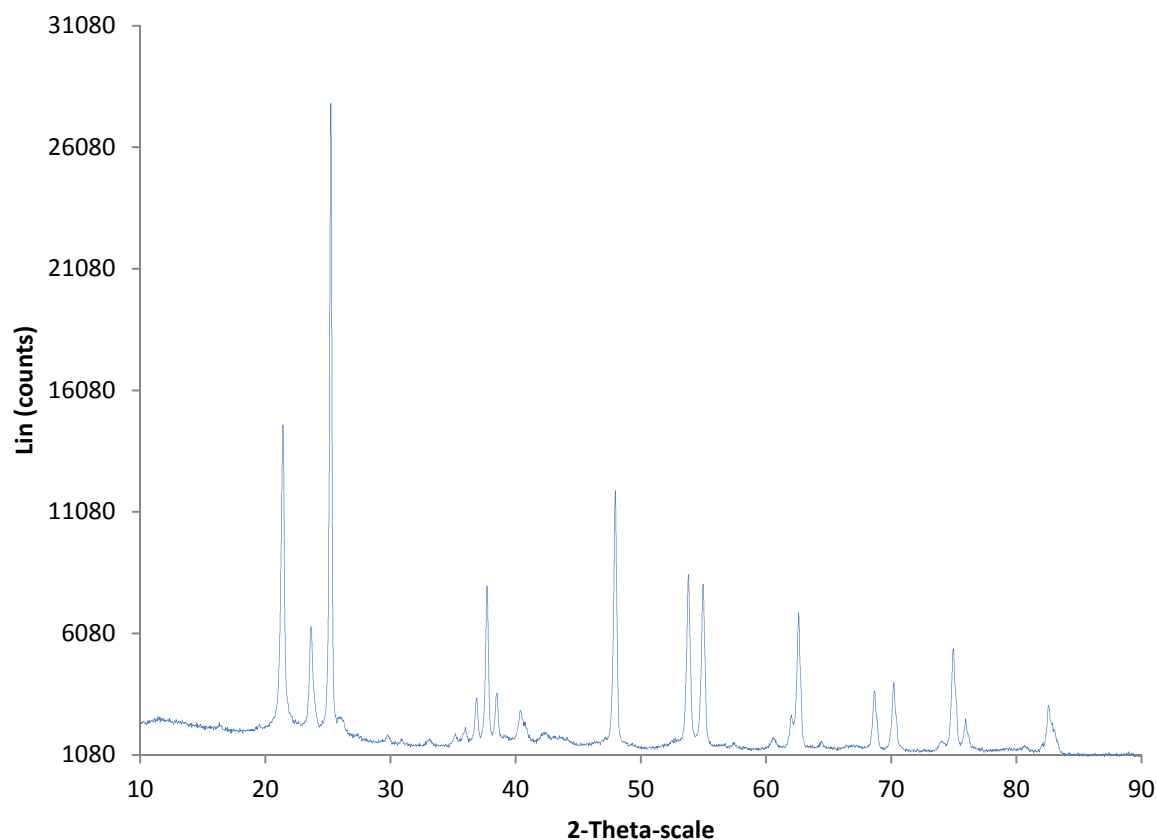
Figure S6.10: X-ray diffactogram for sample A dried in an electric oven at 100 ℃ for one hour. Instrument settings were 2Th/Th locked - Start: 10.000 ° - End: 89.983 ° - Step: 0.034 ° - Step time: 220. s - Temp.: 25 °C (Room) - Time Started: 8 s - 2-Theta: 10.000 ° - Theta: 5.000 ° - χ: 0.00 ° - ψ: 0.00 ° - X: 0.0 mm - Y: 0.0 mm - Operations: Background 0.068,1.000 with Enhanced background 6.761,1.000 and wavelength set at 1.5406 nm.
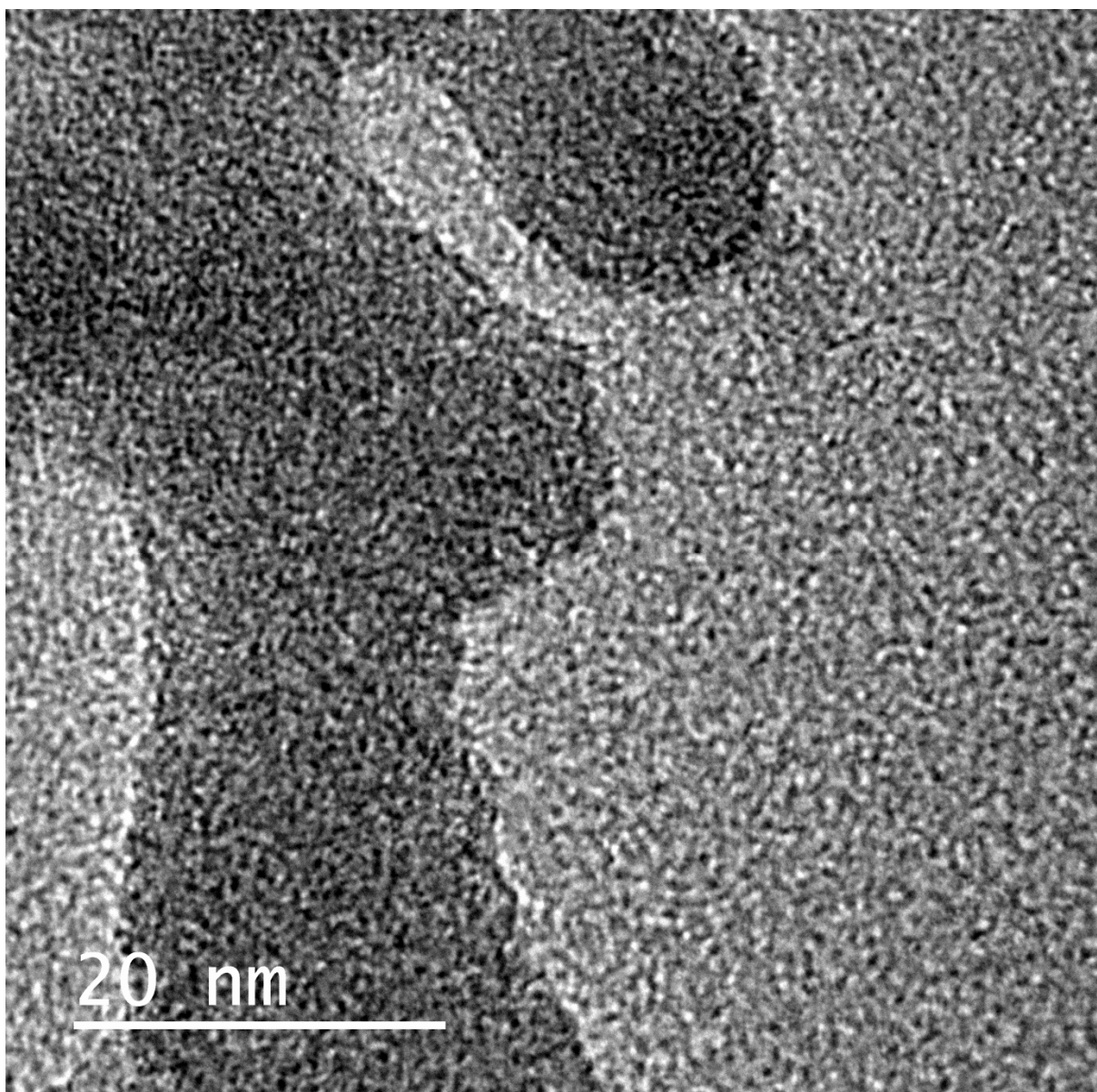
Figure S6.11: High resolution electron microscopy image of sample B observed using high-resolution transmission electron microscopy (HRTEM) on a JEOL JEM-2100 at 200 kV. Structure resolution of microscope was set at 0.2 nm.
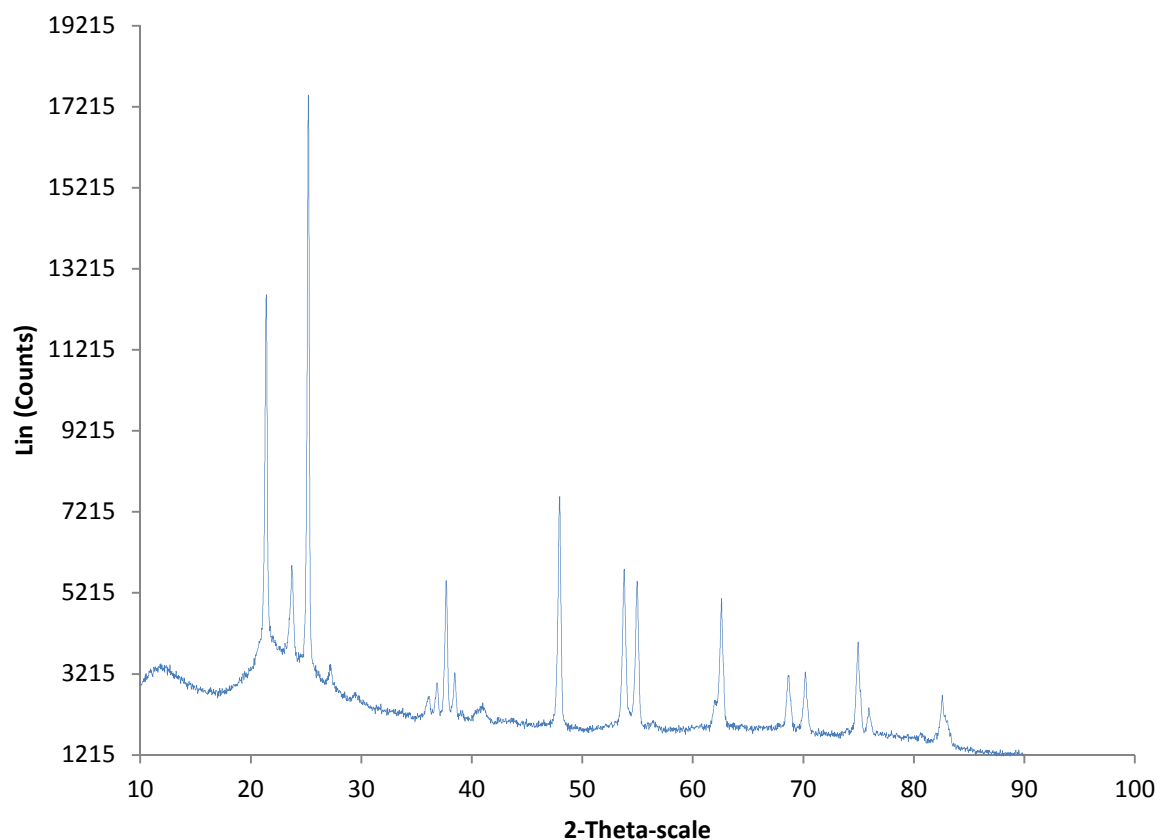
Figure 16: X-ray diffactogram for sample B dried in an electric oven at 100℃ for one hour. Instrument settings were 2Th/Th locked - Start: 10.000 ° - End: 89.983 ° - Step: 0.034 ° - Step time: 220. s - Temp.: 25 °C (Room) - Time Started: 8 s - 2-Theta: 10.000 ° - Theta: 5.000 ° - χ: 0.00 ° - ψ: 0.00 ° - X: 0.0 mm - Y: 0.0 mm - Operations: Background 0.068,1.000 with Enhanced background 6.761,1.000 and wavelength set at 1.5406 nm.
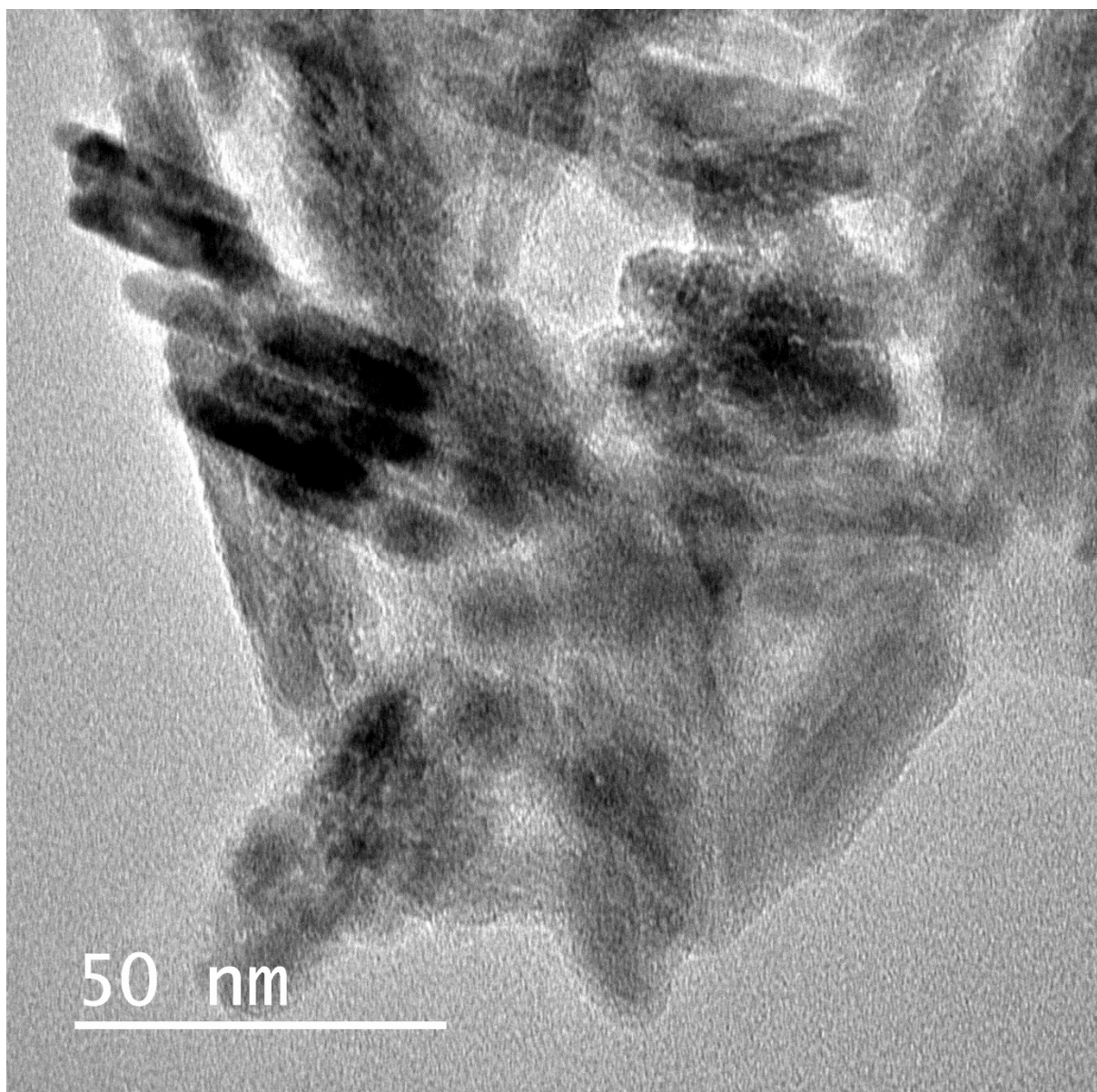
Figure S6.13: High resolution electron microscopy image of sample F observed using high-resolution transmission electron microscopy (HRTEM) on a JEOL JEM-2100 at 200 kV. Structure resolution of microscope was set at 0.2 nm.
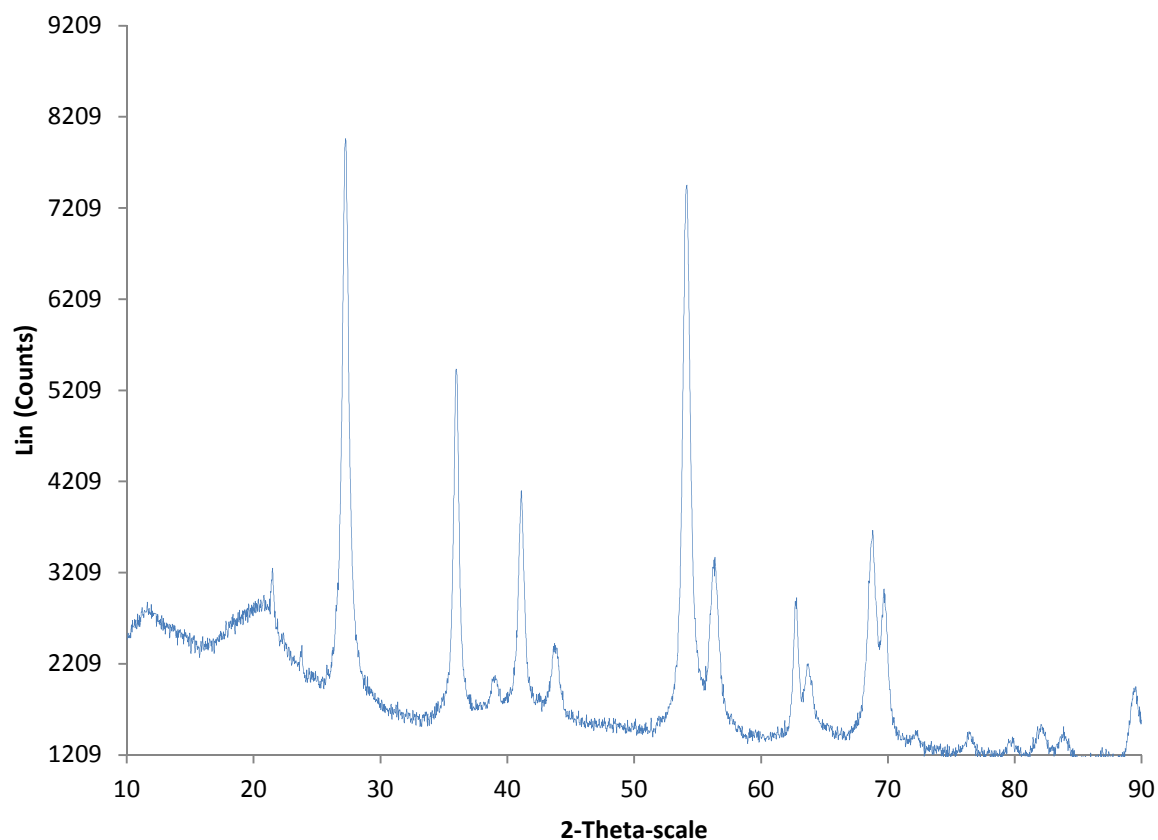
Figure S6.14: X-ray diffactogram for sample F dried in an electric oven at 100 ℃ for one hour. Instrument settings were 2Th/Th locked - Start: 10.000 ° - End: 89.983 ° - Step: 0.034 ° - Step time: 220. s - Temp.: 25 °C (Room) - Time Started: 8 s - 2-Theta: 10.000 ° - Theta: 5.000 ° - χ: 0.00 ° - ψ: 0.00 ° - X: 0.0 mm - Y: 0.0 mm - Operations: Background 0.068,1.000 with Enhanced background 6.761,1.000 and wavelength set at 1.5406 nm.
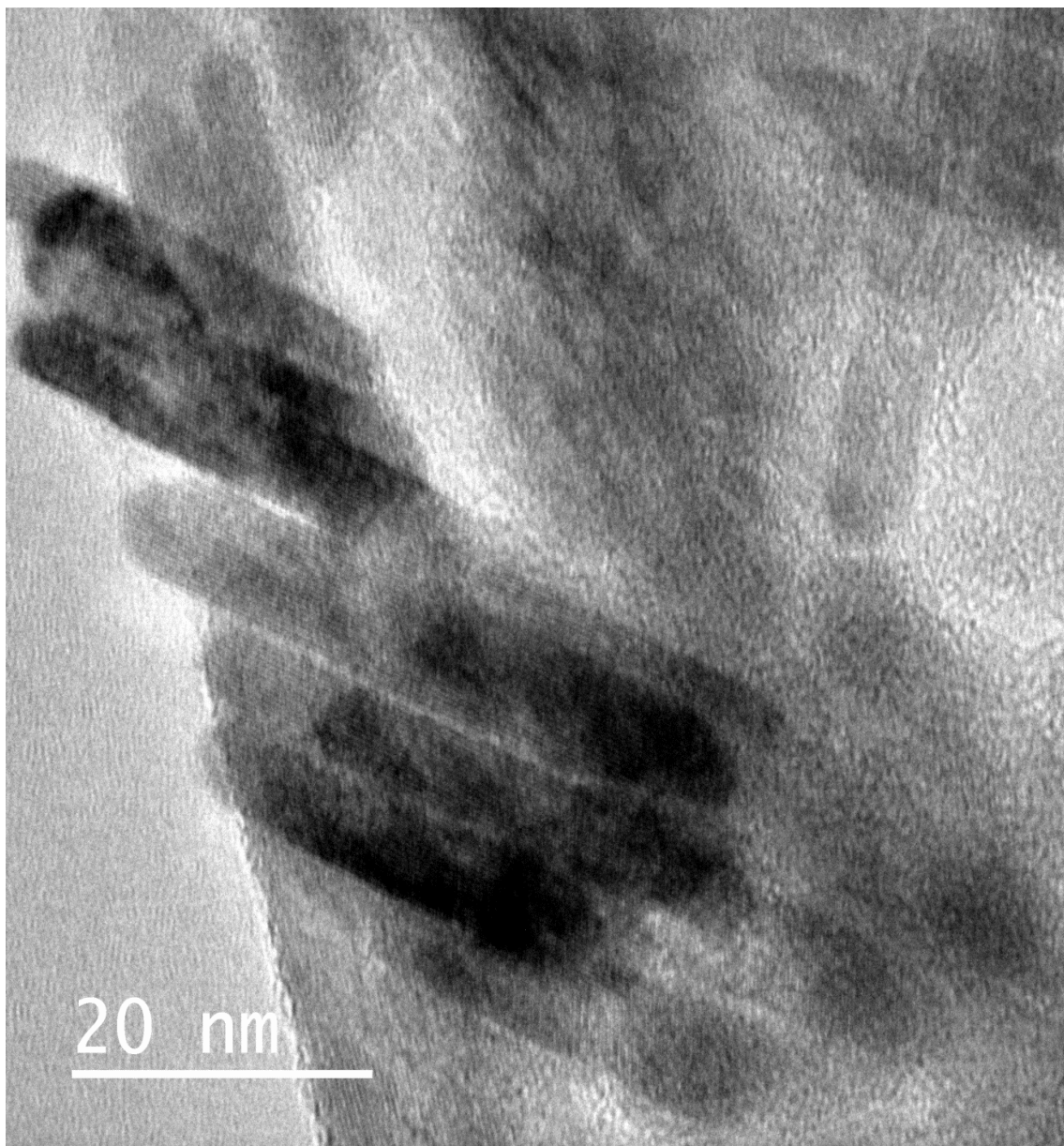
Figure S6.15: High resolution electron microscopy image of sample G observed using high-resolution transmission electron microscopy (HRTEM) on a JEOL JEM-2100 at 200 kV. Structure resolution of microscope was set at 0.2 nm.
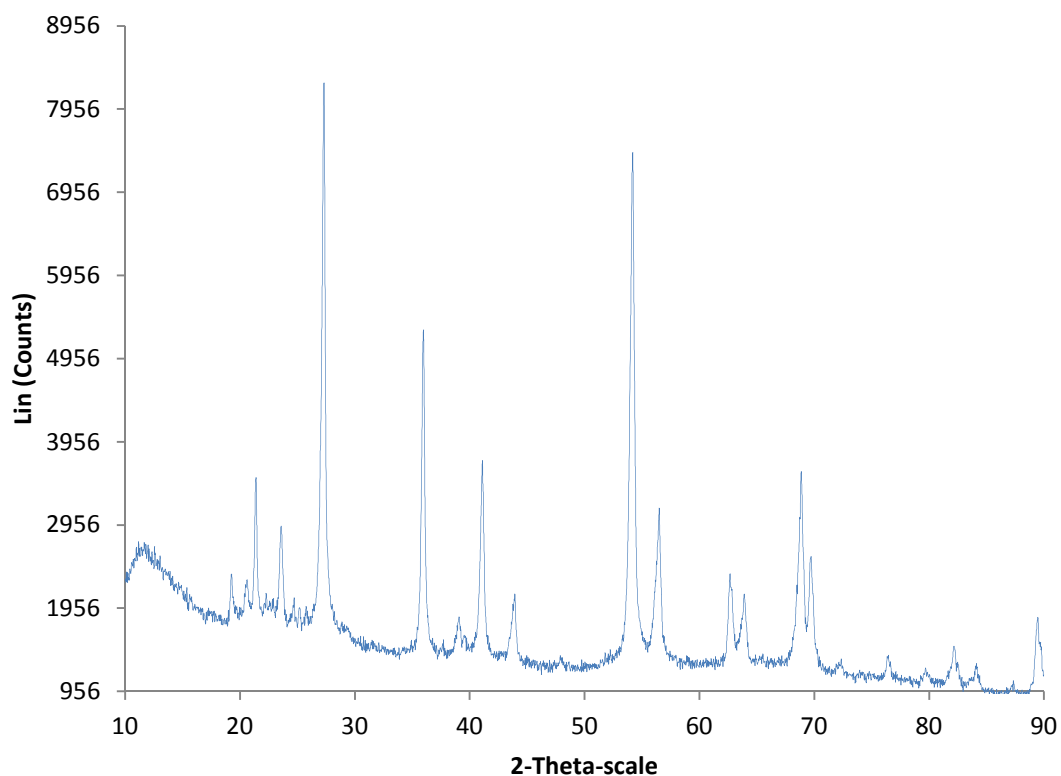
Figure S6.16: X-ray diffactogram for sample G dried in an electric oven at 100℃ for one hour. Instrument settings were 2Th/Th locked - Start: 10.000 ° - End: 89.983 ° - Step: 0.034 ° - Step time: 220. s - Temp.: 25 °C (Room) - Time Started: 8 s - 2-Theta: 10.000 ° - Theta: 5.000 ° - χ: 0.00 ° - ψ: 0.00 ° - X: 0.0 mm - Y: 0.0 mm - Operations: Background 0.068,1.000 with Enhanced background 6.761,1.000 and wavelength set at 1.5406 nm.

Table 15: Duplicate determination of TiO_2 from the XRD difractographic data using Scherrer's equation.

Sample	Kλ	2Θ	Θ	CosΘ	FWHM	β	τ/ nm
A1	0.1448164	27.24341	13.621705	0.97187	0.53643	0.009363684	15.91339479
A2	0.1448164	54.12637	27.063185	0.89051	0.56319	0.009830794	16.54208835
B1	0.1448164	27.26918	13.63459	0.97182	0.30344	0.005296714	28.13360653
B2	0.1448164	54.15218	27.07609	0.8904	0.37802	0.006598549	24.64813945
C1	0.1448164	25.21269	12.606345	0.97589	0.17733	0.003095394	47.94032674
C2	0.1448164	47.94088	23.97044	0.91576	0.24328	0.004246588	37.23882718
D1	0.1448164	25.24339	12.621695	0.97583	0.14599	0.002548337	58.23536441
D2	0.1448164	47.99019	23.995095	0.91358	0.20131	0.003513978	45.10992855
E1	0.1448164	25.19646	12.59823	0.97592	0.18312	0.003196461	46.42309311
E2	0.1448164	21.38227	10.691135	0.98264	0.19902	0.003474005	42.42217301
F1	0.1448164	27.29959	13.649795	0.91776	0.48293	0.008429811	18.71848782
F2	0.1448164	36.16564	18.08282	0.95061	0.32322	0.005641985	27.00122495
G1	0.1448164	27.12458	13.56229	0.543731517	0.32956	0.005752653	46.29830274
G2	0.1448164	36.98547	18.492735	0.937012	0.20234	0.003531957	43.7579707
H1	0.1448164	25.26541	12.632705	0.997800681	0.14258	0.002488813	58.31518598
H2	0.1448164	47.59754	23.79877	0.234617531	0.59856	0.010448197	59.07665825
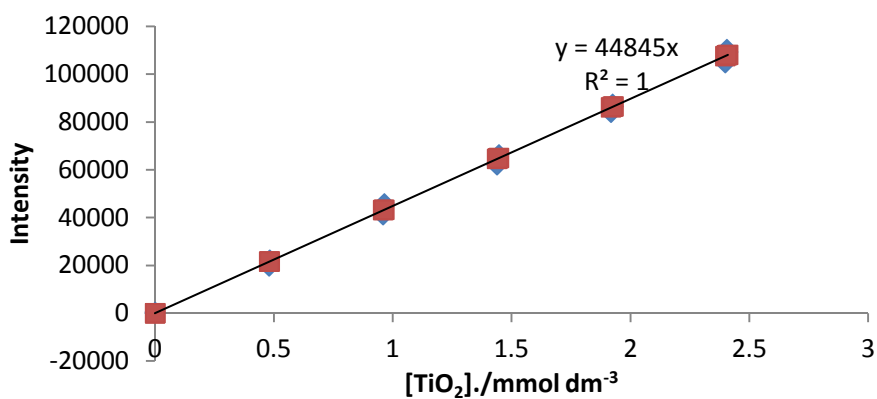
Figure S6.17.1: The calibration curve for quantitation of TiO_2 on ICP-OES operating conditions were: argon gas flow rate of 1.5 litres (L) min^{-1}, auxiliary and nebulizer gas flows at 0.2 L min^{-1} and 0.8 L min^{-1} respectively. The pump flow rate was set at 1.5 mL min^{-1} while plasma radiofrequency working at 1300 W and data acquired at 337.279 nm wavelength.
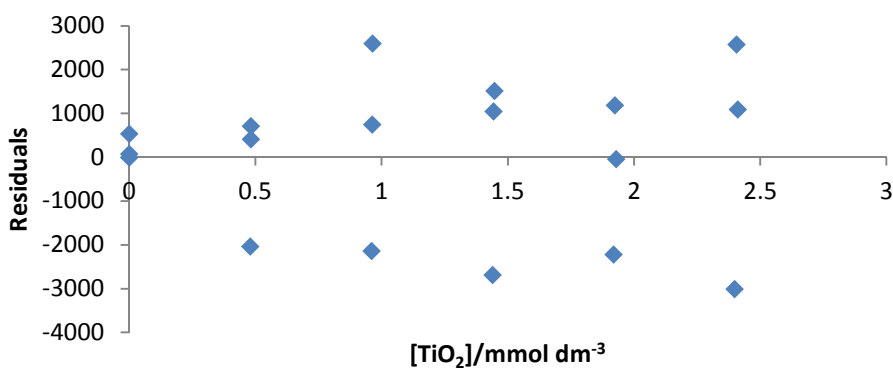
Figure S6.17.2: Residual plot for TiO_2

Chapter Seven

An investigation of the photostabilizing effect of grape seed extract on three common sunscreen absorbers

Moses A. Ollengo and Bice S. Martincigh[*]

School of Chemistry and Physics, University of KwaZulu-Natal, Westville Campus, Private Bag X54001, Durban 4000, South Africa

*Corresponding author: Tel.:+27-31-2601394; Fax: +27-31-2603091; E-mail address: martinci@ukzn.ac.za

Abstract

The photostabilizing ability of grape seed extract on the common sunscreen absorbers: 2-ethylhexyl-*p*-methoxcinnmate (EHMC), benzophenone-3 (BP3) and *tert*-butylmethoxy dibenzoylmethane (BMDBM) was investigated. The chemical composition of the extract was determined by GC-MS. The photostability of the samples was studied by exposure to simulated solar radiation. The change in UV absorption was followed by standard spectrophotometric methods. The major secondary metabolites in this extract were epicatechin and catechin. Exposure of the extract to UV radiation increased the UV absorption capacity of the extract linearly at 280 nm and 320 nm. All sunscreens showed an improved photostability in the extract. The inherent photo-instability of BMDBM when exposed to UV radiation was almost eliminated in the presence of grape seed extract. A mixture of all three sunscreens in the extract showed very high photostability and a red shift covering the entire UVB and UVA regions. The incorporation of the grape seed extract in sunscreens and other cosmetic formulations for topical application is likely to boost photoprotection by stabilizing the sunscreens included. Therefore, when grape seed extracts are combined with sunscreen absorbers photoprotection is enhanced without necessarily adding any other agent. This in turn helps in reducing the amounts of absorbers in a sunscreen product.

7.1   Introduction

Human skin is the principal defence of the entire body against harmful environmental contaminants, various xenobiotic factors and exposure to solar ultraviolet radiation (UV). The solar UV-spectrum can be divided into three regions: UVC (< 280 nm), UVB (280-320 nm) and UVA (320-400 nm) bands (Baliga and Katiyar 2006; Sklar et al. 2013). Approximately 5 % of the total solar UV radiation reaching the earth's surface falls in the UVB. UVB radiation has been shown to possess suppressive effects on the immune system, as well as acting as a tumour initiator, tumour promoter and a co-carcinogen (Santosh 2008). Various biological effects including: inflammation, sunburn cell formation, hyperpigmentation, immunological changes, and induction of oxidative stress, have been associated with exposure to UVB radiation. These biological responses contribute to the development of the many forms of skin cancer (Hruza and Pentland 1993; Krause et al. 2012). Among the various forms of skin cancer, basal cell carcinoma (BCC) and squamous cell carcinoma (SCC), referred to as non-melanoma skin cancer, are by far the most common form of cancer in humans and account for approximately 80 % and 16 %, respectively, of reported cases (Bowden 2004). The remaining part of the solar UV radiation (about 90-95 %) falls in the UVA region. UVA radiation has longer wavelengths and correspondingly deeper penetration through the epidermis into the dermis. Exposure to UVA radiation induces the generation of singlet oxygen ($^1O_2$) and hydroxyl ($^{\cdot}OH$) free radicals, and a host of other reactive oxygen species (ROS), which can cause damage to cellular macromolecules, like proteins, lipids and DNA and suppress some immunological functions (DiGiovanni 1992; Santosh 2008; Sklar et al. 2013; Koksal et al. 2011; Mandal et al. 2009). It is also thought to initiate the worst form of skin cancer, namely, malignant melanoma (Baumler et al. 2012; Krause et al. 2012; Ley and Fourtanier 1997).

Thus, the adverse effect of UV radiation on human health and, particularly, the development of skin cancers cannot be overemphasized. There is therefore a need to develop efficient photoprotective and chemopreventive strategies to combat this hazard. The traditional approach has been the use of sunscreens incorporating both physical blockers and chemical absorbers in combination with other cosmetic agents. This approach has associated advantages and disadvantages; of prime concern is the photoinstability of some chemical absorbers and the cutaneous permeation of physical blockers into the more labile tissues. In the case of chemical absorbers, the photoproducts of some of the commonly used sunscreen agents are unknown and correspondingly their effects still a subject of further investigation. For the physical blockers commonly used, like titanium dioxide, their particle size is a major concern since the current use of nanoparticles poses the danger that these (< 100 nm) particles are likely to permeate deep into the dermis and cause more harm by way of ROS generation. Consequently, various health regulatory authorities have set maximum allowed values of these agents in various cosmetic formulations. However, the standards vary greatly from region to region with need for broad-spectrum protection and high sun protection factor (SPF).

There is a growing trend of incorporating plant extracts in sunscreen formulations with the aim of reducing the amounts of the sunscreening agents. The plant extracts come with other ethnopharmacological benefits though most of them are not yet confirmed. One major advantage of plant extracts is that they have a long history of traditional use for treating various disorders with no adverse effects.

Among the extracts that have attracted scientific interest is the grape seed (*Vitis vinifera*) extract. A number of working groups have shown that grape seed extract products have beneficial effects on vascular disease and wound healing (Khanna et al. 2002). There is a strong indication that these extracts play a preventative role against some cancers (American Cancer Society 2008; Kaur et al.

2006). Results from both *in-vitro* and *in-vivo* models indicate that grape seed extract confers potent protection against oxidative stress and free radical-mediated tissue damage (Bagchi et al. 2000). A major constituent of grape seed extract are proanthocyanidins. These are envisaged to inhibit enzymes integral to the breakdown of the skin, such as collagenase, elastase, hyaluronidase and inhibit tumour growth (Mantena 2005). The proanthocyanidins present in grape seeds are known to have biological effects, including prevention of photocarcinogenesis (Svobodova et al. 2003).

Proanthocyanidins occur naturally in a large variety of fruits, vegetables, nuts, seeds, flowers and bark. This class of phenolic compounds takes the form of oligomers or polymers of polyhydroxy flavan-3-ol units, such as (+)-catechin and (-)-epicatechin (Steinmetz and Potter 1996) (Fig 7.1). The seeds of the grape are a particularly rich source of proanthocyanidins; the major component of polyphenols in red wine. These grape seed proanthocyanidins are mainly dimers, trimers and highly polymerized oligomers of monomeric catechins (Scalbert and Williamson 2000) (Fig. 7.1). Experimental work has shown proanthocyanidins from grape seeds to be potent antioxidants and free radical scavengers, being more effective than either ascorbic acid or vitamin E (Joshi et al. 2001; Bagchi et al. 1997). These secondary metabolites have been shown to have anti-carcinogenic activity in different cancer models (Sudheer et al. 2006). There is overwhelming interest in the use of botanicals for the prevention of various diseases; the main focus has been their consumption as dietary supplements. The topical application of plant extracts in combination with known sun active molecules in cosmetics is on the rise but no literature is available on their actual role. The aim of this study was to investigate the effects of grape seed extract on the photostability of, 2-ethylhexyl-*p*-methoxy cinnamate (EHMC), benzophenone-3 (BP3) and *tert*-butylmethoxy dibenzoylmethane (BMDBM).

(epicatechin)

(2*S*,3*S*)-2-(3,4-dihydroxyphenyl)-3,4-dihydro-2*H*-chromene-3,5,7-triol

(catechin)

(2*R*,3*S*)-2-(3,4-dihydroxyphenyl)-3,4-dihydro-2*H*-chromene-3,5,7-triol

proanthocyanidins

(2*R*,3*S*)-2-(3,4-dihydroxyphenyl)-4-((2*S*)-2-(3,4-dihydroxyphenyl)-4-((2*R*,3*S*,4*R*)-2-(3,4-dihydroxyphenyl)-3,5,7-trihydroxy-4-methyl-3,4-dihydro-2*H*-chromen-8-yl)-6-((2*S*,3*S*)-2-(3,4-dihydroxyphenyl)-3,5,7-trihydroxychroman-4-yl)-5-hydroxy-3,4-dihydro-2*H*-chromen-8-yl)-3,4-dihydro-2*H*-chromene-3,5,7-triol
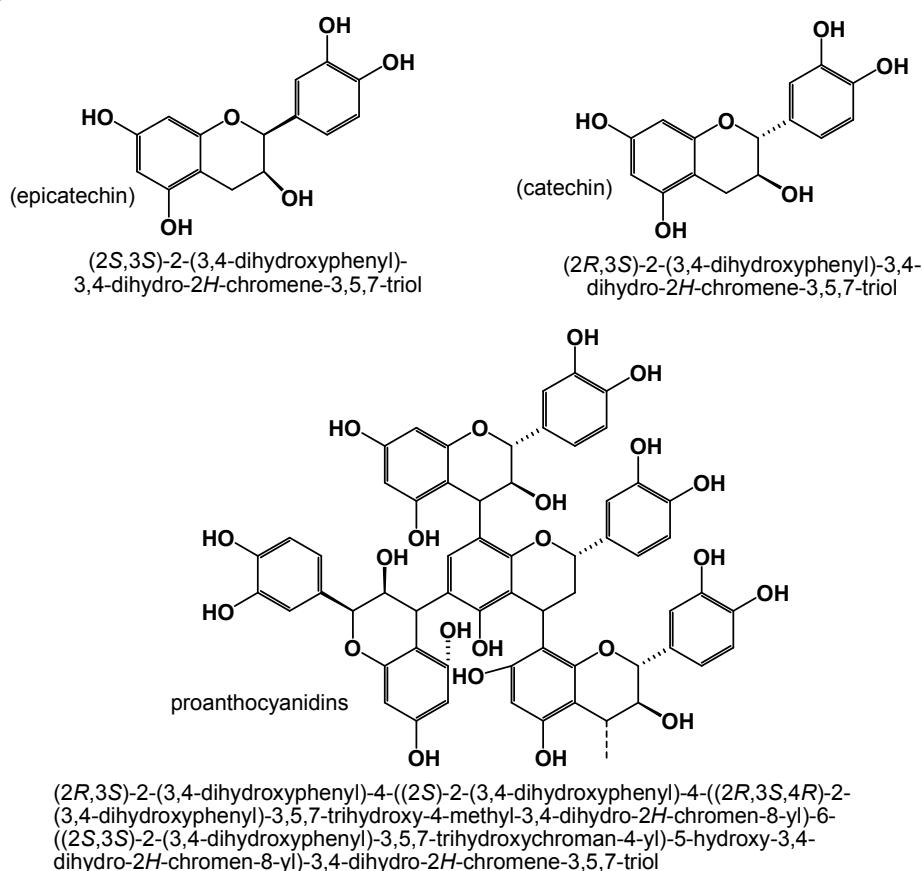
Figure 7.17: Common proanthocyanidins and anthocyanidins found in grape seed (*Vitis vinifera*) extracts.

7.2 Materials and Methods

The grape seed extract was firstly characterised and then its effect on the photostability of the common sunscreen absorbers investigated as detailed below.

7.2.1 Materials

The grape seed extract was purchased from Warren Chem Specialities (Pty) Ltd, South Africa. The solvents, acetonitrile (ACN) and methanol (MeOH), of HPLC-grade were purchased from Merck KGaA. The three chemical UV filters of analytical purity (99.9 %) were purchased as follows: 2-ethylhexyl-*p*-methoxcinnmate (EHMC) and *tert*-butylmethoxy dibenzoylmethane (BMDBM) were kind donation from BASF, benzophenone-3 (BP3) from Sigma-Aldrich and N,O-bis(trimethylsilyl)trifluoroacetamide (BSTFA) was purchased from Supelco.

7.2.2 Characterisation of grape seed extract

The grape seed extract was characterised by gas chromatography-mass spectrometry (GC-MS), gas chromatography-flame ionisation detection (GC-FID), and high performance liquid chromatography-mass spectrometry (HPLC-MS) in order to identify the chemical components present.

7.2.2.1 Sample preparation

About 25 mg of grape seed extract powder was soaked in 25 mL of methanol at 25 °C and placed in an ultrasonic bath for two hours and then left to stand for 24 hours protected from light by aluminium foil. The extraction mixture was then made up to 50 mL in a volumetric flask with methanol. The resultant solution was filtered through a 0.45 μm Millipore Millex-LCR membrane filter and then transferred to an aluminium foil cased glass vial for storage. A 20 μL aliquot of this solution was injected into a high performance liquid chromatography-mass spectrometer (HPLC-MS) for characterisation of the chemical components in the extract. The remaining solution was preserved for photostability studies.

The grape seed extract samples for gas chromatography-mass spectrometry (GC-MS) characterisation were firstly derivatised to volatilise the polyphenols in the extract. This was achieved by dissolving a sample mass of about 2 mg of extract powder in 1.0 mL of ACN in a clean, dry 3 mL reaction vial. To this solution, 0.5 mL of N,O-bis(trimethylsilyl)trifluoroacetamide (BSTFA) was added, then capped tightly, mixed well, and heated at 70 °C for 45 min. The resultant derivatised mixture was filtered through a 0.45 μm Millipore Millex-LCR membrane syringe tip filter after cooling to room temperature. A volume of 0.1 μL of this derivatised sample was then injected into the GC-MS chromatograph.

7.2.2.2 The GC-MS experiment

A 0.1 μL volume of the derivatised grape seed extract sample was delivered into a Shimadzu GCMS (QP2010 SE), with a column temperature set at 70 °C and injection port at 250 °C. Injections were in split mode at a ratio of 20:1. Components were separated in a GL Sciences InertCap 5MS/Sil 30 m × 0.25 μm quartz capillary column with a bound stationary phase consisting of 5% dimethylpolysilphenylene siloxane. The column was held 70 °C for 2 min, a rise to 240 °C at 10 °C min⁻¹, then held for 5 min, followed by raise to 270 °C at 10 °C min⁻¹ and held there for 10 min. The linear velocity was set at 30.0 cm s⁻¹. The MS ion source temperature was 200 °C and the interface

temperature was set at 250 °C. The MS detector was programmed to run in scan mode in the *m/z* range 35-1000 at a scan speed of 3333. The total run time was 37 min with helium as the carrier gas.

7.2.2.3 The GC-FID experiment

To check method interconvertability a GC-FID experiment was carried out on the same samples (derivatised grape seed extract) with the same temperature program. The GC-FID used was a Shimadzu GC-2010, fitted with an autosampler AOC 20i and a flow unit type AFC-2010. Components were separated in a DB-5 30 m × 0.25 µm quartz capillary column with a bound stationary phase consisting of 5% phenyl polysilphenylene-siloxane. The make-up gas was nitrogen/air flowing at 10 mL min^{-1}, the carrier gas was hydrogen with a flow rate of 40 mL min^{-1} and oxygen/air flowing at 400 mL min^{-1}. The injection port was set at 250 °C, operating in a split mode of 20:1 for an injection volume of 0.1 µL. The velocity flow control mode was adopted keeping the pressure at 61.9 kPa, the total flow rate at 5.0 mL min^{-1}, the column flow of 0.68 mL min^{-1}, and a linear velocity of 20.0 mL s^{-1}.

7.2.2.4 HPLC-MS analysis

The grape seed extract dissolved in methanol (see Section 7.2.2.1) was characterised by means of HPLC-PDA-ESI-MS/MS. The analysis was carried out on an Agilent 1200 series LC MSD Trap, equipped with a photodiode array detector, a binary pump, a degasser, autosampler, and an ESI Trap MS. This employed a G1312A binary pump, a G1316A autosampler, a G1322A degasser and a G1315D photodiode array detector controlled by Chemstation software (Agilent, v.08.04). The chromatographic separation was achieved on an Agilent Zorbax Eclipse XDB C-18 reversed-phase column (150 × 4.6 mm i.d.; 5 µm particle size). The mobile phase was composed of water:formic acid (99:1, v/v volume; solvent A) and acetonitrile (solvent B). The mixtures were resolved by a gradient elution as follows: 5–13 min; 16 % B; 13-18 min; 45 % B and held for 5 min, 23-28 min; 75 % B, held for 5 min; 33-40 min; 99 % B, then held 5 min and then dropped linearly to 16 % B for 15 min. The experiment was performed at ambient temperature with a flow rate of 1 mL min^{-1} and an injection volume of 20 µL. The chromatograms were collected at detection wavelengths of 275 nm, 280 nm, 286 nm, 310 nm, 320 nm and 358 nm with a bandwidth of 4 nm simultaneously in each of the 60 min run time. The photodiode array detector was set to collect the UV-vis spectra of the chemical species separated over the range 190 to 800 nm. Analyses were interfaced to an Agilent-SL LC MSD trap equipped with an electrospray ionization source and operated in the negative-ion mode. The mass detector was a G2445A ion-trap mass spectrometer controlled by LCMSD software (Agilent, v.4.1). The nebulizing gas was nitrogen set at a pressure of 65 psi and flow rate adjusted to 116 mL min^{-1}. A heated capillary and voltage was maintained at 350 °C and 4 kV respectively. The instrument was programmed to scan over a mass range from *m/z* 90 to *m/z* 2000. The target ion accumulation in the trap was put at 30000 counts for a maximum accumulation time of 50 ms. MS^{2} data were acquired in the negative ionization automatic smart mode to obtain MS^{n-1}; primary precursor ion. The target ion was set at *m/z* 350, the compound stability at 100 %, and the trap drive level at 90 %. One precursor was selected each cycle; each precursor was excluded after 3 spectra; the release time was 0.3 minutes. All collision-induced fragmentation experiments were performed in the ion-trap with helium as the collision gas, and the voltage was increased in cycles from 0.3 up to 2 V. The fragmentation time was 20 ms at an activation width of 10 amu and the cut-off for the daughter ion range set at 30 %. MS^{3} data were obtained by manual fragmentation, targeting the most abundant ions in the precursor ion in the MS spectra.

7.2.3   Photostability experiments

The sunscreen mixtures with grape seed extract were prepared by adding about 20 mg of the sunscreen agents to 25 mL of the methanol extract (see Section 7.2.2.1). This solution was then made up to 50 mL in a volumetric flask with methanol. To obtain working solutions, appropriate dilutions were carried out in order to obtain a sunscreen agent concentration of about 200 μmol dm^{-3} in the extract before photostability studies were done.

Samples of grape seed extract with and without sunscreens added were exposed to simulated solar light in a Newport research lamp housing (M66901) fitted with a mercury-xenon lamp, powered by an arc lamp power supply (69911). The power output of the lamp was controlled by a digital exposure controller (68951) maintaining the output at 500 W. The output from the lamp was passed through a 10 mm-thick Pyrex filter to ensure that only wavelength greater than 300 nm impinged on the samples (see Supplementary Materials Fig. S7.1). The exposure time was varied incrementally from 0 hour in steps of 30 min to 4 hours of continuous exposure. Each exposed sample was contained in a stoppered 1.00 mm pathlength quartz cuvette. After each irradiation interval a UV-visible spectrum of the sample was recorded on a Perkin Elmer Lambda 35 spectrophotometer. A 20 μL aliquot of these same solutions were then injected into HPLC chromatograph to monitor the chemical transformations in the extract and the included sunscreen(s). Samples of the sunscreens alone dissolved in methanol were similarly irradiated and monitored by UV spectrophotometry.

7.2.3.1   HPLC analysis of the irradiated samples

The chemical transformations in the irradiated samples were monitored on a Shimadzu Prominence LC chromatograph with PDA detector. The chromatographic separation was achieved on Agilent Zorbax Eclipse XDB C-18 reversed-phase column (150 × 4.6 mm i.d.; 5 μm particle size). The mobile phase was composed of water (solvent A) and acetonitrile (solvent B). The mixtures were resolved by a gradient elution as follows: 5–13 min; 16 % B; 13-18 min; 45 % B and held for 5 min, 23-28 min; 75 % B, held for 5 min; 33-40 min; 99 % B, then held 5 min and then dropped linearly to 16 % B for 15 min. The experiment was performed at ambient temperature with a flow rate of 1 mL min^{-1} and an injection volume of 10 μL. The chromatograms were collected at detection wavelengths of 275 nm, 280 nm, 286 nm, 310 nm, 320 nm and 358 nm with a bandwidth of 4 nm simultaneously in each of the 60 min run time. The photodiode array detector was set collect the UV-vis spectra of the chemical species separated over the range 190 to 800 nm.

7.3   Results and discussion

The UV-Vis spectrum of the grape seed extracts showed absorbance in the UVC and UVB range, a very close similarity to the spectrum of catechin (Santos-Buelga et al. 1995; Plumb et al. 1998) (Fig 7.2). This observation was supported by HPLC analysis of the extract. The chromatogram detected at 280 nm exhibited one prominent broad peak with a similar UV spectrum (Fig. 7.3) to catechin. The broadness of this peak is a result of the co-elution of the two stereoisomers which could not be resolved under the current chromatographic conditions. However, both GC-FID and GC-MS analyses resolved the two isomers as epicatechin and catechin (Fig. 7.4) at retention times of 31.970 and 32.581 min respectively. GC-MS analysis of the derivatized grape seed extract showed very high amounts of the two stereomeric isomers of flavan-3-ols; epicatechin and catechin (Fig. 7.4). Exposure of the grape seed extract dissolved in methanol to solar simulated radiation showed an increase in the absorbance with increasing irradiation time (Fig. 7.5 and 7.6). This indicates an increase in photoprotection. The two isomers are known to undergo oligomeric polymerization to yield

proanthocyanidins catalysed by UV light (Fig. 7.7). The observed phenomenon can be envisaged to be due to the polymerization of the oligomers in three fashions: either a *cis – cis*, *trans – trans* or *trans – cis* assembly of oligomers (Fig. 7.7). This results in different conjugation patterns that result in an increase in absorption extending to the UVA range. The linear increase in absorption capacity observed at 280 nm and 320 nm suggest that the same type of molecules come together in the same fashion to form the polymer achieving a linear reaction relation (Fig. 7.6). From the linear increase in absorbance at 280 nm and 320 nm it is proposed that the molecules combine in a *cis-trans* configuration. This stereochemistry provides better conjugation and n to π^* and π to π^* electronic transitions are enhanced thus increasing the UV absorption in the UVA range. This is apparent from the prominent peaks seen at 320 nm and 358 nm on the HPLC chromatogram (Fig. 7.8).
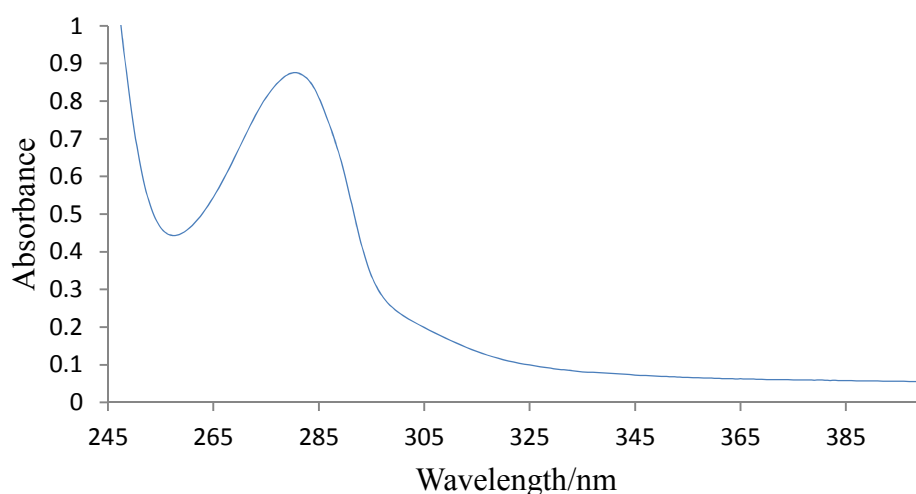
Figure 7.2: UV spectrum of a 0.06 mg mL^{-1} solution of grape seed extract dissolved in methanol. The spectrum was acquired with a Perkin Elmer Lambda 35 UV-Vis spectrophotometer in a 1 mm pathlength quartz cuvette with air as the reference.
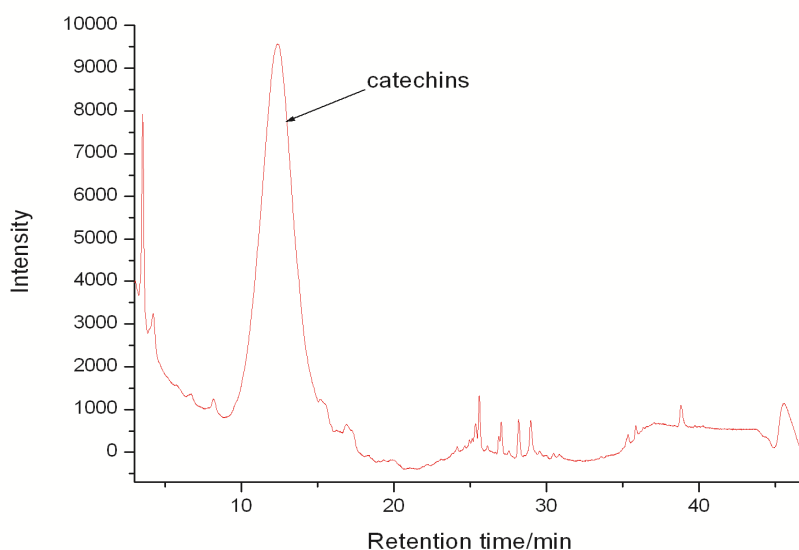
Figure 7.3: HPLC chromatogram of grape seed extract detected at 280 nm. The separation was achieved on a reversed-phase Zorbax Eclipse XDB C-18 column (150 mm × 4.6 mm, i.d., 5 µm), under a gradient elution of acetonitrile-water at flow rate of 1 mL min^{-1}and an injection volume of 20 µL.
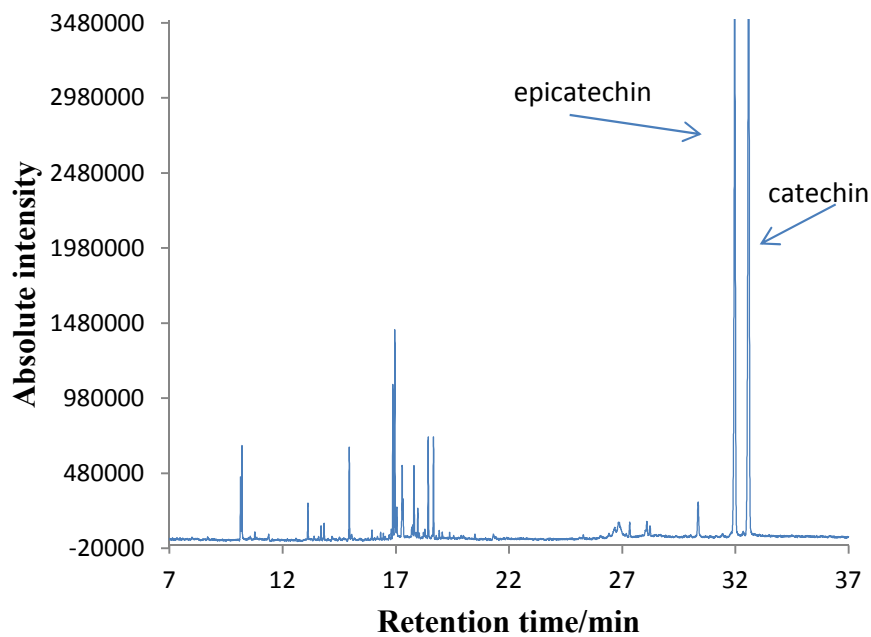
Figure 7.4: Total ion chromatogram of TMS-derivatized grape seed extract showing epicatechin and catechin. The separation was effected on a GL Sciences InertCap 5MS/Sil 30 m × 0.25 quartz capillary column under the condition described in section 7.2.2.2.
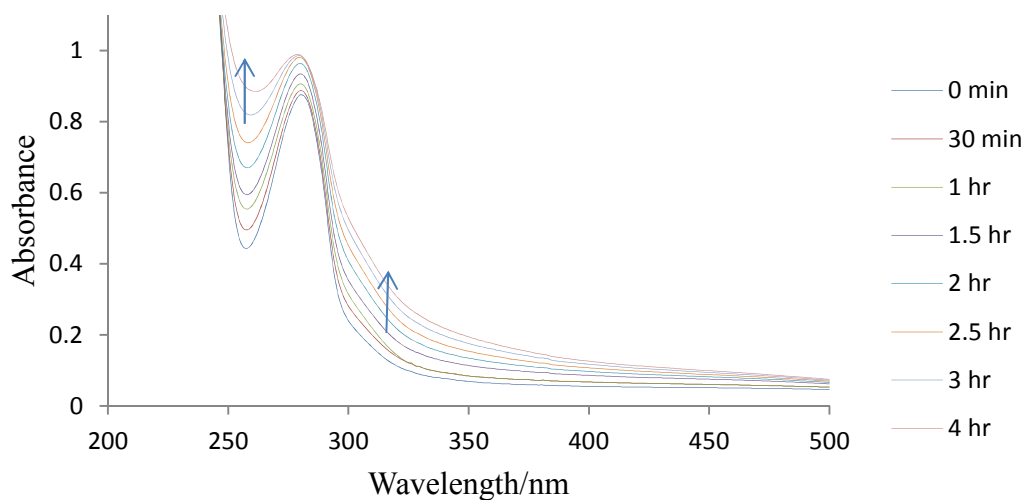
Figure 7.5: The photostability of 0.06 mg mL^{-1} grape seed extract dissolved in methanol, exposed to solar simulated radiation, in a 1 mm pathlength quartz cuvette. Each exposure cycle involved the use of a fresh sample extract. The spectra were recorded on a Perkin Elmer Lambda 35 UV-vis dual beam spectrophotometer.
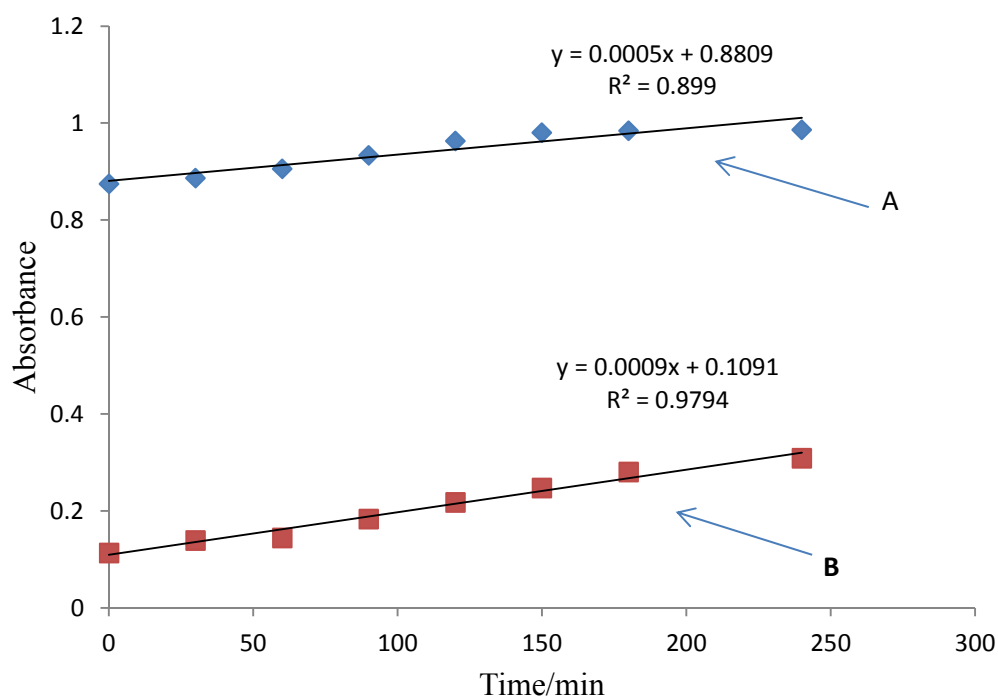
Figure 7.6: Increase in the photo-absorptive potential of grape seed extract dissolved in methanol at A, 280 nm and B, 320 nm. The data were obtained from spectra acquired with a Perkin Elmer Lambda 35 UV-vis dual beam spectrophotometer in a 1 mm pathlength quartz cuvette with air as the reference.

The proposed UV-catalysed polymerization sequence of the proanthocyanidin oligomers that enhances the absorptive efficacy in grape seed extract is shown in Fig. 7.7.
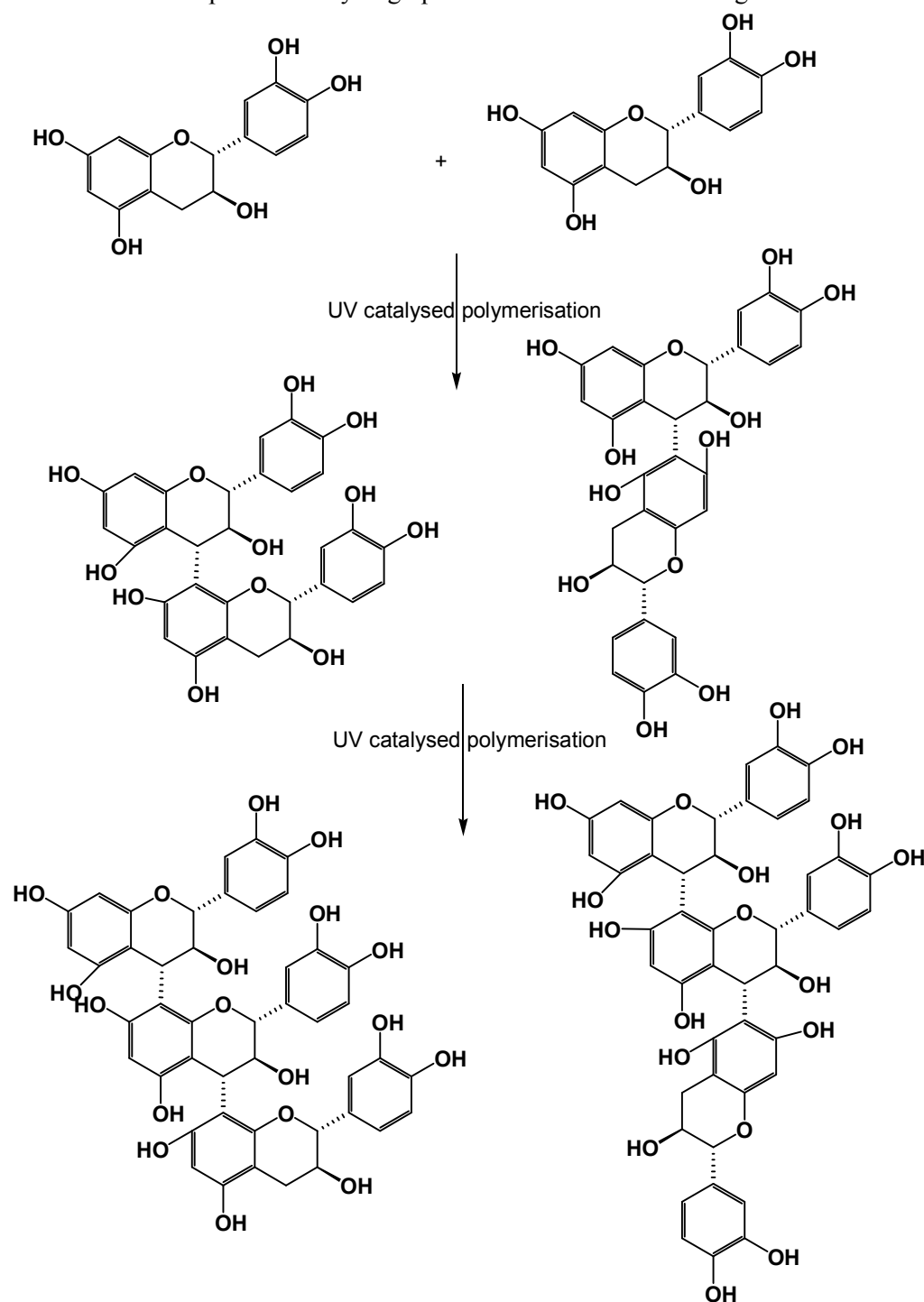
Figure 7.7: Proposed polymerisation scheme of proanthocyanidins that enhance UV absorption.
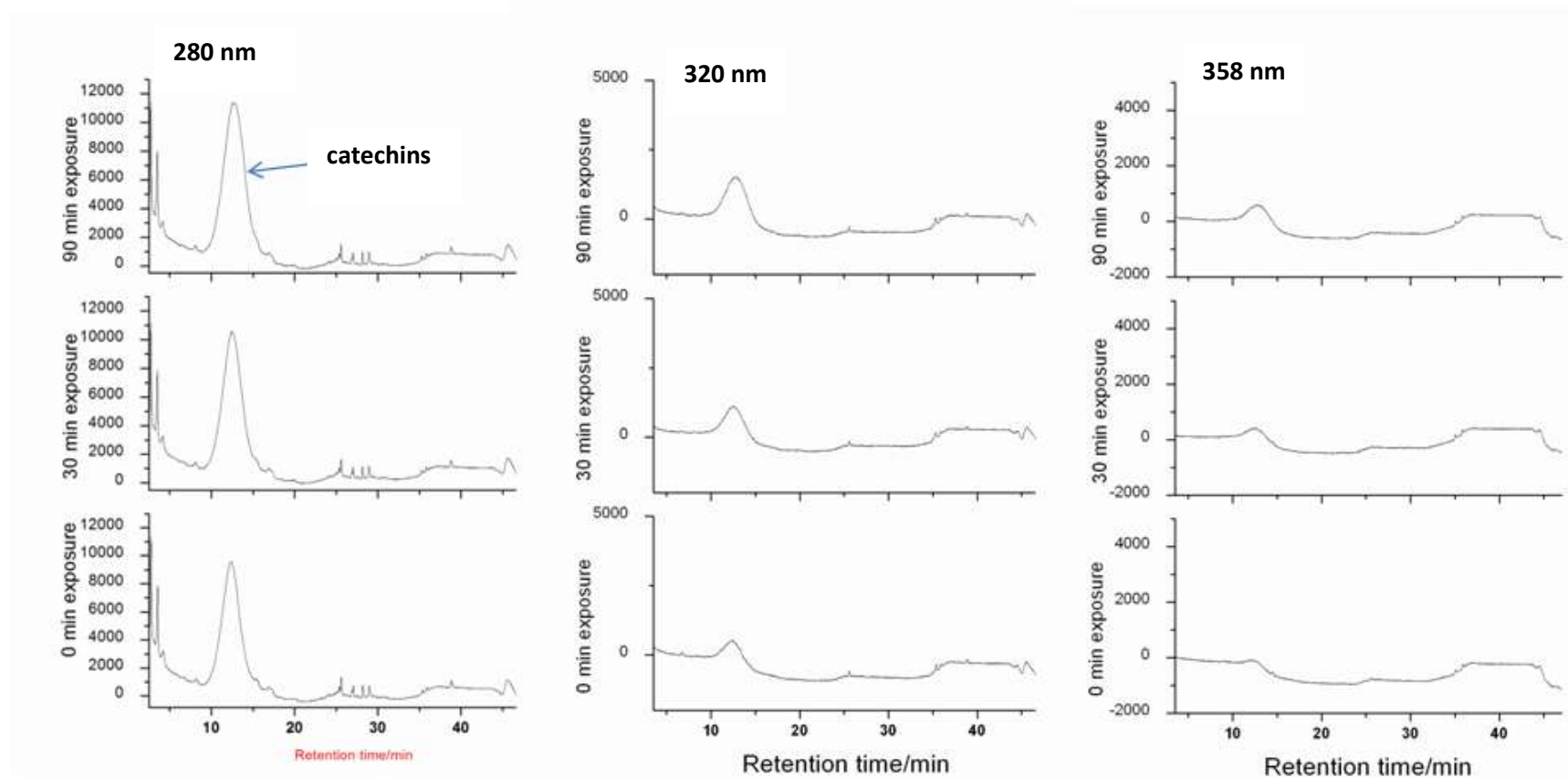
Figure 7.8: Photochemical changes of a methanolic solution of grape seed extract monitored at 280 nm, 320 nm and 358 nm showing the increasing catechin peak area with increase in irradiation time. The separations were achieved on a reversed-phase Zorbax Eclipse XDB C-18 column (150 mm × 4.6 mm, i.d., 5 µm), under a gradient elution of acetonitrile-water at flow rate of 1 mL min^{-1}and an injection volume of 20 µL.

The GC-MS analysis of the grape seed extract showed the presence of various fragments of polyphenols: phenolic acids, flavonoids, catechins, proanthocyanidins, and anthocyanins (Fig. 7.9). The observed lower molecular weight polyphenols could be attributed to fragmentation of the catechins during derivatization. The HPLC-ESI-MS/MS fragmentation of catechin can be rationalized by first a retro-Diels Alder fragmentation for ring A and other subsequent fragments seem to involve only ring B (Fig. 7.10). From the results of the GC-MS analysis we conclude that the grape seed extract contains various classes of phenolic compounds. Among these compounds are the phenolic acids which are simple molecules and form a diverse group that includes the widely distributed hydroxybenzoic and hydroxycinnamic acids (Dai and Mumper 2010). The isolated compounds: 3,4-dihydroxybenzoic acid, 3-hydroxy-4-methoxybenzoic acid and 2-(3,4-dihydroxyphenyl)-2-hydroxyacetic acid, can conveniently be associated with hydroxycinnamic acid derivatives. These compounds occur most frequently as simple esters with hydroxy carboxylic acids or glucose, and the hydroxybenzoic acid compounds are present mainly in the form of glucosides.

The 2-(3,4-dihydroxyphenyl)-3,4-dihydro-2H-chromene-3,5,7-triol identified from this extract is a flavonoid. This class of phenolic compounds is widely distributed in nature and its polyphenolic structure makes these compounds very sensitive to oxidative enzymes (Ghafar et al. 2010). In this grape seed extract catechins were identified as the major constituents. Catechins are documented to mainly occur in tea leaves and grape seeds and the monomeric flavan-3-ols: catechin, epicatechin, gallocatechin, epigallocatechin, epicatechingallate and epigallocatechin-3-gallate. The oligomeric polymerization of catechins produces proanthocyanidins found in grape seeds, red wine and pine bark. The presence of these compounds in the extract under study leads us to expect that this extract exhibits reducing capacity and metal ion chelating ability like other polyphenols. The main cause of reactive oxygen species (ROS) generation in living tissues is the presence of metal ions and they play an important role in generation of oxidative stress, DNA damage and cell death. The biological properties of polyphenols depend on their molecular structure (Farrukh and Santosh 2011). The GC-MS results show the presence of benzene-1,2,3-triol commonly known as pyrogallol. This is a tri-functonal benzene derivative positioning it as a powerful metal chelator, like catechol, for instance, which is a conjugate acid of a chelating agent used widely in coordination chemistry.

Apart from that, di-functional benzene derivatives like catechol, are known to readily condense to form heterocyclic compounds. It is well documented that catechol and gallol are effective metal ion chelators. Catechol reduces silver ions in solutions at ambient temperature and alkaline copper on heating (Donovan et al. 1999; Ferreira and Slade 2002; Soobrattee et al. 2005). Consequently, the reactivities of proanthocyanidins and gallate esters with hydroxyl radicals, azide radicals, or superoxide anions correlate with catechol and pyrogallol groups in their molecular structures that provide evidence of the antioxidant properties of these agents (Ferreira and Slade 2002). The scavenging activity of different grape catechin molecules is also related to the number of *o*-dihydroxy and *o*-hydroxyketo groups, C2-C3 double bonds, concentration and solubility, the accessibility of the active group to the oxidant and on the stability of the reaction product. Polyphenols also affect signal transduction pathways, modulate many endocrine systems, and alter hormones and other physiological processes, as a result of their binding to metal ions and enzyme cofactors. We envisage that coupled with the shown UVB absorbing potential of the extract in this work, the inclusion of the grape seed extract in sunscreens is likely boost the photoprotection and increase the antioxidant effect.
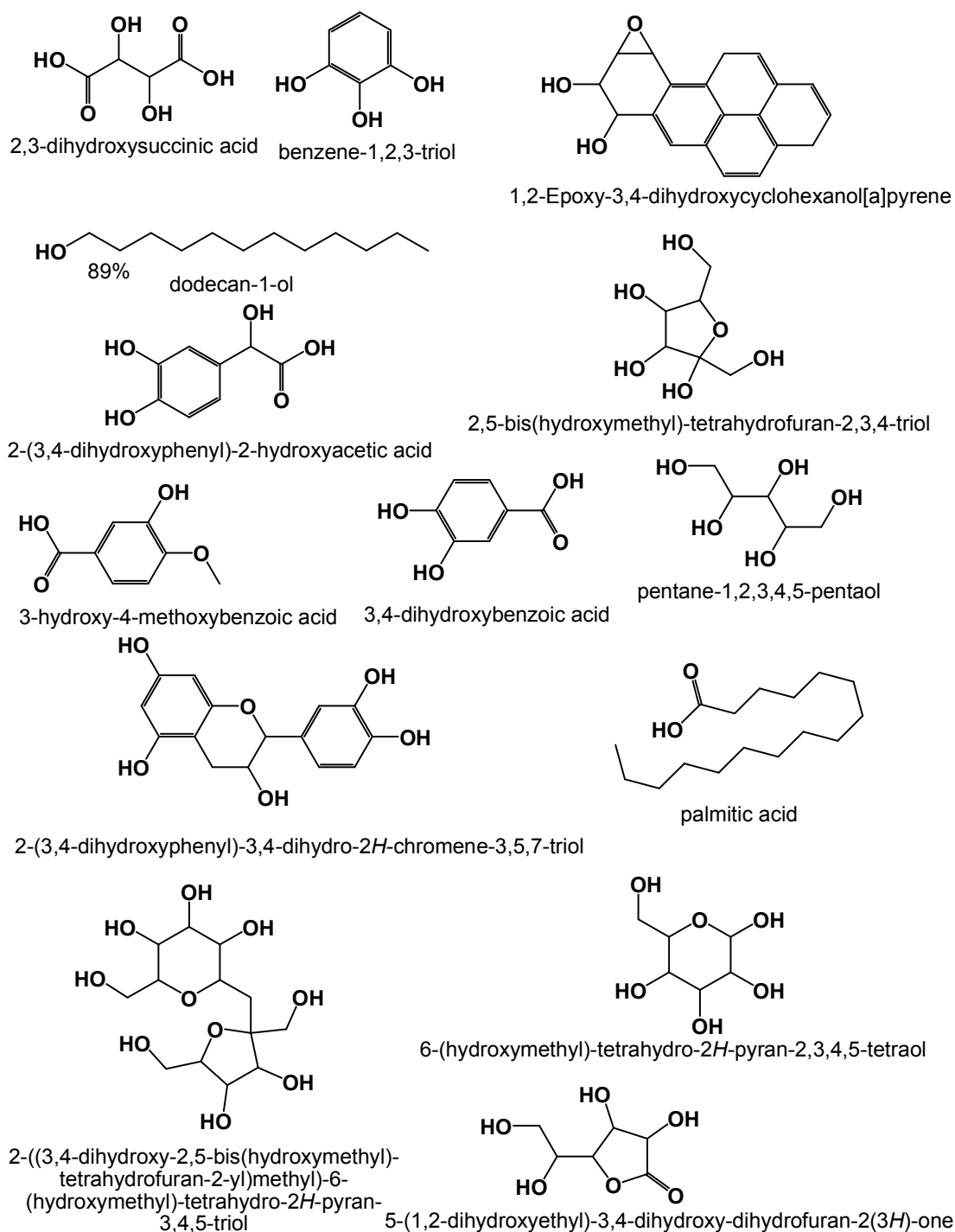
Figure 7.9: Secondary metabolites identified in grape seed extract by GC-MS.
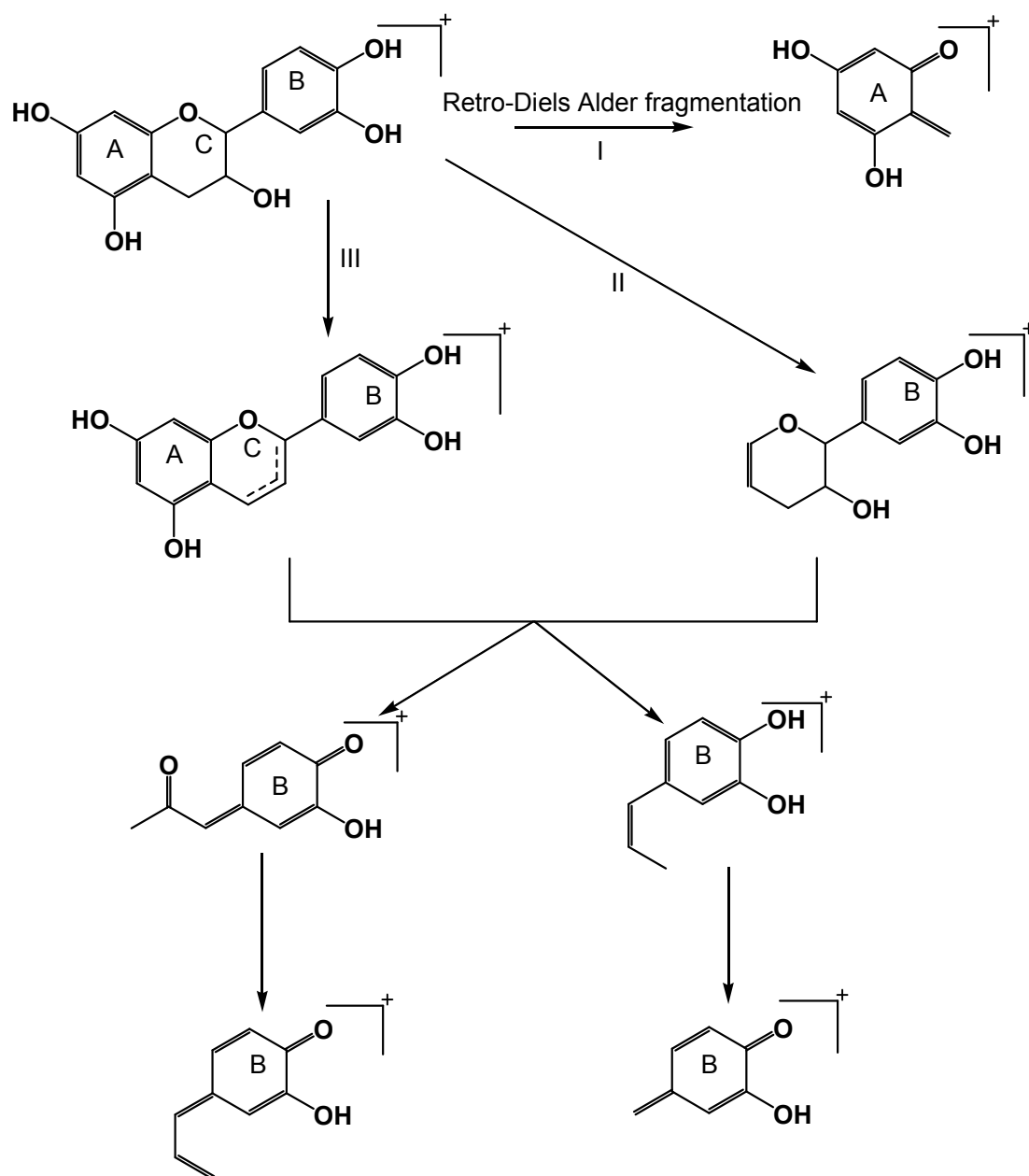
Figure 7.10: The proposed fragmentation of catechin and epicatechin in ESI-MS/MS (Sisa et al. 2010; Benavides et al. 2006).

7.3.1   Photostability of BP3 incorporated in grape seed extract

The spectral stability of a BP3 solution in methanol alone was observed when irradiated with a solar radiation simulator (Fig. 7.11). The irradiated solution on HPLC analysis did not show any other peak an indication that there is likely to be no photodegradation products (Fig. 7.12). Similarly the methanolic solutions of BP3 with grape seed extract were exposed to simulated solar radiation for increasing exposure times without appreciable change in their UV spectra (Fig. 7.13). This indicated good photostability of the agent in the plant extract. However, the HPLC chromatogram showed an additional two peaks observable at 280 nm and 358 nm (Fig. 7.15). These two peaks could be attributed to exclusive photo-reactivity of the benzophenone moiety albeit to a small extent. From a comparison of the UV spectra of BP3 in methanol (Fig. 7.11) and in grape seed extract (Fig. 7.13) we note that one of the three peaks of the BP3 spectrum is missing in the latter namely, that at 240 nm. This could be due to reactions involving BP3 induced by light that do not necessarily destroy the carbonyl chromophore, characterised by an absorption maximum at 286 nm. It is known that upon irradiation of ketones with radiation of wavelengths from 280 to 330 nm an n to π^* transition takes place and because the triplet-singlet energy gap is small (20 - 70 kJ mol^{-1}) intersystem crossing occurs readily (Wilkinson 1997). We envisage that the triplet state photochemical reactions lead to formation of two UV-absorbing entities **A** and **B** exclusively from the triplet state (Fig. 7.14). The high conjugation of species B makes it able to absorb at longer wavelength due to additional π to π^* transitions. The formation of these two species and other absorbing chemical entities observed from the HPLC chromatographic results (Fig. 7.15) are unique to these extracts and suggests synergistic UV absorption efficacy.

Schallreuter et al. (1996) showed that BP3 is rapidly photo-oxidized, yielding benzophenone-3 semiquinone, a potent electrophile, capable of reacting with thiol groups on important antioxidant enzymes and substrates, such as thioredoxin reductase and reduced glutathione, respectively. This group argued that the rapid oxidation followed by the inactivation of important antioxidant systems indicates that this substance may be rather harmful to the homeostasis of the epidermis. But from this work, given that its incorporation in the grape seed extract and subsequent prolonged UV exposure does not significantly alter the secondary metabolite composition (see Supplementary Materials Table S7.2), it can be argued that the grape seed extract is likely to modulate the photochemical response of BP3 and thereby improve its efficacy as a UV absorber.
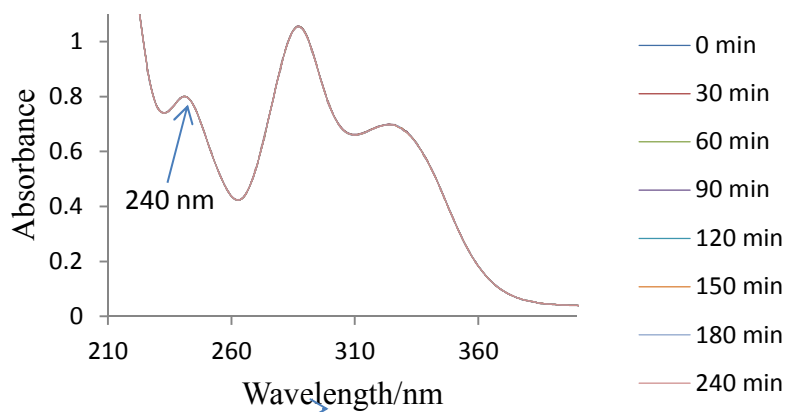
Figure 7.11: The spectral stability of BP3 in methanol irradiated by a solar simulated source. The spectra were acquired with the Perkin Elmer Lambda 35 UV-vis dual beam spectrophotometer in a 1 mm pathlength quartz cuvette with air as the reference.
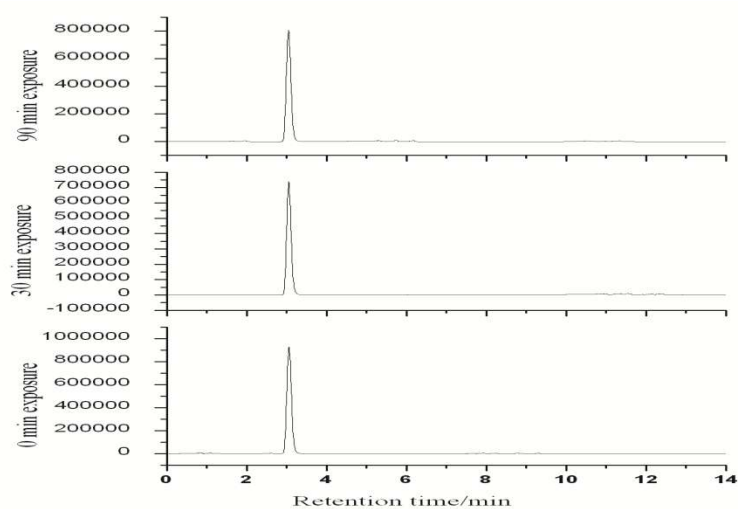
Figure 7.12: The photostability of BP3 monitored at 286 nm. The separation was achieved on a reversed-phase Zorbax Eclipse-XDB C-18 column (150 mm × 4.6 mm) was used with mobile phase of methanol-water (84:16 % v/v). The injection volume was 20 μL and the flow rate was set at 1 mL min^{-1}.
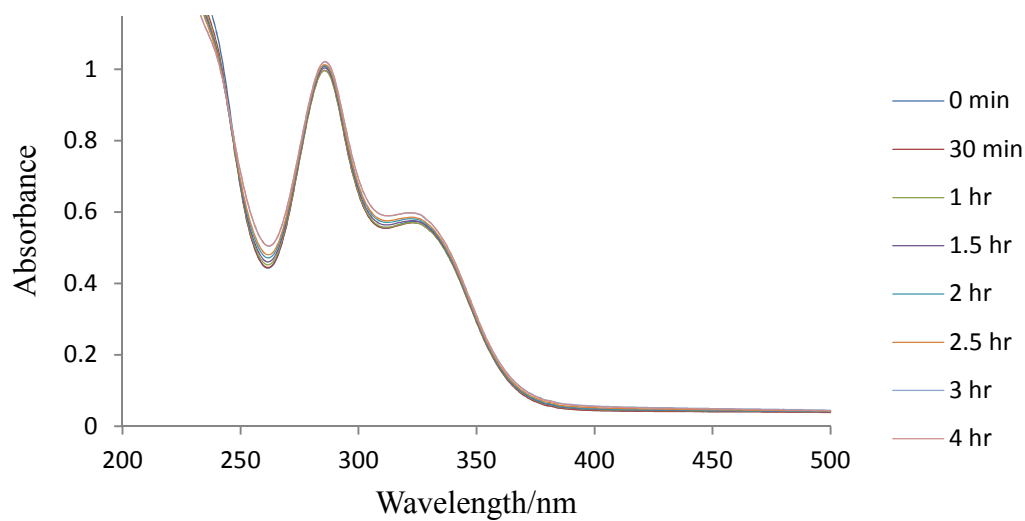
Figure 7.13: Photostability of grape seed extract with BP3 in methanol. The spectra were acquired with a Perkin Elmer Lambda 35 UV-vis dual beam spectrophotometer in a 1 mm pathlength quartz cuvette with air as the reference.
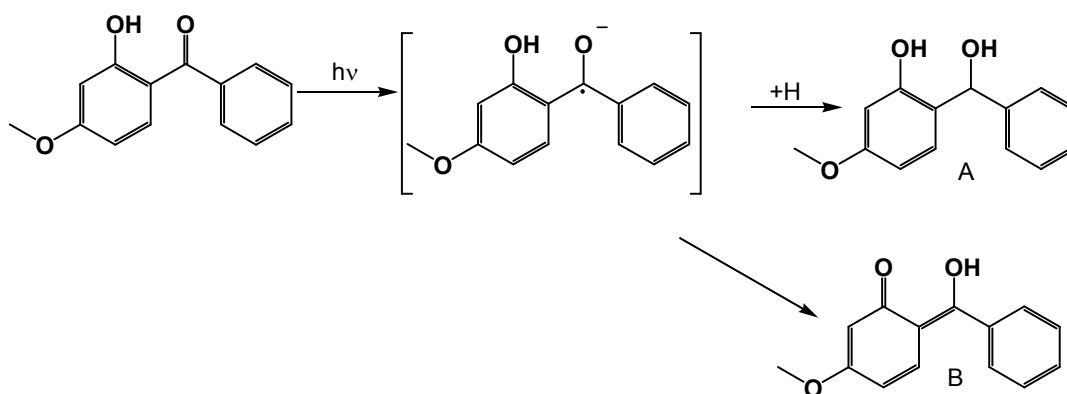
Figure 7.14: Proposed triplet state rearrangement of BP3 yielding UV absorbing species **A** and **B.**
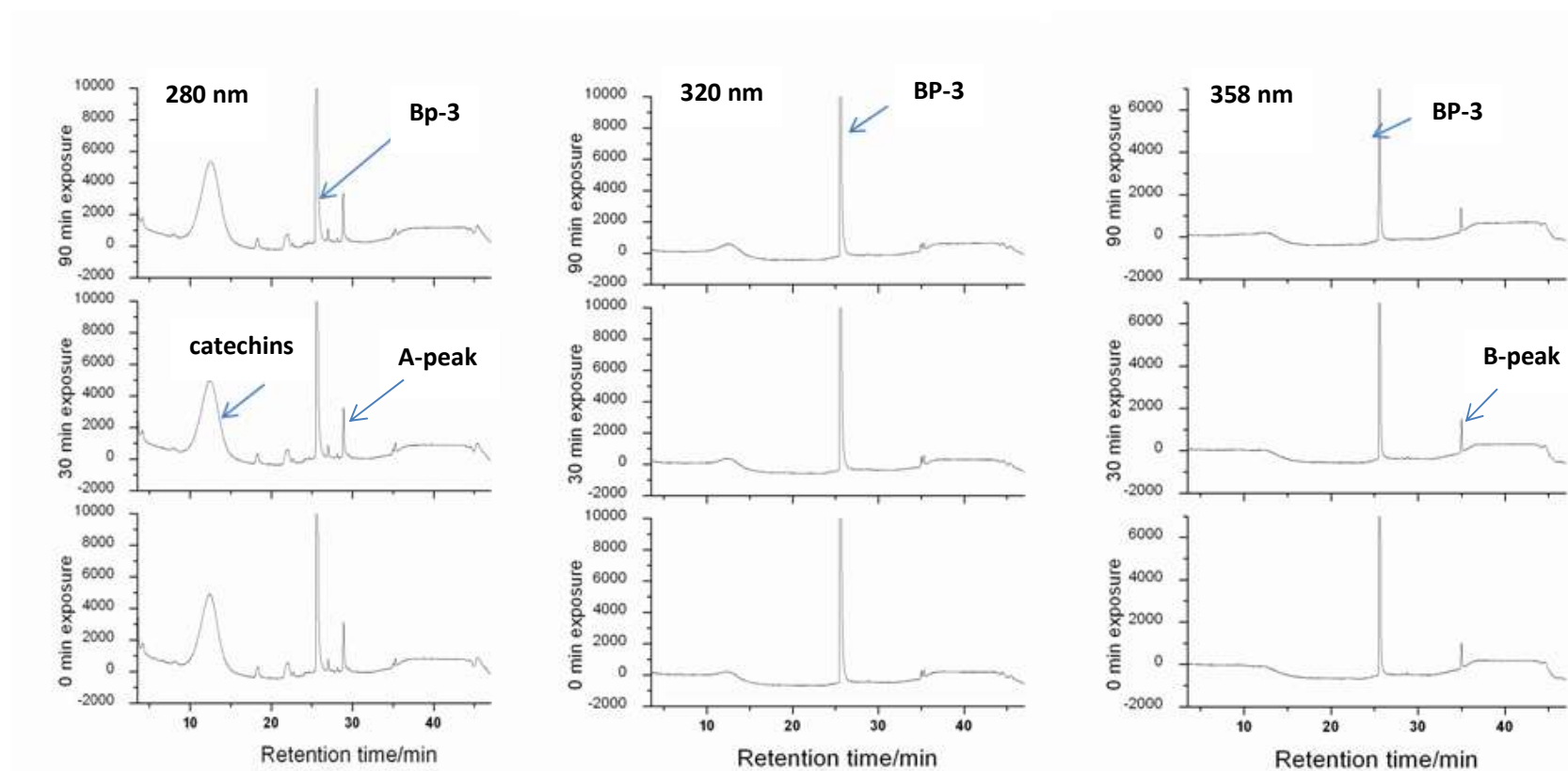
Figure 7.15: Photochemical changes of BP3 and grape seed extract mixture at 280 nm, 320 nm and 358 nm showing increasing catechin peak area with increase of the irradiation time and peaks of compounds **A** and **B**. The separations were achieved on a reversed-phase Zorbax Eclipse XDB C-18 column (150 mm × 4.6 mm, i.d., 5 μm), under a gradient elution of acetonitrile-water at a flow rate of 1 mL min^{-1} and an injection volume of 20 μL.

7.3.2   The photostability of BMDBM in grape seed extract

BMDBM is a common sunscreen absorber incorporated in most cosmetics to protect human skin against deleterious UV effects. In this work the irradiation of a solution of BMDBM in methanol showed a steady decay at 358 nm and an increase at 260 nm (Fig. 7.16). The enol tautomer of BMDBM has a maximum absorption at 358 nm and the keto tautomer shows a maximum around 260 nm. We therefore assign the decrease in absorption at 358 nm as enol decay and the observed growth at 260 nm as increase of the keto tautomer. However, the HPLC chromatograms for the photostability studies did not show much decrease of the enol-tautmer (Fig. 7.17). This apparent photostability could be due to a solvent effect because BMDBM has been shown to be stable in polar protic solvents such as methanol (Mturi and Martincigh 2008). The *keto-enol* tautomerization is therefore be accompanied by a loss in the photo-absorption efficacy of this sunscreening agent. BMDBM is also known to photodegrade upon irradiation in a nonpolar medium by way of radical formation (Fig. 7.18) which may completely destroy UV absorption potential. However, our photostability studies of the methanolic solution of BMDBM with grape seed extract over a four hour illumination period showed a drop in the first 30 minutes and then relative photostability thereafter (Fig. 7.19). The spectra extended to the visible region with the wavelength of maximum absorption shifting to 400 nm. From a comparison of the two spectra, Fig. 7.16 and Fig. 7.19, we conclude that the incorporation of grape seed extract was the cause of the observed red shift. The shift towards much longer wavelength makes the mixture a better UV absorber and effectively covers the entire UVB and UVA spectrum. The UV spectra (Fig. 7.19) showed an increase at 320 nm indicating the formation of other UV absorbing entities. This was supported by the HPLC chromatogram that showed very prominent peaks at 280 nm and 358 nm although the HPLC chromatographic data at 320 nm show those peaks to be smaller (Fig. 7.20). It can be concluded that those chemical species do not strongly absorb at 320 nm   Hence, the shift observed in the UV spectra is associated with photochemical reactions that yield strongly UV-absorbing species (see Supplementary Materials Table S7.3) and since the spectral shape of BMDBM essentially remains the same, we conclude that a chelated enol form is photostabilized.
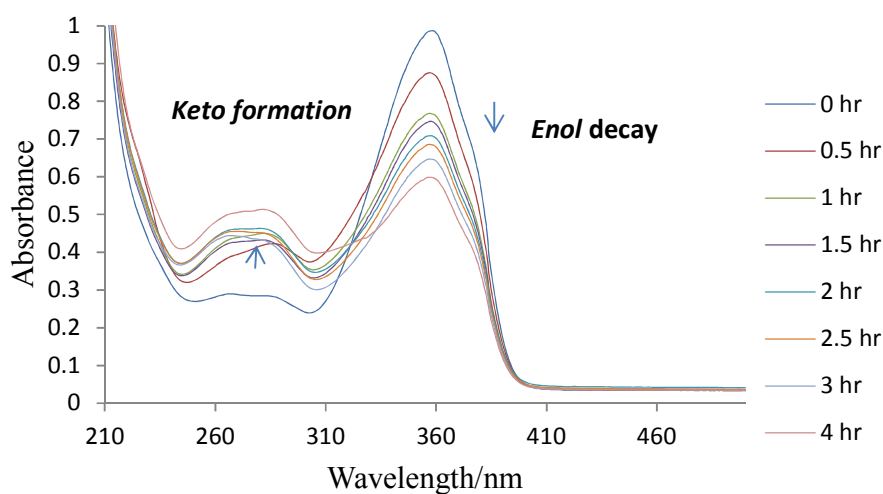
Figure 7.16: The spectral changes of BMDBM dissolved in methanol and irradiated by a solar simulated light source. The spectra were acquired with a Perkin Elmer Lambda 35 UV-vis dual beam spectrophotometer in a 1 mm pathlength quartz cuvette with air as the reference.
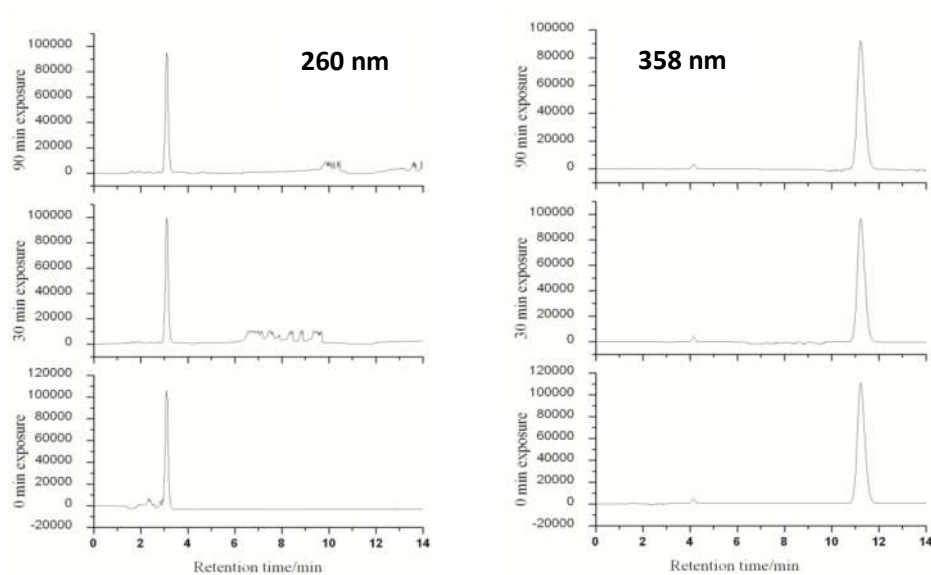
Figure 7.17: The photochemical changes of BMDBM monitored at 260 and 358 nm on a reversed phase Zorbax Eclipse-XDB C-18 column (150 mm × 4.6 mm) with a methanol-water (84:16 % v/v) mobile phase. The injection volume was 20 µL and the flow rate set at 1 mL min^{-1}.
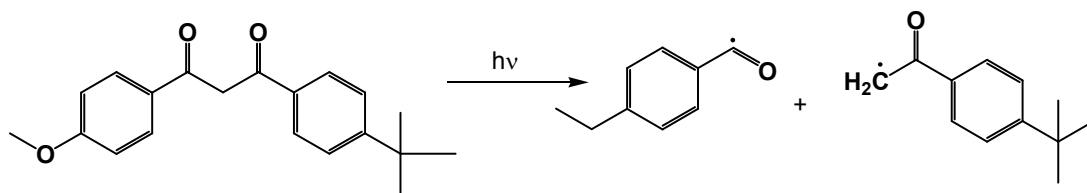
Figure 7.18: The photolysis of BMDBM in UV light adapted from Schwack and Rudolph (1995).
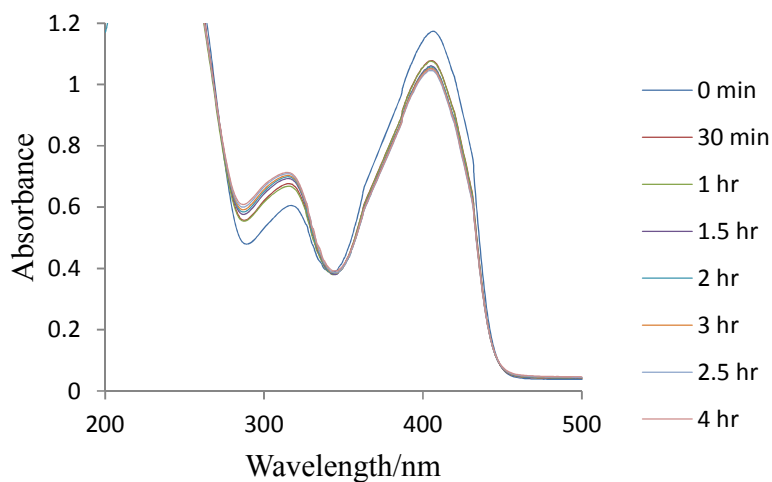
Figure 7.19: Photostability of BMDBM with grape seed extract in methanol. The spectra were acquired with a Perkin Elmer Lambda 35 UV-vis dual beam spectrophotometer in a 1 mm pathlength quartz cuvette with air as the reference.
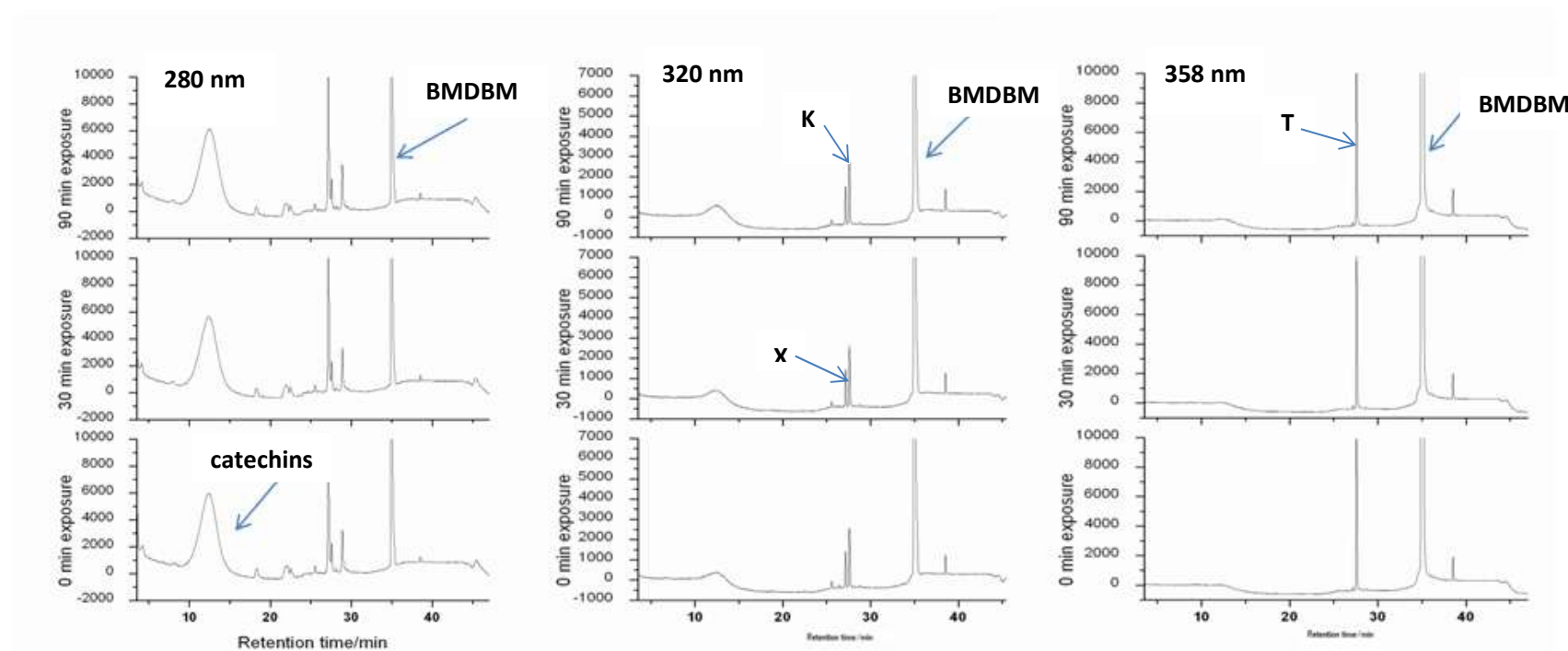
Figure 7.20: Photochemical changes of a BMDBM and grape seed extract mixture at 280 nm, 320 nm and 358 nm showing increasing catechins peak area with increase of the irradiation time and the emergence of UV absorbing species **K, T** and **X**. The separations were achieved on a reversed-phase Zorbax Eclipse XDB C-18 column (150 mm × 4.6 mm, i.d., 5 μm), under a gradient elution of acetonitrile-water at a flow rate of 1 mL min^{-1} and an injection volume of 20 μL.

As indicated above BMDBM under UV irradiation is known to photodegrade into two radical species: a benzyl radical and a phenacyl radical (Fig. 7.18). The presence of these radicals is likely to trigger free radical reactions especially given that flavan-3-ols at 300 nm are known to undergo homolysis of the hetercyclic 1,2-(O-C) and 3,4-(C-C) bonds (Fig. 7.21), (Sisa et al. 2010). We speculate radical disproportionation reactions involving the benzyl and phenacyl radical with the new photochemical products. We then invoke the Woodward-Fieser prediction rules for calculating the wavelength of maximum absorption in the UV for the proposed products to give λ_{max} values for compounds **K**, **T** and **X** as 325 nm, 355 nm and 315 nm respectively formed from the scheme in Figure 7.19. Our prediction agrees with the observed peaks at 320 nm and 358 nm (Fig. 7.20). We therefore propose that the phenacyl radical couples with the catechin radical to give **X** and the benzyl radical couples with the catechin radical to give **K**. However, the photo-induced rearrangement of the catechin radical yields the long wavelength absorbing species **T** in a manner proposed by Fourie et al. (1977). The other peaks appearing at 280 nm could result from various photo-induced radical disproportionation reactions in numerous fashions. The end result for this mixture of grape seed extract and BMDBM is a more effective and stable UV absorbing medium.
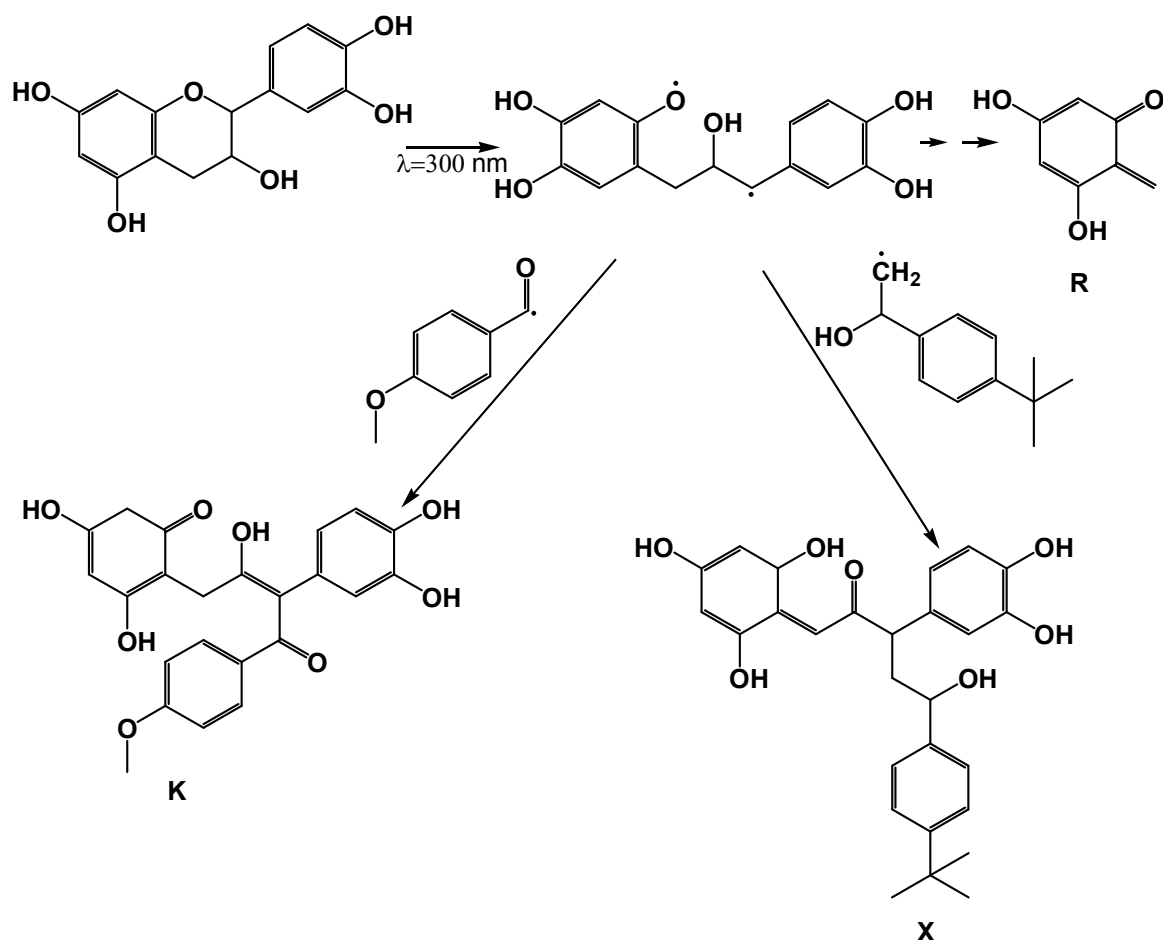
Figure 7.21: Proposed photo-induced radical disproportionation reactions of BMDBM photolysis products and triplet state flavan-3-ols.

7.3.3 Photostability of EHMC in grape seed extract

The exposure of a methanolic solution of EHMC to solar simulated radiation showed the characteristic cinnamic acid moiety decay (Fig. 7.22). The HPLC analysis of this solution showed the formation of *cis*-EHMC (Fig. 7.23) as the only photoproduct, this is in agreement with the findings of Broadbent et al. (1996). Contrary to the argument fronted by these authors that the *trans-cis* isomerisation of EHMC reaches a photostationary state after 4 hours, the UV spectra in this work (Fig. 7.22) indicate an earlier pseudo-photostationary state followed by a further drop in the UV absorption in the fourth hour. This view is supported by our HPLC analysis that shows that the peak areas of the *trans-isomer* for the 30 min exposure of this solution and 90 min exposure period were nearly the same (56.17 % and 53.00 %, of the initial peak area). When this chromatogram was monitored at 260 nm the *cis*-isomer shows maximum absorption. This explains the loss in photoprotection attributed to this isomerisation of EHMC because this particular wavelength does not reach the earth's surface. However, when EHMC was combined with grape seed extract dissolved in methanol and exposed to solar simulated radiation for four hours, a new spectral decay characteristic was observed. The UV spectra of this mixture dropped sharply after the first

30 min and subsequently stabilized for the remaining three and half hours of exposure (Fig. 7.24). The characteristic UV isomerisation that is normally accompanied with photo-loss was completely halted. This could imply a speedy establishment of the photostationary state with higher preference for the *trans*-isomer. It could also be argued that there is no further breakdown of the absorbing molecules but the HPLC chromatogram showed a number of peaks at 280 nm which could be associated with decay products of [2+2] cycloaddition (Broadbent et al. 1996; Lyambila 2003) of EHMC and other unsaturated secondary metabolites in the extracts (Fig 7.25, see also Table S7.4). The [2+2] cycloaddition is usually accompanied by a reduction in double bond conjugation in the molecular structure of a compound and hence likely to diminish the light absorption capacity of the molecule in question. The cyclobutane ring moieties formed are strained structures that are likely to breakdown in light-induced ring opening metathesis reactions yielding less absorbing chemical species as observed in this work. Lack of the higher absorbing species from photo-induced reactions of the flavan-3-ols indicates no radical formation of catechins. These could imply that phenolics remain in their natural state; hence better antioxidant activity is expected of this formulation. The formulation seems to have an efficient excited state self-deactivation mechanism by way of vibrational states depriving the molecules sufficient photon energy to combine and form other products. We do not rule out possible *cis-trans*-isomerization of EHMC but state that the decay life of the *cis*-EHMC is greatly reduced and thus likely to offer longer protection. From the UV spectra, the *trans*-isomer has a shoulder which appears to vanish upon exposure to light. The overall effect is a stable sunscreen product, with antioxidant effect.
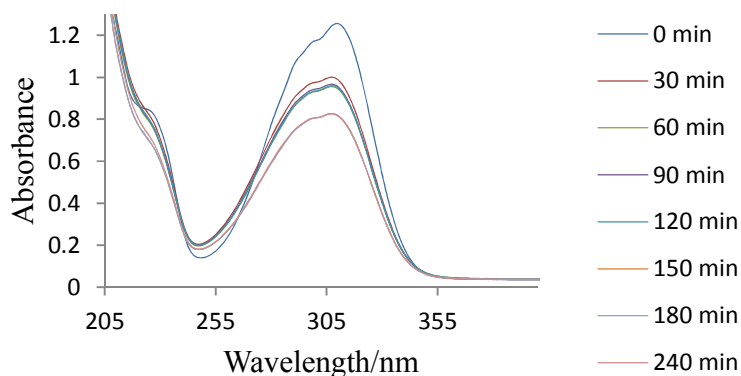
Figure 7.22: Photoinstability of EHMC dissolved in methanol under solar simulated irradiation. The spectra were acquired with a Perkin Elmer Lambda 35 UV-vis dual beam spectrophotometer in a 1 mm pathlength quartz cuvette with air as the reference.
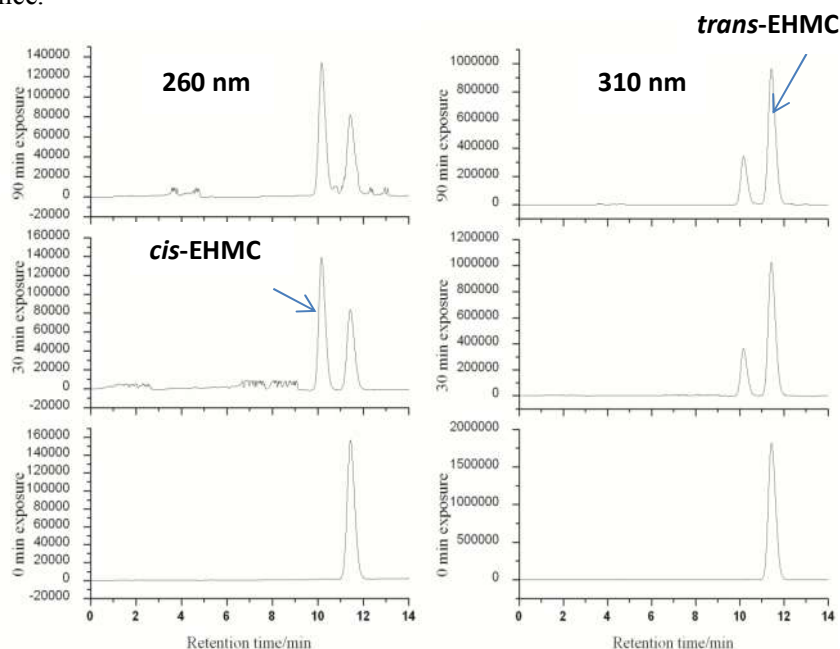

Figure 7.23: Isomerisation of EHMC under simulated solar irradiation monitored at 260 and 310 nm on a reversed-phase Zorbax Eclipse-XDB C-18 column (150 mm × 4.6 mm) with a methanol-water (84:16 % v/v) as the mobile phase. The injection volume was 20 μL and the flow rate set at 1 mL min^{-1}.
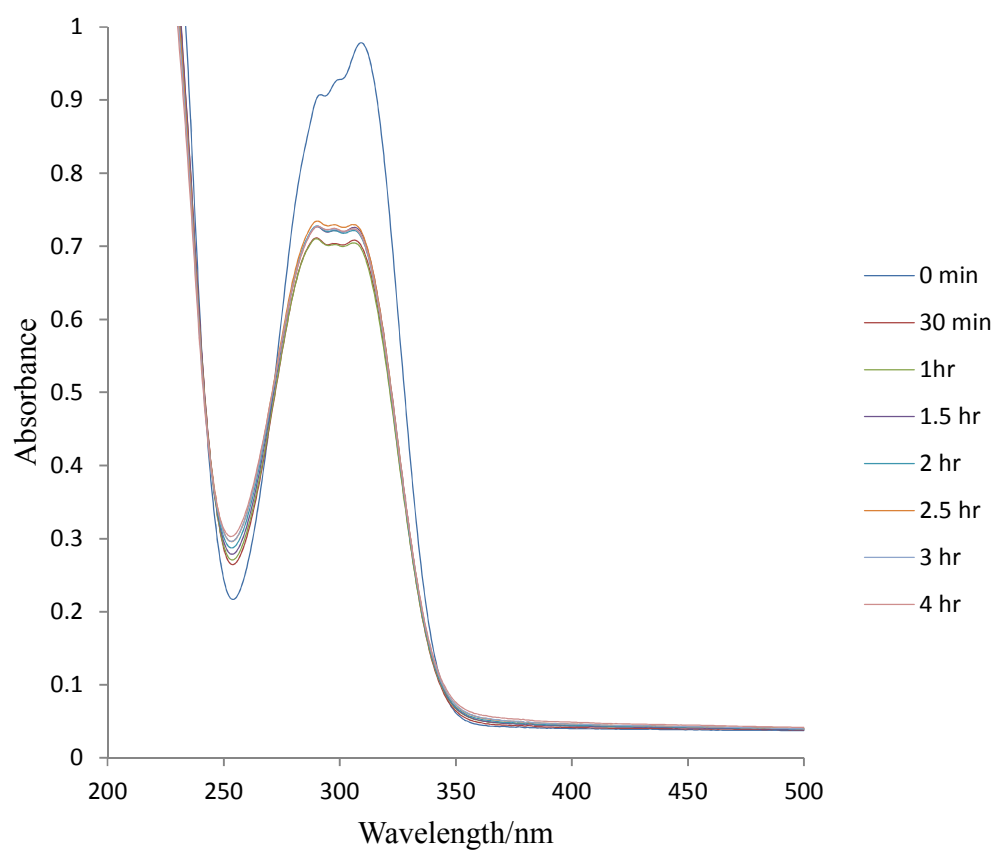
Figure: 7.24. The photostability of EHMC with grape seed extract in methanol under solar simulated radiation. The spectra were acquired with a Perkin Elmer Lambda 35 UV-vis dual beam spectrophotometer in a 1 mm pathlength quartz cuvette with air as the reference.
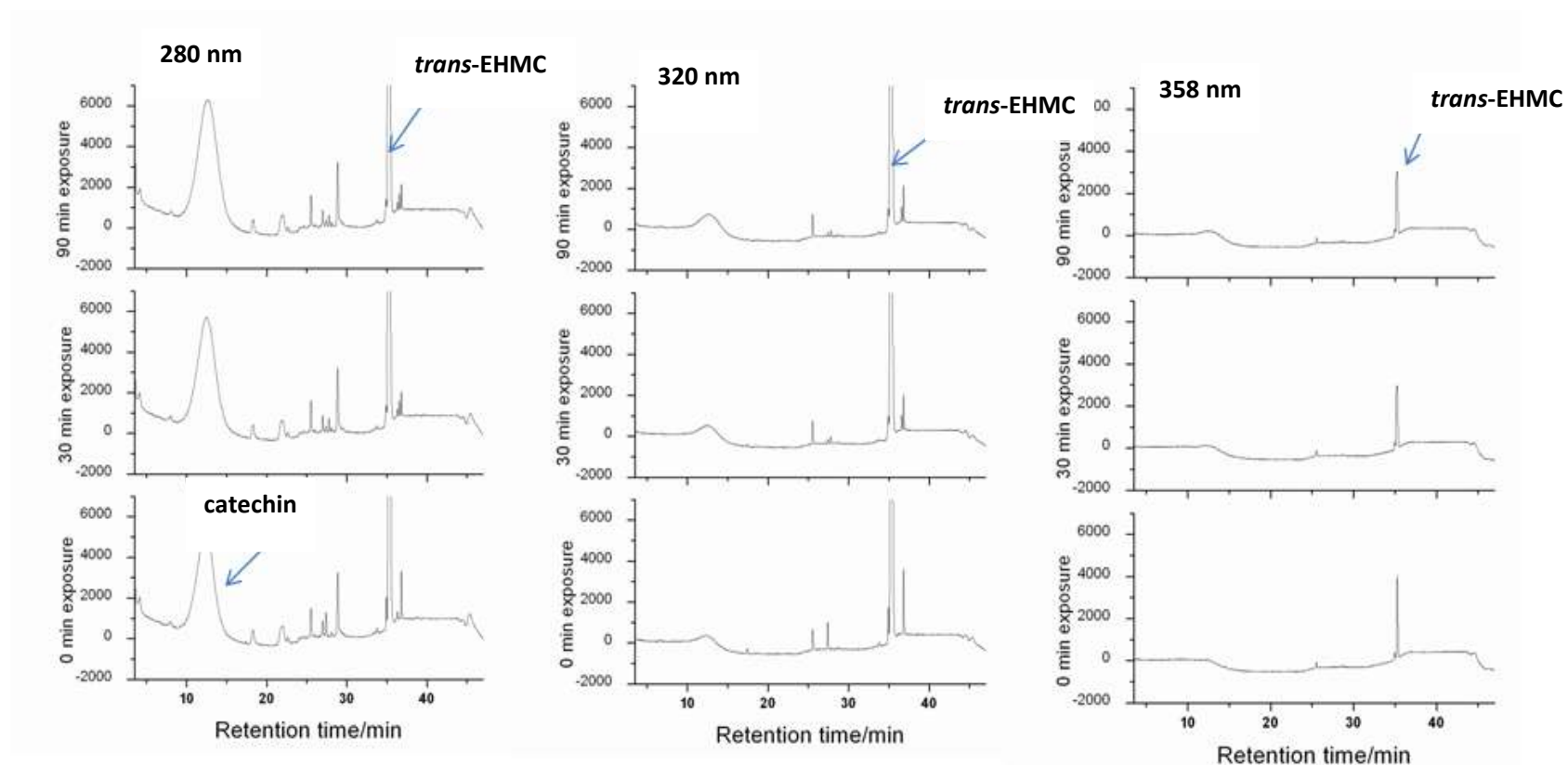
Figure 7.25 Photochemical changes of EHMC and grape seed extract monitored at 280 nm, 320 nm and 358 nm showing an increase in the catechin peak area with an increase in irradiation time and relatively stable EHMC. The separations were achieved on a reversed-phase Zorbax Eclipse XDB C-18 column (150 mm × 4.6 mm, i.d., 5 μm), under a gradient elution of acetonitrile-water at a flow rate of 1 mL min^{-1} and an injection volume of 20 μL.

7.3.4   Photostability of a mixture of BMDBM, BP3 and EHMC in grape seed extract

It is common practice by most sunscreen product manufacturers to combine organic absorbers in a formulation with a view to producing a broad-spectrum product. The common combination is BMDBM for UVA absorption, EHMC for UVB and BP3 to provide a link between UVA and UVB. BP3 shows appreciable absorption in the UVA1 (320-340 nm) region (Fig. 7.11) and sufficient absorption in the UVB region and hence is considered as a suitable combination with any of the sunscreen agents. The irradiation of a methanolic solution of a mixture of BMDBM, BP3 and EHMC showed steady spectral drop with increasing time of irradiation (Fig. 7.26).   The HPLC analysis showed a steady photoisomerisation of *trans*-EHMC to *cis*-EHMC (Fig. 7.27). The BMDBM peak monitored at 358 nm, however, did not show any appreciable change in terms of peak area, indicating an amount of photostability (Fig. 7.27). This could be attributed to solvent polarity because methanol is polar and polar and protic such a medium has been shown to photostabilize BMDBM (Mturi and Martincigh 2008). Another notable observation on these spectra is the blue shift casting doubt on the UVA absorption potential of this mixture. It can be argued that in the absence of any other ingredient other than the three sunscreen absorbers, then this mixture is suitable for UVB photoprotection only. The photostability of a mixture of these three commonly used sunscreen absorbers in grape seed extract was investigated (Fig. 7.28). The three were mixed in the ratio 1:2:2, BMDBM:BP3:EHMC in accordance with the maxima allowed by COLIPA, namely a percent composition of 5 % BMDBM, 10 % BP3 and 10 % EHMC. A minimal drop in photo-absorption was observed in the first 30 minutes of exposure and subsequently the mixture was relatively photostable (Fig. 7.28).   This shows that the inherent photoinstability of the BMDBM and EHMC mixture is diminished. The characteristic peaks observed notably peak **T** on the HPLC chromatogram (see Fig. 7.29) when the grape seed extract was exposed together with BMDBM was also observed here (Fig. 7.29 and Table S7.6).   This chemical species absorbs strongly in the UVA region. This indicates a few photo-induced radical reactions take place preferentially to BMDBM with effect of increasing photostability in the UVA region. These radical disproportionation reactions have an effect of generating more UV-absorbing species thus avoiding the depletion of the antioxidant composition in the grape seed extract.

It would be expected that the prevention of the UV-induced depletion of the antioxidant defence system would result in suppression of oxidative stress and the oxidative stress-mediated adverse effects in the skin. Oxidative stress may cause damage at the cellular level, as well as at the molecular level, and this can result in cutaneous inflammation, lipid and protein oxidation, DNA damage, and activation or inactivation of certain enzymes (Bagchi et al. 2003), all are likely to   contribute to UVB-induced photodamage of the skin. The observed absorption maxima of this mixture are in the UVB region and therefore this formulation is likely to offer sufficient UVB photoprotection. Hence, a mixture of these sunscreens in grape seed extract may play a crucial role in minimizing UV-induced immunosuppression which is considered to be a risk factor for the development of skin cancer (Wang et al. 1991), and prevention of UV-induced immunosuppression represents a potential strategy for the management of skin cancer.

The aim of this work is to find a suitable combination of ingredients that affords a stable photoprotection product. This has direct consequences in terms of the possible ingestion of the product by children and hence safety concerns can be raised. Grape seed extract has been demonstrated to be non-genotoxic and

to possess low toxicity as indicated by some *in vitro* tests and *in vivo* animal toxicity studies (Bagchi et al. 2000; Khanna et al. 2002; Mantena 2005). Yakamoshi et al. (2002) investigated the acute and subchronic oral toxicity of grape seed extracts on Fischer 344 rats and for mutagenic potential by the reverse mutation test on *Salmonella typhimurium*, the chromosomal aberration test on CHL cells, and the micronucleus test on ddY mice. This group found no evidence of acute oral toxicity at dosages up to an oral administration dose of 4 g kg^{-1}. There was no evidence of mutagenicity reported. From these studies we envisage that accidental ingestion of grape seed extract may pose neither an immediate or future grave danger. Other working groups have also shown grape seed extract to have higher bioavailability, conferring much more protection against free radical-induced lipid peroxidation and DNA damage than vitamin C, vitamin E, and β-carotene (Bagchi et al. 2000). From this current work we have demonstrated the ability of grape seed extract to attenuate UV radiation and its potential in reducing the adverse UV-induced effects on human skin. Proanthocyanidins, or condensed tannins, are said to have the capacity to stabilize collagen and elastin and thus enhance the elasticity, flexibility, and appearance of the skin (Bagchi et al. 1998). It is expected that UV-induced scars, stretch marks and skin wrinkling will be reduced. The observed stabilizing potential of the grape seed extract on the chemical absorbers in combination and alone make grape seed extract a good candidate as an ingredient in cosmetic formulations.
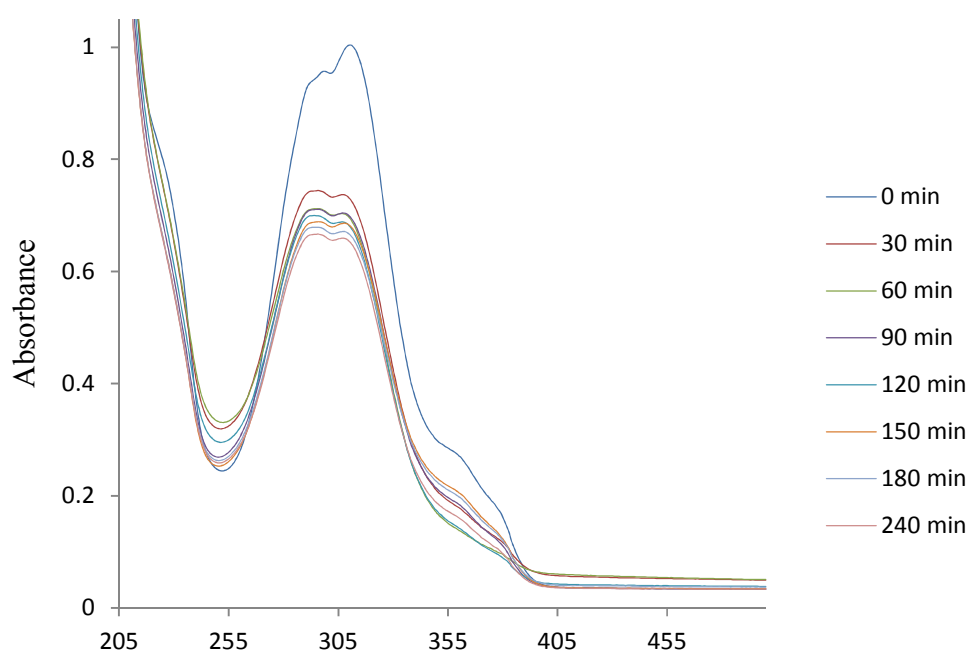
Figure 7.26: The photostability of a mixture of BMDBM, BP3 and EHMC dissolved in methanol, irradiated by a solar simulating source. The spectra were acquired on a Perkin Elmer Lambda 35 UV-vis dual beam spectrophotometer in a 1 mm pathlength quartz cuvette with air as the reference.
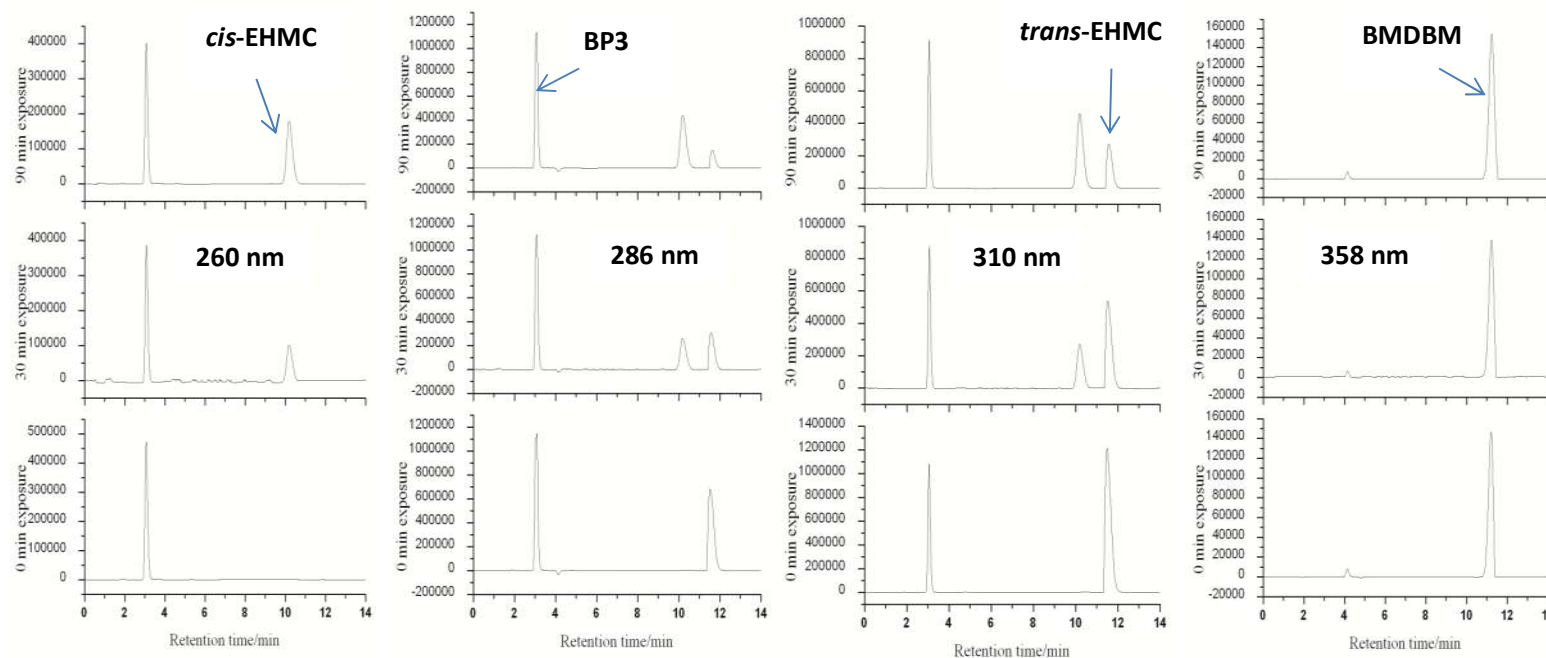
Figure 7.27: The photochemical transformations of a mixture of BMDBM, BP3, and EHMC dissolved in methanol monitored at 260, 286, 310, and 358 nm. The separation was effected on a reversed-phase Zorbax Eclipse-XDB C-18 column. The mobile phase was a gradient elution of acetonitrile-water with a flow rate of 1.00 mL min^{-1} and an injection volume of 20 μL.
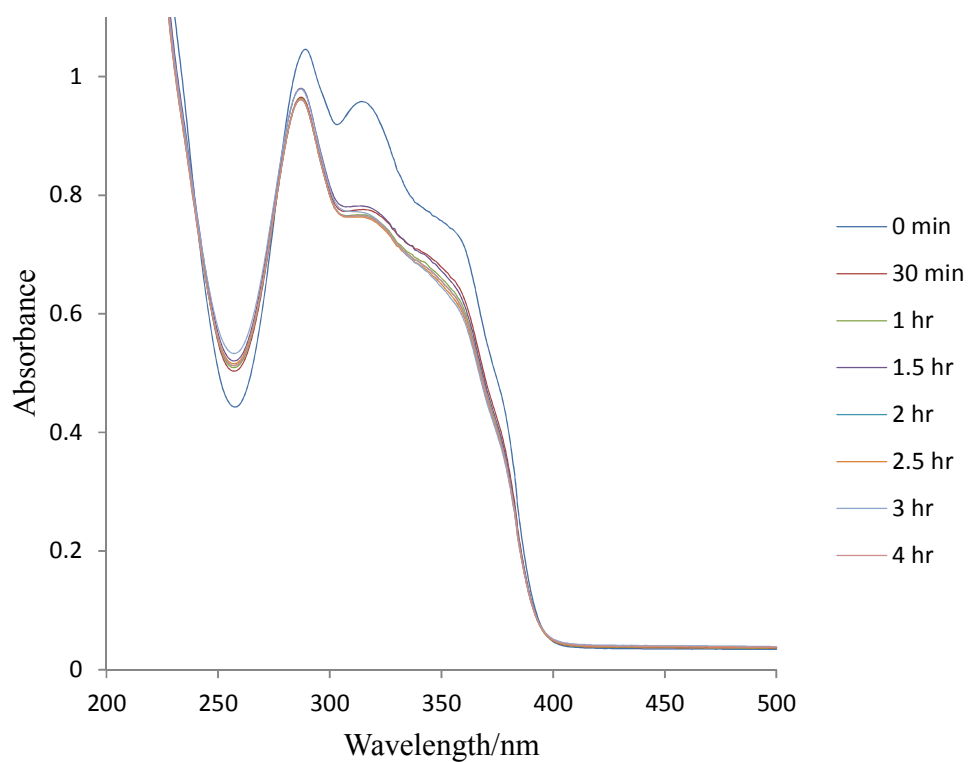
Figure 7.28: Photostability of a mixture of BMDBM, BP3, EHMC and grape seed extract in methanol. The spectra were acquired with a Perkin Elmer Lambda 35 UV-vis spectrophotometer in a 1 mm pathlength quartz cuvette with air as the reference.
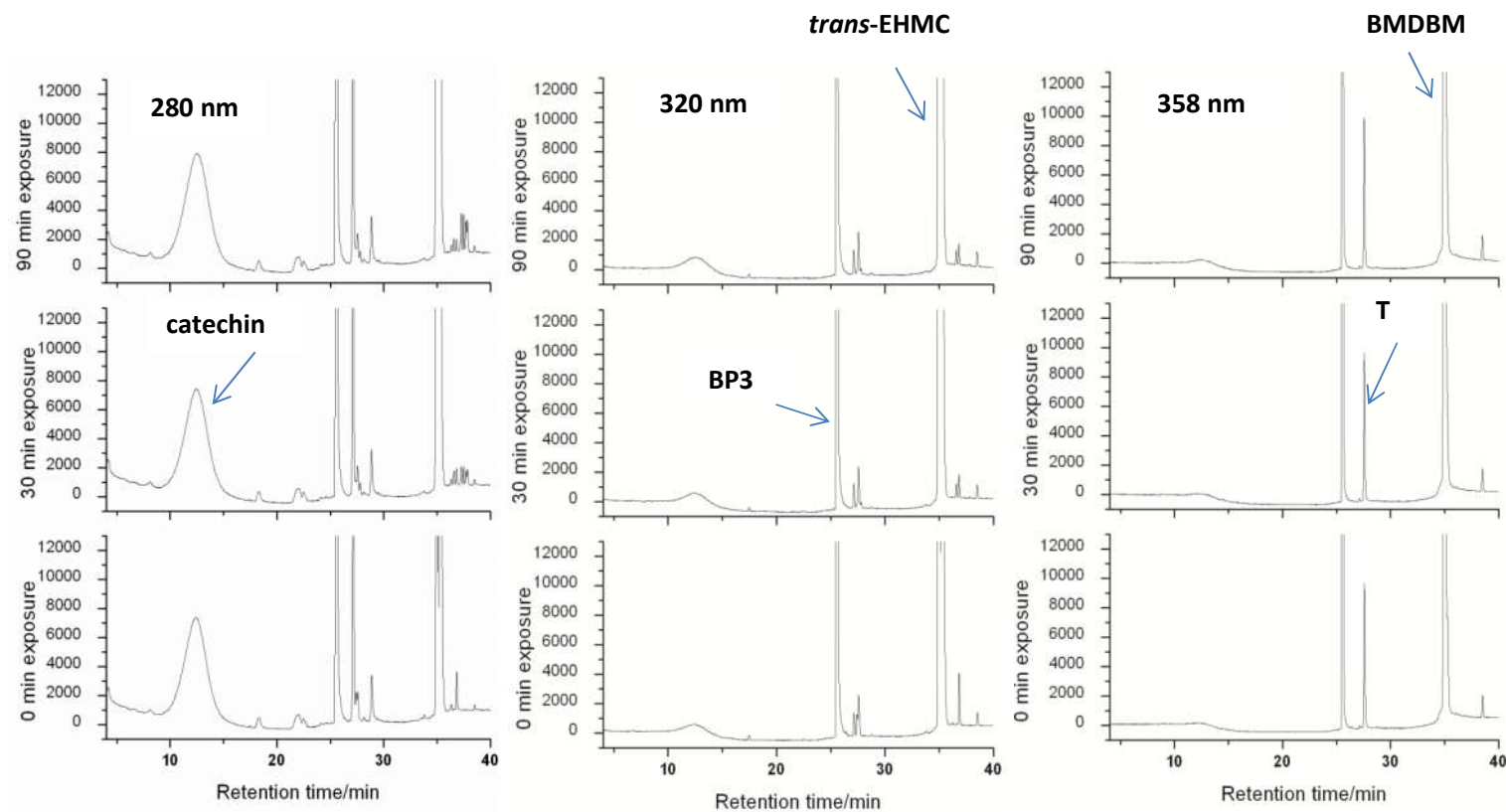
Figure 7.29: Photochemical changes of mixture of BMDBM, BP3, EHMC, and grape seed extracts at 280 nm, 320 nm and 358 nm showing increasing catechins peak area with increase of the irradiation time. The separations were achieved on a reverse phase Zorbax Eclipse XDB C-18 column (150 mm × 4.6 mm, i.d., 5 μm), under a gradient elution of acetonitrile-water at flow rate of 1 mL min^{-1} and an injection volume of 20 μL.

7.4   Conclusions

The secondary metabolites in grape seed extract undergo photochemical reactions yielding photoproducts that act synergistically and in combination with sunscreen absorbers to enhance photoprotection. The photoinstability of the BMDBM and EHMC mixture is highly reduced when mixed with grape seed extract. We propose that inclusion of grape seed extract in sunscreen formulations is likely to enhance the photoprotection potential of the formulation.

Acknowledgements

References

American Cancer Society (2008) Grapes. Ameican Cancer Society. Accessed 5-11-2014 2014

Bagchi D, Bagchi M, Stohs SJ, Das DK, Ray SD, Kuszynski CA, Joshi SS, Pruess H (2000) Free radicals and grape seed proanthocyanidin extract: importance in human health and disease prevention. Toxicology 148 (2):187-197

Bagchi D, Garg A, Krohn RL, Bagchi M, Bagchi D, J, Balmoori J, Stohs SJ (1998) Protective effects of grape seed proanthocyanidins and selected antioxidants against TPA-induced hepatic and brain lipid peroxidation and DNA fragmentation, and peritoneal macrophage activation in, mice. General Pharmacology 30 (5):771-776

Bagchi D, Garg A, Krohn RL, Bagchi M, Tran MX, Stohs SJ (1997) Oxygen free radical scavenging abilities of vitamins C and E, and a grape seed proanthocyanidin extract in vitro. Research Communication on Molecular Pathology and Pharmacology 95 (2):179-189

Bagchi D, Sen CK, Ray SD, Das DK, Bagchi M, Pruess HG, Vinson JA (2003) Molecular mechanisms of cardioprotection by a novel grape seed proanthocyanidin extract. Mutation Research/Fundamental and Molecular Mechanisms of Mutagenesis 523:87-97

Baliga MS, Katiyar SK (2006) Chemoprevention of photocarcinogenesis by selected dietary botanicals. Photochemistry and Photobiological Sciences 5 (2):243-253

Baumler W, Regensburger J, Knak A, Felgentrager A, Maisch T (2012) UVA and endogenous photosensitizers - the detection of singlet oxygen by its luminescence. Photochemical and Photobiological Sciences 11 (1):107-117

Benavides A, Montoro P, Bassarello C, Piacente S, Pizza C (2006) Catechin derivatives in Jatropha macrantha stems: characterisation and LC/ESI/MS/MS quali-quantitative analysis. Journal of pharmaceutical and biomedical analysis 40:639-647

Bowden GT (2004) Prevention of non-melanoma skin cancer by targeting ultraviolet-B-light signalling. Nature Reviews Cancer 4 (1):23-35

Broadbent KJ, Martincigh BS, Raynor WM, Salter FL, Moulder R, Sjoberg P, Markides EK (1996) Capillary supercritical fluid chromatography combined with atmospheric pressure chemical ionisation mass spectrometry for the investigation of photoproduct formation in the sunscreen absorber 2-ethylhexyl methoxycinnamate. Journal of Chromatography A 732:101-110

Dai J, Mumper RJ (2010) Plant Phenolics: Extraction, Analysis and Their Antioxidant and Anticancer Properties. Molecules 15 (10):7313-7352

DiGiovanni J (1992) Multistage carcinogenesis in mouse skin. Pharmacology Therapy 54 (1):63-128

Donovan JL, Luthria DL, Stremple P, Waterhouse AL (1999) Analysis of (+)-catechin and (-)-epicatechin and their 3' - and 4' -O-methylated analogs A comparison of sensitive methods. Journal of Chromatography B 726:277-283

Farrukh A, Santosh KK (2011) Polyphenols: Skin Photoprotection and Inhibition of Photocarcinogenesis. Mini Review Medical Chemistry 11 (14):1200-1215

Ferreira D, Slade D (2002) Oligomeric proanthocyanidins: naturally occuring O-heterocycles. Natural Product Reports 19:517-541

Fourie TG, Ferreira D, Roux DG (1977) Flavanoid synthesis based on photolysis of flavan-3-ols, hydroxyflavanones, and 2-benzylbenzofuranones. Journal of the Chemical Society, Perkin Transactions I 1 (2):125-133

Ghafar MFA, Prasad KN, Weng KK, Ismail A (2010) Flavonoid, hesperidine, total phenolic contents and antioxidant activities from Citrus species. African Journal of Biotechnology 9 (3):326-330

Hruza LL, Pentland AP (1993) Mechanisms of UV-induced inflammation. Journal of Investigative Dermatology 100 (1):35S-41S

Joshi SS, Kuszynski CA, Bagchi D (2001) The cellular and molecular basis of health benefits of grape seed proanthocyanidin extract. Current Pharmaceutical Biotechnology 2 (2):187-200

Kaur M, Agarwal R, Agarwal C (2006) Grape seed extract induces anoikis and caspase-mediated apoptosis in human prostate carcinoma LNCaP cells: possible role of ataxia telangiectasia mutated-p53 activation. Molecular cancer therapeutics 5 (5):1265-1274

Khanna S, Venojarvi M, Roy S, Sharma N, Trikha P, Bagchi D, Bagchi M, Sen KC (2002) Dermal wound healing properties of redox-active grape seed proanthocyanidins. Free Radical Biology and Medicine 33 (8):1089-1096

Koksal E, Bursal E, Dikici E, Tozoglu F, Gulcin I (2011) Antioxidant activity of *Melissa officinalis* leaves. Journal of Medicinal Plants Research 5 (2):217-222

Krause M, Kilt A, Blomberg JM, Soeborg T, Frederiksen H, Schlumpf M, Lichtensteiger W, Skakkebaek NE, Drzewiecki KT (2012) Sunscreens: are they beneficial for health? An overview of endocrine disrupting properties of UV-filters. International Journal of Andrology 35:424 - 436

Ley DR, Fourtanier A (1997) Sunscreen protection against ultraviolet radiation-induced pyrimidine dimers in mouse epidermal DNA. Photochemistry and photobiology 65 (6):1007-1011

Lyambila W (2003) A study of photoinduced transformations of sunscreen chemical absorbers. PhD Thesis, University of Natal, Durban, South Africa

Mandal P, Misra TK, Ghosal M (2009) Free-radical scavenging activity and phytochemical analysis in the leaf and stem of *Drymaria diandra* Blume. International Journal of Intergrative Biology 7 (2):80-84

Mantena SK (2005) Grape seed proanthocyanidins induce apoptosis and inhibit metastasis of highly metastatic breast carcinoma cells. Carcinogenesis 27 (8):1682-1691

Mturi GJ, Martincigh BS (2008) Photostability of the sunscreening agent 4-*tert*-butyl-4'-methoxydibenzoylmethane (avobenzone) in solvents of different polarity and proticity Journal of Photochemistry and Photobiology A: Chemistry 200:410-420

Plumb GW, De Pascual-Teresa S, Santos-Buelga C, Cheynier V, Williamson G (1998) Antioxidant properties of catechins and proanthocyanidins: Effect of polymerisation, galloylation and glycosylation. Free Radical Research 29 (4):351-358

Santos-Buelga C, Bravo-Haro S, Rivas-Gonzalo JC (1995) Interactions between catechin and malvidin-3-monoglucoside in model solutions. Zeitschrift Fur Lebensmittel-Untersuchung Und-Forschung 201 (3):269-274

Santosh KK (2008) Grape seed proanthocyanidines and skin cancer prevention: Inihibition of oxidative stress and protection of immune system. Molecular Nutrition and Food Research 52 (Suppl 1):S71-S76

Scalbert A, Williamson G (2000) Dietary intake and bioavailability of polyphenols. Journal of Nutrition 130 (8S):2073S-2085S

Schallreuter KU, J.M W, Farwell DW, Moore J, Edwards HGM (1996) Oxybenzone oxidation following solar irradiation of skin: Photoprotection versus antioxidant inactivation. Journal of Investigative Dermatology 106 (3):583 - 586

Schwack W, Rudolph T (1995) Photochemistry of dibenzoyl methane UVA filters. Journal of Photochemistry and Photobiology B: Biology 28:229 - 234

Sisa M, Bonnet SL, Ferreira D, Van der Westhuizen JH (2010) Photochemistry of flavanoids. Molecules 15:5196-5245

Sklar LR, Almutawa F, Lim HW, Hamzavi I (2013) Effects of ultraviolet radiation, visible light, and infrared radiation on erythema and pigmentation: a review. Photochemical and Photobiological Sciences 12 (1):54-64

Soobrattee MA, Neergheen VS, Luximon-Ramma A, Aruoma OI, Bahorun T (2005) Phenolics as potential antioxidant therapeutic agents: mechanism and actions. Mutation Research 579 (1-2):200-213

Steinmetz KA, Potter JD (1996) Vegetables, Fruit, and Cancer Prevention: A Review. Journal of the American Dietetic Association 96 (10):1027-1039

Sudheer KM, Manjeshwar SB, Santosh KK (2006) Grape seed proanthocyanidins induce apoptosis and inhibit metastasis of highly metastatic breast carcinoma cells. Carcinogenesis 27 (8):1682-1691

Svobodova A, Psotova J, Walterova D (2003) Natural phenolics in the prevention of UV-induced skin damage. A review. Biomedical Papers 147 (2):137-145

Wang ZY, Agarwal R, Zhou ZC, Bickers DR, Mukhtar H (1991) Inhibition of mutagenicity in salmonella-typhimurium and skin tumor initiating and tumor promoting activities in sencar mice by glycyrrhetinic acid - comparison of 18 alpha-stereoisomers and 18 beta-stereoisomers. Carcinogenesis 12 (2):187-192

Wilkinson F (1997) Quenching of electronically excited states by molecular oxygen in fluid solution. Pure and Applied Chemistry 69 (4):851-856

Yakamoshi J, Saito M, Kataoka S, Kikuchi M (2002) Safety evaluation of proanthocyanidin-rich extract from grape seeds. Food and Chemical Toxicology 40:599-607

Supplementary Materials
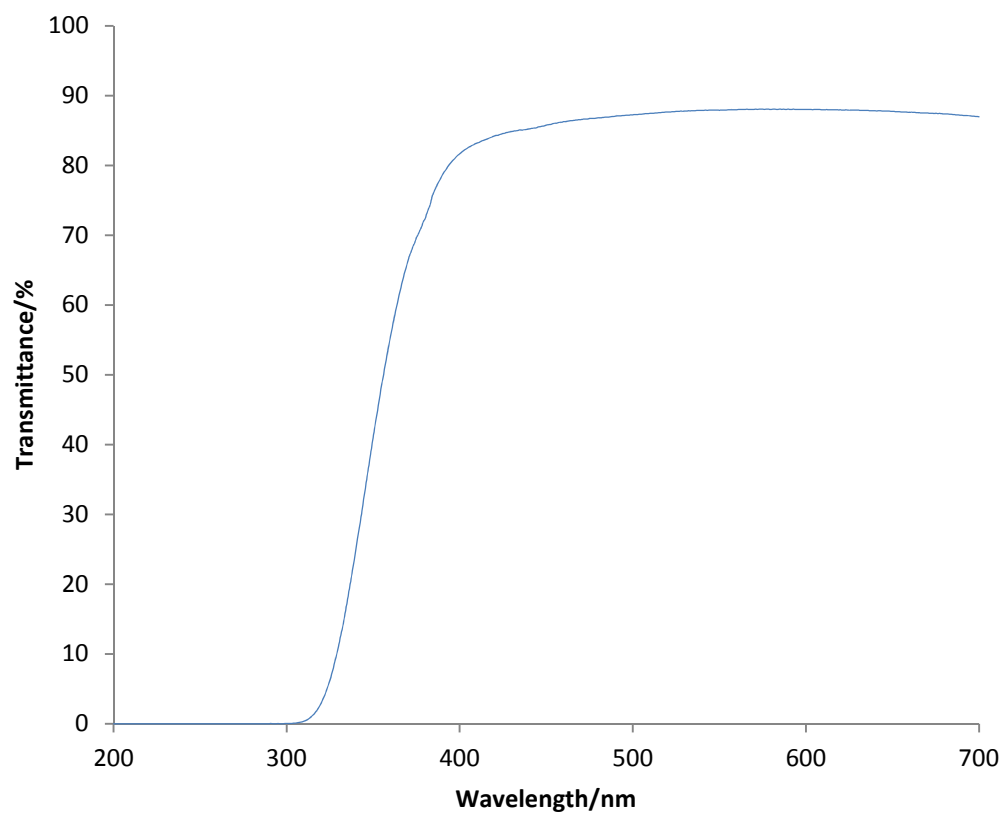
Figure S7.1: The transmittance spectrum of the 10 mm Pyrex glass filter used in this work recorded on a Perkin Elmer Lambda 35 UV-vis spectrophotometer.

Table S7.1 The photochemical changes of the sunscreen(s) dissolved in methanol after irradiation with simulated solar irradiation monitored on HPLC-PDA at 260, 286, 310, 358 nm.

Wavelength/nm	UV-filter	Mixture of BMDBM, BP3 and EHMC			
		Peak Area			
		RT	0 min	30 min	90 min
260	*keto-* BMDBM	3.072	474053	388025	402645
286	BP3	3.08267	1149065	1127671	1136999
	cis-EHMC	10.19733	0	261526	443856
	trans-EHMC	11.53067	683313	303745	148920
310	BP3	3.05067	1076471	879510	915656
	cis-EHMC	10.19733	0	272403	461590
	trans-EHMC	11.488	1212199	538875	272829
358	*enol-* BMDBM	11.21067	146473	139439	154766
		BMDBM			
260	*keto-* BMDBM	2.368	5769	99334	95094
358	*enol-* BMDBM	11.232	110714	96556	92185
		BP3			
286	BP3	3.06133	927540	738944	806767
		EHMC			
260	*cis*-EHMC	10.16533	0	139036	133916
	trans-EHMC	11.43467	156696	83566	81385
310 nm	*cis*-EHMC	10.16533	0	362702	342873
	trans-EHMC	11.44533	1818585	1026119	965827

Table S7.2: The chemical transformations of grape seed extract dissolved in methanol on UV irradiation monitored on HPLC-PDA at 275, 280, 286, 310 and 358 nm..

275 nm						280 nm					
RT	PA-0min	RT	PA-30min	RT	PA-90min	RT	PA-0min	RT	PA-30min	RT	PA-90min
1.402	821754	1.404	810606	1.398	814338	1.402	841527	1.405	827276	1.399	827785
1.562	157219	1.565	138212	1.561	138737	1.562	162778	1.565	142711	1.561	142797
1.851	75411	1.853	80312	1.847	91354	1.852	75001	1.853	79152	1.847	89590
2.048	118953	2.042	112886	2.037	107493	2.049	122437	2.043	115293	2.039	110357
2.392	104562	2.377	110316	2.369	110053	2.394	108431	2.377	109673	2.369	113712
2.745	152558	2.732	153627	2.728	147229	2.745	157294	2.732	156512	2.728	153884
3.061	56112	3.04	46293	3.04	43407	3.053	60422	3.051	52180	3.04	46751
3.537	134134	3.509	134173	3.505	130459	3.537	146947	3.51	137856	3.505	140075
4.225	108880	4.176	88631	4.176	60825	4.223	126170	4.169	91672	4.182	84684
8.159	4921	5.12	3779	8.081	5678	5.195	19163	5.152	5678	5.12	5699
12.357	1353501	8.066	6043	12.605	1842048	5.743	13204	8.097	7424	8.083	5523
15.204	7325	12.462	1556170	16.83	11341	8.166	4710	12.46	1579609	12.597	1861391
16.889	7829	16.898	8440	23.765	1109	12.382	1372515	16.827	7419	16.829	11101
17.28	4266	17.227	4266	24.131	3028	15.142	3030	17.248	4899	17.227	1592
23.083	1238	24.142	1165	24.363	2207	15.499	4539	24.127	2196	24.132	1334
23.829	1429	24.93	2382	24.597	1999	16.892	8312	24.644	3398	24.94	2863
24.165	3655	25.088	1616	24.924	4649	17.28	4859	24.925	3646	25.106	2073
24.427	2903	25.341	8381	25.085	2455	24.164	1435	25.104	2999	25.336	7327
24.619	1832	25.581	13174	25.333	10088	24.655	1056	25.337	7830	25.574	11534
24.946	4475	26.853	2730	25.575	14970	24.975	2651	25.58	11687	26.852	2918
25.142	2415	27.016	6034	26.852	2743	25.145	2601	26.853	2881	27.013	6219
25.367	9733	27.505	1433	27.013	6296	25.361	7067	27.016	6304	28.149	8990
25.607	13282	28.148	10020	27.494	1694	25.606	11647	28.146	8838	28.936	11803
26.878	2718	28.933	11853	28.148	10152	26.876	3025	28.933	11376	29.534	1272

27.047	6270	29.527	1155	28.936	11767	27.044	6281	29.499	1492	30.435	1527
27.543	1535	30.431	1730	30.429	1951	28.186	9068	30.445	1426	30.811	1229
28.183	10173	30.792	1418	30.774	1394	28.977	11481	30.82	1336	35.312	3381
28.977	11856	35.314	3365	35.211	1629	29.563	1317	35.319	3845	35.831	2673
29.558	1107	35.842	2180	35.313	1919	30.468	1153	35.827	2684	38.786	6920
30.46	1616	38.779	6713	35.817	2509	35.351	3391	38.78	6674	45.661	86377
30.821	1818	45.59	78528	36.32	1239	35.863	2521	45.607	88282		
35.347	3341			36.512	1334	38.831	6779				
35.866	2347			38.785	7268	45.589	86824				
38.826	7027			45.623	81154						
45.551	79786										

RT- retention time, PA- peak area

286 nm						310 nm					
RT	PA-0min	RT	PA-30min	RT	PA-90min	RT	PA-0min	RT	PA-30min	RT	PA-90min
1.402	691868	1.405	685360	1.398	695685	1.4	118461	1.403	135185	1.396	165243
1.561	132530	1.564	117089	1.56	119043	1.559	22106	1.563	23431	1.557	26377
1.851	65718	1.852	69386	1.847	75467	1.85	22167	1.851	32067	1.845	34065
2.05	97216	2.044	95267	2.038	96035	2.766	1320	2.082	29938	1.969	10966
2.392	91149	2.377	93260	2.368	96925	3.075	1432	2.364	30168	2.069	22137
2.746	122678	2.732	116779	2.728	118402	3.481	1573	2.735	27430	2.362	32967
3.065	48689	3.042	47944	3.044	43947	3.737	1560	3.058	18944	2.727	24498
3.537	112150	3.509	104589	3.503	105787	4.231	1341	3.418	17621	3.054	16802
3.947	12998	4.168	54555	4.168	52928	6.738	1604	3.702	12160	3.404	15287
4.215	66095	8.095	4752	8.083	4923	11.029	11129	4.169	6845	3.687	5005
5.163	1770	9.515	2196	12.617	1582090	12.171	58919	8.102	1409	6.717	1202
8.168	4083	12.462	1308231	16.855	6063	12.367	58394	10.603	2188	8.157	1103

12.436	1141421	16.847	6683	17.227	4735	13.291	20524	12.139	85222	25.554	1314
15.185	3106	17.248	4283	23.819	1633	25.579	1308	12.555	156053	27.015	1261
15.477	3267	23.787	1432	24.103	1055	27.052	1228	25.549	1241	35.313	4092
16.899	7148	24.133	1204	24.624	1463	35.35	3810	27.023	1040	35.826	1821
17.259	4770	24.617	1259	24.932	2511	35.863	1749	35.321	3839	38.793	2339
24.172	1136	24.949	2059	25.108	3627	38.814	2270	35.841	1505	44.538	2195
24.657	1551	25.11	3626	25.319	6210	45.582	53966	38.786	2339	45.617	59446
24.969	2498	25.339	5898	25.572	8066			45.627	54469		
25.139	3741	25.577	7785	26.851	2734						
25.361	6191	26.852	2557	27.013	6479						
25.599	8057	27.015	5943	27.525	1051						
26.139	1620	28.141	6404	28.141	6811						
26.886	2704	28.926	7598	28.933	8631						
27.044	6111	29.52	1230	29.498	1948						
28.184	6614	30.412	1118	29.93	1609						
28.975	7607	35.312	3373	30.376	1185						
29.551	1465	35.824	2635	35.307	3497						
30.487	1167	38.78	5845	35.827	2781						
35.353	3333	45.596	95733	38.782	6171						
35.865	2614			45.62	97628						
38.818	6043										
45.594	92016										

358 nm					
RT	PA-0min	RT	PA-30min	RT	PA-90min

1.398	33324	1.401	38505	1.394	45755
1.557	7964	1.561	7938	1.555	8422
1.849	18422	1.851	22275	1.845	22889
35.086	1111	1.998	9924	1.977	9811
35.867	1185	2.355	5189	2.363	9329
		35.017	1383	11.989	1106
		35.834	1076	35.004	1446
				35.831	1120

Table S7.3: The chemical transformation of grape seed extract mixed with BMDBM dissolved in methanol on simulated solar irradiation monitored by HPLC-PDA.

275 nm				280 nm			
RT	PA-0min	PA-30min	PA-90min	RT	PA-0min	PA-30min	PA-90min
1.408	571648	619539	612016	1.408	585560	634450	625814
1.568	90745	92438	92092	1.568	94248	96081	95627
1.855	57866	56525	61009	1.855	54728	55661	59921
2.054	77727	73916	76430	2.054	79384	75508	76088
2.398	49912	46431	50549	2.399	74743	49648	54419
2.56	21249	18838	17142	2.518		17058	17678
2.754	101133	100474	103125	2.754	101971	103368	105969
3.093	31948	31083	31607	3.083	34012	31994	35285
3.473		89618	91451	3.474		95084	97927
3.553	86269			3.554	89775		
4.112		49215	46547	4.111		47192	59249
4.24	51543			4.221	50268		
4.875	1813			5.056			2682
6.575	1751			6.564	1307		
7.94		3915	3629	7.941		3771	3751
8.187	3294			8.184	2881		
9.365			2487	9.28		1040	
12.38	814874	739284		9.333			1598
12.428			887456	9.728	2865		
18.35	15642	14621	15120	12.361	822530		
21.867	14274	16813	19341	12.407		771781	901666
22.093	20235	17292	15357	18.343	14864	13719	14585
22.482		12972	13482	21.867	14645		16550
22.512	12353			22.077	18639	31947	15826
24.143	1546	2910	1776	22.486		12833	13368
24.352		1622		22.509	13243		
24.607		1288	1052	24.147	1470	1586	1546
25.499		6551	4420	24.635		1057	1269
25.52	7678			25.532	6828	6861	6704
26.021	1369			26.015	1085		
27.143	378252	389615	402218	27.143	352815	363516	374258
27.569	21930	21289	24635	27.57	22369	23673	22660
28.136	3353	2487	4065	28.124	3135	3672	2409
28.884	40761	40672	43319	28.448		1175	
29.551	1745	2346	1983	28.884	42194	41817	44933
34.656		2137	1423709	29.53		2477	
34.971	1382376	1396290		30.311			1031
38.515	2828	3053	3303	34.971	1420813	1435961	1461669
45.371	31863	28239	18125	38.513	2676	2862	3142
				45.34		35057	35152

				45.416	35035		
	286 nm				310 nm		
RT	PA-0min	PA-30min	PA-90min	RT	PA-0min	PA-30min	PA-90min
1.408	481341	526507	522695	1.405	86260	100627	109291
1.567	76997	79398	79425	1.563	14461	17191	18339
1.855	51367	50065	51396	1.854	28115	29504	30010
2.054	66776	63912	66635	1.973		7502	24845
2.397	45044	42350	46276	2.056		17634	
2.56	16590	16317	14897	2.105	26944		
2.754	80786	80840	83765	2.367	21500	22723	24850
3.085	36541	28563	32663	2.789	17573	20343	20187
3.473			77022	3.089	13866	13678	13314
3.554	71763	79260		3.397			10603
3.979	10036	9133		3.428		8618	
4.113		28045	40231	3.501	7813		
4.237	33440			3.662		4463	4375
4.533		4466		3.722	3301		
4.715	4645			6.776	1001		
7.977		3220	2886	11.712		13353	1168
8.198	2480			12		12762	1499
9.653	1354			12.356		15380	
12.369	685195			12.736		17972	
12.409		646749	742588	22.467		1102	1169
18.349	10349	8616	9737	22.513	1096		
21.877	9329	9428	9516	25.562	2335	2022	1930
22.073		9048	8981	26.384	1051		
22.103	9503			27.143	31009	30985	32352
22.474		10818		27.574	16864	16424	16387
22.507	10793			28.772	1085	1047	1149
24.155	1011	1307		34.613			2200
24.634		1052	1605	34.971	1788683	1802380	1835204
25.141		1432		35.273	3312		
25.546	4709	5235	5649	38.515	4341	4593	5044
27.143	301985	311705	320404	44.582	4109	3218	
27.57	22483	22420	24696	45.389			11968
28.124	2709	1701	2882	45.409	11455	13543	
28.883	27200	26761	29171				
29.565		1988	1972				
34.971	1455159	1470132	1496729				
38.516	2580	2735	3136				
44.559		2219	1322				
45.383	40921	32027	38789				

358 nm

RT	PA-0min	PA-30min	PA-90min
1.403	29669	31744	33448
1.562	7813	7045	7674
1.854	17976	18296	21538
1.973			8792
27.147	1408	1545	1809
27.574	83259	84128	88969
34.971	7224686	7307875	7447378
38.516	11740	12538	13181
44.59	5681	6646	2675

Table S7.4: The chemical transformation of grape seed extract mixed with BP3 dissolved in methanol on simulated solar irradiation monitored by HPLC-PDA.

275 nm				280 nm			
RT	PA-0min	PA-30min	PA-90min	RT	PA-0min	PA-30min	PA-90min
1.406	516446	507024	485679	1.406	528634	519034	495059
1.567	75758	74681	74251	1.567	78670	77518	76878
1.853	51680	52424	54481	1.854	50813	51377	53248
2.046	67225	68522	71194	2.048	68171	69506	71818
2.391	42823	42094	46181	2.388	45344	44639	48342
2.549	16630	16895	17271	2.539	14924	15163	15252
2.744	91236	89518	88067	2.743	90409	90084	87141
3.061	26717	26728	27320	3.062	31906	29464	28946
3.489		79854	78028	3.489		78859	74655
4.132		40942	41626	3.535	79230		
3.535	78713			4.123		40739	30526
4.206	46592			4.201	40225		
4.757		1300	1487	4.533			1261
4.907	1151			4.672	3917		
8.007		3323	2931	4.768		1045	
8.157	2532			7.971			2518
9.397		1392		8.009		3219	
9.589	2645			8.126	2378		
12.347	662858			9.312			1348
12.434		682634	754600	9.579			2252
18.341	16126	15096	15659	12.389	643832		
21.867	16529	16935	16217	12.4		702129	
22.085	21062	19241	20406	12.507			80619

RT	PA-0min	PA-30min	PA-90min	RT	PA-0min	PA-30min	PA-90min
							1
22.666			4622	18.333	14672	14188	13654
22.703	4677	4623		21.877	16421	15059	15814
24.154	2610	1684	1707	22.086	17674	19569	18010
24.341	1242			22.684		4168	4038
25.554	4775428	4789679	4846807	22.725	4137		
26.98			6030	24.151	1501	1525	1373
27.02	6157	6913		24.611		1096	
27.494		1363		25.554	5909379	5930909	5998582
28.099			2592	26.98			6526
28.152	2977	2603		27.017	6408	6746	
28.888	42175	38553	41093	28.097			2181
29.227		3763		28.142	2669	2309	
29.532		1752		28.888	40694	42284	40874
34.983	1762	2458	1781	34.981	1829	2585	1868
35.296	4651	6469	4453	35.298	5433	7488	5162
36.075			1010	44.491		2250	3095
45.375	35671	28750	29652	45.407	40381	35709	35110

286 nm				310 nm			
RT	PA-0min	PA-30min	PA-90min	RT	PA-0min	PA-30min	PA-90min
1.406	436197	431569	413404	1.403	80290	85131	91990
1.566	64749	64188	63936	1.563	13844	15640	16260
1.853	46074	44442	48170	1.853	26874	28421	29565
2.049	57660	59075	61520	2.097	24353	25374	25117
2.388	36839	39631	40254	2.361	17263	21283	23704
2.56	15748	12818	16427	2.768	19969	17374	17784
2.744	70215	70360	70100	3.069	11960	12705	12408
3.076	27653	27301	26883	3.406		8581	10768
3.49		62814	62795	3.507	7004		
3.535	65282			3.715	2942	2485	2682
3.957	5613			12.128			1085
4.14		27341	27342	25.554	4582082	4612760	4646949
4.208	23879			27.018	1440	1532	1381
7.988		2407	2215	28.759	1148	1254	1105
8.124	2032			34.986	2229	3030	2104

RT				RT			
9.365		2222		35.298	7021	9083	6543
9.728	1445			44.546	4046	3850	
12.349	559886			45.364			6226
12.418		330349	662870	45.416	22882	14025	
12.555		262141		45.515			4509
18.333	10685	8800	8348				
21.781			11520				
21.877	10351	9427					
22.085	10527	10933	9217				
22.699	3161	2919	2834				
24.146	1275	1067	1034				
24.602			1232				
25.554	6713939	6755364	6815476				
26.979			6345				
27.019	7220	8894					
28.097			1600				
28.133	1762	1435					
28.887	25350	25054	24881				
29.28	1560	2135	1313				
29.486			2156				
29.551	1744	1700					
34.981	1810	2439	1895				
35.297	6172	8224	6045				
35.84	1025						
44.422		1989					

358 nm			
RT	**PA-0min**	**PA-30min**	**PA-90min**
1.401	**27908**	**28576**	**31082**
1.561	**8035**	**7109**	**8416**
1.853	**18236**	**18203**	**18136**
25.554	**1125806**	**1136514**	**1140015**
34.98	**9668**	**12680**	**9376**
44.563		**5122**	**5384**
45.42	43966	35438	35982

Table S7.5: The chemical transformation of grape seed extract mixed with EHMC dissolved in methanol on simulated solar irradiation monitored by HPLC-PDA.

	275 nm				280 nm		
RT	PA-0min	PA-30min	PA-90min	RT	PA-0min	PA-30min	PA-90min
1.403	551801	579666	525538	1.403	564580	592045	534834
1.563	87707	90706	84373	1.563	90873	94096	87151
1.849	53916	58392	61287	1.849	53091	55028	59887
2.032	73110	69524	76707	2.033	74297	73259	78267
2.369	48402	44513	50714	2.369	68215	47373	52038
2.517	18696	17834	20321	2.533		16085	18770
2.717	96428	94981	94514	2.716	95667	97256	99866
3.04	32526	29373	28418	3.031	33492	29923	28706
3.484	81655	88672		3.484	84755	90640	
3.514			80625	3.514			86568
4.122	48259	45509	33593	4.121	48778	43561	41322
7.975	3300	3431		7.961	2948	3644	
8.076			2872	8.077			2711
9.408	1122			9.504			1342
9.504			2846	12.407	735097	817605	
12.307	723555			12.611			997323
12.462		805143		18.308	14662	14939	15226
12.609			988200	21.792	18047		
18.296		15345		21.803		18778	18466
18.309	15578		15218	22.007	15764	16198	16356
21.813	17947	15722	17761	22.657	4389	4011	4078
22.03	19601	21105	19372	24.134	1463	1373	1536
22.659	5279	5152	4673	24.608		1034	
24.11	2406	1717	2743	25.173		1093	
24.32			1537	25.519	13489	13943	13908
24.613			1351	25.983	1340	1038	1717
25.312		1057		26.988	8310	7258	7269
25.515	11400	12251	11341	27.4	9682	3072	3288
25.971	1274	1398		27.77		5189	4398
26.99	6988	7018	6775	28.111	2618	2252	2433
27.403	8993	3208	3394	28.857	40040	41369	40295
27.771		4724	3947	33.461		1606	1225
28.12	3305	3002	2900	33.791	2599		2369
28.858	41954	41891	41552	34.92	12180	2244	10222
33.472	1004	1335		35.26	8557942	9973	7661832
33.787	2423	1933	2053	36.085	2335	7602718	
34.921	9835	8351	8591	36.32	4904	3320	3193
35.26	6923229	6396703	6442375	36.565	2171	5388	5394
36.085	1725			36.811	15831	7864	7978

RT	PA-0min	PA-30min	PA-90min	RT	PA-0min	PA-30min	PA-90min
36.32	4967	3521	3581	44.419			3068
36.544	1986	4820	5052	45.305	37659	6415	
36.81	12794	6318	6754	45.414		28507	33829
45.317	32035	27956	31738				

286 nm				310 nm			
RT	PA-0min	PA-30min	PA-90min	RT	PA-0min	PA-30min	PA-90min
1.403	464439	490654	448488	1.401	84750	100206	104912
1.563	74413	77578	72839	1.558	14833	16419	17802
1.849	45749	49552	56090	1.848	20843	28210	29698
2.034	64599	60511	64561	1.974			29053
2.367	57733	40963	46725	2.065		25140	
2.526		17212	15814	2.361		19189	26364
2.717	78759	76246	76247	2.738		20060	19450
3.016	29178	30149	25539	3.036	1047	13538	13152
3.483	69883	74645		3.437	1154	9758	13474
3.513			70118	3.675	1198	3612	
3.904	8689			3.733			4815
4.132	30771	37019	23511	12.085		1067	
7.98	2385	2627		12.171			1141
9.515			2980	17.412	1989		
12.403	630439	687468		25.525	8726	8934	8829
12.563			473469	26.986	1347	1781	1437
12.789			333816	27.399	9910	1787	1711
14.432			45445	27.777		3818	3245
18.187	4188			28.733			1108
18.298		9628		33.794	2456	1230	
18.305	5798		9389	33.807			1348
21.99		19569	10638	34.92	17399	13521	13799
22.018	20216		9256	35.26	12244867	9767019	9861700
22.643	2508	2565		36.094		2523	
22.702			2567	36.101	3278		
24.1	1531		1161	36.267	2532	1760	
24.603	1105			36.557	2761	7754	6499
25.522	13323	12961	13235	36.812	24327	13692	13141
25.983			1161	44.498			3770
26.988	7910	7172	7242	44.518	3842		
27.399	10938	3092	3277	45.308	15388	9613	
27.772		5688	4741	45.445			10458
28.099		1631					
28.118	1836		1585				
28.854	26995	26257	26254				
29.527			1500				
33.483		1366					
33.798	2149	1457	1705				

RT			
34.922	14960	11571	11950
35.26	10252311	8842980	8916252
36.085	2530		
36.308	4236	2095	2103
36.562	2390	6208	6159
36.811	18786	9713	9955
45.319	37758		
45.465		39109	40837

358 nm			
RT	PA-0min	PA-30min	PA-90min
1.399	29684	32176	34220
1.556	8346	8104	8308
1.848	18410	18493	18388
25.524	1630	1810	1728
34.94	3104	2830	2538
35.26	32815	40433	40861
44.559			5693

Table S7.6: The chemical transformation of grape seed extract with a mixture of BMDBM, BP3 and EHMC dissolved in methanol on simulated solar irradiation, monitored by HPLC-PDA.

275 nm				280 nm			
RT	PA-0min	PA-30min	PA-90min	RT	PA-0min	PA-30min	PA-90min
1.411	696454	756140	750190	1.411	712897	773027	765720
1.571	114010	112045	114340	1.571	118188	116132	118341
1.858	61706	67382	70616	1.859	60826	66347	69486
2.047	94405	85392	92213	2.049	95706	86720	94307
2.393	56054	56338	59303	2.393	59150	56929	60747
2.56	25196	22133	22634	2.549	20159	22137	20565
2.744	118281	122949	123381	2.744	123243	122637	129829
3.065	41993	36803	37656	3.064	39282	40825	39208
3.533	106630	116478	115066	3.533	103068	110642	120304
4.187	79213	71154	70448	4.204	60588	56373	76616
5.173		2897	2626	5.184			3372
5.28	2754			8.094	4918	3956	
6.522	2167			8.118			4454
6.709			1525	12.35	1040967		
8.082		4615		12.433		1070163	1134387
8.115	4114		4710	18.337	14868	14793	15115
9.525		5103		21.856	17789		
12.35	974547			22.068	15445	33392	33273
12.454		1017324	1172969	22.484	12017	11980	11939
18.332	15937	15722	16056	24.145	1462	1263	1521
21.856	20002		17077	24.604		1303	1081

RT				RT			
22.044	15448	36747	18452	25.142		1032	1009
22.486	11868	12357	12629	25.539	5570159	5701924	5818960
24.125	3018	1861	1799	27.139	314918	321205	327039
24.309	1568			27.393		5848	
24.614	1414			27.416	15961		
25.312			1058	27.561	18236	19107	18821
25.539	4512197	4607830	4702151	27.783		7327	7848
27.139	338038	344763	350399	28.121	3139	2916	3032
27.416	14410	5371		28.384			1022
27.561	18889	19364	19026	28.878	39809	39665	40377
27.784		6938	7358	29.552	1721	2079	2824
28.113	4155	3574	3741	33.483			1290
28.878	40860	40610	40808	33.515		1623	
29.547	1637	2224	2392	33.787		2271	2020
33.545	1155	1391	1228	33.817	2459		
33.777			1829	34.528			1897
33.82	2455	2101		34.958	1290410	1258243	1299389
34.528	1653		1707	35.28	9022547	7869693	7773908
34.958	1259053	1255420	1264415	36.118	2442		
35.28	7298363	6645382	6648113	36.338	5053	3576	3680
36.067			1022	36.576	1783	7237	7682
36.107	1730			36.828	16939	8281	8072
36.338	4935	4030	4151	37.281		9055	17091
36.576	1396	6697	7205	37.5		7408	12613
36.828	13726	7068	7209	37.715		6023	11422
37.281		10382	18612	37.855		7663	15326
37.5		9188	15418	38.51	2624	2776	2767
37.715		7561	13199	45.437	40549	33090	38016
37.858		8403	17012				
38.487			3431				
38.511	2770	2702					
45.391	36991	33581	30411				

286 nm				310 nm			
RT	PA-0min	PA-30min	PA-90min	RT	PA-0min	PA-30min	PA-90min
1.411	586050	631980	636997	1.409	103819	123817	134117
1.571	96617	102345	97669	1.566	17543	19721	20980
1.858	54342	58979	61636	1.856	21177	21326	21880
2.05	77895	72787	78861	2.374		1066	1536
2.39	52032	48274	51049	2.777	1144	1222	1085
2.549	19077	18726	19191	3.068	1146	1371	1178
2.745	94558	98677	100651	3.473	1468	2447	3219
3.067	37335	37317	33990	3.718	1286	1610	1723
3.533	85019	90806	92725	4.198	1032		
4.197	49398	46240	43872	6.737	1368		

RT			
8.094		3702	
8.153	3121		3658
9.579		2188	
12.354	834561		
12.433		874409	999492
17.428	1138		
18.333	10197	11146	10567
21.813	10273		9626
22.062	9034	18389	8771
22.478	10571	9750	10226
24.115	1140	1073	1015
25.539	6332539	6478995	6594770
27.139	268318	274212	274100
27.398		6598	
27.417	16907		
27.563	18667	19060	24316
27.784		8100	7878
28.099			1160
28.135	2033	2249	
28.877	26821	26214	26484
29.543	2062	1846	1936
33.419		1415	
33.791		1412	1423
33.818	2036		
34.496			1038
34.581	1139		
34.958	1320832	1288202	1331422
35.28	10807391	9091783	8918733
36.318	2494	2455	2314
36.566		8019	8393
36.828	19828	9694	9153
37.281		7949	14520
37.5		5284	8708
37.717		4568	8351
37.855		6741	12693
38.513	2433	2651	2691
44.529	3632		3128
45.435	43185	40280	38834

RT			
10.997	6514		
11.477		11525	
12.117	42603	34845	
12.213			1567
12.381	22242	23531	
12.693	25588		
12.779		54334	
13.259	17754		
17.438	2175	1703	1854
22.481	1102		1072
25.539	4317888	4411351	4498009
26.365	1041		
27.139	26810	27845	27197
27.419	10627		
27.567	15846	18031	17284
27.788		4565	4764
28.752	1149	1106	1272
33.792		1058	
33.827	2313		
34.958	1629890	1620001	1630927
35.28	12979343	9008015	9591474
36.284	1213		
36.565		8170	8092
36.829	25177	12011	10716
37.284		1232	1236
37.848			1607
38.509	3901	4198	4545
45.444	14984	22131	11033
46.069	4352		

358 nm			
RT	PA-0min	PA-30min	PA-90min
1.406	31172	36798	39088
1.564	8092	8247	8299
1.856	18094	18381	22368
1.973			13218

2.366			1708
25.54	1058571	1081199	1100750
27.148	1467	1407	1420
27.569	77994	79600	80817
34.958	6689226	6775626	6883434
38.51	10673	11541	12127

Chapter Eight

The photostabilizing potential of mulberry extract on common sunscreen absorbers

Moses A. Ollengo and Bice S. Martincigh[*]

School of Chemistry and Physics, University of KwaZulu-Natal, Westville Campus, Private Bag X54001, Durban 4000, South Africa

*Corresponding author: Tel.:+27-31-2601394; Fax: +27-31-2603091; E-mail address: martinci@ukzn.ac.za

Abstract

The photostability of the sunscreen agents: 2-ethylhexyl-*p*-methoxycinnamate), (EHMC), benzophenone-3 (BP3) and *tert*-butylmethoxy dibenzoylmethane, (BMDBM, avobenzone) in the presence of mulberry extract was investigated. The effect of mulberry extract on the photo-absorption capacity of each sunscreen was studied by exposing the samples to simulated solar radiation. The photochemical transformations were then monitored by means of standard spectrophotometric methods. Any new chemical species formed were monitored by RP-HPLC. The constituents of mulberry extract were identified by means of GC/MS. The absorptive efficacies of the sunscreens were greatly improved when each was mixed with mulberry extract alone in a methanolic solution. The mulberry extract favoured the chelated enol form of BMDBM and hence contributed to enhanced UVA absorption. BP3 remained unchanged for all exposure times indicating no chemical interaction. Hence, no side-reactions of BP3 are envisaged in this mixture. EHMC showed a drop in absorbance but subsequently stabilized. A photochemical isomerisation to a strongly absorbing UVB species was observed. The mulberry extract therefore was found to enhance the UVB absorption potential of EHMC. However, the mixture of the three sunscreens in mulberry extract was found to greatly reduce UVA absorbing chemical species and favour UVB absorbing species. We conclude that mulberry extract is a good photochemical stabilizer of sunscreens and would reduce the amount of sunscreens incorporated in a single product.

8.1   Introduction

The mulberry (*Morus* species) grows wild or is cultivated in many countries for the purpose of providing foliage, that serves as a primary source of food for silkworms (*Bombyx mori*) (Aramwit et al. 2010; Bajpai et al. 2012). The mulberry fruits have been reported to exhibit a variety of biological activities, such as anti-thrombotic, antioxidant, antimicrobial, anti-inflammatory and neuroprotective effects. A review by Bajpai et al. (2012) examines a number of these bioactivities. These activities are associated with anthocyanins; a group of naturally occurring phenolic compounds responsible for the colour of mulberries. Cyanidin-3-glucoside and cyanidin-3-rutinoside are the major anthocyanins (Aramwit et al. 2010; Yadav et al. 2014) present in mulberries.

There is a growing trend of reliance on phytochemically-rich plant extracts containing polyphenolic compounds with good antioxidant properties to cure diverse diseases. This is because of their low toxicity and lack of harmful side-effects compared with synthetic drugs. In addition, the application of antioxidants as preservatives in the food industry (Winkler et al. 2006; Guillard et al. 2009; Brul and Coote 1999) and skin-protective ingredients in cosmetics continues to draw increasing attention and interest (Lupo 2001; Chen et al. 2012). However, exposure of these extracts to light results in the loss of their efficacy. Recently Aramwit et al. (2010) showed that the exposure of mulberry fruit extracts to light significantly deteriorated the total anthocyanin and ascorbic acid content. The anthocyanins have been shown to be responsible for the anti-tyrosinase activity in these extracts, a potentially useful dermatological aspect. Tyrosinase inhibitors are used in topical applications for lightening the skin and also are thought to play a role in cancer and neurodegenerative diseases such as Parkinson's disease (Cavalieri et al. 2002). These findings have generated a great deal of interest leading to widespread screening for compounds with potent anti-tyrosinase activity.

Several authors have investigated the antioxidant potential of the extracts obtained from mulberry leaves and fruits (Wang et al. 2013; Arfan et al. 2012; Mishra et al. 2011). These extracts contain polyphenolic compounds that are some of the most effective antioxidative constituents in fruits, vegetables, and grains; and much interest has been directed to their quantitation and assessment of their contribution to antioxidant activity. However, an emerging aspect is their unique ability to absorb ultraviolet (UV) light. For instance, Arfan et al. (2012) used the absorption bands at wavelengths of 320–350 nm to confirm the presence of phenolic acids in two mulberry species. This UV absorption potential has been speculated to be useful in the sunscreening potential of mulberry extract (Subramaniyan et al. 2013).

A number of investigations are ongoing to make use of naturally occurring UV radiation absorbers targeting anthocyanin in mulberry extract. It is speculated that incorporation of these extracts in sun-protective products could help boost their efficacy. A recent study by Subramaniyan et al. (2013) showed that a higher concentration of anthocyanins yielded a higher sun protection factor (SPF). These authors found no difference in SPF between fabrics treated with crude mulberry fruit extract and fabric treated with anthocyanin extracted from the mulberry fruit. Most sunscreens show loss in photoprotection when irradiated by UV light. However, an investigation of the photostability of sunscreens in skin-lightening products indicated photostability for products containing plant extracts, one of which was mulberry extract (see Chapter Four). We thus sought to study the effect of mulberry extract on the photostability of commonly used sunscreen absorbers. In the current work we set to investigate the stabilizing potential of mulberry extract on some common sunscreen agents in skin-lightening preparations and sunscreen cosmetic products. To the best of our knowledge this is the first comprehensive study on the photostabilizing potential of the mulberry extract on the common

sunscreen agents: 2-ethylhexyl-*p*-methoxycinnamate) (EHMC), benzophenone-3 (BP3) and *tert*-butylmethoxy dibenzoylmethane, (BMDBM).

8.2   Experimental

8.2.1   Materials
The mulberry extract was purchased from Warren Chem Specialities (Pty) Ltd, South Africa. The solvents used were HPLC-grade acetonitrile (ACN) and methanol (MeOH) were purchased from Merck KGaA. The three chemical UV filters of analytical purity (99.9 %) were purchased as follows: 2-ethylhexyl-*p*-methoxcinnmate (EHMC) and *tert*-butylmethoxy dibenzoylmethane (BMDBM) were a kind donation from BASF, benzophenone-3 (BP3) was from Sigma-Aldrich and N,O-*bis*(trimethylsilyl)trifluoroacetamide (BSTFA) was purchased from Supelco.

8.2.2   Characterisation of mulberry extract
The mulberry extract was characterised by gas chromatography-mass spectrometry (GC/MS), gas chromatography-flame ionisation detection (GC/FID), and High performance liquid chromatography-mass spectrometry (HPLC-MS) in order to identify the chemical components present.

8.2.2.1   Sample preparation
About 25 mg of mulberry extract powder was soaked in 25 mL of methanol at 25 °C and placed in an ultrasonic bath for two hours and then left to stand for 24 hours protected from light by aluminium foil. The extraction mixture was then made up to 50 mL in a volumetric flask with methanol. The resultant solution was filtered through a 0.45 µm Millipore Millex-LCR membrane filter and then transferred to an aluminium foil cased glass vial for storage. The remaining solution was preserved for photostability studies.

The mulberry extract samples for gas chromatography-mass spectrometry (GC/MS) characterisation were first derivatised to volatilise the polyphenols in the extract. This was achieved by dissolving a samples mass of about 2 mg of mulberry extract powder in 1.0 mL of ACN in a clean and dry 3 mL reaction vial. To this solution 0.5 mL of N,O-bis(trimethylsilyl)trifluoroacetamide (BSTFA) was added then capped tightly, mixed well, and heated at 70 °C for 45 min. The resultant derivatised mixture was filtered through a 0.45 µm Millipore Millex-LCR membrane syringe tip filter after cooling to room temperature. A volume of 0.1 µL of this derivatised sample was then injected into the GC/MS chromatograph. To monitor any chemical interactions between the mulberry extract and the sunscreen agents, a mixture of the sunscreen(s) with the mulberry extract was prepared and derivatised similarly and injected onto the GC/MS chromatograph. Each mixture contained about 100 µM of the organic sunscreen absorber(s) and the same amount of mulberry extract.

8.2.2.2   The GC/MS experiment
A 0.1 µL aliquot of the derivatised mulberry extract either alone or in combination with a sunscreen(s) was delivered into a Shimadzu GC/MS (QP2010 SE), with a column temperature set at 70 °C and the injection port at 250 °C. Injections were in split mode at a ratio of 20:1. The components were separated in a GL Sciences InertCap 5MS/Sil 30 m × 0.25 µm quartz capillary column with a bound stationary phase consisting of 5 % dimethylpolysilphenylene siloxane. The column was held 70 °C for 2 min, raised to 240 °C at 10 °C min^{-1}, then held for 5 min followed by an

increase to 270 °C at 10 °C min^{-1} and held for 10 min. The carrier gas was helium flowing at linear velocity set at 30.0 cm s^{-1}. The MS ion source temperature was 200 °C and the interface temperature was set at 250 °C. The MS detector was programmed to run in scan mode in the *m/z* range 35-1000 at a scan speed of 3333 and the detector voltage gain set at 2.5 kV. The total run time was 37 min.

8.2.2.3   The GC/FID experiment

To check method interconvertability a GC/FID experiment was carried out on the same samples (derivatised mulberry extract alone and with sunscreen(s) with the same temperature program. The GC/FID used was a Shimadzu GC (GC-2010), fitted with an autosampler (AOC 20i) and a flow unit (AFC-2010). The components were separated in a DB-5 (30 m × 0.25 μm) quartz capillary column with a bound stationary phase consisting of 5% phenyl polysilphenylene-siloxane. The make-up gas was nitrogen/air flowing at 10 mL min^{-1}, the carrier gas was hydrogen with a flow rate of 40 mL min^{-1} and oxygen/air flowing at 400 mL min^{-1}. The injection port was set at 250 °C, operating in a split mode of 20:1 for an injection volume of 2 μL. The velocity flow control mode was adopted keeping the pressure at 61.9 kPa, the total flow rate at 5.0 mL min^{-1}, the column flow of 0.68 mL min^{-1}, and a linear velocity of 20.0 mL s^{-1}.

8.2.3   Photostability experiments

The sunscreen mixtures with mulberry extract were prepared by adding about 20 mg of the sunscreen agents to 25 mL of the methanol extract (prepared as described in Section 8.2.2.1). This solution was then made up to 50 mL in a volumetric flask with methanol. To obtain working solutions, appropriate dilutions were carried out in order to obtain a sunscreen agent concentration of about 200 μmol dm^{-3} in the extract for photostability studies.

Samples of mulberry extract with and without sunscreens added were exposed to simulated solar light in a Newport research lamp housing (M66901) fitted with mercury-xenon lamp, powered by an arc lamp power supply Newport (69911). The power output of the lamp was controlled by a digital exposure controller Newport (68951) maintaining the output at 500 W. The radiation from the lamp was passed through a 10 mm thick Pyrex filter to ensure that only wavelengths greater than 300 nm impinged on the samples. The exposure time was varied incrementally from 0 hour in steps of 30 min to 4 hours of continuous exposure. Each exposed sample was contained in a stoppered 1.00 mm pathlength quartz cuvette. After each irradiation interval a UV-visible spectrum of the sample was recorded on a Perkin Elmer Lambda 35 dual-beam spectrophotometer. A 10 μL aliquot of these same solutions were then injected into the HPLC chromatograph to monitor any chemical transformations between the extract and the included sunscreen(s). Samples of the sunscreens alone dissolved in methanol were similarly irradiated and monitored by UV spectrophotometry.

8.2.3.1   HPLC analysis of irradiated samples

The chemical transformations in the irradiated samples were monitored on a Shimadzu Prominence HPLC chromatograph with a photodiode array (PDA) detector. The chromatographic separation was achieved on an Agilent Zorbax Eclipse XDB C-18 reversed-phase column (150 × 4.6 mm i.d.; 5 μm particle size). The mobile phase was composed of water (solvent A) and acetonitrile (solvent B). The mixtures were resolved by a gradient elution as follows: 5–13 min, 16 % B; 13-18 min, 45 % B and held for 5 min; 23-28 min, 75 B %, held for 5 min; 33-40 min, 99 % B then held 5 min and then dropped linearly to 16 % B for 15 min. The experiment was performed at ambient temperature with a flow rate of 1 mL min^{-1} and an injection volume of 10 μL. The chromatograms were collected at

detection wavelengths of 275, 280, 286, 310, 320, and 358 nm with a bandwidth of 4 nm simultaneously in each of the 60 min run time. The photodiode array detector was set to collect the UV-vis spectra of the chemical species separated over the range 190 to 800 nm.

8.3 Results and discussion

The characterisation of the mulberry extract was firstly done in order to identify the chemical components present that may play a role in any photochemical reactions and consequently give rise to any UV absorption effects observed.

8.3.1 Characterisation of the mulberry extract

In order to investigate the chemical composition of the mulberry extract used in this work, the extract was derivatised and subjected to GC/MS analysis. The components present were identified from their mass spectra. A positive match was obtained by comparison to > 80 % match of the National Institute of Standards and Technology library search. The total ion chromatogram (TIC) of the silylated mulberry extract is shown in Figure 8.1. The prominent peaks P and E were identified as picolinic acid and ethyl-9,12-octadecadienoate respectively (Fig. 8.1). Some of the other compounds identified are shown in Figure 8.2 together with their percentage match of the mass spectra with those of the NIST database.
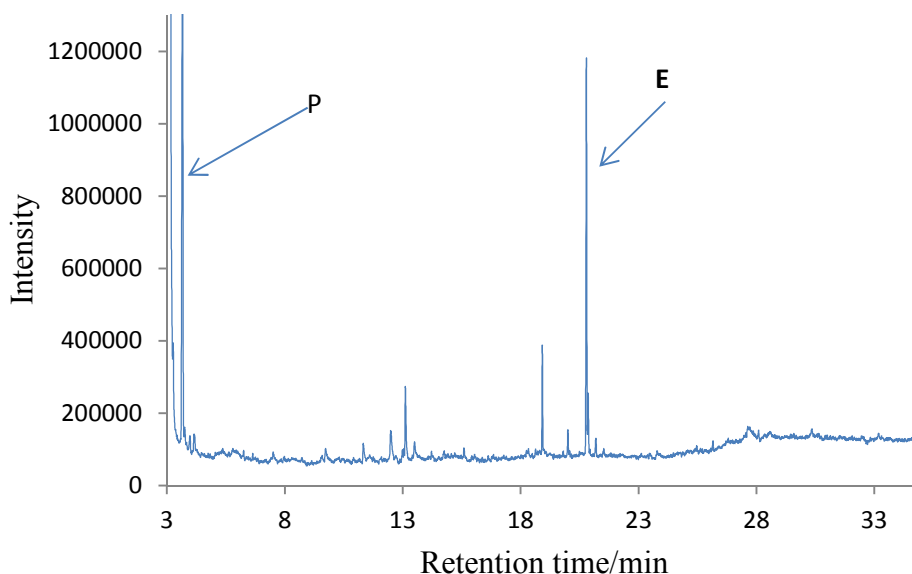
Figure 8.1: The GC/MS total ion chromatogram of a methanolic solution of silylated mulberry extract showing the picolinic acid (P) and ethyl-9,12-octadecadienoate (E) peaks. The separation was effected on a GL Sciences InertCap 5MS/Sil 30 m × 0.25 quartz capillary column under the condition described in Section 8.2.2.2.
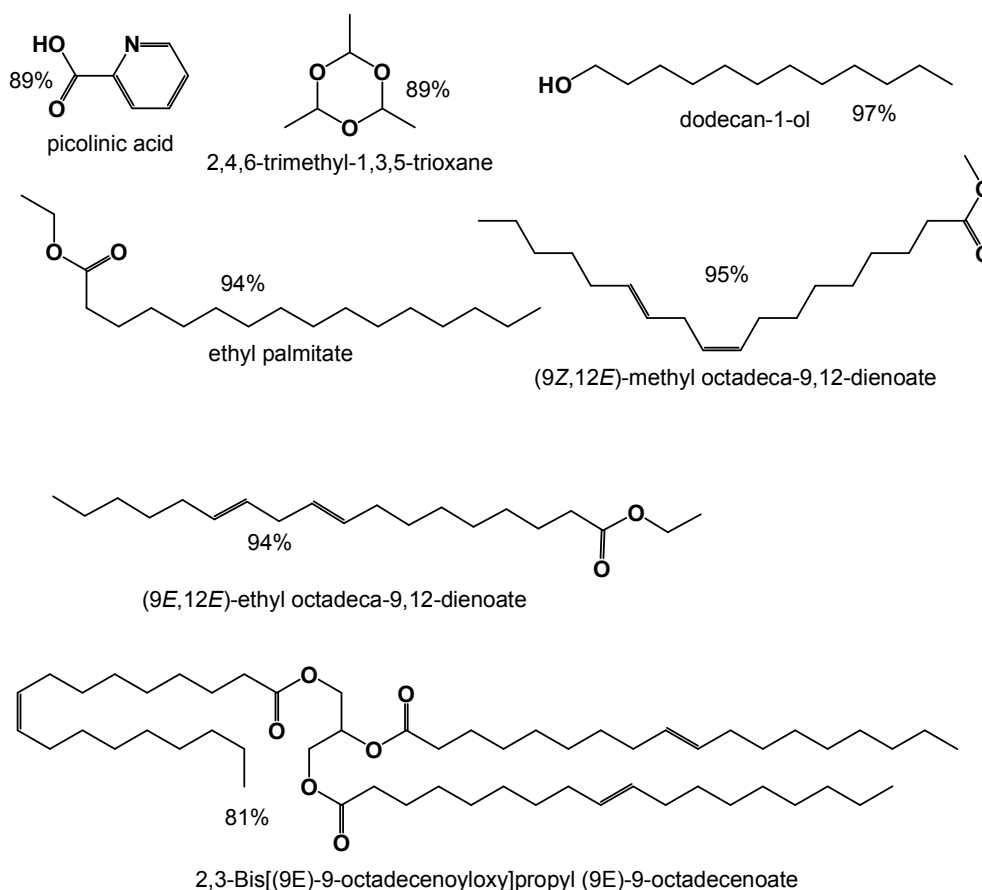
Figure 8.2: Some of the compounds identified in the mulberry extract by GC/MS. Below each structure is given the percentage match of the mass spectrum with that of the NIST database.

According to the library match criteria used in this work, the major constituents of mulberry extract in the methanolic solution were aliphatic esters, in which picolinic acid, an aromatic acid, and ethyl-9,12-octadecadienoate were found to be major methanol extractible components (Fig. 8.1). These compounds may not explain the observed light absorption characteristics exhibited by this extract. However, Wang et al. (2013) isolated a number of flavonoids from various fractions of mulberry by using different solvent systems. These authors concluded that mulberry extract contains high amounts of anthocyanins. Our focus in this work was to investigate the photostabilization potential of the methanol soluble fraction of the mulberry extract on common sunscreen agents. Most sunscreen preparations in the market use alcohol as the solvent. Hence, different extraction solvent compositions were not attempted. However, the absorption of UV observed in this work confirmed, the presence of flavonoids though our GC/MS results did not show any fragments that could relate to flavonoids or flavones. The methanol fraction of mulberry extract has previously been shown to contain anthocyanins (Subramaniyan et al. 2013).

8.3.2 Photostability of the mulberry extract

The extract showed good UV light absorption but this dropped steadily on exposure to solar simulated light (Fig. 8.3). The spectra show good UV absorption which extends to visible region and points to the presence of anthocyanins (Fig. 8.4). The anthocyanins have extended conjugation in the C-ring and hence are better light harvesters than other flavonoids like the catechins. This observation agrees with work by Aramwit et al. (2010); this group showed that light degrades anthocyanins from mulberry fruits. It should be noted that spectral drop is gradual showing relative stability. The

spectral changes observed were monitored by HPLC. The HPLC chromatograms of these samples gave peaks of chemical species seen at 280 nm, 320 nm and 358 nm, with UV spectra characteristic of flavonoids, flavans and flavones (Fig. 5). The lack of flavonoid fragments in the GC/MS results could be due to the low volatility of these compounds and the short derivatisation period employed. A chemical species on the HPLC chromatogram at retention time 15 min decreased steadily with incremental exposure period.
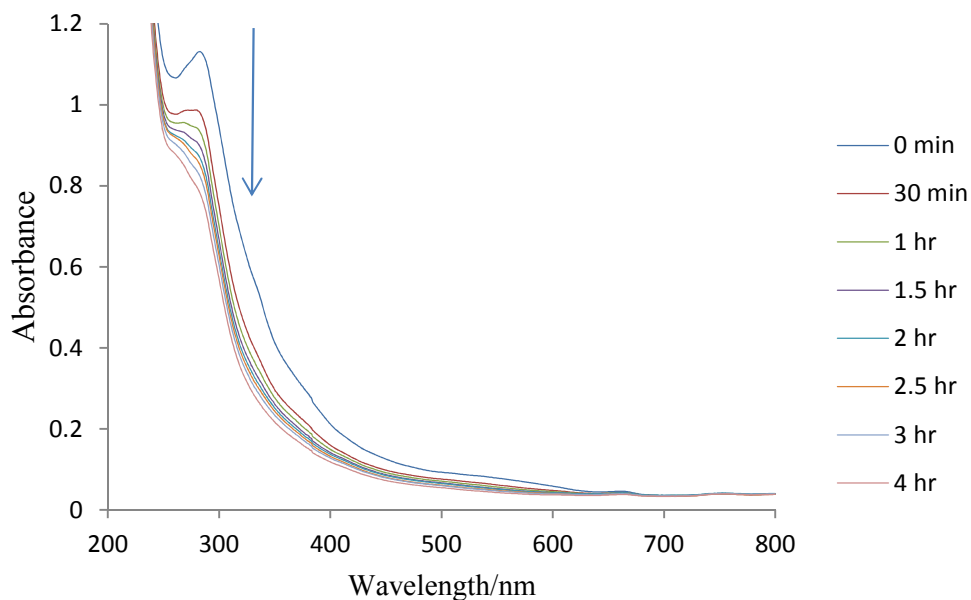
Figure 8.3: Photostability of the mulberry extract dissolved in methanol when exposed to simulated solar radiation. The spectral changes were monitored with a Perkin Elmer Lambda 35 dual beam spectrophotometer, in a 1 mm pathlength quartz cuvette.
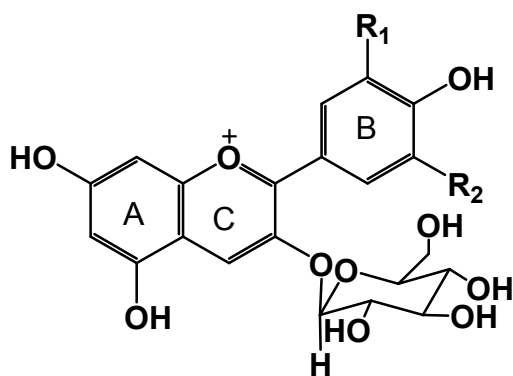
pelargonin: R_1= H, R_2 = H
cyanin: R_1 = OH, R_2 = H
delphinin: R_1 = OH, R_2 = OH

Figure 8.4: The general structure of anthocyanins.
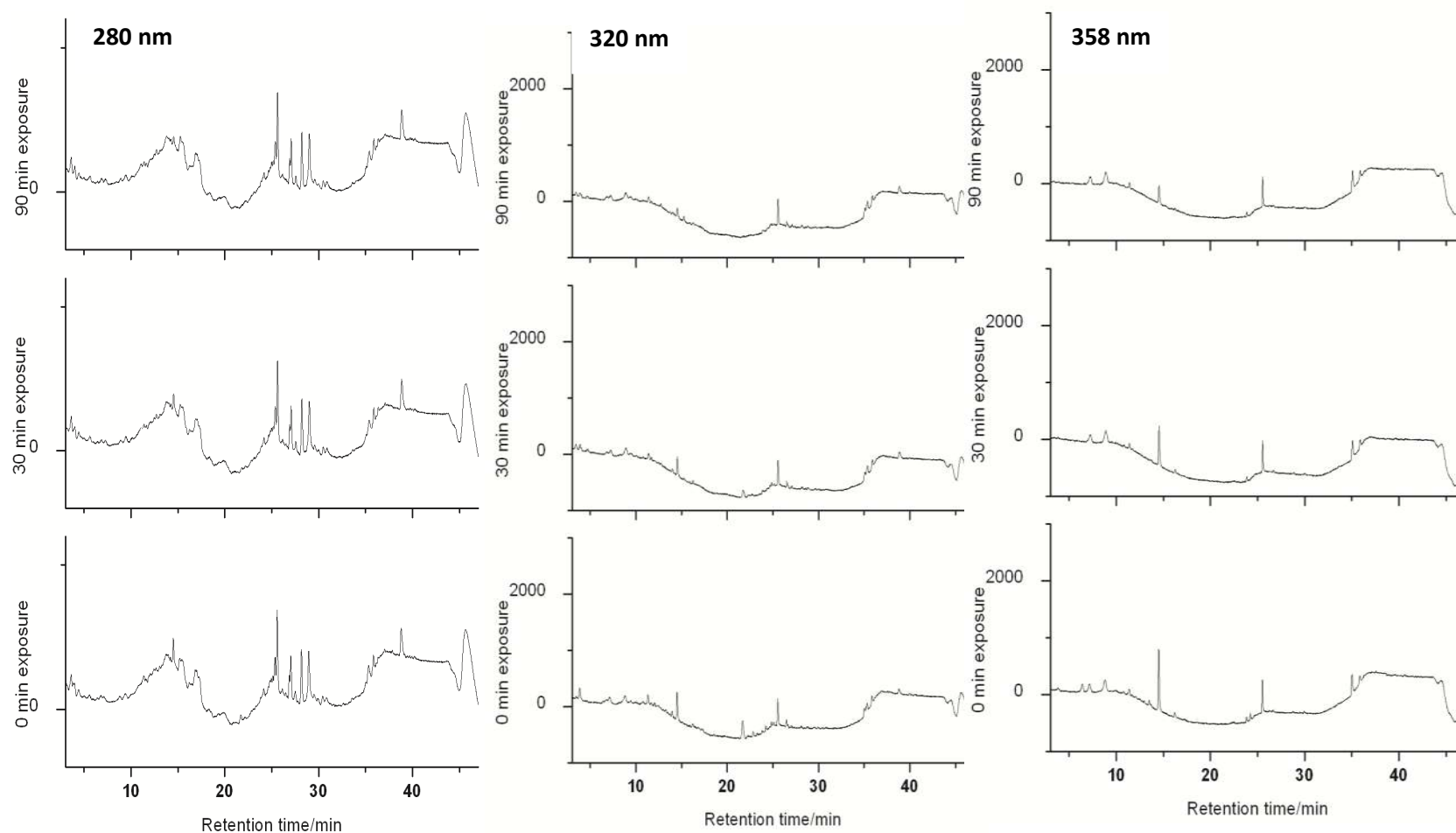
Figure 8.5: HPLC chromatograms recorded at 280 nm, 320 nm, and 358 nm of the photochemical changes undergone by mulberry extract dissolved in methanol when irradiated by simulated solar radiation. The separations were achieved on a reversed-phase Zorbax Eclipse XDB C-18 column (150 mm × 4.6 mm, i.d., 5 μm), under a gradient elution of acetonitrile-water at flow rate of 1 mL min^{-1} and an injection volume of 20 μL.

The observed relative photostability can be attributed to photo-induced electron modulation in the anthocyanins. The extra conjugation in the pyran ring (C-ring) (Fig. 8.4) and the cationic flavylium charge create an electron-hole effect aiding faster electron promotion and transfer on light absorption. The fast conversion of photon energy to kinetic energy of the electrons decreases the probability of molecular excitation and deactivates molecular excitation, blocking possible photolysis of this molecule. The heterocyclic pyran ring thus acts as an efficient energy transducer unit. Our claim is informed by the fact that the anthocyanins are known sources of electrons in dye-sensitized solar cells when they absorb appropriate photons of light. They are also known to readily protonate and deprotonate depending on the pH of the surroundings (Fig. 8.6). At a pH of 1-2 the anthocyanin exists in its cationic flavylium form whereas at a pH of 3-5 it deprotonates from the B-ring to form the quionoidal molecular form (Fig. 8.6). This event creates a *keto-enol* tautomerism phenomenon only possible upon absorption of a photon of light by electrons in this conjugated system. The absorption of photons of sufficient energy by an anthocyanin causes an excitation in the chromophore, which is the anthocyanidin part of the molecule. Generally, lower excitation energies contribute to excitations in the vibrational, rotational and conformational energies of anthocyanins. The rotational and vibrational transitions allow the continuous band spectrum of a molecule. Higher excitation energies from shorter wavelengths, for example UV light, contribute to excitations in the conjugated π-orbital systems where a π-orbital electron is excited to a π-antibonding orbital (π to π^*). In the cationic flavylium form, the aromatic B-ring is an isolated π-orbital system with 6 delocalized π-orbitals, whereas its nonaromatic quinonoidal counterpart has only 5 delocalized π-orbitals due to the *keto*-group at position 4' (Fig. 8.6). The absorbed photon needs to have sufficient frequency to excite the anthocyanin so that it has enough energy to release an electron. After a successful release the molecule drops back to ground state and in the case of cyanin the release occurs on the femtosecond timescale, which prevents any decomposition from occuring. This fast regeneration may sustain excitement and relaxation cycles without photodegradation of the molecule.
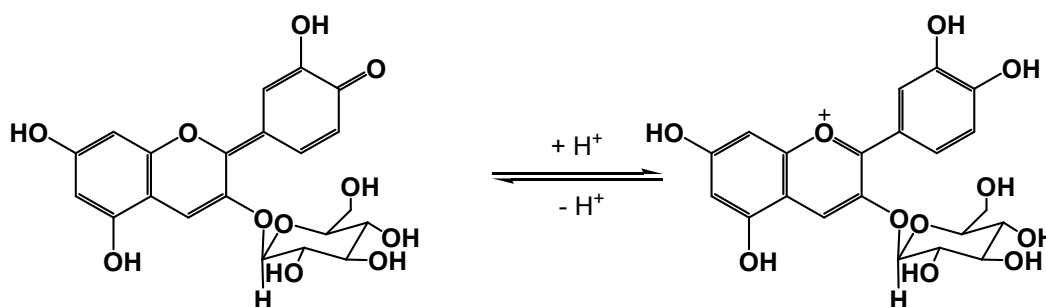
Figure 8.6: The *keto-enol* tautomers of cyanin, showing protonation and deprotonation reactions during photo-induced electron transfer.

The relative energy of an absorbed photon is related to the maximum absorbance value of the sample. Among the anthocyanins the different absorption maxima of these compounds can be accounted for from the increasing number of hydroxyl groups in the B-ring. This B-ring is known to mostly contain the LUMO electron density of the anthocyanin (Cherepy et al. 1997). The increasing number of hydroxyl groups in the B-ring decreases the HOMO-LUMO gap, allowing photons of smaller energy to be absorbed. This is due to a stronger electron affinity of the substituted oxygen compared to hydrogen relative to the sp^2 hybridized carbons (Est'evez and Mosquera 2009). Apart from changing the HOMO-LUMO gap, the hydroxyl auxochromes absorb photons with their non-bonding electrons (n, n*) thus contributing to lower absorption energies. The overall effect of the photo-induced electronic transitions and self-vibrational excited state deactivation is the relative low photolysis of

the molecule and longer wavelength light absorption efficacy. We therefore speculate that this extract could help in the photostabilization of sunscreen absorbers which breakdown upon UV absorption, for example BMDBM.

8.3.2 The effect of mulberry extract on the photostability of BMDBM

The GC/MS total ion chromatogram of an un-exposed derivatised mixture of the mulberry extract and BMDBM (Fig. 8.7) did not show any other new chemical species. The similarity of the total ion chromatograms of the mulberry extract alone and its mixture with BMDBM, save for the BMDBM peak in the latter, indicate that there are no dark reactions and heat does not induce chemical reactions between the mulberry extract and BMDBM. A methanol solution of BMDBM, a common UVA absorber incorporated in most skin-lightening and sunscreen products, was firstly subjected to photostability studies. The irradiation of a solution of BMDBM in methanol showed a gradual drop in UV absorption at 358 nm and an increase at 260 nm (Fig. 8.8). It is known that in solution BMDBM exhibits *keto-enol* tautomerisation (Fig. 8.9). The *enol* tautomer of BMDBM has a maximum absorption at 358 nm and the *keto* tautomer shows a maximum around 260 nm. We therefore assign the decrease in absorption at 358 nm as *enol* photodegradation and the observed growth at 260 nm as increase of the *keto* tautomer. However, the HPLC chromatogram of the same solution did not show any appreciable change in the BMDBM peak (Fig. 8.10). This apparent photostability could be due to the effect of the methanol solvent because BMDBM has been shown to be stable in polar protic solvents (Mturi and Martincigh 2008). The *keto-enol* tautomerization is accompanied by a loss in the photo-absorption efficacy of this sunscreening agent because the *keto* tautomer has maximum absorption at a much shorter wavelength, namely 260 nm. In nonpolar solvents BMDBM is known to photodegrade upon irradiation by way of radical formation which may completely destroy UV absorption potential (Roscher et al. 1994; Mturi and Martincigh 2008).

The photostability of BMDBM in the mulberry methanol extract was greatly improved. Though there was an initial drop in photo-absorption of about 0.2 absorption units thereafter no further significant drop was observed alone (Fig. 8.11) compared to the spectral decay observed when BMDBM is dissolved in methanol (Fig. 8.8). The major component of mulberry extract, anthocyanin, and BMDBM both can undergo light induced *keto-enol* tautomerism. However, the presence of a charge on the anthocyanin provides an added advantage as a major driving force for the electronic transitions and safe deactivation pathway. Considering the foregoing discussion, it is prudent to envisage that in a mixture of anthocyanin and BMDBM, a relationship of donor–acceptor is established, in which the *enol* form of BMDBM is favoured. We expect two tautomeric fast regenerative reactions: the *keto-enol* tautomers of BMDBM and *keto-enol* tautomers of anthocyanin to be synergistically sustained by light. The anthocyanin may act as a quencher thus denying BMDBM sufficient energy to initiate its own break-up via free radical generation. This system preserves the identity of BMDBM in the chelated *enol* form (Fig. 8.9) for a longer time hence no drop in absorption is observed. It is known that molecular reorganization of an organic quencher represents the activation of the vibrational modes of the reactants, which is insignificant for electron transfer into and out of the orbitals (Clark and Hoffman 1997). Such molecular transformations do not result in significant molecular structural changes and may not result in bond breakage or formation but isomerization is possible. Consequently the anthocyanin-BMDBM system may be said to be photostabilized via an electron donor-acceptor effect. The triplet excited state of *keto*-BMDBM may also be quenched by ground state oxygen via triplet-triplet energy transfer to form a ground state *keto*-BMDBM and singlet oxygen, ($^1O_2$) (Cantrell and McGarvey 2001; Mturi and Martincigh 2008). The singlet oxygen may oxidise enolate-BMDBM to BMDBM radical that can rapidly attract hydrogen from the solvent

(methanol) and anthocyanin in the medium since both are rich sources of hydrogen. This route could be favoured in this mixture further stabilizing the *enol*-BMDBM, thus demonstrating the observed photostability (Fig. 8.11). The total ion chromatogram of the mixture does not show any *keto* BMDBM (Fig. 8.7). However, the HPLC chromatogram of a solution of BMDBM alone before irradiation did show a peak with a UV spectrum that matches the UV spectrum of the *keto* form of BMDBM at 260 nm (Fig. 8.10).
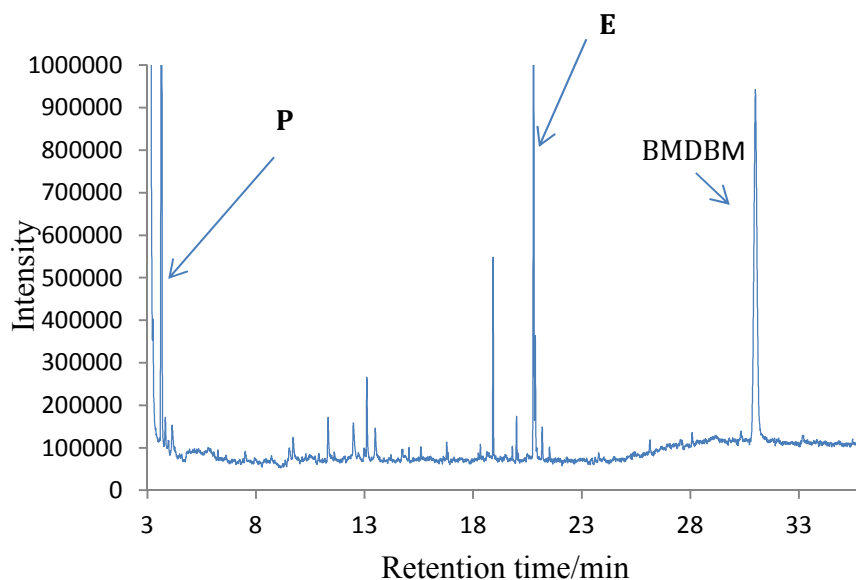
Figure 8.7 The GC/MS total ion chromatogram of a methanol solution of mulberry extract and BMDBM derivatised with BSTFA. The separation was effected on a GL Sciences InertCap 5MS/Sil 30 m × 0.25 quartz capillary column under the conditions described in Section 8.2.2.2.
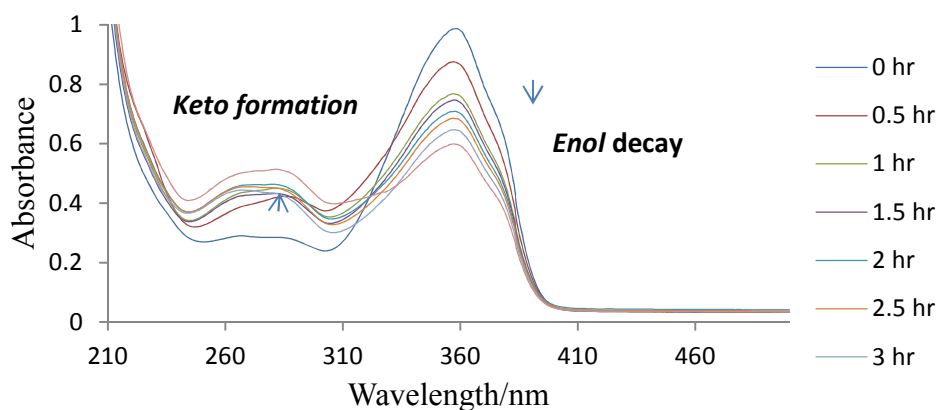
Figure 8.8: The spectral changes of BMDBM dissolved in methanol when irradiated with a solar simulated radiation. The spectra were acquired with a Perkin Elmer Lambda 35 UV-Vis spectrophotometer in a 1 mm pathlength quartz cuvette with air as the reference.

Figure 8.9: The *keto-enol* tautomerism of BMDBM.
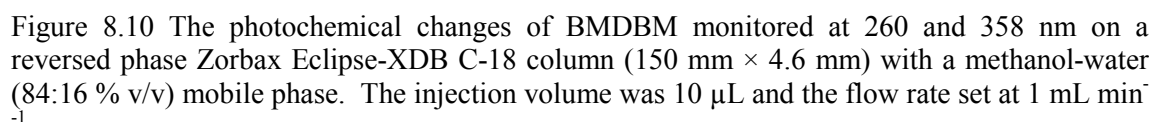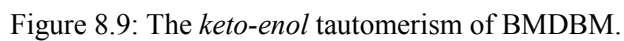
Figure 8.10 The photochemical changes of BMDBM monitored at 260 and 358 nm on a reversed phase Zorbax Eclipse-XDB C-18 column (150 mm × 4.6 mm) with a methanol-water (84:16 % v/v) mobile phase. The injection volume was 10 µL and the flow rate set at 1 mL min^{-1}.

The HPLC chromatograms of the irradiated mixture of mulberry extract and BMDBM show evidence of a photochemical reaction. The lack of detection the BMBDM peak; with a retention time of 34.954 min (Fig. 8.12), and the emergence of a new peak (retention time 25.542 min) **D** observable at all the three detection wavelengths on exposure for a period of 1.5 hours is proof that there are photo-induced reactions. The photochemical product **D** was characterised by UPLC-TOF-MS and gave a molecular mass of 310 (note that the peak for compound D in Figure 7.12 is the same peak in Figure 7.13 UPLC chromatogram and that there is a time delay between the mass spectrum detector and UPLC PDA detector and so the observed small differences in time of data acquisition). The molecular mass obtained and the corresponding UV spectrum (see Fig. 8.13) led us to speculate that the structure could closely resemble the BMDBM structure. Consequently, from the mass spectrum fragments we propose the structure of compound **D** as shown in Figure 8.14. This particular structure may afford the observed longer wavelength absorption exhibited due to the increase in double bond conjugation and the fact that the *cis*-diene structures favour longer wavelength absorption. More so, the structure retains the *enol*-BMDBM chromophore with a consequence of a possible bathochromic shift.

It is known that the n−π* triplet state behaves as a 1,2-biradical and in reactions with hydrocarbons or alcohols, the triplet excited ketones are considered to behave like radicals. It is commonly accepted that for hydrogen abstraction reactions, n−π* excitation is much more favourable than π−π* excitation. Consequently, because of the phenolic constituents of the composition, we propose a chelated *enol* chromophore of the BMDBM is retained, which shows maximum absorption at ~355 nm (Cantrell and McGarvey 2001) (Fig. 8.11 and 8.12) but with a new structural reorganization or conformation, thus, changing the retention time. It is therefore worthwhile to note that mulberry extract is a likely stabilizing candidate of for BMDBM. This composition may not need the addition of any other organic or inorganic sunscreen agents. The advantage, therefore, is the reduction in the number of active agents in a formulation and a significant reduction in the number of related side-effects.
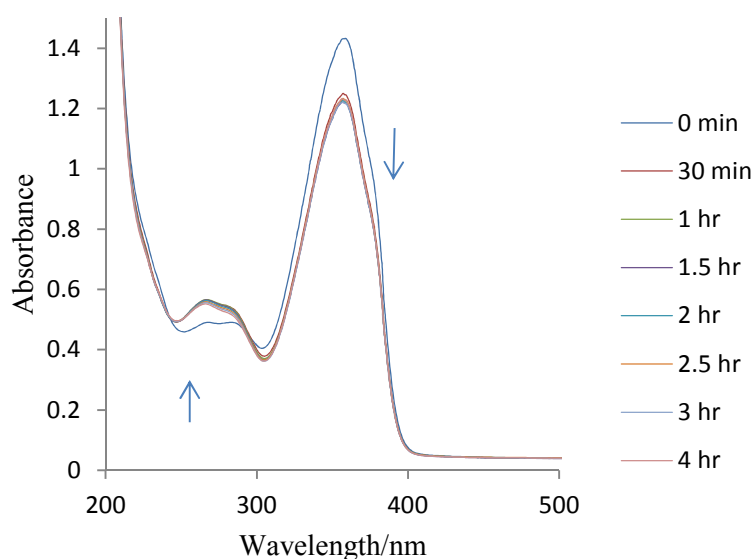
Figure 8.11: Photostability of BMDBM incorporated in mulberry extract dissolved in methanol when exposed to simulated solar radiation. The spectral changes were monitored on a Perkin Elmer Lambda 35 spectrophotometer in a 1 mm pathlength quartz cuvette.
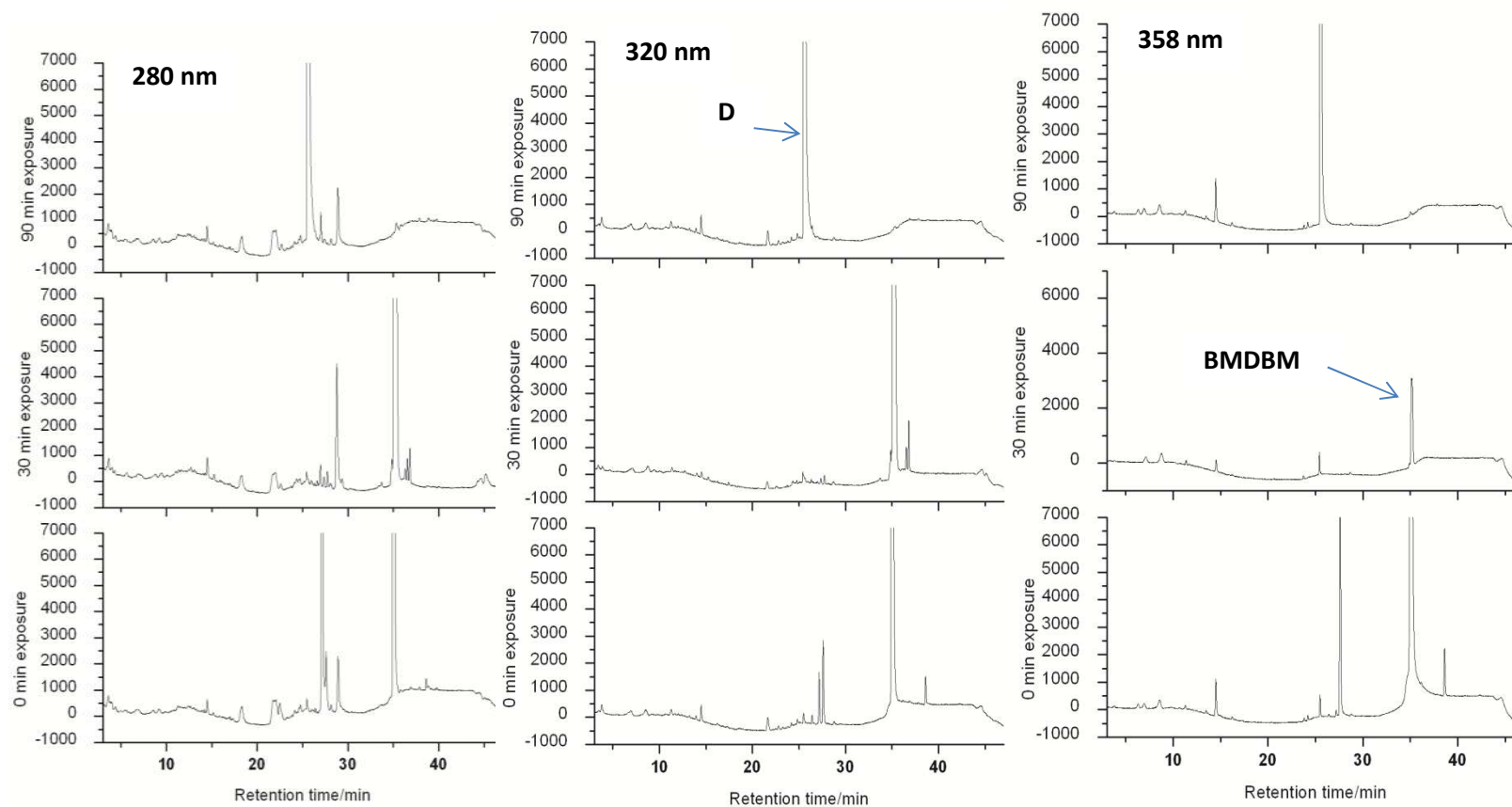
Figure 12: HPLC chromatograms acquired at 280 nm, 320 nm, and 358 nm of the photochemical changes observed when BMDBM is incorporated in mulberry extracts dissolved in methanol and irradiated by simulated solar radiation. The separation effected on a reverse phase Zorbax Eclipse XDB C-18 (150 mm × 4.6 mm, i.d., 5 μm) under a gradient elution of acetonitrile-water at a flow rate of 1 mL min⁻¹ and an injection volume of 20 μL.
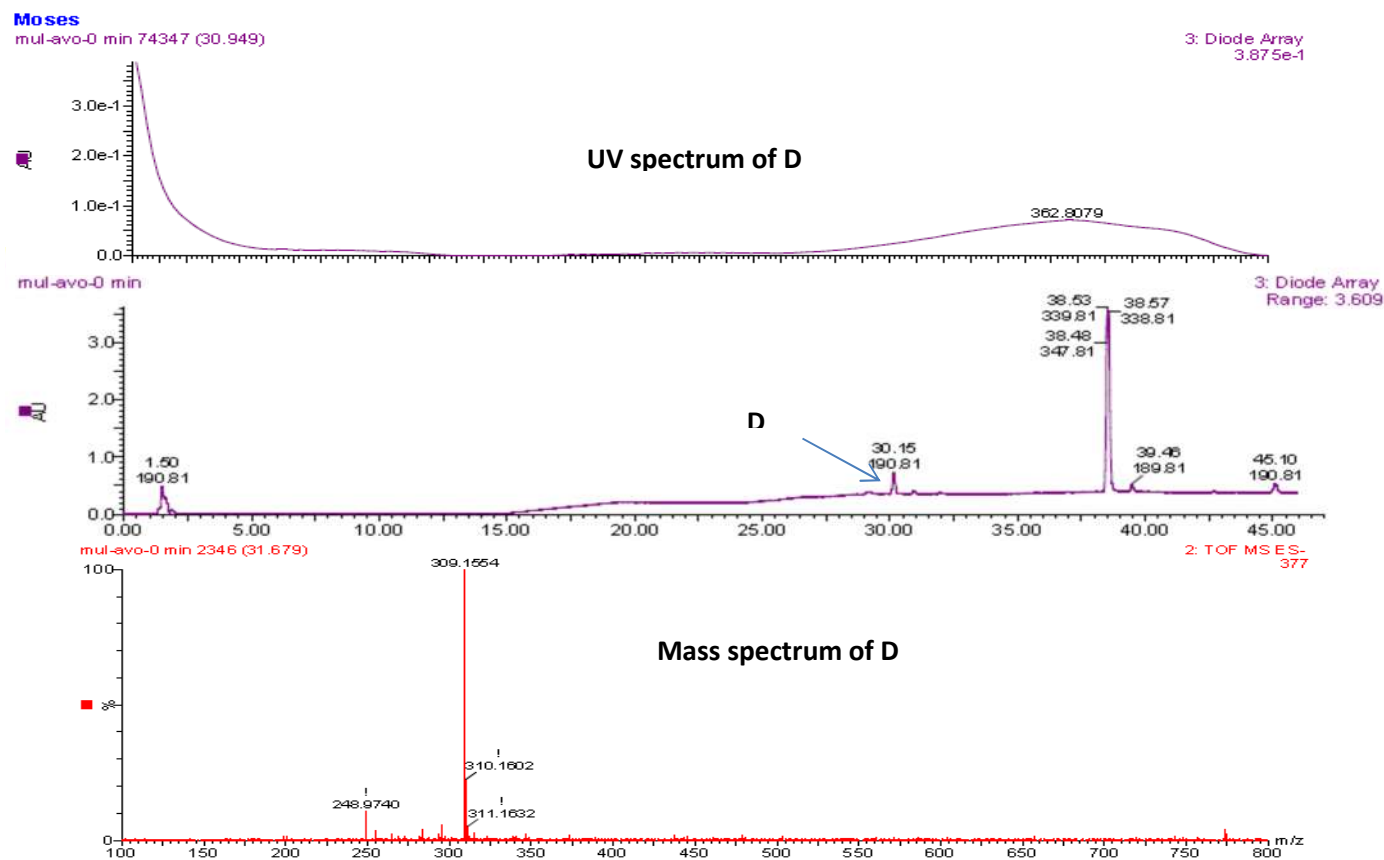
Figure 8.13: The UV spectrum, UPLC chromatogram and mass spectrum of compound **D.** The data was acquired on a Waters Acquity UPLC connected to a Waters Micromass LCT Premier TOF-MS in negative ionisation mode. Characterisation effected using a reversed phase C-12 column (Phenemonex Synergi 4μ Max-RP 80 Å, 150 mm × 4.6 mm) was used with a gradient elution of acetonitrile-water. The injection volume was 7 μL and flow rate set at 1 mL min^{-1}, The detection wavelength was 358 nm.
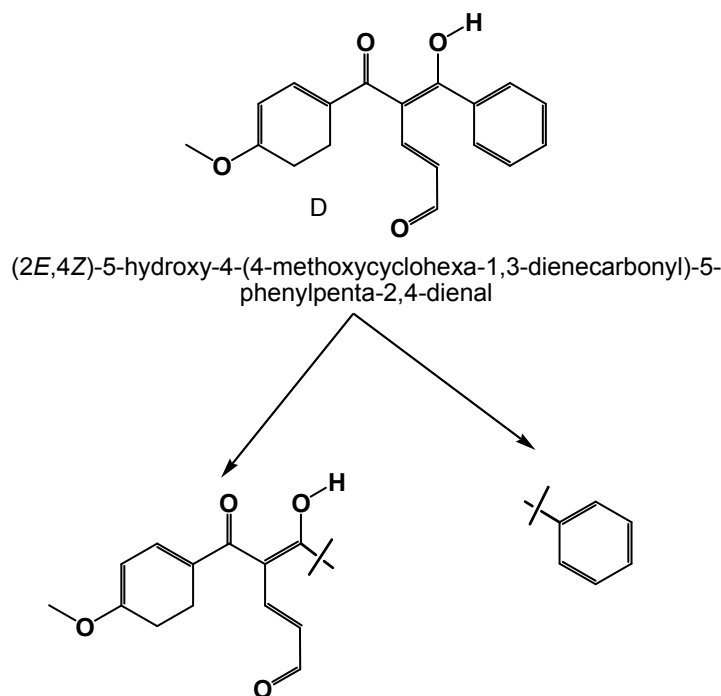
Figure 8.14: The proposed structure of compound **D** and possible fragmentation products that gives the observed mass spectrum

8.3.3 The effect of mulberry extract on the photostability of BP3

The GC/MS total ion chromatogram of the derivatised mixture containing mulberry extract and BP3 showed a BP3 peak, with a library match of 95 % at a retention time of 19.745 min (Fig. 8.15). This indicates that there was no thermally-initiated reaction during the derivatization procedure. The photostability study of a BP3 solution in methanol alone showed a marked expected photostability (Fig 8.16). The HPLC analysis of the solution of irradiated BP3 in methanol also did not show any other peak indicating no photodegradation of BP3 under these exposure conditions (Fig. 8.17). The UV spectra of the mixture of the mulberry extract with BP3 remained unchanged only showing a very slight hypsochromic shift (Fig. 8.18). A comparison with the spectra of BP3 in methanol (Fig. 8.16) shows close similarity in all respects. An inspection of the HPLC chromatograms of the time-dependent irradiance experiment with the solar simulated source, shows no apparent chemical transformation of BP3 (Fig. 8.19). It is reported by several working groups that after absorbing a photon, triplet BP3 is formed in a very efficient intersystem crossing (ISC) process with a quantum yield of one. This triplet may disappear in energy dissipative processes including: the first-order phosphorescence and ISC, as well as the second-order triplet−triplet annihilation reaction (Demeter et al. 2013). The overall effect is the preservation of the BP3 chemical identity.

In the presence of mulberry extract, we propose a new deactivation pathway for BP3. We suspect that the triplet excited state energy of BP3 is higher than the electron excitation in the anthocyanins. Consequently, BP3 loses the excitation energy quickly to the excited anthocyanin which drops to ground state via a vibrational deactivation pathway. Hence, because of the high phenolic concentration in the mulberry extract and the fact that the solvent used is methanol (an alcohol) (all are possible hydrogen donors), the chances of hydrogen-bond complexation known to induce a blue shift for carbonyl chromophores are curtailed. The presence of a large quantity of hydrogen-bond donor phenolic reactants may help to confer further photostabilisation. Multiple complex formation equilibria may be established that mask the activation energy of the actual hydrogen atom transfer

step in a bid to photo-reduce the BP3. This extract therefore enhances the photostability of BP3 greatly and in turn preserves the chemical composition of the mulberry extract as shown by the HPLC data (see Supplementary Materials Table S8.4) and HPLC chromatograms (Fig. 8.19). We envisage the same preservative effect may be replicated in sunscreen preparations incorporating other cosmetic agents like antioxidants that decompose in light.
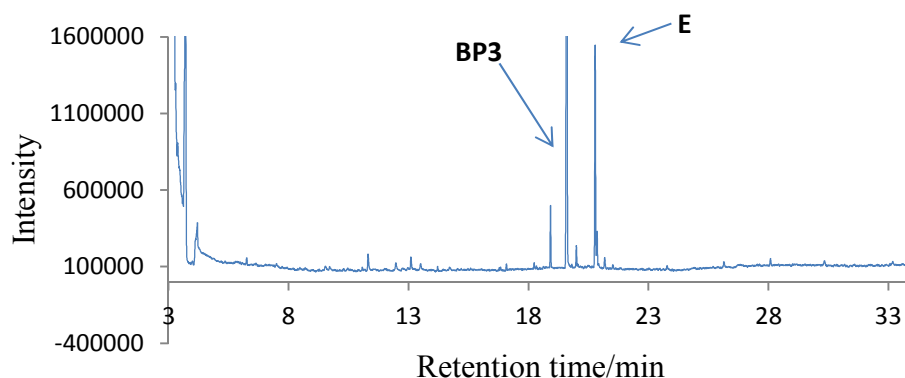
Figure 8.15 The GC/MS total ion chromatogram of a methanolic solution of silylated mulberry extract mixed with BP3. The separation was effected on a GL Sciences InertCap 5MS/Sil 30 m × 0.25 quartz capillary column under the conditions described in Section 8.2.2.2.
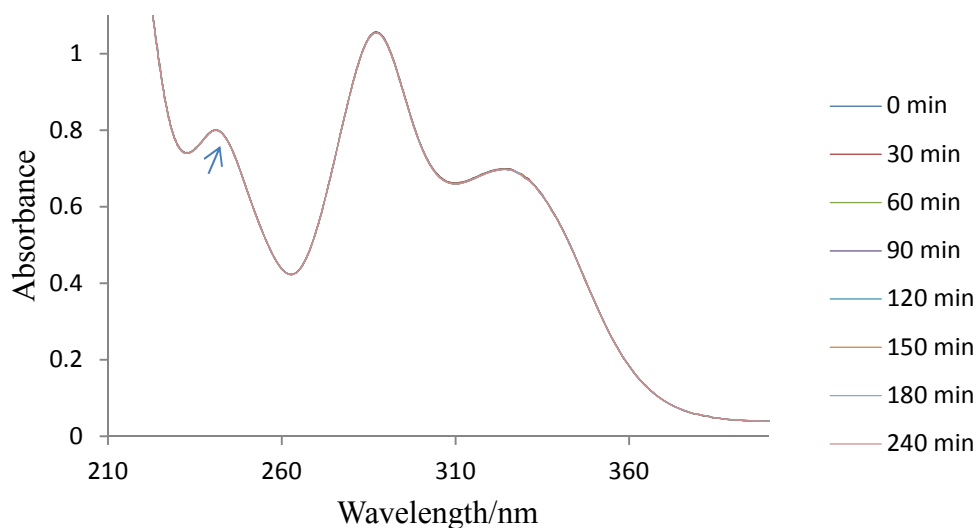
Figure 8.16: The spectral stability of BP3 in methanol irradiated by a solar simulated source. The spectra were acquired with a Perkin Elmer Lambda 35 UV-Vis dual beam spectrophotometer in a 1 mm pathlength quartz cuvette with air as the reference.
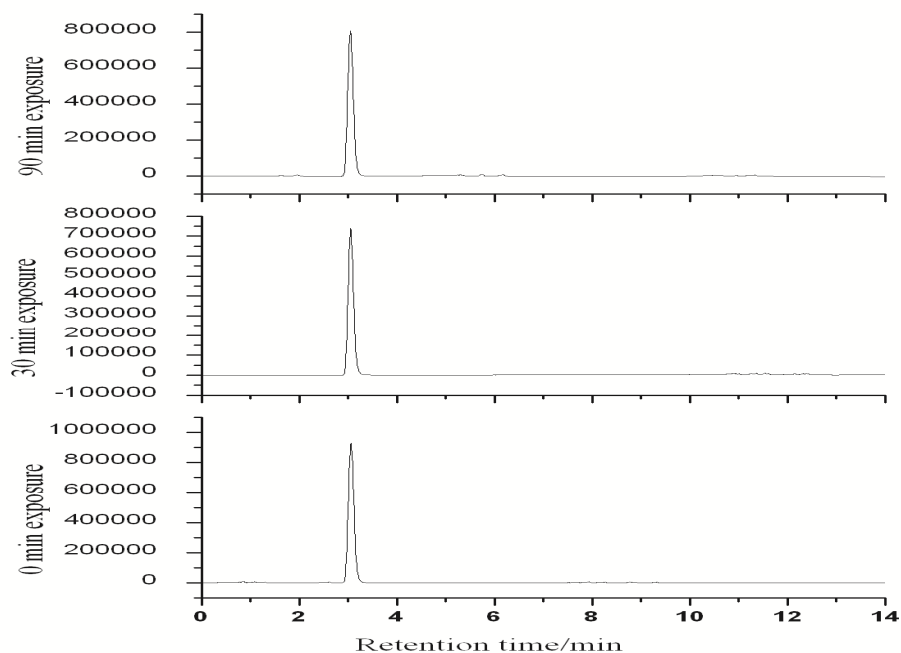
Figure 8.17: The photostability of BP3 monitored by HPLC at 286 nm. A reversed phase Zorbax Eclipse-XDB C-18 column (150 mm × 4.6 mm) was used with a mobile phase of methanol-water (84:16 % v/v). The injection volume was 10 µL and the flow rate set at 1 mL min^{-1}.
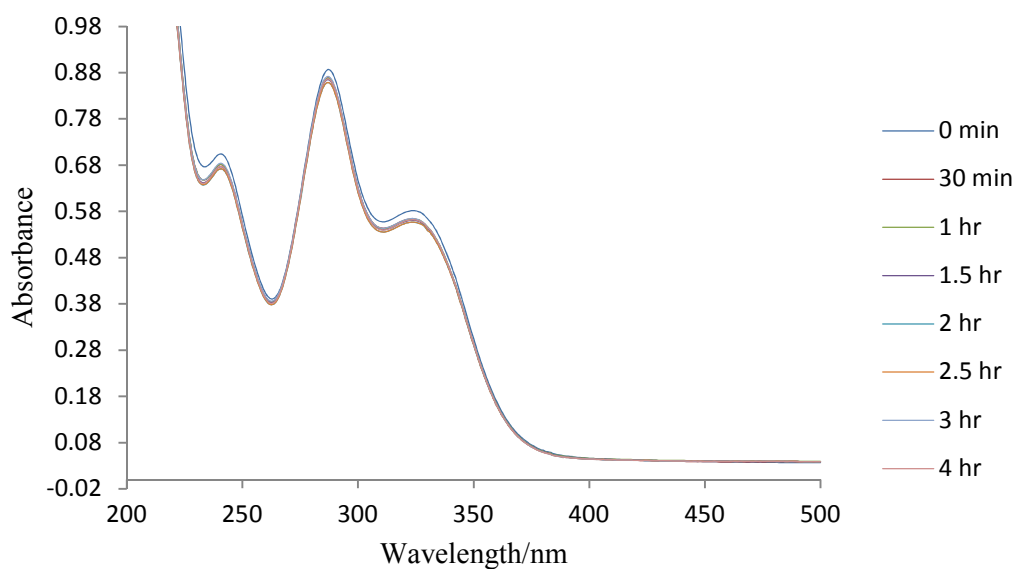
Figure 8.18: Photostability of BP3 incorporated in mulberry extract dissolved in methanol when exposed to simulated solar radiation. The spectral changes were monitored on a Perkin Elmer Lambda 35 UV-vis dual beam spectrophotometer, in a 1 mm pathlength quartz cuvette.
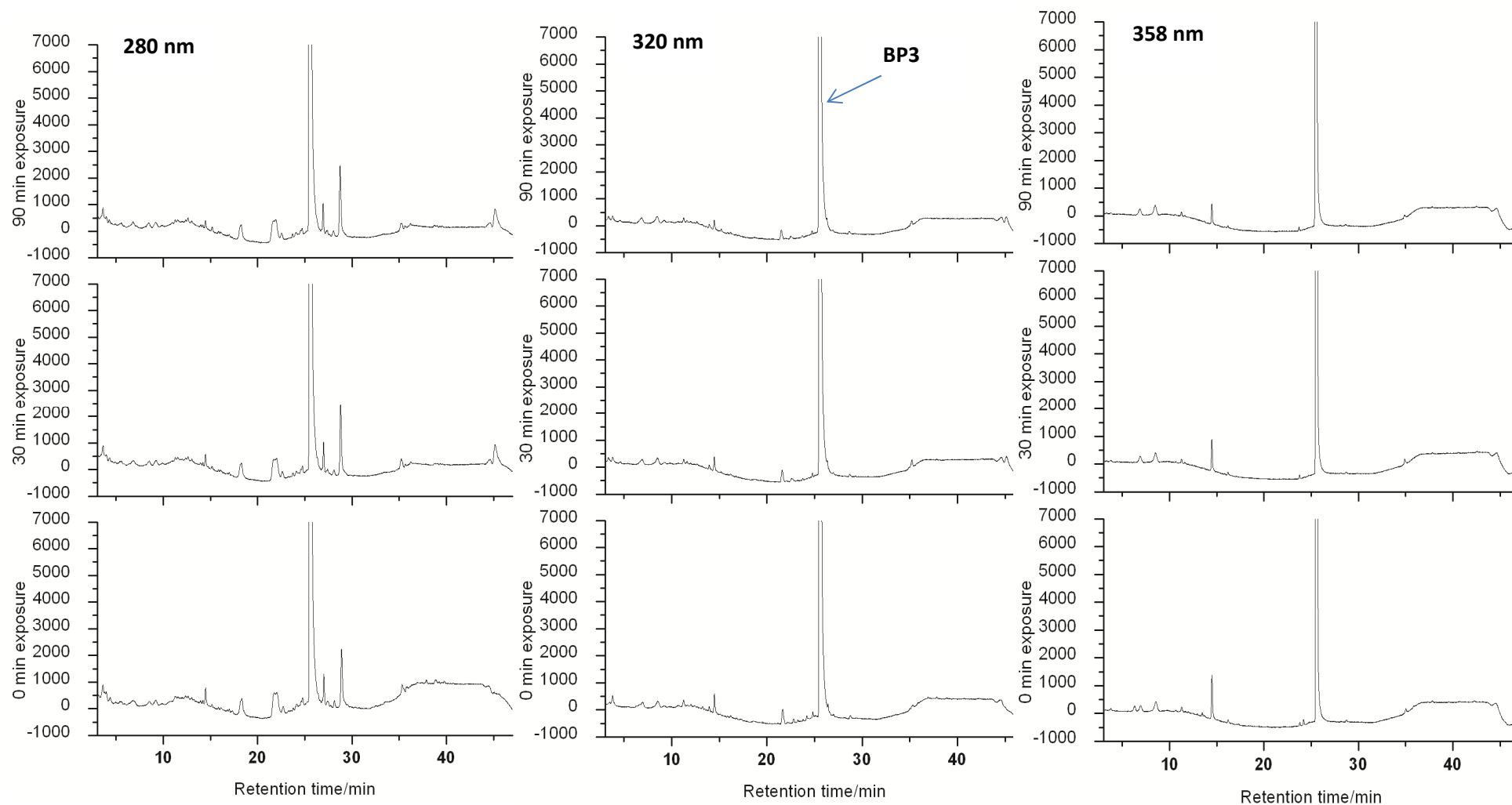
Figure 8.19: HPLC chromatograms acquired at 280 nm, 320 nm and 358 nm of the photochemical changes when BP3 is incorporated in mulberry extract dissolved in methanol and irradiated by simulated solar radiation. The separation was effected on a reversed-phase Zorbax Eclipse XDB C-18 column (150 mm x 4.6 mm, i.d., 5 µm), under a gradient elution of acetonitrile-water at flow rate of 1 mL min^{-1} and an injection volume of 20 µL.

8.3.4 The effect of mulberry extract on the photostability of EHMC

The behaviour of a methanolic solution of EHMC under simulated solar irradiation indicated spectral lability characteristic to the photo-loss by isomerisation of *trans*-EHMC to *cis*-EHMC (Fig. 8.20, 8.21 and 8.22). The HPLC chromatogram of this solution showed the formation of the *cis*-isomer (Fig. 8.21) in the first 30 min of exposure. The peak area of the *trans*- and *cis*-EHMC do not show much difference even after 90 min of exposure indicating an attainment of a photostationary state (Fig. 8.21). When this isomerisation is monitored at 260 nm, the *cis*-EHMC peak was found to be much bigger than *trans*-EHMC peak since the former absorbs more strongly at this wavelength. This shows that the photostationary state is populated by the *cis*-isomer. This in turn is taken as photo-loss because absorption of UVB (290-320 nm) radiation is compromised. The photostability of EHMC was similarly examined in the mulberry extract firstly by investigating possible ground state reactions between EHMC and the mulberry extract. The mixture was derivatised with BSTFA and subjected to GC/MS analysis. The total ion chromatogram remained essentially the same as the original mulberry extract total ion chromatogram (Fig. 8.23). This indicates that thermal reactions involving EHMC, other than derivatisation, did not occur. This was confirmed by the RP-HPLC experiment of the unexposed samples whose result was identical to the chromatogram of the mulberry extract alone (Fig. 8.25). The interpretation then is that the mulberry extract does not react with EHMC in the ground state. Exposure of this mixture to solar simulated radiation for thirty minutes resulted in a 0.3 drop in absorbance units (Fig. 8.24). This drop could be attributed to cinnamic bond decay via *trans-cis* isomerisation. However, the characteristic cinnamic decay observed for an EHMC methanolic solution (Fig. 8.20) is not replicated. For the replication of this decay, the rotation of a C atom around the C=C bond to result in *trans–cis* isomerisation is required. However, this rotation around the π--C=C bond is symmetry forbidden. Therefore isomerization is proposed to occur through a biradical intermediate state in which the π--C-C bond is cleaved (Fig. 8.22). This cleavage requires high energy and therefore it is probably from the singlet state because of the high energy consumed.

Its speculated that in olefins the *trans–cis*-isomerisation occurs with high activation of the singlet excited state. Normally the excited singlet state is stabilized by splitting of the two lowest $\pi\pi^*$ states resulting in large activation barrier for non-radiative decay. This stabilization has been shown to be largest for *meta*, intermediate for *ortho* and smallest for *para*-substituted cinnamates. However, lifetimes for cinnamates are too short to sensitize any oxygen species or form undesired chemical reactions (Karpkird et al. 2009). As seen above the anthocyanins are good activated electron sources necessary for hydrogenation of the cinnamic moiety. But this does not seem to occur because the overall protonation of the methoxy cinnamate radical by phenolics requires two electrons per molecule to be consumed to produce the hydrogenated product (Parker 1981). Hence, we propose that the EHMC *trans-cis*-isomerization favours the *trans*-isomer on prolonged exposure (Fig. 8.24). This, therefore, generates the perceived stable absorption characteristics observed in this work.
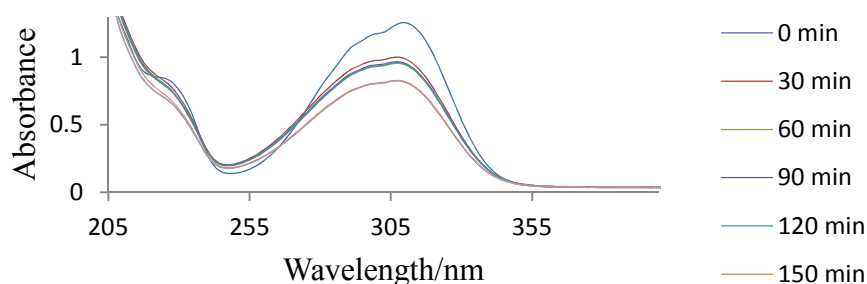
Figure 8.20: Photoinstability of EHMC dissolved in methanol under solar simulated irradiation. The spectra were acquired with a Perkin Elmer Lambda 35 UV-VIS spectrophotometer in a 1 mm pathlength quartz cuvette with air as the reference.
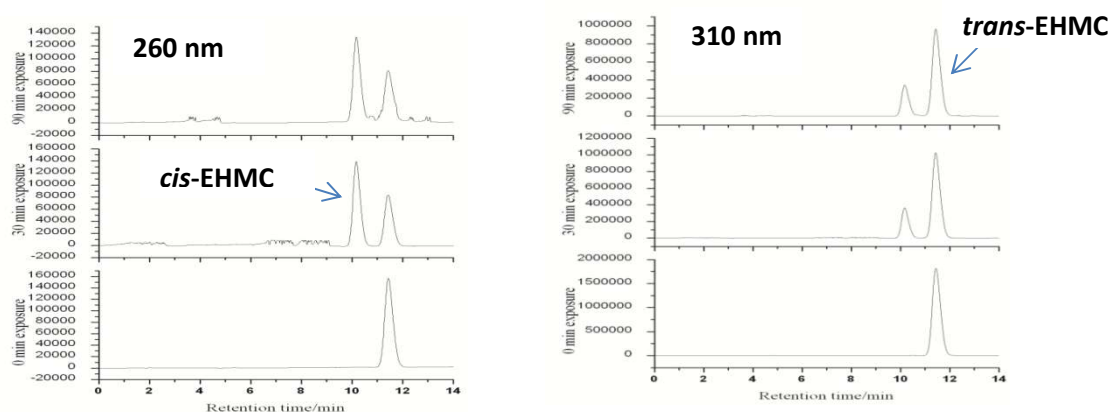
Figure 8.21: Isomerisation of EHMC under simulated solar irradiation monitored by HPLC at 260 and 310 nm on a reversed phase Zorbax Eclipse-XDB C-18 column (150 mm × 4.6 mm) with a methanol-water (84:16 % v/v) mobile phase. The injection volume was 10 µL and the flow rate set at 1 mL min^{-1}.
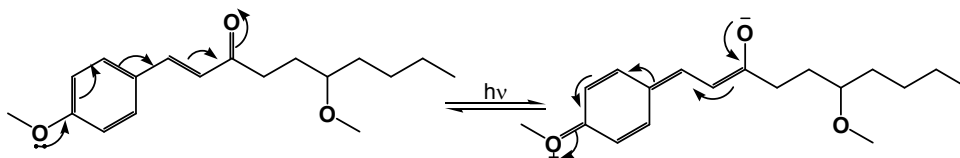
Figure 8.22: Proposed electron movement during photo-induced biradical C=C bond cleavage of EHMC to effect *trans – cis*-isomerisation.
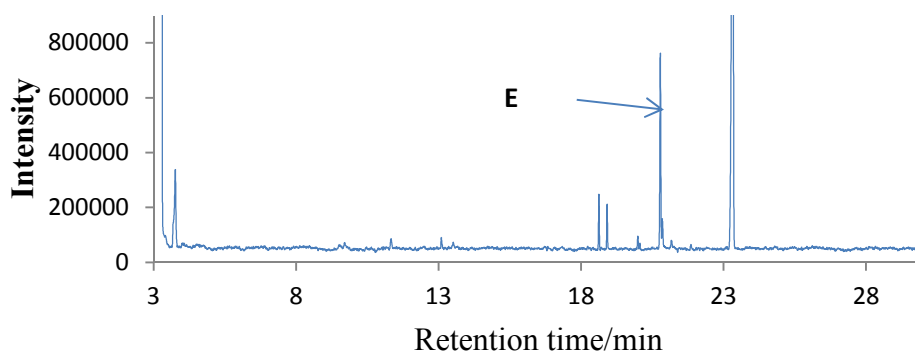
Figure 8.23: The GC/MS total ion chromatogram of methanolic solution of silylated mulberry extract mixed with EHMC. The separation was effected on a GL Sciences InertCap 5MS/Sil 30 m × 0.25 quartz capillary column under the condition described in section 8.2.2.2.
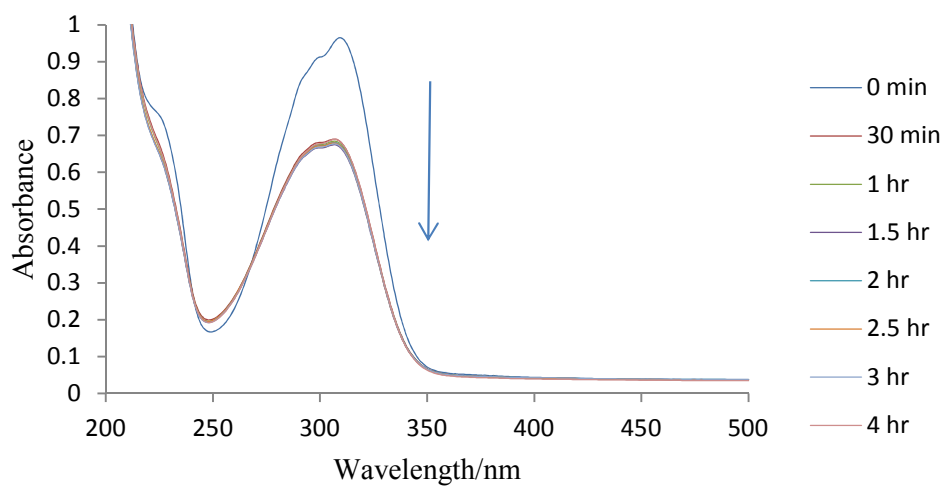
Figure 8.24: Photostability of EHMC incorporated in mulberry extract dissolved in methanol when exposed to simulated solar radiation. The spectral changes were monitored with a Perkin Elmer Lambda 35 spectrophotometer, in a 1 mm pathlength quartz cuvette.
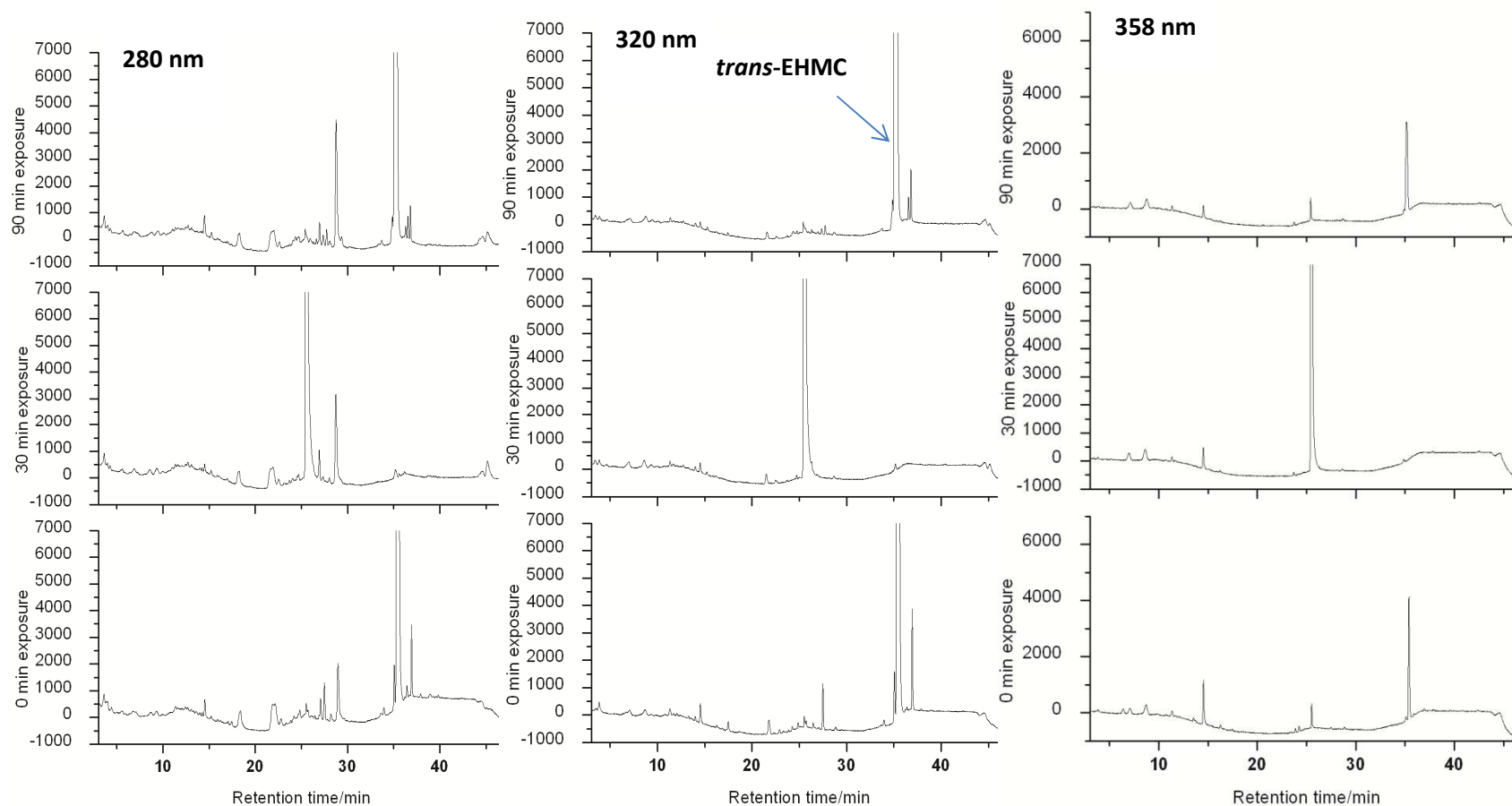
Figure 8.25: Chromatograms recorded at 280 nm, 320 nm, and 358 nm of the photochemical changes when EHMC is incorporated in the mulberry extract dissolved in methanol and irradiated by simulated solar radiation. The separation were effected on a reversed-phase Zorbax Eclipse XDB C-18 column (150 mm × 4.6 mm, i.d., 5 μm), under a gradient elution of acetonitrile-water at a flow rate of 1 mL min^{-1} and an injection volume of 20 μL.

8.3.5   **The effect of mulberry extract on the photostability of a mixture of BMDBM, BP3 and EHMC**

A mixture of the three commonly used sunscreen absorbers with mulberry extract was derivatised and subjected to GC/MS analysis. The total ion chromatogram (Fig. 8.26) of the unexposed sample indicated peaks for all the sunscreens incorporated, eliminating the possibility of any reaction between the sunscreens and mulberry extract that could be thermally-driven during the derivatisation process. The observed smaller molecular weight products obtained by GC/MS can be attributed solely to the derivatisation process (Fig. 8.27). This is because the same procedures were adopted when the sunscreens were incorporated and derivatised singly.

A mixture of the three sunscreen absorbers was prepared and subjected to photostability studies. Spectral lability was observed (Fig. 8.28), with an accompanying blue shift. The exposure of the samples to simulated solar radiation saw a drop in the absorption of the mixture of approximately 0.25 absorbance units in the first thirty minutes (Fig. 8.28). HPLC analysis of these solutions over the 90 min irradiation period shows the isomerisation of EHMC and the steady formation of *cis*-EHMC which explains the photo-loss (Fig. 8.29). In this mixture photostationary state observed earlier between *cis*- and *trans*-EHMC appears seem not to be attained. This could be attributed to enhanced photosentization reaction due to the presence of BMDBM (Paris et al. 2009; Kumasaka et al. 2014). A mixture of the three sunscreens with mulberry extract dissolved in methanol and similarly irradiated demonstrated a unique photostability (Fig. 8.30). The spectral change was confirmed by the lack of detection of BP3 and the reduction of BDBDM. A shift in the retention time of the EHMC peak also observed (Fig. 8.31). These occurred on irradiation by the solar simulated source. It can be safely argued that all the sunscreens underwent photochemical reaction or transformation in the first thirty minutes of exposure (Fig. 8.30). The most significant observation is the disappearance of chemical species absorbing at 358 nm as has been observed when the BDBDM and BP3 were incorporated singly into the mulberry extract (Fig. 8.12, and Fig. 8.19).

From the Frank-Condon principle the position of the 0−0 transition is the measure of the energy of the singlet excited state at the ground state geometry. It has been reported that both the structural and solvent relaxations are expected to be small for the excited benzophenone derivatives and this energy decreases with the increase of the electron withdrawing ability of the substituent on the phenyl group (Kumasaka et al. 2014). Recently, Demeter et al. (2013) have shown that the substitution on the aromatic rings induces a remarkable change in the reactivity of triplet benzophenone towards alcohols which is the primary photoreduction step of the carbonyl chromophore. It is also known that aromatic ketones can form hydrogen-bonded complexes with alcohols, the proton acceptor being the C=O group, which is also the chromophore. Hence, the blue shift observed in the absorption spectrum of the $n\pi^*$ excitation of a carbonyl molecule is due to the reduction of the electron density on the oxygen atom with excitation. This solution is highly polar and therefore it is expected that for an $n\pi^*$ transition, the energy of the first singlet state increases while the energy of the higher $\pi\pi^*$ states, corresponding to symmetry allowed transitions, decreases (Demeter et al. 2013). The resultant effect is the concerted photoreactions culminating in the reduction of the BP3 chromophore, decay of the cinnamate, and breakup of the dibenzoylmethane derivative. The GC/MS results revealed a sizeable composition of aliphatic alcohols in the mulberry extract. Since aromatic ketones undergo hydrogen bonded complex formation in the presence of aliphatic alcohols, it explains why this mixture has a significant blue shift and is thus only suitable as a UVB photoprotector.
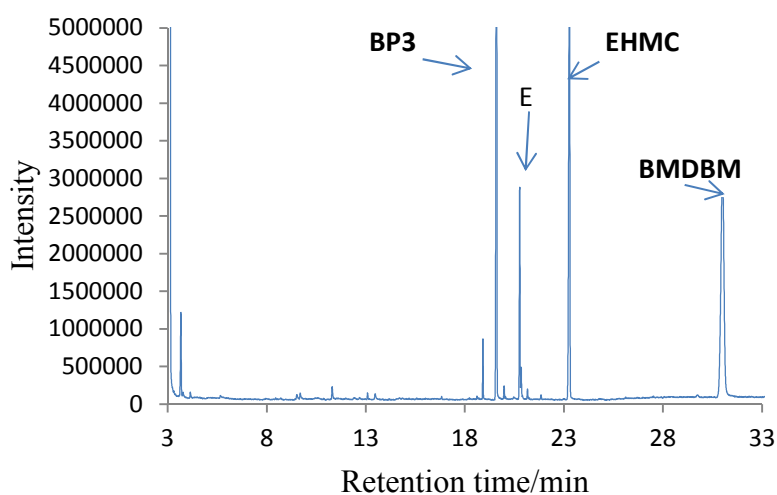
Figure 8.26: The GC/MS total ion chromatogram of a methanolic silylated solution of mulberry extract mixed with BMDBM, BP and EHMC. The separation was effected on a GL Sciences InertCap 5MS/Sil 30 m × 0.25 quartz capillary column under the conditions described in Section 8.2.2.2.
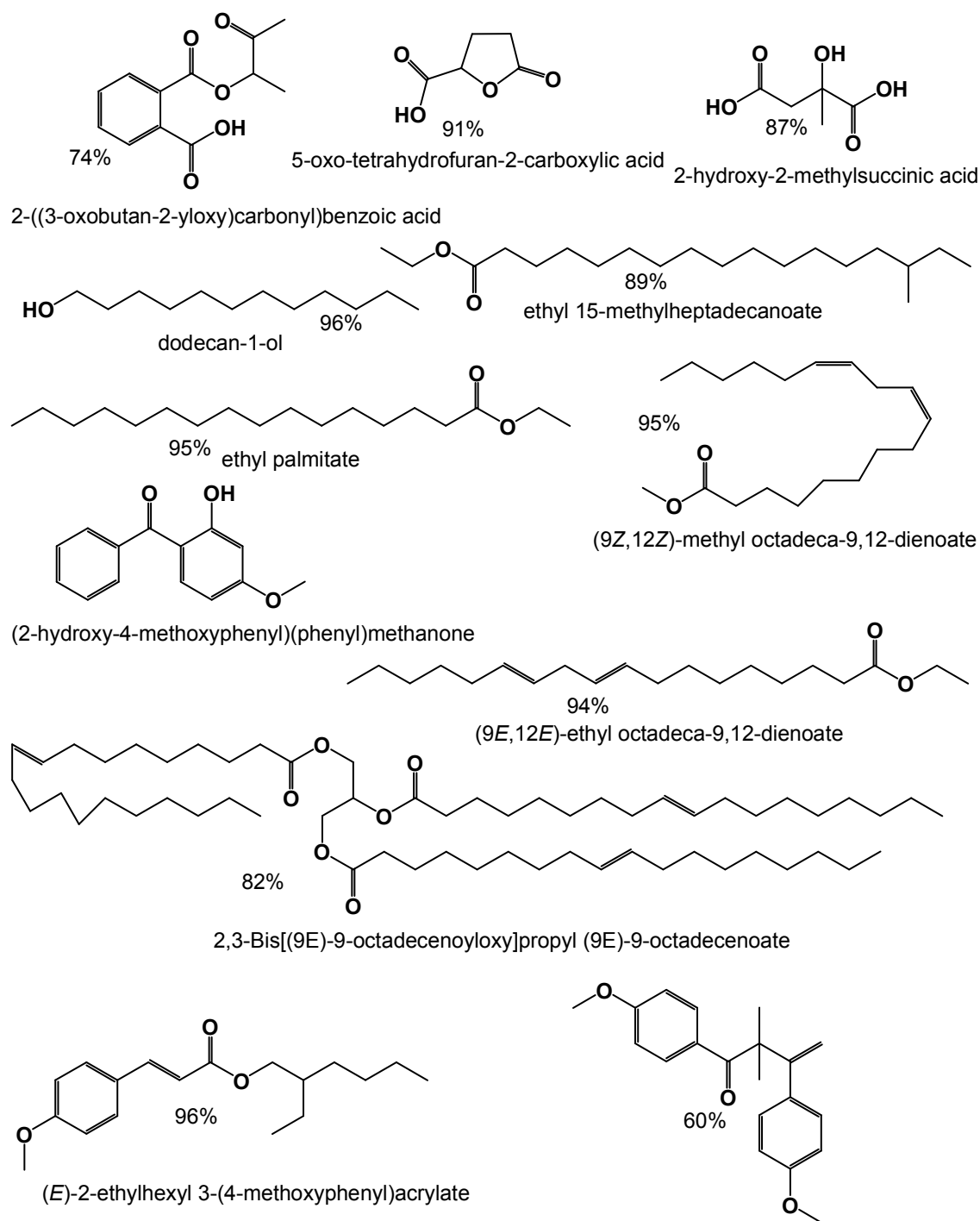
Figure 8.27: Compounds identified by GC/MS when all the sunscreens were mixed with silylated mulberry extract prior to exposure to UV radiation.
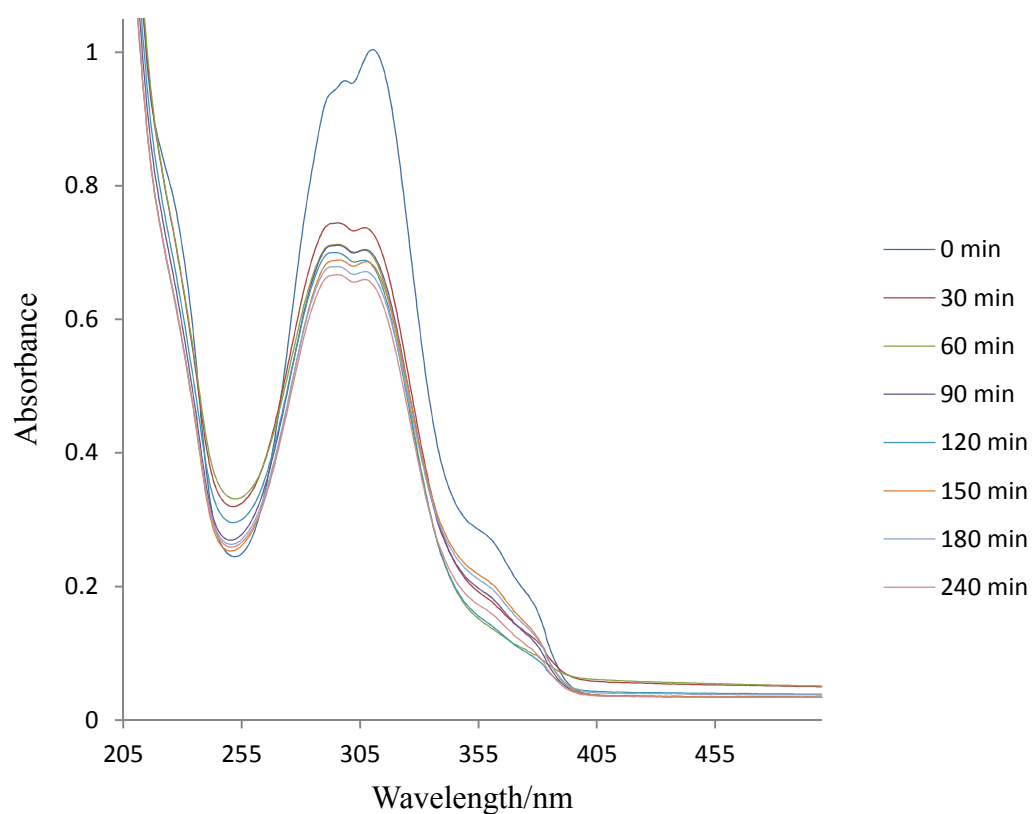
Figure 8.28: The photostability of a methanolic solution containing the sunscreen absorbers: BDBDM, BP3 and EHMC under solar simulated irradiation. The spectral changes were monitored with a Perkin Elmer Lambda 35 UV-vis dual beam spectrophotometer, in a 1 mm pathlength quartz cuvette.
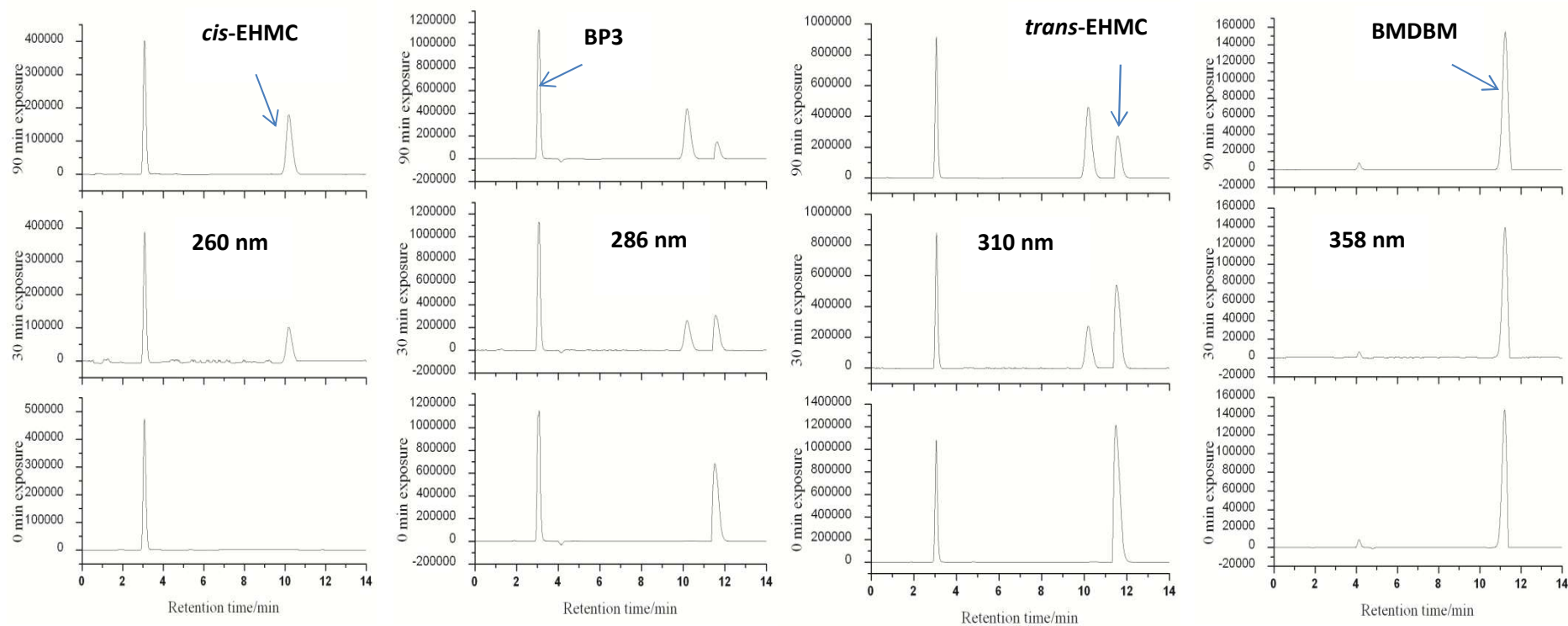
Figure 8.29: The photochemical transformations of a mixture of BMDBM, BP3, and EHMC dissolved in methanol monitored by HPLC at 260, 286, 310, and 358 nm the separation was effected on a Zorbax Eclipse-XDB C-18 column. The mobile phase was a gradient elution of acetonitrile-water with a flow rate of 1.00 mL min^{-1} and an injection volume of 20 μL.
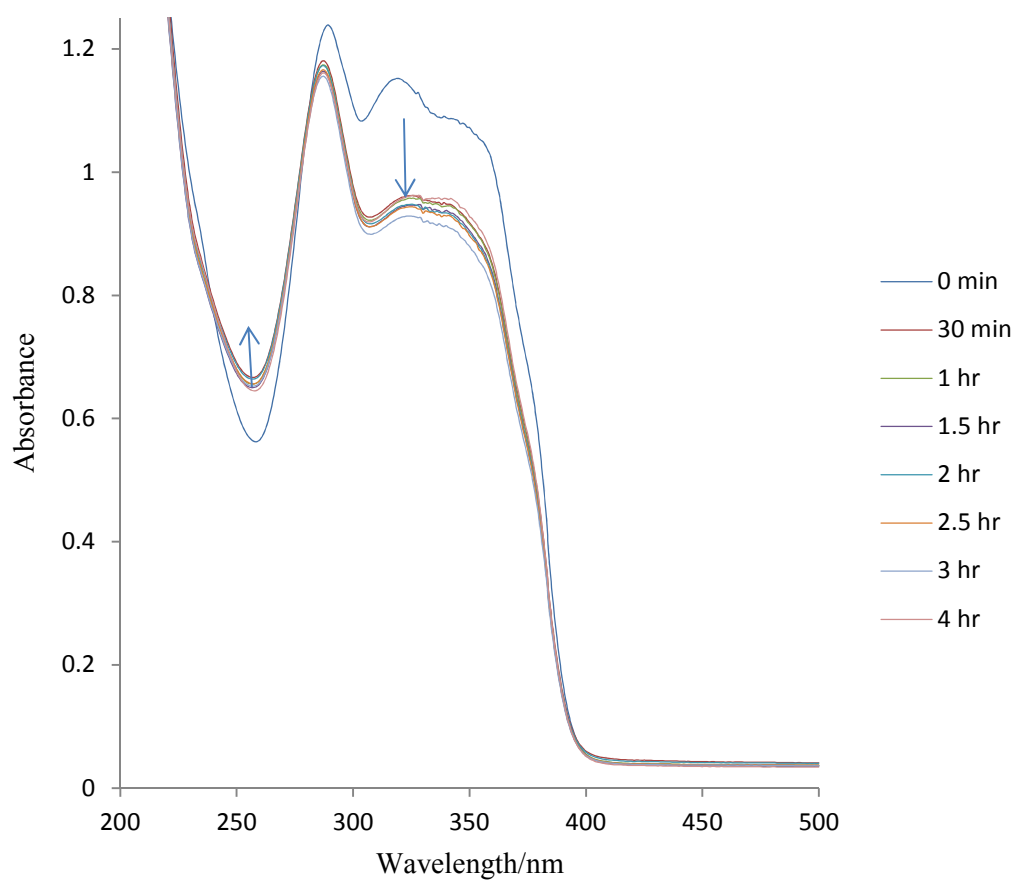
Figure 8.30: Photostability of BDBDM, BP3 and EHMC incorporated in mulberry extract dissolved in methanol when exposed to simulated solar radiation. The spectral changes were monitored on a Perkin Elmer Lambda 35 dual beam spectrophotometer, in a 1 mm pathlength quartz cuvette.
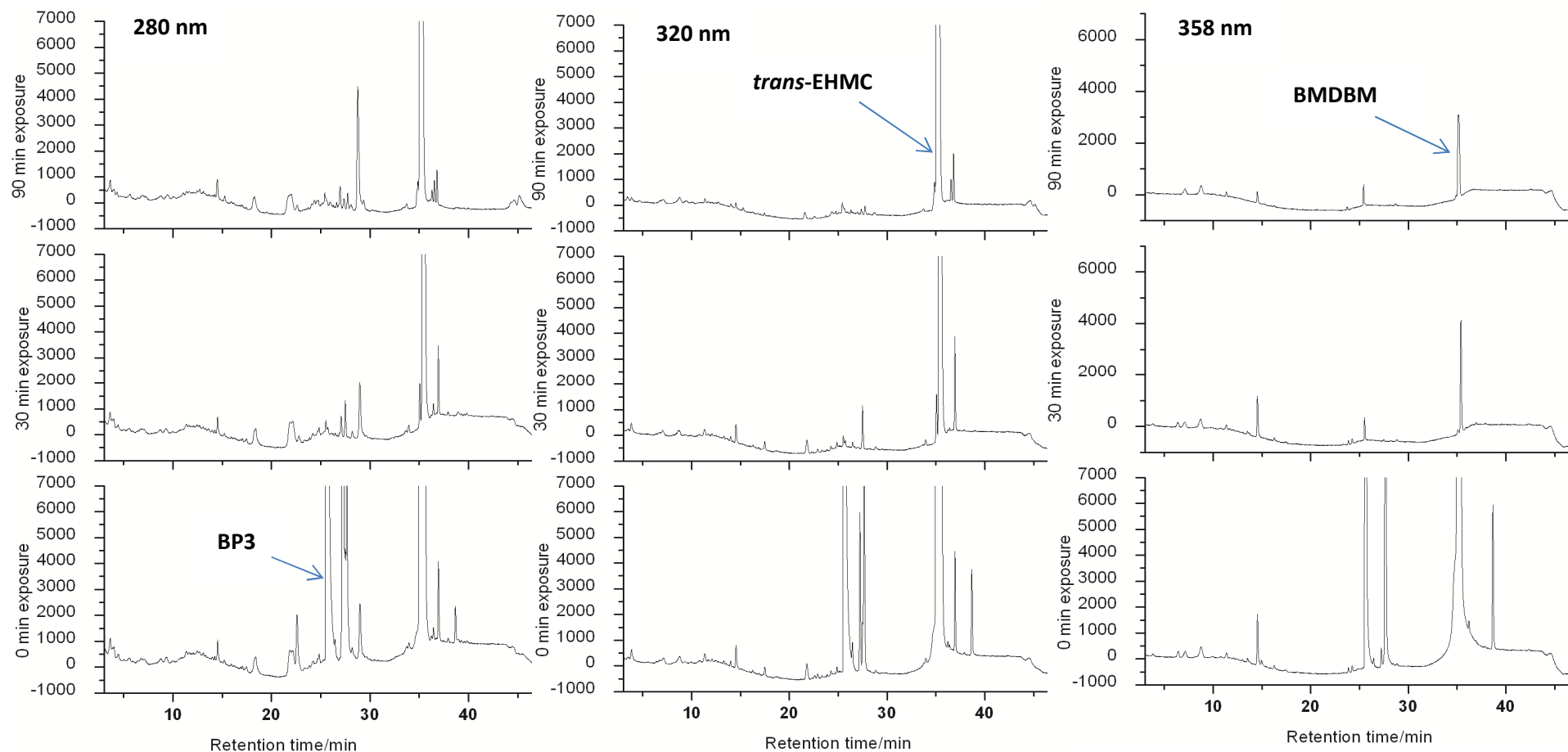
Figure 8.31: HPLC chromatograms recorded at 280 nm, 320 nm, and 358 nm of the photochemical changes when BDBDM, BP3, and EHMC is incorporated with mulberry extract dissolved in methanol and irradiated by simulated solar radiation. The separation was effected on a reverse phase Zorbax eclipse XDB C-18 column (150 mm × 4.6 mm, i.d., 5 µm), under a gradient elution of acetonitrile-water at a flow rate of 1 mL min^{-1} and an injection volume of 20 µL.

8.4 Conclusions

The aim of this work was to investigate the effect of mulberry extract on the photostability of three common sunscreen absorbers. The methanolic mulberry extract solution degraded when subjected to UV-irradiation. However, the extract did photostabilize sunscreens when they were incorporated singly in a mixture. The mixing of the three sunscreens with mulberry extract greatly lowers the UV range of photoprotection offered. The red shift exhibited by BMDBM and BP3 may help in reducing amount of the organic absorbers incorporated in a cosmetic formulation. This may lower the risk associated with photoproducts of these absorbers that may form upon photodegradation.

Acknowledgements

References

Aramwit P, Bang N, Srichana T (2010) The properties and stability of anthocyanins in mulberry fruits. Food Research International 43:1093-1097

Arfan M, Khan R, Rybarczyk A, Amarowicz R (2012) Antioxidant Activity of Mulberry Fruit Extracts. Molecular Sciences 13:2472-2480

Bajpai S, Rao BAV, Muthukumaran M, Nagalakshmamma K (2012) History of active pharmacokinetic principles of mulberry: a review. IOSR Journal of Pharmacy 2 (4):13-16

Brul S, Coote P (1999) Review preservative agents in foods modes of action and microbial resistance mechanisms. International Journal of Food Microbiology 50:1-17

Cantrell A, McGarvey JD (2001) Photochemical studies of 4-*tert*-butyl-4'-mathoxydibenzoylmethane (BM-DBM). Journal of Photochemistry and Photobiology B: Biology 64:117-122

Cavalieri LE, Li K-M, Balu N, Saeed M, Devanesan P, Higginbotham S, Zhao J, Gross LM, Rogan GE (2002) Catechol ortho-quinones: the electrophilic compounds that form depurinating DNA adducts and could initiate cancer and other diseases. Carcinogenesis 23 (6):1071-1077

Chen L, Hu YJ, Wang QS (2012) The role of antioxidants in photoprotection: A critical review. Journal of American Academy of Dermatology 67:1013-1024

Cherepy JN, Smestad PG, Gratzel M, Zhang ZJ (1997) Ultrafast electron injection: Implications for photoelectrochemical cell utilizing an anthocyanin dye-sensitized TiO_2 nanocrystalline electrode. Journal of Physical Chemistry B 101:9342-9351

Clark DC, Hoffman ZM (1997) Effect of solution medium on the rate constants of excited-state electron-transfer quenching reactions of ruthenium(II)-diimine photosensitizers. Coordination Chemistry Reviews 159:359-373

Demeter A, Horvath K, Boor K, Molnar L, Soos T, Lendvay G (2013) Substituent effect on the photoreduction kinetics of benzophenone. Journal of Physical Chemistry A 117:10196-10210

Est'evez L, Mosquera AR (2009) Conformational and substitution effects on the electron distribution in a series of anthocyanidins. Journal of Physical Chemistry A 113:9908-9919

Guillard V, Issoupov V, Redl A, Gontard N (2009) Food preservative content reduction by controlling sorbic acid release from a superficial coating. Innovative Food Science and Emerging Technologies 10:108-115

Karpkird TM, Wanichweacharungruang S, Albinson B (2009) Photophysical characterization of cinnamates. Photochemical and Photobiological Sciences 8:1455-1460

Kumasaka R, Kikuchi A, Yagi M (2014) Photoexcited States of UV Absorbers, Benzophenone Derivatives. Photochemistry and photobiology 90 (4):727-733

Lupo PM (2001) Antioxidants and Vitamins in Cosmetics. Clinics in Dermatology 19:467-473

Mishra AK, Mishra A, Chattopadhyay P (2011) Herbal cosmeceuticals for photoprotection from ultraviolet B radiation: A review. Tropical Journal of Pharmaceutical Research 10 (3):351-360

Mturi GJ, Martincigh BS (2008) Photostability of the sunscreening agent 4-*tert*-butyl-4'-methoxydibenzoylmethane (avobenzone) in solvents of different polarity and proticity Journal of Photochemistry and Photobiology A: Chemistry 200:410-420

Paris C, Lhiaubet-Vallet V, Jimenez O, Trullas C, Miranda MA (2009) A blocked diketo form of avobenzone: photostability, photosensitizing properties and triplet quenching by a triazine-derived UVB-filter. Photochemistry and photobiology 85 (1):178-184

Parker DV (1981) Mechanisms of the electrohydrodimerization of activated olefins IV The protonation of methyl cinnamate anion radical. Acta Chemica Scandinavica B 35:295-301

Roscher NM, Lindemann MKO, Kong SB, Cho CG, Jiang P (1994) Photodecomposition of Several Compounds Commonly Used as Sunscreen Agents. Journal of Photochemistry and Photobiology A: Chemistry 80 (1-3):417-421

Subramaniyan G, Sundaramoorthy S, Andiappan M (2013) Ultraviolet protection of property of mulberry fruit extract on cotton fabrics. Indian Journal of Fibre and Textile Research 38:420-423

Wang Y, Xiang L, Wang C, Tang C, He X (2013) Antidiabetic and antioxidant effects and phytochemicals of mulberry fruit (*Morus alba* L.) polyphenol enhanced extract. PLOS ONE 8 (7):1-11

Winkler C, Frick B, Schroecksnadel K, Schennach H, Fuchs D (2006) Food preservatives sodium sulfite and ascorbic acid suppress mitogen-stimulated peripherical blood mononuclear cells. Food and Chemical Toxicology 44:2003-2007

Yadav P, Garg N, Kumar S (2014) Improved shelf stability of mulberry juices by combination of preservatives. Indian Journal of Natural Products and Resources 5 (1):62-66

Supplementary Materials
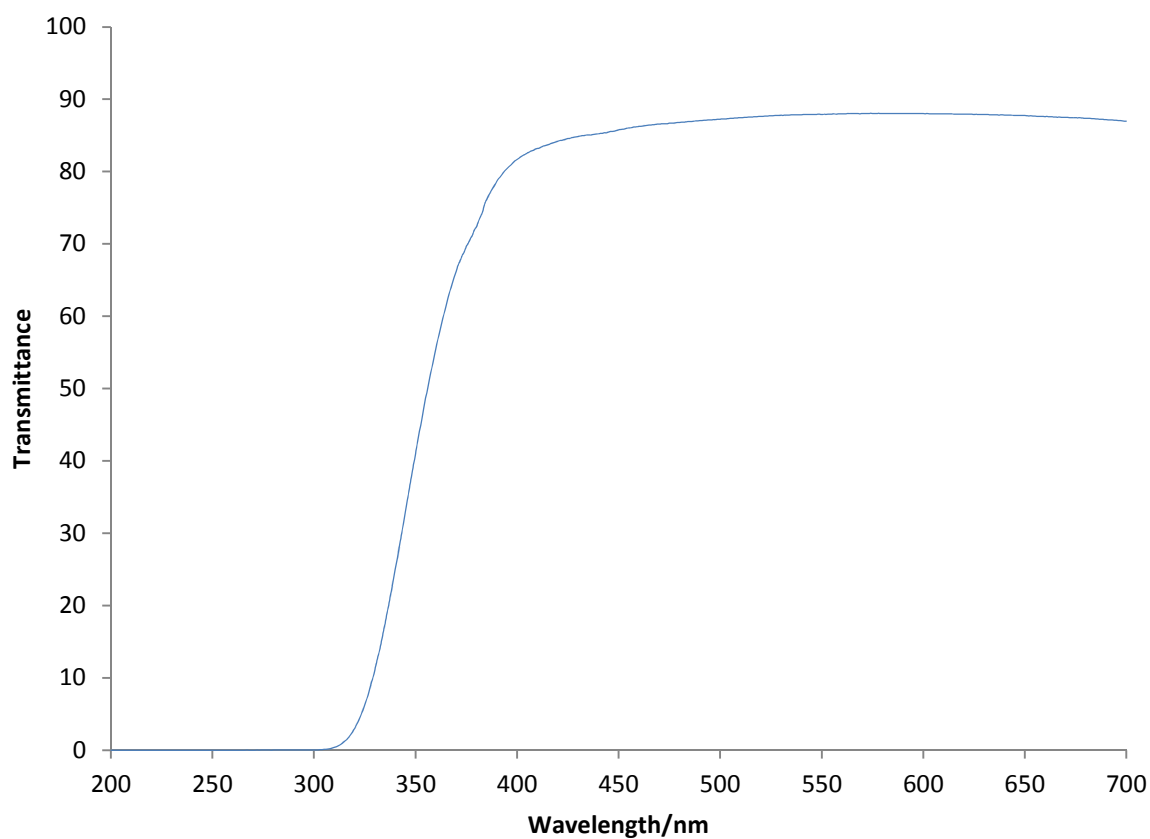
Figure S8.1: The transmittance spectrum of the 1 cm pyrex glass filter used in this work recorded on a PerkinElmer Lambda 35 UV-vis spectrophotometer.

Table S8.1: The photochemical changes of the sunscreen(s) dissolved in methanol after irradiation with simulated solar irradiation monitored on HPLC-PDA at 260, 286, 310, 358 nm.

Wavelength/nm	UV-filter	RT	0 min	30 min	90 min
Mixture of BMDBM, BP3 and EHMC					
			Peak Area		
260	*keto*-BMDBM	2.372	474053	388025	402645
	BP3	3.08267	1149065	1127671	1136999
286	*cis*-EHMC	10.19733	0	261526	443856
	trans-EHMC	11.53067	683313	303745	148920
	BP3	3.05067	1076471	879510	915656
310	*cis*-EHMC	10.19733	0	272403	461590
	trans-EHMC	11.488	1212199	538875	272829
358	*enol*-BMDBM	11.21067	146473	139439	154766
BMDBM					
260	*keto*-BMDBM	2.368	5769	99334	95094
358	*enol*-BMDBM	11.232	110714	96556	92185
BP3					
286	BP3	3.06133	927540	738944	806767
EHMC					
260	*cis*-EHMC	10.16533	0	139036	133916
	trans-EHMC	11.43467	156696	83566	81385
310 nm	*cis*-EHMC	10.16533	0	362702	342873
	trans-EHMC	11.44533	1818585	1026119	965827

Table S8.2: The chemical transformation of mulberry extract dissolved in methanol exposed to simulated solar irradiation monitored by HPLC-PDA.

| | 275 nm | | | | | | 280 nm | | | | |
RT	PA-0min	RT	PA-30min	RT	PA-90min	RT	PA-0min	RT	PA-30min	RT	PA-90min
1.395	136189	1.4	106124	1.394	96619	0.939	2142	1.4	102921	1.394	92546
1.556	15239	1.561	10325	1.557	10324	1.395	141002	1.561	9752	1.557	9972
1.845	64876	1.851	52471	1.846	50793	1.556	15351	1.851	52290	1.846	48267
1.982	36847	1.992	25345	2.001	20097	1.845	65360	1.992	27027	1.999	18723
2.201	33917	2.208	30295	2.204	27720	1.981	35797	2.208	34702	2.204	27781
2.369	24156	2.379	33762	2.374	25116	2.201	35884	2.378	47549	2.374	20486
2.517	30110	3.04	3366	3.6	3490	2.369	21404	3.033	19296	3.626	3122
3.023	19859	3.613	3445	7.267	1364	2.542	30119	3.232	6703	3.984	1461
3.221	8502	4.436	1246	8.912	1156	3.021	23191	3.625	21075	4.429	1107
3.607	20599	11.051	1719	11.029	2853	3.615	21250	3.829	3811	9.401	1287
3.843	12335	11.378	1532	11.377	2247	3.83	11994	3.99	6266	11.019	1489
4.404	4750	11.637	1029	11.659	1734	4.418	4423	4.416	2847	12.064	1854
7.158	1227	12.71	1526	11.968	5591	9.413	1267	9.403	1594	12.7	1051
8.81	1438	13.074	1897	12.267	1587	10.763	1729	11.04	1689	14.53	1883
11.324	1115	13.757	13326	12.437	4059	11.32	1903	11.377	1381	15.239	1758
12.032	4490	14.225	2201	12.708	7151	12.683	2139	14.538	2983	16.904	8843
12.416	3761	14.531	6012	13.077	9425	13.03	1451	15.235	1237	17.269	5867
12.659	4426	15.247	1042	13.773	29259	13.28	1891	16.889	3694	23.445	1124
13.035	7639	16.883	4008	14.251	6735	13.547	2505	17.045	5057	23.829	1624
13.28	3880	17.035	5169	14.526	13762	13.744	8715	17.291	4836	24.156	4745
13.775	24015	17.259	5122	15.241	12994	14.186	2363	24.164	1805	24.437	1552
14.208	5018	24.174	1564	15.509	10375	14.494	7481	24.657	1141	24.629	2792
14.496	16364	24.973	3489	16.901	8041	15.17	1109	24.821	1939	24.811	2463
15.173	22027	25.142	1787	17.269	5668	16.811	4369	24.957	2053	24.967	3367
16.827	8729	25.368	8568	24.174	1625	16.976	4288	25.146	2499	25.137	3477

17.269	6010	25.607	14978	24.821	1832	17.227	6346	25.371	7240	25.371	8143
21.699	1132	26.896	3011	24.971	1515	21.676	1412	25.604	13181	25.605	14126
24.137	1412	27.052	6431	25.141	1680	24.135	1448	26.896	3207	26.887	3293
24.806	4428	27.53	1899	25.368	8630	24.619	1005	27.05	6462	27.055	6925
25.094	2118	28.194	10913	25.607	15138	24.8	2213	27.548	1284	27.54	1819
25.34	9777	28.984	12548	26.889	3011	24.925	1932	28.191	9825	28.192	9637
25.572	16823	29.572	1154	27.053	6581	25.095	2517	28.985	12466	28.987	12801
26.106	2895	30.494	2099	27.551	2036	25.338	7153	29.566	1624	29.563	1175
26.853	2869	30.885	2138	28.191	11388	25.571	13230	30.492	1578	30.491	1838
27.015	6542	35.403	4429	28.988	14175	26.852	2919	30.872	1484	30.923	2050
27.498	2493	35.861	2253	30.486	1961	27.012	6500	35.406	3571	35.405	3536
28.15	10563	38.833	7812	30.873	1386	27.497	1777	35.876	2716	35.877	2845
28.931	12195	45.653	83945	35.406	4070	28.147	9301	38.833	7542	36.365	1028
29.498	1032			35.875	2419	28.926	12142	45.646	91196	38.835	7454
30.419	1944			36.366	1034	29.498	1469			45.68	90565
30.831	1612			38.833	6849	30.409	1984				
35.051	1120			45.651	82412	30.808	1779				
35.3	4678					35.008	1036				
35.829	3220					35.304	4178				
36.117	1078					35.828	2901				
36.331	1668					38.79	6436				
36.512	1230					45.641	91671				
38.781	6829										
45.609	81151										
286 nm						310 nm					
RT	PA-0min	RT	PA-30min	RT	PA-90min	RT	PA-0min	RT	PA-30min	RT	PA-90min
1.395	128990	1.4	96118	1.394	85211	1.394	77490	1.4	60039	1.394	54644
1.556	14056	1.561	9147	1.557	9411	1.555	8970	1.56	8115	1.556	8539

1.845	65272	1.851	50211	1.846	46070	1.845	55218	1.851	37890	1.846	34580
1.981	35072	1.991	25387	1.994	17578	1.984	22777	1.987	17130	1.985	14287
2.201	34924	2.208	33360	2.204	27338	2.2	15411	2.206	12039	2.204	11096
2.369	20869	2.377	44798	2.374	20639	2.365	13651	2.378	11979	2.372	9832
2.525	30020	3.032	13763	3.621	2421	2.543	24590	2.551	12527	2.542	5863
3.022	22149	3.2	6707	3.989	2286	3.017	10350	3.019	2187	3.999	1742
3.618	17736	3.621	14570	4.391	1103	3.221	5398	3.965	1852	14.54	1082
3.844	13592	3.988	7045	6.864	1050	3.513	7604	14.532	2574	24.848	1171
4.423	5697	9.447	1021	9.394	2038	3.825	8152	21.76	1326	25.557	3215
9.372	1810	12.7	1032	12.688	1268	11.315	1375	25.124	1181	27.061	1157
11.331	1068	14.053	5135	13.707	5161	14.499	3658	25.554	3537	35.36	2699
12.028	1018	14.24	2188	14.022	2655	21.661	3669	27.046	1120	35.878	1680
12.43	1350	14.539	5389	14.235	3896	24.822	1132	35.371	2711	38.84	2622
14.493	4063	15.22	1386	14.533	8120	25.096	1500	35.879	1947	45.692	58673
16.821	4024	16.864	3905	15.244	9447	25.524	3772	38.835	2274		
16.995	4594	17.032	4254	15.563	7798	27.004	1088	45.708	54023		
17.28	5360	17.269	4859	17.03	7574	35.313	2340				
21.664	1595	23.84	1676	17.259	5108	35.825	1488				
23.797	1681	24.011	1190	23.861	1041	38.808	2187				
24.134	1887	24.161	2505	24.17	3272	45.673	57298				
24.607	2495	24.658	3749	24.64	3260						
24.757	2930	24.821	2901	24.779	2208						
24.936	2130	24.947	2555	24.957	2527						
25.105	4587	25.146	4876	25.145	4767						
25.335	5855	25.37	6233	25.362	6304						
25.56	10110	25.598	10497	25.599	10659						
26.852	2721	26.895	2711	26.902	2738						
27.016	6539	27.049	6740	27.053	6905						
27.511	1618	27.56	1629	27.559	1827						

RT	PA	RT	PA	RT	PA
28.141	6803	28.189	7043	28.194	6988
28.932	8488	28.983	9152	28.987	9144
29.482	1820	29.543	2133	29.556	1677
29.928	1031	29.989	1351	29.958	1204
30.423	1249	30.493	1244	30.497	1604
35.303	3715	35.38	3586	30.87	1497
35.822	3198	35.868	3066	35.368	3331
38.79	5281	38.836	6029	35.875	3036
45.689	97323	45.688	93875	38.843	6918
				45.684	95161

358 nm					
RT	PA-0min	RT	PA-30min	RT	PA-90min
1.394	42881	1.399	34567	1.393	33795
1.555	7440	1.56	7336	1.556	7698
1.845	25207	1.851	22819	1.846	22605
1.999	7303	2.003	5908	2	5754
6.393	1697	7.237	1371	7.226	1484
7.163	2149	8.885	4051	8.878	3235
8.825	3391	14.53	5888	14.533	2681
14.498	8758	25.525	3847	25.526	3377
25.494	3550	35.056	2591	35.056	2917
35.011	3237	35.866	1093	35.87	1211
35.818	1163				

Table S8.3: The chemical transformation of mulberry extract mixed with BMDBM dissolved in methanol exposed to simulated solar irradiation monitored by HPLC-PDA.

275 nm				280 nm			
RT	PA-0min	PA-30min	PA-90min	RT	PA-0min	PA-30min	PA-90min
1.401	147420	148269	141520	1.401	157719	144659	138081
1.552	11410	15591	15254	1.552	15988	15062	14603
1.849	71921	64822	60722	1.849	72920	65575	60819
1.98	43684	38827	34631	1.98	44377	41621	36953
2.197	39495	34458	32929	2.197	39900	39144	37280
2.358	68291	29730	39350	2.356	59720	36357	53340
2.624		10940		2.613		19881	
2.974	21930	3676		2.974	19007	19856	21342
3.006			4125	3.2	7744	11448	
3.221	11278			3.603	22426	17256	26289
3.601	32597	4314	4116	3.779	5732		
3.808	7241			3.959	9029	9995	8448
3.944	14414			4.36	6847	3168	2795
4.371	17605	1193	1018	5.559	1379		1273
4.951	9912			6.88		3205	1639
5.423	7047	1071	1519	8.559	1396	2532	1604
6.843		3342		9.209	2718	3379	2572
6.917	2933		2983	11.271	1074	1127	1084
8.56	3296	3081	2637	11.593		1035	1040
9.17	1500			12.369	1310		
9.284		2381	1972	12.634	1031	1446	2660
11.279	1814	1117	1003	14.48	4302	3719	2920
11.561		1394	1312	18.144			5037
12.378	1007			18.267			7432
12.605	1272	1956	3525	18.31	14362	11485	
13.026			1245	21.738	16278	13633	14335
14.481	5704	4956		22.053	17983	17748	17079
18.308	15512	11975	12933	22.459	12707	12565	12802
21.749	17314	17991	17778	23.705			1115
22.029	18846	15310	16006	24.063			1346
22.467	12722	12799	12332	24.121	3825	1133	
23.709		1023		24.352	1698		
24.081			1518	24.565		1039	1050
24.115	1930	3540	1513	24.601	2748		
24.363		2081		24.762	5129	2127	1954
24.565		2194		25.195	5953	2245	2213
24.604	1181			25.467	7576	4142	4561
24.759	2030	3787		25.581		2832	2574
25.12		3902	1111	26.002	4811	1183	1683
25.323	1086			26.187			1008

RT	PA-0min	PA-30min	PA-90min	RT	PA-0min	PA-30min	PA-90min
25.468	4188	5934	4149	26.397	2076	1031	
25.565		3687	2008	27.152	376984	397167	397865
25.968	1123	1516		27.579	27157	27946	27002
26.311			1472	28.115	3321	3634	
27.152	404257	427821	428052	28.047			3803
27.101		1234		28.326		1159	1262
27.577	2691	26761	27088	28.767		24334	25346
28.114	3520	3522	4146	28.9	29396		
28.304		1225	1246	35.004	1517432	1538617	1533588
28.767		23636	25537	35.827	1703		
28.903	29651			37.852	1008		
34.592	1806	1119	1428	38.605	3303	3154	3397
35.004	1478800	1505309	1497079	38.842	2263		
35.772	1378			44.596		3393	4675
37.871	1071			45.191		15861	19598
38.605	3387	3383	3433				
38.852	2445						
44.595		4462	3815				
45.178		13391	17953				

286 nm				310 nm			
RT	PA-0min	PA-30min	PA-90min	RT	PA-0min	PA-30min	PA-90min
1.401	151344	137312	129223	1.401	90066	78116	73323
1.552	15781	14661	14037	1.552	9878	8357	8815
1.849	73763	64702	59221	1.849	59968	54101	48838
1.979	44004	40739	35798	1.977	28719	26791	24065
2.197	39312	38431	36537	2.195	14557	16529	16139
2.356	56919	33937	35284	2.356	12687	16446	16109
2.603		20640	16053	2.518	18015	27409	27307
2.999	16771	17108	19324	2.96	2084	11336	11115
3.168	7777			3.377		12542	17017
3.371		14177	12346	3.499		5605	
3.599	20597	12320	12301	3.785	2491	5366	8200
3.787	6890		4343	3.936	1366	2687	
3.946	7753	11212	5579	6.909		1500	
4.374	4808	2661	2671	8.509	2483	1968	1985
5.535	1490	1155		9.187	1282	1082	
6.738	2539		2659	11.256	2197	1362	1258
6.882		1722		13.932	1176	1054	1002
6.965	1119			14.484	4811	4702	3216
8.527	1873	1651		21.562		4403	3546
9.212	3692	3730	3765	21.639	5303		
11.267	1654	1071		22.46	1062		2345
12.378	1137			22.53		2048	
12.615	1108	1360	1436	24.8	2029		

RT	PA-0min	PA-30min	PA-90min
14.48	3971	3279	2643
18.133			4649
18.309	9577	7621	4204
21.664		3478	9464
21.705	11404		
21.977			9206
22.022	10098		
22.462	11032	9013	11436
23.717			1013
24.14	1417	1038	1240
24.576		1022	1212
24.601	1548		
24.78	3114	2802	2210
25.124		2395	2431
25.216	3296		
25.474	4866	3391	4039
25.589		2292	2746
25.999	1912		1931
26.321			1181
26.404	1696		
27.152	322291	340764	339842
27.579	26664	27741	28172
28.041			3638
28.12	2044	3078	
28.324		1464	1344
28.895	17413	16679	16407
35.004	1551232	1577477	1569313
35.831	1732		1974
36.032			1031
38.6	3149	3026	3226
38.833	2041		
44.594		4032	3030
45.177		16360	19174

RT	PA-0min	PA-30min	PA-90min
24.742		1700	1654
25.077	1197		2299
25.107		1549	
25.471	2476	4788	4294
25.959		1255	1313
26.399	2040	1431	1352
27.152	32814	33530	33642
27.584	18321	17688	18074
28.751	1063		
35.004	1907370	1932042	1922224
38.601	4519	4907	5301
44.61		4233	3246
44.516	2110	9718	11090

358 nm			
RT	PA-0min	PA-30min	PA-90min
1.4	46057	40135	38348
1.552	8060	6958	6789
1.848	25360	25114	24761
1.99	5295	5444	6131
2.504	1040		
6.278	1973		
6.936	2357	3081	2924
8.517	5222	6091	
8.603			5237

11.274	1164	1052	1086
14.482	10923	10317	8000
24.187	1202		
25.469	4524	4516	4415
27.156	1564	1621	1489
27.584	87889	89387	89347
35.004	7838740	7947571	7932074
38.602	12927	13483	14291
44.52	7383	7747	8305

Table S8.4: The chemical transformation of mulberry extract mixed with BP3 dissolved in methanol exposed to simulated solar irradiation monitored by HPLC-PDA.

275 nm				280 nm			
RT	PA-0min	PA-30min	PA-90min	RT	PA-0min	PA-30min	PA-90min
1.393	179253	162251	154020	1.393	179061	159352	150418
1.546	17214	17070	16259	1.545	17235	16664	15793
1.842	76363	66492	64967	1.842	77876	67446	63828
1.974	49837	41182	37885	1.974	51395	44672	38168
2.191	40895	36340	41471	2.191	44059	41942	42795
2.352	66700	41583	40756	2.351	62831	37335	37428
2.603			23156	2.581			24623
2.991	21993	3803	21206	2.603		24056	
3.243	9520			2.983	26778	20482	25030
3.591	25485	5039	42882	3.599	25673	40092	35042
3.787	6937			3.787	7174		
3.934	8697		8581	3.808		3632	
4.271			6665	3.951	8946	11968	13035
4.373	7266	1187		4.296		9198	9647
4.587			1618	4.368	7648		
5.394	1765			4.587			3693
5.54		1866	1961	4.629		3113	
6.843	4298	3230	2075	4.892			1481
8.414			3654	4.903		2396	
8.547	2920	3387		5.369	1360		
9.157	2359			6.293	1058		
9.241		2099	2317	6.756	4818		2498
11.294	2173	1369	1359	6.811		2273	
11.512	1204	1449	1601	8.423			3000
12.352	1139			8.514	1696	2400	
12.594			1655	9.196	3579		3832
12.602	1116	1525		9.242		2906	
14.472	6899	4598	2857	11.268	2225	1319	1105

RT				RT			
15.18			1763	11.56	1143	1155	1311
17.318	1033			12.344	1386		
18.259		12714	13224	12.606	1136	1296	1732
18.306	15113			14.473	5131	3430	2234
21.643			17857	15.153		1135	1845
21.745	15907	17147		18.272		12332	12051
21.902			15931	18.31	13553		
22.03	21981	17865		21.675		18103	17962
22.524			3982	21.712	15035		
22.681	4559	4232	1163	21.921			13486
24.095		2716	4425	22.032	20525	14639	
24.123	2178			22.598		4141	3529
24.395		1246	2185	22.682	3851		
24.57		1317	2400	23.683			1023
24.6	1082		4168	23.726		1013	
24.76	2325	2367		24.137	1885	1255	
25.131			3709	24.576		1013	
25.269	1229			24.695			2007
25.532	7930651	7949779	8248403	24.757	2894	2191	
26.993	8256	7910	7932	25.195	2054		
27.362			2220	25.532	9765378	9775067	10109536
27.46	2658	2109		26.994	9304	8689	8733
28.071		2752	2717	27.362	1033	1132	1150
28.108	3203			28.061		2381	2611
28.776		35444	35110	27.467	1167		
28.883	30655			28.106	2564		
35.168			1961	28.777		34735	34904
35.299	5158	5431	2269	28.881	30176		
35.744	1648			35.166			4477
37.853	1108			35.299	5183	5959	
38.883	2046			35.837	1724		
39.04		1687		37.857	1103		
44.501		2634		38.731		1060	
44.621		2769	4490	38.884	2046		
45.153		19262	18318	44.405		1490	1120
				44.589		3439	3123
				45.138		19578	18986
286 nm				310 nm			
RT	PA-0min	PA-30min	PA-90min	RT	PA-0min	PA-30min	PA-90min
1.394	173146	150541	142574	1.393	110613	83964	79694
1.545	17042	16227	15314	1.545	14848	9059	8679
1.842	78974	66481	61785	1.842	66577	54663	48209
1.973	49423	43568	36819	1.97	30474	28212	27319
2.191	45034	40765	41463	2.19	14792	17295	17299

2.351	26826	56938	35823	2.349	14538	17235	17464
2.496	34873		22330	2.509	19237	27619	28234
2.981	17278	17618	17953	3.008	2714	11215	11707
3.157	8352			3.366		18668	18077
3.349		15617	14663	3.485	1306		
3.602	22641	11474	10567	3.776	3627	6315	6093
3.779	7697			3.925	1458	1966	2199
3.944	8776	11653	11356	6.796			3182
4.288		2551	2870	6.841		3154	
4.359	6413			8.489		2765	3138
6.336		1102		8.539	2800		
6.757	5979	5217	2559	9.176	1327		1603
8.477		2056	2503	9.231		1491	
8.529	2646			11.236	2261	1302	1356
9.167	4272			12.631			1144
9.201		3929	4476	13.927	1253	1204	1149
11.251	1848	1248	1242	14.471	5448	3672	2281
12.367	1116			21.59		4833	3995
12.601	1071	1395	2029	21.637	6141		
14.472	4533	3027	1988	22.585		1368	
15.167		1065	1668	22.787	1069		1726
18.27		7617	8015	24.789	2528	1806	
18.308	8834			25.075	2085	1850	2001
21.68		3764		25.532	7728714	7724284	8001178
21.701	4602			26.995	2111	1837	1768
22.693	2132	2052	1877	35.21		4378	2459
23.667			1021	35.306	1777		
24.03			1148	44.466	3079		
24.144	2989			45.141		12100	11287
24.587		1164					
24.69			2681				
24.755	5109	2802					
25.532	11014667	11015851	11372246				
26.994	9573						
27.366	1807						
27.413		1469					
28.061		1640	1680				
28.12	1885						
28.774		21184	21302				
28.882	18237						
35.297	4371	5600	3981				
35.837	1562						
38.887	2109						
44.563		3038	2296				
45.175		20312	18677				

358 nm			
RT	PA-0min	PA-30min	PA-90min
1.393	49747	42667	40758
1.545	7355	7286	7473
1.842	26398	25743	25158
1.987	5770	6695	5012
2.505	1140		
6.288	2324		
6.885		3425	3459
6.93	3173		
8.489		6028	6374
8.539	7121		
11.269	1493	1145	1332
13.436	1007		
14.473	13543	9465	6026
16.168	1029		
24.17	1364		
25.532	1896447	1888780	1950667
34.886		1758	
35.024	1345		
44.61		7701	6206

Table S8.5 The chemical transformation of mulberry extract mixed with EHMC dissolved in methanol exposed to simulated solar irradiation monitored by HPLC-PDA.

275 nm				280 nm			
RT	PA-0min	PA-30min	PA-90min	RT	PA-0min	PA-30min	PA-90min
1.398	181538	157729	146136	1.398	182449	154472	140891
1.551	17387	16256	16607	1.551	17441	15707	15902
1.847	77330	69350	65113	1.848	78919	68095	62846
1.982	48974	39100	35734	1.982	48868	39342	35429
2.201	40183	43766	40631	2.201	44944	45106	42852
2.364	66407	42555	40710	2.363	27436	38797	36049
2.592		23422		2.528	34771		
2.613			24923	2.603		25373	22776
2.995	20932	23481		3.004	27473	21922	21072
3.027			19139	3.413			12138
3.264	10622			3.61	23953	31963	16701
3.605	24928	34871	34597	3.829	6057	4461	
3.84	6125	4391		3.965	10190	7353	10962
3.963	10442	5578	10463	4.267		4084	4182
4.269		3710	3849	4.409	7407		
4.429	8672			5.573	1450		1709
5.482	1370			5.62			

5.595		1979		6.885		2901	
5.607			1902	6.916			3311
6.916		3800		7.328			1041
8.589		4957		8.55		3432	
8.699	2547			8.636	1560		
8.782			2056	8.782			1263
9.328	1886	3381		9.329	2486	4472	
9.437			2451	9.451			3287
10.993		1103		11.335	1647	1555	
11.028			1636	11.6		1212	
11.338	2320	1780	1335	12.445	1057		
11.589	1166	1551		12.669	1065	1873	1733
11.63			1415	13.065		1092	
12.648	1144	1904	1405	14.496		2204	6747
13.062		1138		14.523	5473		
14.492			7148	15.213		1461	1989
14.524	6940	2813		17.453	1115		
15.213		1388	1813	18.24		10827	11704
17.435	1555			18.379	13326		
18.176			5029	21.643		16692	
18.228		11835	7450	21.728			15393
18.384	14567			21.884	18164	12691	
21.653		14009		21.99			13275
21.76			17317	22.131	18022		
21.884	16438			22.512		3981	3683
21.923		16522	13404	22.765	3822		
22.13	21305			24.023		1442	2091
22.52		4446	4289	24.204	1643		
22.759	4402			24.349			3552
24.043		2590		24.523		1207	1532
24.189	1903		2521	24.661	1142	1898	
24.267		1211	6363	24.821	2532		
24.518		1442	2196	25.248	1006		
24.678		1946		25.481		10265491	
24.712			1662	25.405			2892
24.822	2082			25.513	4317		2808
25.376	1871			25.709	1871		
25.481		8358346	5945	25.924			1888
25.511	4714			26.014	1363		
25.694	2301			26.6			1295
25.923			1617	26.919		8322	7403
26.022	1846			27.054	6525		
26.599			1589	27.337		1780	3482
26.918		7949	6587	27.476	11388		
27.054	6200			27.727			5010

RT	PA-0min	PA-30min	PA-90min	RT	PA-0min	PA-30min	PA-90min
27.355		2099	3665	28.021		1941	2910
27.475	10048			28.184	3094		
27.725			4485	28.72		49486	67528
28.007		2358	3114	28.958	29499		
28.179	3252			29.338			2019
28.723		51083	69102	33.344			1261
28.962	30618			33.633	1978		2299
29.341			1757	33.927	3109		
33.657	2016			34.848			10882
33.702			2053	35.046	13736		
33.926	3131			35.162		4841	8089850
34.844			9597	35.381	9186283		
35.045	10872			36.213	2994		4239
35.152		2745	6808804	36.432	5672		
35.264		1949		36.529			6165
35.381	7427395			36.672	2175		
36.213	2206		4486	36.785			8689
36.431	5529			36.922	18079		
36.528			5443	37.904	1085		
36.672	1739			38.916	2113		
36.785			6793	44.267		1243	2607
36.921	14625			44.594		5164	6010
37.913	1239			45.15		15064	12220
38.936	2209						
44.288			4388				
44.621		6345	7678				
45.155		14297	12516				

286 nm				310 nm			
RT	PA-0min	PA-30min	PA-90min	RT	PA-0min	PA-30min	PA-90min
1.398	175247	144150	131452	1.398	111771	80344	72243
1.551	17123	14951	15158	1.551	14143	8782	8320
1.848	79957	66179	60007	1.848	68173	51411	45414
1.982	49967	38386	35473	1.979	31242	28553	25169
2.201	42707	44739	40549	2.199	16346	18333	17513
2.363	27294	39313	34438	2.362	17084	18789	16867
2.517	34083			2.521	29586	29342	
2.624		25495	22438	2.603			26899
2.985		18404		2.988	11439	12891	
3.01	24215		15905	3.029			11290
3.189		9038	5868	3.232	5236		
3.42		13564	11222	3.397		20398	
3.611	20690	13554	12459	3.412			17981
3.811	7476	6316	3951	3.506	10600		
3.964	9622	8968	7647	3.807	8138	6650	7891

4.302			2958	3.979	1630	2210	
4.409	5955	7209		6.677	2427		
4.651		1363		6.886		3753	
5.625			1272	7.004	2208		
6.778	3265			8.595		4013	
6.89		3538	4297	8.675	3491		
7.051	2327			8.752			1327
7.221			1210	9.311		1842	
7.328			1204	9.417			1114
8.573		3382		11.306	2981	1533	1212
8.686	1533			11.669	1308		
				12.699		1507	
9.296	3672			12.702			1312
9.337		5422		13.98	1278	1211	
9.448			4083	14.007			1302
9.967		1421		14.527	5736	2370	2322
11.314	1956	1196	1059	15.248			1636
12.42	1498			17.473	2182		
12.669	1067	2017		21.499		3865	
12.703			2041	21.583			2993
14.495		1821	6400	21.778	5670	1534	
14.523	4871			22.873	1025		
15.215		1710	2149	24.847	1742		
17.456	1702			24.981		1394	
18.233		6942	7415	25.481		8131585	2171
18.365	9882			25.515	2717		1696
21.568		10367		25.633			1780
21.728			9601	25.715	2403		
21.828	12553	7157		25.943			1571
21.959			7391	26.299			1077
22.149	10727			26.471	1830		
22.501		2801	2514	26.913		1961	1786
22.788	3060			27.047	1593		
23.671		1029		27.354			1801
24.008		1442	2476	27.475	12846		
24.217	3232			27.728			3531
24.368			2121	28.684			1225
24.523		1531	2704	28.808	1112		
24.651	3918	2183		33.461	1421		
24.717			3573	33.7			1749
24.824	5282			33.937	3026		
24.981			1638	34.853			13804
25.109	1894		3729	35.046	19119		
25.237	4224			35.161		3105	
25.481		11518356	3968	35.201			10400344

RT	PA-0min	PA-30min	PA-90min	RT	PA-0min	PA-30min	PA-90min
25.517	5971		3163	35.381	13302675		
25.643			2912	36.384	1290		
25.712	4664			36.529			6793
25.932			5312	36.651	1409		
26.035	3355			36.786			13396
26.293	1573			36.923	26762		
26.301			2017	44.535	2670	4148	3317
26.457	2967			45.141		8571	5310
26.589			2712				
26.917		9104	9892				
26.891	2324						
27.056	8333						
27.358			4856				
27.475	14404						
27.726			6410				
28.006		1562	2806				
28.168	2300						
28.716		32281	43431				
28.954	19958						
29.348			3850				
33.323			1328				
33.611	2082						
33.718			1872				
33.943	2817						
34.852			13395				
35.047	16458						
35.163		4920	9403148				
35.382	11003208						
35.573		1081					
36.021			3475				
36.213	3077		4970				
36.421	4855						
36.529			8096				
36.672	2672						
36.786			11116				
36.922	21795						
37.9	1022						
38.907	1584						
44.385	2381	1320	2485				
44.591		3759	5549				
45.153		14103	12124				

358 nm			
RT	PA-0min	PA-30min	PA-90min
1.398	49950	41153	37385

1.551	6889	7700	6814
1.847	25921	25542	24572
1.995	5926	7300	5834
2.542	1375		
6.372	2509		
6.975		4258	
7.077	3387		3485
8.594		7590	
8.696	6279		
8.752			6035
11.332	1445	1368	1250
13.501	1113		
14.526	13038	5927	3581
24.24	1358		
25.407			4974
25.511	4915	1981402	
34.904		1076	
35.111		43670	
35.068	1387		
35.381	35133		
44.288			1633
44.545	6924		1040
44.641			8254

Table S8.6: The chemical transformation of mulberry extract mixed with BMDBM, BP3 and EHMC dissolved in methanol exposed to simulated solar irradiation monitored by HPLC-PDA.

275 nm				280 nm			
RT	PA-0min	PA-30min	PA-90min	RT	PA-0min	PA-30min	PA-90min
1.412	215569	204054	197621	1.412	215403	201422	193034
1.565	21433	19870	19422	1.565	21364	19377	18828
1.862	86358	80811	76106	1.862	88460	80949	78511
1.997	56854	52259	48229	1.997	58788	53465	46263
2.216	48985	48679	47377	2.216	51037	50341	49123
2.379	73585	42220	42219	2.378	31996	38993	38276
2.635		23938	22909	2.539	35479		
3.035	22591	21732	23608	2.635		24785	23089
3.253	8340	9917		3.024	29871	24186	26980
3.627	27379	26961	35810	3.627	25345	26842	27966
3.851	6935			3.823	7103	5106	5454
3.99	9792	12626	11318	3.987	11601	6964	6777
4.295		5354	4080	4.294		4162	4036
4.45	8489			4.451	7288		
5.554	2094	2022	1892	5.577	2032		
6.368	1124			5.633		1600	1877

6.731	2638			6.421	1435		
6.981			5102	6.755	3622		
7.066		4943		6.976			4685
7.102	3359			7.115	3237		
8.657			4456	8.639			1760
8.766	4127	3970		8.727	2157	1852	
9.345	3072			9.32	4007	3652	4122
9.461		2544	2714	11.334	2997	1939	1463
11.345	1977	1844	1743	11.597	2501		
11.575			1687	11.64		1504	1576
11.601	1319	1902		11.861	2054		
12.473	1306	1100		12.075	1505		
12.673	1424			12.431	4204	1224	1108
12.729		2997	4482	12.676	2996		3669
13.073		1494	1663	12.729		2486	
14.53	8771	8702	8399	13.063	1908	1321	1590
15.199	1059	1182	1836	14.53	6594	6520	7079
17.379			1166	15.198	1065	1287	1576
17.435	1887			17.449	1643	1056	1019
18.123			5155	18.103			5301
18.241			7761	18.291		11529	6903
18.392	16354	11833		18.392	13605		
21.632			16683	21.685		16200	15612
21.707		16917		21.849	19112		
21.882	18448			21.919			13780
21.923			13796	22.017		12610	
22.019		13402		22.118	15864		
22.166	17757			22.489		31347	32896
22.491		30260	29579	22.576	31298		
22.577	30388			23.104			3071
23.108			1220	23.413			2349
24.139		2827		23.685			2435
24.064			3008	24.053			5335
24.214	3503			24.134		2604	
24.395	1930	8139	8117	24.209	1783		
24.561		2223	2428	24.347		4412	5920
24.657	1843		4493	24.565		2605	3813
24.731		4762		24.661	1216		5592
24.819	2882			24.725		4300	
25.074			6531	24.828	3009		
25.109		5381		24.907			1845
25.355	1064			25.081			7751
25.596	10856136	11082875	11217752	25.119		5645	
26.431	1671			25.28	1419		
27.095		1357524	1328855	25.596	13213981	13470802	13636683

27.207	1373297			26.428	2048		
27.477	2271		95834	27.095		1257009	1230469
27.506		91796		27.207	1201179		
27.633	36481			27.475	28942		93687
27.961			7985	27.507		89837	
28.024		7594		27.634	82428		
28.189	2817			27.951			6522
28.299		9276	13871	28.001		5760	
28.694			70089	28.185	7726		
28.757		70088		28.241			12646
28.974	29044			28.3		7865	
29.28			4722	28.694			66759
29.357		4735		28.756		66681	
30.157		1559	1599	29.283			6039
33.454		3085	3412	28.971	30238		
33.699		4262	4253	29.341		4989	
33.716	3252			29.664	1150		
33.93	4328			30.119			1176
34.881		4913615	4927658	33.365			3054
35.073	4892530			33.461		3176	
35.207		7452176	7215427	33.631			4292
35.393	7901745			33.714	3773	4733	
35.982			1343	33.946	5131		
36.065		1210		34.881		5039112	5053772
36.227	1167	3866	4174	35.073	5012594		
36.445	4156		6053	35.144			8519858
36.533		4187		35.208		8960556	
36.788		9715	8012	35.393	9759167		
36.931	17242			35.99			1446
37.257		12485	25393	36.069		1343	
37.476		15556	27084	36.211	1173	3992	4170
37.692		9945	20101	36.535		5351	
37.836		13552	26378	36.439	4023		7528
37.925	1396			36.672	1227		
38.461		11598	12632	36.788		12208	10096
38.661	11444			36.932	21227		
38.987	1898		1028	37.257		11405	23897
39.048		1227		37.477		12364	22416
39.284	1100			37.69		8360	17365
44.288		3121	4959	37.788			23462
44.448			2328	37.835		11978	
44.612		6617	5696	37.925	1547		

RT	PA-0min	PA-30min	PA-90min	RT	PA-0min	PA-30min	PA-90min
45.165		11942	13269	38.462		11096	11588
				38.661	11061		
				38.987	2013		
				39.035		1059	
				39.284	1035		
				44.288		2943	3413
				44.662		5708	6272
				45.169		12034	13170

286 nm				310 nm			
RT	PA-0min	PA-30min	PA-90min	RT	PA-0min	PA-30min	PA-90min
1.412	207433	191334	181931	1.412	131443	119263	114237
1.565	20900	18847	18238	1.565	16881	15288	14834
1.862	89870	80337	76698	1.862	74926	65329	58783
1.997	58328	52769	45236	1.994	34043	32695	31946
2.216	50353	49660	48439	2.215	16759	19713	19141
2.378	30773	38662	39073	2.376	15272	18906	20119
2.54	36106			2.544	19994	29927	30409
2.635		23746	22582	3.031	2518	10452	16785
3.03	26218	16347	23748	3.427		17915	25521
3.221		5750		3.529	1264		
3.413			11144	3.827	3836	10005	10602
3.627	23747	23597	13868	3.989	1547		6595
3.842	7775		6976	4.288			3914
3.985	11476	13286	7132	4.653			3280
4.294		3550	3518	6.699	3688		
4.439	7005			6.763			1897
5.583	1835			6.979			3052
5.624		1086	1450	7.084	3438		
6.421		1038		8.685			3214
6.768	3819			8.75	4085		
6.854		7254	5285	9.318	2082	3296	1387
7.09	3320			9.463		1064	
8.687			1426	11.329	3085	1893	1850
8.763	1741	1557		12.698		1102	1125
9.334	4951		4907	13.983	1504		1799
9.435		4239		14.001		1403	
11.332	2430	1655	1786	14.484			4778
11.661			1021	14.531	6847	6362	
12.439	1813	1026	1105	17.393			2264
12.678	1184		2922	17.471	2486	2208	
12.702		1782		18.016			1176
12.95			1751	21.592		6502	5487
14.476			6728	21.768	7019		
14.53	5982	6455		22.493		6104	5922

15.197		1267	1604	22.584	4277		
16.96			1047	22.879	1275		
17.044	1074			24.341		3654	
17.371			1286	24.745		3073	1297
17.457	1391	1255		24.858	2801		
18.089			5077	25.055			1622
18.288		7870	4150	25.152	1853	4553	
18.355	8945			25.208			1119
21.652		10252		25.596	10786855	11005524	11088304
21.838	12757			26.319		1651	1581
22.02		7823		26.438	4098		
22.165	9176			27.095		103483	100531
21.573			9622	27.207	101757		
21.932			7479	27.488	13000		70561
22.489		30190	29066	27.511		70944	
22.575	29721			27.638	61509		
24.071			2241	28.303		2168	3408
24.115		2320		28.7		1078	
24.204	1514		1868	28.822	1151		
24.352		1721		33.504		1719	
24.576		2220	2062	33.645			1931
24.661	1149		3897	33.746	1646	3282	
24.726		4438		33.955	3555		
24.834	3326			35.073	6297845	6326346	6357046
24.907			1149	35.393	14167282	11975206	10845502
25.066			5324	36.056		1225	1122
25.116		6041		36.215	1472		
25.596	14558977	14810740	14937533	36.387	1054		
26.43	2383			36.534		6151	8386
27.095		1071504	1046413	36.792		16612	12483
27.207	1022719			36.935	28259		
27.48	29724		94059	37.255		1059	1914
27.508		90252		37.835		1397	2710
27.635	82635			38.461		16356	17725
28.006		4903	4645	38.661	15119		
28.166	5733			44.32		1146	
28.302		6623	10944	44.624		3896	
28.753		43033	41976	45.135		4720	5182
28.972	18363						
29.356		4326	3811				
30.122			1071				
33.483		3026	1547				

RT						
33.662			1609			
33.727	3377	4264				
33.949	4425					
35.073	5131048	5164413	5168966			
35.393	11653052	10523724	9843225			
36.057		1267	1406			
36.217	1454	2413	2459			
36.436	2685		8195			
36.534		6033				
36.789		14265	11306			
36.933	24335					
37.257		10486	21042			
37.478		9098	16016			
37.692		6360	13040			
37.834		10387	20488			
37.925	1048					
38.461		10394	11081			
38.661	10050					
38.976	1486					
44.288			2744			
44.464	2582		5713			
45.136		10162	12452			

358 nm

RT	PA-0min	PA-30min	PA-90min
1.412	54714	48636	48727
1.565	6891	6999	7378
1.862	27335	27012	26725
2.005	7214	5999	6493
2.547	1593	1210	
6.401	2978		
7.034			4307
7.123	4092	4385	
8.698			7654
8.74	7953	7802	
11.347	1931	1534	1591
13.52	1208		
14.484			12569
14.531	16196	15424	
14.938	1984		
16.229	1385	1043	
23.719		1026	
23.851	1032		
24.248	1681		
25.207			1110
25.596	2622995	2658048	2658915

26.426	1516		
27.1		5533	5428
27.209	5907		
27.639	305930	307344	315782
35.075	29243953	29592356	29881041
36.2	2245	2151	2180
38.661	41587	43742	47180
44.516	7311		

Chapter Nine

The efficacy of liquorice root extract in enhancing the UV stability of three commonly used sun-active agents

Moses A. Ollengo and Bice S. Martincigh[*]

School of Chemistry and Physics, University of KwaZulu-Natal, Westville Campus, Private Bag X54001, Durban 4000, South Africa

*Corresponding author: Tel.:+27-31-2601394; Fax: +27-31-2603091; E-mail address: martinci@ukzn.ac.za

Abstract

The photostabilizing potential of liquorice root extract on commonly used UV absorbers in the market was investigated. The effect of UV light on the photochemical stability of 2-ethylhexyl-*p*-methoxy cinnamate (EHMC), benzophenone-3 (BP3), and *tert*-butylmethoxy dibenzoylmethane (BMDBM, avobenzone) mixed with liquorice root extract was studied by irradiating the mixture(s) with simulated solar radiation. The photochemical transformations were monitored by standard spectrophotometric methods; GC-MS, and HPLC-UV-ESI-MS-MS. The extract showed good UV absorption but degrades on prolonged UV exposure. The mixture of BP3 with liquorice root extract showed enhanced photostability arising from the chemical interaction of BP3 with the extract. EHMC showed photostability upon prolonged exposure and BMDBM showed spectral photodegradation. This extract may not be good photostabilizer for BMDBM but reacts with EHMC to yield compounds that are photostable. Liquorice root extract stabilizes EHMC and BP3 and diminishes the *keto-enol* tautomerism of BMDBM in favour of *enol*-BMDBM. The phenolic secondary metabolites present in liquorice root extract may participate in free radical scavenging activity.

Keywords: Liquorice root extract, 2-ethylhexyl-*p*-methoxy cinnamate, benzophenone-3, *tert*-butylmethoxy dibenzoylmethane, photostability, sunscreens.

9.1 Introduction

Plant extracts are commonly added to most cosmetic products, including sunscreens. The list of plant extracts added to cosmetic formulations grows each day but the most common ones are derived from aloe vera, liquorice root, mulberry, grape seed, and soybean. Despite the widespread use of these extracts in sunscreens, the fate of their photodegradative products and role in ultraviolet (UV) photoprotection remain largely unknown and requires further investigation.

The medicinal properties of liquorice extract (*Glycyrrhiza glabra*) belonging to the *Leguminosae* family have been known since ancient Greece, Rome, and China (Fiore et al. 2005; Patil et al. 2012). The extracts have anti-inflammatory, immune-boosting, and anti-cancer effects, including protective effects against DNA damage. It is reported that in Japan liquorice extracts have been used to treat chronic hepatitis, offering therapeutic benefit against other viruses, including human immunodeficiency virus (HIV), cytomegalovirus (CMV), and *Herpes simplex* (Patil et al. 2012). There is a demonstrated efficacy of these extracts in treating atopic dermatitis, an allergy-related, and intensely itchy swelling of the skin (Morteza-Semnani et al. 2003). Liquorice root extracts are commonly used in skin-lightening preparations because of one of its major components, glycyrrhizin (Fig. 9.1), is associated the whitening effect.

Some organic sunscreens undergo photodegradation when exposed to sunlight, specifically UV light. Our investigation of the photostability of sunscreens in skin-lightening preparations showed a unique photostability of formulations containing plant extracts. Preparations containing among other ingredients, liquorice root extract showed an enhanced photoprotective effect. A major component of the liquorice root extract, glycyrrhizin (Fig. 9.1), first isolated and identified in the early 1990's is shows good absorption of harmful UVB (290-320 nm) and UVA (320-400 nm) radiation. It has been reported to protect human skin against UVB light-induced damage (Yokota et al. 1998; Rossi et al. 2005). Therefore, there may be benefit in incorporating liquorice root extract in sunscreen preparations because of its UV protective effects.
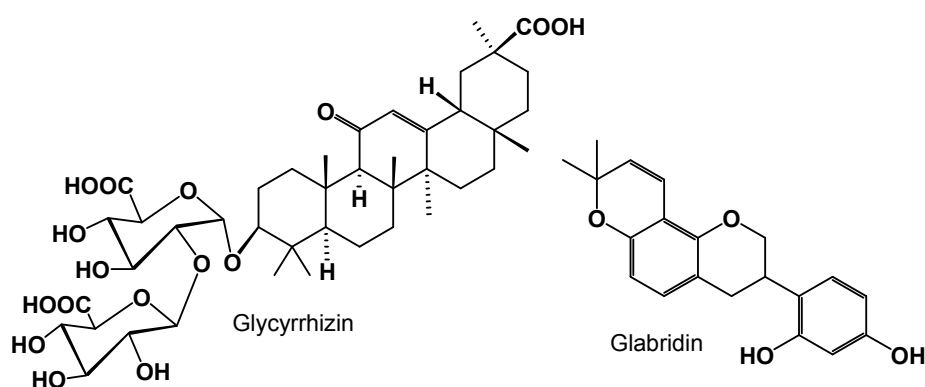
Figure 9.1: The major constituents of liquorice root extract.

A glycyrrhizin-rich liquorice extract has been shown to reduce inflammation resulting from UV light exposure when applied to the skin before exposure to UV light, thereby preventing redness and pigmentation (Yokota et al. 1998). There are claims that enzymes in liquorice extract aid in stimulating cell renewal following damage from UV rays for healthier glowing skin. Studies investigating the inhibitory effects of glycyrrhizin on melanogenesis and inflammation have shown that it inhibits tyrosinase activity of melanocytes. This is its proposed mechanism in the treatment of hyperpigmentation and in reversing the damage caused by acne scars. Another major constituent of liquorice root extract, namely, glabridin (Fig. 9.1), has been shown to protect against skin tumour

initiation and promotion (Wang et al. 1991). Other studies have shown that liquorice root extract antioxidant activity enhances the photostability of other compounds when added to a topical dermatological cream (Morteza-Semnani et al. 2003). The aim of this work was to investigate the effect of a methanolic liquorice root extract on the photostability of some commonly used sunscreens, namely, 2-ethylhexyl-*p*-methoxy cinnamate (EHMC), benzophenone-3 (BP3) and *tert*-butylmethoxy dibenzoylmethane (BMDBM).

9.2 Experimental

The effect of liquorice root extract on common sunscreen agents was investigated by firstly characterizing the constituents of the extract and then subjecting it to photochemical stability studies alone and when mixed with the sunscreen(s).

9.2.1 Materials

The liquorice root extract was purchased from Warren Chem Specialities (Pty) Ltd, South Africa. The solvents used HPLC-grade acetonitrile (ACN) and methanol (MeOH) were purchased from Merck KGaA. The three chemical UV filters of analytical purity (99.9 %) were purchased as follows: 2-ethylhexyl-*p*-methoxy cinnamate (EHMC) and *tert*-butylmethoxy dibenzoylmethane (BMDBM) were a kind donation from BASF, benzophenone-3 (BP3) was from Sigma-Aldrich and N,O-bis(trimethylsilyl)trifluoroacetamide (BSTFA) was purchased from Supelco.

9.2.2 Characterisation of liquorice root extract

The liquorice root extract was characterised by gas chromatography-mass spectrometry (GC-MS), gas chromatography-flame ionisation detection (GC-FID), and high performance liquid chromatography-mass spectrometry (HPLC-MS) in order to identify the chemical components present.

9.2.2.1 Sample preparation

About 25 mg of liquorice root extract powder was soaked in 25 mL of methanol at 25 °C and placed in an ultrasonic bath for two hours and then left to stand for 24 hours protected from light by aluminium foil. The extraction mixture was then made up to 50 mL in a volumetric flask with methanol. The resultant solution was filtered through a 0.45 μm Millipore Millex-LCR membrane filter and then transferred to an aluminium foil cased glass vial for storage. A 20 μL aliquot of this solution was injected into a high performance liquid chromatography-mass spectrometer (HPLC-MS) for characterisation of the chemical components in the extract. The remaining solution was preserved for photostability studies.

The liquorice root extract samples for gas chromatography-mass spectrometry (GC-MS) characterisation were firstly derivatised to volatilise the polyphenols in the extract. This was achieved by dissolving a sample mass of about 2 mg of extract powder in 1.0 mL of ACN in a clean, dry 3 mL reaction vial. To this solution 0.5 mL of N,O-bis(trimethylsilyl)trifluoroacetamide (BSTFA) was added, then capped tightly, mixed well, and heated at 70 °C for 45 min. The resultant derivatised mixture was filtered through a 0.45 μm Millipore Millex-LCR membrane syringe tip filter after cooling to room temperature. A volume of 0.1 μL of this derivatised sample was then injected into the GC-MS chromatograph.

9.2.2.2 The GC-MS experiment

A 0.1 µL volume of the derivatised liquorice root extract sample was delivered into a Shimadzu GC-MS (QP2010 SE), with a column temperature set at 70 °C and injection port at 250 °C. Injections were in split mode at a ratio of 20:1. Components were separated in a GL Sciences InertCap 5MS/Sil 30 m × 0.25 µm quartz capillary column with a bound stationary phase consisting of 5 % dimethylpolysilphenylene siloxane. The column was held 70 °C for 2 min, raised to 240 °C at 10 °C min^{-1}, then held for 5 min followed by a rise to 270 °C at 10 °C min^{-1} and held for 10 min. Helium was the carrier gas flowing with a linear velocity of 30.0 cm s^{-1}. The MS ion source temperature was 200 °C and the interface temperature was set at 250 °C. The MS detector was programmed to run in scan mode in the *m/z* range 35-1000 at a scan speed of 3333. The total run time was 37 min.

9.2.2.3 The GC-FID experiment

To check method interconvertability a GC-FID experiment was carried out on the same sample (derivatised liquorice root extract) with the same temperature program. The GC-FID used was a Shimadzu GC-2010, fitted with an autosampler AOC 20i and a flow unit type AFC-2010. Components were separated in a DB-5 (30 m × 0.25 µm) quartz capillary column with a bound stationary phase consisting of 5 % phenyl polysilphenylene-siloxane. The make-up gas was nitrogen/air flowing at 10 mL min^{-1}, the carrier gas was hydrogen with a flow rate of 40 mL min^{-1} and oxygen/air flowing at 400 mL min^{-1}. The injection port was set at 250 °C, operating in a split mode of 20:1 for an injection volume of 0.1 µL. The velocity flow control mode was adopted keeping the pressure at 61.9 kPa, the total flow rate at 5.0 mL min^{-1}, the column flow of 0.68 mL min^{-1}, and a linear velocity of 20.0 mL s^{-1}.

9.2.2.4   HPLC-MS analysis

The liquorice root extract dissolved in methanol (see Section 9.2.2.1) was characterised by means of HPLC-PDA-ESI-MS/MS. The analysis was carried out on an Agilent 1200 series LC MSD Trap, equipped with a photodiode array detector, a binary pump, a degasser, auto sampler, and an ESI Trap MS. This employed a G1312A binary pump, a G1316A autosampler, a G1322A degasser and a G1315D photodiode array detector controlled by ChemStation software (Agilent, v.08.04). The chromatographic separation was achieved on an Agilent Zorbax Eclipse XDB C-18 reversed-phase column (150 × 4.6 mm i.d.; 5 µm particle size). The mobile phase was composed of water:formic acid (99:1, v/v, solvent A) and acetonitrile (solvent B). The mixtures were resolved by a gradient elution as follows: 5–13 min, 16 % B; 13-18 min; 45 % B and held for 5 min; 23-28 min, 75 % B, held for 5 min; 33-40 min, 99 % B, then held 5 min and then dropped to 16 % B for 15 min. The experiment was performed at ambient temperature with a flow rate of 1 mL min^{-1} and an injection volume of 20 µL. The chromatograms were collected at detection wavelengths of 275 280, 286, 310, 320, and 358 nm with a bandwidth of 4 nm simultaneously in each of the 60 min run time. The photodiode array detector was set to collect the UV-vis spectra of the chemical species separated over the range of 190 to 800 nm. Analyses were interfaced to an Agilent-SL LC MSD trap equipped with an electrospray ionization source and operated in the negative-ion mode. The mass detector was a G2445A ion-trap mass spectrometer controlled by LCMSD software (Agilent, v.4.1). The nebulizing gas was nitrogen set at a pressure of 65 psi and flow rate adjusted to 116 mL min^{-1}. A heated capillary and voltage was maintained at 350 °C and 4 kV respectively. The instrument was programmed to scan over a mass range from *m/z* 90 to *m/z* 2000. The target ion accumulation in the trap was put at 30000 counts for a maximum accumulation time of 50 ms. MS[2] data were acquired in the negative ionization automatic smart mode to obtain MS[n-1]; primary precursor ion. The target ion was set at

m/z 350, the compound stability at 100 %, and the trap drive level at 90 %. One precursor was selected in each cycle; and excluded after averaging 3 spectra; the release time was 0.3 minutes. All collision-induced fragmentation experiments were performed in the ion-trap with helium as the collision gas, and the voltage was increased in cycles from 0.3 up to 2 V. The fragmentation time was 20 ms at an activation width of 10 amu and the cut-off for the daughter ion range set at 30 %. MS[3] data were obtained by manual fragmentation, targeting the most abundant ions in the precursor ion in the MS spectra.

9.2.3   Photostability experiments

The sunscreen mixture(s) with liquorice root extract were prepared by adding about 20 mg of the sunscreen agents to 25 mL of the methanol extract (see Section 9.2.2.1). This solution was then made up to 50 mL in a volumetric flask with methanol. To obtain working solutions, appropriate dilutions were carried out in order to obtain a sunscreen agent concentration of about 200 µmol dm^{-3} in the extract before photostability studies were done. Samples of liquorice root extract with and without sunscreens added were exposed to simulated solar light in a Newport research lamp housing (M66901) fitted with mercury-xenon lamp, powered by an arc lamp power supply (Newport 69911). The power output of the lamp was controlled by a digital exposure controller (Newport 68951) maintaining the output at 500 W. The radiation from the lamp was passed through a 10 mm thick Pyrex filter to ensure that only wavelengths greater than 300 nm impinged on the samples. The exposure time was varied incrementally from 0 hour in steps of 30 min to 4 hours of continuous exposure. Each exposed sample was contained in a stoppered 1.00 mm pathlength quartz cuvette. After each irradiation interval a UV-visible spectrum of the sample was recorded on a Perkin Elmer Lambda 35 UV-vis dual beam spectrophotometer. A 20 µL aliquot of these same solutions was then injected into a HPLC chromatograph to monitor the chemical transformations in the extract and the included sunscreen(s). Samples of the sunscreens alone dissolved in methanol were similarly irradiated and monitored by UV spectrophotometry.

9.2.3.1   HPLC analysis of the irradiated samples

The chemical transformations in the irradiated samples were monitored on a Shimadzu Prominence LC chromatograph with a PDA detector. The chromatographic separation was achieved on an Agilent Zorbax Eclipse XDB C-18 reversed-phase column (150 × 4.6 mm i.d.; 5 µm particle size). The mobile phase was composed of water (solvent A) and acetonitrile (solvent B). The mixtures were resolved by varying the concentration of B as follows: 5–13 min, 16 % B; 13-18 min, 45 % B and held for 5 min; 23-28 min, 75 % B, held for 5 min, 33-40 min, 99 % B then held 5 min and then dropped back to 16 % B for 15 min. The experiment was performed at ambient temperature with a flow rate of 1 mL min^{-1} and an injection volume of 10 µL. The chromatograms were collected at detection wavelengths of 275, 280, 286, 310, 320, and 358 nm with a bandwidth of 4 nm simultaneously in each of the 60 min run time. The photodiode array detector was set to collect the UV-vis spectra of the chemical species separated over the range of 190 to 800 nm.

9.3   Results and discussion

The components of liquorice root extract were first characterised before photostability studies were done on the extract alone and on its mixture(s) with the sunscreen agents.

9.3.1 Characterisation of liquorice root extract

Most plant extracts contain polar N-H and O-H groups which are responsible for strong hydrogen bonding that makes them essentially nonvolatile. Hydrogen on these functional groups can be substituted with a trimethysilyl (TMS) group in order to break the hydrogen bonding thus making them volatile. The presence of each TMS group on any GC-MS fragment is normally taken as 'acidic' hydrogen substitution by the TMS group during derivatization. The qualitative elucidation of the molecular ion can then be done by replacement of the TMS by a hydrogen atom. The chemical composition of the liquorice root extract was therefore identified by replacing the TMS group by H-on the phenolic and alcoholic GC-MS results. This is because a typical derivatization of hydroxylated polycyclic aromatic hydrocarbons into TMS ethers using BSTFA follows the scheme in Fig. 9.2 under hydrophobic conditions. The hydrophobic conditions must be attained because the TMS group substitutes exchangeable, 'acidic' protons and therefore hydrolysis of water may prevent any further derivatization of the analyte (Fig. 9.2 and 9.3).
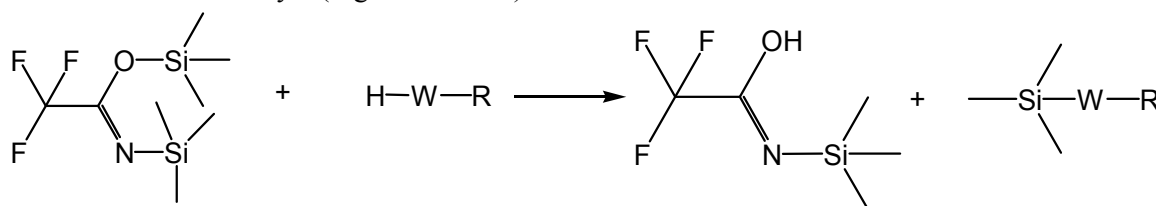
Figure 9.2: General scheme for silylation reaction using N,O–bis(trimethylsilyl)trifluoro-acetamide: TMS = $Si(CH_3)_3$, W = O, S, NH, NR', COO, R, R' = Alk, Ar.
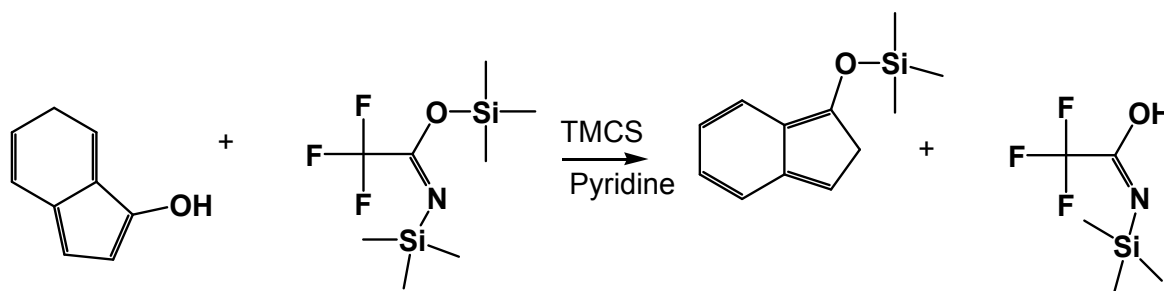
Figure 9.3: Typical derivatization reaction of a secondary metabolite by BSTFA.

However, the reconstructions of the parent secondary metabolites in the liquorice root extract pose a challenge owing to the complex composition of the extract. The total ion chromatogram from the GC-MS (Fig. 9.4) showed high intensities of the fructopyranose and fructofuranose silylated fragments indicating high abundance of glycyrrhizin in these extracts (Fig. 9.5). The remaining less intense signals could be attributed to the fragmentation of glabridin giving rise to hydroxyl cinnamic acid moieties (Fig. 9.6).

The methanolic extract considered in this work is expected to have a high concentration of flavonoids. The major constituents in liquorice root extract are glabridin and glycyrrhizin (Fig. 9.1). These compounds are known to dissociate upon electron impact through a limited number of assumed pathways. The origin of diagnostically valuable fragments can be explained by a retro-aldo fragmentation of the molecular ion and the daughter fragment (Denisova et al. 2006). The flavanolic cleavage forms a set of fragments including the A- and B-rings and cleavage of the pyran ring at the third C atom. The many alcoholic fragments observed in this work can be attributed to the high concentration of glycyrrhizin, whose sugar cleavage gives fructofuranose and fructopyranose moieties (Fig. 9.5). The hydroxycinnamic acid moieties could similarly be attributed to the fragmentation of

glabridin, another known constituent of liquorice root extracts (Fig. 9.6). The successive cleavage of a silyl substituent as CH_2SiMe_3 or $\cdot SiMe_3$ gives rise to various identified chemical components (Fig. 9.7 and Fig. 9.8).
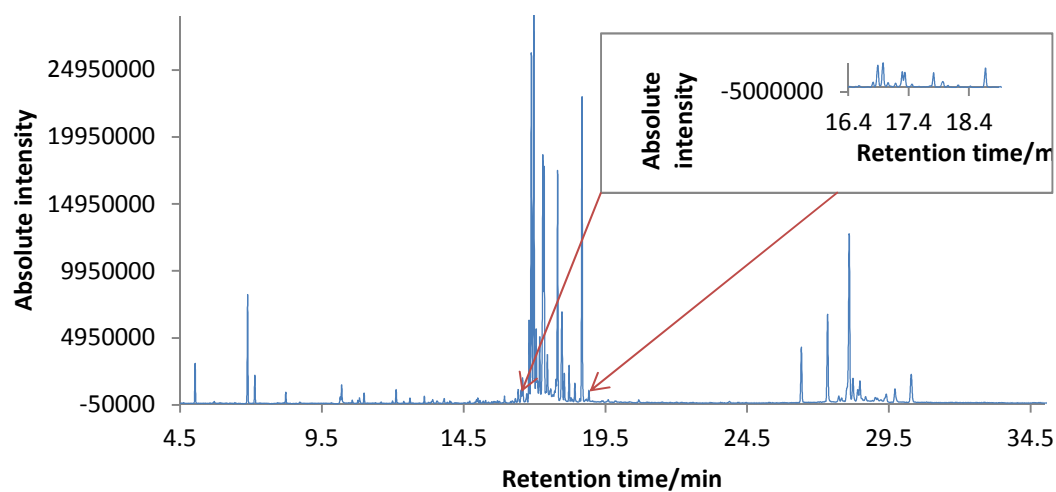
Figure 9.4: The total ion chromatogram of a derivatized sample of liquorice root extract on GC-MS. The separation was effected on a GL Sciences InertCap 5MS/Sil 30 m × 0.25 μm quartz capillary column under the conditions described in Section 9.2.2.2.
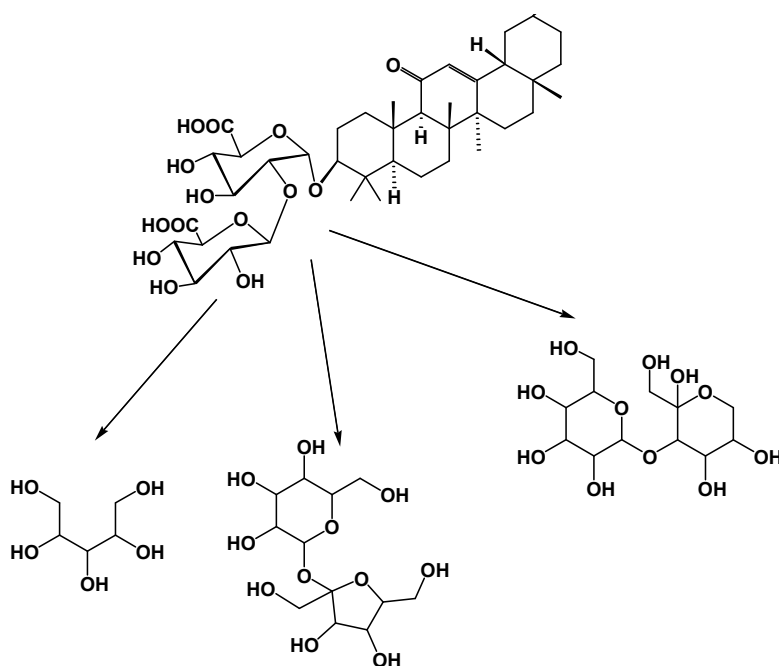
Figure 9.5: The proposed fragmentation scheme of the sugar moiety of glycyrrhizin.
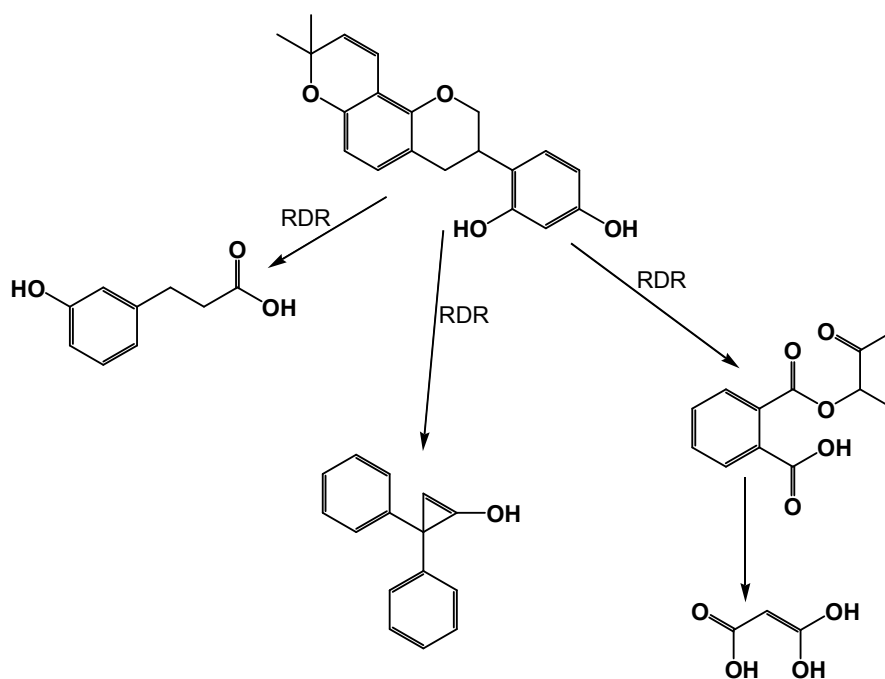
Figure 9.6: An anticipated fragmentation pattern of glabridin in a retro-diene reaction fashion modified by trimethyl silyl groups.

3-(4-hydroxyphenyl)propanoic acid

pentane-1,2,3,4,5-pentaol

(Z)-3-hydroxy-2-isopropylbut-2-enoic acid

3-(3-hydroxyphenyl)propanoic acid

3,3-dihydroxyacrylic acid

2-((3-oxobutan-2-yloxy)carbonyl)benzoic acid

2,4-dihydroxybutanoic acid

2-hydroxyacetic acid

2-(hydroxymethyl)-6-(2,4,5-trihydroxy-2-(hydroxymethyl)-tetrahydro-2H-pyran-3-yloxy)-tetrahydro-2H-pyran-3,4,5-triol

2,3-dihydroxypropanoic acid

3,3-diphenylcycloprop-1-enol

3-hydroxypropanoic acid

2-(3,4-dihydroxy-2,5-bis(hydroxymethyl)-tetrahydrofuran-2-yloxy)-6-(hydroxymethyl)-tetrahydro-2H-pyran-3,4,5-triol

2-hydroxypropanoic acid   4-(2-(4-methoxyphenyl)propan-2-yl)phenol

propane-1,2,3-triol

5-(hydroxymethyl)-6-(5-methyl-2-(prop-1-en-2-yl)phenoxy)-tetrahydro-2H-pyran-2,3,4-triol

Figure 9.7: Some of the chemical constituents of liquorice root extract identified in this work.

(*Z*)-3-hydroxy-2-isopropylbut-2-enoic acid

2-hydroxysuccinic acid

3,4-dihydroxybutanoic acid

pentane-1,2,4,5-tetraol

79%

3,4,5,6-tetrahydroxy-2-oxohexanoic acid

5-(1,2-dihydroxyethyl)-3-hydroxy-dihydrofuran-2(3*H*)-one

2,5-bis(hydroxymethyl)-
tetrahydrofuran-2,3,4-triol

(2*R*)-2,3,4,5-tetrahydroxy-2-methylpentanoic acid

3,4,5-trihydroxybenzoic acid

5-(2,3-dihydroxypropyl)-
tetrahydrofuran-2,3,4-triol

fumaric acid

6-methoxycyclohexane-1,2,3,4,5-
pentaol

3,3-dihydroxyacrylic acid

6-(hydroxymethyl)-tetrahydro-2*H*-pyran-2,3,4,5-tetraol

Figure 9.8: More constituents of liquorice root extract identified by GC-MS.

9.3.2 Photostability studies of the liquorice root extract

The prolonged exposure of a methanolic solution of liquorice root extract to simulated solar radiation showed a notable degree of photodegradation (Fig. 9.9). This photodegradation is observed mainly in the UVB region as the drop in absorption in the UVA1 (340-400 nm) region remains fairly stable. The HPLC chromatograms of the same samples show rearrangement of the two major constituents of the liquorice root extract initially present (Fig. 9.10). The photo-absorptive capacity observed with this extract can be attributed in part to the -enone, π-bond conjugation in glycyrrhizin and the –diene, π-bond conjugation in glabridin. The Woodward-Fieser predictive calculation for the glycyrrhizin chromophore gives a wavelength of absorption > 259 nm. Imposing similar selection rules on the – diene system of the glabridin molecule gives a wavelength > 319 nm (Fig. 9.11). However, it should be noted that these rules only give benchmark values. The actual absorbance may differ by about 5-6 nm or higher. These absorption explain why the liquorice root extract shows good absorption in the UVB and fair absorption in the UVA (Fig. 9.9).

Figure 9.9: The photodegradation of the liquorice root extract dissolved in methanol exposed to simulated solar radiation, in a 1 mm pathlength quartz cuvette. Each exposure circle involved use of fresh sample extract. The spectra were recorded on a Perkin Elmer Lambda 35 UV-vis deal beam spectrophotometer.
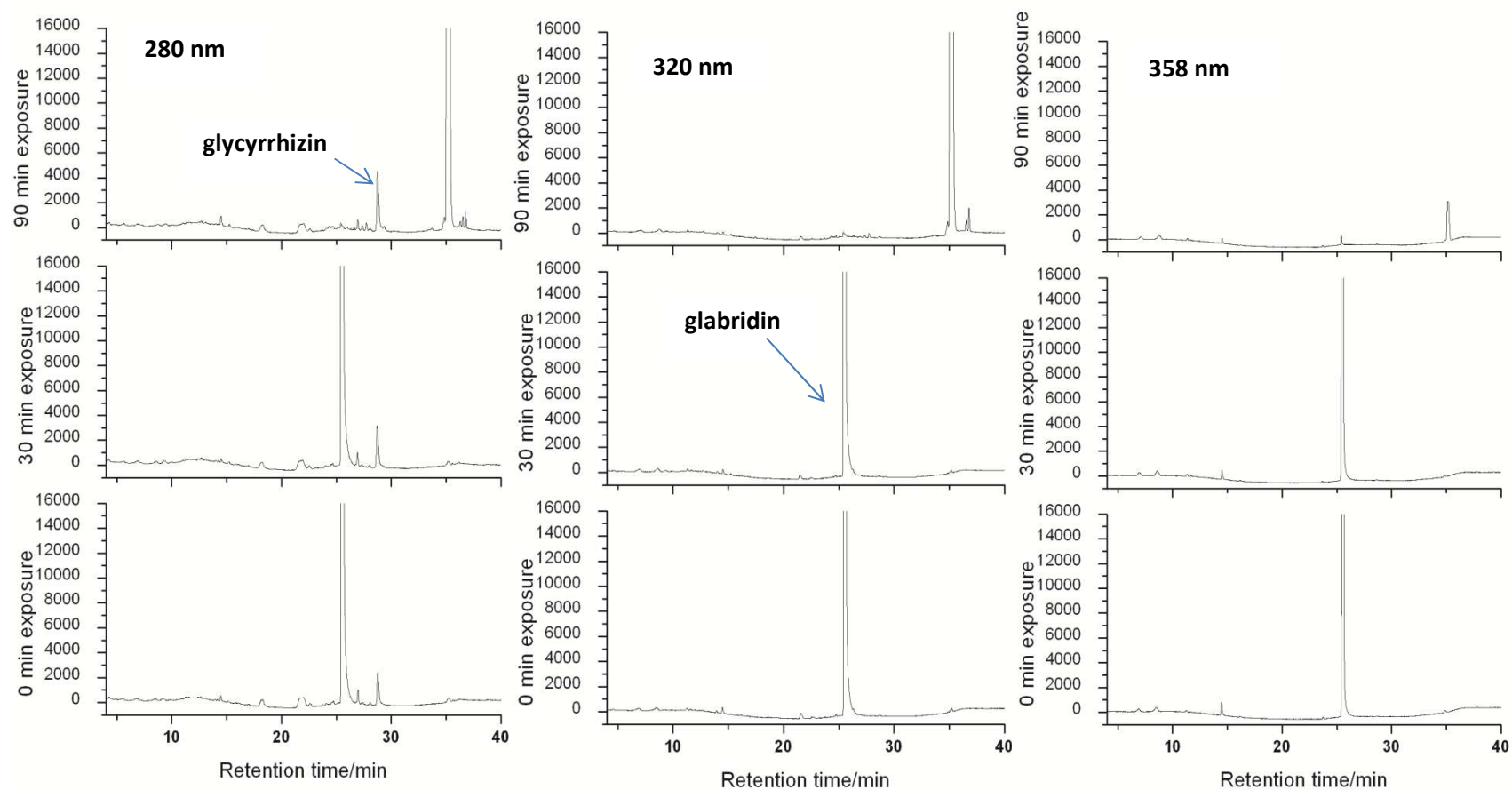
Figure 9.10: Photo-induced chemical changes in liquorice root extract secondary metabolites exposed to simulated solar radiation, monitored on a HPLC at 280, 320, and 358 nm. The separation was effected on a Zorbax Eclipse-XDB C-18 column (150 mm × 4.6 mm, i.d., 5 µm). The mobile phase was a gradient elution of acetonitrile-water with a flow rate of 1.00 mL min^{-1} and the injection volume was 20 µL.

Base value = 253 nm
exo conjugation = 30 nm
4- alkyl groups = 20 nm
2- exo cyclic = 10 nm
1- OR = 6 nm
λ_{max} = 319 nm

Base value = 215 nm
β– ring reisdues = 24 nm
4 exo cyclics = 20 nm
λ_{max} = 259 nm
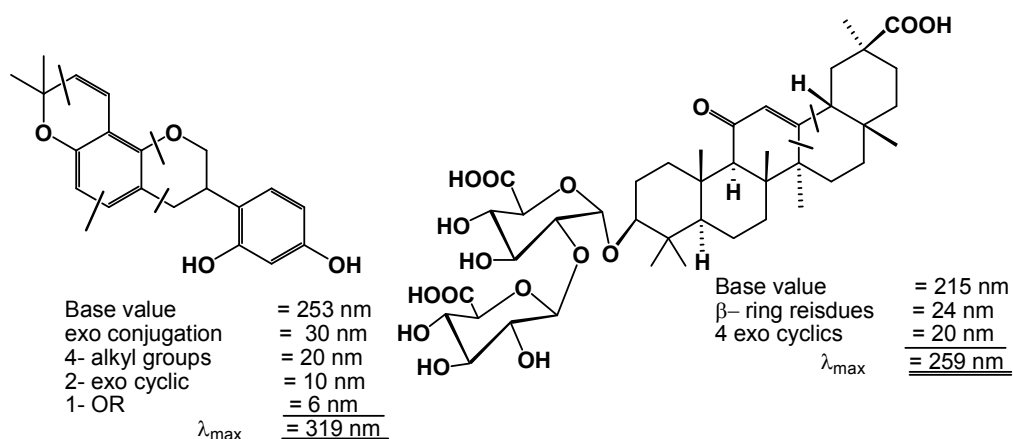
Figure 9.11: Predicted wavelengths of maximum absorption for glycyrrhizin and glabridin based on the Woodward-Fieser selection rules.

The chromatogram of the unexposed sample at 358 nm shows a very small peak for the prominent peak observed at 280 nm (Fig. 9.10). This indicates that, this species does not absorb sufficiently at a longer UV wavelength (358 nm), consistent with the predicted value from Woodward-Fieser values calculated above (Fig. 9.11). The photochemical reactions are observed after 30 minutes of exposure for which a number of peaks appear and others disappear. These can be explained in terms of photo-induced, repeated Norrish type I processes yielding a range of substituted flavonols and other associated photochemical rearrangement products. These chemical species show the relative absorbance in the long wavelength region as indicated by the new peak observed at 358 nm (Fig. 9.10).

9.3.3   Effect of liquorice root extract on the photostability of BP3

The photochemical response of a methanol solution of BP3 irradiated with solar simulated radiation was firstly investigated. The UV spectra of BP3 showed photostability (Fig. 9.12). The HPLC analysis of these same solutions also showed only one peak at 286 nm indicating that BP3 did not photodegrade in the present conditions (Fig. 9.13). This could be attributed to hydrogen bonding between the carbonyl and *ortho*-hydroxyl group that interferes with the n, π* excitation of the carbonyl chromophore. It is known that *ortho*-hydroxybenzophenone does not undergo photoreduction (Placzek et al. 2013) and stabilises the chromophore, namely, the carbonyl group.
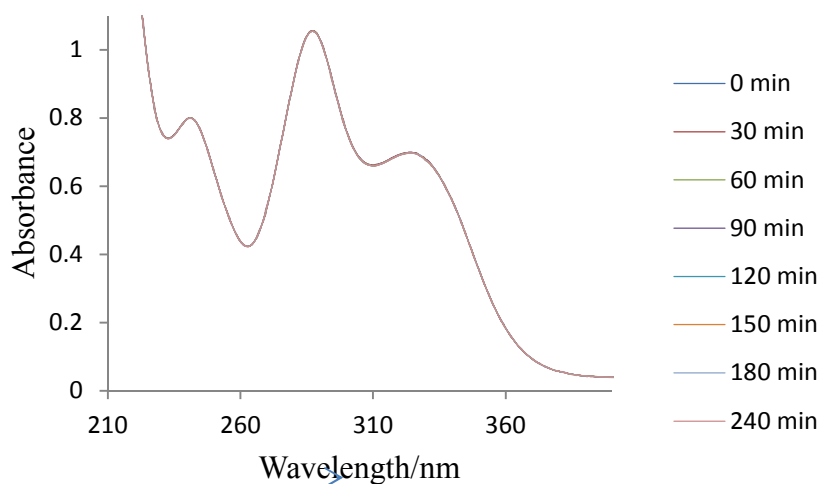
Figure 9.12: The spectral stability of BP3 in methanol irradiated by a solar simulated source. The spectra were acquired on a Perkin Elmer Lambda 35 UV-vis spectrophotometer in a 1 mm pathlength quartz cuvette with air as the reference.
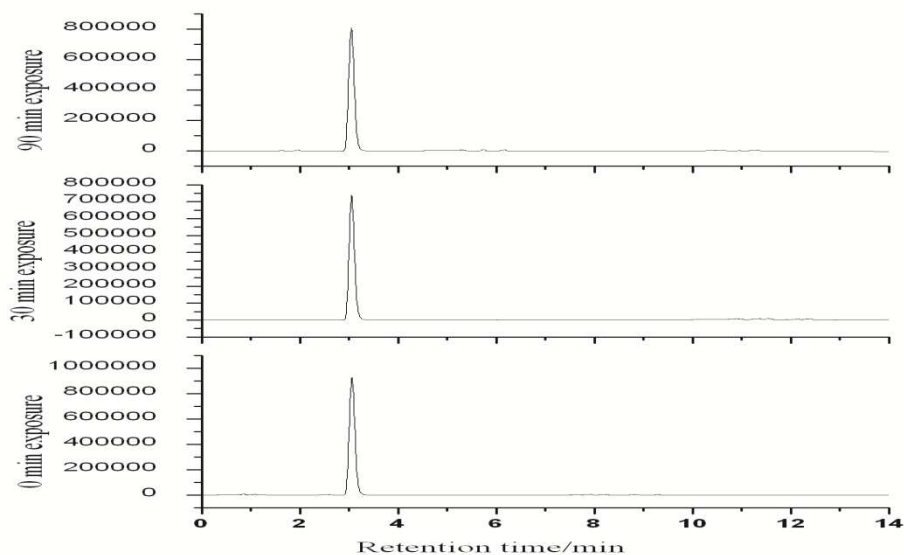
Figure 9.13: The photostability of BP3 monitored by HPLC at 286 nm. A reversed phase Zorbax Eclipse-XDB C-18 column (150 mm × 4.6 mm) column was used with mobile of methanol-water (84:16 % v/v). The injection volume was 20 μL and the flow rate set at 1 mL min^{-1}.

The irradiation of a methanolic solution of BP3 and liquorice root extract showed a small photodegradation followed blue a blue shift in the spectra of BP3 (Fig. 9.14). The HPLC chromatograms of the liquorice root-BP3 mixture gave rather interesting results. The retention time of the BP3 peak varied on the chromatograms and incremental exposure time gave varying retentions for various prominent peaks at various wavelengths of analysis (Fig. 9.15). We speculate that because the UV spectra remained essentially the same, then the carbonyl chromophore is not affected by the reactions and the attack is on the phenyl rings. These reactions could be responsible for the variation of the BP3 peaks and these reactions do not necessarily require light. This observation may in part agree with work by Schallreuter et al. (1996), who proposed possible photoreactions of BP3 culminating in the photo-oxidation of BP3 to semiquinone. But the HPLC analysis from the current work, however, suggests a possible dark reaction that may not necessarily lead to semiquinone formation. It can be further speculated that inclusion of BP3 in the solution containing liquorice root extract introduces proton-type photochemical reactions. We envisage ground state reactions of BP3 that could involve C-C coupling of a radical pair generated by H-abstraction on the BP3 phenyl ring with the fructopyranose moiety (Fig. 9.16).

It is known that BP3 is a derivative of benzophenone and absorbs UV radiation up to 360 nm. The intersystem crossing quantum yield of benzophenones is about 1, and the energy of its n, π^* lowest triplet excited state (TET) is about 290 kJ mol^{-1} (Cowley 1997; Murai et al. 1978; Cai et al. 2005). These compounds are known photosensitizers with singlet oxygen ($^1O_2$) production quantum yields of about 0.3. We associate the peaks observed at 358 nm on prolonged exposure (at 90 min) with reactions of the triplet excited state, of BP3, with photosentised liquorice root extract components. The chemical species formed therefore alter the retention time of BP3 without affecting the chromophore (C=O). The other observed peaks arise from various reaction pathways. Upon light absorption, the triplet-triplet energy transfer (TTET) initiated reactions together with both type I (hydrogen atom or electron transfer) and type II (singlet oxygen) processes take effect. These reactions are sustained by thermal population of the upper vibrational states of the excited triplet state of BP3. Both glycyrrhizin and glabridin may be photosensitized by the triplet excited state of BP3 and therefore undergo a Patternò-Büchi [$_\sigma$2+$_\pi$2] photo-cycloaddition giving rise to oxetanes (Fig. 9.17 and Fig. 9.18). These reactions are known to compete with TTET and are favoured for n,π^* triplets when the excited state of the alkene is comparable to or higher than that of the carbonyl compound.
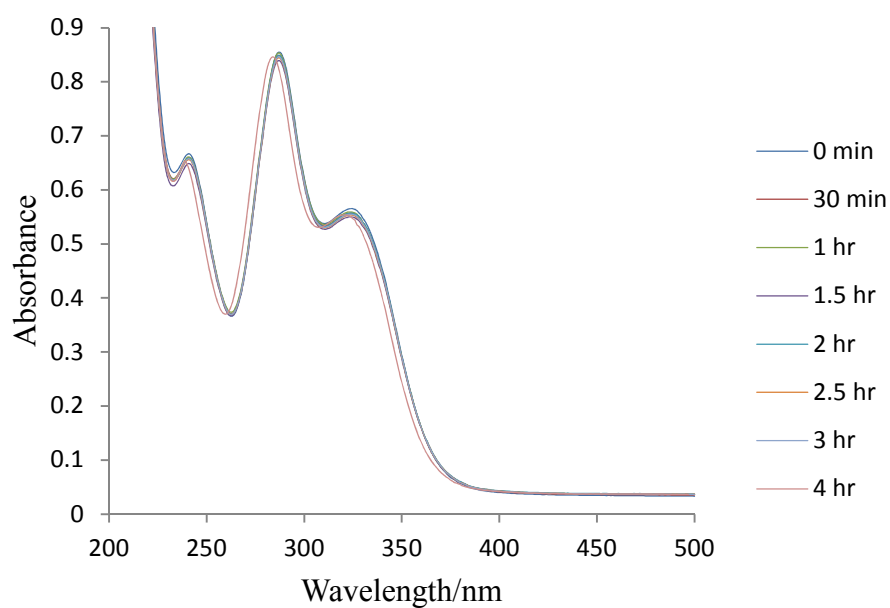
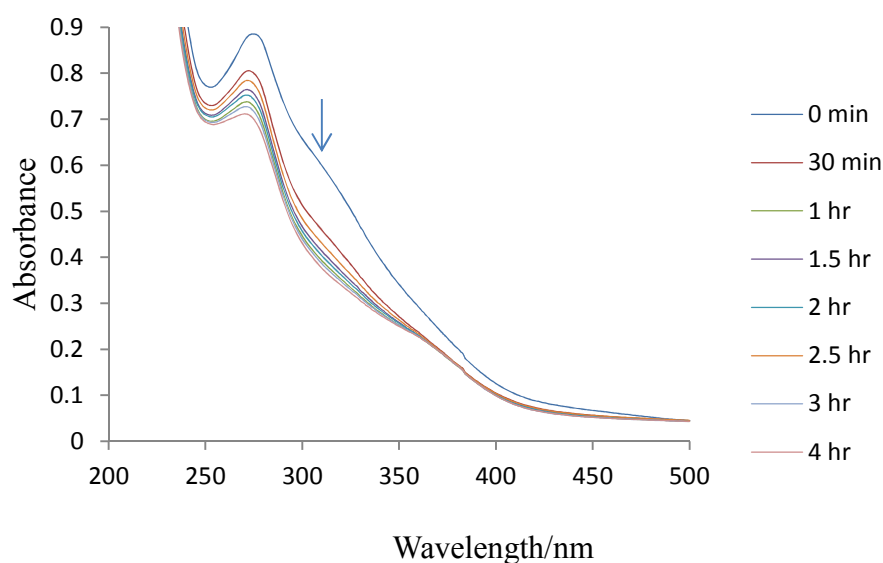Figure 9.14: The photostability of BP3 incorporated in liquorice root extract dissolved in methanol when exposed to simulated solar radiation, in a 1 mm pathlength quartz cuvette. Each exposure event involved use of fresh sample solution. The spectra were recorded on a Perkin Elmer Lambda 35 UV-vis dual beam spectrophotometer.
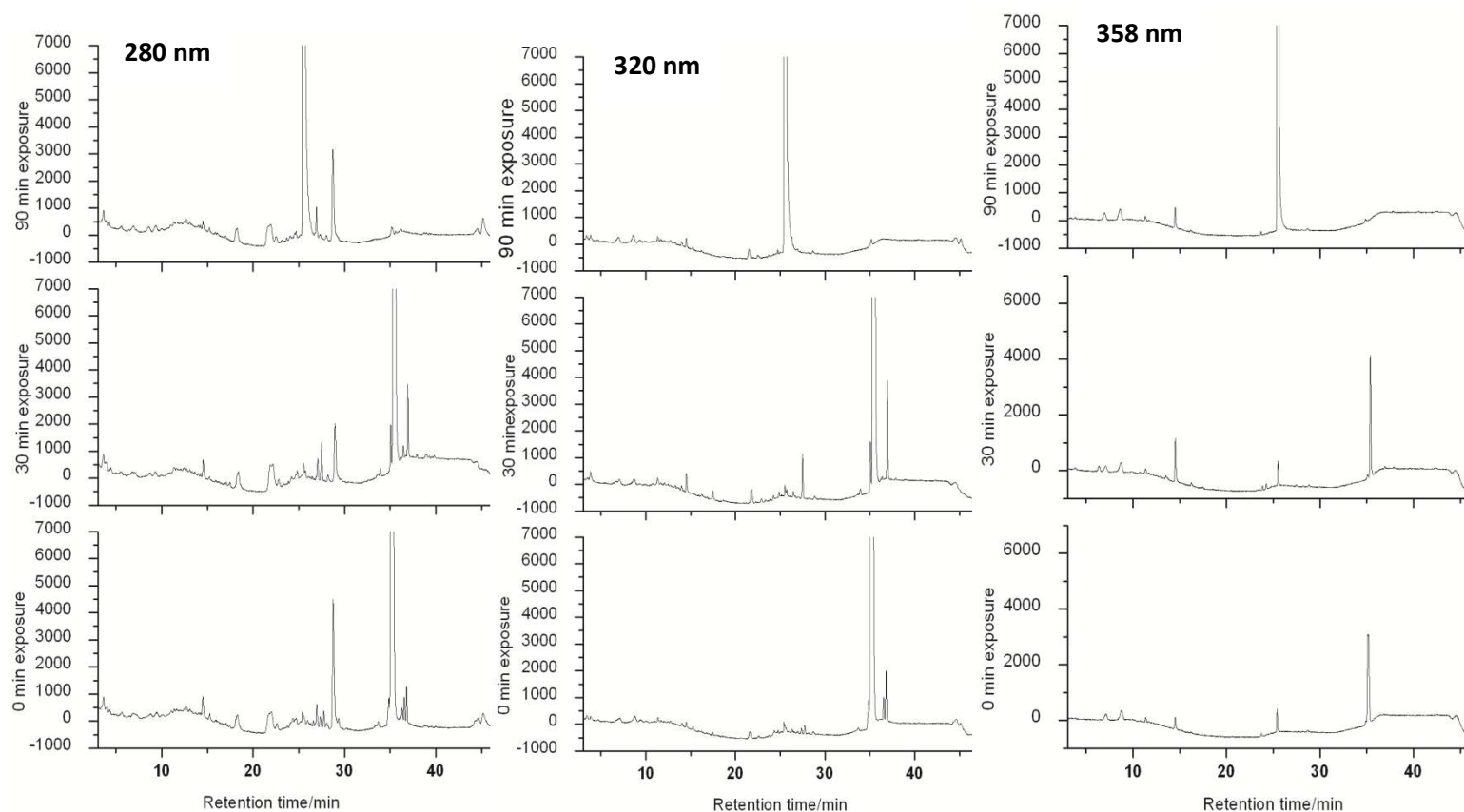
Figure 9.15: HPLC chromatograms of the photochemical changes when BP3 is incorporated in the liquorice root extract dissolved in methanol and irradiated by simulated solar radiation. The chromatograms were monitored at 280, 320, and 358 nm. The separation was effected on a Zorbax Eclipse-XDB C-18 (150 mm x 4.6 mm, i.d., 5 μm) column. The mobile phase was a gradient elution of acetonitrile-water with flow rate of 1.00 mL min^{-1} and the injection volume was 20 μL. The BP3 could not be identified because the retention time changed from the one shown under these conditions.
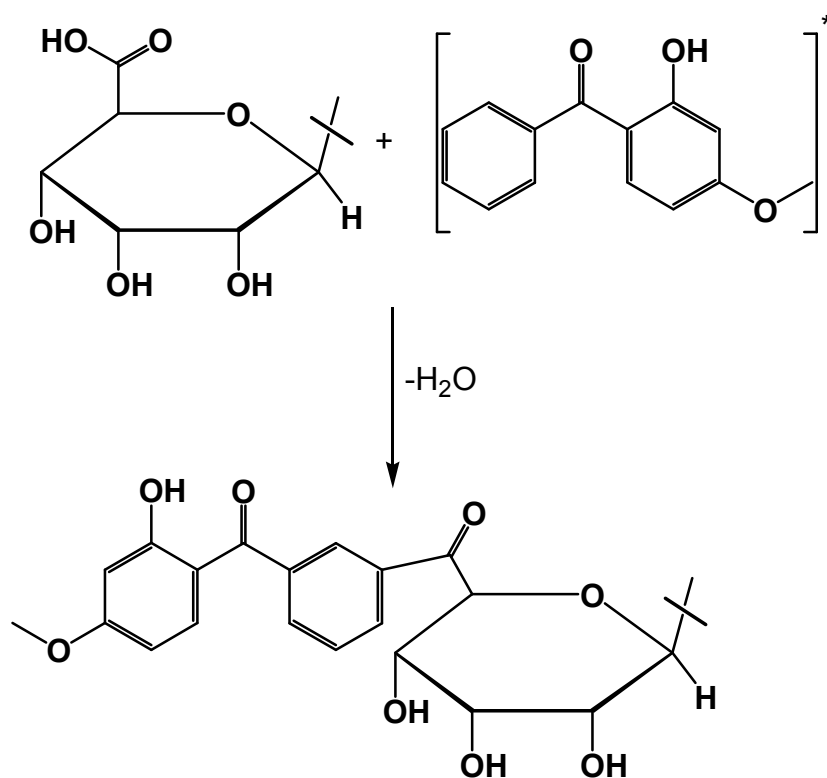
Figure 9.16: Proposed reaction of the excited state BP3 with the fructopyranose moiety of glycyrrhizin.
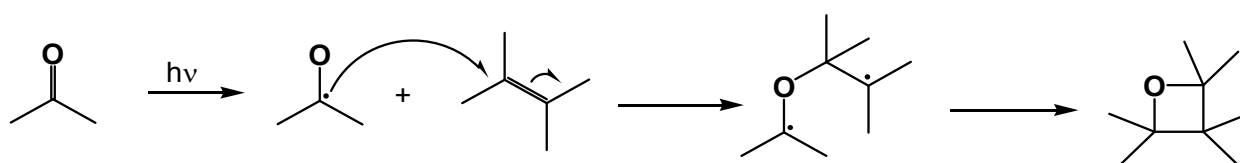
Figure 9.17: The Patternò-Büchi mechanism proposed for the photodegradation of BP3 and BMDBM in the liquorice root extract.
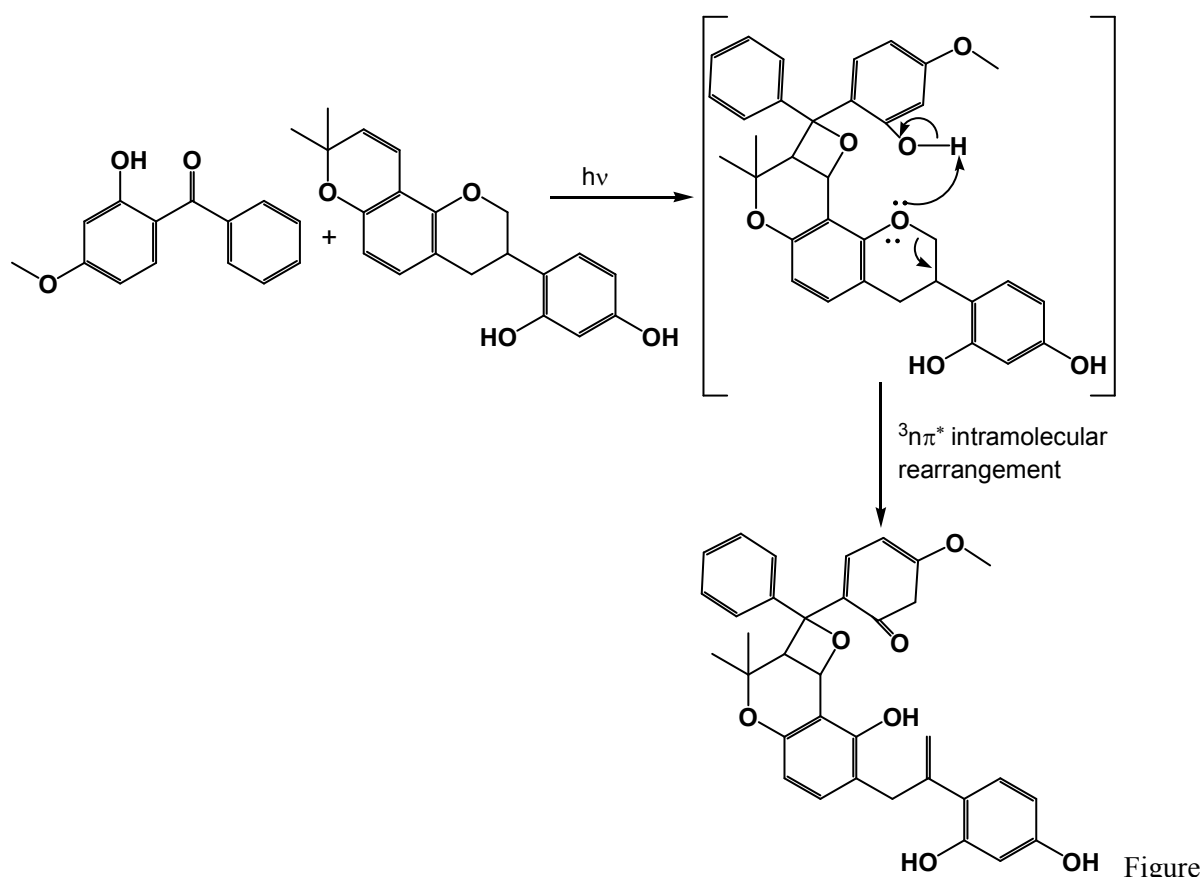
Figure 9.18: Proposed photo-induced reactions of BP3 with glabridin exposed to solar simulated radiation.

9.3.4 Effect of liquorice root extract on the photostability of BMDBM

The photostability of a methanol solution of BMDBM was first investigated by irradiation of the solution with a simulated solar source. The characteristic photodegradation of BMDBM was demonstrated by the spectral lability observed in the UV spectra (Fig. 9.19). A drop of 0.4 absorbance units was recorded in this work for a four-hour period of continuous exposure. The HPLC analysis did not show a sufficient decrease in the peak area of the *enol*-BMDBM at 358 nm (Fig. 9.20). Several working groups have demonstrated the photostability of *enol*-BMDBM in polar protic solvents (Mturi and Martincigh 2008). The UV spectra show an increase in the absorbance at 260 nm but the HPLC chromatograms monitored at 260 nm did not show an appreciable change. This could be attributed to the difference in the sensitivity of the instruments and the fact that *keto*-BMDBM formation is not favoured by a highly polar protic medium. The UV spectra of BMDBM in a mixture with liquorice root extract show a drop in absorption capacity with increase in irradiation time (Fig.9.21). A comparison of the spectral changes under the same conditions with those of BMDBM alone (Fig. 9.19), shows that the absorbance drop is smaller. A notable difference is the reduction in the *keto*-form of BMDBM observed at 260 nm against the decay of the *enol*-form of BMDBM. The assumption here is that in this mixture the BMDBM *keto-enol* tautomerism may only occur to a limited extent but rather decomposition to other chemical species takes place. This indicates that, liquorice root extract diminishes the *keto*-formation but fails to completely protect against *enol*-BMDBM degradation. It can be concluded that liquorice root extract may only partially photostabilize BMDBM. BMDBM is known to photodegrade in UV light in a nonpolar solvent and to break into two radicals: the phenacyl and benzoyl radicals (Schwack and Rudolph 1995). The HPLC chromatogram shows chemical species absorbing in the UVA region, characteristic with the

photo-rearrangement and radical disproportionation reaction of BMDBM (Fig. 9.22, Supplementary Materials Table S9.3). Here also we envisage the participation of BMDBM in Patternò-Büchi type reactions but preserving the *enol*-chromophore (Fig. 9.17).
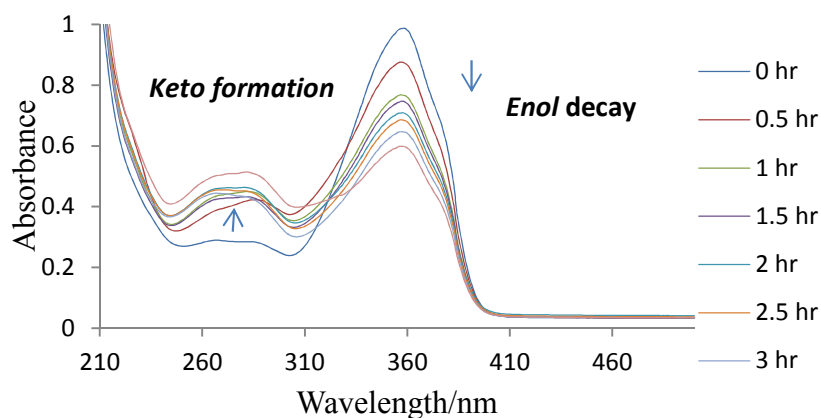
Figure 9.19: The spectral changes of BMDBM dissolved in methanol and irradiated by a solar simulated light source. The spectra were acquired with a Perkin Elmer Lambda 35 UV-Vis spectrophotometer in a 1 mm pathlength quartz cuvette with air as the reference.
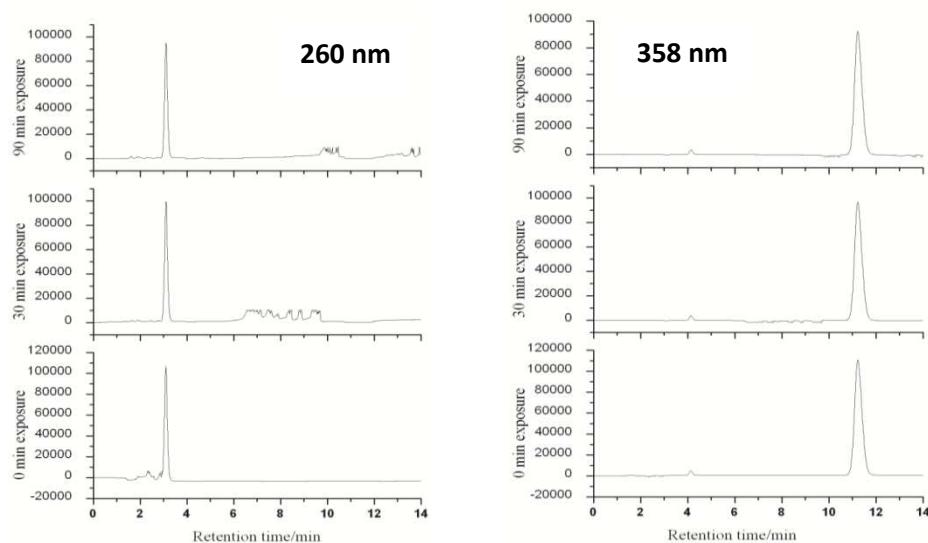
Figure 9.20: The photochemical changes of BMDBM monitored at 260 and 358 nm on a reversed-phase Zorbax Eclipse-XDB C-18 (150 mm x 4.6 mm) column with methanol-water (84:16 % v/v) mobile phase. The injection volume was 10 μL and the flow rate set at 1 mL min^{-1}.
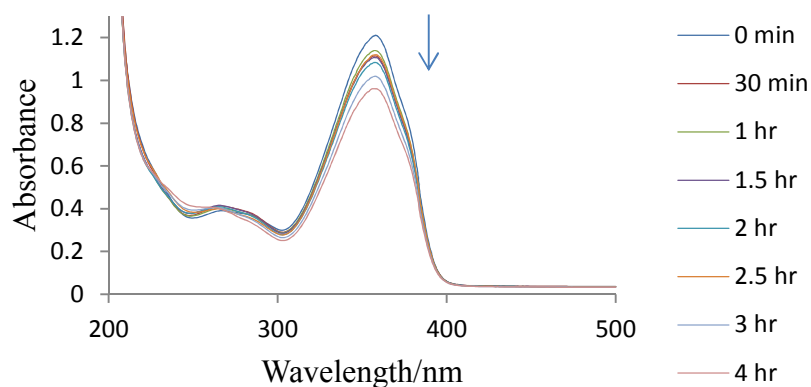
Figure 9.21: The photodegradation of BMDBM in liquorice root extract exposed to UV radiation in methanol, in a 1 mm pathlength quartz cuvette. Each exposure event involved the use of a fresh sample mixture. The spectra were recorded on a Perkin Elmer Lambda 35 spectrophotometer.

Figure 9.22: The photo-induced chemical transformations of a mixture of BMDBM and liquorice root extract in methanol. The HPLC chromatograms were detected at 280, 320, and 358 nm. The separation was effected on a Zorbax Eclipse-XDB C-18 column (150 mm × 4.6 mm, i.d., 5 μm). The mobile phase was a gradient elution of acetonitrile-water with a flow rate of 1.00 mL min^{-1} and the injection volume was 20 μL.

9.3.5 Effect of liquorice root extract on the photostability of EHMC

The irradiation of a methanolic solution of EHMC with solar simulated radiation for an incremental period of time shows a spectral lability (Fig. 9.23).   The HPLC analysis indicates formation of *cis*-EHMC which absorbs shorter wavelengths (Fig. 9.24).   This could explain the spectral lability observed during the photo-isomerisation of *trans*-EHMC to *cis*-EHMC. Pattanaargson et al. (2004) and Broadbent et al. (1996) have previously reported the photoisomerisation of EHMC under UV irradiation.
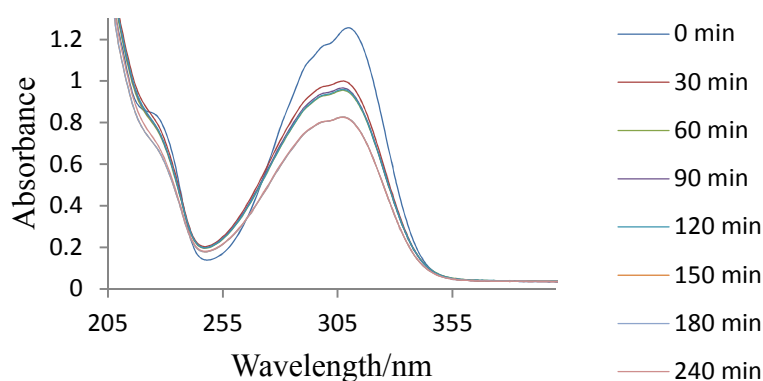
Figure 9.23: Photoinstability of EHMC dissolved in methanol under solar simulated irradiation. The spectra were acquired with a Perkin Elmer Lambda 35 UV-VIS spectrophotometer in a 1 mm pathlength quartz cuvette with air as the reference.
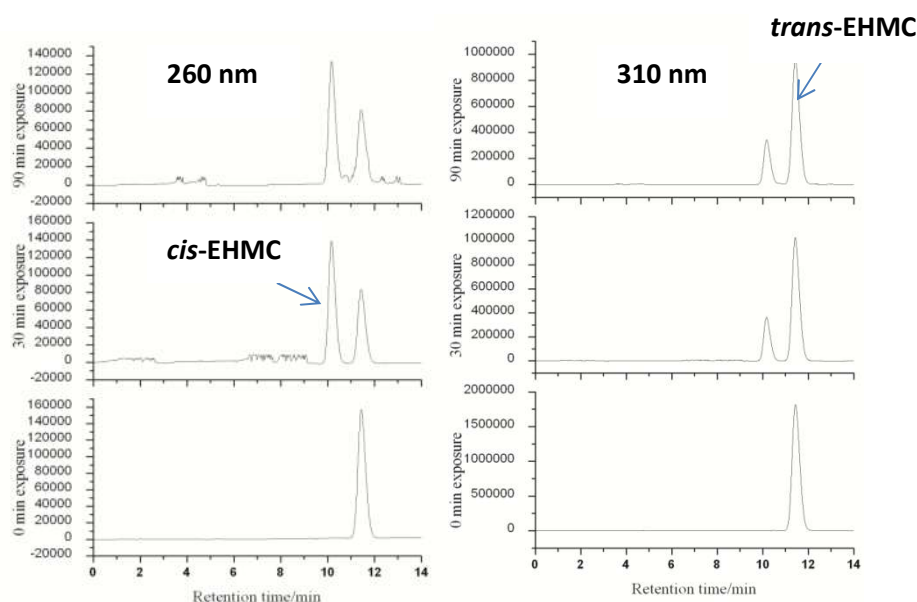
Figure 9.24: Isomerisation of EHMC under simulated solar irradiation monitored by HPLC at 260 and 310 nm on a reversed phase Zorbax Eclipse-XDB C-18 column (150 mm × 4.6 mm) with a methanol-water (84:16 % v/v) mobile phase. The injection volume was 20 µL and the flow rate set at 1 mL min^{-1}.

The photo-response of the mixture of EHMC with liquorice root extract was eratic with a sudden increase in the photo-absorption and then a fall (Fig 9.25). This is unlike the cinnamate spectral decay observed when EHMC is dissolved in methanol (Fig 9.23). The HPLC analysis of these solutions showed the formation of strongly absorbing chemical species on continued exposure above 30 min (Fig. 9.26). This could be attributed to [2+2] cycloaddition and Patternò-Büchi carbonyl-alkene reactions from the nπ* (Fig. 9.27).
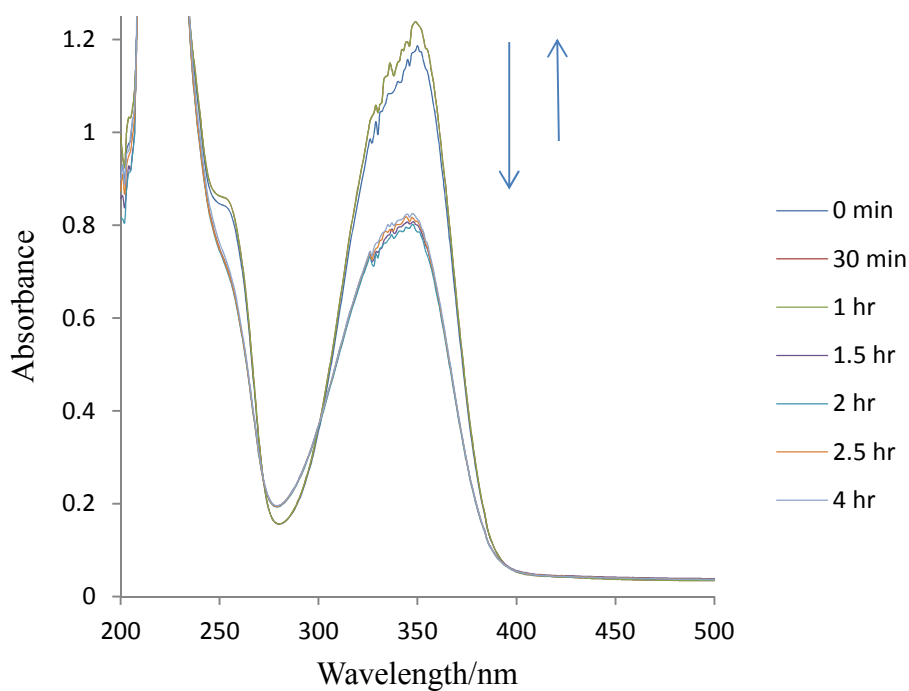
Figure 9.25: The photoinstability of EHMC in liquorice root extract dissolved in methanol when exposed to simulated solar radiation, in a 1 mm pathlength quartz cuvette. Each exposure event involved use of a fresh sample solution. The spectra were recorded on a Perkin Elmer Lambda 35 dual beam spectrophotometer.
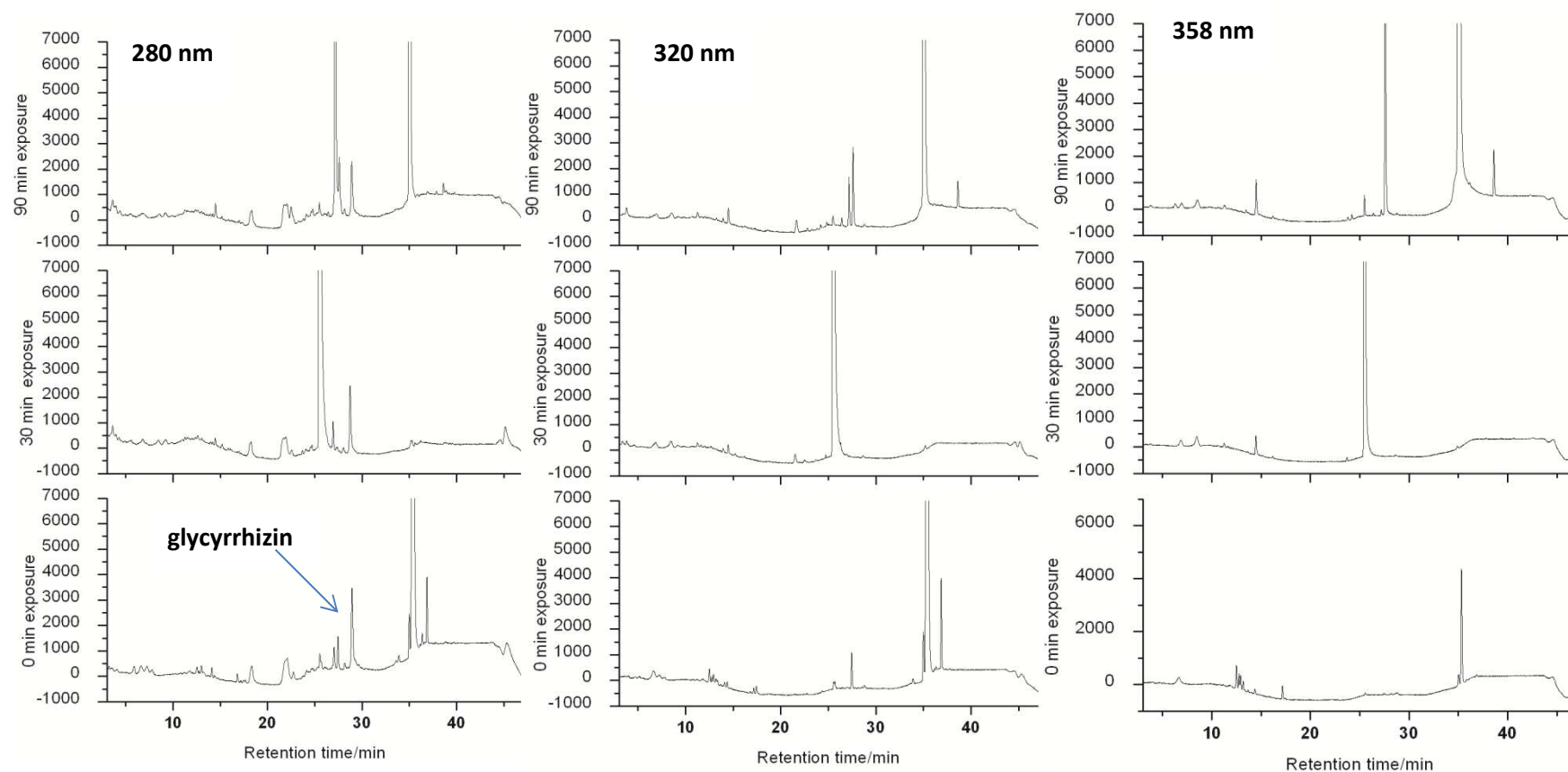
Figure 9.26: HPLC chromatograms of the photo-induced chemical reaction of EHMC with liquorice root extracts dissolved in methanol, irradiated by solar simulated radiation. The chromatograms were monitored at 280, 320, and 358 nm. The separation was effected on a Zorbax Eclipse-XDB C-18 (150 mm × 4.6 mm, i.d., 5 μm) column. The mobile phase was a gradient elution of acetonitrile-water with a flow rate of 1.00 mL min^{-1} and the injection volume was set 20 μL. The EHMC peak and the glabridin could not be resolved under these conditions. .
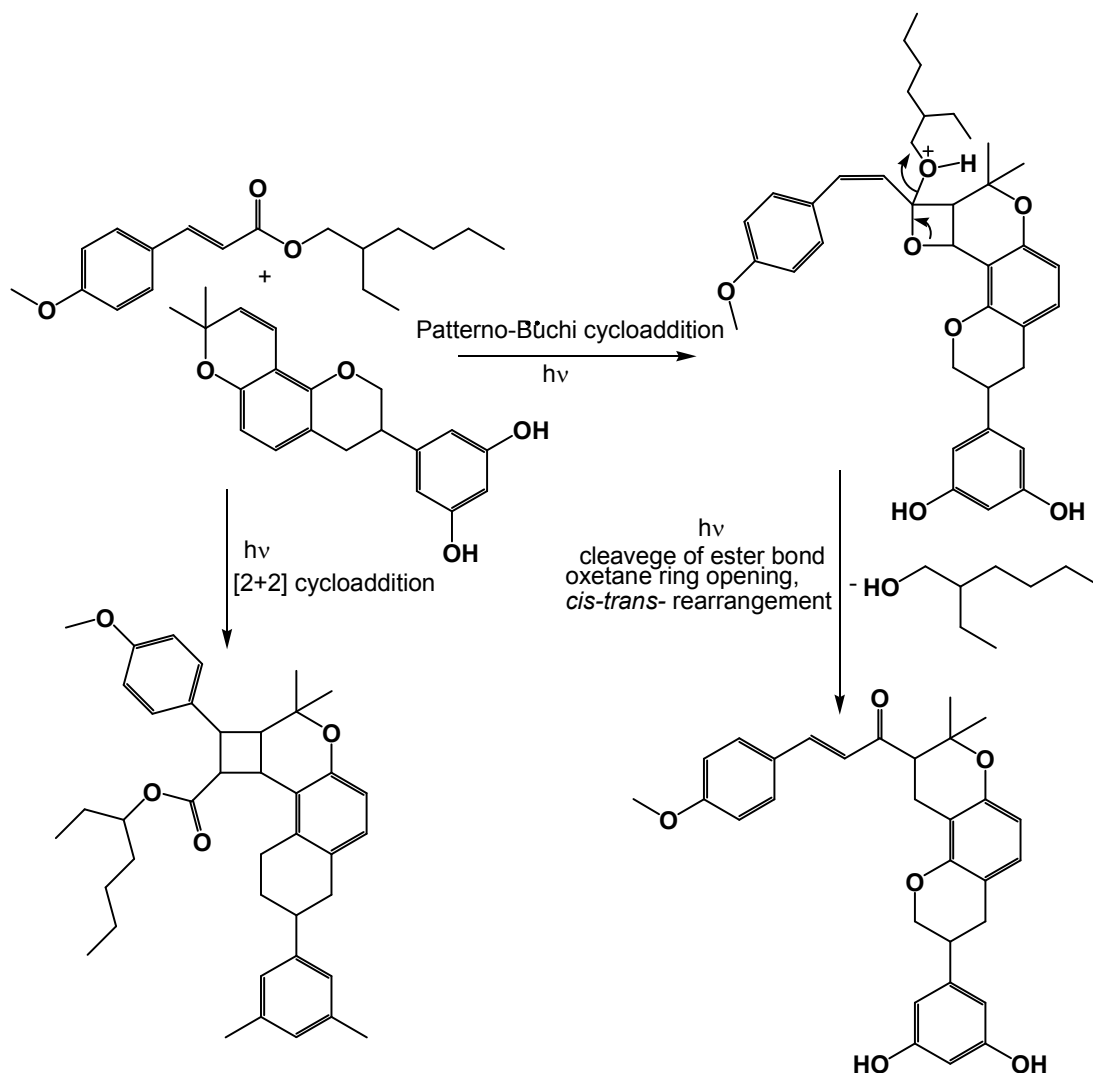
Figure 9.27: Proposed mechanism for the ethylhexylmethoxy cinnamate reaction of EHMC with glabridin.

The proposed mechanism is informed by the fact that the UV spectra of the mixture retain the same shape as the UV spectra of EHMC, and therefore the cinnamate moiety is assumed to be retained. The observed initial drop in the absorption of UV light can be attributed to competitive $[_\pi2+_\pi2]$ cycloaddition and Patternò-Büchi $[_\sigma2+_\pi2]$ cycloaddition involving glabridin which forms an oxetane. We propose that the Patternò-Büchi reaction dominates the $[_\pi2+_\pi2]$ cycloaddition upon UV light exposure, which would require a homolytic ring opening of the cyclobutane ring to retain the easily cleavable ester bond (Fig. 9.27). On prolonged UV exposure the oxetane assumes a *cis*-conformation, which absorbs at a longer wavelength for the cinnamic moiety but with a very low absorption coefficient (ε_o). The oxetane becomes more strained leading to oxidative heterocyclic ring opening with cleavage of the ester bond. The overall result is the retained cinnamic acid moiety with higher ε_o, and a bathochromic shift attributed to the proximity of the cyclic pyran ring of the glabridin moiety. This explains the observed stability of this mixture covering the entire UV spectrum and without further photo-degeneration (Fig. 9.25) and the source of the peaks observed at 358 nm (Fig. 9.26). We conclude that a mixture containing liquorice root extract and EHMC is likely to produce a broad spectrum sunscreen product owing to the photochemical reactions between EHMC and the liquorice root extract constituents.

9.3.6 Effect of liquorice root extract on the photostability of a mixture of EHMC, BP3 and BMDBM

The three sunscreen absorbers investigated are frequently mixed together in a formulation in order to obtain a broad-spectrum photoprotective product. A mixture of the three sunscreen agents was prepared by dissolving the three UV absorbers in methanol and subjected to photostability studies. This solution showed photodegradation (Fig. 9.28), with absorption maxima in the UVB region. The HPLC analysis of this mixture showed the relative photostability of BP3 and BMDBM and photoisomerisation of EHMC (Fig. 9.29). This mixture, therefore cannot guarantee broad-spectrum photoprotection. Efforts were thus made to investigate the effect of liquorice root extract on a mixture of EHMC, BP3 and BMDBM. Most working groups have reported the inherent photoinstability of a BMDBM and EHMC mixture in which EHMC is reported to undergo photoisomerisation photosentised by BMDBM occasioning photo-loss (Dondi et al. 2006; Pattanaargson et al. 2004). These two are may also undergo a [2+2] cycloaddition reaction that breaks down rapidly to give other less absorbing photoproducts. In this work the UV spectra of the three sunscreens combined with liquorice root extract showed a drop after 30 minutes and then stabilized (Fig. 9.30). The spectral decay of this mixture in methanol is accompanied by a blue shift (Fig. 9.28) a phenomenon that is reversed in this mixture containing liquorice extract. An inspection of the corresponding HPLC chromatogram showed the EHMC and BMDBM peaks only. However, the BP3 peak was again not seen on the HPLC chromatogram. This could be due to reactions explained in Section 9.3.3. A study by Sayre et al. (2005) suggested that the photo-loss of EHMC may be enhanced by the free radicals formed in the photodegradation of BMDBM present in the mixture. The overall observed effect of these reactions is the emergence of one major absorbing species (Fig. 9.31). The HPLC chromatographic data reveal several other chemical species (Supplementary Materials Table S9.6,). This mixture achieves an improved absorption efficacy but does not stop the photo-degradation of BMDBM and photoisomerisation of EHMC as chemical entities but reaction occurs to produce long wavelength absorbing species.
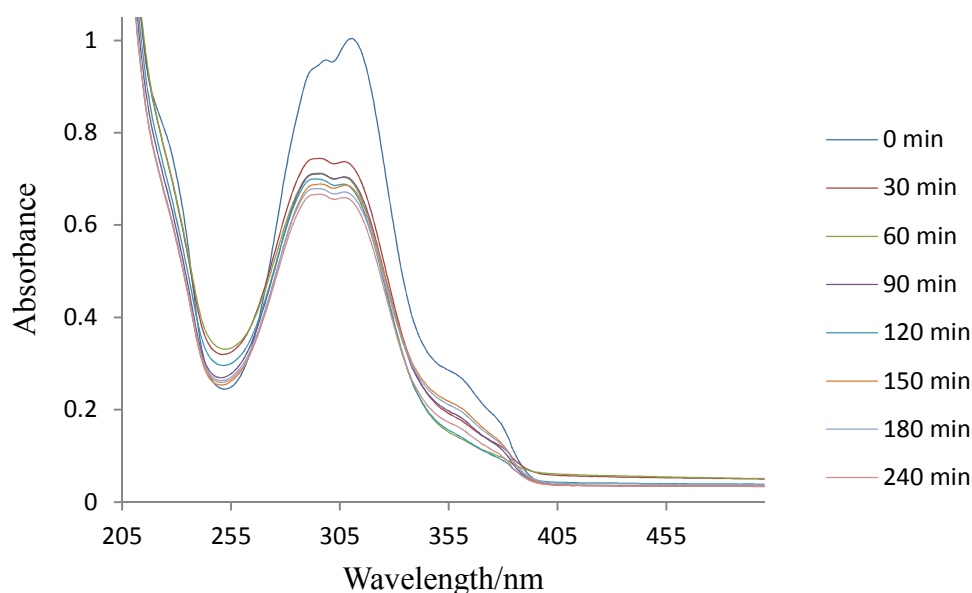
Figure 9.28: The spectral transformations of a mixture of the organic UV absorbers: EHMC, BP3 and BMDBM, under solar simulated irradiation, in a 1 mm pathlength quartz cuvette. Each exposure event involved use of a fresh sample solution. The spectra were recorded on a Perkin Elmer Lambda 35 spectrophotometer.
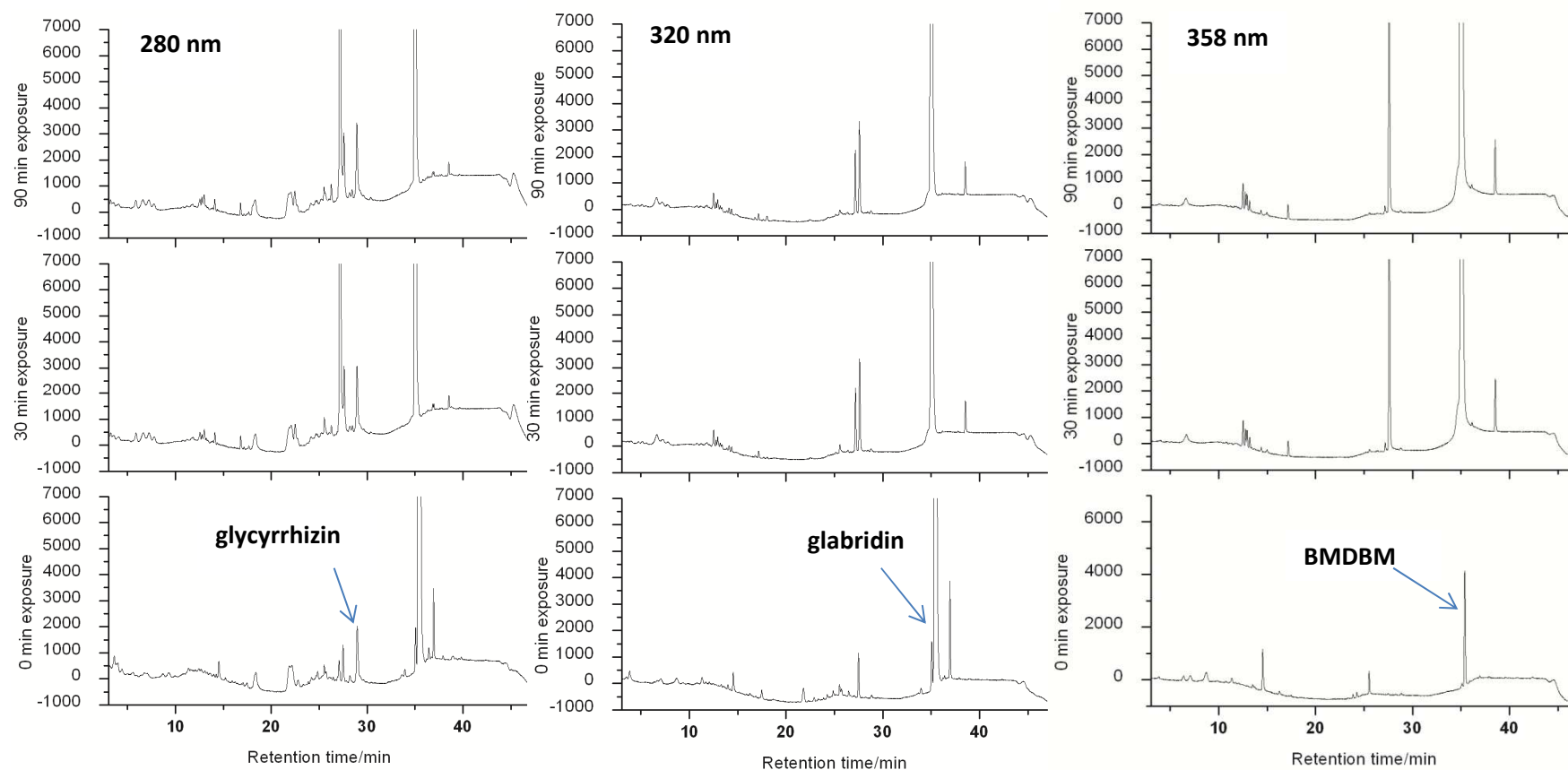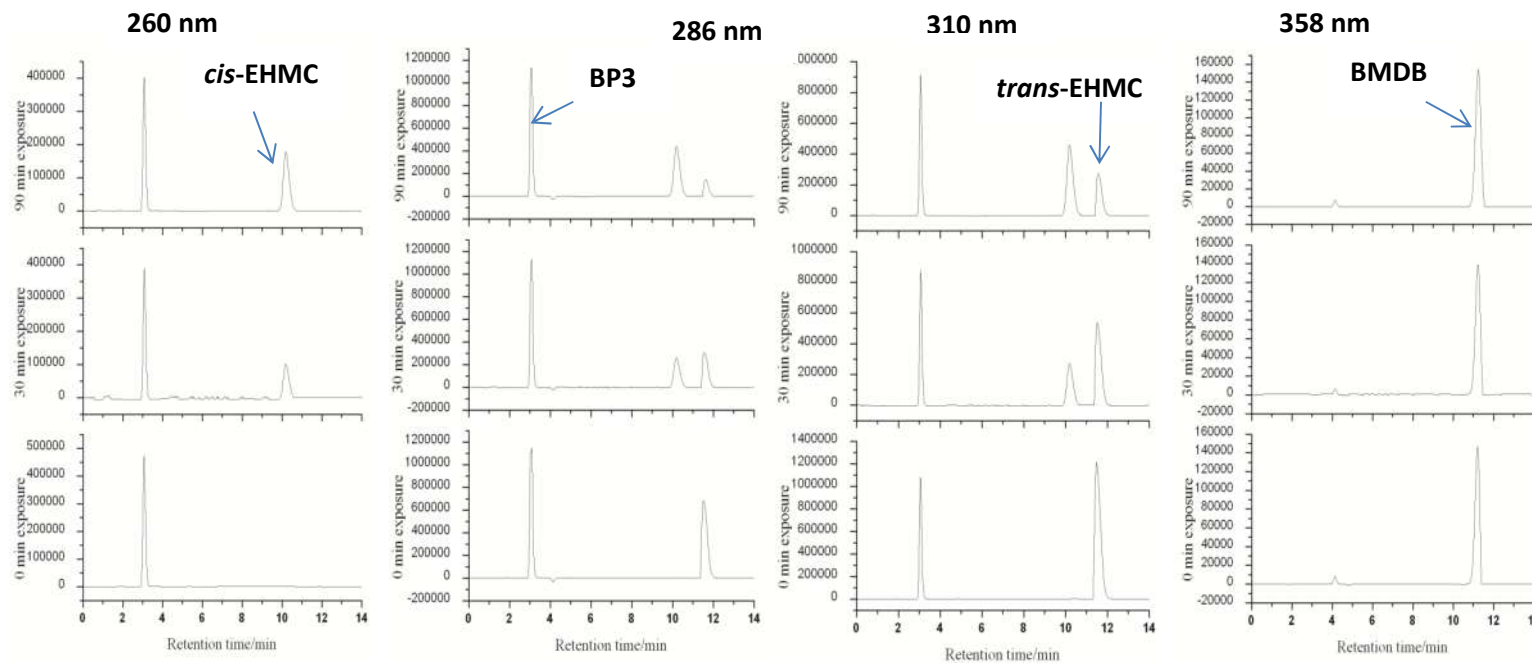
Figure 9.29: The photochemical transformations of a mixture of BMDBM, BP3, and EHMC dissolved in methanol monitored by HPLC at 260, 286, 310, and 358 nm. The separation was effected on a Zorbax Eclipse-XDB C-18 column (150 mm × 4.6 mm, i.d., 5 μm). The mobile phase was a gradient elution of acetonitrile-water with a flow rate of 1.00 mL min^{-1} and the injection volume was 20 μL.
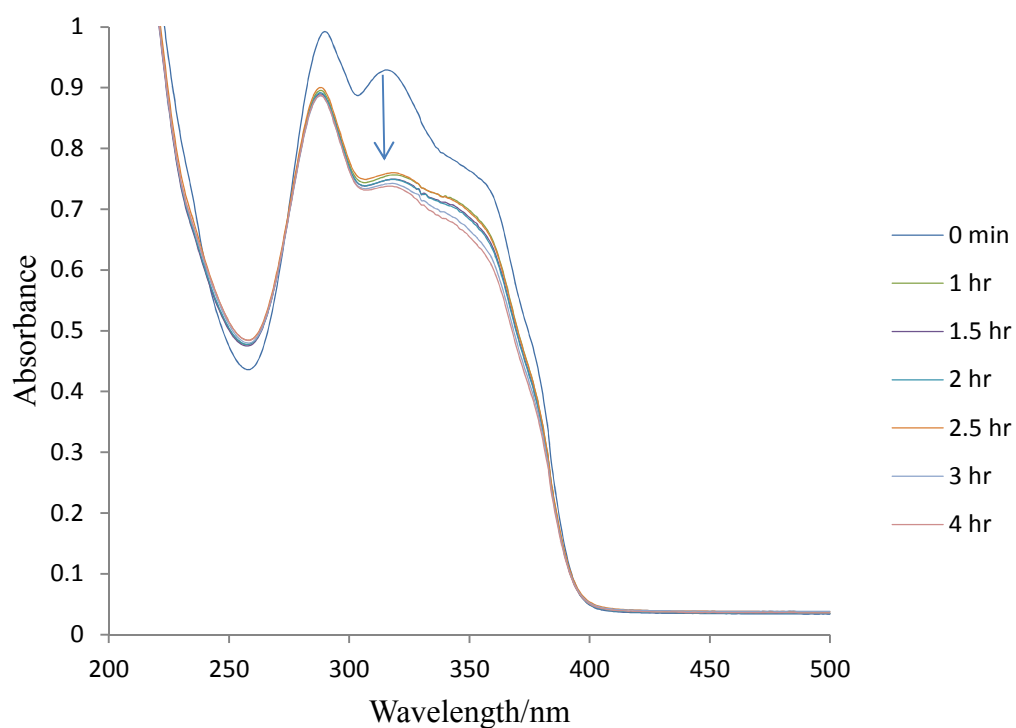
Figure 9.30: The photostability of a mixture of EHMC, BP3, BMDBM, and liquorice root extract dissolved in methanol when exposed to simulated solar radiation, in a 1 mm path-length quartz cuvette. Each exposure event involved use of a fresh sample solution. The spectra were recorded on a Perkin Elmer lambda 35 UV-vis dual beam spectrophotometer.
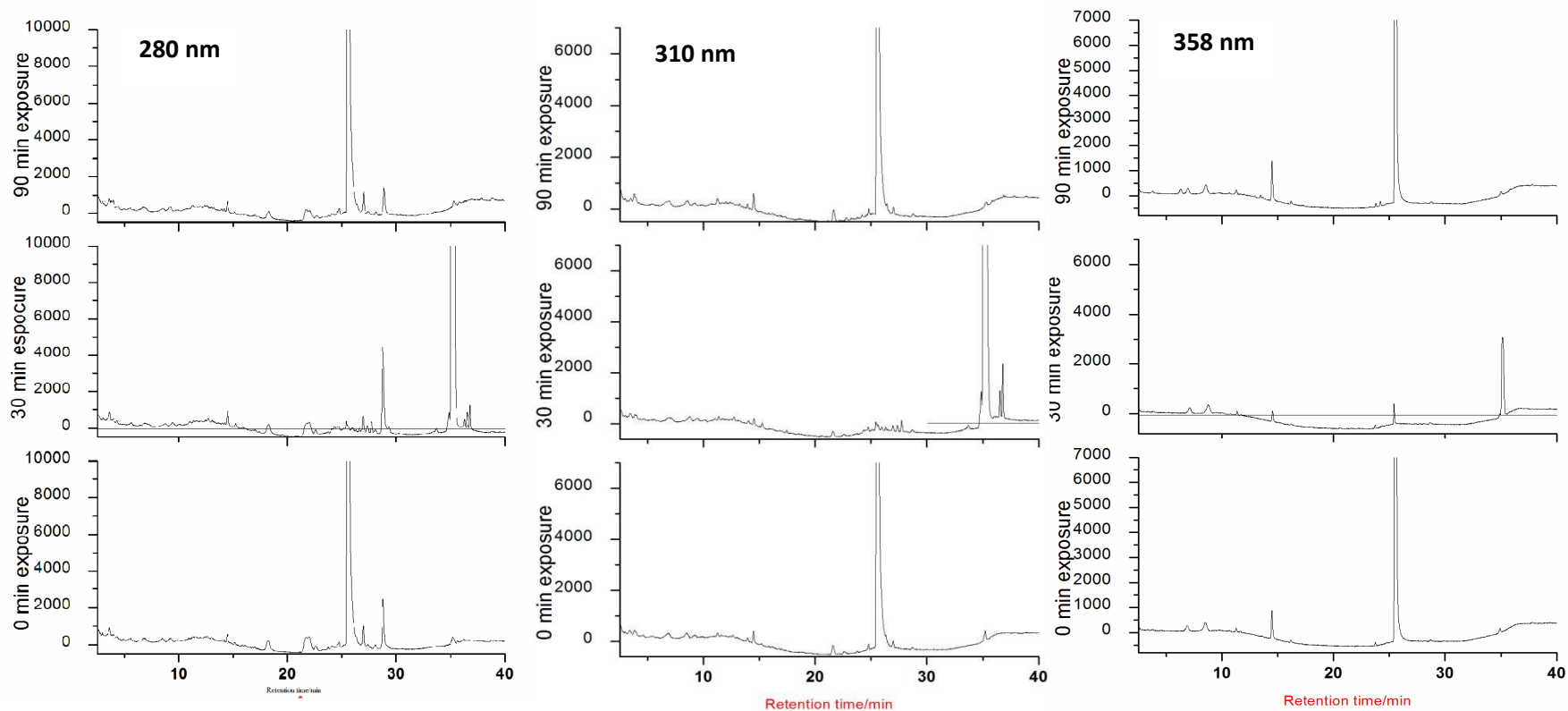
Figure 9.31: Photochemical changes when liquorice root extract is incorporated in in a mixture of EHMC, BP3 and BMDBM in methanol, monitored by HPLC at 260, 286, 310, and 358 nm. The separation was effected on a Zorbax Eclipse-XDB C-18 column (150 mm x 4.6 mm, i.d., 5 µm). The mobile phase was a gradient elution of acetonitrile-water with flow rate of 1.00 mL min^{-1} and an injection volume of 20 µL. No peak be could be identified conclusively.

9.4 Conclusions

The aim of this work was to investigate the effect of liquorice root extract on the photostability of some commonly used sunscreen absorbers. The liquorice root extract alone showed appreciable photo-absorption. However, irradiation of the extract with simulated solar radiation for increasing exposure periods showed a drop in UV-light absorption. We conclude that the photo-absorbing species in the liquorice root extract degrade upon exposure to UV light. The inclusion of common UV-absorbing agents into the liquorice root extract dissolved in methanol, showed different photo-degenerative responses depending on the agent. For example, a mixture containing BP3 in the liquorice root extract showed no appreciable change or drop in UV absorption. But a significant chemical transformation was observed from the HPLC data. No peak for BP3 could be detected on the chromatogram; the observed variation in the retention time indicates both dark and light-promoted reactions between the secondary metabolites of the liquorice root extract and BP3. We propose that the reactions between these metabolites and BP3 do not affect the carbonyl chromophore but rather add onto the phenyl rings. This causes the slight bathochromic shift observed suggesting that the added groups are electron-donating groups. These effects predominate even when all the three absorbing molecules are mixed together. The HPLC chromatograms of the mixture of the three sunscreen absorbers with liquorice root extract resemble those of BP3 alone with the liquorice root extract. The UV spectra resemble those of BP3. These results indicate the stability of the *ortho*-hydroxybenzophenone moiety but do not rule out C-C and C-O linkages on the phenyl rings.

EHMC showed an unusual photodegradation response with a drop-increase and drop fashion. This is attributed to a photochemical reaction involving both Patternò-Büchi and [2+2] cycloaddition reactions followed by a rearrangement. The resultant species is stable or has a longer life-time. There is need to investigate, isolate and characterize this species due to its photostability and may provide a lead to a stable synthetic UV absorber.

The addition of liquorice root extract to a solution of BMDBM in methanol did not show significant change on its photostability. A steady drop in UV absorption was observed at 358 nm the wavelength of maximum absorption for the *enol* form of BMDBM. This indicates photo-induced degradation of this UV absorber. There was a slight increase in absorbance at about 260 nm on the UV spectra indicating a possible isomerization to the *keto* form but to a very limited degree. The *keto* form of BMDBM has maximum wavelength of absorption at 254 nm. A close inspection of the HPLC data shows that exposure to UV radiation of this mixture leads to photochemical reactions similar to those observed and proposed for EHMC. This could be true given that BMDBM can split down to a phenacyl radical and a benzoyl radical upon UV irradiation. The phenacyl radical may rearrange to produce the cinnamic acid moiety which is likely to react in similar fashion as EHMC.

The overall analysis of liquorice root extract is that it may not be a very good stabilizer for all the chemical absorbers investigated, but it reacts with the agents to yield products with varying absorption characteristics. We conclude that these photoreactions with the absorbers produce UV-active species which may photostabilize the absorption efficacy of the formulation and not the individual sunscreen agent. It is expected that the phenolic compounds in the liquorice root extract may also contribute to absorption and scavenging of radical species.

References

Broadbent KJ, Martincigh BS, Raynor WM, Salter FL, Moulder R, Sjoberg P, Markides EK (1996) Capillary supercritical fluid chromatography combined with atmospheric pressure chemical ionisation mass spectrometry for the investigation of photoproduct formation in the sunscreen absorber 2-ethylhexyl methoxycinnamate. Journal of Chromatography A 732:101-110

Cai X, Sakamoto M, Fujitsuka M, Majima T (2005) Higher triplet excited states of benzophenones and bimolecular triplet energy transfer measured by using nanosecond-picosecond two-color/two-laser flash photolysis. Chemistry 11 (22):6471-6477

Cowley JN (1997) The mechanistic photochemistry of 4-hydroxybenzophenone. MSc Thesis, Queen's University, Ontario, Canada

Denisova SB, Galkin EG, Murinov YI (2006) Isolation and GC-MS determination of flavanoids from *Glycyrrhiza glabra* root. Chemistry of Natural Compounds 42 (3):285-289

Dondi D, Albini A, Serpone N (2006) Interactions between different solar UVB/UVA filters contained in commercial suncreams and consequent loss of UV protection. Photochemistry and Photobiological Sciences 5 (9):835-843

Fiore C, Eisenhut M, Ragazzi E, Zanchin G, Armanini D (2005) A history of the therapeutic use of liquorice in Europe. Journal of Ethnopharmacology 99 (3):317-324

Morteza-Semnani K, Saeedi M, Shahnavaz B (2003) Comparison of antioxidant activity of extract from roots of licorice (Glycyrrhiza glabra L.) to commercial antioxidants in 2% hydroquinone cream. Journal of Cosmetic Science 54 (6):551-558

Mturi GJ, Martincigh BS (2008) Photostability of the sunscreening agent 4-*tert*-butyl-4'-methoxydibenzoylmethane (avobenzone) in solvents of different polarity and proticity Journal of Photochemistry and Photobiology A: Chemistry 200:410-420

Murai H, Jinguji M, Obi K (1978) Activation energy of hydrogen atom abstraction by triplet benzophenone at low temperature. The Journal of Physical Chemistry 82 (1):38-40

Patil SK, Salunkhe VR, Mohite SK (2012) Development and validation of UV spectrometric method for the estimation of glycyrrhetic acid in hydroalcoholic extract of *Glycyrrhiza Gabra*. International Journal of Pharmaceutical, Chemical and Biological Sciences 2 (4):617 - 621

Pattanaargson S, Munhapol T, Hirunsupachot P, Luangthongaram P (2004) Photoisomerization of octyl methoxycinnamate. Journal of Photochemistry and Photobiology A: Chemistry 161:269-274

Placzek M, Dendorfer M, Przybilla B, Gilbertz KP, Eberlein B (2013) Photosensitizing properties of compounds related to benzophenone. Acta Dermato-Venereologica 93 (1):30-32

Rossi T, Benassi L, Magnoni C, Ruberto AI, Coppi A, Baggio G (2005) Effects of glycyrrhizin on UVB-irradiated melanoma cells. In Vivo 19 (1):319-322

Sayre MR, Dowdy CJ, Gerwig JA, Shields JW, Lloyd VR (2005) Unexpected photolysis of the sunscreen octinoxate in the presence of the sunscreen avobenzone. Photochemistry and photobiology 81:452-456

Schallreuter UK, Wood MJ, Farwell WD, Moore J, Edwards GMH (1996) Oxybenzone oxidation following solar irradiation of skin: photoprotection versus antioxidant inactivation. Journal of Investigative Dermatology 106:583-586

Schwack W, Rudolph T (1995) Photochemistry of dibenzoyl methane UVA filters. Journal of Photochemistry and Photobiology B: Biology 28:229 - 234

Wang ZY, Agarwal R, Zhou ZC, Bickers DR, Mukhtar H (1991) Inhibition of mutagenicity in salmonella-typhimurium and skin tumor initiating and tumor promoting activities in sencar mice by glycyrrhetinic acid - comparison of 18 alpha-stereoisomers and 18 beta-stereoisomers. Carcinogenesis 12 (2):187-192

Yokota T, Nishi H, Kubota Y, Mizoguchi M (1998) The inhibitory effect of glabridin from licorice extracts on melanogenesis and inflammation. Pigment Cell Research 11 (6):355-361

Supplementary Materials
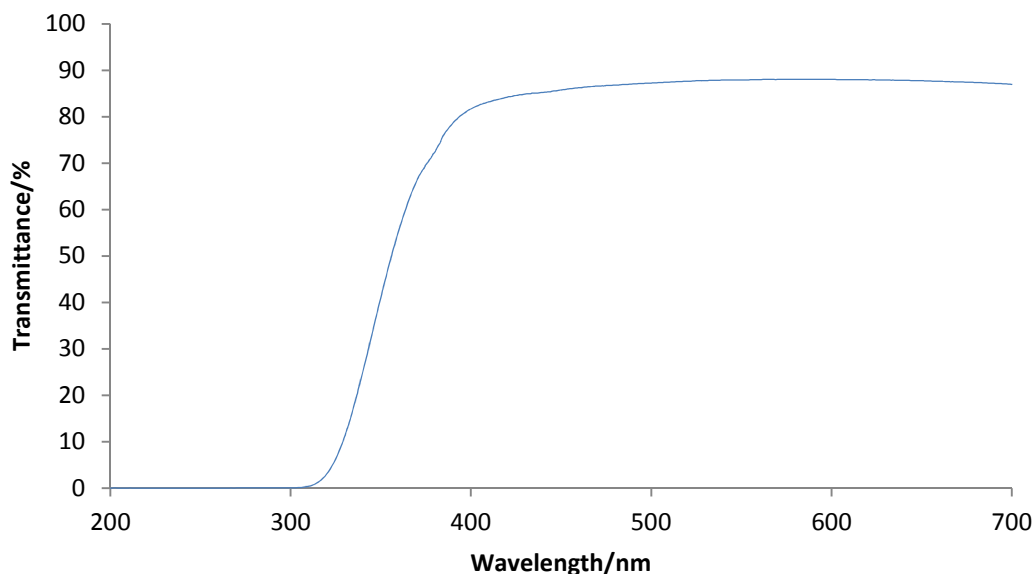
Figure S9.1: The transmittance spectrum of the 10 mm-thick Pyrex glass filter used in this work recorded on a Perkin Elmer Lambda 35 UV-vis dual beam spectrophotometer.

ble S9.1: The photochemical changes of the sunscreen(s) dissolved in methanol after irradiation with simulated solar irradiation monitored on HPLC-PDA at 260, 286, 310, 358 nm.

			Mixture of BMDBM, BP3 and EHMC		
				Peak Area	
Wavelength/nm	UV-filter	RT	0 min	30 min	90 min
260	*keto*-BMDBM	3.072	474053	388025	402645
	BP3	3.08267	1149065	1127671	1136999
286	*cis*-EHMC	10.19733	0	261526	443856
	trans-EHMC	11.53067	683313	303745	148920
	BP3	3.05067	1076471	879510	915656
310	*cis*-EHMC	10.19733	0	272403	461590
	trans-EHMC	11.488	1212199	538875	272829
358	*enol*-BMDBM	11.21067	146473	139439	154766
			BMDBM		
260	*keto*-BMDBM	2.368	5769	99334	95094
358	*enol*-BMDBM	11.232	110714	96556	92185
			BP3		
286	BP3	3.06133	927540	738944	806767
			EHMC		
260	*cis*-EHMC	10.16533	0	139036	133916
	trans-EHMC	11.43467	156696	83566	81385
310 nm	*cis*-EHMC	10.16533	0	362702	342873
	trans-EHMC	11.44533	1818585	1026119	965827

Table S9.2: The chemical transformations of liquorice root extract dissolved in methanol on UV irradiation monitored on HPLC-PDA at 275, 280, 286, 310 and 358 nm.

275 nm						280 nm					
RT	PA-0min	RT	PA-30min	RT	PA-90min	RT	PA-0min	RT	PA-30min	RT	PA-90min
1.309	78395	1.4	172727	1.394	161441	1.4	197880	1.4	164602	1.394	153166
1.4	125300	1.562	15298	1.555	15375	1.562	15560	1.562	15089	1.555	14317
1.562	16397	1.854	72975	1.845	71214	1.854	107730	1.854	88445	1.845	85167
1.854	88278	2.022	18149	2.011	19968	2.22	31271	2.216	37495	2.206	33554
2.027	21072	2.216	26449	2.205	36121	2.517	6452	2.757	20510	2.719	21933
2.221	39948	2.748	9341	2.724	22961	2.781	24284	3.25	14370	3.228	14328
2.784	25109	3.259	3330	3.248	16351	3.276	19671	3.496	5238	3.517	4502
3.282	23805	3.555	2439	3.533	5203	3.523	12519	4.154	1049	5.664	1227
3.567	14525	4.132	2395	4.092	1133	4.148	7474	5.95	6528	5.921	6458
4.021	4028	5.947	7197	5.643	1081	5.998	6965	6.798	13275	6.759	10975
4.144	3238	6.809	14776	5.917	6597	6.906	12869	7.418	12235	7.355	9499
6.001	6048	7.418	12488	6.737	14641	7.528	12518	7.953	6444	7.91	4403
6.898	14706	7.944	5997	7.352	11345	8.069	6043	11.912	1382	11.28	2137
7.536	13172	10.882	1058	7.901	4869	11.311	1672	12.583	4305	11.663	2106
8.088	5917	11.252	1807	10.832	1265	11.975	1877	12.787	1013	11.872	3793
11.326	1816	11.908	1927	11.233	1627	12.606	5577	13.045	4156	12.085	2076
11.731	1026	12.134	1207	12.577	4872	12.822	1807	13.76	1865	12.256	1214
11.934	2247	12.597	6939	12.769	1457	13.075	6156	13.905	2479	12.55	9860
12.625	6858	12.787	1817	13.025	6175	13.29	3862	14.154	5489	12.769	4199
12.818	1950	13.047	7418	13.221	2001	13.771	5782	16.83	9816	13.021	10183
13.074	7962	13.252	2553	13.76	6396	14.179	5678	17.191	6551	13.222	6476
13.29	4126	13.472	2591	13.869	2915	16.841	10004	24.191	3523	13.451	3681
13.837	6761	13.792	4757	14.133	6350	17.202	6637	24.405	1670	13.792	11063
14.179	7461	13.904	3411	16.805	11655	24.205	1850	24.661	2589	13.873	6130

16.833	12529	14.153	6518	17.161	5130	24.83	1939	24.836	2841	14.136	13546
17.202	5331	15.207	4589	24.17	1172	24.987	1565	24.987	2501	14.4	4997
23.819	1293	15.509	5854	24.821	1666	25.162	3014	25.158	4024	14.635	5925
24.195	3412	16.824	12017	24.966	1669	25.395	7132	25.389	8081	14.805	6105
24.448	2798	17.19	5209	25.109	1729	25.632	12822	25.626	14176	14.955	1342
24.683	2476	23.84	1075	25.373	8901	26.165	2388	26.161	2455	15.198	8253
24.839	3608	24.189	4524	25.613	15070	26.918	2545	26.907	2741	15.371	3716
24.992	2643	24.405	3611	26.141	1796	27.076	6111	27.067	6258	15.573	9162
25.153	3659	24.661	3171	26.887	2405	28.221	7975	28.209	8291	16.813	9160
25.401	10775	24.836	4015	27.054	6315	29.013	10996	29	11372	17.167	6391
25.634	16855	25.003	3933	27.544	1451	29.602	1315	29.575	1581	24.161	1822
26.162	3465	25.157	3808	28.198	9866	35.378	2199	30.503	1421	24.815	1377
26.916	2139	25.385	12948	28.99	11003	35.897	2802	30.916	1150	24.967	2037
27.077	5866	25.627	20643	29.581	1168	38.855	6493	35.365	2998	25.142	2773
27.567	1445	26.154	6365	30.471	1302	45.407	73254	35.884	2535	25.375	7305
28.222	8928	26.389	2930	30.845	1292			38.845	6575	25.611	12880
29.016	10101	26.707	3395	35.334	2613			45.425	76008	26.139	2533
30.511	1397	26.91	4040	35.877	2168					26.894	2939
30.906	1239	27.068	8430	38.825	7190					27.057	6602
35.264	1520	27.556	3550	45.519	70622					27.538	1414
35.385	1098	28.21	9439							28.198	8584
35.896	2256	29.003	11027							28.991	11378
38.852	6680	29.576	1145							29.581	1304
45.368	64862	30.501	1551							30.476	1148
		30.885	1639							30.925	1287
		35.364	3573							35.354	2604
		35.889	2018							35.877	2542
		38.844	6775							38.839	6253
		45.424	68933							45.503	80618

286 nm						310 nm					
RT	PA-0min	RT	PA-30min	RT	PA-90min	RT	PA-0min	RT	PA-30min	RT	PA-90min
1.4	179253	1.4	144361	1.394	132810	1.401	117829	1.401	79864	1.394	71480
1.562	15204	1.561	13259	1.554	12573	1.562	13061	1.562	7929	1.554	8089
1.854	101727	1.854	82722	1.845	76137	1.855	84946	1.854	61847	1.846	54745
2.22	21236	2.217	32451	2.206	27452	2.216	6871	2.213	7507	2.196	7721
2.56	4328	2.756	26603	2.716	17942	2.349	8470	2.349	9284	2.336	9731
2.786	6404	3.238	16707	3.217	5148	2.775	8876	2.746	8219	2.725	5312
4.154	1984	3.491	8919	5.643	1188	4.017	1233	4.072	1301	6.768	9748
6.009	4223	3.904	2751	5.928	3553	6.963	9592	6.819	10507	7.369	5435
6.936	9297	3.979	1225	6.778	8895	7.546	6491	7.417	6950	7.881	2298
7.537	9764	4.123	2278	7.356	7821	8.045	2733	7.972	3015	12.525	6607
8.047	4491	5.653	1261	7.928	3827	11.912	1878	11.857	1519	12.772	2124
11.929	1567	5.948	4067	11.864	1093	12.574	6022	12.546	6716	12.949	5481
12.594	4556	6.805	10757	12.537	4608	12.812	2142	12.788	2270	13.209	2647
12.814	1576	7.443	9768	12.773	1453	13.001	5722	12.973	5673	14.13	1932
13.066	4943	7.95	4520	13.02	4363	13.272	2977	13.233	3111	17.171	2284
13.291	2787	11.877	1403	13.209	1287	13.44	1600	14.152	2018	25.58	1703
13.792	2862	12.563	4593	13.884	3447	14.177	1915	14.396	1152	27.047	1207
14.178	3988	12.789	1475	14.131	3965	14.416	2061	17.199	2180	35.363	2979
16.858	6839	13.042	4163	16.827	6369	17.207	2240	25.601	1661	35.87	1616
17.213	6925	13.245	1138	17.169	7483	17.72	1029	35.365	3765	38.841	2344
23.861	2764	13.91	2463	24.159	4599	25.136	1011	35.88	1792	45.5	49753
24.203	3118	14.152	4127	24.658	3673	25.609	1752	38.856	2016		
24.683	3997	16.846	6847	24.808	2131	27.081	1242	45.456	50759		
24.822	2856	17.194	7124	24.974	2451	35.384	2736				
24.981	2489	24.174	1206	25.15	4571	35.896	1990				
25.175	5014	24.681	1339	25.369	7150	38.864	1909				

25.393	7027	24.824	1852	25.608	9505	45.388	46468				
25.631	10179	24.997	1691	26.14	1653						
26.166	2742	25.162	3970	26.896	2610						
26.923	2405	25.383	6244	27.056	6096						
27.077	6350	25.622	9680	28.202	6356						
27.557	1226	26.158	2270	28.987	8318						
28.219	5967	26.914	2449	29.602	2451						
29.014	7711	27.066	5979	29.978	1109						
29.624	1345	27.557	1073	35.347	2726						
35.38	2422	28.214	5937	35.868	2615						
35.896	2991	29	7985	38.842	6211						
38.846	5699	29.583	1419	45.5	86146						
45.403	78502	35.368	3412								
		35.883	2870								
		38.845	5464								
		45.464	83324								

Table S9.3: The chemical transformations of liquorice root extract mixed with BMDBM dissolved in methanol on irradiation with simulated solar irradiation monitored by HPLC-PDA.

275 nm						280 nm					
RT	PA-0min	RT	PA-30min	RT	PA-90min	RT	PA-0min	RT	PA-30min	RT	PA-90min
1.4	126755	1.408	119601	1.394	113945	1.4	122530	1.408	114605	1.394	109236
1.557	9811	1.565	9235	1.552	9863	1.557	9176	1.565	8650	1.552	9333
1.85	89030	1.858	65665	1.844	61528	1.85	84368	1.858	76589	1.844	72687
2.207	30723	2.027	17112	2.007	14993	2.203	29505	2.214	28474	2.202	22385
2.718	35299	2.215	34105	2.198	23068	2.731	13701	2.74	13763	2.696	6839
3.234	20722	2.731	27942	2.697	8490	3.225	4724	3.234	6005	3.225	1138
3.504	14930	3.241	20932	3.227	2086	5.849	3726	4.133	1643	3.553	1039
3.861	3225	3.558	14287	3.53	2058	6.59	4687	5.894	3285	5.869	3338
4.048	3878	3.947	3432	4.047	2006	6.688	3168	6.703	6355	6.661	7522
5.855	3712	4.097	2936	5.87	4163	7.224	7392	7.268	6666	7.215	7397
6.599	9010	5.9	4569	6.658	10175	7.765	3623	7.833	2836	7.75	3594
7.223	8096	6.668	9745	7.258	8271	12.528	2705	12.558	2752	12.525	2702
7.738	3618	7.311	8742	7.78	3739	12.989	3210	13.015	3101	12.987	3061
12.539	3191	7.844	3773	12.545	3251	13.214	1650	14.113	2754	14.082	2765
12.995	4141	11.816	1029	12.993	4105	14.088	2687	14.457	3412	14.428	5047
13.248	1798	12.561	2205	13.195	1079	16.788	2382	16.81	2431	16.777	2195
14.089	3479	13.016	3221	14.081	2985	17.443	1022	18.379	14586	18.323	14745
16.786	4171	14.114	2970	14.438	4911	18.325	14638	21.899	17976	21.856	15228
17.64	1315	14.46	3150	16.779	4085	21.824	16457	22.108	17745	22.045	19557
18.334	15988	16.809	4415	17.64	1127	22.06	19058	22.765	4373	22.72	4377
21.835	19066	17.679	1189	18.326	16192	22.726	4199	24.176	1733	24.12	1520
22.061	18172	18.374	15318	21.856	17094	24.133	1453	24.648	1124	24.608	1094
22.724	5368	21.899	19092	22.052	20446	24.645	1101	25.366	1539	25.28	1913
24.14	2006	22.113	18819	22.72	5131	25.341	1096	25.552	8189	25.517	7534

25.323	1921	22.756	5726	24.13	1689	25.52	5339	26.88	1145	25.982	1119
25.512	7826	24.17	3613	25.323	1913	25.685	2057	27.051	7959	26.837	1034
25.999	1254	24.373	2048	25.517	7283	26.848	1182	27.473	2877	27.015	7800
27.023	7353	24.655	1808	25.98	1573	27.023	7950	27.858	5661	27.432	2991
27.441	9214	24.813	1032	26.827	1003	27.44	10515	28.194	2314	27.816	5027
28.154	2444	25.376	1464	27.019	7511	28.158	2297	28.968	41965	28.145	2320
28.932	41921	25.549	7968	27.44	3184	28.932	42564	33.6	1522	28.922	42210
33.578	1423	26.036	1718	27.816	4592	33.557	1424	33.896	2263	33.557	1709
33.873	2593	26.88	1112	28.144	2749	33.865	2631	35.007	11086	33.856	2379
34.975	11024	27.054	7481	28.923	42344	34.975	13596	35.341	8216264	34.958	10618
35.312	7386906	27.479	3227	33.557	1443	35.312	9133380	36.392	3656	35.295	8038959
36.128	1744	27.856	5059	33.854	1974	36.356	4133	36.628	6055	36.349	3716
36.356	5402	28.187	2838	34.958	8836	36.587	1340	36.878	8626	36.588	5833
36.597	1731	28.968	42313	35.294	6759428	36.847	16705	45.326	31940	36.841	8511
36.847	14111	33.579	1330	36.352	3676	45.304	28032			45.298	31081
45.295	26970	33.893	1995	36.589	5099						
		35.007	9458	36.841	6588						
		35.339	6905276	45.295	25516						
		36.396	3995								
		36.626	5490								
		36.879	7039								
		45.262	20725								
286 nm						310 nm					
RT	PA-0min	RT	PA-30min	RT	PA-90min	RT	PA-0min	RT	PA-30min	RT	PA-90min
1.4	112075	1.408	102256	1.394	96685	1.4	74738	1.408	65625	1.394	61705
1.556	8708	1.565	8161	1.551	8888	1.557	8315	1.565	8129	1.551	8536
1.85	80083	1.859	70106	1.844	68414	1.851	65391	1.859	57246	1.844	48532

2.206	19056	2.218	21028	2.201	23449	2.208	6371	2.229	5495	2.208	4902
2.485	4015	2.714	6156	2.717	5581	2.332	8314	2.357	10290	2.338	1909
2.745	7023	4.097	1043	5.864	2564	2.706	7820	2.716	5026	6.64	4398
5.849	1940	5.893	2307	6.633	6905	6.626	4448	6.683	4291	12.484	3462
6.626	6289	6.706	5398	7.266	6233	7.236	2827	7.273	2425	12.906	2535
7.225	5991	7.309	5568	7.79	3443	12.488	3893	11.823	1163	14.08	1549
7.772	2961	7.826	3081	11.79	1050	12.735	1461	12.512	3401	14.358	1343
12.517	2761	12.53	2286	12.493	2626	12.914	3619	12.934	2243	17.136	1190
12.737	1050	13.01	2175	12.986	2831	13.183	1926	14.111	1448	25.548	2298
12.987	3224	14.113	2077	13.185	1068	13.355	1258	14.38	1107	25.675	1636
13.208	1952	14.463	3461	14.081	2177	14.085	1368	17.172	1155	27.013	1428
14.088	2141	16.808	1048	14.432	5026	14.359	1443	25.574	3269	27.431	1590
14.366	1154	18.36	10058	16.778	1035	17.139	1193	25.717	1512	27.818	3687
16.79	1065	22.086	21330	18.324	8705	17.425	2205	27.054	1833	33.854	1478
17.432	1155	22.75	2836	21.824	10558	25.552	1662	27.47	2010	34.962	14137
18.329	9176	24.175	1483	22.041	9983	25.674	2573	27.854	4221	35.298	10355312
21.856	11328	24.655	1081	22.694	2800	27.023	1662	28.825	1148	36.117	2738
22.052	9921	24.798	1111	24.143	1333	27.439	10742	33.905	1581	36.288	1778
22.722	3306	25.28	1906	24.62	1095	28.786	1006	35.01	14250	36.588	8264
24.125	1396	25.561	7717	25.205	1705	33.873	2660	35.343	10614079	36.841	14248
24.619	1123	27.05	7783	25.529	5188	34.977	19318	36.626	6644	45.296	17649
25.227	1107	27.47	2826	25.675	1162	35.311	13160482	36.879	13996		
25.533	4440	27.854	6030	27.012	7710	36.306	1330	45.299	17587		
25.664	2215	28.201	1552	27.445	2784	36.576	1197				
27.023	7838	28.966	27477	27.815	5305	36.848	25586				
27.44	11898	29.702	1557	28.127	1462	45.3	17600				

RT	PA	RT	PA	RT	PA						
28.148	1519	33.568	1759	28.922	27003						
28.928	26690	33.894	1804	29.637	1387						
29.636	1301	35.007	13087	33.525	1557						
33.573	1521	35.342	9565410	33.853	1623						
33.874	2466	36.381	2268	34.96	12685						
34.976	16316	36.627	6663	35.296	9349185						
35.312	10934005	36.878	10448	36.117	2566						
36.345	2962	45.329	33436	36.342	3963						
36.597	1614			36.589	7647						
36.848	20108			36.841	11232						
45.317	31685			45.298	35132						

358 nm					
RT	PA-0min	RT	PA-30min	RT	PA-90min
1.4	39570	1.409	33411	1.395	32197
1.557	7811	1.565	7370	1.552	8203
1.851	22731	1.859	21170	1.844	21167
1.968	2217	1.983	2114	1.962	1889
6.633	3633	6.703	4428	6.68	4639
12.484	5464	12.508	5245	12.481	5775
12.734	3458	12.759	3445	12.731	3634
12.904	3294	12.926	3330	12.899	3531
13.167	2010	13.192	2097	13.167	2018
14.369	1311	17.165	3312	17.134	3339
17.141	3307	35.039	4133	34.99	2363
28.755	1006	35.318	44567	35.273	43048
35.001	3397				

35.311	34877				

Table S9.4: The chemical transformations of liquorice root extract mixed with BP3 dissolved in methanol on irradiation with simulated solar irradiation monitored by HPLC-PDA.

275 nm						280 nm					
RT	PA-0min	RT	PA-30min	RT	PA-90min	RT	PA-0min	RT	PA-30min	RT	PA-90min
1.402	125182	1.395	120802	1.398	115884	1.402	121025	1.395	115669	1.398	110460
1.562	8783	1.553	9522	1.555	9587	1.562	8251	1.553	8844	1.555	8905
1.855	83159	1.846	78538	1.849	65079	1.855	82144	1.846	79598	1.849	74888
2.211	30904	2.203	24289	2.011	18245	2.211	32844	2.204	33705	2.206	20137
2.726	23112	2.714	7483	2.205	38274	2.744	24365	2.709	22169	2.716	8790
3.257	13213	3.242	1851	2.715	29243	3.239	17111	3.237	20006	3.22	1330
3.539	6379	3.535	2035	3.225	21267	3.507	11586	3.455	10733	3.523	1474
5.891	3607	4.076	1924	3.538	13977	4.086	7030	3.893	3622	4.059	1648
6.706	7255	5.891	3155	4.088	6841	5.898	3657	4.077	2354	5.872	4250
7.275	7262	6.678	8960	5.871	4801	6.712	6051	5.866	4587	6.608	8478
7.823	3376	7.28	7832	6.609	10881	7.27	6888	6.714	6983	7.238	8238
11.823	1083	7.832	3423	7.235	8922	7.826	3153	7.291	7175	7.749	3861
12.563	3160	12.56	2616	7.75	3774	11.802	1432	7.833	3467	11.809	1822
13.021	4192	13.016	3340	11.784	1184	12.56	2742	11.813	1038	12.545	3060
13.301	1695	14.108	2768	12.547	2908	13.019	3704	12.54	2833	13.002	3083
14.116	3108	16.8	3936	13.004	3580	13.222	1983	13.002	3399	14.102	2664
16.81	3897	17.658	1331	13.865	1114	14.116	3219	13.205	1475	16.798	2268
17.672	1244	18.362	14257	14.1	3156	16.812	2212	14.107	2603	18.344	14318
18.38	15678	21.867	18868	16.796	3989	18.361	15117	16.801	2184	22.067	35200
21.931	17058	22.088	19076	17.659	1460	21.888	14342	18.345	13734	22.742	4283
22.128	20824	22.74	5293	18.358	15504	22.123	21340	21.909	16297	24.15	1573
22.781	5285	24.144	2159	22.068	36988	22.786	4634	22.09	18854	24.641	1120

24.186	2034	25.355	1194	22.746	5070	24.186	1587	22.741	4199	25.269	1355
25.355	1861	25.555	3417206	24.154	1833	25.355	1133	24.141	1426	25.558	4233071
25.575	3348181	27.039	6564	24.634	1059	25.575	4148590	24.638	1334	27.043	7026
27.062	7117	28.167	2787	25.333	1556	27.062	7100	25.269	1198	28.168	2397
27.546	1838	28.953	42473	25.558	3415015	28.204	3130	25.555	4241154	28.958	43942
28.207	3335	35.323	2314	27.043	7140	28.544	1132	27.038	6727	35.338	4189
28.986	44812	45.296	25590	27.516	1544	28.985	47471	28.168	2639	45.305	30412
35.076	1127			28.173	2932	35.038	1120	28.953	43520		
35.365	2416			28.958	40055	35.362	2972	35.332	2723		
35.865	1126			35.035	1005	35.897	1464	45.309	27934		
45.308	23156			35.336	3334	45.326	31391				
				36.32	1089						
				45.304	20702						
286 nm						310 nm					
RT	PA-0min	RT	PA-30min	RT	PA-90min	RT	PA-0min	RT	PA-30min	RT	PA-90min
1.402	110184	1.396	103415	1.398	99198	1.403	74503	1.396	68054	1.398	63705
1.562	7756	1.553	8154	1.555	8689	1.562	7981	1.553	8323	1.555	8490
1.855	77095	1.846	70971	1.849	69845	1.856	60911	1.847	58359	1.849	56071
2.212	20411	2.204	20567	2.203	21204	2.208	3908	2.208	6563	2.205	7421
2.736	9198	2.709	6961	2.704	7082	2.357	1999	2.357	8703	2.333	6715
5.897	1714	4.11	1232	4.055	1156	6.724	4998	2.715	6185	2.689	8704
6.716	5433	5.892	2087	5.867	2255	7.326	2834	6.654	3644	6.62	5678
7.29	5916	6.685	4205	6.622	5973	11.826	1535	12.51	3433	7.224	3699
7.845	2899	7.294	3728	7.245	5568	12.515	3852	12.939	2251	7.789	1603
12.54	2897	7.84	1627	7.79	3173	12.764	1262	14.102	1292	11.803	1151

12.762	1198	12.521	2086	11.79	1438	12.946	3518	17.15	1189	12.496	3598
13.025	3553	13.005	2546	12.506	2514	13.227	2187	25.555	3276888	12.932	2557
13.221	2206	13.193	1332	12.997	2467	14.113	1292	27.035	1908	14.098	1388
14.115	2073	14.104	2000	14.103	2040	14.38	1378	28.795	1138	17.154	1135
16.829	1043	16.806	1056	16.805	1087	17.174	1095	35.33	3614	25.558	3267662
18.364	9903	18.229	3275	18.353	8517	25.575	3204247	45.296	16662	27.036	1348
21.888	8981	18.351	5432	21.867	10911	27.049	1381			35.044	1308
22.128	11241	21.92	10052	22.098	9956	28.83	1086			35.335	5459
22.761	2569	22.094	10499	22.737	2939	35.055	1216			45.307	12863
24.672	1076	22.717	2550	24.144	2730	35.364	3787				
25.575	4733540	24.162	1179	24.65	3197	45.337	14161				
27.06	7060	24.648	1252	24.794	1767						
28.195	1931	25.248	1302	25.269	3974						
28.984	28465	25.555	4839071	25.558	4835065						
29.702	1179	27.036	6852	27.039	7027						
35.373	3157	28.175	1857	28.17	1737						
35.869	1585	28.951	25752	28.955	28284						
45.351	28805	29.28	2353	29.666	1710						
		29.672	1161	35.046	1033						
		35.326	3379	35.341	4914						
		45.298	36714	45.311	34645						

358 nm					
RT	PA-0min	RT	PA-30min	RT	PA-90min

1.403	37881	1.396	34813	1.398	34243
1.562	7570	1.553	7586	1.555	8389
1.855	20296	1.847	22269	1.849	21321
6.717	4036	1.975	4693	1.988	2240
12.512	5562	6.725	2899	6.638	4363
12.763	3525	12.504	5156	12.492	6030
12.934	3226	12.754	3350	12.744	3808
13.195	1916	12.925	3100	12.912	3689
14.388	1172	13.19	2008	13.178	2131
17.169	3448	17.155	3337	17.155	3340
25.575	793990	25.556	810399	25.558	809566
35.056	5055	35.016	4126	35.027	4963

Table S9.5: The chemical transformations of liquorice root extract mixed with BMDBM dissolved in methanol on irradiation with simulated solar irradiation monitored by HPLC-PDA.

275 nm						280 nm					
RT	PA-0min	RT	PA-30min	RT	PA-90min	RT	PA-0min	RT	PA-30min	RT	PA-90min
1.402	138090	1.402	138410	1.395	131685	1.402	133501	1.402	133358	1.395	126014
1.562	9563	1.561	10240	1.553	9755	1.561	8963	1.561	9601	1.553	9099
1.853	91355	1.853	72024	1.845	68964	1.853	88965	1.853	83991	1.845	84000
2.205	36440	2.027	14754	2.016	14398	2.206	29917	2.209	22710	2.202	27777
2.713	26418	2.209	25969	2.2	23487	2.475	3784	2.721	9435	2.699	26977
3.224	23672	2.725	7154	2.68	8309	2.702	26585	3.218	1200	3.204	13706
3.526	14436	3.229	2335	3.21	2299	3.213	20085	3.557	1322	3.403	3273
3.84	2481	3.534	2269	3.537	2104	3.492	13279	4.088	1052	3.547	2289
4.039	5206	5.862	4023	5.836	3978	4.038	8047	5.862	4701	5.832	4050
5.844	3923	6.621	10312	6.587	10075	5.85	3917	6.62	9637	6.585	8068
6.573	10073	7.196	9267	7.189	9434	6.586	8702	7.21	9201	7.176	8484

7.185	8789	7.779	4449	7.722	4043	7.181	8190	7.761	4090	7.731	3747
7.765	4285	11.804	1447	11.763	1108	7.737	4283	11.803	1815	11.78	1024
11.762	1251	12.548	3677	12.537	3637	11.751	1156	12.533	3142	12.531	3220
12.526	3492	12.743	2731	12.739	5592	12.513	2946	12.742	1726	12.734	3166
12.976	4762	12.998	4771	12.98	5656	12.737	1154	12.996	3709	12.982	4560
13.216	1922	13.184	1216	14.077	3531	12.974	4083	14.101	3010	14.079	3255
14.074	3698	14.1	3614	16.774	6253	13.159	2202	16.792	3378	16.776	3305
16.767	6205	16.791	6463	17.419	2048	14.068	2931	18.349	13861	17.626	1067
17.624	2306	17.643	2321	17.636	1561	16.768	3298	21.867	15592	18.325	17266
18.312	16333	18.34	14434	18.326	18081	18.32	13988	22.067	16353	21.803	16307
21.867	18863	21.835	17921	21.824	20140	21.835	18226	22.472	12169	22.049	16265
22.031	16832	22.074	16403	22.024	15394	22.013	14432	22.741	3295	22.446	12640
22.426	11652	22.471	11780	22.444	11663	22.428	11830	24.15	1513	22.688	3130
22.709	4425	22.731	4402	22.684	4437	22.677	3428	24.627	1651	24.131	4965
24.13	2018	23.755	1420	24.115	1945	23.748	1278	24.79	1324	24.612	6379
25.323	2382	24.134	5859	24.606	1104	24.107	6291	25.184	3610	24.759	3220
25.495	6606	24.624	8681	25.227	3403	24.597	4098	25.523	9371	25.184	8688
26.005	1431	24.785	3761	25.499	5054	24.767	2911	26.021	1421	25.502	7237
26.22	1887	25.205	7457	25.628	3969	25.035	2198	26.256	4220	25.643	6816
26.837	1170	25.333	2706	25.984	2592	25.184	4651	26.848	1020	26.032	3893
27.138	499064	25.523	14780	26.247	7123	25.504	8890	27.157	480336	26.248	8557
27.566	26948	26.005	5105	26.645	1089	26.009	2688	27.589	28329	26.635	2620
28.136	5370	26.255	8385	26.837	1398	26.219	2658	28.177	4018	26.848	2057
28.448	1510	26.667	2615	27.14	504644	26.37	1406	28.426	3403	27.14	471925
28.914	44457	26.848	2316	27.569	28962	26.837	1308	28.934	35944	27.57	30604
29.632	1488	27.157	520028	28.153	5477	27.138	463262	29.643	1384	28.151	5211
34.977	1558150	27.588	32718	28.421	4998	27.567	26136	34.994	1672256	28.418	4903
38.519	3126	28.163	6371	28.914	43593	28.133	3015	36.829	1119	28.913	41484

45.275	21115	28.429	4488	29.611	2195	28.914	41718	36.954	1199	29.632	1641
		28.933	38964	30.371	1320	34.977	1599042	38.529	3644	30.377	1148
		29.653	1354	34.974	1590505	35.812	1180	45.295	34447	34.974	1631321
		34.994	1629840	36.937	1040	38.516	3080			36.94	1048
		36.835	1210	38.506	3827	45.277	24338			38.512	3517
		36.951	1294	45.253	26680					45.257	31373
		38.531	3847								
		38.768	1018								
		45.243	21792								

286 nm						310 nm					
RT	PA-0min	RT	PA-30min	RT	PA-90min	RT	PA-0min	RT	PA-30min	RT	PA-90min
1.402	122188	1.402	120685	1.395	113461	1.402	82238	1.403	79177	1.396	73738
1.561	8547	1.561	9137	1.553	8996	1.561	8248	1.561	8752	1.553	8702
1.853	81715	1.853	81453	1.845	76936	1.854	71013	1.854	66351	1.846	61640
2.205	22340	2.209	20973	2.202	21395	2.208	6552	2.219	6313	2.197	9752
2.715	6186	2.507	2026	2.703	8954	2.339	9552	2.336	8921	2.315	9253
4.057	1539	2.716	6594	5.859	1958	2.706	12762	2.724	5729	2.688	12227
5.852	2125	4.089	1381	6.584	7139	6.598	6084	6.617	5726	3.019	1328
6.562	6640	5.851	2093	7.224	6662	7.196	3234	7.216	3073	6.578	5671
7.194	6132	6.639	7613	7.731	3303	12.474	4192	12.499	4475	7.184	2792
7.737	3334	7.216	7027	12.505	3074	12.716	1557	12.747	1608	12.486	4497
12.477	3248	7.769	3415	12.733	1637	12.895	3958	12.931	3995	12.731	1589
12.721	1407	11.823	1490	12.97	4171	13.183	2153	13.187	1650	12.912	4320
12.979	3858	12.517	2925	14.086	2203	13.333	1226	13.361	1236	13.169	1632
13.187	2642	12.742	1072	16.779	1467	14.07	1461	14.09	1564	13.347	1415

14.067	2242	12.989	3289	18.011	4162	14.344	1502	14.37	1185	14.082	1376
16.773	1424	14.091	2235	18.197	2571	17.116	1295	17.144	1403	14.354	1089
18.311	10365	16.804	1619	18.322	4881	22.434	1284	22.478	1430	17.129	1356
21.835	9605	18.327	9085	21.781	10837	25.555	1129	25.554	4269	18.003	2963
22.042	9054	21.877	11511	22.049	7690	26.368	1130	27.157	41842	22.438	1572
22.426	11861	22.056	7232	22.44	13976	27.138	40423	27.592	20400	25.557	2906
22.709	2101	22.471	11983	24.122	1257	27.571	19537	28.777	1039	26.243	1197
24.117	2746	22.731	2014	24.614	1158	34.977	2016290	34.994	2107348	27.14	40681
24.633	2885	24.136	1255	24.761	1235	38.518	5054	38.53	5421	27.573	20217
24.764	2047	24.634	1399	25.201	3333	45.336	14390	45.266	18032	34.974	2056519
25.195	4478	24.767	1290	25.513	3991					38.513	5476
25.511	6710	25.212	2318	25.632	3466					44.527	2208
26.004	1694	25.535	9265	26.013	1723					45.286	14160
26.224	1274	26.021	1963	26.244	5364						
27.138	395911	26.254	3297	27.14	400165						
27.568	27209	27.157	409390	27.57	28229						
28.142	3898	27.59	28935	28.146	3211						
28.427	1162	28.167	3155	28.403	3815						
28.913	25384	28.44	2824	28.913	24638						
29.184	2961	28.932	21400	29.28	1463						
29.602	1581	29.237	2262	29.596	1552						
34.977	1637345	29.645	1266	34.974	1668522						
35.805	2417	34.994	1710141	36.93	1013						
36.107	1064	36.833	1034	38.517	3328						
36.288	1923	36.949	1105	45.298	33916						

| 38.516 | 2934 | 38.53 | 3554 | | | | | | | | | |
| 45.316 | 31101 | 45.293 | 38072 | | | | | | | | | |

358 nm					
RT	PA-0min	RT	PA-30min	RT	PA-90min
1.402	42088	1.403	38772	1.396	38846
1.562	7917	1.561	7986	1.554	7997
1.853	23869	1.853	20587	1.845	22894
1.968	2638	6.636	4702	1.961	2832
6.587	4700	11.843	1077	6.595	5158
11.868	1009	12.496	6769	12.482	6164
12.469	6047	12.745	4406	12.734	3926
12.723	3790	12.915	3964	12.902	3802
12.89	3594	13.179	2354	13.169	2227
13.157	2224	17.146	3942	14.357	1116
14.345	1340	27.159	2192	17.128	3838
17.123	3674	27.593	99325	27.146	2304
27.148	2229	34.994	8593920	27.574	98791
27.572	94559	38.529	14544	34.974	8401211
34.977	8220439			38.512	14932
38.518	13417				
44.496	2717				

Table S9.6: The chemical transformation of liquorice root extract with a mixture of BMDBM, BP3 and EHMC dissolved in methanol on simulated solar irradiation, monitored by HPLC-PDA.

275 nm	280 nm

RT	PA-0min	RT	PA-30min	RT	PA-90min	RT	PA-0min	RT	PA-30min	RT	PA-90min
1.41	133174	1.402	132743	1.398	131131	1.41	129019	1.402	127941	1.398	125938
1.571	9152	1.561	9936	1.556	9099	1.57	8547	1.561	9340	1.556	8567
1.864	90514	1.853	83649	1.85	86510	1.864	79026	1.853	79070	1.85	85121
2.223	27602	2.128	45008	2.199	38439	2.224	10817	2.201	36363	2.203	35514
2.75	31214	2.71	25085	2.734	26796	2.755	1233	2.716	23264	2.705	22856
3.261	14820	2.993	13859	3.221	21549	3.257	1525	2.992	10043	3.215	20545
3.558	6296	3.229	12563	3.525	12840	3.486	1584	3.205	7930	3.508	12851
4.099	1034	3.539	13223	4.035	8653	5.91	3694	3.536	5376	4.031	8198
5.918	4004	3.851	3579	5.839	3868	6.775	8547	5.845	4214	5.867	3471
6.738	10327	4.042	3187	6.582	10587	7.288	8603	6.584	8580	6.618	7816
7.342	9043	5.833	3528	7.195	9167	7.871	3851	7.207	7880	7.199	8055
7.877	3972	6.562	8694	7.739	4331	11.825	1178	7.759	3365	7.741	3844
11.855	1139	7.173	8360	12.573	3509	12.579	3020	12.528	2756	12.545	3318
12.583	2799	7.76	4015	12.769	4341	12.783	1104	12.735	1302	12.772	2987
13.037	4442	11.787	2415	13.026	5435	13.034	4018	12.979	3349	13.015	5118
13.28	1747	12.529	4274	13.227	1252	13.269	1829	14.078	2781	13.232	1399
14.135	3276	12.73	2331	14.13	3137	14.137	3061	14.378	1845	14.131	3235
16.823	5840	12.98	5128	14.471	2969	16.825	3078	16.782	3087	14.468	3040
17.483	1161	13.173	1035	16.836	5830	17.68	1192	17.434	1067	16.838	3093
17.676	1454	14.078	3539	17.493	1466	18.392	15670	17.62	1148	17.5	1443
18.389	16071	14.384	1689	17.699	2027	21.931	16599	18.337	15271	17.701	1130
22.142	35751	16.781	5819	18.414	17199	22.133	17525	21.803	17278	18.406	16809
22.539	12531	17.408	1404	21.963	17545	22.54	13648	22.035	15671	21.92	16452
22.805	4205	17.619	1554	22.157	17550	22.805	3286	22.44	12985	22.141	16402
24.177	2069	18.339	16469	22.541	11959	24.205	1668	22.699	2909	22.54	12708
25.376	1917	21.824	18286	22.795	3603	24.815	1029	23.744	1032	22.773	3454
25.585	3868155	22.038	17528	24.154	1972	25.585	4798003	24.124	5179	23.691	1545

27.201	529829	22.444	11456	24.994	1988	27.201	493177	24.618	6084	24.156	4826
27.484	15370	22.72	4263	25.288	3383	27.485	16819	24.766	3784	24.651	6173
27.633	25748	24.114	2294	25.557	3985436	27.634	25291	24.967	2764	24.794	3089
28.2	2420	25.275	2939	26.255	3396	28.216	2196	25.152	2684	24.995	4411
28.997	41815	25.537	3875195	27.151	534477	28.996	41469	25.272	4551	25.284	6957
33.69	1523	26.236	1299	27.582	30889	33.666	1541	25.537	4839913	25.557	4966928
33.926	1919	27.149	522326	27.797	9553	33.947	1808	26.237	1156	26.253	2797
35.052	1677431	27.578	27040	28.146	5561	35.052	1722737	27.149	483037	27.151	492744
35.369	6786418	27.804	8916	28.416	7474	35.369	8404158	27.579	25719	27.582	28144
36.405	3927	28.146	4983	28.928	48654	36.406	3738	27.809	8324	27.799	8253
36.64	1085	28.425	4996	29.644	7941	36.64	1257	28.151	3536	28.142	3008
36.892	15850	28.927	46026	30.598	3581	36.893	18523	28.427	3855	28.423	4496
38.587	3484	29.632	3799	30.848	1348	38.59	3293	28.925	44247	28.927	41650
45.313	27993	33.6	1599	33.632	1488	45.34	30790	29.631	4345	29.638	5155
		33.86	1748	33.844	1050			33.589	1380	33.557	1461
		34.99	1631523	34.995	1644479			33.86	1712	33.851	1064
		35.296	6035815	35.219	2733896			34.99	1676243	34.995	1688954
		36.101	1046	35.287	3321049			35.298	7117289	35.293	7062640
		36.356	3803	36.08	1768			36.354	3688	36.1	1439
		36.596	6159	36.357	3890			36.597	6694	36.357	3602
		36.842	10240	36.596	6922			36.843	11316	36.596	7464
		37.309	6803	36.839	8970			37.309	6056	36.839	14840
		37.531	7452	36.949	5423			37.531	6105	37.309	11168
		37.747	6699	37.31	11870			37.748	5827	37.529	10517
		37.889	8195	37.53	12658			37.886	7494	37.745	11729
		38.531	3727	37.745	13356			38.531	3522	37.883	15045
		45.274	23866	37.882	16386			45.316	29383	38.532	3721
				38.532	4284					45.32	32358
				45.317	24454						

286 nm						310 nm					
RT	PA-0min	RT	PA-30min	RT	PA-90min	RT	PA-0min	RT	PA-30min	RT	PA-90min
1.41	117480	1.402	116590	1.398	113733	1.411	78585	1.403	76980	1.398	73711
1.57	8398	1.56	8880	1.556	8125	1.57	7916	1.56	8587	1.556	8324
1.864	80741	1.853	75284	1.85	80343	1.864	69593	1.853	59779	1.85	65105
2.223	19896	2.203	38338	2.204	30683	2.229	6953	2.193	4392	2.203	7993
2.755	8839	2.715	17142	2.692	21387	2.347	6452	2.347	2473	2.325	7190
5.915	2241	3	9325	3.216	10538	2.528	4240	6.57	5436	2.701	9409
6.772	6934	3.215	5558	3.429	2722	2.738	5680	7.171	2662	6.627	4697
7.354	6319	3.411	4879	3.605	2278	3.992	1137	11.792	1162	7.741	1033
7.875	3131	5.857	1916	5.847	2510	6.748	4440	12.479	3563	12.517	4161
11.866	1085	6.588	5597	6.601	6186	11.848	1408	12.91	2519	12.772	1524
12.557	3045	7.202	5707	7.218	6036	12.531	4032	14.079	1443	12.947	4075
12.783	1239	7.73	2676	7.736	2892	12.777	1496	14.351	1310	13.219	1618
13.035	3635	11.791	1390	11.791	1370	12.957	3897	17.133	1254	13.397	1146
13.263	2388	12.492	2676	12.537	3087	13.243	2388	17.415	1579	14.128	1542
14.133	2109	12.722	1058	12.773	1794	13.397	1002	22.464	1538	14.422	1439
14.396	1136	12.976	3024	13.012	4691	14.128	1319	25.272	1328	17.194	1224
16.828	1539	14.082	2168	13.218	1252	14.394	1472	25.537	3702028	17.471	1653
17.477	1131	14.383	1784	14.138	2245	17.178	1257	27.149	41317	18.079	1924
18.376	9688	16.784	1265	14.453	3056	17.471	2068	27.583	22721	22.551	1474
21.952	11741	18.338	9549	16.842	1368	22.543	1494	27.814	4369	24.997	1765
22.155	7422	21.792	9460	17.472	1246	25.585	3721421	28.45	1168	25.294	3101
22.541	12340	22.053	9136	18.414	11352	27.201	43081	28.769	1054	25.557	3808448
22.752	2775	22.446	12060	21.963	9993	27.49	9681	33.86	1123	27.15	41574
24.178	1983	22.709	1934	22.161	8757	27.638	21213	34.99	2103404	27.585	22446
24.661	1483	24.134	2446	22.543	14157	28.838	1459	35.302	8968159	27.816	4547
24.816	1005	24.632	2866	24.185	2437	33.938	2288	36.596	6977	28.431	1475

25.269	1016	24.77	1924	24.649	2819	35.052	2167809	36.848	10517	28.772	1002
25.585	5472912	24.977	2149	24.795	2013	35.369	12085707	38.531	5557	33.867	1462
27.201	421370	25.12	2006	24.997	3272	36.356	1163	44.538	2211	34.995	2120166
27.487	17701	25.271	2917	25.293	5535	36.651	1035	45.348	14185	35.302	8669005
27.635	26531	25.537	5482690	25.557	5635900	36.896	23569			36.596	7739
28.211	1783	27.149	406645	26.253	2448	38.586	5356			36.848	10341
28.995	27496	27.421	5824	27.151	421696	45.332	14320			37.887	1371
33.653	1636	27.58	26899	27.583	28257					38.533	5977
33.939	2248	27.81	8186	27.807	9086					45.312	13772
35.052	1764193	28.126	2185	28.138	2294						
35.369	10077322	28.43	3001	28.421	4084						
36.189	1051	28.924	25094	28.926	26708						
36.397	2609	29.259	1997	29.641	4059						
36.894	21629	29.636	2582	30.574	1380						
38.588	3256	33.589	1387	33.536	1262						
45.329	32129	34.99	1715995	34.995	1729985						
		35.3	8221614	35.297	8090041						
		36.348	2202	36.112	1180						
		36.595	7446	36.348	2233						
		36.845	12062	36.596	8002						
		37.309	5308	36.841	15166						
		37.53	4342	37.309	9887						
		37.748	4390	37.53	7428						
		37.888	6391	37.745	8884						
		38.533	3380	37.884	12891						
		45.32	30879	38.533	3581						
				45.327	35448						

358 nm					
RT	PA-0min	RT	PA-30min	RT	PA-90min
1.411	40421	1.403	37652	1.398	36925
1.571	7723	1.561	7647	1.556	8325
1.864	23012	1.853	22650	1.85	23211
1.985	3273	1.969	2802	1.986	4106
6.77	5418	6.609	4534	6.638	5580
12.528	6201	12.477	5396	12.514	6398
12.777	4041	12.729	3632	12.773	4193
12.949	3679	12.898	3442	12.941	3807
13.218	2113	13.161	2162	13.216	2160
14.394	1225	14.359	1047	14.416	1069
17.181	3637	17.133	3656	17.193	3478
25.585	921858	25.276	1959	24.997	1019
26.419	1405	25.537	913296	25.295	2930
27.199	2453	27.15	2284	25.557	935616
27.64	102648	27.584	102185	27.154	2451
35.052	8927220	34.99	8839924	27.587	104278
38.586	14392	38.531	14900	30.818	1322
				34.995	8989042
				38.532	15854

Chapter Ten

The effect of lavender oil on the photostability of commonly used sunscreen absorbers in suncare products

Moses A. Ollengo and Bice S. Martincigh[*]

School of Chemistry and Physics, University of KwaZulu-Natal, Westville Campus, Private Bag X54001, Durban 4000, South Africa

*Corresponding author: Tel.:+27-31-2601394; Fax: +27-31-2603091; E-mail address: martinci@ukzn.ac.za

Abstract

The ability of lavender oil to photostabilize common sunscreening agents in cosmetics was investigated. The samples were exposed to simulated solar radiation in a 1 mm pathlength cuvette and the spectral changes were monitored with a UV-vis spectrophotometer. The photochemical changes were also monitored by GC-MS. The absorption spectrum of lavender oil shows a maximum at 260 nm indicating no significant ultraviolet B (UVB) (290-320 nm) and UVA (320-400) absorption. The absorption capacity of lavender oil decreases with increasing time of irradiation showing a steady photodegradation on exposure to light. When lavender oil was irradiated with *tert*-butylmethoxy dibenzoylmethane (BMDBM) photoinstability was observed. GC-MS analysis of these solutions showed a [2+2] cycloaddition reaction. The spectra of lavender oil and 2-ethylhexyl-*p*-methoxy cinnamate (EHMC) showed an erratic increase followed by a steady drop of light absorption with increased irradiation. There was no observed spectral change for benzophenone-3 (BP3) in combination with lavender oil, an indication of a good degree of photostability, however, more photochemical products were observed by GC-MS. These could indicate photosensitization reactions initiated by the triplet excited state of BP3. A mixture of lavender oil with all the three studied chemical absorbers showed relative photostability but with a blue shift indicating any cosmetic product with lavender oil cannot guarantee UVA protection to the consumer. We conclude that lavender oil may not photostabilize any of the sunscreens under investigation and itself cannot be used as UVB/UVA absorber. The inclusion of EHMC, BP3 and BMDBM in a lavender oil cosmetic product formulation, may pose a health risk due to unknown photoproducts formed.

10.1   Introduction

Lavender oil has been used in a wide range of products in the food, aromatherapy, fragrance and pharmaceutical industries due to its exceptional chemical composition associated with both aromatic and biological activities (Danh et al. 2012; Salah et al. 2009; Cavanagh and Wilkinson 2005). Proponents of alternative medicine, advocate the use of lavender oil as an antiseptic and pain reliever and so it can be applied to minor burns and insect bites and stings. The use of lavender oil to treat a variety of common ailments, such as sunburn and sunstroke (Hanamanthagouda et al. 2010; Salah et al. 2009; Cavanagh and Wilkinson 2005), has been reported. This essential oil is reported to be used in massage oil mixtures, and believed to be effective in the relief of joint and muscle pain, or in chest rub mixtures for the relief of asthmatic and bronchitic spasm (Hanamanthagouda et al. 2010; Sheikhan et al. 2012). It is also said to treat head lice when used in a hair rinse mixture, or on a fine comb to eliminate nits. One study suggests application of lavender essential oil instead of povidone-iodine for episiotomy wound care (Sheikhan et al. 2012; Sosa et al. 2005; Vakilian et al. 2011).

Despite its good therapeutic claims a number of *in vitro* studies indicate that lavender oil is cytotoxic and photosensitizing.   Recent work on the cytotoxicity of lavender oil to human skin cells demonstrated an *in vitro* cytotoxic effect on endothelial cells and fibroblasts at a concentration of 0.25 %.   In this work, linalool, a component of lavender oil, reflected the activity of the whole oil, indicating that linalool may be the active component of lavender oil (Cavanagh and Wilkinson 2005; Prashar et al. 2004). Other studies investigating the aqueous extracts of lavender *spp* showed that they reduce the mitotic index, but significantly induce chromosome aberrations and mitotic aberrations. The aqueous extracts induced breaks, stickiness, pole deviations and micronuclei. The authors observed that these effects were related to extract concentrations (Sosa et al. 2005).

Cavanagh and Wilkinson (2005) reported that lavender oil, and its major constituent linalyl acetate, are toxic to human skin cells *in vitro*. Contact dermatitis to lavender oil appears to occur at only a very low frequency. The relevance of this *in vitro* toxicity to dermatological application of *lavandula* oil remains unclear. For example, an investigative report by Placzek et al. (2007) on photo-toxicity of fragrances concluded that lavender oil and sandalwood oil do not induce photo-haemolysis. A clinical review by Groot and Frosch (1997) documents photosensitivity reactions due to these substances on patients with persistent light reaction but more recently a positive photo-patch test exonerating sandalwood oil has also been reported (Cavanagh and Wilkinson 2005).

The topical application of lavender oil has been implicated in gynecomastia, the abnormal development of breasts in pre-puberty teens. An investigation by Henley et al. (2007) showed that lavender and tea tree oil have compounds which suppress male hormones and mimic female hormones. This led the authors to suspect that lavender and tea tree oils, present in various personal care products including shampoos and lotions, may contribute to the increased incidence of early breast development in girls. However, an *in vivo* study on rats gave no evidence of estrogenic activity of lavender oils (Politano et al. 2013).

Considering all the claims and widespread use of lavender oils in cosmetics, aromatherapy and other forms of alternative medicine, we report for the first time photo-activity of lavender oil incorporated in sunscreen mixtures.   The aim of this work was to investigate the effects of this oil on the sunscreens: 2-ethylhexyl-*p*-methoxy cinnamate, benzophenone-3 and *tert*-butylmethoxy dibenzoylmethane. These sunscreen agents are commonly used in skin care products containing lavender oil among other ingredients.

10.2 Experimental

The investigation of the effect of lavender oil on common sunscreen absorbers was done by firstly characterising the components of the lavender oil and studying their UV absorption efficacy. The oil was then mixed with the sunscreen agents singly and then in a mixture following the procedure detailed here-under.

10.2.1 Materials

The lavender oil was purchased from the South Africa distributor: Vital Health Foods. The solvents acetonitrile (ACN) and methanol (MeOH) of HPLC-grade were purchased from Merck KGaA. The three chemical UV filters of analytical purity (99.9 %) were purchased as follows: 2-ethylhexyl-*p*-methoxy cinnamate (EHMC) and *tert*-butylmethoxy dibenzoylmethane (BMDBM) were a kind donation from BASF, and benzophenone-3 (BP3) was from Sigma-Aldrich.

10.2.2 Characterisation of lavender oil

The lavender oil was characterised by gas chromatography-mass spectrometry (GC-MS) and gas chromatography-flame ionisation detection (GC/FID) in order to identify the chemical components present.

10.2.2.1 Sample preparation

About 20 mg of lavender oil was dissolved in 25 mL of methanol at ambient conditions and protected from light by aluminium foil. The mixture was then made up to 50 mL in a volumetric flask with methanol. The resultant solution was filtered through a 0.45 µm Millipore Millex-LCR membrane filter and then transferred to an aluminium foil-cased glass vial for storage. This solution was used for both characterisation experiments and photostability studies. To study the effect of lavender oil on the photostability of sunscreen absorbers, the above solution was mixed with approximately 200 µM solution(s) of the sunscreens.

10.2.2.2 The GC/MS experiment

A 0.1 µL volume of the lavender oil alone and mixed with sunscreen was delivered into a Shimadzu GC/MS (QP2010 SE), with a column temperature set at 70 °C and injection port at 250 °C. Injections were in split mode at a ratio of 20:1. Components were separated in a GL Sciences InertCap 5MS/Sil 30 m × 0.25 µm quartz capillary column with a bound stationary phase consisting of 5 % dimethylpolysilphenylene siloxane. The column was held 70 °C for 2 min, raised to 240 °C at 10 °C min^{-1}, then held for 5 min followed by a rise to 270 °C at 10 °C min^{-1} and held for 10 min. The linear velocity was set at 30.0 cm s^{-1}. The MS ion source temperature was 200 °C and the interface temperature was set at 250 °C. The MS detector was programmed to run in scan mode in the *m/z* range 35-1000 at a scan speed of 3333. The total run time was 37 min with helium as the carrier gas.

10.2.2.3 The GC-FID experiment

To check method interconvertability a GC-FID experiment was carried out on the same samples (lavender oil alone and in sunscreen mixture(s)) with the same temperature program. The GC/FID used was a Shimadzu GC (GC-2010), fitted with an autosampler (AOC 20i) and a flow unit type (AFC-2010). Components were separated in a DB-5 (30 m × 0.25 µm) quartz capillary column with a bound stationary phase consisting of 5 % phenyl polysilphenylene-siloxane. The make-up gas was

nitrogen/air flowing at 10 mL min^{-1}, the carrier gas was hydrogen with a flow rate of 40 mL min^{-1} and oxygen/air flowing at 400 mL min^{-1}. The injection port was set at 250 °C, operating in split mode of 20:1 for an injection volume of 2 μL. The velocity flow control mode was adopted keeping the pressure at 61.9 kPa, the total flow rate at 5.0 mL min^{-1}, the column flow of 0.68 mL min^{-1}, and a linear velocity of 20.0 mL s^{-1}.

10.2.3   Photostability experiments

The sunscreen mixtures with lavender oil were prepared by adding about 20 mg of the sunscreen agents to 25 mL of the methanolic lavender oil solution (see Section 10.2.2.1). This solution was then made up to 50 mL in a volumetric flask with methanol. To obtain working solutions, appropriate dilutions were carried out in order to obtain a sunscreen agent concentration of about 200 μmol dm^{-3} in the lavender oil solution before photostability studies were performed.

Samples of the lavender oil with and without sunscreens added were exposed to simulated solar radiation in a Newport research lamp housing (M66901) fitted with mercury-xenon lamp, powered by an arc lamp power supply (Newport 69911). The power output of the lamp was controlled by a digital exposure controller (Newport 68951) maintaining the output at 500 W. The radiation from the lamp was passed through a 10 mm thick Pyrex filter to ensure that only wavelengths greater than 300 nm impinged on the samples. The exposure time was varied incrementally from 0 hour in steps of 30 min to 4 hours of continuous exposure. Each exposed sample was contained in a stoppered 1.00 mm pathlength quartz cuvette. After each irradiation interval a UV-visible spectrum of the sample was recorded on a Perkin Elmer Lambda 35 UV-vis dual beam spectrophotometer. A 0.1 μL aliquot of these same solutions was then injected into the GC-MS to monitor the chemical transformations in the lavender oil solution and the included sunscreen(s). The chemical changes in the solutions of sunscreens alone without the oil were monitored by HPLC by injecting a 20 μL aliquot after every irradiation cycle and their UV spectra recorded by a UV-visible spectrophotometer .(The HPLC results can be seen in the Supplementary Material section.)

10.2.3.1 GC-MS experiment for the irradiated samples

A 0.1 μL aliquot of irradiated lavender oil solution with or without the sunscreen absorbers was injected on to the GC-MS chromatograph to monitor the photochemical transformations by using the method described in Section 10.2.2.2.

10.2.3.2 HPLC analysis of the irradiated sunscreen absorbers

The chemical transformations in the irradiated samples were monitored on a Shimadzu Prominence LC chromatograph with a PDA detector. The chromatographic separation was achieved on an Agilent Zorbax Eclipse XDB C-18 reversed-phase column (150 × 4.6 mm i.d.; 5 μm particle size). The mobile phase was composed of water (solvent A) and acetonitrile (solvent B). The mixtures were resolved by varying the concentration of B as follows: 5–13 min, 16 % B; 13-18 min, 45 % B and held for 5 min; 23-28 min, 75 % B, held for 5 min; 33-40 min, 99 % B then held 5 min and then dropped back to 16 % B for 15 min. The experiment was performed at ambient temperature with a flow rate of 1 mL min^{-1} and an injection volume of 10 μL. The chromatograms were collected at detection wavelengths of 275, 280, 286, 310, 320, and 358 nm with a bandwidth of 4 nm simultaneously in each of the 60 min run time. The photodiode array detector was set to collect the UV-vis spectra of the chemical species separated over the range of 190 to 800 nm.

10.3   Results and discussion

The components of lavender oil were identified and their UV absorption capacity determined by using UV spectrophotometry before mixing with sunscreen(s) solution(s).

10.3.1   Characterisation of lavender oil

The constituents of unexposed lavender oil were analyzed by using GC-MS. The total ion chromatogram showed 39 peaks (Fig. 10.1). The identity of each peak was determined by comparison with the National Institute of Science and Technology (NIST) library. The criterion used for a positive match was a > 80 % similarity with a five hit threshold per peak. The components identified in this way are shown in Figure 10.2. By considering the peak height and peak area, linalool (35.23 %) and linalyl acetate (32.97 %) were found to be the major constituents of lavender oil. This is in agreement with the results of Umezu et al. (2006), who showed with the aid of standards that linalool and linalyl acetate were the major constituents of lavender oil. The other components found were: α-pinene, camphene, β-myrcene, *p*-cymene, limonene, cineol, borneol, terpinen-4-ol, geranyl acetate and caryophyllene, these too have been shown by other working groups. HPLC analysis of the lavender oil was done to compare the number of species identified by GC-MS and those on HPLC and the two were found comparable (Supplementary Materials Table S10.1). All the components identified by GC-MS analysis, and their retention indices and area percentages are summarised in Supplementary Materials Table S10.2. These compounds have been reported to have several valuable properties. The main fragrance compounds of lavender essential oil are linalool and linalyl acetate. They are used in decorative cosmetics, fine fragrances, household cleaners, detergents, shampoos and other toiletries (Letizia et al. 2003). Linalool has been shown to possess antibacterial, antifungal and insecticidal properties. These bioactivities are useful for treatment of minor cuts, insect bites, scratch or fungal infections and for the preparation of a natural disinfecting solution. Camphor and menthol are readily absorbed through skin and produce a feeling of cooling and acs as a slight local anaesthetic and antimicrobial substance. In addition, camphor has been used as an antimicrobial substance with several applications for treating insects and improving sleep quality (Fismer and Pilkington 2012). It is also used as a natural flavouring agent and an ingredient for food processing (Karapandzova et al. 2012). In traditional Chinese medicine borneol is used as a moxibustion and it is a natural insect repellent (Duke 2014). Lavender is a popular aromatherapy plant that has an appealing scent that has been incorporated into numerous products. In aromatherapy, lavender is believed to possess anticonvulsive, sedative and anti-depressive effects, and to be useful for treating nervous breakdown, nervous tension and depression.
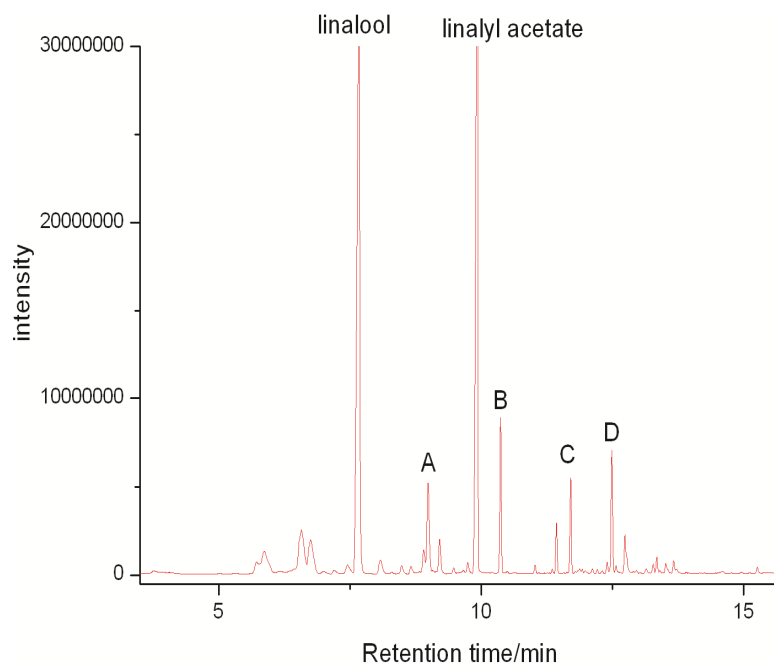
Figure 10.1: The total ion chromatogram of the unexposed lavender oils on GC/MS showing the major chemical constituents: linalool, terpinen-4-ol (A), linalyl acetate, lavandulyl acetate (B), geranyl acetate (C) and caryophyllene (D). The separation was effected on a GL Sciences InertCap 5MS/Sil 30 m × 0.25 µm quartz capillary column under the conditions described in Section 10.2.2.2.
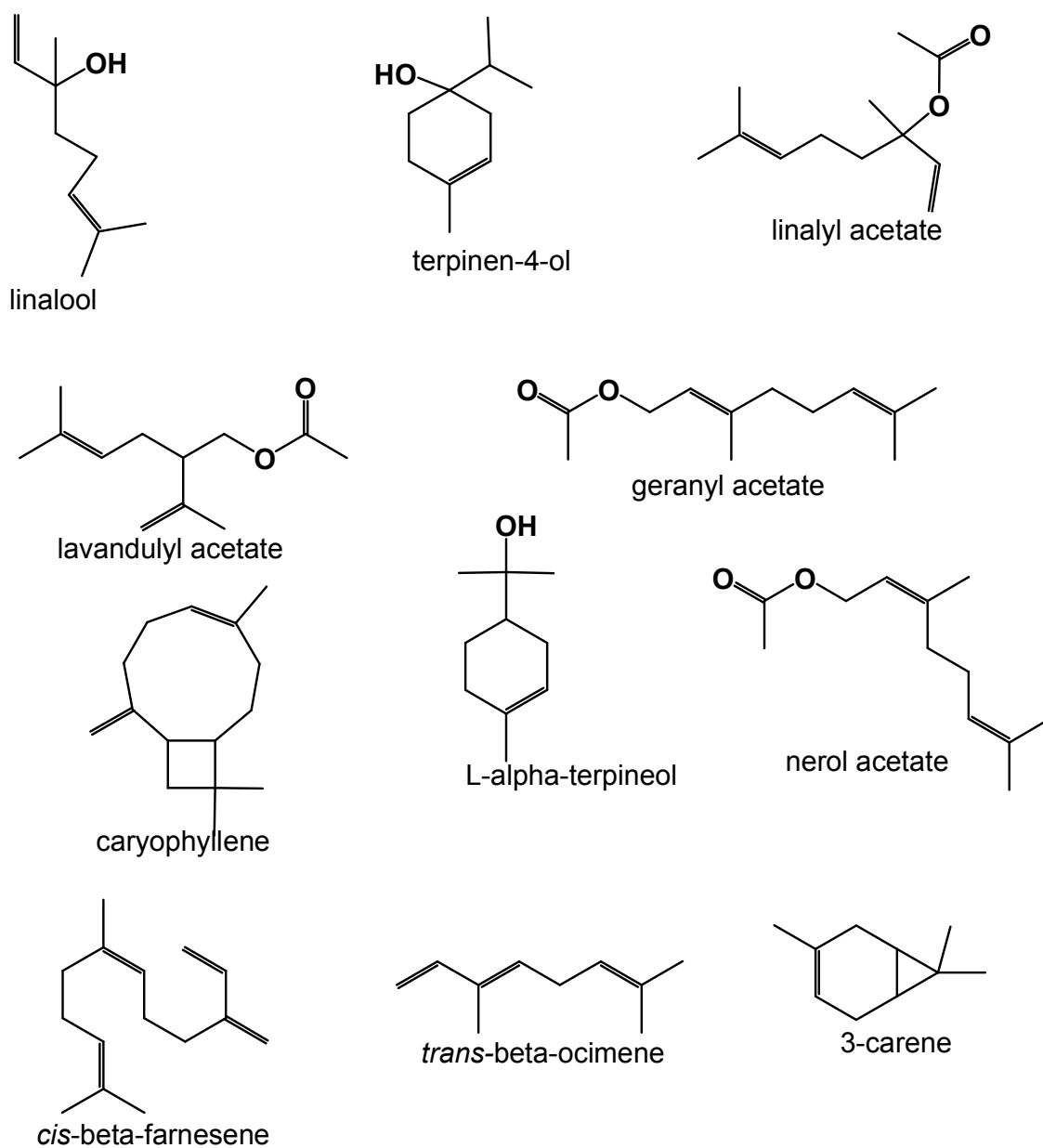
Figure 10.2: Chemical constituents of lavender oil.

10.3.2   The photostability experiments

The photostability of lavender oil alone and when mixed with sunscreen absorbers was investigated by examining the spectral changes arising from simulated solar irradiation. The chemical species formed were monitored by GC-MS.

10.3.2.1The photostability of the lavender oils

Lavender oil was exposed to simulated solar radiation for increasing time intervals in a 1 mm pathlength quartz cuvette. The spectral changes were recorded on a Perkin Elmer Lambda 35 UV-vi dual beam spectrophotometer. Each irradiated sample was then injected into the GC-MS chromatograph to monitor photochemical products. The oils showed weak absorption in the UVB and a maximum in the UVC range (absorption maximum wavelength, 263 nm) (Fig. 10.3). The UVC region of the spectrum does not reach the earth's surface. Hence the oil on its own is not suitable as a UV absorber. The absorbance of the oil decreased with increasing exposure time indicating a steady degradation of the chromophores in the oil (Fig. 10.3). The photoproducts also varied depending on the length of time of exposure. The major components of lavender oil: linalool and linalyl acetate, decreased significantly when the samples were exposed for 120 minutes, and then increased again when the samples were exposed for 240 minutes (Fig. 10.4 and Supplementary Materials Table S10.1). These compounds have some level of unsaturation in their carbon skeleton and therefore the drop in absorption of UV light may be due to photo-induced [2+2] cycloaddition reactions which cause a loss in the concentration of these compounds. A large number of chemical species were observed in the chromatogram for the sample exposed for 120 minutes. This could be due to the formation of self-dimers causing inter-and intra-molecular cleavages with the resultant effect of producing low UV absorbing species formed. Most of the compounds identified by comparison with the GC-MS library did not meet the library match criteria adopted in this work (> 80 %) and hence they were not considered as true photoproducts. It can be concluded that these cleavages gave rise to new chemical entities whose identities require further investigation. Very recently Gismondi et al. (2014) demonstrated that UV light induces a significant deterioration of lavender oil biochemical profile. This is, however, evidence that topical application of the lavender oil may expose the user to risk of photodegradation. The penetrative dermal effects of these photoproducts was demonstrated by Salah et al. (2009), in their study on rat skin exposed to ultraviolet radiation. These authors speculated a reversible change of stratum corneum behaviour when lavender oils were applied on the rat skin leading to accumulation of these compounds in the epidermis. These could explain the photo-dermatitis effect reported in other studies (Wu and James 2011).
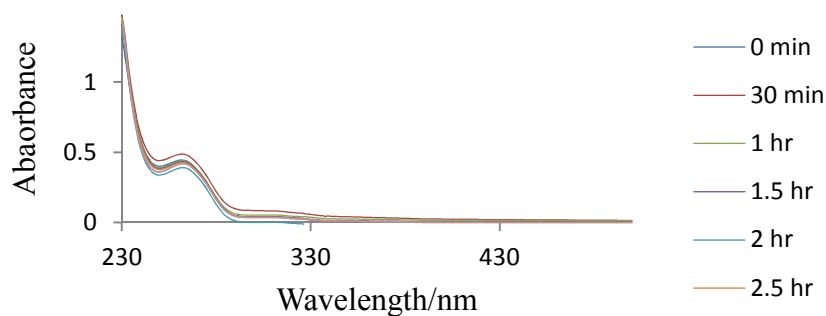
Figure 10.3: Photostability of lavender oil dissolved in methanol when exposed to simulated solar radiation. The spectral changes were monitored on a Perkin Elmer Lambda 35 UV-vis dual beam spectrophotometer, in a 1 mm pathlength quartz cuvette.
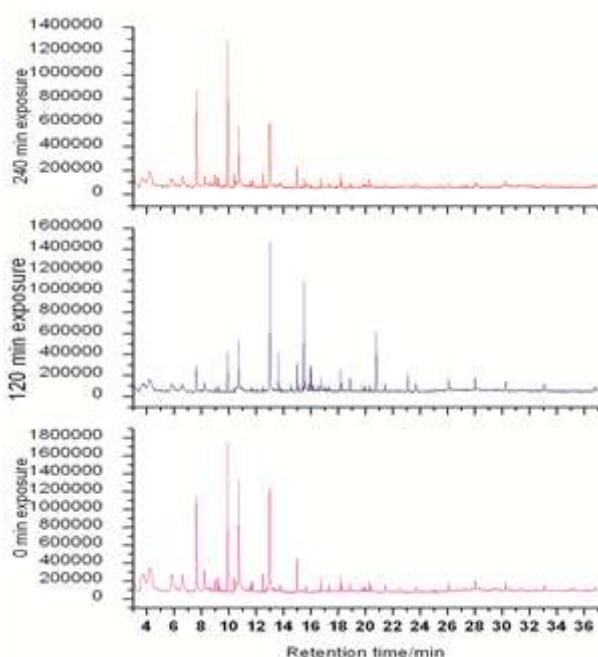

Figure 10.4: Selected photochemical transformations for exposed samples of lavender oils monitored by GC/MS. The separation was effected on a GL Sciences InertCap 5MS/Sil 30 m × 0.25 μm quartz capillary column under the conditions described in Section 10.2.2.2.

## 10.3.2.2 The effect of lavender oil on the photostability of EHMC

The irradiation of a solution of EHMC in methanol showed characteristic spectral decay (Fig. 10.5). The GC/MS total ion chromatogram (TIC) showed the isomerisation of *trans*-EHMC to *cis*-EHMC (Fig. 10.6). The peak areas of *trans*- and *cis*-EHMC seem not to change after 30 min of exposure which indicates that the process attains a photostationary state within a 30 min exposure period. No other products were observed to form. We conclude that exposure of EHMC dissolved in methanol to UV radiation only leads to isomerisation and therefore that formation of photodimers may only occur to a very limited degree (Fig. 10.7) if any are formed. This observation is in agreement with Broadbent et al. (1996) who showed a neat solution of EHMC forms dimers when irradiated, but indicated that a solution of *trans*-EHMC only yields *cis*-EHMC on UV irradiation. This current work only differs in the time taken to attain a photostationary state: ours is attained in the first 30 min

whereas theirs took longer but this dependent on the intensity of the irradiation sourc, and the concentration of the solution.

The spectral lability of the mixture of EHMC with lavender oil in methanol was not entirely characteristic of the cinnamate degradation (Fig 10.8). A drop greater than 0.3 in absorbance units was observed in the first 30 minutes indicating loss in the cinnamate chromophore. The GC-MS TIC showed the characteristic formation of *cis*-EHMC and an increase in the number of peaks (Fig. 10.9). There are a number of likely reaction pathways expected. The absorption of light of the order of 300 nm triggers $\pi\pi^*$ and $n\pi^*$ transitions, these events results in the electronic rearrangement of excited state *trans*-EHMC that leads to transition state cleavage of the C=C bond to allow rotation to *cis*-EHMC. This is accompanied by a drop in absorption due to the smaller absorption coefficient of *cis*-EHMC. However, the margin of loss in absorption observed in this mixture points to other reactions that characterise rapid loss of the cinnamic chromophore. The increase in the number of peaks and chemical species identified may be associated with photo-induced dimerization of EHMC leading to formation of strained dimer structures (Fig. 10.7). The strained cyclobutane structural moieties may break to form less UV absorbing species.

Other reactions involving unsaturated hydrocarbons and excited state EHMC may occur. Most unsaturated hydrocarbons are known to undergo [2+2] cycloaddition reactions within themselves and this may involve the incorporated EHMC. The four-membered rings formed are strained and therefore likely to participate in concerted ring opening metathesis reactions giving rise to several ring fragments. In this work exposure of the solution to solar simulated radiation for 180 minutes resulted in a further decrease of both *trans-* and *cis*-EHMC peaks and most peaks from the components of lavender oil (Fig. 10.9). Most striking is that the peaks that increased after sixty minutes of exposure also vanished. We therefore propose that ring fragmentations yield less volatile species that could not be detected by GC-MS.
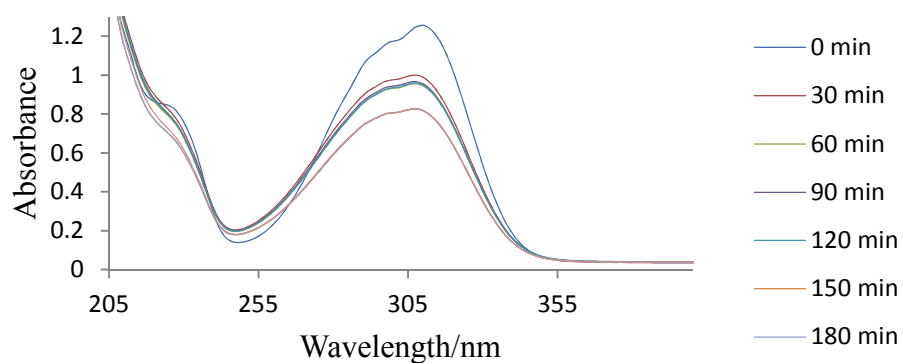
Figure 10.5: The spectral changes of a methanolic solution of EHMC irradiated by a solar simulated light source. The spectral changes were monitored with a Perkin Elmer Lambda 35 spectrophotometer, in a 1 mm pathlength quartz cuvette.
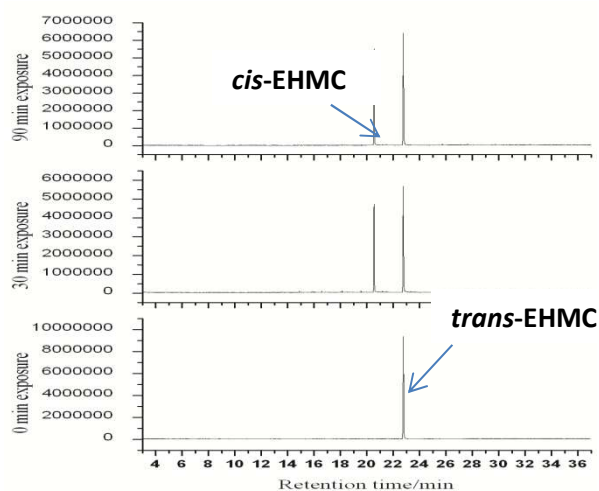
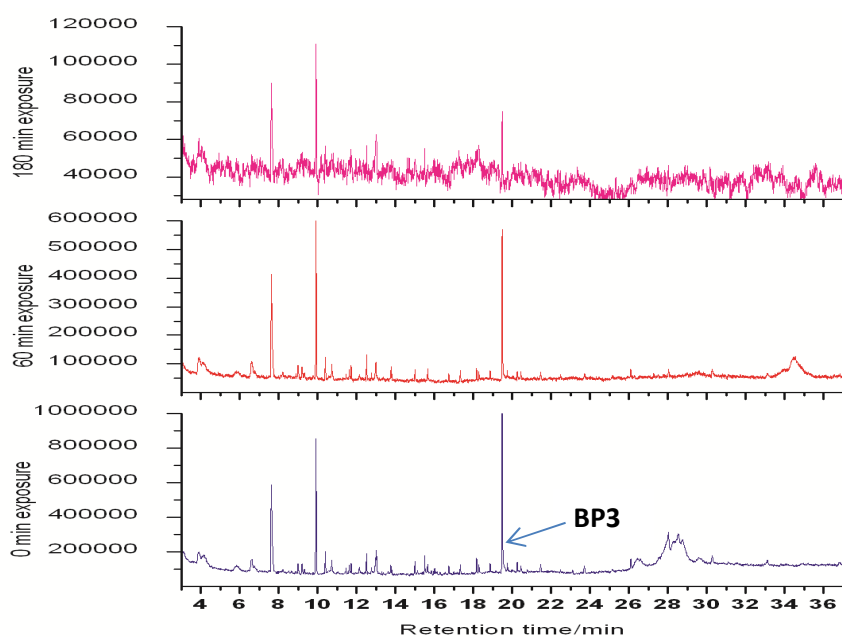Figure 10.6: The total ion chromatogram showing the photochemical changes of an exposed methanolic solution of EHMC. The separation was effected on a GL Sciences InertCap 5MS/Sil 30 m × 0.25 μm quartz capillary column under the conditions described in Section 10.2.2.2.
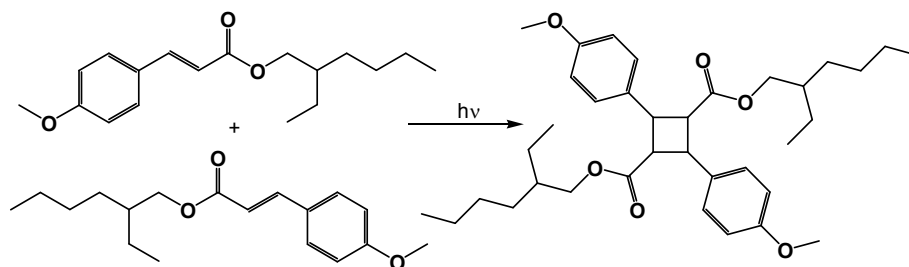
Figure 10.7: Photo-induced dimeration of EHMC.
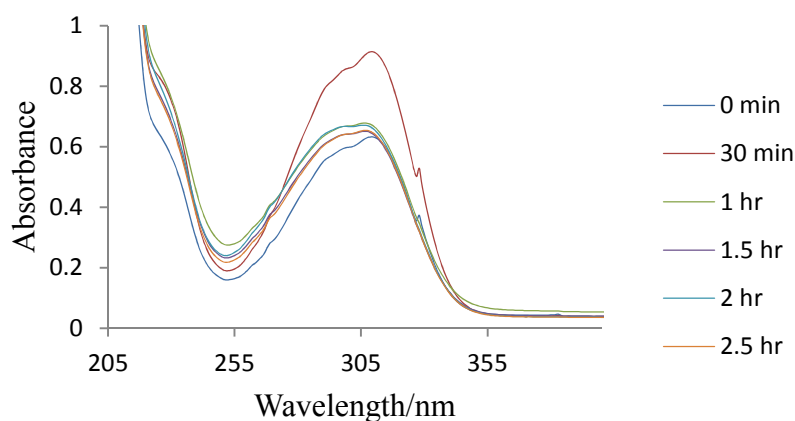
Figure 10.8: Photodegradation of EHMC incorporated in lavender oil dissolved in methanol when exposed to simulated solar radiation. The spectral changes were monitored on a Perkin Elmer Lambda 35 UV-vis dual beam spectrophotometer, in a 1 mm pathlength quartz cuvette.
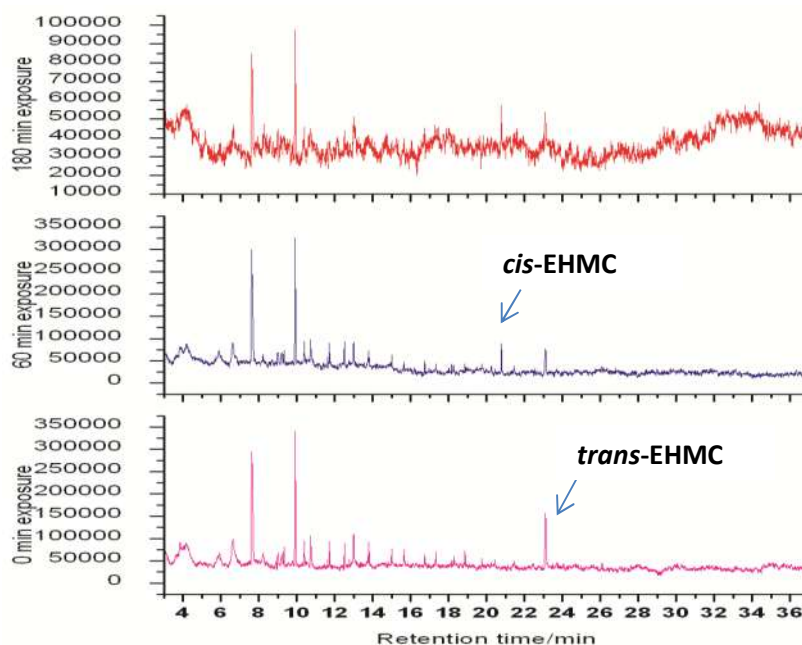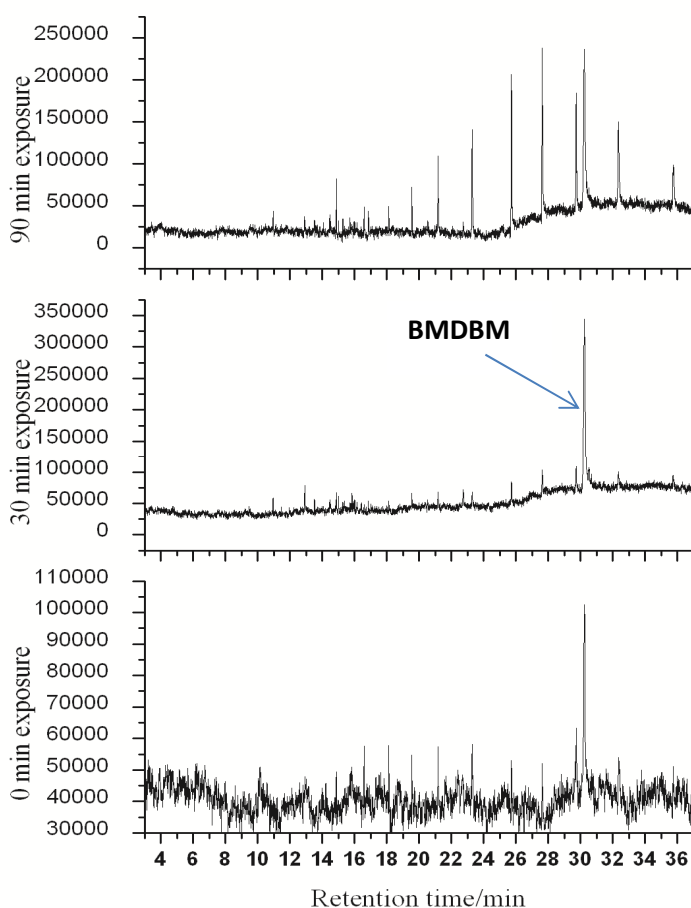

Figure 10.9: The total ion chromatograms showing photochemical changes of an exposed sample of lavender oil and EHMC. The separation was effected on a GL Sciences InertCap 5MS/Sil 30 m × 0.25 μm quartz capillary column under the conditions described in Section 10.2.2.2.

10.3.2.3 The effect of lavender oil on photostability of BP3

The irradiation of a solution of BP3 with a simulated solar light source showed spectral stability of BP3 (Fig. 10.10). The GC-MS analysis of this solution did not show any other peak for all samples and exposure periods (Fig. 10.11). This indicated that BP3 is photostable in methanol. The inclusion of BP3 in the solution of the lavender oil indicated a very small amount of degradation upon irradiation. This implied fairly high photostability on absorption of UV light for this sunscreen absorber (Fig. 10.12) in this mixture. The GC-MS TIC, however, indicates differently, particularly in the number of identified compounds. For an exposure period of 180 minutes only three significant peaks for linalool, linalyl acetate and BP3 could be seen on the chromatogram (Fig. 10.13). Even so these peaks are greatly reduced in magnitude indicating a loss of these components through participation in photochemical reactions. BP3 is a derivative of benzophenone which is a known photosensitizer in its triplet excited state ($^3\pi\pi^*$) (Kumasaka et al. 2014). Consequently there is high chance of BP3-photosensitized induced reactions giving rise to less volatile species and hence a loss in the number of volatile species.

The carbonyl chromophore of BP3 has lone pairs of electrons and is therefore capable of a n to π^* electronic transition upon absorption of light in the range 290 to 320 nm. This forms the lowest triplet state of BP3. The lowest triplet state ($^3n\pi^*$) of benzophenone is known to deactivate by abstraction of a hydrogen atom from hydrogen containing solvent molecules and to form the diphenylketyl radical at room temperature (Murai et al. 1978). This may initiate radical reactions in the mixture we have leading to production of various less volatile products. The solvent used in this experiment is methanol and components of lavender oil all have abstractible hydrogens and therefore it is a likely event in diverse forms. The unsaturation in linalool and linalyl acetate could also aggravate the situation for the excited state BP3 by engaging in photo-Fries reactions resulting in the formation of oxetane moieties that fragment yielding phenolic products detected by the GC-MS. The overall result is the multiplication of photochemical products. Because absorption by the benzophenone chromophore (C=O) is not lost as observed in the UV-spectra, we speculate that photo-Fries reactions are minimal but that the lowest excited state relaxation mechanism via hydrogen abstractions could be enhanced and hence cause the reduction in the BP3 peak observed in the TIC.
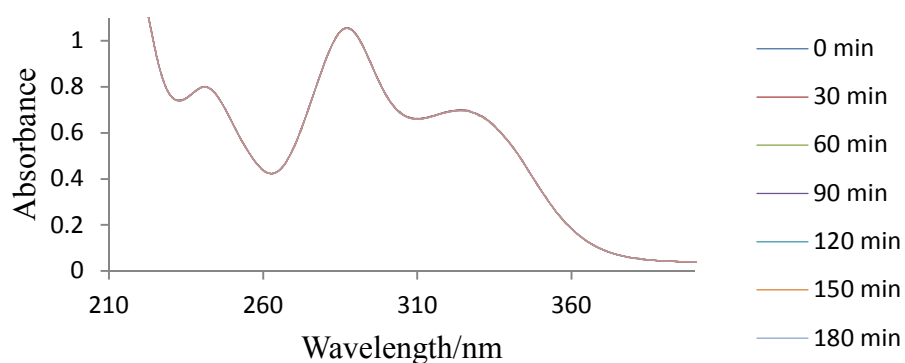
Figure 10.10: The photostability of BP3 in methanol irradiated by solar simulated light source. The spectral changes were monitored on a Perkin Elmer Lambda 35 UV-vis dual beam spectrophotometer, in a 1 mm pathlength quartz cuvette.
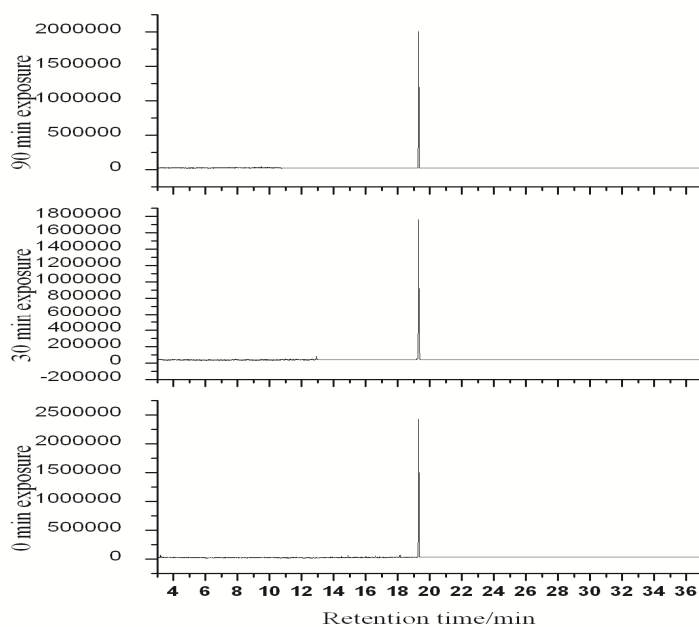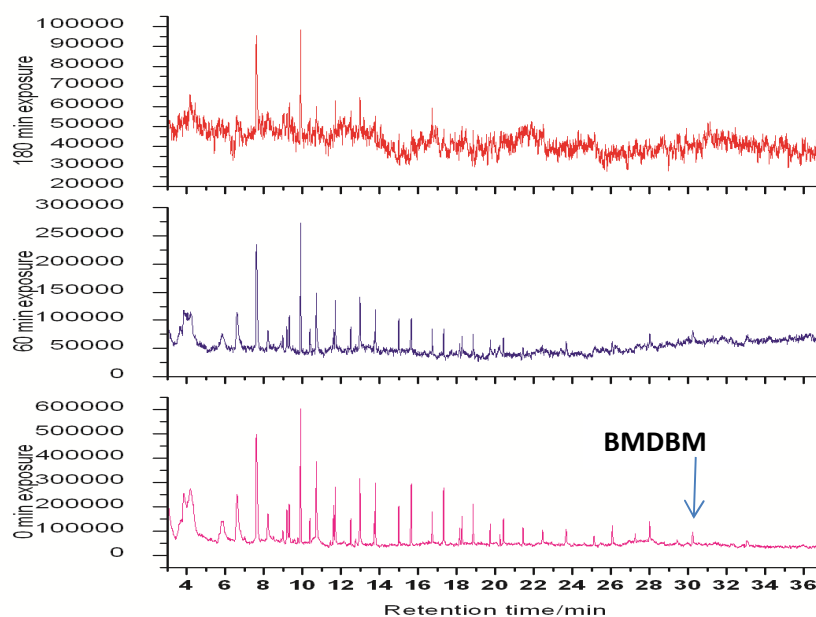

Figure 10.11: The total ion chromatogram of BP3 dissolved in methanol showing photochemical stability. The separation was effected on a GL Sciences InertCap 5MS/Sil 30 m × 0.25 µm quartz capillary column under the condition described in section 10.2.2.2.
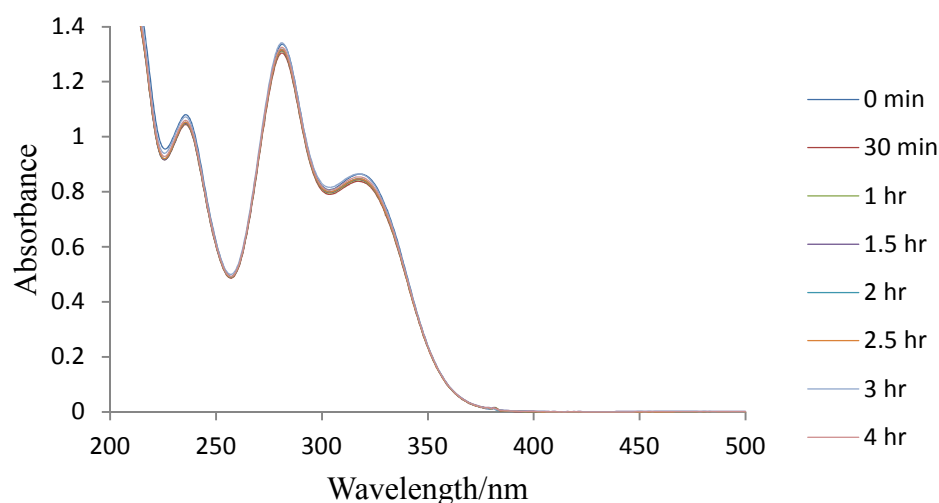
Figure 10.12: Photostability of BP3 incorporated in lavender oil dissolved in methanol when exposed to simulated solar radiation. The spectral changes were monitored on a Perkin Elmer Lambda 35 UV-vis dual beam spectrophotometer, in a 1 mm pathlength quartz cuvette.

Figure 10.13: The total ion chromatogram of BP3 and lavender oil showing photochemical changes. The separation was effected on a GL Sciences InertCap 5MS/Sil 30 m × 0.25 μm quartz capillary column under the conditions described in Section 10.2.2.2.

10.3.2.4The effect of lavender oil on the photostability of BMDBM

A solution of BMDBM in methanol when irradiated by simulated solar radiation showed photoinstability (Fig. 10.14). The TIC chromatogram showed formation of several chemical peaks after 90 min of exposure (Fig. 10.15). This observation indicates that it is not only the *keto-enol* tautomerism that occurs. A mixture involving lavender oil and BMDBM showed characteristic photodegradation of this photo-absorber (Fig. 10.16). However, the degradation was not as pronounced as for BMDBM alone for the same concentration of BMDBM. The TIC chromatogram not only shows a total disappearance of the BMDBM peak but also rapid reduction in the number of volatiles profiled by the mass spectrometer (Fig. 10.17). BMDBM in known to break down into two radicals, the benzoyl radical and the phenacyl radical, the mechanism of which is well presented by Schwack and Rudolph (1995). However, Mturi and Martincigh (2008) demonstrated that this photodegradation of BMDBM is solvent dependent and that polar protic solvents tend to photostabilize BMDBM. In this work we observed a steady decomposition of BMDBM in methanol in the presence of lavender oil. Contrary to their observation there was a significant drop in absorption in the first 30 minutes (~ 0.3 absorbance units). We envisage not only radical-initiated reactions but also concerted cycloaddition reactions. A thorough mechanistic investigation is required to establish the life-time of BMDBM in this mixture. BMDBM is a common sunscreen and lavender oils are frequently used in cosmetics. Most of these products also have a long shelf-life before they are sold. Our work demonstrates a rapid degradation of BMDBM and formation of less volatile compounds within 90 minutes of exposure. This raises concerns on the nature of the photoproducts and their fate on topical application on the living skin.
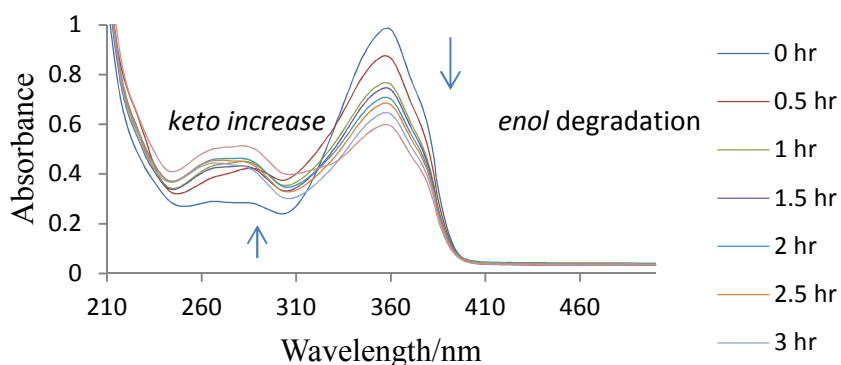
Figure 10.14: The spectral lability of BMDBM in methanol when exposed to solar simulated radiation. The spectral lability was monitored on a Perkin Elmer Lambda 35 UV-vis spectrophotometer, in a 1 mm pathlength quartz cuvette.

Figure 10.15: Total ion chromatograms for the solution of BMDBM in methanol irradiated with a solar simulated light source. The separation was effected on a GL Sciences InertCap 5MS/Sil 30 m × 0.25 μm quartz capillary column under the condition described in section 10.2.2.2.
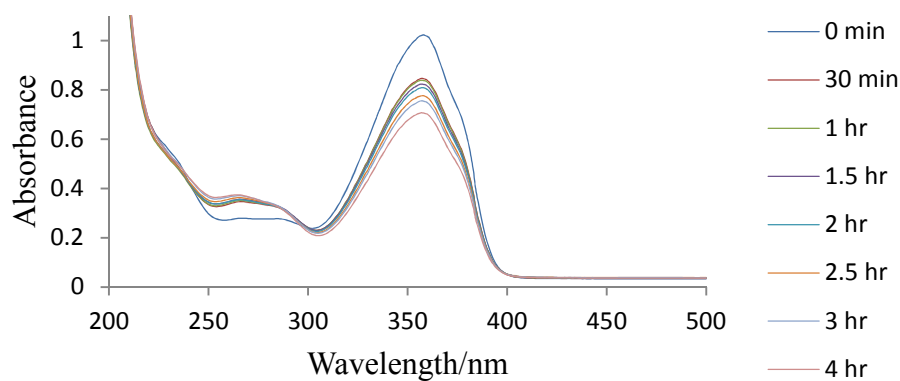
Figure 10.16: Photostability of BMDBM incorporated in lavender oil dissolved in methanol when exposed to simulated solar radiation. The spectral changes were monitored on a Perkin Elmer Lambda 35 UV-vis dual beam spectrophotometer, in a 1 mm pathlength quartz cuvette.

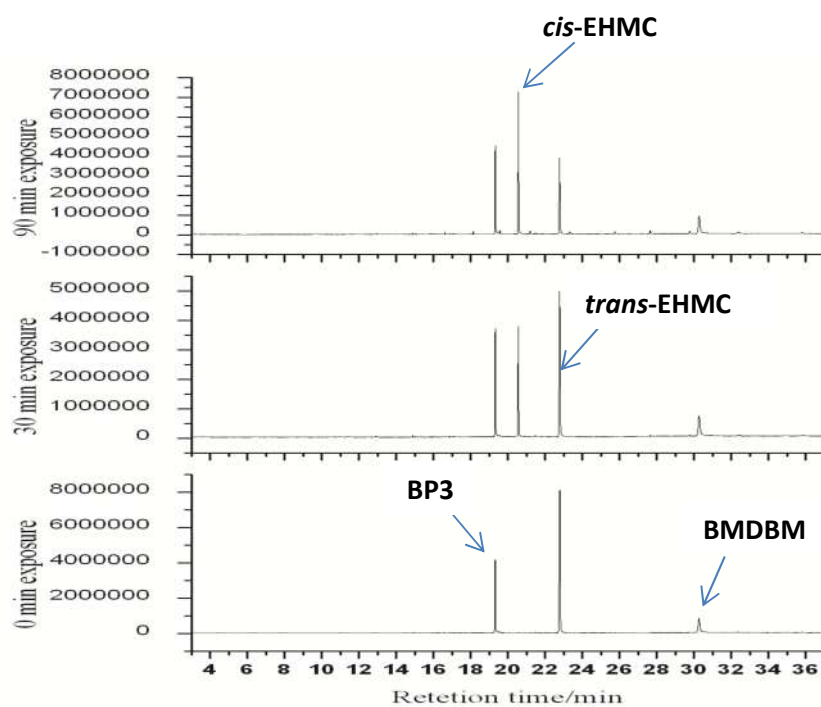Figure 10.17: Total ion chromatograms for an exposed sample of lavender oil and BMDBM. The separation was effected on a GL Sciences InertCap 5MS/Sil 30 m × 0.25 μm quartz capillary column under the conditions described in Section 10.2.2.2.

**10.3.2.5 The effect of lavender oil on the photostability of a mixture of BMDBM, BP3 and EHMC**

The photostability of a mixture incorporating all three common sunscreen absorbers with the lavender oil was investigated. First; ground state reactions were investigated by GC-MS. The unexposed mixture of the three absorbers was injected on the GC-MS and the constituents profiled (Fig. 10.18). The TIC chromatogram of the unexposed samples showed the presence of all three sunscreens and nearly all the components of lavender oil (Fig. 10.18 and Fig. 10.19). This shows that any other chemical transformations observed are as a result of exposure to solar simulated radiation. A mixture of the three sunscreens was irradiated by solar simulated radiation and monitored on a UV-vis spectrophotometer and GC-MS. Spectral lability was observed (Fig. 10.20). The observed drop in absorbance was accompanied by a blue shift (Fig. 10.20). The GC-MS TIC chromatogram showed the formation of *cis*-EHMC and the BP3 and BMDBM peaks do not show any change (Fig. 10.21). Whereas our previous experiment indicated attainment of a photostationary state in the isomerisation process of EHMC (see Section 10.3.2.2) in the first 30 min, this does not occur here. *Cis*-EHMC doubles its peak area after 90 min exposure with respect to *trans*-EHMC (see Supplementary Materials Table S10.1). This can be attributed to enhanced photosentization of EHMC by the excited state BMDBM (Kumasaka et al. 2014; Sayre et al. 2005). A mixture of EHMC and BMDBM has been shown to be inherently photo-unstable because BMDBM can photo-induce the isomerisation of EHMC to *cis*-EHMC (Panday 2002; Gonzenbach et al. 1992). The BMDBM has also been shown to form a mixture of *enol*-transient-*keto* forms yielding UVB absorbing species (Andrae et al. 1997). Our earlier work has shown that the *keto*-BMDBM strongly absorbs in the shorter wavelength UV region (see Chapters 7, 8, and 9).

A solution of a mixture of the three sunscreens with lavender oil was similarly irradiated and monitored by both UV-vis spectrophotometry and GC-MS. Mixing all the three sunscreen absorbers with lavender oil was expected to enhance the photostability of the sunscreen absorbers by synergistic effects or otherwise. The spectral changes observed in this experiment show an initial drop and thereafter the mixture becomes relatively stable only showing a much smaller spectral drop (Fig. 10.22). An inspection of the TIC chromatograms of exposed samples for incremental time intervals shows an increase in the number of peaks that is a sign of the formation of new chemical species (Fig. 10.23, and Supplementary Materials Table S10.6).

This solution has many likely reaction routes and the lower energy pathways are likely to be favoured. The total disappearance of the BMDBM peak is expected because it is a low energy activated $n\pi^*$ transition; lower than the lowest $^3n\pi^*$ of BP3 (Demeter et al. 2013; Yamaji et al. 2010; Shaath 2010; Azusa et al. 2009; Wilkinson 1997). Thus, the radical reactions dominate as a result of photosentization by BP3. The photosensitization reactions are envisaged as seen from the UV spectra of the mixture, the maximum at 290 nm is characteristic of the BP3 absorption spectrum. This implies that the C=O chromophore is un-affected though one of its aromatic rings may have acquired an electron-withdrawing auxochrome. Auxochromes are groups of atoms or functional groups that modify the absorption characteristic of a given chromophore. Electron withdrawing auxochromes reduce the wavelength of maximum absorption and so the BP3 shoulder in the UVA region dropped (Fig. 10.22). The aromatic ring bearing the methoxy group also carries the hydroxyl group at the *ortho* position. The methoxy group is an electron-donating group and the hydroxyl group at the *ortho* position has been argued to stabilize the carbonyl chromophore. Hence, we envisage no hydrogen abstraction relaxation mechanism for BP3 in this mixture but an excited state pseudo-transition state aromatic ring addition reaction. This would involve substitution of the acidic hydrogen by a

nucleophile. This claim requires further investigation to establish the molecular structure of this UV absorbing species. The various products formed would therefore result from photochemical decay of the intermediate products of the reactions between the sunscreen absorbers EHMC and BMDBM and
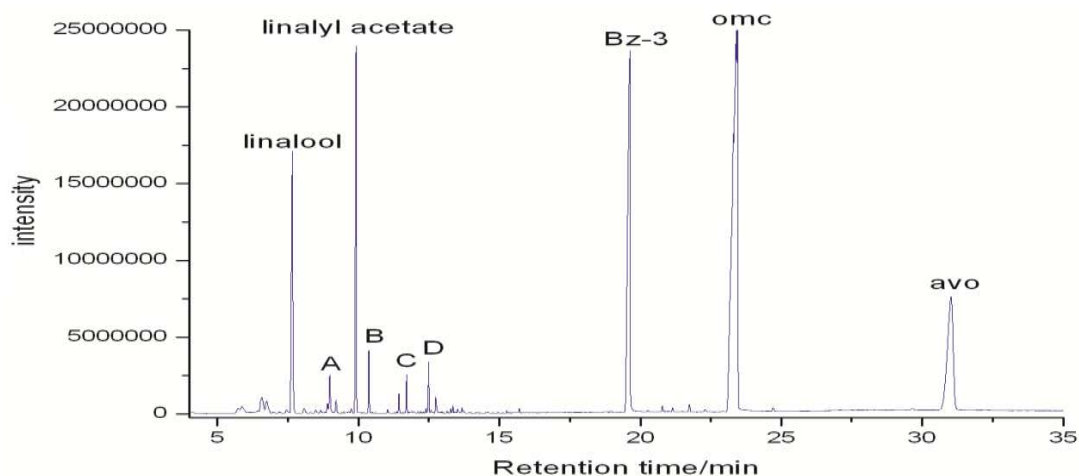
Figure 10.18: The GC/MS total ion chromatogram of an unexposed mixture of lavender oil (linalool, terpinen-4-ol (A), linalyl acetate, lavandulyl acetate (B), geranyl acetate (C) and caryophyllene (D)), EHMC, BP3 and BMDBM BMDBM. The separation was effected on a GL Sciences InertCap 5MS/Sil 30 m × 0.25 µm quartz capillary column under the conditions described in Section 10.2.2.2.

the unsaturated components of lavender oil.
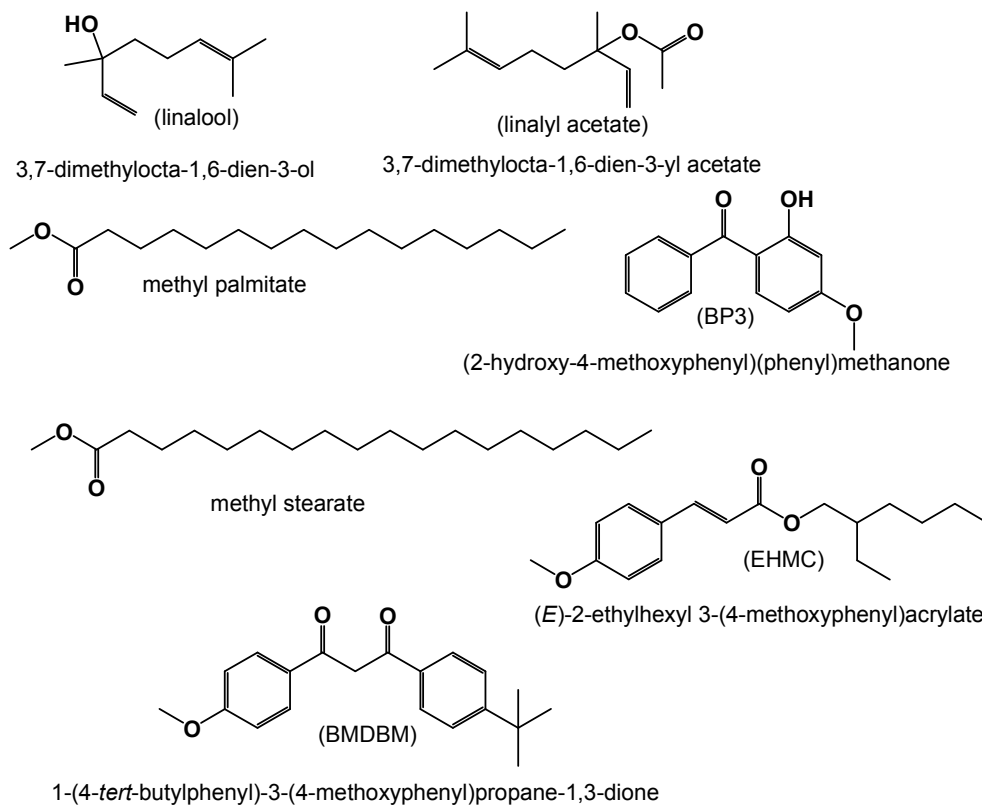
Figure 10.19: Major compounds identified by comparison with the NIST library from the GC-MS analysis of a solution of lavender oil, EHMC, BP3 and BMDBM in methanol.
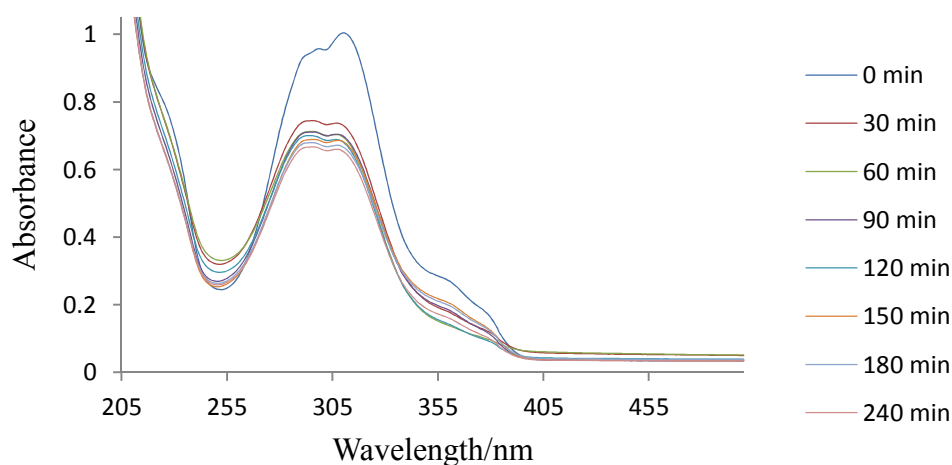
Figure 10.20 The spectral changes of a mixture of the sunscreens: EHMC, BP3 and BMDBM exposed to solar simulated light. The spectral change was monitored with a Perkin Elmer Lambda 35 UV-vis dual beam spectrophotometer, in a 1 mm pathlength quartz cuvette.

Figure 10.21: The total ion chromatogram of mixture of EHMC, BP3 and BMDBM showing photochemical changes. The separations were effected on a GL Sciences InertCap 5MS/Sil 30 m × 0.25 µm quartz capillary column under the conditions described in Section 10.2.2.2.
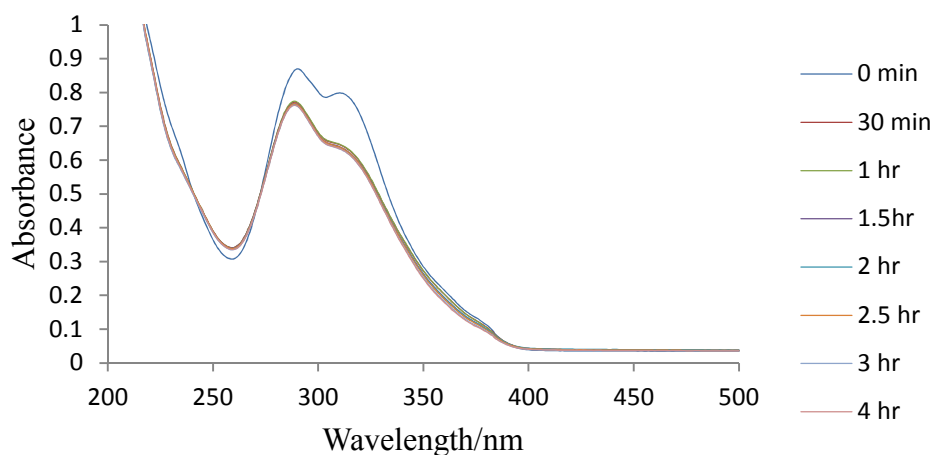
Figure 10.22: Photostability of EHMC, BP3 and BMDBM incorporated in lavender oils dissolved in methanol when exposed to simulated solar radiation. The spectral changes were monitored with a Perkin Elmer Lambda 35 spectrophotometer, in a 1 mm pathlength quartz cuvette.
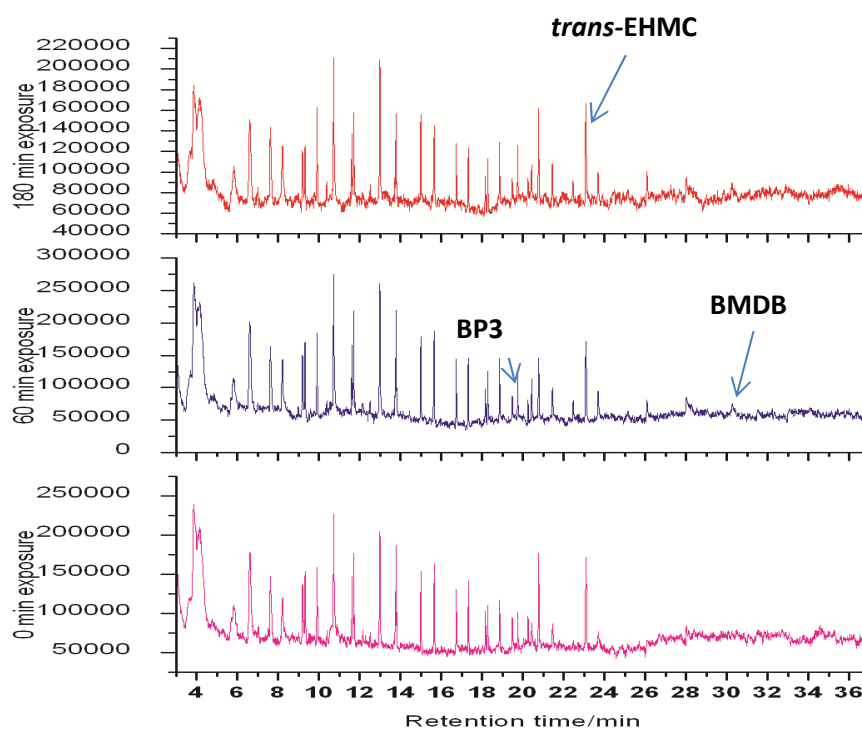
Figure 10.23: The photochemical transformation for the formulation containing EHMC BP3 and BMDBM and lavender oils exposed to simulated solar radiation. The separation was effected on a GL Sciences InertCap 5MS/Sil 30 m × 0.25 μm quartz capillary column under the condition described in section 10.2.2.2.

10.4   Conclusions

This study aimed at investigating the photo-activity of lavender oil and its effect on the photostability of the common sunscreen absorbers: EHMC, BP3 and BMDBM. The composition of the lavender oil was investigated and chemical components were identified. The major components were linalool and linalyl acetate. These were speculated to participate in the photochemical response of lavender oil. The lavender oil was found to adversely reduce the photostability of all the sunscreens investigated and more so generate a number of chemical species whose fate on the skin require further investigation. A mixture of lavender oil with all the three studied chemical absorbers showed a blue shift indicating any cosmetic product with lavender oil cannot guarantee UVA protection to the consumer. However, the oil seemed to photostabilize BMDBM to small degree and the mixture of the three sunscreens was more stable. We conclude that sunscreen preparations and skin-lightening preparation for outdoor workers incorporating lavender oil with any of these chemical absorbers is unsuitable to offer broad-spectrum photoprotection and should be applied with caution.

References

Andrae I, Bringhen A, Bohm F, Gonzenbach H, Hill T, Mulroy L, Truscott TG (1997) A UVA filter (4-*tert*-butyl-4'-methoxydibenzoylmethane): photoprotection reflects photophysical properties. Journal of Photochemistry and Photobiology B: Biology 37:147-150

Azusa K, Nozomi O, Mikio Y (2009) Optical and Electron Paramagnetic Resonance Studies of the Excited States of 4-*tert*-Butyl-4'-Methoxydibenzoylmethane and 4-*tert*-Butyl-4'-Methoxydibenzoylpropane. Journal of Physical Chemistry 113:13492-13497

Broadbent KJ, Martincigh BS, Raynor WM, Salter FL, Moulder R, Sjoberg P, Markides EK (1996) Capillary supercritical fluid chromatography combined with atmospheric pressure chemical ionisation mass spectrometry for the investigation of photoproduct formation in the sunscreen absorber 2-ethylhexyl methoxycinnamate. Journal of Chromatography A 732:101-110

Cavanagh HMA, Wilkinson JM (2005) Lavender essential oil: a review. Australian Infection Control 10 (1):35-37

Danh LT, Triet NDA, Han LTN, Zhao J, Mammucari R, Foster N (2012) Antioxidant activity, yield and chemical composition of lavender essential oil extracted by supercritical CO_2. The Journal of Supercritical Fluids 70:27-34

Demeter A, Horvath K, Boor K, Molnar L, Soos T, Lendvay G (2013) Substituent effect on the photoreduction kinetics of benzophenone. Journal of Physical Chemistry A 117:10196-10210

Duke Jk (2014) Chemicals in: *Lavandula latifolia* MEDIK (*Lamiacea*) Apic, broad leaved, Lavender, Spike Lavender. doi:http://www.ars-grin.gov/cgi-bin/duke/farmacy2.pl?545(Accessedon13/08/2014)

Fismer KL, Pilkington K (2012) Lavender and sleep: A systematic review of the evidence. European Journal of Integrative Medicine:e436-e447

Gismondi A, Canuti L, Grispo M, Canini A (2014) Biochemical composition and antioxidant properties of *Lavandula angustifolia* Miller essential oil are shielded by propolis against UV radiations. Photochemistry and photobiology 90 (3):702-708

Gonzenbach H, Hill TJ, Truscott TG (1992) The triplet energy levels of UVA and UVB sunscreens. Journal of Photochemistry and Photobiology B: Biology 16 (3–4):377-379

Groot CA, Frosch JP (1997) Adverse reactions to fragrances: A clinical review. Contact Dermatitis 36:57-86

Hanamanthagouda MS, Kakkalameli SB, Naik PM, Nagella P, Seetharamareddy HR, Murthy HN (2010) Essential oils of *Lavandula bipinnata* and their antimicrobial activities. Food Chemistry 118:836-839

Henley VD, Lipson N, Korach SK, Bloch AC (2007) Prepubertal gynecomastia linked to lavender and tea tree oils. The New England Journal of Medicine 356:479-485

Karapandzova M, Cvetkovikj I, Stefkov G, Stoimenov V, Crvenov M, Kulevanova S (2012) The influence of duration of the distillation of fresh and dried flowers on the essential oil composition of lavandin cultivated in Republic of Macedonia. Macedonian Pharmaceutical Bulletin 1 (2):31-38

Kumasaka R, Kikuchi A, Yagi M (2014) Photoexcited States of UV Absorbers, Benzophenone Derivatives. Photochemistry and photobiology 90 (4):727-733

Letizia CS, Cocchiara J, Lalko J, Api AM (2003) Fragrance material review on linalyl acetate. Food and Chemical Toxicology 41:965-976

Mturi GJ, Martincigh BS (2008) Photostability of the sunscreening agent 4-*tert*-butyl-4'-methoxydibenzoylmethane (avobenzone) in solvents of different polarity and proticity Journal of Photochemistry and Photobiology A: Chemistry 200:410-420

Murai H, Jinguji M, Obi K (1978) Activation energy of hydrogen atom abstraction by triplet benzophenone at low temperature. The Journal of Physical Chemistry 82 (1):38-40

Panday R (2002) A photochemical investigation of two sunscreenabsorbers in a polar and non polar medium. MSc. Dissertation, University of Natal, Durban, South Africa

Placzek M, Fromel W, Eberlein B, Gilbertz K-P, Przybilla B (2007) Evaluation of phototoxic properties of fragrances. Acta Dermato-Venereologica 87:312-316

Politano TV, McGinty D, Lewis ME, Hoberman MA, Christian SM, Diener MR, Api AM (2013) Uterotrophic assay of percutaneous lavender oil in immature female rats. International Journal of Toxicology 32 (2):123-129

Prashar A, Locke IC, Evans CS (2004) Cytotoxicity of lavender oil and its major components to human skin cells. Cell Proliferation 37:221-229

Salah MB, Abderraba M, Tarhouni MR, Abdelmelek H (2009) Effects of ultraviolet radiation on the kinetics of in vitro percutaneous absorption of lavender oil. International journal of pharmaceutics 382:33-38

Sayre MR, Dowdy CJ, Gerwig JA, Shields JW, Lloyd VR (2005) Unexpected photolysis of the sunscreen octinoxate in the presence of the sunscreen avobenzone. Photochemistry and photobiology 81:452-456

Schwack W, Rudolph T (1995) Photochemistry of dibenzoyl methane UVA filters Part 1. Journal of Photochemistry and Photobiology B: Biology 28:229-234

Shaath NA (2010) Ultraviolet filters. Photochemistry and Photobiological Sciences 9 (4):464-469

Sheikhan F, Jahdi F, Khoei EM, Shamsalizadeh N, Sheikhan M, Haghani H (2012) Episiotomy pain relief: Use of Lavender oil essence in primiparous Iranian women. Complementary Therapies in Clinical Practice 18:66-70

Sosa S, Altinier G, Politi M, Braca A, Morelli I, Loggia RD (2005) Extracts and constituents of *Lavandula mutlifida* with topical anti-inflammatory activity. Phytomedicine 12:271-277

Umezu T, Nagano K, Ito H, Kosakai K, Sakaniwa M, Morita M (2006) Anticonflict effects of lavender oils and identification of its active constituents. Pharmacology, Biochemistry and Behaviour 85:713-721

Vakilian K, Atarha M, Bekhradi R, Chaman R (2011) Healing advantages of lavender essential oils during episiotomy recovery: A clinical trial. Complementary Therapies in Clinical Practice 17:50-53

Wilkinson F (1997) Quenching of electronically excited states by molecular oxygen in fluid solution. Pure and Applied Chemistry 69 (4):851-856

Wu PA, James WD (2011) Lavender. Dermatitis 22 (6):344-347

Yamaji M, Cecilia P, Miguel AM (2010) Steady-state and laser flash photolysis studies on photochemical formation of 4-t*ert*-butyl-4'-methoxydibenzoylmethane from its derivative *via* the Norrish Type II reaction in solution. Journal of Photochemistry and Photobiology A: Chemistry 209:153 - 157
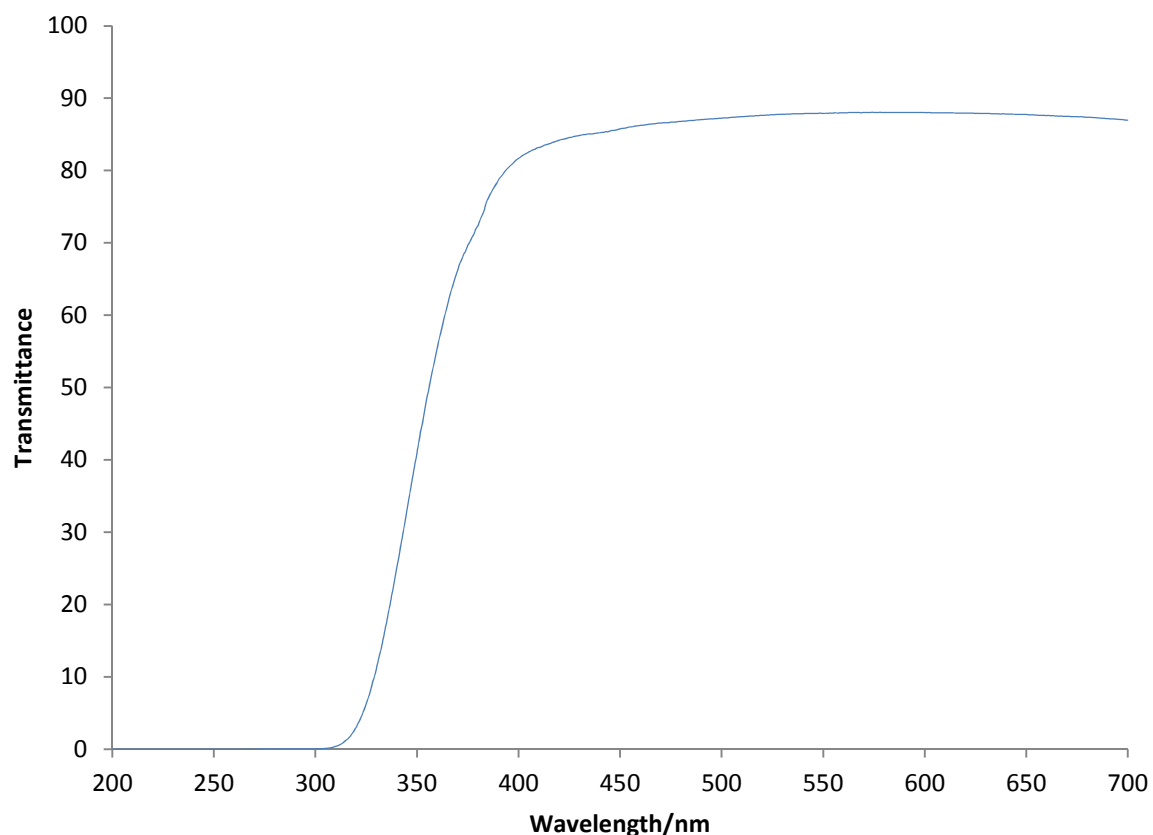
Figure S10.1: The transmittance spectrum of the 10 mm-thick Pyrex glass filter used in this work recorded on a Perkin Elmer Lambda 35 UV-vis spectrophotometer.

Table S10.2: The GC-MS results of the sunscreens: EHMC, BP3 and BMDBM exposed to solar simulated radiation for incremental period of time.

Exposure time/min		0	30	90	30	90
Sunscreen	type		peak area		Ratio of *cis*-EHMC/*trans*-EHMC	
cis-EHMC			12346471	23247414		
trans-EHMC	mixture	12611552	23016741	17031488	0.536	1.365
BP3		40997159	10855687	135589934		
BMDBM		6998458	6063437	6760110		
cis-EHMC	single		15480633	30137737	0.609	0.618
trans-EHMC		4457545	25404416	48759010		
BP3	single	6357540	4551065	5425680		
BMDBM	single	257520	2395318	1454228		

Table S10.3: The photochemical changes of irradiated lavender oil monitored by HPLC-PDA.

	275 nm				280 nm		
RT	PA-0min	PA-30min	PA-90min	RT	PA-0min	PA-30min	PA-90min
1.401	24010	24331	23849	1.4	24034	23478	23929
1.568	11081	11451	11424	1.567	10647	10838	10840
1.852	22986	23270	23024	1.852	24961	21976	22006
13.338	62356	60292	58067	1.986	1826		
15.459		10085		13.338	61243	58834	56839
16.16	1846	1937	1555	15.25		10657	
16.486	5393	4127	3730	16.139	1800		1617
16.889	13227	14208	14438	16.427	5004	1284	4314
17.269	8081		7675	16.868		2656	12370
17.312		7702		16.929	11573		
18.32	1518			17.269	9055		7891
19.515	5366	5351	5921	18.31	1089		
20.034	4076	4694	4225	19.525	5093	5435	5220
22.499		3663		20.036	4551	4894	4949
22.508	3655		3888	22.495		3056	
23.35	2311			22.511	3752		3196
23.825	4638	2784	2700	22.933	1394		
24.125	4240	1227	1131	23.338	3333		
24.395	3291			23.824	5306	2482	2279
24.629	2093			24.142	4620	1343	1398
24.942	4852	2296	2739	24.427	3674		
25.094			1648	24.662	2682		
25.112	2603	1670		24.943	5415	2453	2202
25.348	9230	7954	7822	25.115	3795	2339	2290
25.591	16282	15052	15081	25.343	7720	6384	6242
26.124	2119	2285	1854	25.591	14706	12334	12069
26.867	2148	2351	2656	26.117	3157	2320	2080
27.029	6074	6183	6229	26.866	2693	2810	3203
27.507	1020	1008	1036	27.033	6283	6061	6741
28.165	10688	10834	10215	27.502			2112
28.956	16112	15388	13800	28.163	8860	9112	9084
29.54	1270	1215	1152	28.957	13268	13043	12751
30.427	1649	1944	2195	29.543	1318	1260	1425
30.863	1710	2091	2186	30.426	1248	1489	
31.72	61768	59620	57530	30.796			1592
32.365		1058	1240	30.842	1526		1834
35.078	4246	4192	4981	31.719	60629	58802	56390
35.489	1125	1063	2586	32.315		1084	1361
35.853	2473	2853	4900	35.071	2587	1284	1188
36.139			1878	35.307	1516		
36.341			3226	35.849	3059	3123	3351

RT	PA-0min	PA-30min	PA-90min	RT	PA-0min	PA-30min	PA-90min
36.533			3752	38.445	6314	6541	6579
36.757			3239	38.794		5520	
37.042			4609	38.809	4776		5759
37.583			1735	38.959	3482	2755	2559
38.447	10024	10186	10045	39.157	1367	1253	1353
38.79		5358		39.784	1476	1315	1086
38.807	5246	2790	5559	45.29	111742	113956	109665
38.976	3298		2682				
39.136	1250	1464	1325				
39.763	1977	1427					
45.288	101020	103492	99930				

286 nm				310 nm			
RT	PA-0min	PA-30min	PA-90min	RT	PA-0min	PA-30min	PA-90min
1.4	23146	22639	23237	1.4	21194	21496	22149
1.567	10164	10271	10256	1.566	10665	10556	10500
1.852	21764	21485	21624	1.852	19808	19891	19908
13.337	54540	52771	51013	13.338	35524	34738	33393
15.225	1826		1327	15.213	1271	1225	1071
16.153				16.429	1045		
16.432	1526	1236	3472	22.579	1578		
16.891		2033	10361	25.556	1465	1175	1112
17.28			6687	27.015	1043	1133	1275
19.515		1045		31.73	1431	1372	1387
20.031	2466	2262	1977	35.316	2236	1848	1866
22.49		1779		35.839	2172	2157	2090
22.521	1991		1974	38.802	2339	2399	2211
23.341	2189	2356		45.327	75474	70191	71310
23.797			2693				
23.819	4822						
24.13	2547	1291	1055				
24.427	1662						
24.636	2835	1244	1249				
24.937	4420	2668	2689				
25.118	4650	3947	3830				
25.331	6252	5602	5193				
25.589	9767	8972	8339				
25.995	1292						
26.139	1741	3059	2300				
26.87	2471	2653	2523				
27.032	6388	6655	5900				
27.512		2078	1010				
28.159	6558	6630	6650				
28.946	8736	8098	9515				
29.501	1915		1650				

RT							
29.937			1264				
30.396	1158	1087					
30.416			1414				
30.834			1570				
31.718	51482	49464	47991				
35.323	1411	1431					
32.368			1143				
35.338			1598				
35.853	3437	3324	3685				
38.442	2472	2869	2824				
38.792		4662					
38.81	4481		4606				
38.965	2530	2403	2566				
39.157	1195	1166	1264				
39.782	1426	1006					
45.334	120358	123040	115133				

358 nm		
RT	PA-0min	PA-30min	PA-90min
1.4	20048	20303	18675
1.566	10787	10532	10815
1.853	18202	18234	18254
22.572	2217		
35.053	1359		
35.86	1083	1234	1326
44.452	3121		

Chapter Eleven

Quantitation and antioxidant Activity of phenolic acids from *Sutherlandia frutescens*

Moses A. Ollengo, Anis Mangenda and Bice S. Martincigh[*]

School of Chemistry and Physics, University of KwaZulu-Natal, Westville Campus, Private Bag X54001, Durban 4000, South Africa

*Corresponding author: Tel.:+27-31-2601394; Fax: +27-31-2603091; E-mail address: martinci@ukzn.ac.za

Abstract

The aim of this work was to investigate the phenolic acid content and antioxidant activity of the plant *Sutherlandia frutescens* subspecies *microphylla* commonly known as the cancer bush (CB). The medicinal value of CB and its reported role in the management of chronic ailments like HIV/AIDS generates interest for the identification and quantitation of the total phenolic acid content. The antioxidant properties of phenolic acids are known to reduce the risk of chronic diseases including cancer and heart sicknesses linked to oxidative stress. Phenolic acids were extracted from the leaves of the CB by Soxhlet (SXE) and ultrasonication (USE) extraction methods. These extracts were analysed by ultraviolet (UV) spectroscopy, high performance liquid chromatography (HPLC), and liquid chromatography-mass spectrometry (RP-HPLC-PDA-ESI-MS). Six phenolic acids were identified and quantitated by RP-HPLC-PDA, under isocratic elution conditions with an external standard method. The identified phenolic acids were: gallic, *p*-hydroxybenzoic, vanillic, caffeic, syringic and *p*-coumaric acids. The concentration of p-coumaric acid was the highest in all the extracts. RP-HPLC-PDA-ESI-MS was used to characterise three novel phenolic acids: 5-hydroxy-2-vinylbenzoic acid, an isomer of *p*-coumaric acid (**C-1**); (Z)-3-(4-hydroxy-2-methoxyphenyl)acrylic acid (**C-2**); and (Z)-2-hydroxy-3-(4-methoxyphenyl)acrylic acid (**C-3**) ferulic acid isomers. The Folin-Ciocalteu protocol was used to determine the total phenolic content of the extracts. The ultrasonication-diethyl ether (USDE) fraction gave GAE = 0.1247 mg g^{-1} and ultrasonication-ethyl acetate (USEA) GAE = 0.0769 mg g^{-1} as the highest and lowest total phenolic content respectively. Antioxidant activity was investigated by the DPPH free radical scavenging assay and the FRAP assay. The USDE extract (EC_{50} = 30.38 µg mL^{-1}) and the Soxhlet-diethyl ether extract (SXDE) (EC_{50} = 48.63 µg mL^{-1}) exhibited the highest and lowest antioxidant activity by DPPH assay respectively. The FRAP assay showed higher activity for USDE (EC_1 = 41.53 µg mL^{-1}) and lower value for SXDE extract (EC_1 = 33.05 µg mL^{-1}). The CB extracts with higher phenolic content had higher antioxidant activity and are thus a suitable remedy for free radical mediated ailments. Also the UV-vis spectra of the CB extracts had significant absorption in the UV region, and hence are viable ingredients in sunscreen preparations.

Keywords: *Sutherlandia frutescens,* radicals, antioxidants, phenolic acids, UV-photoprotection.

11.1 Introduction

Qualitative and quantitative investigations of the phenolic acid content of plants are of great interest due to their antioxidant properties especially for reported medicinal plants. Several working groups have reported the anti-inflammatory, antiseptic, antibiotic, antitumour and antioxidant properties of phenolic acids (Tarnawski et al. 2006; Baublis et al. 2000; Arimboor et al. 2008). The antioxidant properties of phenolic compounds draw attention for research because of their effect in preventing diseases related to oxidative stress (Yashin et al. 2011). Antioxidants have also been shown to be inhibit the formation of ultraviolet B (UVB) induced cyclopyrimidine dimers in human HaCaT cells (Guahk et al. 2010; Thongrakard et al. 2013). These dimers are the precursor lesions to skin cancer. Antioxidants are also known to offer systemic protection by stimulating cellular defence mechanisms (Thongrakard et al. 2013), remaining active for days. A body is considered to be under oxidative stress when there are excess reactive oxygen species (ROS) or reactive nitrogen species (RNS) conditions relative to its endogenous antioxidant capacity. This excess leads to "oxidation" of a variety of biomacromolecules, such as enzymes, proteins, DNA and lipids (Dai and Mumper 2010; Marxen et al. 2007). The oxidation of these biomacromolecules is linked to health complications such as cancer, heart disease, rheumatoid arthritis, inflammatory bowel disease, ageing and cataracts (Tarnawski et al. 2006; Dai and Mumper 2010). Humans can be exposed to oxidative stresses by exposure to pollutants and UV radiation; by smoking cigarettes; by ingestion of oxidized or burnt foods; and from cellular metabolism (Tarnawski et al. 2006; Baublis et al. 2000). These are initiators of ROS such as the hydroxyl radical ($^{\bullet}OH$); superoxide anion ($^{\bullet}O_2^-$); and hydrogen peroxide (H_2O_2) (Tarnawski et al. 2006; Marxen et al. 2007).

To prevent an imbalance between reactive oxidising species and the body's natural antioxidant capacity requires dietary antioxidant supplements (Baublis et al. 2000; Tarnawski et al. 2006; Paulo et al. 1999). The proposed mechanisms linked to the antioxidant properties of phenolic compounds include scavenging radical species, the suppression of ROS/RNS formation by inhibiting some enzymes or chelating trace metals involved in free radical production; and the protection of antioxidant defence (Dai and Mumper 2010). As antioxidants, phenolic acids enhance the protection against the above mentioned diseases by scavenging free radicals in the body (Baublis et al. 2000; Tarnawski et al. 2006; Cvetkovic and Markovic 2011). In general, phenolic compounds have been found to be more potent antioxidants *in vitro* than vitamin C and E and carotenoids (Baublis et al. 2000). For example, caffeic acid has been found to inhibit intracellular free radical production, not achievable with vitamin C (Kadoma and Fujisawa 2008). Epidemiological data show that the presence of phenolic acids in the diet can act as a preventive measure for various diseases (Biglari et al. 2008; Ramos 2008).

Phenolic acids are aromatic carboxylic acids, containing a single benzene ring bearing hydroxyl or methoxyl substituents. They are generally classified into two groups: benzoic acid derivatives and cinnamic acid derivatives (Fig. 11.1). Structurally, they can be distinguished by the number and position of the hydroxyl or methoxyl substituents on the benzene ring of benzoic acid. They are plant secondary metabolites, for fighting external stresses including pathogens, predators, UV radiation, mechanical damage, and low temperature conditions (Stalikas 2007). A commonly known phenolic acid is salicylic acid (*m*-hydroxybenzoic acid), an active signal molecule in plants.
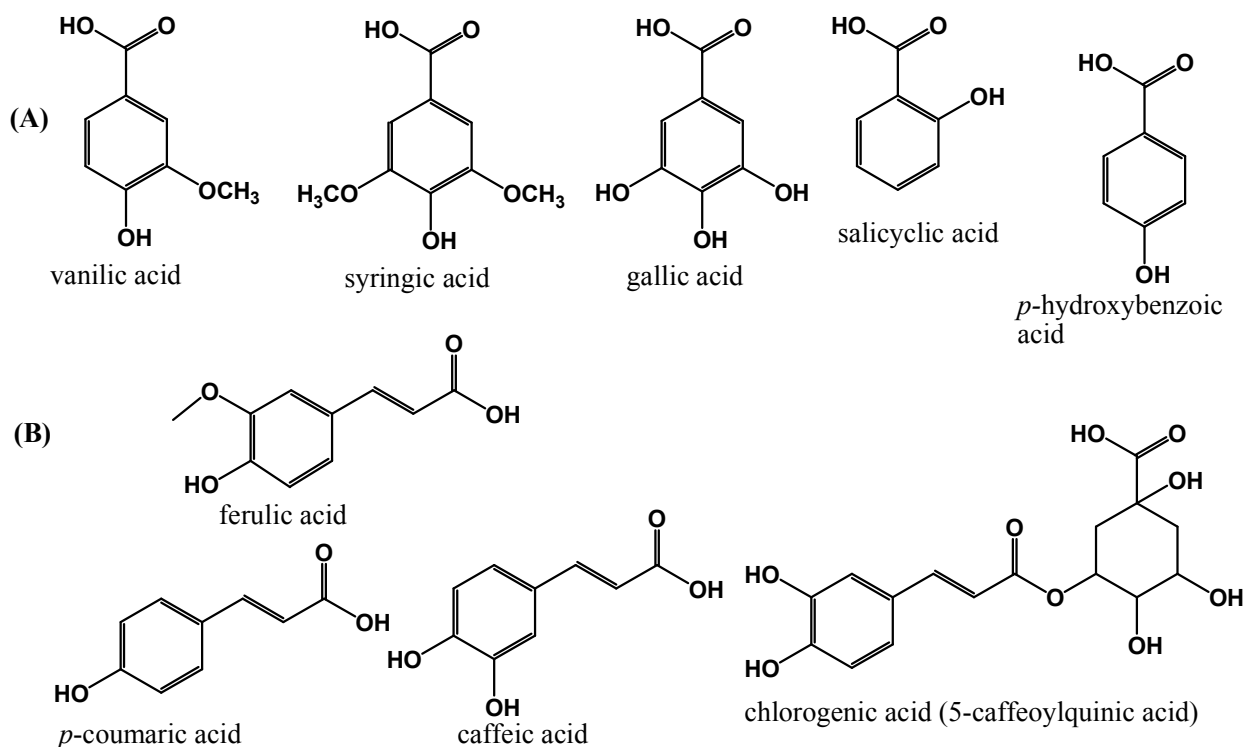
Figure 12.1: Structure of some phenolic acids: (A) benzoic acid derivatives; (B) cinnamic acid derivatives.

Sutherlandia frutescens (Fig. 11.2) is a medicinal plant, indigenous to dry parts of Southern Africa, and occurs mainly in the Western Cape up to Namibia and Botswana and in the western Karoo up to the Eastern Cape (Shaik et al. 2010). In South Africa it has various names such as *kankerbos* (Afrikaans), cancer bush (CB), and *unwele* (Zulu) (Shaik et al. 2010; Directorate of Plant Production 2009). The name cancer bush emanates from the ethnopharmacological belief that it cures cancer (Shaik et al. 2008). It serves different purposes including: washing of wounds and the treatment of colds, flu, rheumatism, bronchitis and dysentery. It is a reputed immune booster in the treatment of HIV/AIDS (Shaik et al. 2010; Shaik et al. 2008; Directorate of Plant Production 2009). The therapeutic effect of the cancer bush like in many other herbal medications is related to the presence of polyphenols. The role of polyphenols as antioxidants has been widely reported especially their ability to modify immune cell functions. The antioxidant activity of the cancer bush has previously been demonstrated by Fernandes et al. (2004) but a comparison of the total phenolic content to antioxidant activity has not been exhaustively reported. Therefore, an investigation of the cancer bush phenolic acid content and the relationship with the antioxidant activity is relevant, given its popularity in Southern African traditional medicine. In this work, phenolic acids present in the leaves were extracted, identified, quantified and their antioxidant activity and photoprotection ability investigated.

Figure 11.2: Leaves, pods and flower of *Sutherlandia frutescens* (Directorate of Plant Production 2009).

11.2 Experimental

11.2.1 Materials and Equipment

Leaves from the *Sutherlandia frutescens* (family: *Fabaceae*) plant were harvested and air-dried in the shade in the vicinity of Murraysburg in the Karoo, South Africa by W. Grobler. The plants were identified as *Sutherlandia frutescens* (L.) R. Br. Var. *microphylla* (Burch. Ex DC) Harv., by Professor B.-E. van Wyk of the Botany and Biotechnology Department of the University of Johannesburg [voucher specimen from W. Grobler: C. Albrecht s.n. sub. B.-E. van Wyk 4126 (JRAU)]. The phenolic acid standards supplied were: gallic acid (Hopkin and William), *p*-hydroxybenzoic acid (Aldrich Chemicals), vanillic acid (Merck kGaA), caffeic acid (Sigma-Aldrich), syringic acid (Sigma-Aldrich) and *p*-coumaric acid (Sigma-Aldrich) were all supplied at high purity (> 99%). 2,2-Diphenylpicryl-1-hydrazyl (DPPH) was obtained from Aldrich, 2,4,6-tripyridyl-s-triazine (TPTZ) was purchased from Merck KGaA, ammonium ferrous sulphate was from BDH, ferric chloride from UniLAB, glacial acetic acid was from ACE, anhydrous sodium carbonate and sodium sulphate from BDH Chemicals Ltd, and Folin-Ciocalteu phenol reagent from Merck kGaA and acetic acid was from Sigma-Aldrich. The solvents used were deionised water obtained from a Millipore Milli-Q® water purification system (Millipore, Bedford, MA, USA), methanol (BDH Prolabo), ethanol (Sigma-Aldrich), diethyl ether (DE) (Sigma-Aldrich), ethyl acetate (EA) (SMM Instruments) and petroleum ether (Sigma-Aldrich).

11.2.2 Sample preparation, extraction and purification of phenolic acids

A sample of dried CB leaves (84 g) was ground to a fine powder by using a mechanical grinder. To obtain crude extracts two methods were employed: Soxhlet extraction (SXE) and an ultrasonication (USE) method. After the crude extraction in methanol and soaking the extract in water, diethyl ether (DE) and ethyl acetate (EA) were used to extract the phenolic acids from the aqueous phase. Both DE and EA have been used extensively in literature for the extraction of phenolic acids, giving similar extraction efficiencies (Stalikas 2007). In this work, both solvents were used in order to compare their effectiveness in isolating phenolic acids from the rest of the methanolic extract.

11.2.2.1　　　　Soxhlet extraction

About 20 g of dry CB powder was extracted with approximately 100 mL of methanol by means of Soxhlet extraction. The extraction was carried out for 18 hours, and then the crude extract was filtered through Munktell grade (3hw) filter paper under gravity into a clean pre-weighed round bottomed flask. The methanol was removed from the crude extract by means of rotary evaporator to dryness under vacuum at 56 °C to give a dark green tar-like residue. The extractible amount of the crude phenolic extract by this method was calculated on a dry weight basis (Table 11.1) by using equation 11.1.

$$\% \, \textbf{yield} \; = \frac{\textbf{weight of dry extract}}{\textbf{weight taken for extraction}} \times \textbf{100} \qquad\qquad \textbf{equation 11.1}$$

11.2.2.2　　　　Ultrasonic extraction

About 10 g of CB was placed in conical flask and 50 mL of methanol was added. The mixture was ultrasonicated for 30 min and then filtered under gravity through a Munktell grade (3hw) filter paper. The procedure was repeated with a further 10 g of CB. The filtrates from the two extractions were combined and the solvent was evaporated by means of a rotary evaporator under vacuum conditions at 56 °C. The percentage amount extracted by this method was similarly calculated from equation 11.1.

11.2.2.3　　　　Liquid-liquid extraction

A volume of about 120 mL of boiling water was added to each the crude Soxhlet and ultrasonication extracts in a round-bottomed flask and left to stand for 16 hours to allow water extractible phenolics to dissolve. The solutions were filtered through Whatman No. 1 filter paper under gravity. The filtrates were then divided into two portions and re-extracted with 30 mL portions of petroleum ether (PE) six times in order to remove lipophilic components. After extraction with PE, half of the aqueous phase from SXE or USE was re-extracted with 6 × 30 mL diethyl ether (DE) and the other half with 6 x30 mL ethyl acetate (EA). The EA or DE layers were dried by adding some anhydrous sodium sulphate (Na_2SO_4). The DE or EA was removed from the extract by rotary evaporation under vacuum, at temperatures of about 30 ºC for DE and about 45 ºC for EA. Each residue was reconstituted in methanol to achieve a concentration of approximately 12.5 mg mL^{-1}.

11.2.3　　　　HPLC separation and quantification of phenolic acids

Shimadzu LC-20 AD XR liquid chromatograph fitted with Zorbax Eclipse XDB C-18 column of dimensions 4.6 × 150 mm, 5 μm particle size, with a photodiode array (PDA) detection was used for identification and quantitation of the phenolic acids. The phenolic extracts were analysed by isocratic elution with a mobile phase consisting of 2 % (v/v) acetic acid in water-methanol 88:12 (v/v), and the flow rate was 1.00 mL min^{-1}. The column temperature was 25 °C. A 500 μL aliquot of each CB extract was diluted with an equal volume of mobile phase and a 10 μL volume of this resultant solution (now approximately 6.25 mg mL^{-1}) was injected into the chromatograph. The chromatograms were detected at 255, 260, 271, 274, 309 and 323 nm. All samples and standards were filtered through 0.45 μm Millipore Millex-LCR syringe filters before being injected into the chromatograph. The identification of phenolic acids was done by matching the retention time and UV spectra of the extract components with those of six phenolic acid standards. The quantitation of identified phenolic acids was done by an external calibration method. Stock solutions of each of the six acids containing approximately 10^3 mg dm^{-3} were prepared in methanol. Aliquots of these

standard stock solutions were diluted with the mobile phase to obtain multi-standard solutions with approximate concentration of 10, 20, 80 and 100 mg dm^{-3} of each acid. These solutions were used to obtain the calibration curves for each standard acid. Method validation was done by spiking extracts with 10 µL of each of the six phenolic acid stock solutions.

11.2.4　　　　Identification of novel phenolic acids by RP-HPLC-PDA-ESI-MS/MS

A reverse phase, Zorbax Eclipse-XDB C-18 column of dimensions 150 mm × 4.60 mm, 5 µm particle size protected with a 4 mm × 4 mm Zorbax Eclipse-XDB guard column under isocratic conditions of 12 % methanol; 88% water with 2 % acetic acid was used to achieve chromatographic separation at a flow rate of 1 mL min^{-1} and with 50 µL injection volumes. The HPLC system consisted of an Agilent 1100 series equipped with an Agilent 1100 series photo diode array detector and a mass detector in series (Agilent Technologies, Waldbronn, Germany). It consisted of a G1312A binary pump, a G1313A autosampler, a G1322A degasser and a G1315B photodiode array detector controlled by ChemStation software (Agilent, v.08.04). The chromatograms were detected at 255, 260, 271, 274, 309 and 323 nm. The mass detector was a G2445A Ion-Trap Mass Spectrometer equipped with an electrospray ionization (ESI) system and controlled by LCMSD software (Agilent, v.4.1). The nebulizing gas was nitrogen set at a pressure of 65 psi and a flow rate adjusted to 116 mL min^{-1}. A heated capillary and voltage was maintained at 350 °C and 4 kV respectively. The detector was programmed to scan masses in the range m/z 90 up to m/z 2000. All collision-induced fragmentation experiments were performed in the ion trap with helium as collision gas, with the voltage being ramped in cycles from 0.3 up to 2 V. MS^{2} data were acquired in the negative ionization automatic smart mode to get MS^{n-1}; primary precursor ion. MS^{3} data were obtained by manual fragmentation, targeting the most abundant ions in the precursor ion MS spectra. Targeting much lower abundant mass values on MS^{3} only yielded the primary precursor ion of the series. Frequent characteristic fragment ions shown in Table 11.2 were used to elucidate the structures of compounds C-1, C-2 and C-3.

11.2.5　　　　Determination of total phenolic content

The determination of the total phenolic content of each extract was done by using the Folin-Ciocalteu assay. A 150 µL of extract, 2400 µL of Millipore water and 150 µL of 0.25 N Folin–Ciocalteu reagent were combined in a plastic vial and then mixed thoroughly. The mixture was allowed to react for 3 min and then 300 µL of 1 N Na$_2$CO$_3$ solution was added and mixed well. The solution was incubated at room temperature (25 °C) in the dark for 2 hr. The absorbance was measured at 765 nm with a Perkin Elmer Lambda 35 UV-Vis dual beam spectrophotometer and the results were expressed in gallic acid equivalents (GAE; mg g^{-1} dry mass) based on an external calibration of gallic acid standards ranging from 50 mg dm^{-3} to 500 mg dm^{-3}. The measurements for both gallic acid standards and the samples were done in triplicate.

11.2.6　　　　DPPH scavenging assay

The free radical scavenging activity of the extracts was assessed by using the 2,2-diphenylpicryl-1-hydrazyl (DPPH) assay according to the method reported by Blois (1958). The reaction mixture contained 1.8 mL of 0.1 mM DPPH methanolic solution and 0.2 mL of each serial dilution of cancer bush extracts. Simultaneously a control was prepared without sample extract and both reaction mixture sets were incubated at room temperature for 1 hour in the dark. The antioxidant activity of each fraction was quantitated by the loss in colour at 522 nm on a Perkin Elmer Lambda 35 UV-Vis dual beam spectrophotometer. The percentage DPPH scavenged was calculated by using equation

11.2, where $A_{control}$ is the absorbance of the solution containing only DPPH diluted with the solvent, and A_{sample} is the absorbance of the DPPH solution after incubation with different concentrations of the CB extracts.

$$\% \textbf{ DPPH scavenged} = \frac{A_{control} - A_{sample}}{A_{control}} \textbf{ x 100} \qquad \textbf{equation 11.2}$$

The percentage DPPH scavenged and the absorbance due to the remaining DPPH were plotted against the volume of each extract. The EC_{50} value for each extract was obtained by reading off the linear section of the curve.

11.2.7 FRAP Antioxidant Assay

The FRAP assay was performed according to the protocol described by Benzie and Strain (1996). The stock solutions included 300 mM acetate buffer (3.1 g $C_2H_3NaO_2 \cdot 3H_2O$ and 16 mL $C_2H_4O_2$) of pH 3.6, 10 mM 2,4,6-tripyridyl-s-triazine (TPTZ) solution in 40 mM HCl, and 20 mM $FeCl_3 \cdot 6H_2O$ solution. A fresh working solution was prepared by mixing 25 mL acetate buffer, 2.5 mL TPTZ solution, and 2.5 mL $FeCl_3 \cdot 6H_2O$ solution. The standards were then incubated for 4 and 30 minutes at 37 ºC in a water bath before analysis in a 1 cm pathlength glass cuvette with Perkin Elmer lambda 25 UV-vis spectrophotometer fitted with a Peltier temperature controller set at 37 ºC. The absorbance of the solutions were measured at 596.00 nm. Standard graphs were constructed using known concentrations of ammonium ferrous sulphate dissolved in 80 % (v/v) aqueous methanol. All tests were done in triplicate and mean values were used to calculate EC_1 values. EC_1 is defined as concentration of an antioxidant having a ferric reducing ability equivalent to that of mM ferrous salt (Sarla et al. 2011). An aliquot of 5 mg mL^{-1} solution of cancer bush extracts (150 µL) were allowed to react with 2850 µL of the FRAP solution for 4 min and 30 min in the dark condition before absorbance measurements were taken.

11.2.4 Potential role of phenolic acid extracts in photoprotection

The potential role of the CB extracts in photoprotection was investigated by recording the UV-vis spectra of each extract. The UV-vis spectrum of a mixture of the six phenolic acids was also measured for comparison. All UV spectra were recorded on a Perkin Elmer Lambda 35 UV-vis dual beam spectrophotometer. For this experiment, the CB extracts and the phenolic acid standard solutions were diluted with methanol to achieve concentrations of 0.0625 mg mL^{-1} and 0.005 mg mL^{-1} respectively.

11.3 Results and discussion

The extraction of phenolic acids from the CB leaves was carried out by both Soxhlet extraction (SXE) and ultrasonic extraction (USE), due to the sample matrix dependence of phenolic acids (Waksmundzka-Hajnos et al. 2007). An additional step was introduced to remove lipophilic components so as to avoid masking the HPLC determination of phenolic acids (Ćetković et al. 2004). The effect of pH on the extraction of phenolic acids by releasing ester bound phenolics (Ayaz et al. 2005) was investigated and compared with un-acidified samples (Table 11.1). A comparison of the percentage yields of crude extracts indicated the USE yield to be higher than the SXE yield. The yields of purified extracts from the two solvents (Table 11.1) show that re-extraction with ethyl acetate (EA) has a higher yield of extract than re-extraction with diethyl ether (DE) for all extraction

methods. Acidified extracts: UHDE, SHDE, and SHEA showed a yield increase effect for SXE with EA (SXEA; 0.91% and SHEA; 1.58%) and a decrease in yield for DE (SXDE; 0.63% and SHDE; 0.48%) (Table 11.1).

Table 11.16: Yield of crude extract and purified extract obtained from each extraction method.

Method	Solvent for LLE	Extract	Mass of dried CB powder used/g	Mass of crude (methanolic) extract/g	Mass of purified extract/g	% Yield of crude extract/g	% Yield of purified extract/g
USE	DE	USDE	10.23	2.68	0.0442	26.2	0.43
USE	EA	USEA	10.23	2.68	0.0742	26.2	0.73
USE	DE*	UHDE	10.24	3.02	0.0808	29.5	0.79
SXE	DE	SXDE	10.06	1.94	0.0629	19.3	0.63
SXE	EA	SXEA	10.06	1.94	0.0919	19.3	0.91
SXE	DE *	SHDE	10.16	1.60	0.0492	15.7	0.48
SXE	EA *	SHEA	10.16	1.60	0.1601	15.7	1.58

* pH was adjusted to 2.1 with HCl before purification by LLE.

RP-HPLC-PDA quantitation was based on ultraviolet (UV) spectra and retention times (RT) of the phenolic acid standards after optimising column conditions (Fig. 11.3). Each phenolic acid was identified and quantitated at its wavelength of maximum absorption. Diluting the standards and extract samples with the mobile phase gave better peak profiles with baseline resolution (Figure 11.4 and 11.5).
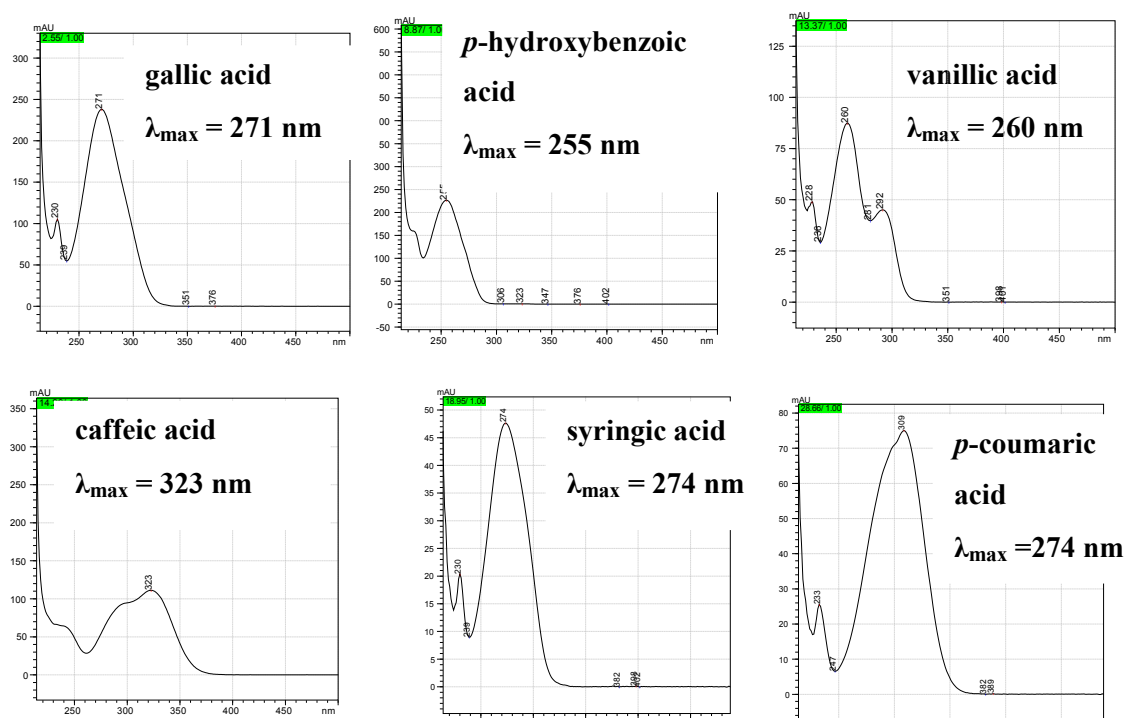
Figure 11.3: UV spectra of the six phenolic acid standards recorded by the PDA detector. The separation was effected on a reversed-phase, Zorbax Eclipse-XDB C-18 (150 mm × 4.60 mm, 5 μm particle size) column protected with a 4 mm × 4 mm Zorbax Eclipse-XDB guard column under isocratic conditions of 12 % methanol; 88 % water with 2 % acetic acid the flow rate was 1.00 mL min^{-1}and the injection volume was 10 μL.

Figure 11.4: Comparison of partial HPLC chromatograms of the SXDE extract diluted in MeOH (A), and in the mobile phase (B). The separation was effected on a reversed-phase, Zorbax Eclipse-XDB C-18 (150 mm × 4.60 mm, 5 μm particle size) column protected with a 4 mm × 4 mm Zorbax Eclipse-XDB guard column under isocratic conditions of 12 % methanol; 88 % water with 2 % acetic acid, the flow rate was 1.00 mL min^{-1}and the injection volume was 10 μL.
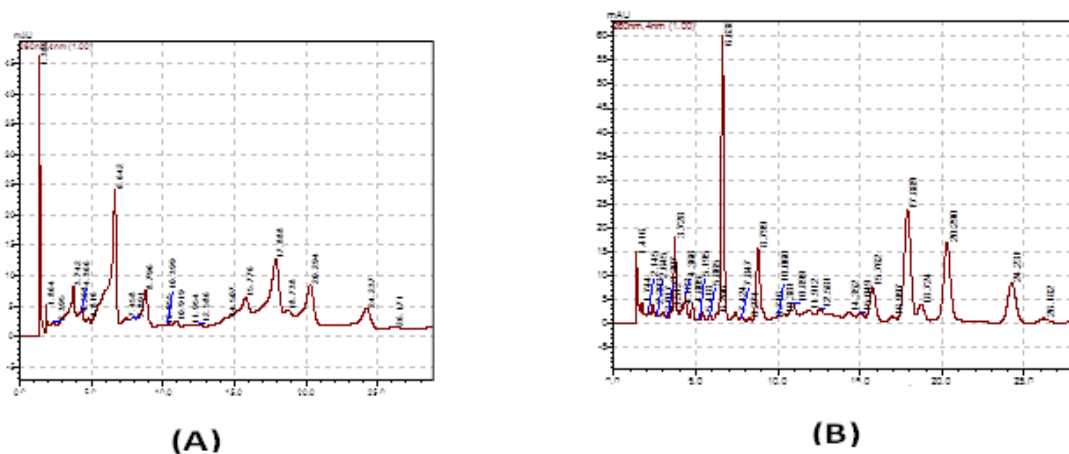
The HPLC chromatogram of SXDE showed three other prominent peaks at 274 nm (Fig. 11.5) with unique UV spectra (Fig. 11.6). These three new compounds had retention times 33.2 min, 44.2 nm, and 53.3 nm. Characterisation targeting these peaks on HPLC-DAD-ESI-MS[n] revealed the presence of a *p*-coumaric acid isomer (peak **C-1**) and two ferulic acid isomers (peaks **C-2** and **C-3**) (Figs. 11.5 and 11.6). Each peak had unique MS fragmentation pattern allowing for differentiation (Fig. 11.7, 11.8 and 11.9) and structure speculation. An isomer of *p*-coumaric acid, 5-hydroxy-2-vinylbenzoic acid, (**C-1**); and (Z)-3-(4-hydroxy-2-methoxyphenyl)acrylic acid (**C-2**), and; (Z)-2-hydroxy-3-(4-methoxyphenyl)acrylic acid (**C-3**), both isomers of ferulic acid were similarly elucidated by manual target ion fragmentation (Fig. 11.10). An MS[3] mode targeting smaller molecular weights did not yield tangible mass fractions hence the MS[2] precursor ion was used (Table 11.2). This could be attributed to low currents and, hence, the low field frequencies of MS[3] mode.
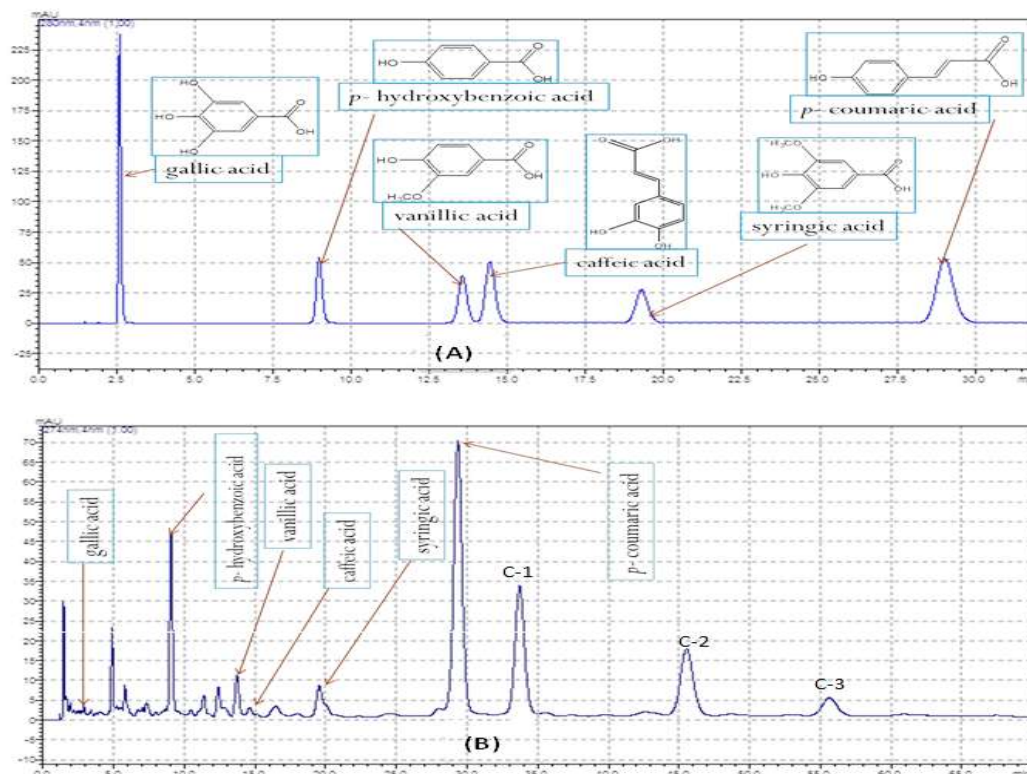
Figure 11.5: HPLC chromatograms of six phenolic acid standards monitored at 280 nm (A), and of the SXDE extract monitored at 274 nm (B). The labelled phenolic acids were identified by matching the retention times and UV spectra of the extract and of the phenolic acid standards. The separation was effected on a reversed-phase, Zorbax Eclipse-XDB C-18 (150 mm × 4.60 mm, 5 μm particle size) column protected with a 4 mm × 4 mm Zorbax Eclipse-XDB guard column under isocratic conditions of 12 % methanol; 88 % water with 2 % acetic acid, the flow rate was 1.00 mL min^{-1} and the injection volume was 10 μL.
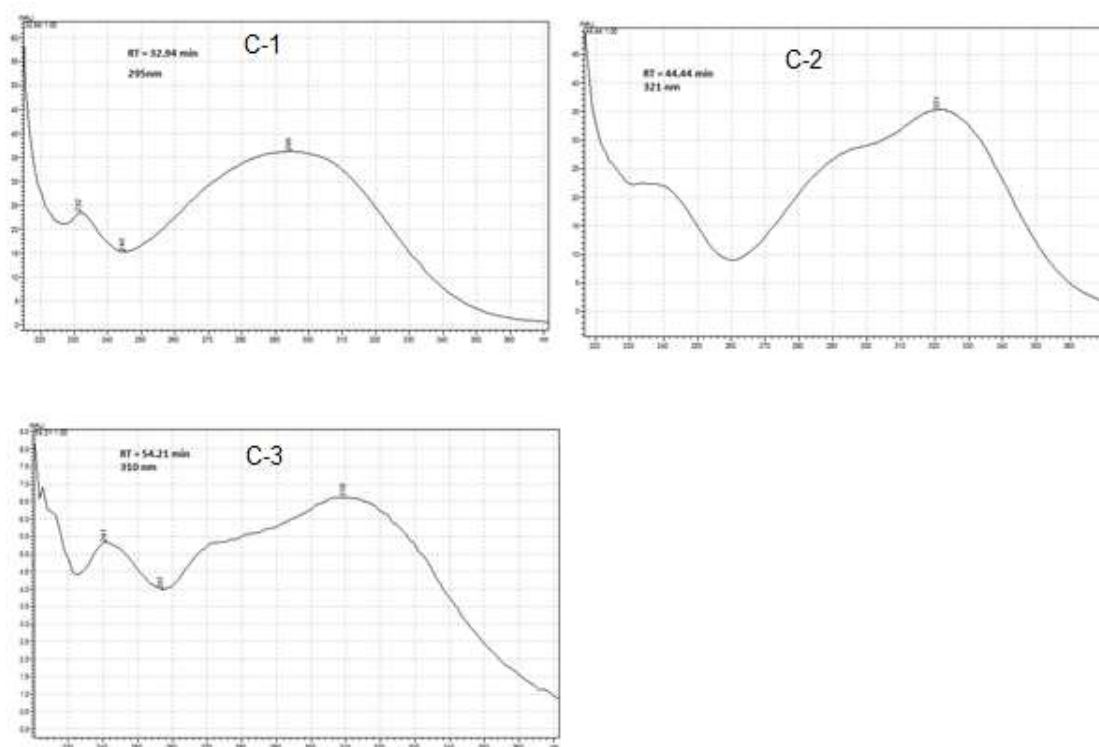
Figure 11.6: The UV spectra of predicted compounds C-1, C-2 and C-3 of the SXDE extracts. The separation was effected on a reverse phase, Zorbax Eclipse-XDB C-18 (150 mm × 4.60 mm, 5 μm particle size) column protected with a 4 mm × 4 mm Zorbax Eclipse-XDB guard column under isocratic conditions of 12 % methanol; 88 % water with 2 % acetic acid, the flow rate was 1.00 mL min^{-1} and the injection volume was 10 μL.

Table 11.2: MS^n fragmentation pattern of three phenolic acids.

Compound	RT/min	MS^2 [M-H]$^-$	MS^3 [(M-H)$^-$ →(M-H-X)$^-$]	MS^3 [(M-H)$^-$ →(M-H-Y)$^-$]	MS^3 [(M-H)$^-$→(M-H-Z)$^-$]
C-1	33.2	164	119	134	75.2
C-2	44.2	194	137	117	75.2
C-3	53.3	194	149	117	75.2

*Masses that were not structurally helpful are not considered.
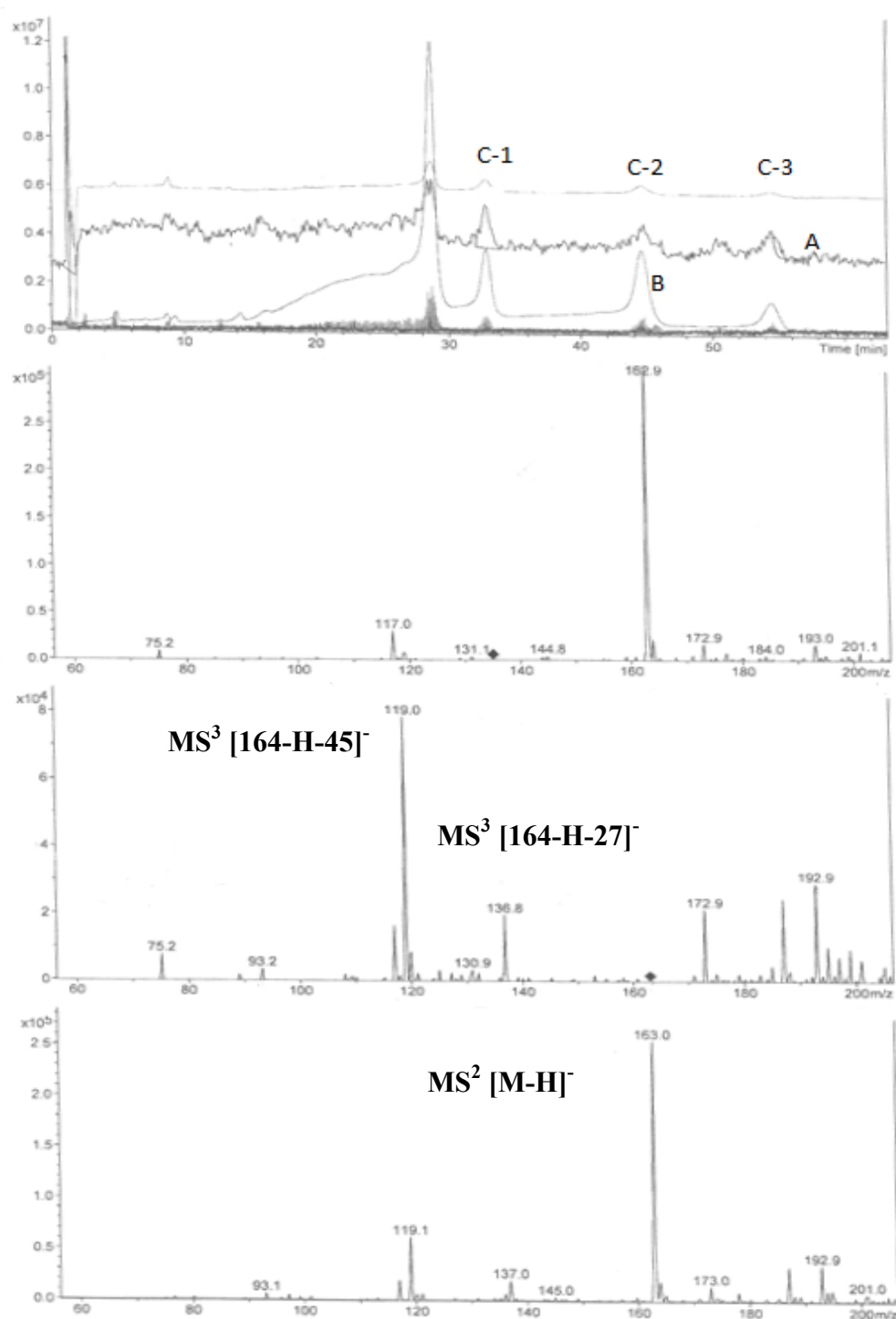
Figure 11.7: MS^n analysis of 5-hydroxy-2-vinylbenzoic acid (C-1) in the negative mode. MS^2 [M-H]$^-$; MS^3 [M-H]$^-$ → MS^3 [164-H-27]$^-$; MS^3 [164-H-45]$^-$. A is the and total ion mass spectrum and B is the HPLC chromatogram monitored at 309 nm respectively
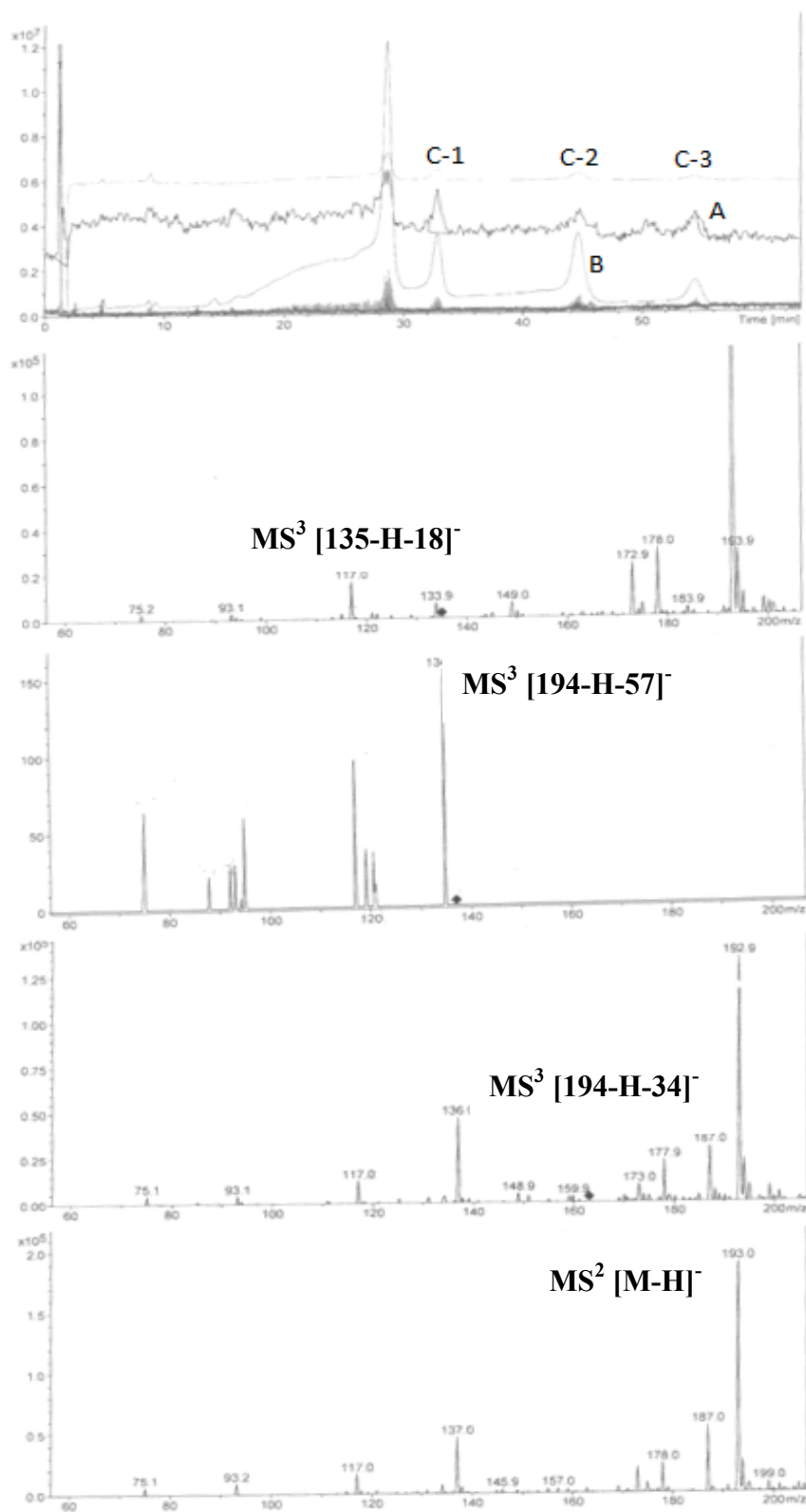
Figure 11.8: MS^n analysis of (Z)-3-(4-hydroxy-2-methoxyphenyl)acrylic acid (C-2) in the negative mode. MS^2 [M-H]$^-$; MS^3 [M-H]$^-$ →MS^3 [194-H-31]$^-$; MS^3 [194-H-57]$^-$; MS^3 [135-H-18]$^-$. A is the total ion mass spectrum and B is the HPLC chromatogram monitored at 309 nm respectively
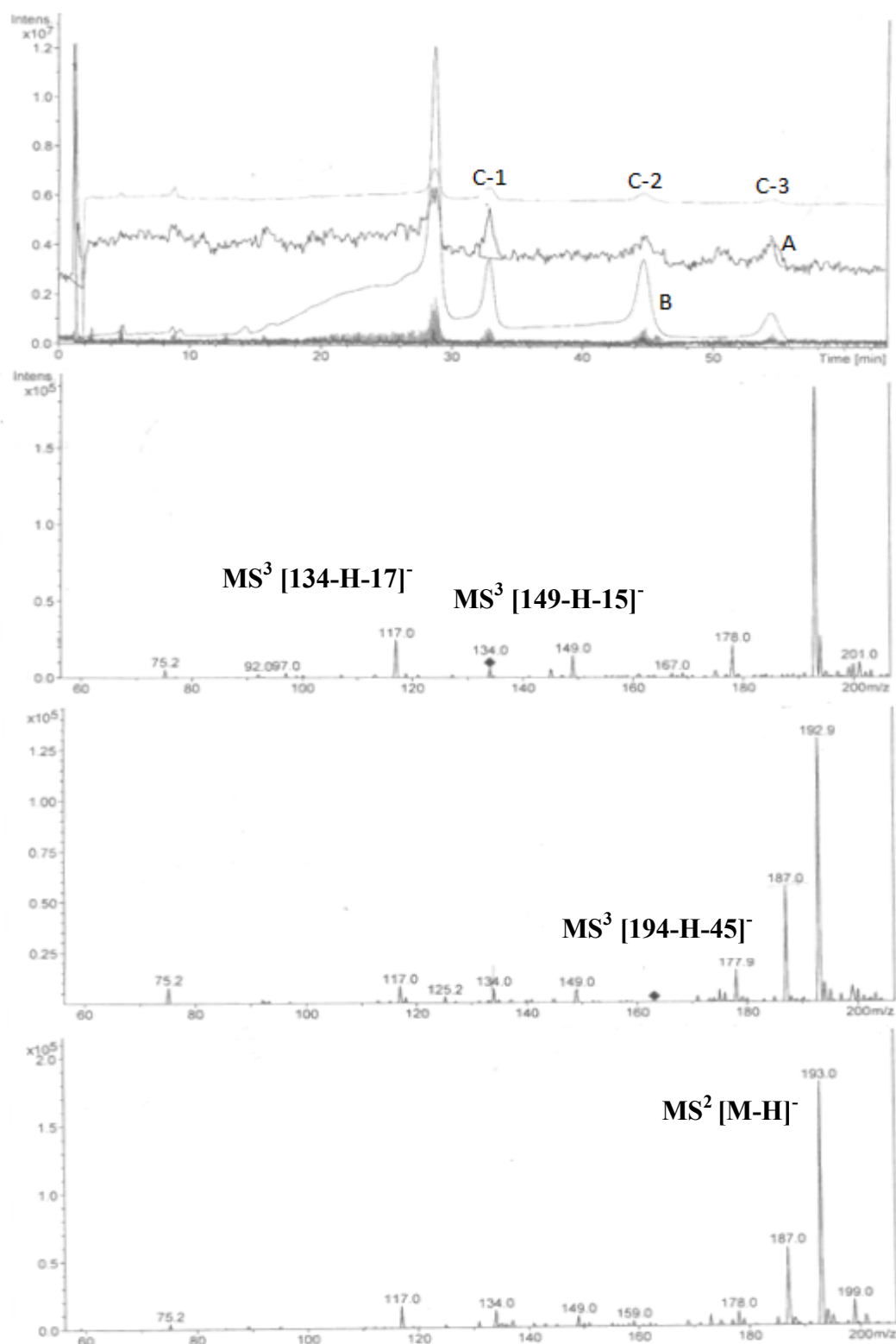
Figure 11.9: MS^n analysis of (Z)-2-hydroxy-3-(4-methoxyphenyl)acrylic acid (C-3) in the negative mode. MS^2 [M-H]$^-$; MS^3 [M-H]$^-$ →MS^3 [194-H-45]$^-$; MS^3 [149-H-15]$^-$; MS^3 [134-H-17]$^-$. A is the total ion mass spectrum and B is the HPLC chromatogram monitored at 309 nm respectively.
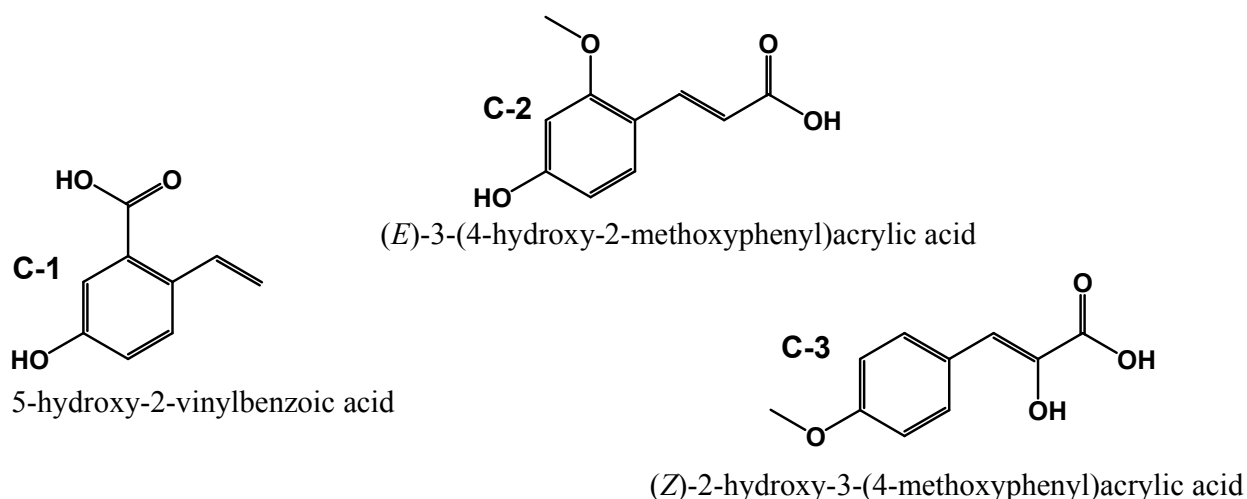
Figure 11.10: Predicted structures of compounds C-1, C-2 and C-3 from the chromatogram of the SXDE extract monitored at 274 nm, based on LC-MS precursor ion identification in MS^2 mode.

The limit of detection (LOD) and limit of quantitation (LOQ) for each phenolic acid was calculated by using an external standard method (Thomsen et al. 2003; Bunhu 2006). The LOD and LOQ were calculated as $3S_{y/x}/b$ and 3.3LOD respectively where $S_{y/x}$ is the standard error of the slope and b is the slope (Miller and Miller 1984). Among the six phenolic acids analysed, caffeic acid (4.33 μg mL^{-1}) and gallic acid (1.31 μg mL^{-1}) had the highest and lowest LOD (Table 11.3) respectively.

Table 11.3: Summary of results from the linear regression of the calibration curves of phenolic acids.

Phenolic acid	Conc. range/μg mL^{-1}	RT/min	Absorb λ_{max}/nm	slope/ 10^4/mL μg^{-1}	S_b/10^2	R^2	LOD/μg mL^{-1}	LOQ/μg mL^{-1}
Gallic acid	13.10 - 131.0	2.17	271	2.94	1.29	0.9992	1.31	4.37
p-hydrobenzoic acid	13.21 - 132.1	6.64	255	6.13	3.14	0.9979	1.54	5.12
Vanilic acid	12.68 - 126.8	8.81	260	3.64	2.47	0.9964	2.04	6.78
Caffeic acid	11.39 - 113.9	9.10	323	5.38	7.76	0.9877	4.33	14.42
Syringic acid	11.22 - 112.2	10.93	274	3.26	3.41	0.9945	3.13	10.43
p-coumaric acid	10.76 - 107.6	17.9	309	7.71	8.35	0.9922	3.25	10.81

λ_{max} = wavelength of maximum absorption, S_b = standard error of slope

The concentration of p-coumaric acid ranging from 2860 μg g^{-1} to 14520 μg g^{-1} was highest in all the extracts, followed by p-hydroxybenzoic acid; 106 μg g^{-1} to 500.5 μg g^{-1} (Table 11.4, Fig. 11.11). Notably the concentrations of vanilic acid (48 μg g^{-1} to 193.5 μg g^{-1}) and gallic acid (80 μg g^{-1} to 180 μg g^{-1}) were much lower compared to the other four phenolic acids. Syringic acid was present in all extracts (360 μg g^{-1} to 1730 μg g^{-1}) (Table 11.4).

The total phenolic acids of the USDE (17584 μg g^{-1}) extract had the highest concentration, followed by SXDE (13859 μg g^{-1}); SXHDE (13667 μg g^{-1}); USHDE (10834 μg g^{-1}); USEA (8840 μg g^{-1}); SXEA (6349 μg g^{-1}); and SXHEA (4604 μg g^{-1}) extracts in decreasing order (Table 11.4). Total

phenolic content of the eight CB extracts was determined by using the Folin-Ciocalteu (F-C) assay. The total phenolic content of each CB extract ranged from SXDE, 7.69 mg g^{-1} GAE to USDE, 12.12 mg g^{-1} GAE (Table 11.5). However, the total phenolic content may not correlate to phenolic acids content determined by HPLC as other phenolic compounds could be present in the extracts that may reduce the F-C reagent. A comparison of the SXE and USE shows that in general there are more phenolic compounds in the USE extract than the SXE extract. The effect of acidifying the aqueous phase before extraction with DE or EA did not show any significant trend.

Beside the determination of total phenolic content, the F-C assay is also an indicator of antioxidant capacity of the extract. This is because the hexavalent phosphomolybdic/phosphotungstic acid complexes of the F-C reagent can be reduced to W_8O_{23} and Mo_8O_{23} by phenolic compounds (Kasavel 2008). Therefore, USDE extract is likely to have the highest antioxidant capacity, while the SXHEA extract may show lowest antioxidant capacity because it had the lowest total phenolic content (Table 11.4).

Table 11.4: Concentrations of phenolic acids in cancer bush extracts ($n = 3$).

Extracts	Gallic acid/µg g^{-1}	p-hydrobenzoic acid/µg g^{-1}	Vanilic acid/µg g^{-1}	Caffeic acid/µg g^{-1}	Syringic acid/µg g^{-1}	p-coumaric acid/µg g^{-1}	ΣPA/µg g^{-1}
USDE	140 ± 0.02	500.5 ± 0.03	193.5 ± 0.01	605 ± 0.03	1625 ± 0.02	14520 ± 0.20	17584
USEA	80 ± 0.01	271 ± 0.01	119 ± 0.08	340 ± 0.02	1180 ± 0.01	6850 ± 0.60	8840
USHDE	180 ± 0.04	296 ± 0.01	148 ± 0.21	380 ± 0.01	1200 ± 0.13	8630 ± 0.01	10834
SXDE	100 ± 0.01	431 ± 0.01	178 ± 0.01	380 ± 0.01	1680 ± 0.01	11090 ± 0.01	13859
SXEA	100 ± 0.10	177 ± 0.02	82 ± 0.04	70 ± 0.03	750 ± 0.01	5170 ± 0.01	6349
SXHEA	110 ± 0.11	106 ± 0.02	48 ± 0.03	1120 ± 0.03	360 ± 0.10	2860 ± 0.01	4604
SXHDE	130 ± 0.10	130 ± 0.01	167 ± 0.02	1670 ± 0.02	1730 ± 0.03	9840 ± 0.19	13667

ΣPA is the sum of the six phenolic acid concentrations
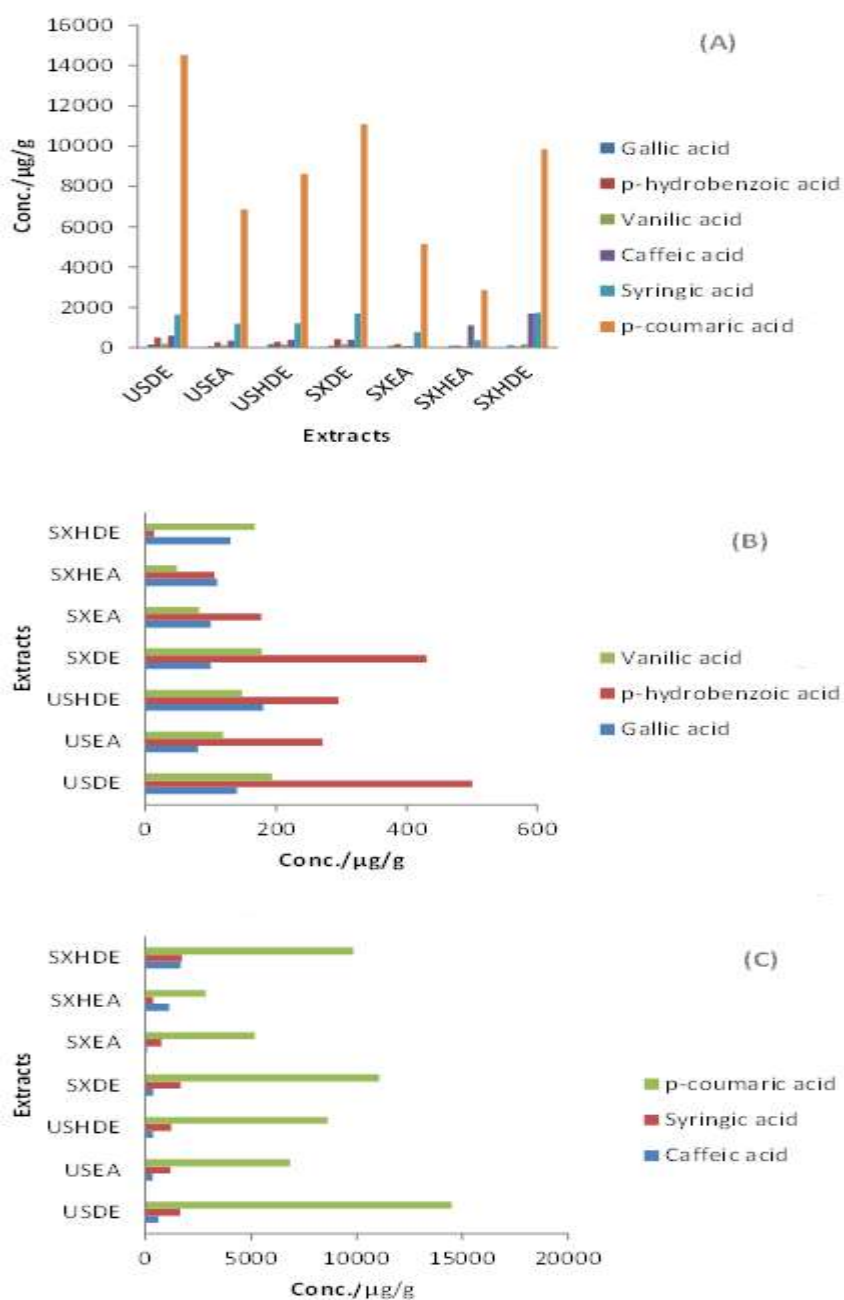
Figure 11.11: A comparison of (A) all the phenolic acids concentration in all extracts, (B) the minor phenolic acids: vanilic acid, *p*-hydrobenzoic acid and gallic acid, and (C) the major phenolic acids: *p*-coumaric acid, syringic acid and caffeic acid in all the cancer bush extracts.

The antioxidant activity of the extract was assessed by the 1,1-diphenylpicryl-2-hydrazyl (DPPH) assay. This assay is based on the scavenging of DPPH by an antioxidant through a hydrogen atom transfer (HAT) mechanism. In this study percentage DPPH scavenged extracts ranged from USDE (30.43 µg mL^{-1}) to SXDE (48.65 µg mL^{-1}) (Table 11.5).

This model was compared to the ferric reducing ability of plasma (FRAP), a single electron transfer (SET) antioxidant model. Electron donating species can be taken as antioxidant and the resulting deactivation of the species results in a redox reaction. Hence, total antioxidant power can be analogously referred to as total reducing power (Sarla et al. 2011). In this study all the fractions exhibited a total reducing capacity in the range of SXDE, 33.05 µg mL^{-1} to USDE, 41.53 µg mL^{-1} see Table 11.5.

Table 11.17: Comparison of the total phenol (F-C), FRAP values and DPPH, IC_{50} values of the extracts (n = 3).

Extract	GAE/mg g^{-1}	DPPH/EC_{50}/µg mL^{-1}	FRAP value/µg mL^{-1}
USDE	12.12 ± 1.2	30.43 ± 0.92	41.53 ± 3.77
USEA	7.85 ± 0.3	42.92 ± 0.15	36.95 ± 3.09
SXEA	7.94 ± 0.03	38.75 ± 0.50	36.26 ± 2.59
SXDE	7.69 ± 2.8	48.65 ± 0.36	33.05 ± 6.03

(*n* = 3)

A low EC_{50} value for DPPH indicates that the antioxidant extract has a high free radical scavenging capacity which would mean a higher FRAP value. In the present work, the USDE extract had the highest free radical scavenging capacity (EC_{50} = 30.43 ± 0.92 µg ml^{-1}), and the SXDE extract showed the lowest free radical scavenging capacity (EC_{50} = 48.65 ± 0.36 µg ml^{-1}). Their corresponding FRAP results were 41.53 ± 3.77 µg mL^{-1} and 33.05 ± 6.03 µg mL^{-1} respectively (Table 11.5). Thus there is a good correlation between the models and the total phenolic content in the extracts in line with findings by Arora and Chandra (2010) studied the total phenolic content from *Aspergillus sp* isolate. These authors argued that the higher the total phenolic content the higher the antioxidant activity. By the same argument, the marked antioxidant activity of the CB extracts, should imply that these extracts can be effective remedies for free radical mediated ailments.
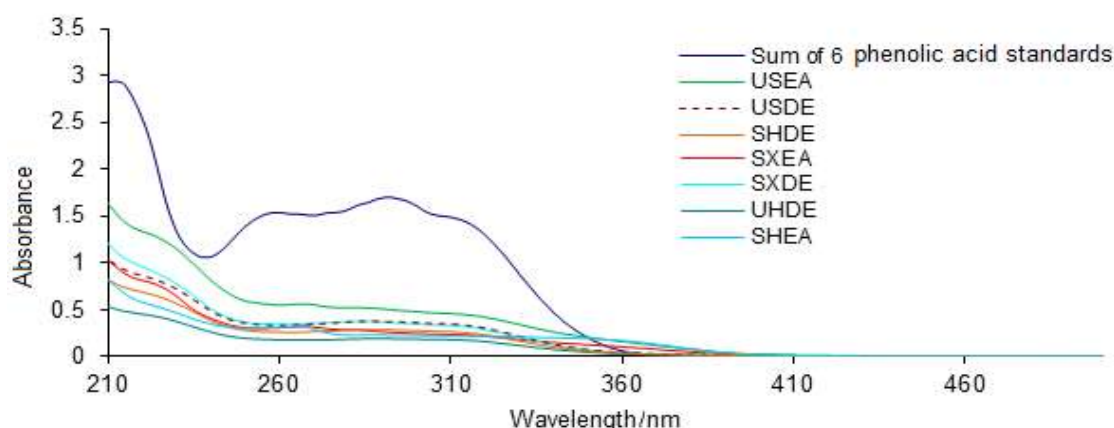
Figure 11.12: UV-vis spectra of the CB extracts and the sum of the six phenolic acids. The spectra are recorded on Perkin Elmer lambda 35 UV-vis dual beam spectrophotometer in a 1 cm pathlength quartz glass cuvette.

UV-vis spectra of 0.0625 mg mL^{-1} solutions of each of the extracts were recorded (Figure 11.12). These spectra show that all the extracts have significant absorption throughout the UVB (280-315 nm) region and part of the UVA (315-400) region. The combined absorbance of a solution of the six phenolic acids is similar to that of the extracts indicating the potential of using these extracts as photoprotectors against UVB and UVA radiation in sunscreen preparations. This corroborates the findings of Shapiro et al. (2009) who showed that caffeic acid, gallic acid and chlorogenic acid provided UV photoprotection to Beet armyworms at much lower concentrations of up to 0.005 M.

Another recent work by Oresajo et al. (2008) on the photoabsorption potential of phenolic compounds demonstrated that a mixture of vitamin C, ferulic acid and phloretin gave sufficient UV protection at a concentration of 100 ppm. This group observed that the thymine dimers were substantially inhibited an indication of UVA damage photoprotection afforded to the DNA. Though in their work, limited UV absorption was shown in the 320-400 nm bands, our work shows appreciable absorption in the region 280-360 nm (Fig. 11.12). Because of the intrinsic existence of conjugated double bonds and a benzene moiety, every phenolic acid exhibits some degree of photo absorption in the ultraviolet (UV) and/or ultraviolet/visible (UV-vis) region. This structural property may present proof for sufficient sun protection factor (SPF) afforded by these phenolic compounds. It is probable that phenolic acids may offer photoprotection by both absorption of UV radiation and scavenging of ROS. Thus, phenolic acids impart two important biological benefits if incorporated in sunscreen preparations and other cosmetic products.

11.4   Conclusions

The cancer bush extracts were extracted by two extraction procedures, Soxhlet extraction and an ultrasonic extraction method. Six known phenolic acids, namely gallic acid, caffeic acid, vanilic acid, syringic acid, ferulic acid and p-coumaric acid were identified and quantified. The acid with the highest concentration was *p*-coumaric. In addition, three other acids were identified. These were 5-hydroxy-2-vinylbenzoic acid, (Z)-3-(4-hydroxy-2-methoxyphenyl)acrylic acid and (Z)-2-hydroxy-3-(4-methoxyphenyl)acrylic acid. The extracts showed remarkable antioxidant activity proportional to the total phenolic content. The two antioxidant assays investigated in this work showed very good correlation implying both hydrogen atom transfer and single electron transfer can conveniently be used to describe the antioxidant activity of these plant extracts. The phenolic acid standards and the cancer bush extracts showed similar photoabsorption characteristics in the UV region. We speculate that the absorption potential demonstrated by the cancer bush extracts is mainly due to the phenolic acid content. The characteristic spectra of the three identified compounds in the extracts also show good absorption in the UVB and UVA region. We conclude that these extracts have high potential for use in the sun protection preparations as absorbers of UV light. Combining the UV absorption and antioxidant activity of the cancer bush we propose that cancer bush extracts can be useful ingredients in sunscreens and other cosmetic preparations.

References

Arimboor R, Kumar KS, Arumughan C (2008) Simultaneous estimation of phenolic acids in sea buckthorn (*Hippophae rhamnoides*) using RP-HPLC with DAD. Journal of Pharmaceutical Biomedical Analysis 47 (1):31-38

Arora DS, Chandra P (2010) Assay of antioxidant potential of two *Aspergillus* isolates by different methods under various physio-chemical conditions. Brazilian Journal of Michrobiology 41:765-777

Ayaz FA, Hayirlioglu-Ayaz S, Gruz J, Novak O, Strnad M (2005) Separation, characterization, and quantitation of phenolic acids in a little-known blueberry (*Vaccinium arctostaphylos L.*) fruit by HPLC-MS. Journal of Agricultural and Food Chemistry 53 (21):8116-8122

Baublis AJ, Lu CR, Clydesdale FM, Decker EA (2000) Potential of wheat-based breakfast cereals as a source of dietary antioxidants. Journal of the American College of Nutrition 19 (3):308S-311S

Benzie IFF, Strain JJ (1996) Ferric reducing antioxidant power assay: Direct measure of total antioxidant activity of biological fluids and modified version for simultaneous measurement of total antioxidant power and ascorbic acid concentration. Oxidants and Antioxidants, Pt A 299:15-27

Biglari F, AlKarkhi AFM, Easa AM (2008) Antioxidant activity and phenolic content of various date palm (*Phoenix dactylifera*) fruits from Iran. Food Chemistry 107 (4):1636-1641

Blois MS (1958) Antioxidant Determinations by the Use of a Stable Free Radical. Nature 181 (4617):1199-1200

Bunhu T (2006) An Assessment of the Photostability of South African Commercial Sunscreens. MSc Dissertation, University of KwaZulu-Natal, Durban, South Africa

Ćetković GS, Djilas SM, Čanadanović-Brunet JM, Tumbas VT (2004) Antioxidant properties of marigold extracts. Food Research International 37 (7):643-650

Cvetkovic D, Markovic D (2011) Beta-carotene suppression of benzophenone-sensitized lipid peroxidation in hexane through additional chain-breaking activities. Radiation Physics and Chemistry 80 (1):76-84

Dai J, Mumper RJ (2010) Plant Phenolics: Extraction, Analysis and Their Antioxidant and Anticancer Properties. Molecules 15 (10):7313-7352

Directorate of Plant Production (2009) Cancer bush. Department of Agriculture, Pretoria

Fernandes AC, Cromarty AD, Albrecht C, van Rensburg CE (2004) The antioxidant potential of Sutherlandia frutescens. Journal of Ethnopharmacology 95 (1):1-5

Guahk G-H, Ha SK, Jung H-S, Kang C, Kim C-H, Kim Y-B, Kim SY (2010) Zingiber officinale Protects HaCaT cells and C57BL/6 Mice from Ultraviolet B-Induced Inflammation. J Med Food 13 (3):673-680

Kadoma Y, Fujisawa S (2008) A Comparative Study of the Radical-scavenging Activity of the Phenolcarboxylic Acids Caffeic Acid, p-Coumaric Acid, Chlorogenic Acid and Ferulic Acid, With or Without 2-Mercaptoethanol, a Thiol, Using the Induction Period Method. Molecules 13 (10):2488-2499

Kasavel JE (2008) A study of the activity of polyphenolic extracts from *Sutherlandia frutescens*. MSc Dissertation, University of KwaZulu-Natal, Durban, South Africa

Marxen K, Vanselow KH, Lippemeier S, Hintze R, Ruser A, Hansen U-P (2007) Determination of DPPH Radical Oxidation Caused by Methanolic Extracts of Some Microalgal Species by Linear Regression Analysis of Spectrophotometric Measurements. Sensors 7:2080 - 2095

Miller JC, Miller JN (1984) Statistics for Analytical Chemistry. Wiley, New York

Oresajo C, Stephens T, Hino PD, Law RM, Yatskayer M, Foltis P, Pillai S, Pinnell SR (2008) Protective effects of a topical antioxidant mixture containing vitamin C, ferulic acid, and phloretin against ultraviolet-induced photodamage in human skin. Journal of Cosmetic Dermatology 7 (4):290-297

Paulo GM, Marques CMH, Morais AGJ, Almeida JA (1999) An isocratic LC method for the simultaneous determination of vitamins A, C, E and b-carotene. Journal of pharmaceutical and biomedical analysis 21:399 - 406

Ramos S (2008) Cancer chemoprevention and chemotherapy: Dietary polyphenols and signalling pathways. Molecular Nutrition & Food Research 52 (5):507-526

Sarla S, Prakash MA, Apeksha R, Subhash C (2011) Free Radical Scavenging (DPPH) and Ferric Reducing Ability (FRAP) of *Aphanamixis polystachya* (Wall) Parker. International Journal of Drug Development and Research 3 (4):271 - 274

Shaik S, Dewir YH, Nicholas A (2008) Influences of pre-sowing seed treatments on germination of the cancer bush (Sutherlandia fruitescens), a reputed medicinal plant in arid environments. Seed Science and Technology 36:795 - 801

Shaik S, Dewir YH, Singh N, Nicholas A (2010) Micropropagation and bioreactor studies of the medicinally important plant *Lessertia (Sutherlandia) fruitescens L*. South African Journal of Botany 76:180 - 186

Shapiro M, Salamouny SE, Shepard BM (2009) Plant Phenolics as Radiation Protectants for Beet Armyworms (*Lepidoptera: Noctuidae*) *Nucleopolyhedrovirus*. Journal of Agricultural and Urban Entomology 26 (1):1-10

Stalikas CD (2007) Extraction, separation, and detection methods for phenolic acids and flavonoids. Journal of Separation Science 30 (18):3268-3295

Tarnawski M, Depta K, Grejciun D, Szelepin B (2006) HPLC determination of phenolic acids and antioxidant activity in concentrated peat extract-a natural immunomodulator. Journal of pharmaceutical and biomedical analysis 41 (1):182-188

Thomsen V, Schatzlein D, Mercuro D (2003) Limits of detection in spectroscopy. Spectroscopy 18:112-114

Thongrakard V, Ruangrungsi N, Ekkapongpisit M, Isidoro C, Tencomnao T (2013) Protection from UVB Toxicity in Human Keratinocytes by Thailand Native Herbs Extracts. Photochemistry and photobiology

Waksmundzka-Hajnos M, Petruczynik A, Ciesa G (2007) Temperature - the tool in separation of alkaloids by RP-HPLC. Journal of Liquid Chromatography and Related Technologies 30 (13-16):2473-2484

Yashin A, Yashin Y, Nemzer B (2011) Determination of antioxidant activity in tea extracts, and their total antioxidant content. American Journal of Biomedical Sciences 3 (4):322 - 335

Chapter Twelve

Antioxidant capacity of South African beverages

Moses A. Ollengo, Lynette Komarsamy, Georges J. Mturi and Bice S. Martincigh[*]

School of Chemistry and Physics, University of KwaZulu-Natal, Westville Campus, Private Bag X54001, Durban 4000, South Africa

*Corresponding author: Tel.:+27-31-2601394; Fax: +27-31-2603091; E-mail address: martinci@ukzn.ac.za

Abstract

Polyphenols from plants draw increasing attention due to their potent antioxidant properties and marked effects in prevention of various oxidative stress associated diseases such as cancer. In this work teas and fruit juice samples from the local South African market were investigated for their phenolic content and antioxidant activity. The Folin-Ciocalteu protocol was used for the total phenolic content and expressed as gallic acid equivalents. The antioxidant activity was done by assessing free radical scavenging activity of stable 1,1-diphenylpicryl-2-hydrazyl radical (DPPH) and the ferric reducing antioxidant power (FRAP) of the samples. The two models compared well with determined total phenolic content of tea and fruit juice samples expressed in gallic acid equivalents per gram of dry sample: green tea (GT) (758.6 ± 20.48 mg g^{-1}) > black tea (BT) (580.1 ± 5.80 mg g^{-1}) > Rooibos-Honeybush (RH) (573.5 ± 8.47 mg g^{-1}) > Rooibos-Honeybush-blck tea (RHB) (485.4 ± 6.70 mg g^{-1}) > Rooibos-black tea (RB) (520.2 ± 6.40 mg g^{-1}). The DPPH IC_{50} : GT(3.60 ± 0.02 µg mL^{-1}) > BT (4.50 ± 0.01 µg mL^{-1}) > RH (10.79 ± 0.06 µg mL^{-1}) > RHB (11.69 ± 0.01 µg mL^{-1}) > RB (14.35 ± 0.04 µg mL^{-1}). This sequences were supported by the results of the FRAP analysis in mM of Fe(II) showing; GT (0.204 ± 0.03 mM)> BT (0.268 ± 0.03 mM) > RH (0.290 ± 0.04 mM) > RHB (0.321 ± 0.01 mM) > RB (0.441 ± 0.06 mM). Thus green tea had a higher antioxidant activity followed by black tea. All the tea samples showed presence of other polyphenols. Fruit juices sampled also gave differences in total phenolic content: orange (611.7 ± 18.87 mg L^{-1}) > grape (503.5 ± 11.07 mg L^{-1}) > apple (334.4 ± 7.41 mg L^{-1}) and subsequently varying antioxidant activity. The free radical scavenging activity done by using the stable DPPH radical indicated a stronger activity (IC_{50}) in gallic acid equivalent for orange (2.11 ± 0.02 mg L^{-1} GAE), > grape (2.63 ± 0.02 mg L^{-1} GAE) > apple (4.23 ± 0.07 mg L^{-1} GAE) and similar trend for FRAP, EC_1: orange ($2.52 \pm 0.0\ 2$ mM Fe(II)), > grape (4.47 ± 0.05 mM Fe(II)) > and apple (4.55 ± 0.02 mM Fe(II)). HPLC-UV analysis of fruit juices indicated orange juice had the highest number of polyphenols. All the beverages had a good activity and correlated well with the total phenolic content. Increased dietary intake of these beverages should be encouraged as a remedy for various oxidative stress related degenerative ailments and to prolong life expectancy.

Keywords: Fruit juices, teas, antioxidant activity, DPPH, FRAP, phenolic content.

12.1   Introduction

Experimental evidence links many pathophysiological disorders such as anthritis, cancer, skin irritations and inflammation, arteriosclerosis, genotoxicity (Mandal et al. 2009; Koksal et al. 2011; Sidddiqua et al. 2010) and neurodegenerative diseases like Alzheimer's ailment (Pulido et al. 2000) to reactive oxygen species (ROS). The six major reactive oxygen species causing oxidative damage to a living body are superoxide anion ($O_2^{\bullet-}$); hydrogen peroxide (H_2O_2), peroxyl radicals ($ROO^{\bullet}$); hydroxyl radical ($HO^{\bullet}$); singlet oxygen ($^1O_2$); and peroxynitrite ($ONOO^-$) (Dejian et al. 2005). These species initiate degenerative disorders in living systems by oxidizing nucleic acids, lipids and proteins (Pisoschi et al. 2009). To counteract the assault of these ROS, biological defence systems composed of enzymatic antioxidants convert ROS and reactive nitrogen species (RNS) to harmless species. However, no enzymatic action is known to scavenge $ROO^{\bullet}$, $HO^{\bullet}$, $^1O_2$, and $ONOO^-$. Therefore, the burden of defence relies on nonenzymatic antioxidants, such as vitamins C and E and other phytochemicals that have the ability to scavenge oxidants and free radicals.

It has been shown that antioxidants can inhibit oxidative reactions *in vivo*, aiding the functional performance of enzyme systems for the self-defence of mechanisms within cells (Lu et al. 2011). Thus, dietary intake of antioxidants is necessary to maintain a physiological balance of antioxidants and oxidant generation in living organisms (Sidddiqua et al. 2010). A number of working groups have shown a good correlation between increased dietary intake of phenolic acids, and generally polyphenols, to reduced coronary heart disease and cancer mortality with longer life expectancy (Ghafar et al. 2010). Antioxidants are known to deactivate radicals via three major mechanisms: hydrogen atom transfer (HAT), electron transfer (ET) and a combination of both HAT and ET (Dejian et al. 2005). Hydrogen atom transfer measures the ability of an antioxidant to quench free radicals by hydrogen atom donation within their environs. Electron transfer determines the ability of an antioxidant to transfer one electron to reduce radicals, metals and carbonyls in a medium (Lu et al. 2011).

One easy way of introducing these polyphenolic antioxidants in the diet is through beverages. South Africa has a wealth of plant materials and there is a long history of their use by the indigenous people as traditional medicines. South Africa also has a thriving fruit industry and produces a variety of fruit juices both for export and local consumption. It was therefore of interest to determine the polyphenolic content of beverages in the South African market. The aim of this study was to determine the total phenolic content of common South African beverages by using an electron transfer based mechanism (Folin-Ciocalteau) and to correlate the results with the antioxidant capacity of these beverages based on similar mechanistic assays; namely, the FRAP assay a purely ET based assay and the DPPH assay which combines both HAT and ET. Information about their relative composition will help in determining nutritional value of these beverages to consumers. Common non-alcoholic beverages in the South African market are teas and fruit juices. Rooibos (*Aspalathus linearis*) tea is known to be a source rich in polyphenols. The plant is also indigenous to South Africa. These were compared with green tea and black tea. Then, three common fruit juice samples, namely, orange, grape and apple were also investigated. In this study brand names have been dropped and replaced by code names for simplicity of reference in the text. Fruit juices investigated have also been coded for purposes of ease of naming.

12.2   Experimental

12.2.1   Samples and reagents

Commercial fruit juices namely, orange, red grape and clear apple were purchased from Liqui-Fruit[TM] South Africa. Apart from orange juice which was a blend of grape, apple and pear juice, all other juices were 100 % pure. A total of five tea brands were also randomly selected and bought from a local market for study. These were: green tea produced by Entyce beverages (GT), Joko black tea (BT) from Unilever, Rooibos All-in-one (a blend of Rooibos, Honeybush and black tea) (RHB) and Honeybush blend (a blend of Rooibos and Honeybush) (HB) from Joekels tea packers and Rooibos Vital (RB) from Vital Health Foods. The phenolic standard used was gallic acid purchased from Hopkin and Williams. The Folin-Ciocalteau phenol reagent, 2,4,6-tripyridyl-s-triazine, and sodium acetate were from Merck kGaA, acetic acid and 1,1-diphenylpicryl-2-hydazyl (DPPH) radical from Sigma-Aldrich, and ferric chloride hexahydrate, from Associated Chemicals, SA. The solvents used were deionised water obtained from a Millipore Milli-Q[®] water purification system (Millipore, Bedford, MA, USA), and methanol was from BDH Prolabo.

12.2.2   Ethanol-water extraction of polyphenols from teas

A study by Lin et al. (2003) found that significantly more polyphenols were extracted from tea leaves by 75% ethanol than by boiling water. Hence this was also attempted here. About 5 g of extractable material was ground by using a mortar and pestle, and then immersed in 40 ml 75:25 (v/v) ethanol-deionised water solution. The mixture was placed in an oil bath at 65 ºC with stirring for 30 min. The mixture was then filtered through Whatman No. 4 filter paper and the filtrate evaporated under reduced pressure by means of a rotary evaporator. The crude extract was re-dissolved in 25 ml deionised water (Miketova et al. 1998). The aqueous solution was extracted three times with an equal volume of ethyl acetate (Miketova et al. 1998; Mukhtar et al. 1992; Lin et al. 1996) to extract the polyphenols. The ethyl acetate extracts were combined and filtered through Whatman No. 4 filter paper. The ethyl acetate was evaporated under reduced pressure in a rotary evaporator. A few drops of dichloromethane were added to ensure complete removal of water (Soleas et al. 1997; Soleas and Goldberg 1999).   This provided a solid extract. A mass of about 30 mg of each tea extract was re-dissolved in 2 mL of methanol and a 10 μL aliquot of the solution injected into the HPLC for analysis. This ethanol-water extraction method was used to extract polyphenols from all the teas investigated.

12.2.3   Extraction of polyphenols from fruit juices

The extraction of polyphenols was carried out by using a solvent composition consisting of methanol:water:acetic acid (30:69:1 % (v/v)).   This composition has been shown to extract intracellular polyphenols (Abad-García et al. 2007). The fruit juice samples were centrifuged at a speed of 6000 rpm for two minutes with a Labofuge 200 centrifuge and then the supernatants were decanted into clean vials. A 1 mL aliquot of each juice sample was diluted with 2 mL of extraction solvent in the absence and presence of 0.2 % (w/v) ascorbic acid. The 0.2 % (w/v) ascorbic acid was used to as an antioxidant to prevent the oxidation of the extracted polyphenols. The samples were sonicated for 15 minutes at 25 °C in an ultrasonic bath and then filtered through 0.45 μm Millex LCR syringe filters into HPLC vials. Aliquots of 10 μL of these samples were injected into the reversed-phase high performance liquid chromatograph with diode array detector (RP-HPLC-DAD) for analysis.

12.2.3 Reversed-phase HPLC analyses

The HPLC analysis of the tea extract samples was done on a Waters 600 multisolvent delivery system connected to Perkin Elmer series 200 autosampler. A waters 996 photodiode array (PDA) detector was used to detect sample components. All chromatograms were monitored at a wavelength of 272 nm. The PDA detector and acquisition of the chromatograms was controlled by Waters Millennium Version 4.00 software. The separation was effected on a Nucleosil 100 C-18 (250 mm × 4.6 mm, 5 μm particle size) column. All samples were filtered through 0.45 μm Millex LCR syringe filters and solvents were filtered through 0.45 μm Durapore filters before being injected into the HPLC. Helium was used to sparge the mobile phase prior to use. The solvent flow rate was 1 mL min^{-1} and injection volume was 10 μL. The samples passed through a Waters Guard-Pak μ-Bondapak C-18 before entering the column. A gradient elution method reported by Zuo et al. (2002) was used to separate the extracted polyphenols. The mobile phase composition was varied as follows: 100 % solvent A (97:3 % (v/v) deionised water-acetic acid) for 1 min, then a linear change to 63 % solvent B (methanol) over 56 min and brought back linearly to 100 % solvent A over 3 minutes, and left at solvent A for 10 min. A mass of about 30 mg of the tea extract was dissolved in 2 mL of methanol. A 10 μL aliquot of this solution was eluted with the above mobile phase.

The HPLC analysis of fruit juice samples was carried out on an Agilent 1200 series HPLC, equipped with a photodiode array detector (G1315D), a binary pump (G1312A), a degasser (G1322A), autosampler (G1316A) all controlled by Chemstation software (Agilent, v.08.04). The chromatographic separation was achieved on a reversed-phase Phenomenex Luna ODS, C18 column (250 mm × 4.6 mm, i.d., 5 μm). A gradient elution with mobile phase composition of 0.25 % (w/v) acetic acid in Millipore water (solvent A) and methanol (solvent B) was employed. The solvent composition was varied as follows: initially held at 5 % (v/v) B for 4 min then linearly increased to 10 % (v/v) B in 4 min; followed by an increase to 20 % (v/v) B in 1 min and held for 4 min, then increased to 35 % (v/v) B in 7 min and held for 4 min. It was then followed by a rise to 100 % (v/v) B in 4 min and held for 2 min before being dropped back to 5 % (v/v) B in 5 min and held for 5 min. Helium gas was used to spurge the mobile phase prior to use. The flow rate was set at 0.5 mL min^{-1}; the injection volume was 5 μL; and the column temperature kept at 30 °C for a run time of 40 min. The chromatograms were acquired at 265, 280, 300 and 350 nm.

12.2.4 Folin-Ciocalteu total phenol assay

The total concentration of polyphenols in the tea and fruit juice extracts was determined according to the Folin-Ciocalteu method (Singleton et al. 1999). This method measures the phenolic content by UV spectrophotometry based on a colorimetric redox reaction in which the reduced form of the phosphomolybdic-tungstic mixed acid chromagen is measured at approximately 750 nm. Gallic acid was employed as the standard. Singleton et al. (1999) reported that linear calibration curves for gallic acid are obtained only between concentrations ranging from 3 to 300 mg dm^{-3}. Hence, a calibration curve was prepared from standard gallic acid solutions ranging in concentration from 5 mg dm^{-3} to 50 mg dm^{-3}. These standards were prepared by dissolving 0.500 g of gallic acid in 10 mL of ethanol and diluting to 100 mL with Millipore water. Sodium carbonate solution was prepared by dissolving 200 g of anhydrous sodium carbonate in 800 mL of millipore water and brought to a boil. After cooling, a few crystals of sodium carbonate were added then left to stand for 24 hour; the solution was then filtered and made to 1 L by adding water. From each calibration solution, sample, or blank, 20 μL was pipetted into separate cuvettes, followed by addition of 1580 μL water, and then 100 μL of Folin-Ciocalteu reagent, and mixed well. After 8 min, 300 μL of sodium carbonate solution was added, and shaken to mix. The solutions were left at 25 °C for 2 hours and the absorbance of each solution was

determined at 765 nm against a blank. A plot of absorbance vs. concentration was made for the gallic acid standards. Each measurement was performed in triplicate. The total phenolic content of the samples was calculated and expressed as gallic acid equivalents (GAE) mg g^{-1} of dry sample according to equation 12.1

$$\textbf{GAE}\left(\frac{\textbf{mg}}{\textbf{g}}\right) = \textbf{Conc. GA}\left(\frac{\textbf{mg}}{\textbf{L}}\right) \times \textbf{0.1 L} \times \frac{\textbf{mass of extract/g}}{\textbf{mass used/g} \times \textbf{total mass taken/g}} \qquad \textbf{equation 12.1}$$

12.2.6   DPPH scavenging assay

The free radical scavenging activity of fruit juice and tea extracts was assessed by using stable 1,1-diphenylpicryl-2-hydrazyl (DPPH) assay according to a standard method reported by Blois (1958). Briefly a 40 mg dm^{-3} stock solution of DPPH was prepared by dissolving 4 mg of DPPH in 80 % (v/v) aqueous ethanol and made up to 100 mL by the same solution in a standard flask. An aliquot of 2 mL of the 40 mg dm^{-3} DPPH in 80 % aqueous ethanol was mixed with 1 mL of 1.8 mg mL^{-1} of tea or fruit juice extracts and 1 mL of 80 % aqueous ethanol. Simultaneously a control was prepared without sample extracts and both reaction mixture sets were incubated at room temperature for 1 hour in the dark. The antioxidant activity of each sample was quantitated by the loss in colour at 522 nm by using a Perkin Elmer Lambda 35 UV-vis dual beam spectrophotometer. The percentage DPPH scavenged was calculated using equation 12.2, where $A_{control}$ is the absorbance of the solution containing only DPPH diluted with solvent (80 % (v/v) aqueous ethanol), and A_{sample} is the absorbance of the DPPH solution after incubation with different concentration of fruit juice and tea extracts.

$$\textbf{\% DPPH scavenged} = \frac{\textbf{A}_{\textbf{control}} - \textbf{A}_{\textbf{sample}}}{\textbf{A}_{\textbf{control}}} \textbf{x 100} \qquad \textbf{equation 12.2}$$

A double axes plot of mean % DPPH scavenged, mean absorbance of three replicate against concentrations was drawn. The IC_{50} volume was read by interpolation for each tea and fruit juice sample. On average about 45 mg of each tea or fruit juice sample was weighed and dissolved in 15 mL 80 % (v/v) aqueous ethanol and made up to 25 mL with 80 % (v/v) aqueous ethanol to make a concentration of 1.8 mg mL^{-1} of the extract. From this solution 1 mL of extract was combined with 1 mL of 80 % (v/v) aqueous ethanol and then added 2 mL of 40 mg dm^{-3} DPPH solution. Considering these dilutions then IC_{50} was calculated from the equation below, expressed interms of µg mL^{-1} of tea and fruit juice samples solution equation 12.3.

$$\textbf{IC}_{\textbf{50}}$$
$$= \left(\frac{\textbf{mass of extract/µg}}{\textbf{25 mL}}\right)\left(\frac{\textbf{volume at 50\% DPPH/µL}}{\textbf{1 mL}}\right)\left(\frac{\textbf{1 mL}}{\textbf{4 mL}}\right)\left(\frac{\textbf{1 mL}}{\textbf{1000µL}}\right) \quad \textbf{equation 12.3}$$

12.2.7   FRAP Antioxidant Assay

The FRAP assay was performed according to the protocol reported by Benzie and Strain (1996). Stock solutions contained 300 mM acetate buffer (3.1 g $C_2H_3NaO_2 \cdot 3H_2O$ and 16 mL $C_2H_4O_2$) at pH 3.6, 10 mM TPTZ (2,4,6-tripyridyl-s-triazine) solution in 40 mM HCl, and 20 mM $FeCl_3 \cdot 6H_2O$ solution. A fresh working solution was prepared by mixing 25 mL acetate buffer, 2.5 mL TPTZ solution, and 2.5 mL $FeCl_3 \cdot 6H_2O$ solution. Ferrous ammonium sulphate standards in the range of 100 – 1000 µM were prepared from a 0.01 M stock solution with 80 % aqueous methanol. A 100 µL aliquot of each standard was then added to 3 mL of the FRAP reagent and incubated for 4 and 30 min at 37 °C in a waterbath before analysis in a 1 cm pathlength glass cuvette with Perkin Elmer Lambda

25 UV-vis dual beam spectrophotometer fitted with a Peltier temperature controller set at 37 ºC and the absorbance measured at 596 nm. A standard calibration curve was consequently constructed. The tea and fruit juice extracts (150 µL) dissolved in 80 % aqueous methanol were allowed to react with 2850 µL of the FRAP solution for 4 min and 30 min in the dark condition before absorbance measurement were similarly taken. All tests were run in triplicate and mean values were used for the determination of EC_1 values. EC_1 is defined as concentration of an antioxidant having a ferric reducing ability equivalent to that of 1 mM Fe^{+2} (Sarla et al. 2011).

12.3   Results

The identification of phenolic groups present in the beverages was first done by comparison of the retention time of standards and their corresponding UV spectra from the HPLC chromatograms and literature.

12.3.1   HPLC analysis of the tea extracts

One-third of dietary polyphenols consist of phenolic acids that are ubiquitous in plants in free and bound forms. The main linkage of bound phenolics to various plant components is through ester, ether, or acetal bonds (Robbins 2003). Identification of these phenolics was done by elution of standards and compared to sample eluents by matching retention times and respective UV spectra and by classifying polyphenolic groups according to their UV spectra. For example in this work gallic acid peaks were observed at 9.7 min for both the standard (Fig. 12.1) and the RHB extract (Fig. 12.2).

The HPLC chromatograms of the Rooibos tea extracts are displayed in Fig 12.4 for rooibos tea, Fig. 12.5 for RH tea and for RHB tea in Fig. 12.5. Table 12.1 summarises the chromatograms by listing and categorising all the compounds present in the extracts. The extracts from RB and RH teas contain a similar range of compounds but differ from RHB tea. However, the RHB tea extract contains the largest number of compounds. Rooibos tea is a rich source of flavonoids (Erickson 2003), and honeybush teas is also known to contain various polyphenols (Ferreira et al. 1998; Kamara et al. 2003) such as hydroxycinnamic acids, isoflavones, flavanones, flavones, coumestans and xanthones. The polyphenolic substances in black tea are different from those in rooibos and honeybush tea they tend to be rich in dimeric flavanols and polymeric polyphenols known as theaflavins and thearubigins formed from the oxidation of catechins (Zhao et al. 1999). This is the reason that the RHB tea chromatogram showed a greater variety of compounds than those of the other rooibos teas. The method extraction determines the chemical composition of the extractable polyphenols.
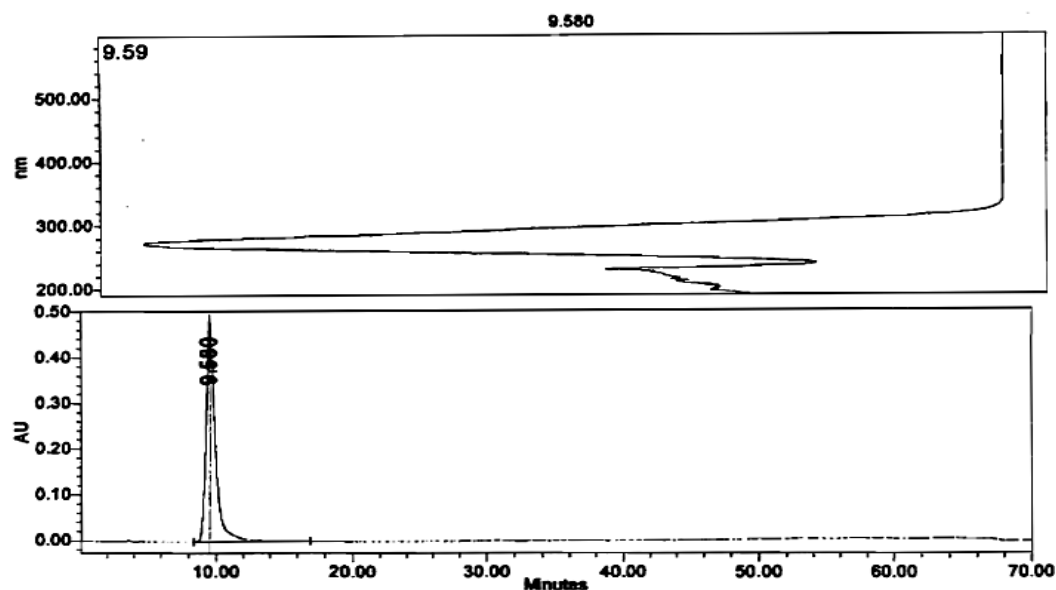
Figure 12.1: HPLC chromatogram of the elution of gallic acid standard through a Nucleosil 100 C18 column (250 mm × 4.5 mm, i.d., 5 µm) by a gradient mobile phase of composition water/acetic acid (97:3 v/v) solvent A and methanol solvent B at flow rate of 1 mL min^{-1}. The chromatogram was monitored at a detection wavelength of 272 nm. Gallic acid elutes at 9.6 min and the top window shows its UV spectrum.
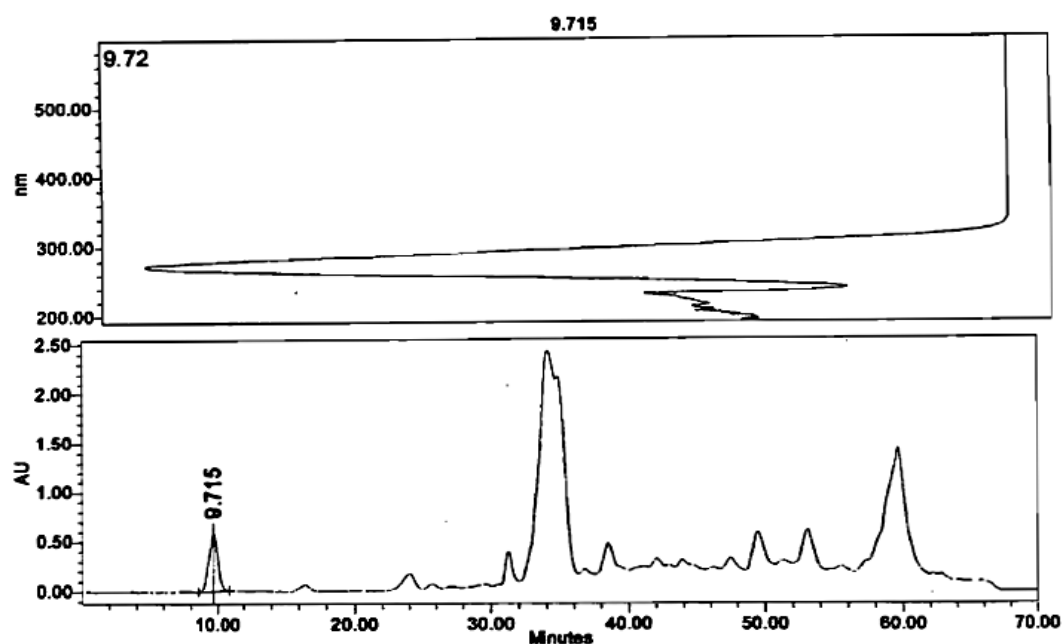
Figure 12.2: HPLC chromatogram of boiling water Rooibos-black tea extract eluted through a Nucleosil 100 C18 column (250 mm × 4.5 mm, i.d., 5 µm) by a gradient mobile phase of composition water/acetic acid (97:3 v/v) solvent A and methanol solvent B at flow rate of 1 mL min^{-1}. The chromatogram was monitored at a detection wavelength of 272 and shows gallic acid eluting at 9.7 min.
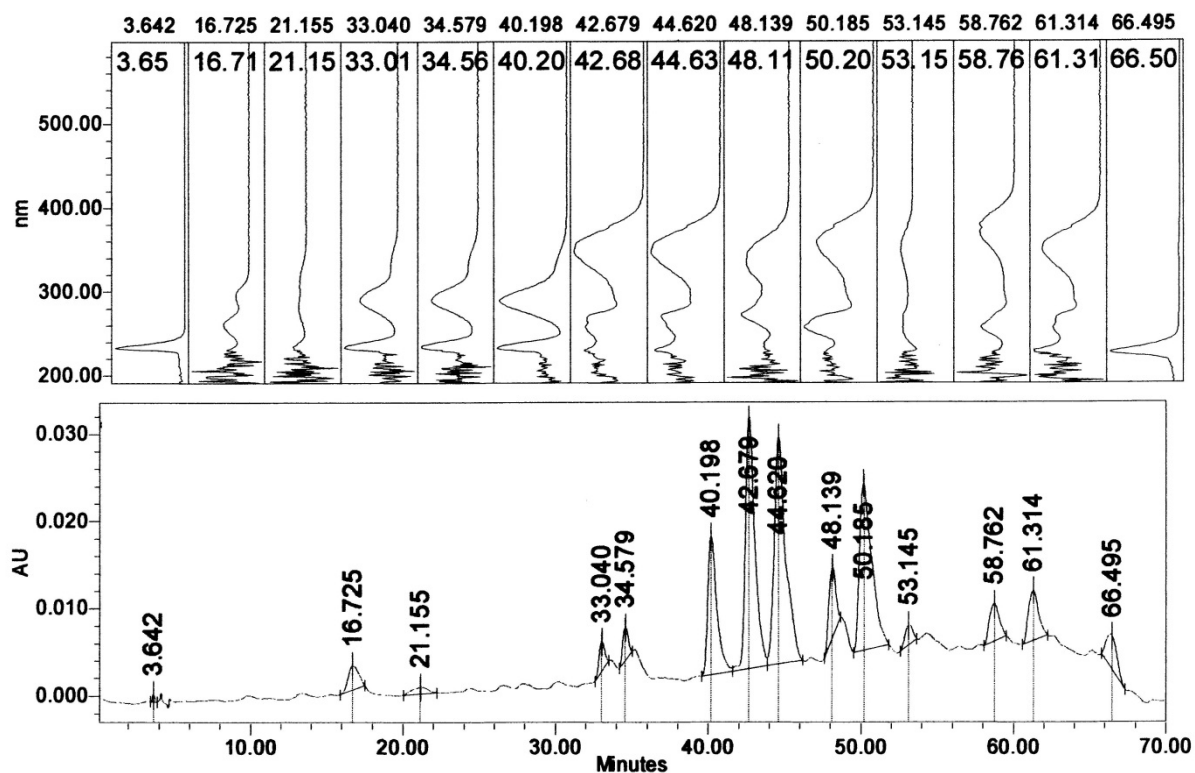
Figure 12.3: HPLC chromatogram of the boiling water Rooibos tea extract eluted through a Nucleosil 100 C_{18} column (250 mm × 4.5 mm, i.d., 5 μm) by a gradient mobile phase of composition water/acetic acid (97:3 v/v) solvent A and methanol solvent B at flow rate of 1 mL min^{-1}. The wavelength of detection was 272 nm, and the top window shows the corresponding UV spectra of eluents.
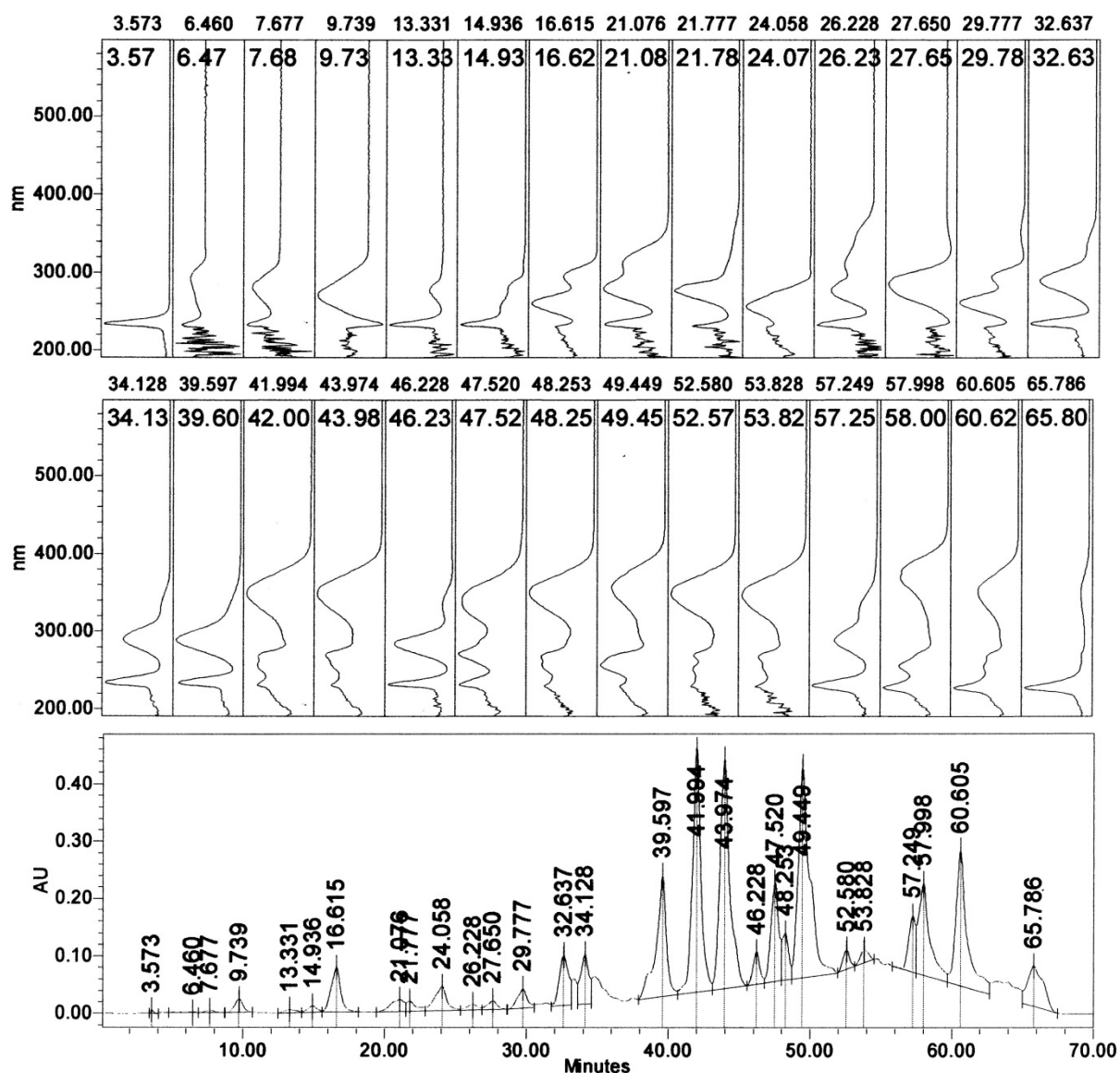
Figure 12.4: HPLC chromatogram of the ethanol-water Rooibos-honeybush tea extract eluted through a Nucleosil 100 C_{18} column (250 mm × 4.5 mm, i.d., 5 µm) by a gradient mobile phase of composition water/acetic acid (97:3 v/v) solvent A and methanol solvent B at flow rate of 1 mL min^{-1}. The wavelength of detection was 272 nm, and the top window shows the corresponding UV spectra of eluents.
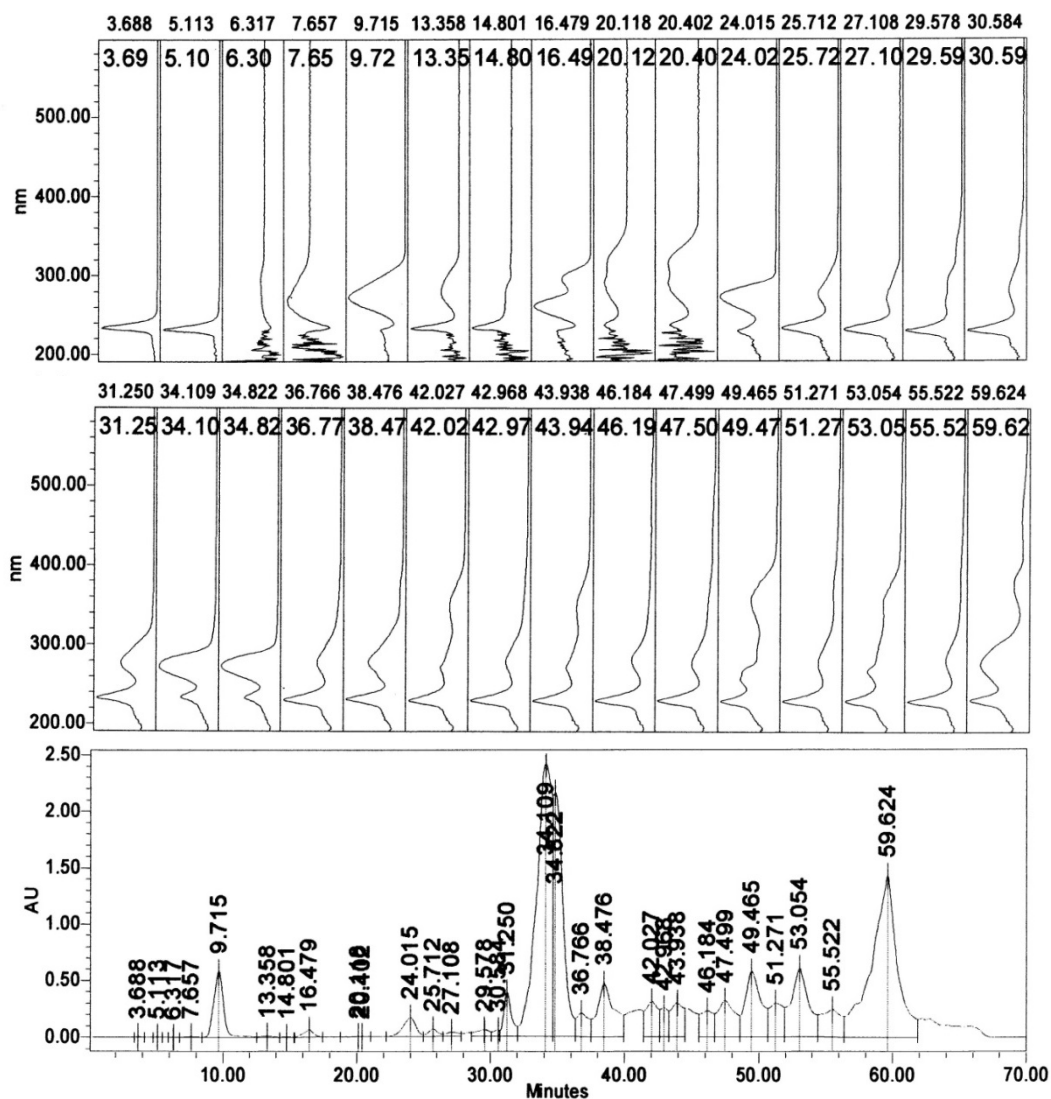
Figure 12.5: HPLC chromatogram of the boiling-water RHB tea extract eluted through a Nucleosil 100 C_{18} column (250 mm × 4.5 mm, i.d., 5 μm) by a gradient mobile phase of composition water/acetic acid (97:3 v/v) solvent A and methanol solvent B at flow rate of 1 mL min^{-1}.   The wavelength of detection was 272 nm, and the top window shows the corresponding UV spectra of eluents.

Table 12.18: Matched HPLC peaks, based on their retention times and UV spectra, from extracts of various Rooibos teas. These compounds are grouped into known polyphenolic groups based on their UV spectra.

polyphenols		Retention times of the compounds extracted by the ethanol-water extraction method		
		RB tea	RHB tea	RH
	1	3.642	3.688	3.573
	2		5.113	
	3		6.317	6.468
	4		7.657	
	5			7.677
Gallic acid			9.715	9.739
	7		13.358	13.331
	8		14.801	14.936
	9	16.725	16.479	16.615
	10		20.118	
	11		20.402	
Flavan-3-ol/Benzoic acid (Ryan and Robards 1998)		21.155		21.076
Flavan-3-ol/Benzoic acid (Ryan and Robards 1998)				21.777
	14			24.058
Flavan-3-ol/Benzoic acid (Ryan and Robards 1998)			24.015	
Flavan-3-ol/Benzoic acid (Ryan and Robards 1998)			25.715	
Flavan-3-ol/Benzoic acid (Ryan and Robards 1998)				26.238
	18		27.108	
	19			27.65
	20		30.578	
Flavan-3-ol/Benzoic acid (Ryan and Robards 1998)			30.584	
Flavan-3-ol/Benzoic acid (Ryan and Robards 1998)			31.25	
	23	33.04		32.637
Flavan-3-ol/Benzoic acid (Ryan and Robards 1998)			34.109	
	25	34.579		34.128
Flavan-3-ol/Benzoic acid (Ryan and Robards 1998)			34.822	
Flavan-3-ol/Benzoic acid (Ryan and Robards 1998)			36.766	
Flavan-3-ol/Benzoic acid (Ryan and Robards 1998)			38.476	
	29	40.198		39.597

	No			
Flavone/Flavanol/Chalcone (Ryan and Robards 1998)		42.676	42.027	41.994
Flavan-3-ol/Benzoic acid (Ryan and Robards 1998)			42.968	
Flavone/Flavanol/Chalcone (Ryan and Robards 1998)		44.62	43.938	43.974
	33		46.184	46.288
	34		47.499	
Flavone/Isoflavone (Ryan and Robards 1998)		48.138		47.52
Flavone/Flavanol/Chalcone (Ryan and Robards 1998)				47.52
Rutin		50.185	49.465	49.449
Flavanol/Chalcone (Ryan and Robards 1998)			51.271	
Flavone/Flavanol/Chalcone (Ryan and Robards 1998)				52.58
Flavone/Flavanol/Chalcone (Ryan and Robards 1998)		53.145	53.054	53.828
	41		55.522	
	42			57.998
Flavanol/Chalcone(Ryan and Robards 1998)		58.762		57.998
	44		59.624	
Flavanol/Chalcone (Ryan and Robards 1998)		61.314		60.605
	46	66.495		65.786

12.3.1.2 HPLC analysis of components of fruit juices

Reverse phase high-performance liquid chromatography ultraviolet (HPLC-UV) analysis was performed to identify various polyphenols in each of the fruit juice extracts. Retention times, UV spectra and library data provided structural information of compounds obtained without need for individual compounds isolation. Phenolic acids: gallic acid, ascorbic acid; and hydroxycinnamic acid were identified alongside caffeine and catechin. Three flavonoids: flavanone, flavan-3-ol and flavonol were identified. The wavelengths of detection employed were 265, 280, 300, 350 and 500 nm. Fig. 12.6 to 12.8 show the chromatograms obtained for each fruit juice extract and the UV-vis spectra for peaks obtained in three chromatograms. Tables 2 to 12.4 shows identifications made based on UV spectra, retention times and literature data.

Figure 12.6: HPLC chromatogram of the apple juice extract which was profiled on the Agilent 1200 series HPLC system comprising of a reversed-phase Phenomenex Luna ODS C18 column (250 mm × 4.6 mm, i.d., 5 µm), with a 35 minute gradient elution programme at a flow rate of 0.5 mL min⁻¹ and a PDA detection wavelength of 280 nm.

Figure 12.7: HPLC chromatogram of the grape juice extract which was profiled on the Agilent 1200 series HPLC system comprising of a reversed-phase Phenomenex Luna ODS, C18 column (250 mm × 4.6 mm, i.d., 5 µm) with a 35 minute gradient elution programme at a flow rate of 0.5 mL min⁻¹ and a PDA detection wavelength of 280 nm.

Figure 12.8: HPLC chromatogram of the orange juice extract which was profiled on the Agilent 1200 series HPLC system comprising of a reversed-phase Phenomenex Luna ODS, C-18 column (250 mm x 4.6 mm, i.d., 5 µm), a 35 minute gradient elution programme at a flow rate of 0.5 mL min-1 and a PDA detection wavelength of 300 nm.

Table 12.2: Description of the peaks observed in the HPLC chromatogram seen in Fig. 12.6. The UV-vis spectrum of each peak is displayed together with its absorption maxima. The retention times of the correlating peaks in the apple juice extract are listed.
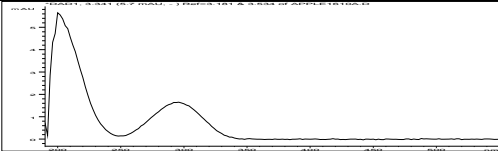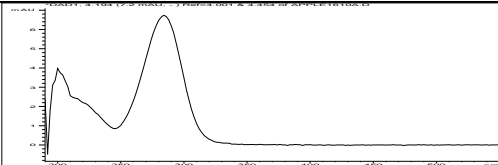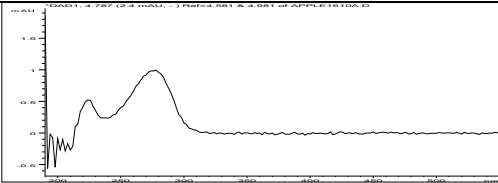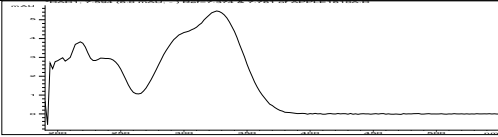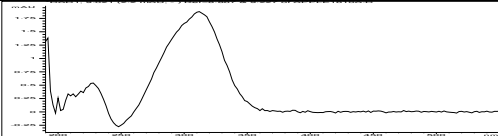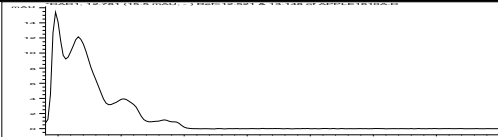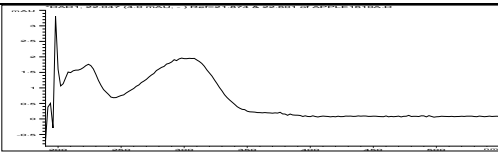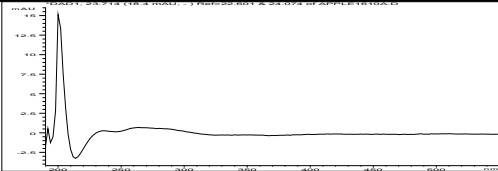
Retention time/min	UV/VIS spectrum	UV-vis absorption maxima/nm	Polyphenol identification
3.308		200, 296	-
4.214		202, 284	Flavanone (Abad-García et al. 2007)
4.749		226, 276	Flavan-3-ol (Abad-García et al. 2007)
7.525		206, 220, 234, 300, 326	Hydroxycinnamic acid (Tsao et al. 2003)
8.999		228, 312	Hydroxycinnamic acid (Tsao et al. 2003)[b]
12.758		198, 216, 252, 284	Flavanone (Abad-García et al. 2007)
21.993		214, 302	Hydroxycinnamic acid (Abad-García et al. 2007)
23.693		200, 236, 264	-

Table 12.3: Description of the peaks observed in the HPLC chromatogram seen in Fig. 12.7. The UV-vis spectrum of each peak is displayed together with its absorption maxima. The retention times of the correlating peaks in the grape juice extract are listed.

Retention time/min	UV-vis spectrum	UV-vis wavelength of maximum	Polyphenol identification
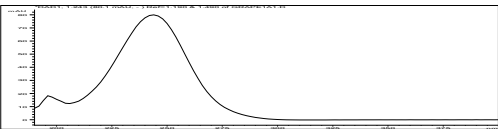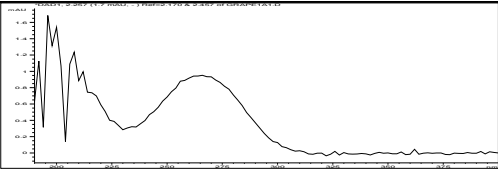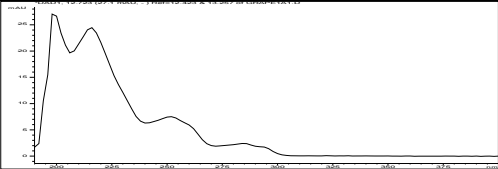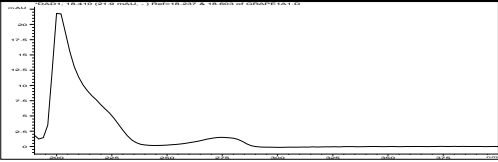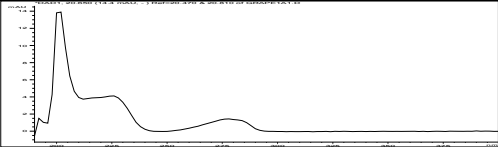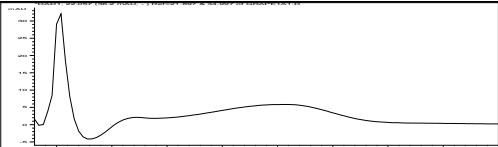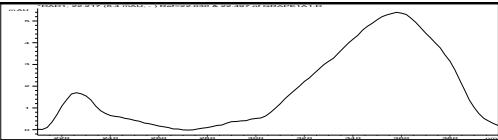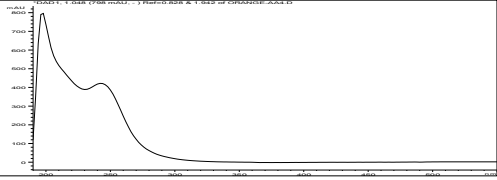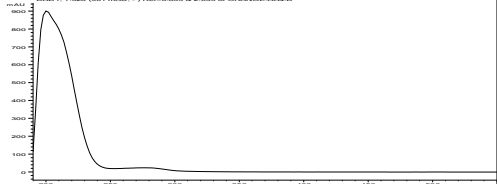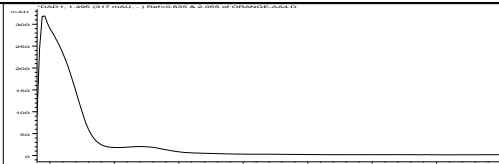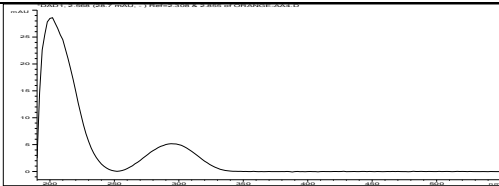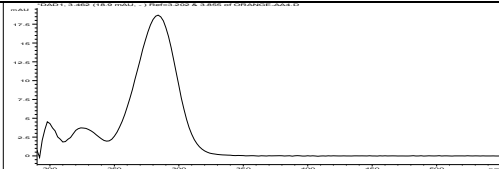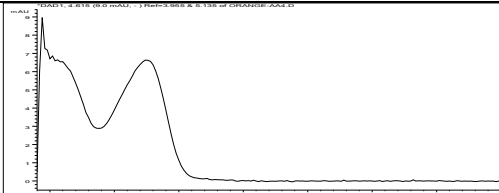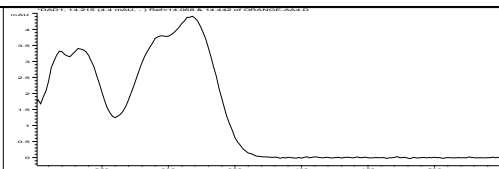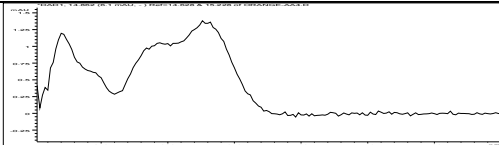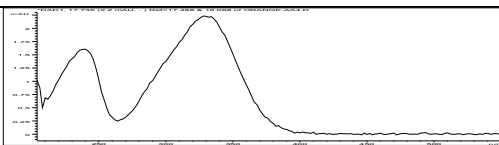
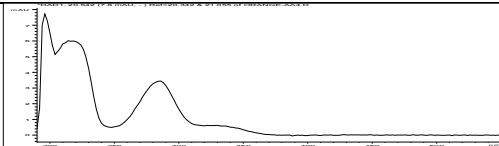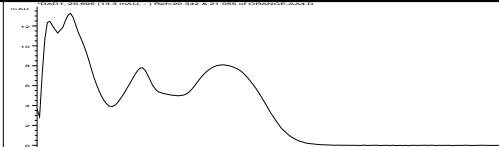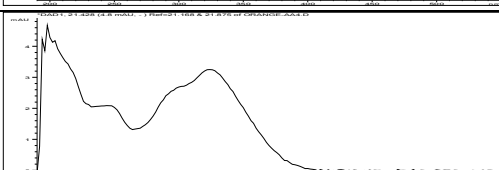|	absorption/nm	
1.270		196, 244	Ascorbic acid
2.279		264, 270	Hydroxybenzoic acid (Tsao et al. 2003; Abad-García et al. 2007)[a,b]
12.760		198, 216, 252, 284	-
18.378		200, 274	Catechin (Tsao et al. 2003)
20.589		202, 224, 278	Catechin (Tsao et al. 2003)
22.006		202, 236, 304	-
22.175 (at 350 nm)		226, 358	Flavonol (Howard and Mabry 1970)

Table 12.4: Description of the peaks observed in the HPLC chromatograms seen in Fig. 12.8. The UV/VIS spectrum of each peak is displayed together with its absorption maxima. The retention times of the correlating peaks in the orange juice extract are listed.

Retention time/min	UV/VIS spectrum	UV-vis absorption maxima/nm	Polyphenol identification
1.045		198, 242	Ascorbic acid
1.323		200, 276	-

1.493		196, 270	-
2.547		202, 294	-
3.459		198, 224, 284	Flavanone (Abad-García et al. 2007)
4.624		194, 274	Flavan-3-ol (Abad-García et al. 2007)
4.218		218, 232, 294, 318	Hydroxycinnamic acid (Abad-García et al. 2007)
14.867		220, 294, 326	Hydroxycinnamic acid (Abad-García et al. 2007)
16.322		220, 268, 322	-
17.734		238, 328	Hydroxycinnamic acid (Abad-García et al. 2007)
20.534		196, 214, 218, 286	-
20.709		200, 216, 272, 334	Flavone (Abad-García et al. 2007)
21.463		198, 244, 302, 324	Hydroxycinnamic acid (Abad-García et al. 2007; Tsao et al. 2003)

22.657		196, 228, 282	Flavanone (Abad-García et al. 2007)
25.284		196, 216, 224, 284, 328	Flavanone (Abad-García et al. 2007)
27.397		200, 284 , 332	Flavanone (Abad-García et al. 2007)
28.726		218, 286, 338	-
29.346		212, 254, 325	Hydroxycinnamic acid (Abad-García et al. 2007)
29.575		198, 208, 230, 256	-
30.356		312, 358	-

12.3.3   Total phenolic content

The Folin-Ciocalteu reaction method is a simple, yet accurate, method for quantitating phenols in a sample, though, it lacks specificity in the type of phenolics it quantitates. In this method, gallic acid was used as the standard and the phenolic quantity in the beverages is reported in milligram gallic acid equivalents per gram (mg GAE g^{-1} beverage). Antioxidant activity is associated with the presence of phenolic acids whose composition varies from one type of the beverage to another. The total phenolic content of beverages investigated (see Table 12.5) showed that GT (758.6 mg g^{-1} GAE) had the largest total phenolic content of all the samples. The teas were ranked as follows: GT(758.6 ± 20.48 mg g^{-1})> BT (580.1 ± 5.80 mg g^{-1}) > RH (573.5 ± 8.47 mg g^{-1}) > RHB (520.2 ± 6.40 mg g^{-1}) > RB (485.4 ± 6.70 mg g^{-1}). The fruit juices sampled also gave differences in total phenolic content (Table 12.5): orange (611.7 ± 18.87 mg g^{-1}), > grape (503.5 ± 11.07 mg g^{-1}) > apple (334.4 ± 7.41 mg g^{-1}).

Table 12.5: total phenolic content, IC_{50} of DPPH and FRAP value of beverages investigated (n = 3)

Sample	Total phenolic content/mg GAE g^{-1} tea	IC_{50} DPPH/µg mL^{-1}	EC_1/mM Fe(II)
GT	758.6 ± 20.48	3.60 ± 0.02	2.04 ± 0.03
BT	580.1 ± 5.80	4.50 ± 0.01	2.68 ± 0.03
RH	573.5 ± 8.47	10.79 ± 0.06	2.90 ± 0.04
RHB	485.4 ± 6.70	11.69 ± 0.01	3.21 ± 0.01
RB	520.2 ± 6.40	14.35 ± 0.04	4.41 ± 0.06
Orange*	611.7 ± 18.87	2.11 ± 0.02	2.52 ± 0.0 2
Grape*	503.5 ± 11.07	2.63 ± 0.02	4.47 ± 0.05
Apple*	334.4 ± 7.41	4.23 ± 0.07	4.55 ± 0.0 2

* units are in mg GAE dm^{-3}

12.3.4 Antioxidant assays

A lower value of a beverage sample required to scavenge 50 % of the DPPH present is considered to be a good antioxidant. Hence, the for the five tea samples the order of decreasing antioxidant activity is; GT (3.60 ± 0.02 µg mL^{-1}) > BT (4.50 ± 0.01 µg mL^{-1}) > RH (10.79 ± 0.06 µg mL^{-1}) > RHB (11.69 ± 0.01 µg mL^{-1}) > RB (14.35 ± 0.04 µg mL^{-1}). These sequence was supported by the results of the FRAP analysis indicating GT (2.04 ± 0.03 mM) > BT (2.68 ± 0.03 mM) > RH (2.90 ± 0.04 mM) > RHB (3.21 ± 0.01 mM) > RB (4.41 ± 0.06 mM). Thus GT showed a higher antioxidant activity followed by BT (Table 12.5).

The free radical scavenging activity of the fruit juices samples by using the same stable DPPH radical indicated a stronger activity (IC_{50}) in gallic acid equivalent for orange (2.11 ± 0.02 µg mL^{-1} GAE) > grape (2.63 ± 0.02 µg mL^{-1} GAE) > apple (4.23 ± 0.07 µg mL^{-1} GAE) and a similar trend for FRAP, EC_1: orange (2.52 ± 0.0 2 mM Fe(II)), > grape (4.47 ± 0.05 mM Fe(II)) > apple (4.55 ± 0.0 2 mM Fe(II)).

12.4 Discussion

The antioxidant activity of beverages is closely linked to the total polyphenol content. In this study the tea and fruit juice extracts were investigated for their radical-scavenging ability by reacting them with a stable free radical, namely the 1,1-diphenyl-2-picrylhydrazyl radical (DPPH). The progress of the reaction was monitored by measuring the loss of DPPH absorption at its wavelength of maximum absorption (8_{max}) at 522 nm. When the radical was reacted with the tea and fruit juice extracts, a loss in absorbance at its 8_{max} was observed with time. After four hours the tea and fruit juice extracts had scavenged all the DPPH radicals. This implies that the tea and fruit juice extracts acted as hydrogen donor towards the DPPH radical, the stoichiometry of the reaction depends on the number of sites for hydrogen abstraction on the donor compound. Polyphenols would therefore act as ideal donors since they contain conjugated phenyl rings, hydroxyl groups and carbonyl groups that are able to delocalise the radical electron left on the compound. The resulting relatively stable phenoxyl radicals subsequently form orthoquinones.

It is expected that sample extracts with high phenolic content are expected to demonstrate higher antioxidant potential because phenolic compounds (POH) act as free radical acceptors and chain breakers. They are known to interfere with the oxidation of lipids and other molecules by rapid donation of a hydrogen atom to radicals (R):

$$R^{\cdot} + POH \rightarrow RH + PO^{\cdot}$$
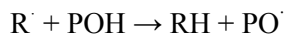
The resonance stabilization effect in the phenoxy radical intermediates (PO$^{\cdot}$) slows down a new chain reaction initiation and propagation thus acting as terminators of propagation route by reacting with other free radicals:

$$PO^{\cdot} + R^{\cdot} \rightarrow POR$$
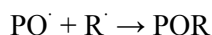
The presence of hydroxyl groups on the molecular structure of phenolic compounds makes them ideal structures for free radical scavenging activities because they readily donate a hydrogen atom or an electron to a free radical. Secondly the extended conjugated aromatic system creates room for delocalization of an unpaired electron thus enhancing its stability.

Consequently, the antioxidant activity of phenolic acids and their esters depends on the number of free hydroxyl groups in the molecule, favoured by steric hindrance. Hydroxycinnamic acids have been shown to be effective reducing agents with resonance effect of –CH=CH–COOH and the phenyl ring as aryloxy-radical stabilizing mechanism. Hence, a high content of hydroxycinnamic acids is likely to contribute to higher antioxidant effect of a given type of beverage. Apart from phenolic acids, green tea is reported to have a large amount of flavan-3-ols known as catechins (-) epigallocatechin-3-gallate (EGCG) is the most abundant catechin with an occurrence of up to 50 % of catechins by weight (Balentine et al. 2000).

Apart from polyphenols, tea is considered a rich source of other antioxidant molecules. Three major forms of antioxidant tea are green teas and black tea differing in mode of production and chemical composition (Balentine et al. 2000; Lambert and Elias 2010). The main antioxidants in tea are catechins, theaflavins, thearubigins, oxyaromatic acids, flavonols, such as kaempferol, myricetin, quercetin; and flavones, such as apigenin; derivatives of gallic acid, such as tannins. Animal model studies on carcinogenesis show that green tea and (-) epigallocatechin-3-gallate (EGCG) can inhibit tumorigenesis during initiation, promotion and progression stages (Lambert and Elias 2010). Results of catechins oxidation is formation of catechins dimers, known as theaflavins. These compounds are responsible for colour, taste, and antioxidant activity.

A qualitative investigation of the fruit juices showed hydroxycinnamic acids to be present in all the fruit juice samples (Tables 12.2 – 12.4) these are known to be potent antioxidants (Soobrattee et al. 2005). A wide variety of polyphenols were found in orange juice and this could be due to the fact that it was a blend of other fruits, hence, polyphenols from these fruits contributed to the observed activity. It was found that fewer polyphenols were present in grape juice and polyphenols that were expected, such as anthocyanidins were not detected. The results show that in comparison with orange juice, apple juice showed less variety of polyphenols and this correlated to its low antioxidant activity (Table 12.5). Both DPPH and FRAP assays showed that fruit juice with highest antioxidant activity was orange followed by grape and then apple juice. It can be concluded that blending of fruit juices increases the polyphenol content and variety thereby improving the antioxidant activity as observed in the case of the orange juice antioxidant activity.

12.5   Conclusions

Total phenolic content determines the antioxidant activity of a beverage as seen for green tea and orange juice blend. Each of the beverage amounts of polyphenols. The Of the beverages considered green tea and orange juice exhibited the best antioxidant activity..

References

Abad-García B, Berrueta LA, López-Márquez DM, Crespo-Ferrer I, Gallo B, Vicente F (2007) Optimization and validation of a methodology based on solvent extraction and liquid chromatography for the simultaneous determination of several polyphenolic families in fruit juices. Journal of Chromatography A 1154 (1–2):87-96

Balentine DA, Wiseman SA, Bouwens LCM, Malvy D (2000) Chemistry of tea flavonoids. Cahiers de Nutrition Dietetique 35:1S13-11S21

Benzie IFF, Strain JJ (1996) Ferric reducing antioxidant power assay: Direct measure of total antioxidant activity of biological fluids and modified version for simultaneous measurement of total antioxidant power and ascorbic acid concentration. Oxidants and Antioxidants, Pt A 299:15-27

Blois MS (1958) Antioxidant Determinations by the Use of a Stable Free Radical. Nature 181 (4617):1199-1200

Dejian H, Boxin O, Ronald LP (2005) The chemistry behind antioxidant capacity assays. Journal of Agricultural and Food Chemistry 53:1841-1856

Erickson L (2003) Rooibos Tea: Research into Antioxidant and Antimutagenic Properties. HerbalGram 59:34-45

Ferreira D, Kamara BI, Brandt EV, Joubert E (1998) Phenolic compounds from Cyclopia intermedia (honeybush tea). 1. Journal of Agricultural and Food Chemistry 46 (9):3406-3410

Ghafar MFA, Prasad KN, Weng KK, Ismail A (2010) Flavonoid, hesperidine, total phenolic contents and antioxidant activities from Citrus species. African Journal of Biotechnology 9 (3):326-330

Howard G, Mabry TJ (1970) Myricetin 3-o-methyl ether 3'-O-beta-glucoside, major flavonoid of Oenothera-speciosa (Onagraceae). Phytochemistry 9 (11):2413-2418

Kamara BI, Brandt EV, Ferreira D, Joubert E (2003) Polyphenols from honeybush tea (Cyclopia intermedia). Journal of Agricultural and Food Chemistry 51 (13):3874-3879

Koksal E, Bursal E, Dikici E, Tozoglu F, Gulcin I (2011) Antioxidant activity of *Melissa officinalis* leaves. Journal of Medicinal Plants Research 5 (2):217-222

Lambert JD, Elias RJ (2010) The antioxidant and pro-oxidant activities of green tea polyphenols: A role in cancer prevention. Archives of Biochemistry and Biophysics 501:65-72

Lin YL, Juan IM, Chen YL, Liang YC, Lin JK (1996) Composition of polyphenols in fresh tea leaves and associations of their oxygen-radical-absorbing capacity with antiproliferative actions in fibroblast cells. Journal of Agricultural and Food Chemistry 44 (6):1387-1394

Lin YS, Tsai YJ, Tsay JS, Lin JK (2003) Factors affecting the levels of tea polyphenols and caffeine in tea leaves. Journal of Agricultural and Food Chemistry 51 (7):1864-1873

Lu X, Wang J, Al-Qadiri MH, Ross FC, Powers RJ, Tang J, Rasco AB (2011) Determination of total phenolic content and antioxidant capacity of onion (*Allium cepa*) and shallot (*Allium oschaninii*) using infrared spectroscopy. Food Chemistry 129:637-644

Mandal P, Misra TK, Ghosal M (2009) Free-radical scavenging activity and phytochemical analysis in the leaf and stem of *Drymaria diandra* Blume. International Journal of Intergrative Biology 7 (2):80-84

Miketova P, Schram KH, Whitney JL, Kerns EH, Valcic S, Timmermann BN, Volk KJ (1998) Mass spectrometry of selected components of biological interest in green tea extracts. Journal of Natural Products 61 (4):461-467

Mukhtar H, Wang ZY, Katiyar SK, Agarwal R (1992) Tea components - antimutagenic and anticarcinogenic effects. Preventive Medicine 21 (3):351-360

Pisoschi AM, Cheregi MC, Danet AF (2009) Total Antioxidant Capacity of Some Commercial Fruit Juices: Electrochemical and Spectrophotometrical Approaches. Molecules 14 (1):480-493

Pulido R, Bravo L, Saura-Calixto F (2000) Antioxidant activity of dietary polyphenols as determined by a modified ferric reducing/antioxidant power assay. Journal of Agricultural and Food Chemistry 48 (8):3396-3402

Robbins JR (2003) Phenolic Acids in Foods: An Overview of Analytical Methodology. Journal of Agricultural and Food Chemistry 51:2866-2887

Ryan D, Robards K (1998) Phenolic compounds in olives. Analyst 123:31R-44R

Sarla S, Prakash MA, Apeksha R, Subhash C (2011) Free Radical Scavenging (DPPH) and Ferric Reducing Ability (FRAP) of *Aphanamixis polystachya* (Wall) Parker. International Journal of Drug Development and Research 3 (4):271 - 274

Sidddiqua A, Premakumari KB, Sultana R, Vithya, Savitha (2010) Antioxidant Activity and Estimation of Total Phenolic Content of *Muntingia calabura* by Colorimetry. International Journal of ChemTech Research 2 (1):205-208

Singleton VL, Orthofer R, Lamuela-Raventos RM (1999) Analysis of total phenols and other oxidation substrates and antioxidants by means of Folin-Ciocalteu reagent. In: Packer L (ed) Oxidants and Antioxidants, Pt A, vol 299. Methods in Enzymology. pp 152-178

Soleas GJ, Diamandis EP, Karumanchiri A, Goldberg DM (1997) A multiresidue derivatization gas chromatographic assay for fifteen phenolic constituents with mass selective detection. Analytical Chemistry 69 (21):4405-4409

Soleas GJ, Goldberg DM (1999) Analysis of antioxidant wine polyphenols by gas chromatography mass spectrometry. Oxidants and Antioxidants, Pt A 299:137-151

Soobrattee MA, Neergheen VS, Luximon-Ramma A, Aruoma OI, Bahorun T (2005) Phenolics as potential antioxidant therapeutic agents: mechanism and actions. Mutation Research 579 (1-2):200-213

Tsao R, Yang R, Sockovie E, Dale A, Zhou T (2003) Antioxidant phytochemicals in cultivated and wild Canadian strawberries. Acta Horticultural 626:25-35

Zhao JF, Jin XH, E YP, Zheng ZS, Zhang YJ, Athar M, DeLeo VA, Mukhtar H, Bickers DR, Wang ZY (1999) Photoprotective effect of black tea extracts against UVB-induced phototoxicity in skin. Photochemistry and photobiology 70 (4):637-644

Zuo YG, Chen H, Deng YW (2002) Simultaneous determination of catechins, caffeine and gallic acids in green, Oolong, black and pu-erh teas using HPLC with a photodiode array detector. Talanta 57 (2):307-316

Chapter Thirteen

General conclusions

There are different methods of combating the deleterious effects of ultraviolet radiation: these include sunscreens formulated with filters as well as clothing. The consequences of exposure to UV radiation and its correlation with the development of skin cancer have triggered a public education campaign promoting the use of sunscreens. Several inorganic and organic compounds have been explored and are employed for protection from harmful UV radiation. The challenge has been the localization of the active ingredients on the skin without permeating into the deeper viable layers of the skin and the photodegradation exhibited by some organic UV absorbers. Efforts are therefore ongoing to investigate various ways of reducing the skin penetration of sunscreen active ingredients, oxidative stress management and evaluation of different types of vehicles to prevent photodegradation of absorbers. The major aim is to make an aesthetically acceptable and stable broad-spectrum photoprotection sunscreen product.

The decomposition of sunscreen agents under sunlight exposure leads to a loss in the initial absorptive capacity. Photoproducts and reactive intermediates of photo-unstable filter substances coming into direct contact with skin, may behave as photo-oxidants or promote phototoxic or photoallergic contact dermatitis. Moreover, ultrafine sunscreen-grade TiO_2 irradiated with sunlight is photocatalytically active known to cause single- and double-strand breaks in DNA plasmids (Hidaka et al. 1997; Dunford et al. 1997; Buchalska et al. 2010). In view of the above concerns and the need to improve sunscreen photostability the photophysics and photochemistry of sunscreen absorbers require careful study.

Titanium(IV) oxide (TiO_2) is used as a physical blocker of ultraviolet (UV) radiation in many skin care products. To avoid the whitening effect of TiO_2 on the skin nano-particulate TiO_2 is used. Absorption of nano-TiO_2 through the skin is likely to interact with viable tissues because UV radiation absorption by nano-TiO_2 generates toxic reactive oxygen species such as hydroxyl radicals. Studies on the acute toxicity of TiO_2 nanoparticles in mammals indicate that intra-tracheal instillation, intraperitoneal injection or oral instillation of TiO_2 particles to the animals evoke an inflammatory response as well as certain histopathological changes. Ultrafine particles of the anatase form of titanium dioxide, which are smaller than 0.1 microns, are pathogenic. In this work eight skin-lighteners containing TiO_2 from the South African market were studied. The TiO_2 was extracted by a fusion technique and quantified by inductively coupled plasma-optical emission spectrometry (ICP-OES). Sequential solvent extraction was employed to isolate TiO_2 particles for characterisation by means of high resolution transmission electron microscopy (HR-TEM) and powder X-ray diffraction (PXRD). All samples considered in this study had a TiO_2 % (m/m) composition below the maximum limit specified by health regulatory bodies. In most samples the $TiO2$ content was of the order of 3 % (m/m) which on its own does not afford sufficient protection particularly in a skin-lightening product aimed to reduce melanin formation. Both forms of TiO_2: anatase and rutile, were found to be present. This is a cause of concern because of the greater photocatalytic activity of anatase TiO_2. Most samples contained nano-TiO_2 in the particle size range 16.23 nm to 51.47 nm that could possibly lead to detrimental effects.

The photochemical stability of common sunscreens in skin-lightening preparations was investigated in order to assess the photoprotective capacity of these products. These products contained the sunscreens 2-ethylhexyl-*p*-methoxycinnamate (EHMC), benzophenone-3 (BP3), *tert*-butyl-4-methoxydibenzoylmethane (BMDBM) and titanium dioxide (TiO_2). The percentage composition of the organic absorbers was determined by use of reversed-phase-HPLC. The physical absorber titanium dioxide was quantitated by ICP-OES. The percentage compositions of all the UV filters were found to be within the set maximum allowed limits of the various health regulatory bodies but

some of them were very low (0.066 % (m/m)) casting doubt on the product ability of the product to offer significant photoprotection. Photostability experiments were performed by application of a thin layer of the product on a quartz plate and exposing it to sunlight. The application density was kept at ~1.0 mg cm^{-2}. Skin-lightening preparations with sunscreens but without plant extracts showed an increase in transmittance on increased exposure to solar UV radiation. This indicated photo-instability due to possible degradation of the absorbers to chemical species that are less efficient absorbers. However, products that contained plant extracts in the skin-lightening preparations with sunscreens showed the opposite effect and improved their absorption characteristics particularly in the long wavelength region. This effect could be associated with formation of highly conjugated photoproducts and hence the high long wavelength absorption. We conclude that inclusion of the plant extracts in skin-lightening preparations is likely to photostabilize the UV absorbers. The photoprotection offered is likely to be enhanced but further investigation and profiling of the photo-toxicities of the photochemical products formed needs to be done.

The photo-stabilizing potential of plant extracts on sunscreen absorbers in commercial sunscreen products was also investigated. The amounts of the ultraviolet filters in these products were determined in order to check compliance with applicable regulatory requirements. The reversed-phase high performance liquid chromatographic method, with photo diode array (PDA) detection was used for the simultaneous determination of BP3, EHMC, methylene bis-benzotriazolyl tetramethylphenol (Tinosorb M), octocrylene (OCT), bis-ethylhexyloxyphenol methoxyphenyl triazine (Tinosorb S) and BMDBM. The physical absorbers: titanium dioxide and zinc oxide were quantified by using ICP-OES. The photostability experiment was performed by applying the product on a quartz glass plate with an application density of 1.0 mg cm^{-2} and exposing to sunlight. All samples contained UV filters within accepted maximum limits set by COLIPA. These sunscreen products contained significantly more of the active ingredients than the skin-lightening products. The products containing plant extracts showed remarkable photostability compared with products without the extracts irrespective of the percentage composition of the UV filters in the products. We conclude that plants extracts may contribute synergistically or otherwise to the observed photostability.

Since plant extracts in the skin-lightening and sunscreen products improved the photo-absorption properties it was of interest to investigate this aspect further. To this end four plant extracts were purchased: grape seed extract, mulberry extract, liquorice root extract and lavender oil. These extracts were found in some of the skin-lighteners and sunscreens investigated and so their choice was made to study their possible photostabilization effect on commonly used sunscreens. The effect and photostabilizing ability of grape seed extract on the common sunscreen absorbers: EHMC, BP3 and BMDBM was investigated. The chemical composition of a derivatised sample of grape seed extract was determined by GC-MS. It was found that grape seed contained catechin and epicatechin which can chemically combine to form proanthocyanidins which are likely contributor to the enhanced UV absorption. The photostability of the samples was studied by exposure to simulated solar radiation. The change in UV absorption and chemical transformations were followed by standard spectrophotometric and chromatographic methods. Exposure of the extracts to UV radiation increased the UV absorption capacity of the extracts linearly at 280 nm and 320 nm. All sunscreens showed a higher degree of photostability in the extract. The inherent photoinstability of BMDBM when exposed to UV radiation was almost eliminated. The mixture of all the sunscreens in the extract showed very high photostability and greater bathochromic shift covering the entire UVB and UVA region. The grape seed extract indicated potential to afford broad-spectrum protection and thus, likely to reduce the quantity of absorbers added in a formulation. The incorporation of the grape seed

extract in sunscreens and other cosmetic formulations for topical application is likely to boost photoprotection by stabilizing sunscreens included.

The photostability of EHMC, BP3 and BMDBM in a methanolic solution of mulberry extract was investigated. The effect of mulberry extract on the photo-absorption capacity of each sunscreen was studied by exposing the samples to simulated solar radiation. The photochemical transformations were then followed by standard spectrophotometric methods. The new chemical species were monitored by means of reversed-phase-HPLC and derivatised constituents of mulberry extract were identified by GC-MS. The absorptive efficacies of the sunscreens were greatly improved when each was mixed with mulberry extract alone. The mulberry extract seemed to favour the chelated enol form of BMDBM and hence contributed to enhanced UVA absorption. BP3 remained unchanged for all exposure periods indicating no chemical interaction. Hence no side reactions of BP3 are envisaged in this mixture. EHMC showed a drop in absorption but subsequentlystabilized. A photochemical isomerisation to a strongly absorbing UVB species was observed. The mulberry extract therefore was found to enhance the UVB absorption potential of EHMC. However, a combination of the three sunscreens in mulberry extract was found to greatly reduce UVA absorbing chemical species and favour UVB absorbing species. We conclude that mulberry extract may be good a photochemical stabilizer of sunscreens and would reduce the amount of sunscreens incorporated in a single product.

The photostabilizing potential of liquorice root extract on commonly used UV absorbers in the market was investigated. The effect of UV light on the photochemical stability of EHMC, BP3 and BMDBM was studied by irradiating the extract incorporated samples by simulated solar radiation. The photochemical transformations were monitored by standard spectrophotometric and chromatographic methods: UV, GC-MS, and HPLC-UV-ESI-MS/MS. The extract showed good UV absorption but degrades on UV exposure. The incorporation of BP3 showed enhanced photostability by chemical interaction with the extract. EHMC showed stability with prolonged exposure and BMDBM showed photodegradation. This extract may not be a good stabilizer for BMDBM but reacts with EHMC to yields compounds that are photostable. Liquorice root extract may enhance the photo-absorption of BP3 and EHMC but not BMDBM. The phenolic secondary metabolites present may help free radical scavenging.

The lavender oil was bought from a local market and the photostabilizing potential investigated against common sunscreening agents in cosmetics. The samples were exposed to simulated solar radiation in 1 mm pathlength quartz cuvette and spectral changes recorded on a UV-Vis dual beam spectrophotometer. The photochemical changes were monitored by GC-MS. The absorption spectra of lavender oil showed maximum absorption at 260 nm indicating no significant UVB and UVA absorption. The absorption capacity of lavender oil drops with increasing time of irradiation showing steady photodegradation on exposure to light. The combination of lavender oil and BMDBM showed less photodegradation than BMDBM alone, with the GC-MS results showing fragments characteristic of [2+2] cycloaddition reactions. This indicated some degree of photostabilization of BMDBM in the presence of lavender oil. The spectra of a methanolic solution of lavender oil and EHMC showed an erratic increase then steadily dropped with absorption of light showing a low level of photostabilization of EHMC in lavender oil. There was a small spectral change for BP3 mixture with lavender oil indicating a good degree of stability; however, more photochemical products were observed by GC-MS. These could indicate sensitization reactions initiated by the triplet excited state of BP3. We conclude that lavender oil exhibits some degree of photostabilization of the sunscreens under investigation but it self cannot be used as UVB/UVA absorber. The inclusion of EHMC, BP3

and BMDBM in a lavender oil cosmetic product formulation, may pose a greater health risk due to the unknown photoproducts formed.

Since the plant extracts were shown to be able to enhance photoprotection it was of interest to investigate the properties of a South African plant material for this purpose. Previous work in our laboratories showed the ability of a polyphenolic extract from *Sutherlandia frutescens* to photostabilize BMDBM (Mturi 2005). The phenolic acids form part of the polyphenolic content of plants and also exhibit antioxidant properties, it was therefore important to isolate then, characterise them and determine their UV absorption properties.

Sutherlandia frutescens is a very important ethnopharmacological plant. We set to investigate the phenolic acid content, antioxidant activity and UV absorption potential of *Sutherlandia frutescens* subspecies *microphylla,* commonly known as the cancer bush (CB). *Sutherlandia frutescens* medicinal value and reported role in the management of chronic diseases, like HIV/AIDS, generates interest for total phenolic acid quantitation in this plant. The antioxidant properties of phenolic acids are known to reduce the risk of chronic infections including cancer and heart ailments linked to oxidative stress. Phenolic acids were extracted from the leaves of the CB by both Soxhlet (SXE) and ultrasonication (USE) extraction methods. These extracts were analysed by ultraviolet spectroscopy, high performance liquid chromatography, and liquid chromatography-mass spectrometry. Six phenolic acids were identified and quantitated by means of reversed-phase-HPLC-PDA, under isocratic elution conditions with an external standard method. The identified phenolic acids were: gallic, *p*-hydroxybenzoic, vanillic, caffeic, syringic and *p*-coumaric acids. RP-HPLC-PDA-ESI-MS was used to characterise three novel phenolic acids: 5-hydroxy-2-vinylbenzoic acid, an isomer of *p*-coumaric acid (**C-1**); (Z)-3-(4-hydroxy-2-methoxyphenyl)acrylic acid (**C-2**); and (Z)-2-hydroxy-3-(4-methoxyphenyl)acrylic acid (**C-3**), ferulic acid isomers. The Folin-Ciocalteu protocol was used to determine the total phenolic content of various phenolic acid extracts. The ultrasonication-diethyl ether (USDE) fraction gave GAE = 0.1247 mg g^{-1} and the ultrasonication-ethyl acetate extract (USEA), GAE = 0.0769 mg g^{-1} as the highest and lowest total phenolic content respectively. The antioxidant activity of these extracts was investigated by the 1,1-diphenylpicryl-2-hydrazyl (DPPH) free radical scavenging assay and the ferric reducing antioxidant power (FRAP) assay. The USDE extract (EC_{50} = 30.38 µg mL^{-1}) and soxhlet-diethyl ether (SXDE) (EC_{50} = 48.63 µg mL^{-1}) were the highest and lowest antioxidants by DPPH assay. The FRAP assay showed higher activity for USDE (EC_1 = 41.53 µg mL^{-1}) and a lower value for SXDE extract (EC_1 = 33.05 µg mL^{-1}). The CB extracts with higher phenolic content had higher antioxidant activity and thus suitable remedies for free radical mediated ailments.

The UV-vis spectra of CB extracts had significant absorption in the UV region, and hence viable are ingredients in sunscreening preparations. Further work will entail investigating the photostabilizing potential of CB phenolic acids on individual sunscreen absorbers and their mixtures.

The polyphenols from plants draw increasing attention due to their potent antioxidant properties and marked effects in prevention of various oxidative stress associated diseases such as cancer. In this work teas and fruit juice samples were purchased from a local South African market for determination of their phenolic content and antioxidant activity. The Folin-Ciocalteu protocol was used to determine the total phenolic content and was expressed as gallic acid equivalents. The antioxidant activity was tested by assessing the free radical scavenging activity of the stable radical, DPPH, and FRAP of the samples. The two models compared well with the determined total phenolic content of tea samples expressed in gallic acid equivalent per gram of dry sample: GT (758.6 ± 20.48 mg g^{-1}) >

BT (580.1 ± 5.80 mg g^{-1}) > RH (573.5 ± 8.47 mg g^{-1}) > RHB (485.4 ± 6.70 mg g^{-1}) > RB (520.2 ± 6.40 mg g^{-1}). The DPPH IC_{50}: GT(3.60 ± 0.02 μg mL^{-1}) > BT (4.50 ± 0.01 μg mL^{-1}) > RH (10.79 ± 0.06 μg mL^{-1}) > RHB (11.69 ± 0.01 μg mL^{-1}) > RB (14.35 ± 0.04 μg mL^{-1}). This sequence was supported by the results of the FRAP analysis in mM of Fe(II) showing; GT (0.204 ± 0.03 mM)> BT (0.268 ± 0.03 mM) > RH (0.290 ± 0.04 mM) > RHB (0.321 ± 0.01 mM) > RB (0.441 ± 0.06 mM). Thus, GT (green tea) had a higher antioxidant activity followed by BT (black tea). All the tea samples showed the presence of polyphenols. The fruit juices sampled also gave differences in total phenolic content: orange (611.7 ± 18.87 mg GAE L^{-1}) > grape (503.5 ± 11.07 mg GAE L^{-1}) > apple (334.4 ± 7.41 mg GAE L^{-1}) and subsequently varying antioxidant activity. The free radical scavenging activity done by using the stable DPPH radical indicated a stronger activity (IC_{50}) in gallic acid equivalents for orange (211.3 ± 2.59 mg GAE L^{-1}), > grape (263.2 ± 1.73 mg GAE L^{-1}) > apple (423.3 ± 7.00 mg GAE L^{-1}) and similar trend for FRAP, EC_1: orange (2.52 ± 0.02 mM Fe(II)), > grape (4.47 ± 0.05 mM Fe(II)) > and apple (4.55 ± 0.0 2 mM Fe(II)). HPLC-UV analysis of the fruit juices indicated orange juice had the larger polyphenolic content. All the beverages had a good activity and correlated well with the total phenolic content. A comparison of the total phenolic content shows that the teas have higher phenolic content than the fruit juices. Increased dietary intake of these beverages should be encouraged as a remedy for various oxidative stress related degenerative ailments and to prolong life expectancy.

We investigated systems that could provide a lead to photostable sunscreen products. Our work demonstrates for the first time the photostabilization potential of plant extracts on common UV absorbers in sunscreens and skin-lightening preparations. We have also shown that the incorporation of plant extracts may not require a combination of sunscreen absorbers to achieve broad-spectrum protection. Therefore, the reduction in the number of organic absorbers incorporated in a formulation is likely to decrease potential side-effects. Efforts have been made to profile the photoproducts in various plant extracts with a view to determining their identities as this is important for characterising their photo-toxicities in the future.

References

Buchalska M, Kras G, Oszajca M, Lasocha W, Macyk W (2010) Singlet oxygen generation inthe presence of titanium dioxide materials used as sunscreens in suntan lotions. Journal of Photochemistry and Photobiology A: Chemistry 213:158-163

Dunford R, Salinaro A, Cai L, Serpone N, Horikoshi S, Hidaka H, Knowland J (1997) Chemical oxidation and DNA damage catalysed by inorganic sunscreen ingredients. FEBS Letters 418 (1–2):87-90

Hidaka H, Horikoshi S, Serpone N, Knowland J (1997) In vitro photochemical damage to DNA, RNA and their bases by an inorganic sunscreen agent on exposure to UVA and UVB radiation. Journal of Photochemistry and Photobiology A: Chemistry 111:205-2013

Mturi JG (2005) An investigation of the photostabilisation of the sunscreen absorbers by plant polyphenols. MSc Dissertation, University of KwaZulu-Natal, Durban, South Africa